FUZZY HYBRID APPROACHES FOR SOFT CLASSIFICATION OF SATELLITE IMAGES

Ph.D. THESIS

by

RAKESH KUMAR DWIVEDI

DEPARTMENT OF CIVIL ENGINEERING
INDIAN INSTITUTE OF TECHNOLOGY ROORKEE
ROORKEE-247667 (INDIA)
MAY, 2014

FUZZY HYBRID APPROACHES FOR SOFT CLASSIFICATION OF SATELLITE IMAGES

A THESIS

Submitted in partial fulfilment of the
requirements for the award of the degree
of
DOCTOR OF PHILOSOPHY
in
CIVIL ENGINEERING

by

RAKESH KUMAR DWIVEDI

DEPARTMENT OF CIVIL ENGINEERING
INDIAN INSTITUTE OF TECHNOLOGY ROORKEE
ROORKEE-247667 (INDIA)
MAY, 2014

INDIAN INSTITUE OF TECHNOLOGY ROORKEE

CANDIDATE'S DECLARATION

I hereby certify that the work which is being presented in the thesis entitled **"FUZZY HYBRID APPROACHES FOR SOFT CLASSIFICATION OF SATELLITE IMAGES "** in partial fulfilment of the requirements for the award of the Degree of Doctor of Philosophy and submitted in the Department of Civil Engineering, Indian Institute of Technology Roorkee, Roorkee is an authentic record of my own work carried out during a period from July, 2010 to May, 2014 under the supervision of Prof. S.K. Ghosh, Department of Civil Engineering, Indian Institute of Technology Roorkee, Roorkee and Dr. Anil. Kumar, Indian Institute of Remote Sensing (Indian Space Research Organization), Dehradun.

The matter presented in this thesis has not been submitted by me for the award of any other degree of this or any other Institute.

(RAKESH KUMAR DWIVEDI)

This is to certify that the above statement made by the candidate is correct to the best of our knowledge.

Date: ……

(Anil Kumar)
Supervisor

(S.K. Ghosh)
Supervisor

The Ph.D. Viva-Voce Examination of **Mr**. **Rakesh Kumar Dwivedi**, Research Scholar, has been held on ……

Signature of Supervisors **Chairman, SRC** **External Examiner**

Head of the Department/Chairman, ODC

ABSTRACT

This study is intends to provide an exhaustive treatise on hybrid soft classification algorithm design, analysis and testing using multi-spectral remote sensing imagery. Satellite image classification is a complex process that is affected by various parameters. On the basis of current practices of image classification, the problem area has been examined and better approach of classification using spectral and spatial information have been proposed. The major emphasis has been placed on the use of advanced classification approaches and the techniques used for improving the accuracy of classification. In medium and course resolution images, occurrences of mixed pixels at the scale of measurement are a major problem. Due to this problem, there has been an increasing interest to use contextual information (spectral, spatial or temporal) to eliminate possible ambiguities.

Fuzzy set based classifier such as Fuzzy *c*-Mean (FCM), Possibilistic *c*-Mean (PCM) and Noise Clustering (NC) classifier can be used to handle mixed pixels. Although, these classifiers have the capability to classify mixed pixels by assigning membership value but unable to incorporate entropy and spatial contextual information of an image. Use of entropy as a regularizer and context, eliminates the problem of isolated pixels and improves the accuracy of a classifier. In this study, three Fuzzy set based classifier (FCM, PCM, NC), two entropy based i.e. Fuzzy *c*-Mean with Entropy (FCMWE) and Noise Clustering with Entropy (NCWE) and five contextual based i.e. FCM with contextual, PCM with contextual, NC with contextual, FCMWE with contextual and NCWE with contextual classifier has been considered by using MRF models. To incorporate contextual information of an image, Smoothness Adaptive (SA) prior and four Discontinuity Adaptive (DA), MRF models have been used. The hybridized SA and DA prior have been tested on coarse and medium resolution dataset i.e. AWiFS, LISS-III and LISS-IV of Resourcesat-1 with spatial resolution of 60m, 20m and 5m respectively. The classified fraction images of AWiFS have been tested using finer resolution dataset of LISS-III or LISS-IV as reference.

To resolve the sub-pixel area allocation problem, class membership, Sub-pixel Confusion Uncertainty Matrix (SCM), FERM, MIN-MIN, MIN-LEAST and ENTROPY methods has been

introduced to assess the accuracy of fuzzy, entropy and contextual based hybrid soft classifiers. All the classification algorithms of this study have been tested in supervised mode using Euclidian weighted norm to classify the remote sensing imagery and entropy has been used to measure the accuracy in terms of uncertainty without using any kind of ground reference data.

In FCM classifier, it has been found that irrespective of datasets, the generalized optimum value of weighting exponent (*m*) has also been fixed as 2.4 for classification using FCM classifier. For PCM classifier, it has been found that irrespective of dataset, *m*=2.1 have been found to be more suitable to classify agriculture. However, for barren land, moist land and water body, *m*=2.2 yield good classification result while for sal forest and eucalyptus plantation, *m*=2.3 gives the best result. It has also been found that MIN-LEAST operator is not suitable to assess the accuracy of PCM.

NC classifier has been used to overcome the problem of noisy data points. The performance of NC classifier is dependent upon the optimized value of weighting exponent (*m*=2.4) and by varying value of resolution parameter (δ). It is found that irrespective of datasets, the optimized value of (δ) for agriculture, sal forest, eucalyptus plantation, barren land, moist land and water body is 3.2×10^5, 0.8×10^5, 3.1×10^5, 4.1×10^5, 27.8×10^5, and 3.1×10^5 respectively. Further, it is found that for $\delta = 10^5$, all accuracy measures have highest value and achieve the threshold criterion of accuracy measures of 85% with least uncertainty values when LISS-III and LISS-IV dataset is used as reference data. Thus, the optimum value of δ has been fixed as 10^5 for NC classifier.

The joint effect of two purely fuzzy models (FCM and NC) and entropy models which are similar to statistical model have been investigated. The NCWE classifier is able to extract the multiple land cover class at a time, at sub-pixel level. The performance of this classifier is dependent on the constant value of resolution parameter $\delta=10^5$ and regularizing parameter (ν). It is observed that irrespective of datasets, the optimized value of (ν) for agriculture and barren land is 2.12×10^2, while for sal forest, eucalyptus plantation, moist land and water body, the optimized value is 10^2. In the process of identifying the generalized optimized value of ν, it is found that for $\nu = 10^2$, where all the accuracy indices have high value.

To perform the FCMWE classification, a fixed value of *m*=1 has been used for different values of ν. It has been found that irrespective of datasets used, $\nu = 6.6 \times 10^2$ is found to be most suitable in classifying agriculture and eucalyptus plantation. However, for barren land, moist land and water body, $\nu = 10^2$ is found to be suitable for classification using FCMWE classification approach. For sal forest, $\nu = 7.7 \times 10^2$ is found to be most appropriate for classification.

To incorporate the spatial contextual information along with spectral information, hybridized model has been devised to resolve the problem of mixed pixel. Contextual information has been added into FCM, PCM, NC, NCWE and FCMWE classifiers to generate smoothness effect, preserving the edges and reduce the classification uncertainty. In FCM-S classifier, it has been observed that for optimized values of λ and β are 0.7 and 3.5 respectively for AWiFS, LISS-III and LISS-IV datasets. To incorporate spatial contextual information with FCM, four DA-MRF models have been implemented. The hybridized model of DA approach has been devised to resolve the problems of mixed pixel and over-smoothing. Four objective functions of FCM with Discontinuity Adaptive (DA) prior known as FDM-(H1), FDM-(H2), FDM-(H3), and FDM-(H4) have been defined. It is observed that FDM-(H3) model produces highest accuracy of 95%. The basic advantage of hybridization DA model with FCM classifier is that classes are well classified and edges are not over smoothed. In PCM-S classifier, for λ=0.6 and β=3.0, is found to be more suitable to classify multiple land cover classes. In case PCM-DA-MRF model, it has been found that PDM-(H4) model produces higher accuracy for all cases of λ=0.5 and γ=0.5.

The idea of using hybrid approach for soft classification i.e. Noise Clustering (NC) with contextual is a new approach which helps significantly to eliminate noise pixels while incorporating spatial contextual information. It has been found that for NC-S classifier, for λ=0.7 and β =3.5, class membership lies between 0.90 to 0.99 for all six classes selected for this study and that the computed entropy is lies between 0.005 to 0.65. This trend indicates that pixels of particular interest have been classified properly using context. To perform Noise Clustering with contextual classification with all four DA-MRF models, the optimized value of resolution parameter $\delta = 10^5$ has been taken. For **N**DM-(H1), NDM-(H2), NDM-(H3), NDM-

(H4) classifier, it has been found that the optimized value of λ and γ is 0.4. Further, it has been found that NDM-(H4) model produces highest accuracy in all cases. This classifier uses spatial contextual information in an appropriate manner which helps significantly in the removal of noisy pixels in remote sensing imagery.

For FCMWE-S classifier, it has been found that for λ=0.4 and β =2.0, agriculture, barren land, moist land and water body produces highest membership. However, for λ=0.5 and β =2.5 and λ=0.6 and β=3.0, sal forest and eucalyptus plantation produces highest membership respectively. It has been found that for FCMWE with Discontinuity Adaptive Prior, the optimized value of λ and γ is 0.7. The accuracy values have been compared for all four DA models and it has been found that FDEM-(H1) model produces highest accuracy in all cases. While performing NCWE-S classification, it has been found that for λ=0.6 and β =3.0, all land cover classes produces the highest membership. In case of NCWE-DA-MRF model, the accuracy values have been compared for all four DA models and it has been found that NDEM-(H2) model produces highest accuracy in all cases.

On the basis of SCM accuracy, the comparative performance analysis has been done for all the classifiers, and it is found that NDM (H4) classifiers produce the highest accuracy (99.79%) with minimum entropy (0.005). This output reflects that the combination of noise clustering classifier with contextual information using DA model produces least uncertainty value when compared to other classifiers. Thus, NDM-(H4) model is less affected by uncertainty and hence, it can be used to generate spectrally and spatially consistent thematic maps which preserve the edges between classes.

The hybrid approach of soft classification based upon contextual is effective for the appropriate land cover identification and applicable for the multiple land cover identification at the same time. Thus, this study has explored the applicability of SA and DA MRF models for incorporating spatial contextual information of an image. The finding of the study illustrate that by utilizing appropriate hybrid classification strategy, accurate and meaningful land cover classifications can be produced from remote sensing imagery with minimum level of uncertainty. This study also suggests that suitable use of context allows the elimination of ambiguities, recovery of missing information and helps in correction of errors.

ACKNOWLEDGEMENTS

First of all, Praise to God, the creator, destroyer and the cherisher of this universe

The thesis in your hand is the essence of blessings of elder's, support, guidance and cooperation of many people, friends and family members. In the sequel that follows, some names may or some may not be there, but their contributions have all been of importance.

First and foremost, I would like to express my sincere gratitude to my supervisors **Prof. Sanjay K. Ghosh** and **Dr. Anil Kumar**, for their support, enthusiastic guidance and advice, which were the constant source of inspiration for the completion of this research work. I appreciate their discussions as well as the continuous encouragement to carry out the research reported in this thesis.

Prof. Sanjay K. Ghosh will forever remain my creditor for his caring attitude and emotional backing. On one hand, I have learnt the nuances and fruits produced by hard work from him. He introduced me to the topic of hybrid classification. May be he was in office, home or out of station but he has always provided his guidance, expertise, moral support and encouragement through personal meeting in his office, telephone or Internet. He helped to understand this research work by dividing all objectives into small parts and complete them step-by-step. He provided his precious time for long hour's discussion whenever required to understand this research work. Furthermore, he has always shown for the great enthusiasm for my work and also his humanistic and warm personal approach, which has given me strength to carry out this research on steady and smooth course. I humbly acknowledge my lifetime gratitude to him.

My indebtedness towards the kind hospitality and willful support rendered by **Mrs. Chitrita Ghosh.** I wish to express my deep sense of gratitude to Madam for her encouraging and caring words.

I express my deep sense of gratitude to **Dr. Anil Kumar,** Scientist/Engineer 'SF', IIRS, Dehradun, for his guidance and technical support as supervisor.

I am thankful to **Shri. Suresh Chand Jain**, Honorable Chancellor, Teerthanker Mahaveer University, Moradabad, who permitted me to join Indian Institute of Technology Roorkee for Ph.D research work.

I am also thankful to **Shri. Manish Jain**, Hon'able Group Vice Chairman, Teerthanker Mahaveer University, Moradabad, who has directed university authorities to make a provision of study leave for joining my Ph.D research work at Indian Institute of Technology Roorkee.

I am also thankful to **Prof. R. K. Mittal and Prof. R.K. Mudgal (Vice Chancellor, TMU)**, for providing 'No Objection Certificate', for joining my Ph.D research work at Indian Institute of Technology Roorkee.

I am also grateful to **Prof. (Dr.) P. K. Garg**, Head Geomatics Engineering Section, Department of Civil Engineering, for providing research guidance during the course of this work.

I am also thankful to my S**RC Committee members** at IIT Roorkee, for providing suggestions and corrections at initial stage as well as at final submission stage of this research work.

I acknowledge with gratitude for the financial support provided by Quality Improvement Program (QIP) centre, to pursue this research in the Civil Engineering Department, IIT Roorkee.

My indebtedness towards the kind help by **Mr. Danish Ather**, **Mr. Priyadarshi Upadhyay, Dr. Kapil Govil, Dr. Rajive Kumar, Mr. Rajat Agarwal, Mr. Shambhu Bhardwaj, Dr. Ashendra Saxena** and all my departmental faculty colleagues for their encouraging, caring words and suggestions which have contributed directly or indirectly in a significant way towards completion of this thesis.

I thankfully appreciate and acknowledge my indebtedness to my colleagues **Atul Kant Piyoosh, Veerender Yadav, Siddarth Khare, Upendra Rajput, Abhishek Bhatt, Prateek Verma, Sushila Dahiya, Manish Tiwari, Ajay Tiwari, Pankaj Pratap Singh, Anoop Shukla,**

Surendra Pal Singh, Kapil Rohila and Manoj Gupta for being not only my best friends, but also for the good moments, interesting discussions and significant help during the entire research tenure.

I owe a deep sense of gratitude to All-pervading Spirit whose Divine Light provided me the perseverance, guidance, inspiration, faith and strength to carry on even when the going was tough.

My special sincere, heartfelt gratitude and indebtedness are due to my father **Shri. G.P. Dwivedi**, my mother **Srimathi Sushila Dwivedi**, my brothers **Pankaj Dwivedi** and **Neeraj Dwivedi**, my sister, **Anupa**, my relatives and friends for their sincere prayers, constant encouragements and blessings. One important thing I would like to mention that my brothers are very much special for me, during my entire career struggle, their financial support and mental motivation makes me energetic. My sincere gratitude to both my younger brothers.

I am lucky to get the full support from my wife and also my best friend ***Mrs. Priyanka Dwivedi,*** throughout all the stages of my work. Thanks to my lovely wife for her friendship, love, patience, special humor and assistance, this provided me an inner strength and encouragement. Finally I thank my handsome kids **Mr. Shiv Dwivedi** and **Mr. Iesh Dwivedi** for their love and inspiration, although I was unable to spend as much time with them as they deserved. This thesis is therefore dedicated to my love **Shiv** and **Iesh.**

(Rakesh Kumar Dwivedi)

CONTENTS

LIST OF FIGURES

LIST OF TABLES

LIST OF ABBREVIATIONS

ALCM	-	Automatic Land Cover Mapping
ALOS	-	Advanced Land Observing Satellite
ANC	-	Alternative Noise Clustering
ANN	-	Artificial Neural Networks
AWiFS	-	Advanced Wide Field Sensor
ASTER	-	Advanced Spaceborne Thermal Emission and Reflection Radiometer
ATCOR	-	Atmospheric Correction tool of ERDAS software
ATM	-	Airborne Thematic Mapper
AVINER	-	Advanced Visible and Near Infrared Radiometer
D-Matrix	-	Diagonal Matrix
DEA	-	Differential Evolution Algorithm
DEM	-	Digital Elevation Model
DInSAR	-	Differential Interferometric Synthetic Aperture Radar
DTC	-	Decision Tree Classifiers
D.V-C Matrix	-	Diagonal Variance - Covariance Matrix
ECHO	-	Extraction and Classification of Homogenous Objects
EDSVM	-	Entropy Decomposition and Support Vector Machine
ENVI	-	ENvironment for Visualizing Images
ERDAS	-	Earth Resource Data Analysis System
ETM	-	Enhanced Thematic Mapper

FCC	-	False Color Composite
FCM	-	Fuzzy *c*-Means
FCMWE	-	Fuzzy *c*-Means with Entropy
FDM	-	Fuzzy *c*-Means Discontinuity Adaptive MRF Model
FDEM	-	Fuzzy *c*-Means with Entropy with Discontinuity Adaptive MRF Model
FERM	-	Fuzzy Error Matrix
FFBP	-	Feed-Forward Back-Propagation
FNN	-	Fuzzy Neuron Network
FUZCEN	-	FUZzy soft classification incorporating Contextual, Entropy and Noise
GA	-	Genetic Algorithm
GCP	-	Ground Control Points
GIS	-	Geographic Information System
GMM	-	Gaussian Mixture Models
GPS	-	Global Positioning System
ICM	-	Iterative Conditional Mode algorithm
IDRISI	-	Integrated Geographic Information System (GIS) and Remote Sensing Software
IFOV	-	Instantaneous Field of View
IMD	-	India Meteorological Department
IRS	-	Indian Remote Sensing Satellite
ISODATA	-	Iterative Self-Organizing Data Analysis Technique
KNC	-	Kernel Noise Clustering

LIDAR	-	Light Detection And Ranging
LISS-III	-	Linear Imaging Self Scanning Sensor-III
LISS-IV	-	Linear Imaging Self Scanning Sensor-IV
LMM	-	Linear Mixture Model
LSMA	-	Linear Spectral Mixture Analysis
MDA	-	Mixture Discriminant Analysis
MLC	-	Maximum Likelihood Classifier
MRF	-	Markov Random Field
NC	-	Noise Cluster
NCWE	-	Noise Clustering with Entropy
NDM	-	Noise Clustering with Discontinuity Adaptive MRF Model
NDEM	-	Noise Clustering with Entropy with Discontinuity Adaptive MRF Model
NDVI	-	Normalized Difference Vegetation Index
NDWI	-	Normalized Difference Water Index
NIR	-	Near Infra Red
OA	-	Overall Accuracy
PA	-	Producer's Accuray
PAN	-	PANchromatic
PCA	-	Principal Component Analysis
PCM	-	Possibilistic *c*-Means
PDM	-	Possibilistic *c*-Means Discontinuity Adaptive MRF Model

PDF	-	Probability Density Function
PMLC	-	Possibilistic Maximum Likelihood Classifier
RADAR	-	Radio Detection and Ranging
RBFN	-	Radial Basis Function Network
RMSE	-	Root Mean Square Error
SA	-	Simulated Annealing
SAR	-	Synthetic Aperture Radar
SAVI	-	Soil Adjusted Vegetation Index
SCM	-	Sub-pixel Confusion Uncertainty Matrix
SMA	-	Spectral Mixture Analysis
SPAA	-	Sub-Pixel Accuracy Assessment
SSC	-	Sparse Subspace Clustering
SSSL	-	Supervised Spectral Substratum Classifier
SVM	-	Support Vector Machine
SWIR	-	Short Wave Infra Red
TNDVI	-	Transformed Normalized Difference Vegetation Index
UA	-	User’s Accuracy
VI	-	Vegetation Index
V-C Matrix	-	Variance - Covariance Matrix

LIST OF SYMBOLS

A	-	Weight matrix
c	-	Total no. of clusters
C_i	-	Variance-covariance matrix
C_k	-	k^{th} class on the ground
D_i	-	Diagonal matrix
H	-	Entropy
I	-	Identity matrix
$J_{fcm}(U,V)$	-	Objective function of FCM
$J_{pcm}(U,V)$	-	Objective function of PCM
$J_{nc}(U,V)$	-	Objective function of NC
$J_{fcmwe}(U,V)$	-	Objective function of FCM with Entropy
$J_{ncwe}(U,V)$	-	Objective function of NC with Entropy
m	-	Weighted constant ($1< m < \infty$)
N	-	Total no. of pixels
r	-	Row of pixels belonging to a class
U	-	$N * c$ membership matrix
V	-	Mean vector for class i
v_i	-	Collection of vector of cluster centers of class i
v_j	-	Collection of vector of cluster centers of class j
x_k	-	Vector denoting spectral response of a pixel k
δ	-	Resolution constant ($0 < \delta < \infty$)

ν	-	Regularization parameter ($0 < \nu < \infty$)
η_i	-	Parameter that depends on the distribution of pixels in the cluster i
$\mu_{k,i}$	-	Class membership values of a pixel k belonging to i
$D(x_k, v_i)$	-	Squared distance in feature space between x_k and v_i
$D(x_k, v_j)$	-	Squared distance in feature space between x_k and v_j
$U(u_{ki}/d)$	-	Posterior energy of image u , in a given image d.
λ	-	Weight for spectral and contextual information (smoothness strength).
β	-	weight for neighbors.
n_k	-	Neighborhood window around pixel k.
γ	-	Adaptive Potential Function or interaction range parameter $\in [0,1]$.

CHAPTER-1

INTRODUCTION

"Thought and theory must precede all salutary action; yet action is nobler in itself than either thought or theory"

William Wordsworth

1.1 BACKGROUND

Many countries worldwide, including India, now depend on the satellite data and imageries for various purposes like quantitative analysis of the images and the preparation of thematic maps; use of digital computer is carried out. The basis of analysis is to correlate spectral properties of an object to the digital number recorded by a sensor. This method is commonly referred to as digital image classification, as the images acquired are in digital format.

Remote sensing fraternity has used digital image classification for many applications, such as resource utilization, environmental impact analysis, and other socio-economic applications. The development of suitable algorithms for image classification and assessment of accuracy has lead to significant confidence in extraction of information and generation of thematic maps (Gong and Howarth, 1992; Kontoes *et al.*, 1993; Foody, 1996; San Miguel-Ayanz and Biging, 1997; Aplin *et al.*, 1999a; Stuckens *et al.*, 2000; Franklin *et al.*, 2002; Pal and Mather, 2003; Tso and Mather, 2001; Landgrebe, 2003; Gallego, 2004; Richards and Jia, 2005). However, classifying any remotely sensed data into a thematic map remains a challenge due to many factors, such as, complexity of landscape, selection of remotely sensed data, image-processing and classification approaches, which may affect the success of a classification.

The term classification as defined by Chambers Twentieth Century Dictionary is the "act of forming into a class as per a rank or order of persons or things". Lillesand and Keifer (1994) state that the overall objective of image classification procedure is to automatically categorize all pixels in an image into land cover classes or themes. This is known as the 'hard classification' approach, where the aim is to identify each pixel into a single land cover class. During the last one decade or so, there has been a change in the concept where a pixel does not have a homogeneous coverage of land cover, but it is a heterogeneous one. Therefore, it is imperative that this heterogeneous nature be accommodated when the classification of land cover is under

taken. This procedure of classification is known as 'soft classification' where each pixel has a class membership proportionate to its area (Zhu *et al*., 2002, Kumar and Dadhwal, 2010, Upadhaya *et al*., 2012).

A standard hard classification method such as Maximum Likelihood Classifier uses an effective measure of similarity to determine the class allocation of a particular pixel. If a pixel is not a classifiable object, then hard classification methods will not work except in specific cases. In such cases, soft or fuzzy methods of classification provide, for each pixel, a measure of the degree of similarity (e.g., a membership probability) for every class (Harris, 1983; Bezdek *et al*., 1984; Fisher and Pathirana, 1990; Foody *et al.*, 1992; Maselli *et al.*, 1996; Lucas *et al.*, 2002; Harris, 2005; Stein, 2005; Stein, 2006; Harris, 1980; Jeyakanthan and Sanjeevi, 2006).

1.2 CONCEPT OF IMAGE CLASSIFICATION

Digital image classification of remote sensing images is a complex process and requires consideration of many factors. The major steps of image classification may include determination of a suitable classification system, selection of training samples, image preprocessing, feature extraction, selection of suitable classification approaches, post-classification processing, and assessment of accuracy. In image classification, decision making are not generally deterministic but are usually characterized by some level of fuzziness or uncertainty. Concepts such as *hot, cold, good,* or *difficult* contain elements of subjectivity, and analyst bias and hence it cannot be completely or deterministically specified as analogous to the classification of remotely sensed imagery. A typical soft classification of an image is illustrated in Fig. 1.1.

An analyst attempts to classify features in an image by using the elements of visual interpretation to identify homogenous groups of pixels that represent various features of interest. In digital image classification, the analyst uses the spectral information to classify each individual pixel based on this spectral information (Zia, 1996). This type of classification is termed as *spectral pattern recognition*. In either case, objective is to assign all pixels in the image to particular classes or themes. When talking about classes, it is important to distinguish

between information classes and spectral classes. Information classes are those categories of interest that the analyst is actually trying to identify in the imagery, such as different kinds of crops, different forest types and water bodies etc. Spectral classes are groups of pixels that are uniform with respect to their brightness values in the different spectral channels of data. The objective is to match the spectral classes in the data to the information classes of interest (Chandra and Ghosh, 2006).

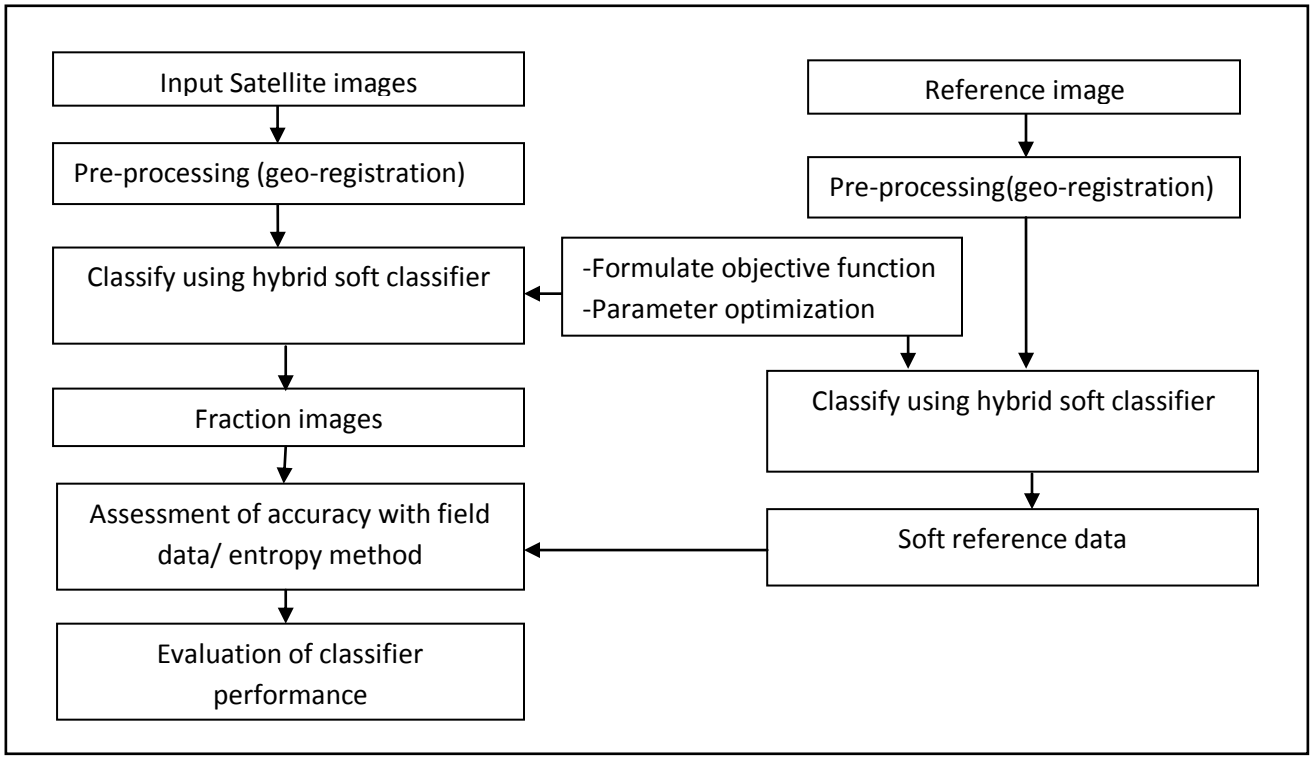

Fig. 1.1 Schematic diagram of soft classification

Commonly, there are two classification procedures, supervised and unsupervised. In supervised classification, the analyst identifies in an imagery, homogenous and representative samples of different surface cover type (information classes) of interest. These samples are referred to as training areas. The selection of appropriate training areas is based on the analyst's familiarity with actual surface cover type present in the image. Thus, the analyst is supervising the categorization of a set of specific classes. In unsupervised classification, spectral classes are grouped and matched by the analyst (if possible). Clustering algorithms are used to determine the

natural groupings or structures in the data. However, it does not start with a predetermined set of classes and it requires analyst intervention.

1.3 PROBLEMS ASSOCIATED WITH CLASSIFICATION

Digital image classification is usually performed to retrieve spectral information using a range of statistical classification techniques such as Maximum Likelihood Classifier (MLC), *k*-means clustering, Minimum Distance to Mean classifier etc. These classifiers allocate each pixel of the image to a single class, thus producing hard classification. However, often the images are dominated by mixed pixels, which do not represent a single class but contains more classes in single pixel area (Shalan *et al*., 2003). This situation is quite prevalent in developing country like India where the development has taken place in a haphazard manner. As a result, the land use land cover classes are generally mixed in nature and inter-grade gradually in an area. A satellite image having coarse resolution, chances of class mixture within a single pixel is higher in heterogeneous landscapes, and in interclass boundaries leading to higher proportion of mixed pixels in an image. Fine resolution satellite data, will be able to remove, by and large, the mixing of information within a pixel, yet the problem may still exist at inter-class boundary, where the number of such pixels may increase many folds.

Whatever be the origin of mixed pixels, these may create problem in image classification. For instance, a mixed pixel displays a composite spectral response that may be dissimilar to the spectral response of each of its component classes and, therefore, the pixel may not be allocated to any of its component classes (Zhang and Foody, 2001). Hence, error may occur in the classification of image containing large number of mixed pixels. Conventional hard classification approaches, force the mixed pixels to be allocated to one and only one class. This may result into a loss of pertinent information present in a pixel. Mixed pixels may thus be treated as error, noise, or uncertainty in class allocation in case of hard classification methods. These methods may therefore tend to over or under-estimate the actual area covered by these classes on ground. The land use land cover areal estimates obtained from hard classification, if used as an input to any Geographical Information System (GIS) based application, it may affect

the accuracy of the end product. Thus, it is clear that conventional hard classification methods may not be appropriate for classification of images fraught with mixed pixels.

The problem of mixed pixels may be resolved by accommodating this in classification process in some way to acquire the hidden information in it (Foody, 2000; Olthof *et al*., 2004). The application of soft classification methods based on spectral mixture analysis (Lu and Weng, 2004), fuzzy set theory (Maulik, 2002) and artificial neural network (Baraldi *et al*., 2001) may thus be adopted. The output from these methods is a set of class membership values for each pixel, also named as soft or fuzzy classification outputs, which are represented as probability, fraction or proportion images (Shalan *et al*., 2003).

The utilization of soft classification methods is an active area of research, which can be gauged from a number of research papers published during the last couple of years (e.g. Eastman and Laney, 2002; Shalan *et al.,* 2003; Oki *et al.,* 2004; Powell *et al.,* 2004). An in-depth review on this subject (Chapter 2) reveals that even although the problem of mixed pixels has been under investigation for some time now, yet it has got renewed interests with the availability of digital data from new sensors at varied spatial, spectral and temporal resolutions. It has been observed that:

i) Hybrid soft classification methods are largely in the exploratory stage and that research needs to be conducted to examine these methods on different types of remote sensing data products acquired for complex and uncertain environments.

ii) Most of the studies have focused on generation of soft classification output (i.e. the allocation stage) only. Incorporation of mixed pixels in training and testing stages of a supervised classification process appears to be necessary and requires extensive study.

iii) Determination of optimum number of parameters and their values for each classifier have to be investigated further.

1.4 SOFT CLASSIFIERS INVESTIGATED

From amongst a large number of soft classification methods, distribution –free classifiers based on fuzzy set is used. One of the most popular fuzzy clustering algorithms is Fuzzy *c*-Mean (FCM), which assigns class membership values to pixels of an image by an iterative process (Bezdek *et al*., 1984; Ji, 2003). The major limitation of FCM is that the sum total of membership must be equal to one (Yannis and Stefanos, 1999, Verhoeye and Robert, 2000). Thus, besides using this classifier, another fuzzy set clustering algorithm namely Possibilistic *c*-Mean (PCM), which relaxes this constraint so as to be robust to the noise present in the dataset, has also been implemented in this study (Krishnapuram and Keller, 1993). However, the basic problem associated with PCM is proper accounting of noise pixels. Therefore, another fuzzy based method, namely, Noise Clustering (NC) algorithm, has been implemented in this study. Attention has also been focused to optimize classification controlling parameters of FCM, PCM and NC classifiers to classify image pixels accurately.

Many factors, such as spatial and spectral resolution of the satellite data, different sources of data, classification system, and availability of classification software must be taken into account when selecting a classification approach. The question is which classification approach is suitable for a data analysis, is not an easy to answer. However, Cihlar *et al*. (1998) has proposed six criteria such as, accuracy, reproducibility, robustness, ability to fully utilize information content of data, uniform applicability and objectiveness. In reality, no classification algorithm can satisfy all these requirements nor be applicable to all studies, due to different environmental settings and data used. DeFries and Chan (2000) suggested to use multiple criteria to evaluate the suitability of any algorithm. Therefore, in this study, the applicability of hybrid algorithms has been tested on the basis of various parameters, such as, performance of algorithm, robustness to noise and classification accuracy etc. Therefore, another group of classifiers used here, considers hybridization, which has its origin in Entropy theory and theory of Markov Random Field (MRF). Two Entropy classifiers, one with FCM and another one with Noise (Li, 1995) and the other based on Markov Random Field for utilizing the contextual information along with FCM, PCM, NC and Entropy (Besag, 1974; Geman and Geman, 1984) have been considered in this study. The use of entropy and MRF has been introduced here as a soft

classification method, which itself is a novelty. The typical structure and taxonomy of soft classifications can be depicted as shown Fig. 1.2 and Table 1.1

In recent years, many soft classification approaches, such as artificial neural network, fuzzy–sets and expert systems have been widely applied for image classification. Tso and Mather (2001) and Landgrebe (2003) specifically focus on image processing approaches and classification algorithms. Table 1.1 provides a description of various soft classification approaches.

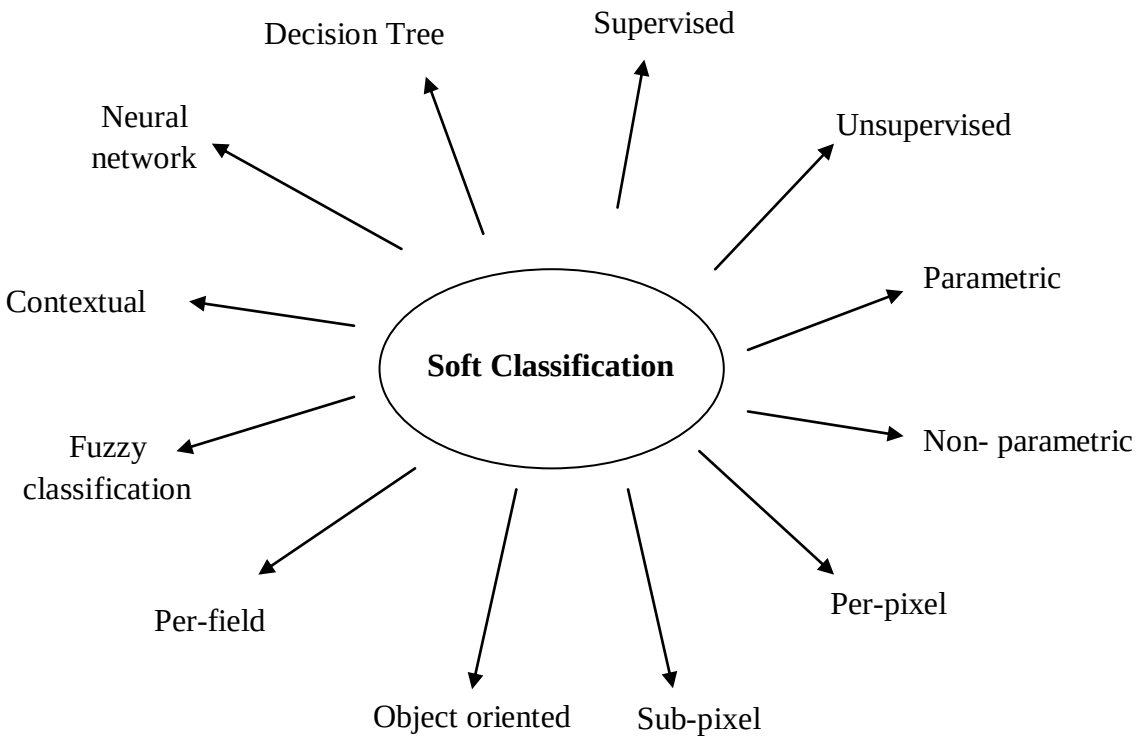

Fig. 1.2: General structure of soft classification

Table 1.1: A Taxonomy of soft classification methods

S. No.	Classification Approaches	Salient Features	Some of the relevant References
1	Supervised i) Maximum Likelihood ii) Minimum Distance to Mean iii) Artificial neural network iv) Decision Tree	Land cover classes are defined. Sufficient ancillary data is available and can be and used in classification procedure. The signatures generated from training samples are then used to train the classifier to classify the spectral data into a thematic map.	Foody *et al*.,1996, 2001, 2002, 2004, Baraldi *et al*., 2001, Eastman *et al*., 2002, Ju *et al*., 2003, Erbek *et al*., 2004, Guo *et al*., 2005, Lee *et al*., 2005 Jeyakanthan *et al*., 2006 Mather *et al*., 2004, Kannan *et al*., 2013, Priyadarshi *et al*., 2014
2	Unsupervised i) ISODATA ii) k-means clustering iii) Support vector machine	Cluster – based algorithms which partition the spectral image into a number of spectral classes based on statistical information inherent in the image. No prior definitions of the classes are required. The analyst performs detection, recognition and enumeration of the spectral classes into meaningful classes.	Bastin, *et al*., 1997, Bruzzone *et al*., 2001, Simone *et al*., 2002, Maulik *et al*., 2003, *Oki, et al*., 2004, Ibrahim *et al*., 2005, Okeke *et al*., 2006, MacAlister *et al*., 2008
3	Parametric i) Maximum Likelihood ii) Linear Discriminant Analysis	Gaussian distribution is assumed. The parameter (e.g. mean vector and covariance matrix) are often generated from training samples.	Hubert-Moy *et al*., 2001, Huang *et al*., 2002, Emrahoglu *et al*., 2003, Pontius *et al*., 2006, Solberg *et al*., 2008, Tolpekin *et al*., 2009, Moser *et al*., 2010.
4	Non –parametric i) Artificial neural network. ii) Decision tree iii) Evidential reasoning iv) Expert system	No assumption about the data is required. This classifier does not employ statistical parameters to calculate class separation.	Penaloza *et al*., 1996, Zhang *et al*., 2001, Mannan *et al*., 2003, Foody *et al*., 2004

5	Per-pixel i) Maximum Likelihood ii) Minimum Distance iii) Artificial neural network iv) Decision Tree	Typically develop a signature by combining the spectra of all training-set pixels from a given feature.	Mercier *et al*., 2003, Mitra *et al*., 2004, Mather *et al*., 2006a, 2006b, 2006c, 2006d, MacKay *et al*., 2009
6	Sub-pixel i) Fuzzy –set classifiers ii) Spectral mixture analysis iii) Fuzzy expert system iv) Fuzzy neural network	The spectral value of each pixel is assumed to be linear or non-linear combination of defined pure end members, providing proportional membership of each pixel to each end member.	Huguenin *et al*., 1997, Solaiman *et al*., 1999, Foody *et al*., 1996, 2001, 2002, 2004, Maselli *et al*., 1996, Zhang *et al*., 2001, Shalan *et al*., 2003, Lu *et al*., 2004, Sengar *et al*., 2013
7	Object Oriented i) eCognition	Image segmentation merges pixels into objects and classification is conducted based on the objects, instead of an individual pixel.	Herold *et al*., 2003, Geneletti *et al*., 2003, Thomas *et al*., 2003, Van der Sande *et al*., 2003, Benz *et al*., 2004, Gitas *et al*., 2004, Walter, 2004.
8	Per-field i) GIS –based classification	GIS plays an important role in per-field classification, integrating raster and vector data in a classification. The vector data are often used to subdivide an image into parcels, and classification is based on the parcels, avoiding the spectral variation inherent in the same class.	Lobo *et al*., 1996, Aplin *et al*., 1999a, Dean and Smith 2003, Aplin and Atkinson 2001.
9	Fuzzy classification i) FCM ii) PCM iii) Noise clustering iv) Spectral mixture analysis	Providing for each pixel a measure of the degree of similarity for every class. Soft classification provides more information and potentially a more accurate result, especially for coarse spatial resolution data classification.	Sohn *et al.* , 1999, Sohn *et al.* ,2002, Ferna´ndez-Prieto 2002, Lee *et al.* , 2000, Barandela *et al.* ,2002, Shah *et al.* , 2004, Emrahoglu *et al.* ,2003, Foody *et al*., 1996,2001,2002,2004

10	Contextual (i) ECHO(Extraction and classification of homogenous objects) (ii) Supervised relaxation classifier (iii)Frequency based contextual classifier (iv)Fuzzy contextual classification	The spatially neighbouring pixel information is used in image classification.	Kontoes *et al.*, 1993,1996, Sharma *et al.*, 1998, Stuckens *et al.*, 2000, Biehl and Landgrebe 2002, Landgrebe, 2003, Lu et al. 2004, Xu et al. 2003, Keuchel et al. 2003, Magnussen et al. 2004,
11	Neural network (i) Back propagation learning algorithm (ii) Competitive learning algorithm	This classifier generalize the relation between the input and the output and it does not follow a distribution	Chen et al. 1995, Foody et al. 1995, Kulkarni and Lulla 1999, Pal and Mather 2003, Foody 2004b, Schmidt et al. 2004, Lawrence et al. 2004, Keramitsoglou, 2006.
12	Decision Tree	Build an accurate model for each class based on the set of attributes	Hansen *et al.*, 1996, Friedl *et al.*, 1997, DeFries *et al.*, 1998, Friedl *et al.*, 1999, DeFries *et al.*, 2000, Pal *et al.*,2003, Lawrence *et al.*, 2004

1.5 HYBRID CLASSIFIERS

Hard classifiers are commonly used in image classification, where a pixel has a membership value of either 0 or 1, thus it is considered as a pure pixel. In actual data, however, a single pixel may contain more than one class, such as a combination of forest, water, bare soil and grass. This happens because real world phenomena change gradually from one class to another as well as due to compatibility of spatial resolution with class size forms mixed pixels. Therefore at the boundaries of different classes uncertainty increases and fuzziness or vagueness occurs.

To overcome the problem of multiple classes at the boundaries, L.A Zadeh in 1965, introduced fuzzy set theory, which is based upon uncertainty and vagueness. Fuzzy sets may have membership values ranging between 0 and 1 where this value defines the proportion of occurrence of information within a pixel (Zadeh, 1965). This concept has been used in many

applications such as sensor signal analysis, uncertainty minimization and business and finance (Wang *et al*., 2004; Sengar *et al*., 2012).

Standard fuzzy-set based classifiers do not incorporate spatial contextual information of the pixels into its classifying algorithm; it only considers the spectral information of the pixels which is not sufficient enough to handle noise, uncertainty and vagueness in a class. To incorporate spatial contextual information, Markov Random Field (MRF) is widely used (Geman and Geman, 1984; Solberg *et al*., 1996; Li, 2009). MRF theory is able to model context dependent entities such as pixels or correlated features in a convenient and consistent way (Li, 2009). Spatial context implies the presence of correlation of class labels within neighbouring pixels (Solberg *et al*., 1996). The actual geographical phenomenon lies in context to others. For example, a vegetation pixel has a high probability to have the same vegetation pixels as its neighbours. So the isolated pixels exist rarely. Use of context eliminates the problem of isolated pixels (Tso and Mather, 2009). In this study, MRF has been used to develop contextual based supervised FCM, PCM and NC classifier.

To incorporate contextual information, it is important to select MRF models carefully to achieve good results. MRF models are also known as MRF priors and regularizers. Some of the MRF models are Standard Regularization model, Weak String and Membrane model, Line Process Model, and Discontinuity Adaptive (DA) MRF models. In this study, standard regularization model (i.e. smoothness prior) and Discontinuity Adaptive (DA) models (i.e. edge preserving priors) have been use to study smoothing effect as well as edge preserving effect in image.

MRF uses smoothness prior models to calculate prior energy using prior probabilities to model the smoothness in an image (Tso and Mather, 2009). It applies smooth contextual concept, which assumes uniform smoothness everywhere in the image. If discontinuities are overlooked (e.g. at boundaries), MRF tends to over-smoothen, leading to loss of information and hence yield less accurate results (Li, 1995; Solberg *et al*., 1996; Li, 2009). Discontinuity Adaptive (DA) models (Li, 1995) or adaptive neighbourhoods (Pinoli and Debayle, 2009) can be used to overcome the problems of discontinuity. Hence, this study proposes to examine the effect of

various Discontinuity Adaptive MRF models in Fuzzy *c*-Means (FCM), Possibilistic *c*-Mean (PCM) and Noise Clustering (NC) classifier.

In general, image classification approaches can be grouped as supervised and unsupervised, or parametric and nonparametric, or hard and soft (fuzzy) classification, or per-pixel, sub-pixel, and per-field. For the sake of convenience, this study categories a classification approach as, sub-pixel, contextual-based, noise clustering based, and a combination of these classifiers with and without entropy.

Sub-pixel classification approaches have been developed to provide a more appropriate representation and better estimation of area for land cover especially when coarse spatial resolution data are used (Foody and Cox, 1994; Binaghi *et al*., 1999; Ricotta, 2004, 2006; Woodcock and Gopal, 2000; Ju *et al*., 2003, 2005; Seetha *et al*., 2007). A fuzzy representation is required when a location/pixel is composed of partial memberships of some or all classes present.

Different approaches have been used to describe a soft classifier, including fuzzy-set theory, Dempster–Shafer theory, Certainty Factor (Bloch 1996), softening the output of a hard classification from maximum likelihood (Schowengerdt , 1996) and neural networks (Foody 1999, Kulkarni and Lulla 1999, Mannan and Ray 2003). The fuzzy-set technique (Foody 1996, 1998, Maselli *et al*., 1996, Mannan *et al*., 1998, Zhang and Kirby 1999, Zhang and Foody 2001, Shalan *et al*., 2003) and Spectral Mixture Analysis (SMA) classification (Adams *et al*., 1993,1995, Roberts *et al*., 1998b, Rashed *et al*., 2001, Lu *et al*., 2003) are some of the commonly used popular approaches to overcome the problem of mixed pixel. One major drawback of sub-pixel classification lies in the difficulty in assessing accuracy when reference data is not obtained from ground survey.

In addition to other classifiers, contextual classifiers have been used to cope with the problem of intra-class spectral variations (Gong and Howarth 1992; Kartikeyan *et al*., 1998; Flygare, 1997; Sharma and Sarkar, 1998; Keuchel *et al*., 2003; Magnussen *et al*., 2004). Contextual classification exploits spatial information among neighbouring pixels to improve image classification results, while minimizing noise in an image (Flygare 1997, Stuckens *et al*.,

2000, Hubert-Moy *et al*., 2001, Magnussen *et al*., 2004). A contextual classifier may use smoothing techniques, Markov random fields, spatial statistics, fuzzy logic, segmentation, or neural networks (Binaghi *et al*., 1997, Cortijo and de la Blanca 1998, Kartikeyan *et al*., 1998, Keuchel *et al*., 2003, Magnussen *et al*., 2004). In general, pre-smoothing classifiers incorporate contextual information as additional bands, and classification is then carried out using normal spectral classifiers, while post-smoothing classification is conducted on classified images developed previously using spectral-based classifiers. However, in pre-smoothing process smoothing filters are used, while post smoothing uses majority of median filters. Markov Random Field-based contextual classifiers, such as Iterated Conditional Modes (ICM), are the some of the frequently used approaches in contextual classification (Cortijo and de la Blanca 1998; Magnussen *et al*., 2004), and have proven to be effective in improving classification results.

From amongst a number of soft classification methods, this study has focused its attention on two fuzzy set theory based algorithms, such as Fuzzy *c*-Mean (FCM) and Possibilistic *c*-Means (PCM), one noise clustering based i.e.(NC), five contextual based and another seven are a combination of entropy along with contextual in FCM, PCM and NC classifier

The concept of "Noise Clustering" has been introduced such that noisy data points may be assigned to a noise class. The approach is developed for objective functional type (K-means or fuzzy *k*-means) algorithms, and its ability to detect 'good' clusters amongst noisy data is demonstrated. The approach is applicable to a variety of fuzzy clustering algorithms as well as regression analysis (Dave, 1991).

In this study, fuzzy as well as entropy based fuzzy classifier, entropy based noise clustering and entropy based contextual classifier has been used to study the effect of entropy on classification output and also to study uncertainty variation across spatial resolution of multi-spectral data sets at pixel level. Uncertainty has been estimated using Sub-pixel Confusion Uncertainty Matrix method (SCM) (Silván-Cárdenas and Wang, 2008) for computing overall

accuracy, Kappa coefficient, as well as, entropy which has been used as an absolute indicator to measure uncertainty.

The information obtained from neighboring pixels is known as spatial contextual information (Richards and Jia, 2005). Spatial contextual information, if exploited tactfully, it may be used for elimination of ambiguities, or recovery of missing information and the correction of errors (Tso and Mather, 2001), and therefore, can provide spatially and spectrally consistent thematic maps (Derin and Elliott, 1987).

Earlier, a few attempts have been made to incorporate the spatial contextual information for traditional hard classifiers and results shows that incorporation of context improves classification result (Tso and Mather, 2001). Thus, there is a scope to improve the accuracy of fuzzy classification results by modeling the spatial context. This aspect requires in-depth investigation. Therefore, one of aim of this study is to explore the contextual classifiers and investigate the possibility of use of spatial contextual information with other classification technique in the context of various land use land cover mapping. Once an efficient contextual algorithm with its various combinations is tested successfully, it may help researchers to produce more accurate maps from remotely sensed data, where the land cover classes are heterogeneous in nature.

1.6 CAPABILITIES OF DIFFERENT AVAILABLE SOFTWARE PACKAGES

The performance of image processing software has improved significantly to perform necessary analysis. During last two decades, a large number of image processing software have been developed by various commercial companies offering a suite of modules related to data input, visualization, enhancement, transformation, classification and accuracy assessment (Ghosh, 2013). Some of the leading GIS software which has well defined image processing modules is ERDAS IMAGINE, IDRISI, ENVI, and ER MAPPER. *e*Cognition, a new image analysis software facilitates fast and accurate geo- information extraction from any kind of remote sensing imagery. Some of these tools have appropriate features to incorporate training data and resolve the problem of mixed pixel. However, it is not able to accommodate the contextual information of an image.

For classification and accuracy assessment of soft classified output, none of the commercially available software packages have FERM and SCM based accuracy assessment algorithms, so an in-house software package, known as **FUZ**zy soft classification incorporating **C**ontextual, **E**ntropy and **N**oise (*FUZCEN*) has been developed for the purpose of hybrid classification to incorporate the contextual information and accuracy assessment. This software package has capabilities to incorporate training data as pure pixel. Using pure training data, FUZCEN package has the capability to incorporate informational features into soft classifier. For testing the classified data, this software package can generate accuracy assessment results in terms of overall accuracy, user's accuracy, producer accuracy, fuzzy kappa coefficients, FERM, SCM and uncertainty in overall accuracy (Binaghi *et al*., 1999, Silvan-Cardenas and Wang, 2008).

1.7 RESEARCH GAPS

The use of soft classification method is still an open research area, due to the relationship between the object and the class label may be one-to-one (producing a *hard classification*) or one-to-many (producing a *fuzzy classification*). Spectral and spatial overlap of classes is one of the main barrier for achievement of high classification accuracy (Townshend *et al.,* 2001).

Selecting suitable optimized variables is another critical step for successful implementation of a soft classification procedure. Many potential variables may be used in image classification, such as spectral signatures, vegetation indices, transformed images, textural or contextual information, multi-temporal images, multi-sensor images, and ancillary data. Due to different capabilities in land-cover separability, use of many variables in a classification procedure may lead to a decrease in classification accuracy (Hughes, 1968; Price *et al.,* 2003). Therefore, it is important to select only those variables that are useful in separating land-cover or vegetation classes, especially when hyper spectral or multi-source , multi-resolution data are used (Mausel *et al*., 1990; Friedman, 1994; Jensen, 1996; Hastie and Tibshirani, 1996; Mather, 1999; Richards and Jia, 1999; Mattera and Haykin, 1999; Mather, 2001; Myint, 2001; Okin *et al.,* 2001; Rashed *et al*., 2001; Peddle and Ferguson, 2002; Asner and Heidebrecht, 2002; Lobell *et al.,* 2002; Landgrebe, 2003; Neville *et al*., 2003; Landgrebe, 2003; Tso and Daniel *et al.*, 2003;

Platt and Goetz, 2004; Pal and Mather, 2001a; 2001b; 2002; 2003a; 2003c; Pal, 2006b, 2006c; Van *et al.*, 2005; Pal, 2006a).

.

Mixed pixel may not be appropriately represented by traditional image classification techniques, which assumes that pixels are pure. Occurrence of mixed pixel may be a problem in mapping and monitoring land cover, and in particular their effect is the most severe in mapping heterogeneous landscape from coarse spatial resolution images (Foody, 2002a). Therefore, there is a need to explore and implement other classification methods that may be grouped as soft classification methods. Based on the broad review of various studies and available algorithms, it is observed that some gaps are existing. It is important to address these gaps in order to ensure the suitability and utility of soft classification approaches. These gaps can be identified as:

i) Advanced hybrid fuzzy based soft classification methods are largely at an exploratory stage. Systematic studies needs to be carried out to examine the suitability of hybrid fuzzy based classification methods for remote sensing images.

ii) Uncertainty is a significant issue in the interpretation of remote sensing data, as it is necessary to completely evaluate a classifier's performance.

iii) In general, it is found that, majority of the studies are focused on generation of soft classification output only. Images acquired over uncertain environments may contain large number of mixed pixels. Therefore, their incorporation in testing stages of a supervised classification process becomes mandatory. A concerted effort in this particular direction is required.

iv) The determination of optimized values for hybrid fuzzy based soft classifiers needs to be investigated further.

v) Suitable method or an approach for assessment of accuracy is required.

vi) A thorough investigation into noise reduction techniques to improve classifier performance needs to be undertaken.

vii) Hybridization of classifiers to improve classifier performance by optimization of relevant parameters requires an in-depth study.

1.8 RESEARCH OBJECTIVES

In view of research gaps, the objective of this study can be identified as:

a) To assess the suitability of fuzzy set theory based algorithm such as Fuzzy *c*-Mean, Probabilistic *c*-Mean and noise clustering based algorithm for sub-pixel classification.
b) To identify the usefulness of contextual based fuzzy classification approaches.
c) To investigate the effect of contextual based fuzzy classification approaches with or without entropy.
d) To investigate the effect of contextual in noise clustering classification approaches with or without entropy.
e) Comparative study on assessment of accuracy for fuzzy classification approach.
f) Development of a dedicated, user-friendly and interactive software package to fulfil the needs of this study.

It is proposed to achieve research objectives using Resourcesat-1 (IRS-P6) multispectral data to extract information for different land use and land cover classes at sub-pixel level. This provides real time remote sensing data of ground turn which in turn helps in assessing the accuracy of a classified imagery.

1.9 ORGANIZATION OF THESIS

This thesis has been organized in seven different chapters. The first chapter provides an input to the soft classification information generated from remote sensing data. It identifies the research question as well as few gaps in this area, which form the research objectives for this work.

Chapter 2 provides a comprehensive literature review on land cover classification. It also covers a review on soft classification presently used on multi-spectral remote sensing data. Soft classification algorithms evaluated in this study have been discussed in detail.

Chapter 3 builds the philosophy and mathematical foundations of various soft classifiers investigated in this study. The constraints and parameters of each method have been critically examined. The assessment of accuracy has also been focused, where mathematical background of various uncertainty and accuracy measures are presented.

Chapter 4 provides details of the datasets used in this study. AWiFS, LISS-III and LISS-IV remote sensing imagery has been used to perform classification and assessing the accuracy of an algorithm. Chapter 5 describes the methodology adopted in this study. It highlights the various steps involved in preprocessing of various dataset, preparation of reference data set, and finally the assessment of classified image. This chapter also provides the details of the *FUZCEN* software.

Chapter 6 provides an in depth analysis of the results obtained from various classifiers and assessment of accuracy. Chapter 7 provides the major conclusion of the study. It also identifies the further scope of this study.

CHAPTER 2

REVIEW OF SOFT CLASSIFICATION METHODS

2.1 INTRODUCTION

Identification of any particular land cover class from remote sensing images has traditionally been viewed as a classification problem where each pixel in the image is allocated to one of the possible classes. However, in reality, different amounts of land cover mixing within a pixel can occur due to continuum of variation in landscape and intrinsic mixed nature of most classes (Ju *et al.,* 2003, Maulik, 2013). Therefore, pixels with a mixture of classes (i.e. mixed pixels) may be problematic.

Mixed pixels may not be appropriately represented by hard image classification techniques, which assume that pixels are pure. Occurrence of mixed pixels may be a problem in mapping and monitoring land cover, and in particular, their effect is most severe in mapping heterogeneous landscape from coarse spatial resolution images (Foody, 2002a, Lu and Weng, 2007). Therefore, there is an urgent need for development and implementation of suitable classification methods that may be grouped as soft classification methods.

During the last few years, there has been resurgence in the application of soft classification methods to classify remote sensing images dominated by mixed pixels. These methods are used to unmixed the classes so as to produce sub-pixel classification (Oki *et al.*, 2004). The methods appear to be have strong suitability under the Indian conditions, where large areas are dominated by a mixture of classes.

Image classification techniques using remote sensing data has attracted the attention of remote sensing fraternity as these classification results are the foundation for many environmental and socio-economic applications. Scientists and analysts have made tremendous

efforts in developing advanced classification approaches and techniques for improving accuracy of classification (Gong and Howarth, 1992; Kontoes *et al*., 1993; Foody 1996; San Miguel-Ayanz and Biging 1997; Aplin *et al.*, 1999a, Stuckens *et al.*, 2000; Franklin *et al.*, 2002; Pal and Mather, 2003; Gallego 2004, Ghosh, 2013). However, classification of remotely sensed data into a thematic map remains a challenge due to many factors, such as, complexity of landscape, selection of remotely sensed data and image-processing and classification approaches, may influence the success of a classification.

In this chapter, current status of some prevalent soft classification methods for extraction of land cover followed by different approaches for assessing the accuracy of soft classification, has been discussed.

2.2 INITIAL INVESTIGATION OF SOFT CLASSIFICATION

Binaghi *et al*., (1997) integrated Fuzzy based knowledge classifier with contextual information using MRF and remote sensing data from multiple sources. The attempt was to emulate the process of human thinking in solving problems pertaining to classification. The classification of satellite image has been modeled as a cognitive process, providing procedures that mimic the rich interaction of human activity in solving classification problems. The key feature of this approach are the definition of a knowledge-based classification methodology designed to integrate contextual information into a multi-source classification scheme, together with a fuzzy knowledge representation framework to model the overall process in a form that closely resembles the mental representation of human experts. An application for the identification of glacier equilibrium line in two different zones of the Italian Alps has been developed to evaluate the performance of their methodology in a real domain where class discrimination requires the simultaneous use of contextual and multi-source information.

Chang (2002) considered an alternative approach, which imposes constraints on target signature vectors rather than target abundance fractions. While Linear Spectral Mixture analysis has been widely used for sub-pixel detection and mixed pixel classification, but when

implemented as constrained LSMA (Linear Spectral Mixture Analysis), the constraints are generally imposed on abundance fractions within the mixture.

Eastman and Laney (2002) examined the assumptions and procedure of Bayesian soft classification procedure for sub-pixel classification and tested its ability to uncover mixture proportions. Mixed pixels were used in the training stage through fuzzy mean and fuzzy variance covariance matrices to estimate the underlying class signatures. The sub-pixel classifications were evaluated by cross-tabulating the actual and predicted class proportions in a manner similar to traditional error matrix. After critical evaluation, it was recommended that the use of fuzzy mean and variance covariance may not be effective in accurately recovering class proportions in pixels unless there exists substantial overlap in the distributions of constituent classes. Therefore, MLC for soft classification should be used with caution.

Kolaczyk (2003) discussed the problems of classification and sub-pixel proportion estimation in remote sensing land cover characterization, in details, using simple, canonical versions of the two problems (i.e. classification and sub-pixel proportion estimation) and during the course of the study, provided analytical expressions to suggest improvements to sub-pixel proportion estimation from a statistical viewpoint.

Blaschke (2004) proposes an efficient extraction approach of information from high resolution imagery of Landsat ETM, and seamless integration of this information into Geographic Information System (GIS) databases using object based contextual classification techniques. This study investigated different approaches to image segmentation techniques and demonstrated through several applications how segmentation and object-based methods improve pixel-based image analysis/classification methods. In contrast to pixel-based procedure, image objects can carry many more attributes rather than only spectral information. This study, addresses to the concepts of object-based image processing, and presents an approach that integrates the concept of object-based processing into the image classification process. Object-based processing not only considers contextual information but also information about the shape and spatial relations between the image regions.

Lee and Lathrop (2005) examined the utility of Linear Mixture Modeling in the sub-pixel analysis of Landsat Enhanced Thematic Mapper (ETM) imagery to estimate three key land cover components in an urban/suburban setting i.e. impervious surface, managed/unmanaged lawn and tree cover. Impervious surface estimates from Landsat ETM showed a high degree of similarity (RMS error between ±10 to 15%) to that obtained from using high spatial resolution digital orthophotography and IKONOS imagery. The partition of vegetation component into tree verses grass cover was problematic due to low spectral similarity between these land cover types.

Myint (2006) examined the effectiveness of a sub-pixel classifier, by using some rules as defined by an expert system, to estimate varying distributions of different types of vegetation within an urban area. Spearman's Rank Order correlation between the vegetation output and reference data for different type of land cover, such as, wild grass, man-made grass, riparian vegetation, tree and agriculture was found to be having high values. This study demonstrated that the expert system rule using NDVI threshold procedure is reliable and that the sub-pixel processor was able to identify signatures relatively well. Further, this study suggested a checklist of the sources of limitation in the application of sub-pixel approaches.

Thornton *et al*., (2006) mapped rural land cover features, such as trees and hedgerows, for ecological applications. The imagery was analyzed using a supervised Fuzzy *c*-Means algorithm. Overall RMSE was between 20 to 30%, resulting in the sub-pixel mapping method producing reasonably accurate results of the order of 50 to 75%. Sub-pixels within pixels were then iteratively swapped until the spatial correlation between sub-pixels for the entire image was maximized using mathematical morphology. Visual inspection of the super-resolved (i.e. dividing each pixel into sub-pixels using a zoom factor of five) output shows that the prediction of the position and dimensions of hedgerows was comparable to the original imagery.

Kumar and Ghosh (2007) carried out a comparison of FCM and PCM as sub-pixel classifiers method using SPOT satellite data. It was found that PCM using Euclidean Norm gives the highest overall accuracy of 99.29%, whereas FCM with Euclidean Norm yielded the overall accuracy of 97.9%.

Saha *et al.* (2010) found that remotely sensed images often display spectral variations over heterogeneous regions in the context of land cover classes (LCCs), which imposes challenges to extraction of information from the images. The Supervised Spectral Substratum Classifier (SSSL) approach has been proposed using Landsat 7 ETM+ dataset. The classifier first builds spectral LCCs (SLCC) from a Training Dataset (TD). A SLCC comprises of spectral signals of a labeled LCC in TD based on the ground truth. This SLCC is further marked as homogeneous or heterogeneous according to the statistical properties of mean value and standard deviation of all spectral cases in this SLCC. When this SLCC is marked as heterogeneous, the spectral space of the SLCC will be disaggregated (or clustered) into substrata by applying statistical cluster analysis. A membership function is then defined for each substratum. To classify images, fuzzy membership functions are applied to measure similarities between corresponding spectral substrata and any new to-be classified cases (pixels). The new cases are classified to the most comparable substrata as determined by the membership functions. As a case study, a vegetation cover classification over typical grassland in Inner Mongolia has been selected using Landsat ETM+ data. Result shows that the proposed classification model gives an overall accuracy of 79.3% and kappa value of 0.76, where the testing data was available from a hybrid fuzzy classifier and maximum likelihood classifier.

Binaghi (2013) carried out studies to examine the utility of Radial Basis Function Network (RBFN) to estimate the thickness of snow cover as a function of climate and topographic parameters. The estimation is modeled in terms of, classification and obtaining continuous and discrete thickness values. The model is based on a minimal set of climatic and topographic data collected from a limited number of stations located in the Italian Central Alps. The RBFN model provided a better results and it was found to be a valuable tool in those situations where conventional techniques was not able to represent or classify information.

2.2.1 FUZZY *C*-MEANS CLASSIFICATION

Fuzzy *c*-Mean is the one of popular fuzzy clustering method and many researchers have used this technique for different application problems related to remote sensing data clustering for both supervised and unsupervised mode.

Wang (1990) used supervised FCM approach to classify Landsat MSS and TM data having seven land cover classes. When compared to Maximum Likelihood classification, it was found that higher classification accuracy could be achieved when using fuzzy classification approach.

Foody (1996) evaluated the performance of FCM and Fuzzy Neuron Network (FNN) approaches for land cover classification using Airborne Thematic Mapper (ATM) data. A detailed investigation was carried on the effect of different fuzzy weight parameter *m* values for the same dataset and it was found that for $m = 2.0$, it gives most accurate fuzzy classification output for large cases. It was concluded that fuzzy classification technique yields more appropriate results in land cover mapping than hard classification techniques.

Atkinson *et al*., (1997) compared three classification techniques of Artificial Neural Networks (ANN), Mixture modeling and Fuzzy *c*-Means for mapping sub-pixel proportions of land cover classes for an area in the New Forest, U.K. It was found that ANN was one of the accurate techniques; however, its successful implementation depends on accurate co-registration and availability of a training data set. Supervised Fuzzy *c*-Means classification gave slightly better results than mixture modeling.

Bastin (1997) made comparison amongst FCM, Linear Mixture Modeling and Maximum Likelihood Classifier for unmixing coarse pixels present in aggregated Landsat TM data. In the absence of ground truth, original TM data was used as a reference map and the image was aggregated using mean and cubic filter having different kernel size. Thereafter, the membership value for each of the three classifier was generated from the classified aggregated image. This information was then compared to continuous membership values with sub-pixel area proportions present in a coarser pixel. It was concluded that FCM gives best estimation of sub-pixel land cover classes for the aggregated TM image at different scale.

Zhang and Foody (1998) used FCM algorithm for sub-urban land cover mapping from SPOT HRV and Landsat TM data. It was concluded that the classification results could be improved significantly when using fuzzy classification and evaluation approaches.

Zhang and Foody (2001) described two approaches for full – fuzzy classification of remotely sensed imagery using a statistical approach based on a modified Fuzzy *c*-Means clustering algorithm in a supervised mode and an Artificial Neural Network based approach. Both approaches were applied to derive a fully- fuzzy classifications of land cover, using fuzzy ground data, derived through Kriging technique. Results confirmed the superiority of fully – fuzzy over partially – fuzzy classification. Further, it was found that fully fuzzy class was more beneficial as it has more relaxed requirements for training pixels i.e. these need not be pure.

Lucas *et al*. (2002) used FCM and linear unmixing techniques for sub-pixel habitat mapping of a coastal dune ecosystem from airborne imaging spectrometer (CASI) image. It was observed that these techniques could be useful to find out land cover class proportions at sub-pixel level.

Okeke and Karnieli (2006) used FCM classification for vegetation change analysis in Adulam Nature Reserve, Israel using historical aerial photographs. The assessment of accuracy was carried using Fuzzy Error Matrix (FERM). Recently, the concept of Fuzzy Error Matrix and Sub-pixel confusion uncertainty matrix has been put forth to assess the accuracy of soft classification (Binaghi *et al*., 1999; Silvan *et al*., 2008). The elements of the error matrix represent class proportions corresponding to reference data and classified outputs respectively. In this work, for evaluation of output, Fuzzy Error Matrix (FERM) was used where ground reference data was not available. It was found that fuzzy overall accuracy for all the datasets was more than 85%.

Bandyopadhyay *et al*. (2007) proposed a multi-objective optimization algorithm to simplify the problem of fuzzy partitioning on SPOT and Indian Remote Sensing (IRS) dataset; where a number of fuzzy cluster validity indexes were simultaneously optimized. The resultant set contains a number of non dominated solutions, which the user can judge relatively and pick up the most promising one according to the problem requirements. Results demonstrated the effectiveness of the proposed technique as remote sensing data was described in terms of feature vectors. Different land cover regions in remote sensing imagery were classified using the proposed technique to establish its efficiency.

Hore *et al*. (2007) proposes a simple Fuzzy c- Means algorithm and measured the performance using image compression technique. It was found that this algorithm produced a better results compared to any other clustering technique. Further, it produces excellent speed – ups in clustering and thus can be used even if the data cannot be fully loaded in to the computer memory.

Volpi *et al*. (2011) suggested an efficient way to select suitable training set for the success of remote sensing image classification. The complexity of the problem is high intra-class variance, which can fail an algorithm, if it is trained with a suboptimal dataset. Active learning aims at building efficient training sets by iteratively improving the model performance through sampling. A user-defined heuristic first ranks the unlabeled pixels according to a function of the uncertainty of their class membership and then the user is asked to provide labels for the most uncertain pixels.

Maulik and Sarkar (2013) suggested an important approach for image classification by clustering of pixels in the spectral domain. Fast detection of different land cover regions or clusters of arbitrarily varying shapes and sizes in satellite images present a challenging task. Here, an efficient scalable parallel clustering technique of multi-spectral remote sensing imagery using a fuzzy based approach has been proposed. This approach is able to correctly identify the presence of overlapping clusters of any arbitrary shape and size and assess whether they are intra-symmetrical or inter-symmetrical in nature. A Kd-tree based approximate nearest neighbor searching technique is used as a speedup strategy for computing the point symmetry based distance. SPOT and IRS satellite images have been used in symmetry analysis of land cover regions. The classified outputs are compared with the available ground truth information.

2.2.2 POSSIBILISTIC *C*-MEANS CLASSIFICATION

In 1993, Krishnapuram and Keller gave a specific implementation of Zadeh's, 1978 possibility based method, called Possibilistic *c*-Means (PCM). It assigns a pixel to more than one cluster in the form of membership value and this membership value does not follow the constraint in FCM called hyper-line constraint.

Barni *et al*., (1996) reported a difficulty with the application of the possibilistic approach to fuzzy clustering (PCM) proposed by Krishnapuram and Keller. While applying this algorithm, it has been observed that it has undesirable tendency to produce coincident clusters. Results illustrating this tendency are reported and a possible explanation for the PCM behavior is suggested. The membership functions are directly related to the typicality of data points with respect to the given classes. In this way, classification tasks are made easier and the impact of spurious points on the final partition is reduced.

Krishnapuram and Keller (1996) gave some recommendations based on their findings and issues raised. The first recommendation was that the value of fuzzy *m* is different for both FCM and PCM since its differs in interpretation. The main motivation to use PCM relates to the relaxation of probabilistic constraints of FCM. The weighting exponent *m* in PCM determines the rate of decay of membership values while, in case of FCM, the value of m represents the degree of sharing. Further, in case of PCM, another parameter η plays an important and is defined as that distance at which membership value of a class becomes 0.5.

Foody (2000) investigated the utility of FCM and Possibilistic *c*-Means (PCM) algorithms which derive relative and absolute measures of class membership strength respectively on Airborne Thematic Mapper (ATM) image for a part of Swansea city, U.K. Both algorithms were able to provide accurate estimates of sub-pixel land cover composition. When all classes had been defined in training a classification, in general, FCM provided better and accurate class composition estimates. The presence of an untrained class, however, could substantially degrade accuracy of sub-pixel land cover composition estimates derived from FCM but has no effect on those from PCM. Since untrained classes are commonly encountered, it may be more appropriate to use approaches such as PCM in addition to FCM to enhance the extraction of land cover information from remotely sensed data. In nutshell, it was concluded that supervised PCM in case of untrained classes gave lower RMS error when compared to Fuzzy *c*-Means.

Ibrahim *et al*. (2005) made a comparative analysis of different fuzzy classification techniques to generate accurate land cover maps in the presence of uncertainties. It was found

that Possibilistic *c*- Means classifier gives highest accuracy in land cover mapping, followed by FCM classifier.

Kumar *et al.* (2007) applied PCM and FCM classifier to (ASTER) data. Initially, only on first three bands were used followed by first nine bands, and then all the 14 bands. The results for all three cases gave the higher performance for PCM when compared to FCM in terms of accuracy. While, overall accuracy of FCM using 3 bands was only 76.4%, in comparison to 86% for PCM. In case of 9 bands and 14 bands, the overall accuracy of FCM was 81.7 % and 80.5% respectively, when compared to PCM 88.9% and 82%. Hence, it was found that the performance of PCM is better than FCM.

Tayyebi *et al*. (2008) proposes a GIS-based Possibilistic approach for simulating land use change. Two historical Landsat imageries of Tehran Metropolitan area was selected for the purpose of study. Supervised PCM classification was used to classify the images into different land use categories. Four classes were identified i.e. road, residential area, service centre, and administrative area. This work introduces a simulation experiment on urban land use change, wherein supervised PCM has been employed in parameterization of the simulation model. GIS has been used to model and monitor land use change and perform spatial analysis on the results. This approach performs with a relatively high predictive ability (72%) at a resolution of 25×25 m. By applying this methodology to the Tehran Metropolitan Area, land use changes have been derived.

2.2.3 NOISE CLUSTERING CLASSIFICATION

The concept of "Noise Cluster" was introduced such that noisy data points may be assigned to noise class. The approach has developed for objective functional type (*k*-means or fuzzy *k*-means) algorithms, and its ability to detect 'good' clusters amongst noisy data. The approach presented is applicable to a variety of fuzzy clustering algorithms as well as regression analysis (Dave, 1990, 1991, 1997). The bias due to noise is a classical problem affecting all clustering algorithms. A satisfactory solution to this problem is much awaited. Although the field of clustering has been in existence for decades, an ideal solution would be one where noise points

get automatically identified and removed from the data. The concept of having an approach where one can define one cluster as noise cluster is also promising, provided there is a way by which all the noise points could be assigned into that single cluster. Noise clustering (NC) is a method, which can be adapted to any prototype-based clustering algorithm like *k*-means and Fuzzy c-Means (FCM) (Rehm *et al.*, 2007).

Dave (1990) carried a study on noise clustering without entropy not only to establish a connection between fuzzy set theory and robust statistics, but also to discuss and compare several popular clustering methods from the point of view of robustness.

Wu and Zhou (2006) proposed a Non-Euclidean distance based algorithm, which proposes an Alternative Noise Clustering (ANC) as an extension to Noise Clustering (NC) algorithm. The ANC algorithm computes the membership values by using a Non-Euclidean Distance instead of Euclidean distance, as in FCM and NC. Based on robust statistic and influence function, it is found that ANC is more robust than FCM and NC. Further, results show that ANC can deal with noises or outliers far better than FCM and NC.

Chotiwattana (2009) proposed Kernel Noise Clustering (KNC) which is based on a distance kernel method, a noise-resistant fuzzy clustering algorithm. KNC is an extension of the noise clustering (NC) algorithm proposed by Dave in 1991. By replacing the Euclidean distance used in the objective function of NC algorithm, a new distance is introduced in NC algorithm. The distance of the kernel method is more robust than Euclidean and its alternative distance. It has also been observed that KNC algorithm is highly suitable for cluster with annular ring data shape, especially when Gaussian kernel function is applied in KNC.

Osoba *et al*. (2013) identified that noise can speedup convergence in many clustering algorithms, including the popular *k*-means clustering algorithm. The clustering noise benefit follows from the general noise benefit for the Expectation–Maximization (EM) algorithm since many clustering algorithms are special cases of the EM algorithm. Simulations show that noise also speeds up convergence in stochastic unsupervised competitive learning, supervised competitive learning, and differential competitive learning.

In 2013, Wang considered the problem of subspace clustering under noise. Specifically, the identification of behavior of Sparse Subspace Clustering (SSC) when either adversarial or random noise is added to unlabelled input data points, which are assumed to lie in a union of low-dimensional subspaces. It is shown that SSC is effective in correctly identifying the underlying subspaces, even with noisy data. In addition, it has been found that fundamental trade-off between robustness to noise and the subspace dimension is insensitivity to the number of subspaces. Thus, the analysis identifies the fundamental relationships between robustness, number of samples and dimension of the subspace.

During the last one decade, a number of robust fuzzy clustering algorithms have been proposed to partition data sets which are affected by noise and outliers. In robust NC, noise is modeled as a separate cluster and is characterized by a prototype that has a constant distance from all data points known as resolution parameter (δ). Distance 'δ' specifies the boundary of noise cluster and therefore is a critical parameter of this algorithm to be optimized (Cimino *et al.*, 2005).

2.3 HYBRIDIZATION OF CLASSIFIERS WITH ENTROPY

A combination of classifiers is a well researched topic in the area of machine learning and speech recognition. The general objective of classifier combination is to exploit the complementary information between the classifiers. In a sense, different classifiers within a classifier combination can be seen as a collection of weak classifiers, where each classifier can solve some problems. Thereafter, the process of combination involves combining the decisions of classifiers or assigning a weight to each classifier's output evidence and combining the evidence in order to reduce the objective error. The weights can be estimated statistically, i.e., *a priori*, on held-out data or development data, such as linear regression, dynamically and inverse entropy combination.

Hung and Ridd (2002) developed a hybrid supervised classifier consisting of Maximum Likelihood Classifier (MLC) and expert system rules to produce soft classification for an urban area using Landsat-TM images. MLC was used to first estimate initial class proportions which

were then redefined by generating expert system rules based on Linear Mixture Model (LMM). Most of the classes showed a significant correlation with the actual class proportions in a typical complex urban area.

Ju *et al*., (2003) presented a Mixture Discriminant Analysis (MDA) model for soft classification of remote sensing data and evaluated its performance *vis a vis LMM* and ARTMAP neural network. The results show that MDA outperformed LMM and produced similar results to ARTMAP neural network. The accuracy of the soft classification was assessed using RMSE thereby signifying that the testing data contained mixed pixels.

Tan (2007) proposed a combined Entropy Decomposition and Support Vector Machine (EDSVM) technique for Synthetic Aperture Radar (SAR) image classification for monitoring rice crop. This study assessed the utility of multi-temporal data for the supervised classification of rice planting area based on different schedules. Since adequate priori information is required for this supervised classification, ground truth measurements of rice fields were conducted. Thereafter, Support Vector Machine is applied to the feature space to perform the image classification. The effectiveness of this algorithm is demonstrated using multi-temporal RADARSAT-1 data. The results are also used for comparison with results based on information of training sets from the image using Maximum Likelihood technique, Entropy Decomposition technique and Support Vector Machine technique. The proposed method of EDSVM has found to be useful in retrieving polarimetric information for each class and it gives a good separation between classes.

Zhou (2007) proposed a new way of hybridization where a fuzzy-rule-based classifier using Genetic Algorithms (GA) was investigated. The optimal parameters of the fuzzy classifier including fuzzy membership functions and the size and structure of fuzzy rules have been extracted from the training data using GA. This was carried by introducing new representation schemes for fuzzy membership functions and fuzzy rules. The performance of the classifier was tested on two real-world databases (Iris and Wine) and a simulated Gaussian database. The results indicate that highly accurate classifiers may be designed by using relatively lesser number of fuzzy rules. The performance was also compared to other fuzzy classifiers tested on the same databases.

Xu *et al*. (2010) investigated the change in urbanization with increased availability and improved quality of multi-spatial and multi-temporal remote sensing data. This study aims to quantify changes in urban area of Antakya located in the Mediterranean region of Turkey, using Landsat and ALOS imagery. Urban changes were identified by using satellite images of Landsat MSS of 1972, Landsat TM of 1987, Landsat ETM of 2001, ALOS of 2008, using a contextual information extraction approach within a GIS. It was noted during the last 36 years that the population had grown by 3.52 times as a result of industrial development, and permanent migration was the main driving force of urbanization. Accordingly, it was found that the extent of urban areas had increased by 132%, 42.8% and 5.60% during the years 1972-1987, 1987-2001, and 2001-2008, respectively.

Debella-Gilo *et al*. (2011) proposed that edge detection is one of the most important and difficult steps in image processing and pattern recognition systems. Its importance arises from the fact that edge often gives an indication of the physical extent of an object within the image. Edge provides sufficient information about the image such that size of image data is reduced to a size which is more suitable for image analysis. The performance of the tasks after edge detection, such as image segmentation, boundary detection, object recognition and classification, and image registration are dependent on the information on the edge. However, noise is a common problem in acquisition, transmission and processing of image, which will degrade image quality seriously. Moreover, it will lead to unexpected results when images containing noise are classified using non hybrid classification approach. However, using context information along with fuzzy set based technique, Differential Evolution Algorithm (DEA), Genetic Algorithm (GA), Particle Swarm Optimization (PSO) and Simulated Annealing Algorithm (SAA) are able to remove the noise and enhances classification results.

2.4 HYBRIDIZATION OF CLASSIFIERS WITH CONTEXTUAL INFORMATION

With improvement in spatial resolution of remotely sensed data, the problem of image being contaminated by mixed pixels has also increased many folds. Conventional soft classification techniques often produce erroneous results when applied to image dominated by mixed pixels. This may lead to unrealistic representation of land cover, thereby, effecting efficient planning,

management, monitoring of natural resources. Consequently, soft hybrid classification techniques which provide sub-pixel land cover information may have to be utilized.

In contextual classifier, spatial neighbouring pixel information is used in image classification to classify homogenous objects. Contextual classifiers have been developed to address with the problem of intra-class spectral variations. This classification approach exploits spatial information among neighbouring pixels to improve classification results (Flygare, 1997, Stuckens *et al*., 2000; Hubert-Moy *et al*., 2001; Keuchel *et al*., 2003; Magnussen *et al*., 2004).

A contextual classifier may use smoothing techniques, Markov Random Fields, spatial statistics, fuzzy logic, segmentation, or neural networks (Binaghi *et al*., 1997). In general, pre-smoothing classifiers incorporate contextual information as smoothing filters, and then classification is carried out using normal spectral classifiers, while post-smoothing contextual classification may be carried out on classified images previously developed using median and mode filters. The Markov random field-based contextual classifiers, such as Iterated Conditional Modes (ICM), are frequently used approaches in contextual classification, and have proven to be effective in improving classification results (Cortijo and de la Blanca 1998; Magnussen *et al*., 2004).

In the field of pattern recognition, Markov Random Field (MRF) has been used to model the spatial context quite successfully. MRF is a mathematical toolbox which characterizes the contextual information and it has been widely used in image segmentation and image restoration (Besag, 1974; Geman and Geman, 1984; Derin and Elliott, 1987).

The importance of shape and size measure could be understood when natural objects are to be identified on satellite imagery. For example, a river and a pond may have same spectral, texture and spatial properties but may differ in shape and size. It is because rivers are linear and unbounded features whereas ponds are non-linear and bounded features. Shape and size measures are mostly utilized as complementary to each other. Further, these are always applied in conjunction with the spectral and texture measures.

Besag (1974) stated in his study that Markov Random Field (MRF) is a useful tool for modeling contextual information and may be widely used for image segmentation and restoration problems. It is also a branch of probability theory that characterizes the spatial or contextual relationship of physical phenomena.

Geman and Geman (1984) and Solberg *et al*. (1996) proposed a MRF based model for classification of remotely sensed data obtained from multiple sources. It was found that MRF based model could successful use both spatial and temporal contextual information successfully. When multi-temporal MRF fusion model was used, the overall improvement in accuracy was reported to be 2.7% when compared to a reference model. Further, with inclusion of crop field border map from GIS data, there was a significant increase in the overall accuracy, which was 79.6%.

Nguyen and Cohen (1993) have proposed a hierarchical unsupervised segmentation method for textured image using Gibbs Random Field (GRF) and fuzzy clustering technique. In the first step, image texture using GRF and fuzzy clustering method was used for feature extraction and model parameter estimation. Afterwards, they performed segmentation, using Bayesian local decisions based on previously obtained model parameters.

Markov Random Field (MRF) use smoothness priors to include spatial contextual information and to avoid over smoothening, Regularizers and Discontinuity Adaptive (DA) models have been introduced. Li (1995; 1995b) suggested DA models may be used as prior models in MRF, in order to take into consideration for discontinuities and avoid over smoothening. Further, it was shown that solution to DA models can be obtained by using Gradient Descent method, but its direct use may cause getting trapped into local minima.

Binaghi *et al*. (1997) proposed a fuzzy hybrid methodology for the classification, conceived as a cognitive process of remote sensing images. The salient aspect of the approach is the combined use of different techniques i.e. linear mixture model, a supervised fuzzy statistical classifier and a fuzzy labeling technique. An application for the identification of rice crops using Landsat Thematic Mapper image has been developed with the aim of experimentally evaluating the performance of the overall strategy in a real domain where fuzzy membership to classes are

essential in class discrimination. The results have then been compared with those obtained by means of the Maximum Likelihood classifier.

Solberg *et al. (*1996*)* used MRF to include context for multisource satellite images. It was found that MRF can model spatial class dependencies as well as temporal class dependencies. MRF model achieved 2% higher classification accuracy when same set of image used for two different models. Finally, it was conclude that MRF model provides better results for classification of multi – source satellite images.

Binaghi *et al*. (1999) used fuzzy knowledge representation framework for multi-source image classification. Both contextual and multisource information was used for identification of glacier equilibrium line in Italian Alps region. It was found that contextual classification provides better and accurate information when compared to conventional classification techniques.

Smits and Dellepiane (1997) gave a 'Discontinuity Adaptive MRF' model for segmentation of SAR images using unsupervised mode of segmentation. Since, it is important to preserve the discontinuities in particular, small structures in SAR images as it is obscured by speckle noise.

Dulyakarn and Rangsanseri (2001) have used contextual information for Fuzzy *c*-Means clustering algorithm by means of 'Geometrical Guided Model' (GG-FCM) and found better segmentation result when compared to the standard FCM method. However, it was not robust since it was carried out by partitioning the image into sub-matrix and determining the mean membership deviation compared to membership of neighbourhood pixels.

Pham (2001) included spatial contextual information with FCM using MRF for image segmentation in Magnetic Resonance Images (MRI) of brain and called it as Robust Fuzzy C-means or RFCM algorithm. Convergence of the objective function was achieved when change in the objective function was less than a defined threshold. To obtain the value of β which controls the smoothness performed by the penalty function (or objective function), cross-validation technique was used. The results were compared using Mis-Classified rate (MCR) which was 14.14% for FCM, whereas for RFCM it was 0.52%.

Kang and Roh (2001) presented a new method to increase the performance of edge-preserving image smoothing of MRF function by parameter tuning. The method was based on an automatic control of smoothing- strength in Discontinuity Adaptive MRF function from discontinuities of image intensity. An algorithm was proposed which used parameter modification to increase the piecewise smoothness of images in a Discontinuity Adaptive (DA) MRF modeling. It was observed that the proposed method was able to preserve the object boundaries in comparison to conventional DA smoothing.

Dean and Smith *et al*. (2003) modified Tree structured MRF model based on binary split of the image regions at each step. Initially, the regions were split in a binary tree pattern based on splitting criterion. In order to reduce fragmentation, estimation of field parameters was locally adaptive and a region merging parameter was also included. The image was modeled as a linear combination of original value plus zero-mean Gaussian noise. Estimation of field parameters was based on local neighbourhood characteristics using maximum pseudo likelihood estimation. Finally, MRF labelling was performed using supervised technique because of Multi-Layer Perceptron (MLP) network. The process was based on intensity values or spectral properties.

Melgani and Serpico (2003) used MRF to integrate contextual and spatio- temporal information for the classification of Landsat TM and ERS-1 SAR images. In this work, a mutual approach was proposed for image classification. It was found that proposed mutual method showed an improvement of 1% to 3% in classification accuracy when compared to reference MRF-based classifier.

Magnussen (2004) elaborated in the context of Landsat TM images that forest stands are a cluster of homogeneous pixels. Contextual classification of forest cover types exploits relationships between neighbouring pixels in order to increase in the accuracy of classification. Results of six contextual classifiers from two sites in Canada were compared to results obtained using Maximum Likelihood (ML) classifier. The comparisons were done at three levels of spectral class separation. Training and validation data were obtained from single-stage cluster sampling of 2km × 2 km Primary Sampling Units (PSU) located on a 20 km × 20km grid. A strong relationship between contextual and ML classification accuracy was explored with logistic regression analysis. Estimates of the spatial autocorrelation of reflectance values within a PSU were deemed consistent with a first-order autoregressive process. Iterative Conditional

Modes (ICM) was the best contextual method; it improved the overall accuracy by 4 to 6 % when ML accuracy was between 50% and 80%. A relaxed ICM and a smoothing algorithm were second and third best.

Kasetkasem *et al,* (2005) used MRF for super-resolution land cover mapping. In this study, a proposed MRF model based approach was applied on IKONOS MSS and Landsat ETM+ images. The results showed a significant improvement in accuracy of land cover maps over that obtained from Land cover mapping at sub pixel scales using Linear Optimization approach given by Verhoeye and Wulf (2002).

Tso and Olsen (2005) used multi scale wavelet based technique to extract line features and fuzzy fusion process to merge resulting multi scale line feature. MRF has been used here to restrict the over smoothness and bias contributed by boundary pixels.

Pal (2005) was first to hybridize PCM with FCM classifier to propose a new classifier called Possibilistic Fuzzy *c*-Mean (PFCM). This produces membership and possibilities simultaneously and avoids various problems such as hyperline constraint, and production of an unrealistic typicality values for large data sets of FCM and PCM classifier. PFCM solves the problem of noise sensitivity in FCM. It also overcomes the coincidence cluster problem of PCM. Thus, it has been observed that PFCM is more effective for identification of an object.

Debayle and Pinoli (2006) used adaptive neighbourhood image processing on a real human retina image. Adaptive neighbourhood approach was used so that context-dependent analysis could utilize radiometric as well as geometric properties of the image.

Salzenstein and Collet (2006) carried out a comparative study between fuzzy Markov Random Field and Markov Random Chain for multispectral image segmentation. It was concluded that fuzzy based approach is a good technique for astronomical data segmentation and for recovery missing data.

Sanchez-Hernandez *et al (*2007*)* used MRF for super resolution image reconstruction using Iterated Conditional Modes (ICM) algorithm to find Maximum-a-Posterior (MAP) solution. Discontinuity Adaptive framework was used to control over smoothness of MAP-MRF formulations for sixteen low-resolution (LR) images.

Hou *et al.* (2007) used modified FCM that included spatial contextual information using moving average filter as a regularizer. The accuracy was tested using different noise levels. The results obtained were in consonant with the results as obtained by Pham (2001).

Zhang and Huang (2007) proposed a Distance-Weighted Markov Random Field (DwMRF) for classification of high–spatial resolution imagery in combination with a fuzzy set based classifier. The proposed DwMRF integrates spectral and spatial information of the image, and coordinates a better interaction between neighbours and the central pixels than the conventional Equal-weighted MRF (EwMRF). In addition, a Serial Iterated Conditional Mode (SICM) method for the solution of the Markov Random Field (MRF) model was also proposed. Studies were carried out on three data sets i.e. HYDICE data of the Mall in Washington, DC, HYMAP data of Purdue University and QuickBird data of Beijing. A comparative analysis has been carried out amongst the proposed DwMRF approach with other methods such as EwMRF, Maximum Likelihood Classification (MLC) and multi resolution segmentation (Fractal Net Evolution Approach (FNEA)) method. It was found that DwMRF is robust and out performs other methods and that the proposed SICM method converges more rapidly than conventional Iterated Conditional Mode (ICM) and provides classification results which are comparable to conventional ICM method.

Tolpekin and Stein (2009) proposed a single point iterative weighted Fuzzy *c*-Means which uses prior knowledge for initializing cluster centres and spatial and spectral information for weighing the original Fuzzy *c*-Means distance calculation.

Tso and Mather (2009) proposed a proper use of context which can improve classification accuracy. Context is important in visual image interpretation and it can be obtained from spectral, spatial or from temporal attributes. This study highlights the use of context to generate a smooth image classification pattern. Use of context eliminates the possible ambiguities; recover missing information and utilizing in correction of errors. In this study, it is further highlighted, that in contextual image classification the pixels are not treated in isolation i.e. statistical dependence with its neighbour pixels should be considered. In this study, spatial contextual information has been exploited for image classification.

Balafar *et al.* (2010) proposed a hybrid clustering method for automatic medical image segmentation. Initially, local features of medical image pixels are extracted to feed a Self-Organizing Map (SOM) after a pre-processing step. The output prototypes of SOM are then filtered with hits map and a hierarchical agglomerative clustering method was applied to the prototypes. Compared to Davies-Bouldin (DB) clustering index and entropy image segmentation index, a quantitative image evaluation index had been selected for identifying best segmentation technique. The segmentation results, after post-processing, shows that the proposed method to be effective and promising.

Moser and Serpico (2010) proposed contextual Support Vector Machines (SVM) classifier based on MRF model. To minimize the execution time and to automatically tune its input parameters, hierarchical clustering and parameter optimization algorithm was also integrated with SVM. The developed method was applied on SAR and multispectral high resolution images. The overall accuracy was found to be 93.92 % and 98.98 % for traditional SVM and proposed MRF based SVM respectively.

Tuia and Camps-Valls (2011) suggested that noise clustering based learning may build efficient training sets by iteratively improving model performance through sampling. A user-defined heuristic ranks the unlabeled pixels according to a function of uncertainty of their class membership and then the user is required to provide labels for the most uncertain pixels. This study reviews and tests the main families of clustering based active learning algorithms which are based upon posterior probability. For each of them, the most recent advances in remote sensing community are discussed and some heuristics are detailed and tested. Several challenging remote sensing scenarios are considered, including very high spatial resolution and hyperspectral image classification.

Zhang and Jia (2011) stated that apart from the rich spectral information provided by multi-spectral and hyper-spectral sensors, spatial information should be given more weightage in remote sensing classification, especially in ease of high spatial resolution images. Pixel-wise spatial features can be generated by applying Gray Level Co-occurrence Matrix (GLCM) locally to describe the texture properties of an image. Morphological filtering provides spatial structure enhancement and watershed processing aims at contextual boundary identification. Further, the

advantages and disadvantages of these spatial treatments are investigated. A combined procedure has been developed to maximize spatial information extraction. Texture feature selection is emphasized for class separability. Morphological filtering is introduced as a preprocessing for watershed segmentation in order to reduce false alarm on contextual boundaries.

Trinder *et al*. (2012) aimed at developing a fuzzy based no-reference image quality assessment system by utilizing human perception and entropy of images. The proposed approach selects important features to reduce the complexity of the system and is based on entropy of feature vector, where images are partitioned into different clusters. To assign soft class labels to different images, continuous weights are estimated using entropy of Mean Opinion Score (MOS) of crisp weights. Finally, Fuzzy Relational Classifier (FRC) has been built using MOS based weight matrix and fuzzy partition matrix to establish correlation between features and class labels. Quality of the distorted/decompressed test images are predicted using the proposed fuzzy system, showing satisfactory results with the existing no-reference techniques.

Vijaya *et al.* (2012) extracted a single crop of interest using PCM and noise clustering (NC) based classifiers with the help of temporal multi-spectral satellite images. The crop grown in Aurangabad district, Maharashtra state, in India was considered. Five spectral indices SR, NDVI, TNDVI, SAVI and TVI were investigated to identify cotton crop using temporal multi-spectral images with fuzzy-based NC classifier. Accuracy assessment has been carried out using FERM. The overall accuracy observed using PCM classifier was 93.12% for SAVI indices with dataset 2. While applying NC classifier, the overall accuracy achieved was 96.02% for TNDVI index with dataset 2.

Kannan *et al.* (2013) used FCM for segmentation of a synthetic MRI image while incorporating noise clustering concept into the entropy based FCM. This FCM method was able to deal with uncertainty presents in the dataset during the segmentation of MR images. The accuracy of the proposed FCM with noise clustering method exceeded when compared to standard FCM.

Li (2013) elaborated that when noise is added inherently by the sensor and image processing techniques also corrupt the image with noise in varying degrees. One of the measures to quantify information content is classification accuracy. This can be attributed that although the

value of a pixel may change as a result of corruption due to noise, the same pixel may, in most cases, will be classified correctly. This study reveals that this loss in information is exponentially related to the variance of the added noise. The model is equally applicable for Landsat TM as well as multi-look and single-look SIR-C imagery. It has been observed that the relationship is independent of the type of noise (Gaussian, Gamma, or exponential). However, the rate of information loss increases with correlation distance, in case of spatially correlated noise. The rate of information loss also increases with the number of classes chosen for classifying the scene. Using the proposed mathematical model for information content as a function of noise variance, one can specify an "allowable" signal-to-noise ratio for a specific application.

A critical step is to develop suitable rules to combine the classification results from different classifiers. Although few attempts were made previously by the researchers to incorporate spatial contextual information for fuzzy classifiers, contextual FCM, PCM, NC, NC with entropy and FCM with entropy classifier with MRF were not introduced earlier by any researcher. As PCM works only in spectral domain thus, a PCM and spatial contextual information based sub-pixel classification method has been developed to incorporate the spatial contextual information.

As seen in the literature survey, MRF has been included into fuzzy based approaches. Extensive use of MRF with FCM, PCM, NC, and NC with entropy and FCM with entropy for soft classification has been carried out, especially in the field of remote sensing imagery. Neither edge preserving models for MRF with FCM, PCM, NC, and NC with entropy and FCM with entropy has been used for soft classification. The idea of using hybrid approach of soft classification using noise clustering with entropy is new which helps significantly to eliminate noise pixels and improves classification accuracy. However, this approach does not incorporate the spatial contextual information, which can be useful for further improvement in fuzzy classification results.

The main objective is to study contextual FCM and NC classifier with entropy by using MRF to judge the importance of spatial contextual information in soft classification techniques. In this mechanism, spatial contextual information has been incorporated in FCM algorithm by using Markov Random Field.

Traditional classification methods based on spectral analysis cannot extract land use and land cover information accurately. A successful approach must take spatial contextual information and entropy into consideration. This approach presents a novel soft-classification approach that can distinguish pixels of each class, produced in spectral analysis so that the overall accuracy of the classification is improved.

2.5 OVERVIEW OF ACCURACY ASSESSMENT

The significance of land cover as an ecological and environmental variable has made remote sensing one of the most attractive tools for the production of thematic maps of the earth's surface. However, in order for remote sensing to be able as a valuable source of land cover information, reliable accuracy measures are needed. Determining land cover information accurately from remote sensing is crucial to understand the environmental processes. Since the spatial pattern of land cover information can be smaller than the sensor footprint, soft classifications offer a flexible way to infer sub-pixel land cover information. However, accuracy assessment of these representations has been recognized to be far more difficult than traditional crisp classifications (Foody, 2002).

In the past one decade, the prevailing concerns on ecological and environmental issues, occurring especially at regional to global scales, have prompted significant advances on the use of remote sensing data for estimation of land cover information at sub-pixel level. However, the quality and performance of such classifications are difficult to quantify. Thus, there is an increasing need for assessment of sub-pixel classification performance in remote sensing (Ozdogan and Woodcock, 2006).

The assessment of accuracy for conventional hard classification has been standardized through the use of confusion matrix. This method is appropriate only for hard classifications, where it assumes that each pixel is associated with only one class in both the assessed and the reference datasets. For soft classifications and hybrid soft classifications, where multiple classes are assigned to a single pixel, a comparable standardized assessment procedure has not been established yet. For the evaluation of soft classifications in general, various suggestions have been made and few of them are mentioned here.

Gopal and Woodcock (1994) have provided an initial attempt in assessing the accuracy of a thematic map based on fuzzy set theory. In this approach, soft reference data is generated by assigning a set of linguistic values by an expert for different classes. The linguistic values are cited, 1 for absolutely wrong, 2 for understandable but wrong, 3 for accepted, 4 for good and 5 for absolutely right. These values may then be converted into numerical values from 1 to 5 for representing the soft reference data.

Binaghi (1999) put forth the concept of Fuzzy Error Matrix (FERM) to assess the accuracy of soft classification. The layout of a fuzzy error matrix is similar to the traditional error matrix used for assessing the accuracy of hard classification. The exception is that elements of fuzzy error matrix can be any non- negative real numbers instead of non-negative integer number.

Congalton and Green (1999) has proposed an error matrix based approach with the help of User and Producer accuracies wherein it is mentioned that maps are rarely 100 percent correct and are widely used with unknown accuracy to perform decision making processes. Every mapping project requires trade-offs and some level of error is accepted as a trade-off in remotely sensed data. Knowing the extent of this error however, is critical for appropriate application of the derived maps. The purpose of quantitative accuracy assessment is identification and measurement of map errors. It involves comparison of classified data against reference data for the same site. In this study, it has been suggested that assessment of accuracy include four fundamental steps: design the sample, collect data, build and test the error matrix, and analyze the results.

An error matrix is an effective way of communicating the accuracy of individual classes as well as overall map accuracy. It is a square array of numbers set in rows and columns that express the number of sample units assigned to a particular category in one classification relative the number of sample units assigned in another classification. The column usually represent reference data and is assumed to be correct, while rows indicate the classification generated from the remotely sensed data. Overall accuracy is the sum of correctly classified samples (i.e., sum of the major diagonal) divided by the total number of samples in the matrix. Producer and User accuracies are ways of representing individual class accuracies based on error of commission (

i.e. including an area into a category when it does not belong to that category) and error of omission errors (i.e. exclusion of an area from the category to which it belongs).

Foody (2002) briefly reviews the background and methods of assessment of classification accuracy, that are commonly used and recommended in literature. It was observed that the community often tends to use, unquestioningly, techniques based on the confusion matrix for which the correct application and interpretation requires the satisfaction of often untenable assumptions such as perfect co-registration of data sets and the provision of rarely conveyed information such as sampling design for ground data acquisition. Eight broad problem areas have been identified that currently limit the ability to appropriately assess, document, and use the accuracy of thematic maps derived from remote sensing. The implications of these problems are that it is unlikely that a single standard method for assessment of accuracy and reporting can be identified; yet some possible directions for future research that may facilitate assessment of accuracy are presented.

Lewis and Brown (2002) utilized the concept of fuzzy operators to evaluate the accuracy of regional scale land cover maps produced from remote sensing data. Results showed that the assessment of soft classification using fuzzy operators resulted in an improvement in map accuracy by about 19% to 23%. This study also emphasized the need of using mixed pixels in testing stage, for the assessment of accuracy of soft classification.

Shalan *et al.* (2003) presented a case study on the use of fully fuzzy classification to map land cover from IRS LISS III imagery. Two classifiers, namely, FCM and MLC were used to produce soft classification. The soft classifications were evaluated with soft reference data using cross entropy, Euclidean distance and correlation coefficient. The values of cross entropy were 0.262 and 0.287 for MLC and FCM respectively whereas corresponding Euclidean distances were 0.057 and 0.060. Although, the results showed that MLC is more accurate than FCM, the same is not clearly reflected by the magnitudes of either cross-entropy or distance measure. Therefore, there is need to develop more effective accuracy measures for sub-pixel classification.

Latifovic and Olthof (2004) have suggested that the sub-pixel class overlap problem can be resolved with the help of interval technique. The intervals defined by these operators are

arranged within a matrix, in the form of a center value plus-minus its uncertainty. It was shown that when at least one class is either under or overestimated at each pixel, the results are in the original matrix, meaning that no uncertainty arise on the interclass confusions. One typical instance of this occurs when at least one of the compared sets is crisp, as in the assessment of continental and global products through moderated resolution images. In this case, crisp classification from coarse resolution images is assessed using fractions derived from moderate or high resolution images.

Shabanov *et al*. (2005) investigated that broadleaf forest has the highest vegetation density. Identification of accurate bio-physical parameters, such as, Leaf Area Index (LAI), is a challenge to remote sensing techniques in view of low sensitivity of surface reflectance to such parameter over dense vegetation. The Moderate Resolution Imaging Spectro-radiometer (MODIS) data of Amazonia was selected for analysis. It is found that there was some anomaly in identification due to inconsistency between simulated and MODIS surface reflectance. LAI retrievals are done using new stochastic radiative transfer model, which poses high numerical accuracy at the condition of saturation. Separate sets of parameters of the LAI algorithm were generated for deciduous and evergreen broadleaf forests to account for the differences in the corresponding surface reflectance properties.

Dehghan and Ghassemian (2006) have suggested that entropy may be used as an absolute measure of uncertainty for the classified output. It is called absolute since it does not take into account any other reference data set like in case of RMSE and correlation coefficient. Further, it states that a single number can be used to specify uncertainty of classified output at per-pixel level or pe- class level or even at image level. It states that higher entropy implies higher degree of uncertainty and vice-versa. A classifier with lower entropy is considered to be a better classifier. This is another measure that can be used to provide the quantitative measure of the reliability of classification.

Ricotta and Avena (2006) initially described a generalized function of entropy which is sensitivity to the presence of abundant class. In topological analysis process, this is completely independent from metric information of an image.

Okeke and Karnieli (2006) investigated cross comparison of crisp classification with soft-classified pixels. This approach suggests a procedure of generating uncertainty free matrix for smaller number of classes. Here, a hard version of a fuzzy classification can be assessed using fuzzy values. This is also significant because many remote sensing methods for producing soft classifications are, typically based on spectral mixing models.

Pontius and Cheuk (2006) provided a set of composite operators for computation of cross-tabulation matrix for soft classified outputs. These composite operators are a combination of single operators including boolean, multiplication and minimum operators. These operators are used in building cross-tabulation matrix and assess the results for the comparison of classifier.

Silvan and Wang (2008) has proposed a more general approach of assessment of accuracy for soft classification. In this study, it has been shown that the accuracy of sub-pixel classification, having multiple classes, is accurately represented. They presented the development of a more ontologically-grounded cross-tabulation matrix that accounts for the sub-pixel distribution uncertainty. The assessment of accuracy using Sub-pixel Confusion Uncertainty matrix (SCM) approach exhibits a diagonalization characteristic that allows identifying perfect matching cases, the agreement measures must be constrained at pixel level. Even though, it was shown that there is no analytical way to determine uniquely the actual confusion based solely on the information of land cover fractions. This problem was termed as sub-pixel area allocation problem. Two new composite operators were introduced to provide minimum and maximum possible sub-pixel class overlap constrained to the unmatched sub-pixel fraction. The intervals defined by these operators are arranged within a matrix, in the form of a center value plus-minus its uncertainty, termed as the Sub-pixel Confusion-Uncertainty Matrix (SCM). Further, accuracy indices from the traditional confusion matrix were also generalized from SCM to account for the sub-pixel distribution uncertainty.

Kumar and Dadhwal (2010) proposed a hybrid model of soft classifier wherein Fuzzy *c*-Means (FCM) is chosen as a base soft classifier and entropy parameter has been added in this. Resourcesat-1 (IRS-P6) datasets from AWiFS, LISS-III and LISS-IV sensors of same date have been used. AWiFS soft classified outputs from entropy based FCM classifiers for AWiFS and

LISS-III datasets have been evaluated using Sub-pixel Confusion Uncertainty Matrix (SCM). It has been observed that output from FCM classifier yields higher classification accuracy with higher uncertainty, but entropy-based classifier with optimum value of regularizing parameter generates classified output with minimum uncertainty.

Heremans *et al*. (2012) investigated different methods, such as, Map-level hard accuracy measures, MIN, PROD and LEAST matrix, MIN-MIN; MIN-PROD and MIN-LEAST matrix, Sub-pixel confusion-uncertainty matrix, soft overall accuracy and kappa, and STATistical CONfusion matrix (STATCON) for validating sub-pixel classifications on artificial data set, and compared it with respect to their ability to correctly represent artificially induced confusion patterns. A distinction has been made between map-level accuracy measures, which allows for a fast comparison and ranking of classifications and confusion matrices that provide a more detailed overview of the confusions between individual classes. A new approach of calculating the soft confusion matrix was also added to the comparison. In terms of performance evaluation, hard accuracy measure does not perform badly, while soft measures appear, almost perfectly, to reproduce the real accuracy of the artificial classifications. With respect to confusion matrices, the results seem to be in perfect correspondence where two or more classes are under-estimated and two or more classes are over-estimated, the newly developed STATCON matrix out performs the existing approaches. Therefore, STATCON matrix may be considered as a valid alternative for assessing the accuracy of sub-pixel land use and land cover classifications.

Accuracy assessment and validation for sub-pixel classifiers is still a subject of research. No standard methods are available for sub-pixel classifiers, unlike in hard-classifiers where well defined approach, such as, Error Matrix and Kappa Coefficient are available. To conclude, FERM and SCM approaches are the most common assessment of accuracy for soft classification. Entropy has been used for uncertainty analysis of classification results and is attracting the attention in effectively employing classification results for decision making.

2.6 SUMMARY

In this chapter, various soft classification methods such as fuzzy based, entropy based and contextual based have been discussed. It is found that recent studies clearly highlight the

problem of mixed pixels in classification and their incorporation in various stages of supervised classification. Main emphasis has been given to fuzzy, noise and newly upcoming contextual based classifiers. In recent years, few attempts have been made to tackle the problem of mixed pixels; however, there is a need to carry out more investigations to define suitable criterion or procedure to perform good classification. Some of the conclusions that may be drawn from this review are:

i) A number of soft classifiers have been devised for classifications; however most of them are more suited for pure pixels and not exactly for mixed pixels.

ii) In various studies, it is found that standard methods such as MLC and ANN measure the similarity to determine class allocation of a pixel, whereas fuzzy methods provide a measure of the degree of similarity for each pixel.

iii) Only a few studies have shown incorporation of mixed pixels in the training and allocation stage of MLC, FCM , PCM and NC classifier along with the hybridization of entropy and contextual.

iv) Review of existing alternatives for assessing accuracy and identifying major drawbacks for sub-pixel assessment of accuracy based on cross-comparison matrices is required.

v) Investigations reveal general cross-comparison of sub-pixel classification accounts for sub-pixel class distribution uncertainty.

vi) Very little work has been done on hybridized model of soft classification using entropy and contextual classifiers.

Further, it is found that little work has been done in the field of soft classification using fuzzy contextual based soft classifiers. Here, some studies have been discussed to illustrate the utility of different classifiers, such as, FCM, PCM, noise clustering , contextual and entropy based hybrid soft classifiers using pure training and testing data.

The next chapter gives details of the different soft classification algorithms which have selected for this study.

CHAPTER 3

SOFT CLASSIFICATION ALGORITHMS AND ASSESSMENT OF ACCURACY

3.1 INTRODUCTION

In remote sensing, both supervised and unsupervised classification techniques may be applied to perform soft classification. This increases the classification accuracy and produces adequate land cover composition. As stated in Section 2.2, 2.3 and 2.4, this study focuses its attention on three fuzzy based soft classifiers, two fuzzy set theory based hybrid algorithms and five contextual based hybrid soft classifier to examine the various aspects as stated in Section 1.7. The three non-contextual non hybrid soft classifiers are Fuzzy *c*-Mean (FCM), Possibilistic *c*-Mean (PCM) and Noise Clustering (NC), have been selected as soft classifiers, while Noise Clustering With Entropy (NCWE) and Fuzzy *c*-Mean With Entropy (FCMWE) are non contextual fuzzy based hybrid algorithms considered for study.

There has been an increasing interest in the use of contextual information for acquiring a smooth image classification pattern. The suitable use of context allows the elimination of possible ambiguities and recovery of missing information (Li, 1995a). In contextual based hybrid classification, all five soft classifiers stated above have been implemented considering two modes i.e. Smoothness prior and Discontinuing Adoptive prior, thus yielding a combination of 10 different algorithms. Fig. 3.1 shows a tree diagram of all the soft classifiers which are proposed to be used in this study. At the top most level, the classifiers are grouped into three major categories i.e. Fuzzy, Entropy and Contextual based classifiers. In the sections 3.2, 3.3, 3.4, 3.5 and 3.6, a detailed treatise of the some of the classifiers and accuracy assessment techniques has been outlined.

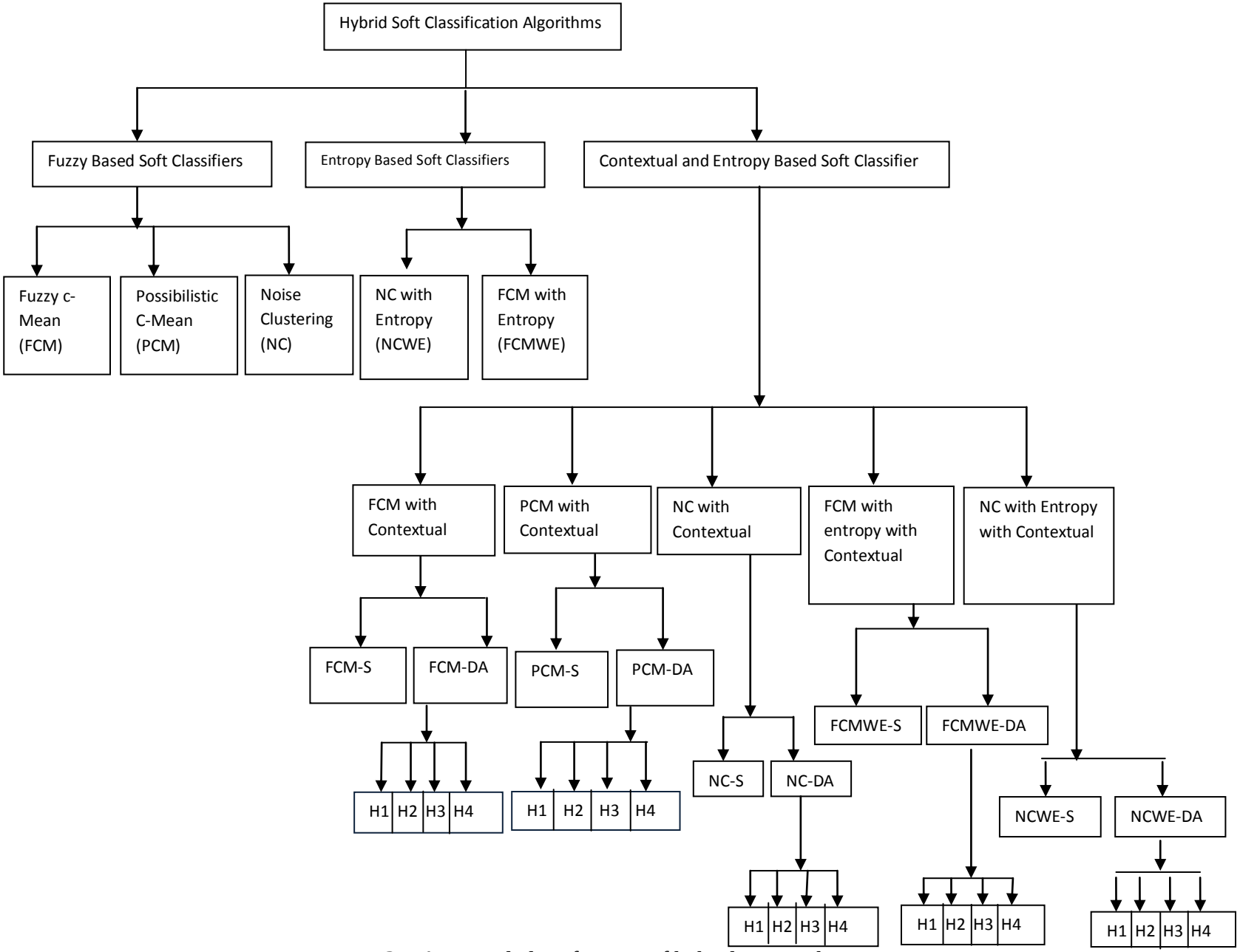

Fig. 3.1 A general classification of hybrid approaches

3.2 FUZZY BASED SOFT CLASSIFIERS

The use of non hybrid fuzzy set based classification methods in remote sensing has received growing interests where the ecological phenomena are inherently fuzzy (Zang and Foody, 2001). The commonly used classifiers are FCM, PCM, and NC which are conceptually unsupervised in nature. However, these can be applied in supervised mode by providing the class means from well defined training data sets in place of cluster centers (Foody, 2000b).

As described by Zhang and Foody (2001), the reason for fuzziness within information is mainly due to:

i) In real world, different land cover types are heterogeneous resulting in intergraded phenomena i.e. classes do not have crisp boundaries. There is fuzziness due to the geographical phenomena.

ii) A pixel value is the result of interaction of electromagnetic waves with the ground objects and/or atmosphere. The sensor records this spectral response which may differ for similar entities, while dissimilar entities may also show similar spectral response, depending on the ground situations.

iii) Finally, due to coarse or medium spatial resolution of sensors (e.g. AWIFS and LISS III), a pixel may not consist of single class but two or more classes. This can be defined as fuzziness due to resolution of the sensor.

3.2.1 FUZZY *C*- MEANS (FCM) CLASSIFIER

The Fuzzy *c*-Means (Bezdek, *et. al.*, 1984) method is a partitioning algorithm; and is widely used in pattern recognition. FCM partitions the feature space and form clusters. It calculates the membership values of the each pixel for different land cover classes. The membership values gives the *degree of sharing* of a single pixel to different land cover classes with values ranges between 0 and 1. Thus, a pixel can belong to several land cover classes with varying degree of membership. Hence, in FCM the clusters are not partitioned as a crisp but as a fuzzy by giving memberships values to each class within an each pixel.

FCM is based on the minimization of the objective function as given in Eq. 3.1,

$$J_m(U,V) = \sum_{j=1}^{n}\sum_{i=1}^{c} u_{ij}^{m}\left\|X_j - V_i\right\|^2, \quad 1 \le m < \infty \qquad \ldots \text{Eq (3.1)}$$

where,

n is the total number of the pixels,

c is the number of classes,

u_{ij} is the fuzzy membership value of the i^{th} pixel for class *j*,

m is the weighing exponent,

X_j is the vector pixel value and,

V_i is the mean vector of cluster *j*.

The fuzzy membership value is calculated through an iterative optimization of Eq 3.1 with update of membership u_{ij} and cluster centers V_i (Dulyakarn, *et. al.,* 2001):

$$u_{ij} = \frac{1}{\sum_{k=1}^{c}\left(\frac{d_{ij}}{d_{ik}}\right)^{\frac{2}{m-1}}} \qquad \ldots \text{Eq (3.2)}$$

$$V_i = \frac{\sum_{j=1}^{n} u_{ij}^{m} X_j}{\sum_{j=1}^{n} u_{ij}^{m}} \qquad \ldots \text{Eq (3.3)}$$

The iteration of Eq 3.1 stops when $\max_{ij}[|u_{ij} - \hat{u}_{ij}|] < \varepsilon$ is satisfied, where ε is a termination criterion between 0 and 1 (Dulyakarn, *et. al.,* 2001).

3.2.2 POSSIBILISTIC *C*- MEANS (PCM) CLASSIFIER

The main advantage of PCM is related to the relaxation of the probabilistic constraint of FCM. Therefore, the formulation of PCM is based on a modified FCM objective function whereby an additional term called as regularizing term is also included.

FCM has been successful in assigning the membership (u_{ij}) of a pixel to multiple classes however, the assignment is relative to total number of classes defined (Krishnapuram and Keller, 1993). This is due to the constraint on the membership values given by the Eq 3.4

$$\sum_{i=1}^{c} u_{ij} = 1, \forall j \qquad \ldots \text{Eq (3.4)}$$

where,

j varies from 1 to *n* (*n* is the total number of pixels in the image) and,

'*c*' is the total number of classes defined by the analyst.

Eq 3.4 can be interpreted as the sum of membership values of a pixel for all the classes and should be equal to one (Bezdek,*et al.*, 1984, Krishnapuram and Keller, 1993). Krisnhapuram and Keller (1993) introduced a relaxation in FCM, such that the sum of membership may exceed beyond 1. This variation of PCM is known as Possibilistic *c*-Means (PCM), where the constraint on membership value is as per Eq 3.4. Thus, similar to FCM, PCM classification is also an iterative process where the class membership values are obtained by minimizing the generalized least square error objective function (Krishnapuram and Keller,1993), given by Eq 3.5,

$$J_m(U,V) = \sum_{i=1}^{n}\sum_{j=1}^{c} u_{ij}^{\ m} \left\| X_i - v_j \right\|_A^2 + \sum_{j=1}^{c} \eta_j \sum_{i=1}^{n} \left(1 - u_{ij}\right)^m \qquad \ldots \text{Eq (3.5)}$$

ensuring that the conditions given below are satisfied.

$$\max_j u_{ij} > 0, \forall i \qquad \ldots \text{Eq (3.6)}$$

$$\sum_{i=1}^{n} u_{ij} > 0 \qquad \textit{for all } j \qquad \ldots \text{Eq (3.7)}$$

$$0 \le u_{ij} \le 1 \qquad \textit{for all } i, j \qquad \ldots \text{Eq (3.8)}$$

where,

η_j is a parameter that depends on the distribution of pixels in the cluster '*j*' and is assumed to be proportional to the mean value of the intra cluster distance.

In Eq 3.5, the first term demands that distances between feature vectors and its prototypes be as low as possible, while the second term forces the u_{ij} to be as large as possible, thus avoiding the trivial solution. Generally, η_j depends on shape and average size of the cluster 'j' and its value may be computed as;

$$\eta_j = K \frac{\sum_{i=1}^{N} u_{ij}^m d_{ij}^2}{\sum_{i=1}^{N} u_{ij}^m} \qquad \text{...Eq (3.9)}$$

where K is a constant and is generally kept as one.

After this, class memberships, u_{ij} are obtained as;

$$u_{ij} = \frac{1}{1 + \left(\frac{d_{ij}^2}{\eta_j} \right)^{1/m-1}} \qquad \text{...Eq (3.10)}$$

In case of PCM, this membership value represents the "degree of belongingness or compatibility or typicality", contrary to FCM, where it is, "degree of sharing" (Krishnapuram and Keller, 1993). Overcoming this constraint gives higher accuracy of supervised classification using PCM as compared to that of FCM (Kumar and Ghosh, 2006, 2007). Also, PCM, as a supervised classifier, works better in case of untrained classes, when compared to FCM (as supervised classifier) (Foody, 2000). Untrained classes are those classes which are present in the image but are not known to the analyst; hence, the classifier is not trained with that unknown class. Thus, the advantages of PCM over FCM are the motivation behind selecting PCM as soft classification approach in this research. Further, PCM can handle noise and outliers (Krishnapuram and Keller, 1996). Noise and outliers affect the prototype parameters i.e. cluster means.

3.2.3 NOISE CLUSTERING (NC) CLASSIFIER

Dave (1991) proposed a method of noise clustering. This method is fundamentally based on FCM, where an additional cluster is introduced such that it supposedly contains all outliers

(Dave and Keller, 1997). Feature vectors that are located close to a noise distance 'δ' or further away from any other prototype vector are assigned high membership values to this noise cluster. The noise prototype is defined such that the distance between the feature vectors from the centre point of line cluster (v_c) is a fixed constant value. To incorporate noise, another cluster (c+1) is added which has no centre and that the dissimilarity $D_{k,c+1}$, between any cluster x_k and this cluster is given by Eq 3.11

$$D_{k,c+1} = \delta \qquad \text{...Eq (3.11)}$$

where

δ = Resolution parameter and δ>0, which is a fixed parameter.

Thus, the objective function of NC classifier is given by Eq 3.12

$$J_{NC}(U,V) = \sum_{i=1}^{c}\sum_{k=1}^{n} u_{ki}^{\ m} D(x_{k,}\, v_i) + \sum_{k=1}^{n} u_{k,c+1}^{\ m}\, \delta \qquad \text{...Eq (3.12)}$$

where,

U is n×(c+1) matrix, while $V=(v_1, \ldots, v_c)$.

The applicable constraints for Eq. 3.12 are

$$u_f = \{U = (u_{ki}) : \sum_{j=1}^{c+1} u_{kj} = 1, \quad 1 \le k \le n;\} \qquad \text{...Eq (3.13)}$$

and

$$u_{ki} \in [0,1], 1 \le k \le n,\ 1 \le i \le c+1 \qquad \text{...Eq (3.14)}$$

where

i= 1,……c+1, k=1,…….n , resolution parameter δ> 0 and weighting exponent or fuzzifier m>1.

n= No. of rows × No. of column (image size).

The distances are defined as mentioned in Eq 3.15

$$D(x_{k,}\, v_i) = (x_k - v_i)^T A_i (x_k - v_i) \qquad \text{...Eq (3.15)}$$

for all 'k' and i=1 to c+1 and A_i is the weight matrix.

When the objective function of NC defined in Eq. 3.12 is used in algorithm, the optimal membership value (u_{ki}) is computed using Eq 3.16.

$$u_{ki} = \left[\sum_{j=1}^{c} \left(\frac{D(\mathrm{x_{k,}}\, \nu_{\mathrm{i}})}{D(\mathrm{x_{k,}}\, \nu_j)} \right)^{\frac{1}{m-1}} + \left(\frac{D(\mathrm{x_{k,}}\, \nu_{\mathrm{i}})}{\delta} \right)^{\frac{1}{m-1}} \right]^{-1}, \quad 1 \le i \le c \qquad \text{...Eq (3.16)}$$

In Eq 3.12 the second term ($u_{k,c+1}$) is computed using Eq 3.17.

$$u_{k,c+1} = \left[\sum_{j=1}^{c} \left(\frac{\delta}{D(\mathrm{x_{k,}}\, \nu_j)} \right)^{\frac{1}{m-1}} + 1 \right]^{-1}, \quad 1 \le i \le c \qquad \text{...Eq (3.17)}$$

where

ν_{i} denotes the mean vector of each class and can be defined as

$$\nu_i \qquad \frac{\sum_{k=1}^{n} (u_{ik})^m x_k}{\sum_{i=1}^{n} (u_{ik})^m}, 1 \le i \le c \qquad \text{...Eq (3.18)}$$

The specification of noise distance depends on several factors, i.e. maximum percentage of the data set to be classified as noise, distance measure, number of assumed clusters and the expansion of the feature space. The noise distance is a simplified statistical average over the non-weighted distances of all feature vectors to all their corresponding prototype vectors (Rehm *et al*., 2007).

3.3 ENTROPY BASED HYBRID SOFT CLASSIFIERS

The measure of information, as per Shannon (1948, 1951) states that it has an intimate relationship with entropy theory as in statistical thermodynamics. Therefore, information theory and thermodynamics must have some common points of interest. The increase in entropy has been regarded as the degradation of energy by Kelvin (Kivinen, J. and Warmuth, 1999). In statistical thermodynamics, entropy is defined as a measure of the disorder of a system. However, in information theory, entropy is a measure of the lack of information about the actual structure of the system (Li and Mukaidono, 1999). It is perceived that fuzzy based information

can become complete by adding entropy to the standard one, since it can observe the nature of both methods more deeply by contrasting these two methods (Dunn, 1974 and Bezdek ,1984).

In this study, it has been observed that entropy based method is similar to a statistical model having Gaussian distribution, since both of them have error functions, while the standard method such as FCM, PCM, etc. are different from a statistical model. For this reason, standard method is purely fuzzy, while entropy based method connects a statistical model and a fuzzy model (Dunn, 1974, Bezdek, 1973, 1981).

In this study, one of the primary motivations is to hybridize FCM and NC based classifier with entropy for the purpose of optimization with respect to membership values and cluster centers and that the constraint is same for both where, the difference between two methods is the use of an objective function.

3.3.1 NOISE CLUSTERING WITH ENTROPY (NCWE) CLASSIFIER

Recently, many researchers have used cluster analysis as one of the main tool to solve problems related with satellite image classification, data analysis and data mining. Generally, it found that use of K-means classifier, which uses K cluster centers, is still popular. A group of data points are collected around a cluster center and which forms a cluster and in turn provides a base for noise clustering classifier.

The term entropy was first used by Rudolf Clausius (1865) to state the Second law of thermodynamics. Though, entropy is a simple term, many people find it difficult to understand its exact meaning. There are three important E's in the study of the thermodynamics: energy, equilibrium and entropy. Entropy is an adaptation of a Greek word 'tropee' which means transformation. Fuzzy or soft classification outputs of images as obtained either in form of class membership or in form of probabilities (Dunn. 1973) and (Bezdek, 1981). Such an idea of regularization has frequently been found in formulation of ill-posed problems. A typical regularization is done by adding a regularizing function. The objective function of Noise Clustering with Entropy classifier (NCWE) is given by Eq 3.19,

$$J_{NCWE}(U,V) = \sum_{i=1}^{c}\sum_{k=1}^{n} u_{ki} \quad D(x_{k,}\nu_{i}) + \sum_{k=1}^{n} u_{k,c+1} \quad \delta + \nu \sum_{i=1}^{c+1}\sum_{k=1}^{n} u_{ki} \log u_{ki} \qquad \text{...Eq (3.19)}$$

where,

ν is regularizing parameter and has a value greater than 0.

u_{ki} denotes the class proportion of class k in pixel i of the image and

c is the number of classes.

The computation formula of u_{ki}, $u_{k,c+1}$ and v_i is given by Eq 3.20, Eq 3.21 and Eq 3.22,

$$u_{ki} = \frac{\exp\left(-\frac{D(x_{k,}\nu_{i})}{\nu}\right)}{\sum_{j=1}^{c}\exp\left(-\frac{D(x_{k,}\nu_{j})}{\nu}\right) + \exp\left(-\frac{\delta}{\nu}\right)}, \quad 1 \le i \le c \qquad \text{...Eq (3.20)}$$

$$u_{k,c+1} = \frac{\exp\left(-\frac{\delta}{\nu}\right)}{\sum_{j=1}^{c}\exp\left(-\frac{D(x_{k,}\nu_{j})}{\nu}\right) + \exp\left(-\frac{\delta}{\nu}\right)}, \qquad \text{...Eq (3.21)}$$

$$v_i = \frac{\sum_{k=1}^{n} u_{ki} x_k}{\sum_{k=1}^{n} u_{ki}}, \quad 1 \le i \le c \qquad \text{...Eq (3.22)}$$

In Eq. 3.19, the first and second terms are similar to the formulation of NC classifier (Eq. 3.12) and all parameters have similar meaning as specified in Section 3.2.3. Further, the third term is a typical regularization, done by adding entropy as a non linear regularizing function in the process of classification.

3.3.2 FUZZY *C*-MEAN WITH ENTROPY (FCMWE) CLASSIFIER

Fuzzy c-Mean with Entropy (FCMWE) is a hybridization approach of classification where the emphasis is to integrate entropy based regularization method with FCM. It is believed that the methods of Fuzzy *c*-Means become *complete* by adding entropy to the standard one as defined in Eq 3.1 (Dunn, 1974; Bezdek, 1984; Li and Mukaidono, 1999; Miyamoto and Mukaidono, 1997).

The primary motivation is to use both alternatives for the purpose of optimization with respect to membership matrix and cluster centers. Moreover, the constraint is same for the both alternatives, difference being the objective functions. There are numerous reasons, to incorporate entropy-based method such as (Li *et al*., 1995; 2002; Little and Rubin, 2002):

i) Methods using entropy functions have been rediscovered repeatedly in fuzzy clustering by different formulations. This hybridization has been proposed, to evaluate the performance of algorithm which is purely fuzzy, while entropy based method is more similar to statistical method.

ii) This method is related to general principle of maximum entropy (Wu, 1997) that has potentiality for further development in various applications.

iii) The method of entropy is closely related to statistical models such as the Gaussian Mixture Model (McLachlan, 2000) and Gibbs distribution (Rose *et al.*, 1990).

iv) Comparison between the methods suggested by Dunn (1974) and Bezdek (1973,1981), and entropy based algorithm reveals more clearly the different features of both methods.

It is observed that the method of Dunn (1974) and Bezdek (1981) also known as the standard method of FCM, is purely fuzzy, while entropy-based method is more similar to statistical models (Tihonov, 1997; Vapnik, 1995, 1998, 1999, 2000). It has been observed that output from FCM classifier has higher classification accuracy with higher uncertainty but entropy based classifier with optimum value of regularizing parameter generates classified output with minimum uncertainty (Kumar and Dadhwal, 2010). As nonlinearity, introduced by Dunn (1974) and Bezdek (1984), smoothens the crisp solution into a differentiable one. Moreover, fuzzy solution approximates the crisp one i.e. the fuzzy solution converges to a crisp solution as *m* approaches to 1. Roughly, it can be stated that fuzzified solution regularizes the crisp solutions.

Fuzzy *c*-Mean introduces non linearity using $(u_{ki})^{m}$. However, use of entropy is another type of nonlinearity. A typical regularization is done by adding a regularizing function. The basic objective function of FCM with entropy classifier is given in Eq 3.23

$$J_{FCMWE}(\mathrm{U},\mathrm{V}) = \sum_{i=1}^{c}\sum_{k=1}^{n} u_{ki} D(\mathrm{x}_{\mathrm{k}}, \nu_{\mathrm{i}}) + \nu \sum_{i=1}^{c}\sum_{k=1}^{n} u_{ki} \log u_{ki}\,, (\nu > 0) \qquad \text{...Eq (3.23)}$$

where ν is regularizing parameter and has a value greater than 0.

The membership value (u_{ki}) and mean vector (v_i) is computed as given in Eq 3.24 and Eq 3.25

$$u_{ki} = \frac{\exp\left(-\frac{D(x_{k,}\, v_i)}{v}\right)}{\sum_{j=1}^{c}\exp\left(-\frac{D(x_{k,}\, v_j)}{v}\right)}, \quad 1 \le i \le c \qquad \text{...Eq (3.24)}$$

$$v_i = \frac{\sum_{k=1}^{n} u_{ki} x_k}{\sum_{k=1}^{n} u_{ki}}, \; 1 \le i \le c \qquad \text{...Eq (3.25)}$$

In the Eq. 3.23, the first term is the objective function of FCM classifier and second term is a nonlinear regularizing entropy function. It is observed that regularizing function is a strictly a convex function, and hence capable of fuzzifying the membership values.

3.4 CONTEXTUAL BASED HYBRID SOFT CLASSIFIERS

Contextual based image classification approach is one where, contextual information of an image is used. This approach focuses on the relationship of the nearby pixels. The overall objective of this approach is to classify images by using the contextual information to resolve the problem associated with uncertain boundaries. Non contextual fuzzy based classification technique such as FCM, PCM, NC, NCWE and FCMWE can be used to handle mixed pixels. Although, these hybrid and non-hybrid classification approaches have the advantage of classifying mixed pixels by assigning a membership value. However, these methods are unable to incorporate the spatial contextual information of pixels into the classification process. Use of context eliminates the problem of isolated pixels and improves classification accuracy (Li, 2009).

Markov Random Field (MRF) is a mathematical toolbox which characterizes the spatial contextual information in terms of Smoothness prior and Discontinuity Adaptive prior models, to improve classification accuracy and also preserves edges at boundaries and generates spectrally and spatially consistent classified output.

3.4.1 THEORY OF MARKOV RANDOM FIELD

In remote sensing image analysis, Bayesian theory has a strong influence on statistical modeling. Bayesian classification consists of prior and conditional Probability Density Functions (PDF). By using these functions, a classification can be obtained in terms of Maximum Posterior (MAP) criteria (Tso and Mather, 2009). In practice, there are problems in using MAP estimates. One of the difficulties is that the prior information of the data distribution may not always be available. So, it may be necessary to use alternative criteria instead of MAP. Maximum Likelihood (ML) criteria can be used, if the knowledge of data distribution is available without the prior information of data. A maximum likelihood criterion is being widely used in remote sensing image classification. Most classification use Gaussian distribution to model class-conditional probability density function. Classification results can be improved, if MAP estimation is carried out by modeling of prior PDF and the class-conditional PDF. For modeling of prior probability context is one assumption (Tso and Mather, 2009).

Proper use of context can improve classification accuracy (Solberg *et al*., 1996; Jackson and Landgrebe, 2002; Magnussen *et al*., 2004; Tso and Olsen, 2005). Context is an important characteristic in visual image interpretation. It can be obtained from spectral, spatial or temporal attributes (Tso and Mather, 2009). Context generates a smooth image classification pattern. Use of context eliminates possible ambiguities; recover missing information and correction of errors (Magnussen *et al*., 2004). In contextual image classification, pixels are not treated in isolation, but as a statistical dependence with its neighbor pixels (Tso and Mather, 2009). In this study, spatial contextual information has been incorporated for image classification to reduce uncertainty and improve classification accuracy.

Markov Random Field (MRF) is a useful tool for modeling contextual information and is widely used for image segmentation and restoration (Besag, 1974; Geman and Geman, 1984). It is based on probability theory that characterizes spatial or contextual relationship of physical phenomena. MRF theory and its formulations described here have been adopted from Tso and Mather (2009).

Let, $d = \{d_1, d_2, \dots, d_n\}$ denote a set of random variables, where a set *S* containing *n* number of sites (pixels) in which each random variable takes a label (membership values) for class L, where family *d* is called a random field. The set S is equivalent to an image containing n pixels; *d* is a set of pixel (DN) values and the label set L depends on user defined application, i.e. *L*={agriculture, sal forest, moist land, barren land, water body}. Based on the definition of random field, the configuration *w* for set *S* may be defined as $w = \{d_1 = w_1, d_2 = w_2, \dots, d_n = w_n\}$ where $w_r \in L(1 \leq r \leq n)$. The notation of *w* can be simplified to $w = \{w_1, w_2, \dots, w_n\}$. A random field, with respect to a neighborhood system is a Markov Random Field, if and only if, the probability density function satisfies the following three properties (Tso and Mather, 2009).

Positivity: $P(w) > 0$, for every possible configuration of *w*. It states that, it has a non-zero probability and $P(w)$ is the probability of given dataset *w*.

Markovianity: $P(w_r|w_{s-r}) = P(w_r|w_{Nr})$**,** it defines the neighborhood system. This property means that, membership value of pixel *r* is only dependent on its neighboring pixels.

Homogeneity: $P(w_r|w_{Nr})$ is same for all pixels *r*, this property specifies the probability for the label of all pixels is dependent on neighboring pixels regardless of the pixel location.

An MRF also satisfy other property such as isotropy. This is the direction independence property among the neighboring pixels. It means that the neighboring pixels surrounding a pixel *r* have same contributing effect to the labeling of pixel *r* (Tso and Mather, 2009).

3.4.2 NEIGHBORHOOD SYSTEM

In image analysis, neighborhood is defined to consider the surrounding pixels in a given systematic manner. Usually, neighborhood system used in image analysis defines the first-order neighborhood that contains four pixels sharing a side with the central pixel, as shown in (Fig. 3.2a). Second-order neighborhood contains four pixels having corner boundaries with the pixel of interest (Tso and Mather, 2009), as shown in (Fig. 3.2b). Higher order neighborhood system can be formed in a similar fashion. In (Fig. 3.2c) neighborhood system order up to five is shown. In this study only the second-order neighborhood system has been considered.

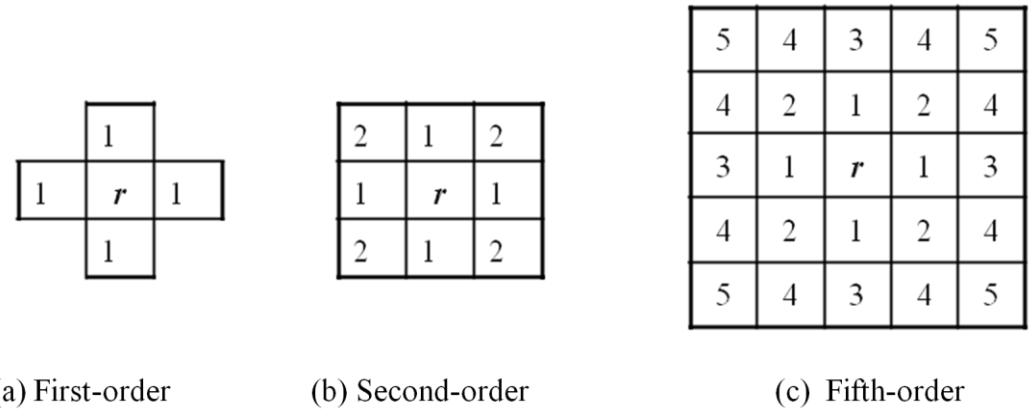

Fig 3.2: Neighborhood system of different order for pixel *r* (Tso and Mather, 2009)

3.4.3 GIBBS RANDOM FIELD

Gibbs Random Field (GRF) defines a global model for an image. GRF provides a global model of an image by specifying a PDF as in Eq 3.26 (Tso and Mather, 2009):

$$P(w) = \frac{1}{Z}\exp\left(-\frac{U(w)}{T}\right) \quad \text{... Eq (3.26)}$$

where,

$P(w)$ is the probability of *w*,

$U(w)$ is the energy function,

T is a constant termed temperature and,

Z is the partition function, and it can be expressed by Eq 3.27:

$$Z = \sum \exp\left(-\frac{U(w)}{T}\right) \quad \text{... Eq(3.27)}$$

In Eq 3.27, Z is the sum of all possible combination of *w*. In case of an image, it is all combinations of pixel values. In practice, Z is not computable except for very simple cases. This difficulty in computation of Z complicates sampling and estimation problems. From Eq 3.26, maximization of $P(w)$ is equivalent to minimization of the energy function $U(w)$ as given by Eq 3.28.

$$U(w) = \sum_{c \epsilon C} V_c(w) \quad \text{... Eq (3.28)}$$

In Eq 3.28, C is a clique. $C = C_1 \cup C_2 \cup C_3 \cup ...$, is the collection of all possible cliques, C is a subset of image and within a clique all pairs of pixels are mutual neighbors $V_c(w)$ and is called the potential function with respect to clique C. As the order of neighborhood system increases, the number of cliques grows rapidly, so does the increase in computational complexity. The energy function $U(w)$ in Eq 3.28 can also be expanded as given below in Eq 3.29 (Tso and Mather, 2009):

$$U(w) = \sum_{\{r\} \in C_1} V_1(w_r) + \sum_{\{r,r'\} \in C_2} V_2(w_r, w_{r'}) + \sum_{\{r,r',r'\} \in C_3} V_3\left(w_r, w_{r'}, w_{r''}\right) + \cdots \quad \text{... Eq (3.29)}$$

where C_1, C_2, C_3 represents a single-site, a pair-site, a triple-site and a quadratic-site clique respectively. In this study, only C_2 has been considered, since it represents a second order neighborhood system.

3.4.4 MRF-GRF EQUIVALENCE

An MRF describes in terms of local properties of an image, whereas GRF describes global properties of an image. According to Hammersley-Clifford theorem, there is an equivalence of GRF and MRF properties and that a unique GRF exists for every MRF as long as GRF is defined in terms of cliques in a neighborhood system. This equivalence provides a simple way to address MRF- based contextual image analysis problems (Tso and Mather, 2009).

3.4.5 PRIOR ENERGY

The energy function represented by $U(w)$ is called as prior energy. From Eq 3.29, $U(w)$ provides *prior knowledge* about the image. In image classification, smoothness assumption is usually adopted to model prior information (Tso and Mather, 2009). To model prior energy, several functions are available and are known as smoothness prior. Some of the commonly used smoothness prior modes are *Auto-models, Multi-level Logistic model, Auto-logistic model, Ising model etc.* (Li, 2009; Tso and Mather, 2009).

3.4.6 SMOOTHNESS PRIOR

Smoothness is a generic constraint of context. It assumes that a physical property does not change abruptly (Li, 2009). In case of an image, Digital Number (DN) of pixels do not change suddenly and present some coherence. This assumption of smoothness has been applied in early applications of vision problem (Grimson, 1981; Horn and Schunck, 1981). To compute image properties, smoothness prior is one of the most popular prior assumption in low-level vision. Smoothness assumption is expressed as prior probability or equivalently as an energy term $U(f)$ (Li., 2009). The analytic regularization model provides a convenient platform for the study of smoothness prior (Li, 2009).

Eq 3.30 defines the general form of these regularizers (Li, 1995):

$$U(f) = \sum_{n=1}^{N} U_n(f) = \sum_{n=1}^{N} \lambda_n \int_a^b g\left(f^{(n)}(x)\right) dx \qquad \text{... Eq (3.30)}$$

where,

$U(f)$ is prior energy and is the smoothness term,

$U_n(f)$ is nth order regularizer,

N is highest order to be considered and,

$\lambda_n \geq 0$ is a weighting factor.

This regularizer model is based on Euler equation, so the order of derivative is to be considered with boundary condition $f(a)$ and $f(b)$. The potential function $g\left(f^{(n)}(x)\right)$ is dependent on irregularity in $f^{(n-1)}(x)$ and all the regularizers vary according to this potential function i.e. $g\left(f^{(n)}(x)\right)$. In this study, *standard regularizer* has been used as smoothness prior. Standard regularizers take the pure quadratic form as expressed by Eq 3.31.

$$g_q(\eta) = \eta^2 \qquad \text{... Eq (3.31)}$$

More irregularity in $f^{(n-1)}(x)$ increases $|f^n|$ and contributes to a higher energy i.e. $U(f)$. This standard regularization based smoothness prior has been used previously with FCM and Possibilistic *c*-Means (PCM) classifier respectively.

Smoothness is generic postulation underlying a wide range of geographical phenomena. It characterizes coherence and homogeneity and its applications are seen widely in image restoration, edge detection, texture and visual interpretation. However, it involves discontinuities, so the disadvantages of this regularization model are (Li, 1995):

i) It considers constant interaction among neighboring points.
ii) Smoothing strength is proportional to derivative magnitudes $|f^n|$.

So, this causes over-smoothing at discontinuities at which the derivative is infinite (Li, 1995).

3.4.7 DISCONTINUITY ADAPTIVE MRF MODELS

Smoothness is a generic assumption underlying a wide range of physical phenomena. This characterizes consistency and homogeneity of an image (Geman and Geman, 1984). Its applications are widely seen in edge detection, region segmentation and texture analysis. However, improper imposition may lead to the problem of over smoothing. Thus, it is necessary to take care of discontinuities.

To resolve the above problem, Li (1995) introduced Discontinuity Adaptive (DA) MRF models to avoid over smoothing. The major differences amongst different DA MRF models lies in the way how these pixels interact with their neighboring points and control the smoothing strength. The principle of DA models states that whenever a discontinuity occurs, it minimizes the smoothing strength according to Li (2009).

Smoothness assumption implies uniform smoothness everywhere (Li, 1995). However, in a real image discontinuity occurs at the boundaries or at edges and the image itself is a piecewise discontinuous surface. Further, improper use or applying smoothness homogeneously over an image can lead to over smoothing and undesirable results. Thus, it is important to take care of discontinuities before using smoothness priors (Li, 1995; Li, 2009). Hence, in this study, Discontinuity Adaptive (DA) priors have been used to model the prior energy and to preserve edges.

The Discontinuity Adaptive smoothness models works on a principle that whenever a discontinuity occurs, interaction should decrease (Li, 2009). There are four possible choices available for the potential function i.e. $g(\eta)$ and is also termed as Adaptive Potential Function (APF). The derivative of APF is expressed by Eq 3.32.

$$g'(\eta) = 2\eta h(\eta) \quad \text{... Eq (3.32)}$$

where,

h is the interaction function, known as *Adaptive Interaction Function* (AIF).

The smoothness strength depends on the shape of AIF and can be determined by h_γ, where γ is a parameter. The strength with which a regularizer performs smoothing is given by Eq 3.33.

$$\left|g'(f')\right| = \left|2f'h(f')\right| \quad \text{... Eq (3.33)}$$

where, $h(f'(x))$ determines the interaction between neighboring pixels.

3.4.7.1 WORKING PRINCIPLE OF DA PRIORS:

The necessary condition for regularization model to be "Discontinuity Adaptive" can be expressed by Eq 3.34 (Li, 1995):

$$\lim_{\eta\to\infty}\left|g'(\eta)\right| = \lim_{\eta\to\infty}|2\eta h(\eta)| = C \quad \text{... Eq (3.34)}$$

where,

$C \in [0, \infty]$ and is a constant.

The condition with $C = 0$, entirely disallow smoothing at discontinuities where $\eta \to \infty$. If $C > 0$, it allows bounded or limited smoothing. However, for large $|\eta|$, the interaction $h(\eta)$ will be small and approaches 0 as $|\eta|$ goes to ∞ (Li, 2009).

3.4.7.2 THE DISCONTINUITY ADAPTIVE (DA) MODELS USED:

The DA models works with energy minimization in MRF. It is found that the fundamental difference amongst different models for dealing with discontinuities lies in their ways of

controlling the interaction between neighboring pixels. DA model is based on the principle that wherever a discontinuity occurs, the interaction should diminish.

Four possible choices of DA models have been given by (Li, 2009). All the four DA models have been incorporated in this study which is based upon Adaptive Potential Function (APF). DA models used in this study are expressed by Eq 3.35 - 3.38:

$$g_{1\gamma}(\eta) = -\gamma e^{-\frac{\eta^2}{\gamma}} \quad \text{... Eq (3.35)}$$

where,

g_γ = Adaptive string

γ = Interaction range parameter lies between 0 and 1.

η = scale parameter >0.

There are various strategies to accelerate the algorithm. In Eq 3.35, to compute the adaptive potential, the exponential nature APF has been chosen, wherein $g_{1\gamma}(\eta)$ is not necessary to be bound. However, it is helpful for analyzing the convexity of energy function mentioned in Eq 3.33.

$$g_{2\gamma}(\eta) = -\frac{\gamma}{1+\frac{\eta^2}{\gamma}} \quad \text{... Eq (3.36)}$$

In Eq 3.36, inverse function has been used to compute the adoptive potential. APF refers to the ability of the system to tolerate a repetitive movement. Inclusion of APF does not essentially lead to an optimal solution. However, it conveys the changing nature of an image.

$$g_{3\gamma}(\eta) = \gamma \ln(1+\frac{\eta^2}{\gamma}) \quad \text{... Eq (3.37)}$$

In Eq 3.37, a small multiplicative constant has been affixed in logarithmic function to compute the adoptive potential. Increase of an interaction range parameter causes slow convergence. However, convergence is no longer guaranteed.

$$g_{4\gamma}(\eta) = \gamma|\eta| - \gamma^2 \ln(1+\frac{|\eta|}{\gamma}) \quad \text{... Eq (3.38)}$$

In Eq 3.38, APF increases monotonically as η increases. This allows bounded but, non-zero smoothing. The standard regularizer as given in Eq. 3.31 and all the four DA models as mentioned in Eq.3.35 - 3.38 have been used separately and their output have been compared as fraction images. The qualitative shapes of these models are shows in Fig 3.3. These figures help in visualizing regarding the manner by which DA models perform smoothing. The quadratic regularizer imposes smoothness constraint everywhere. It determines the constant interaction between neighboring points. The homogeneous or isotropic application of smoothness constraint inevitably leads to over smoothing at discontinuities at which the derivative is infinite. Furthermore, function g_γ increases monotonically as |η| increases.

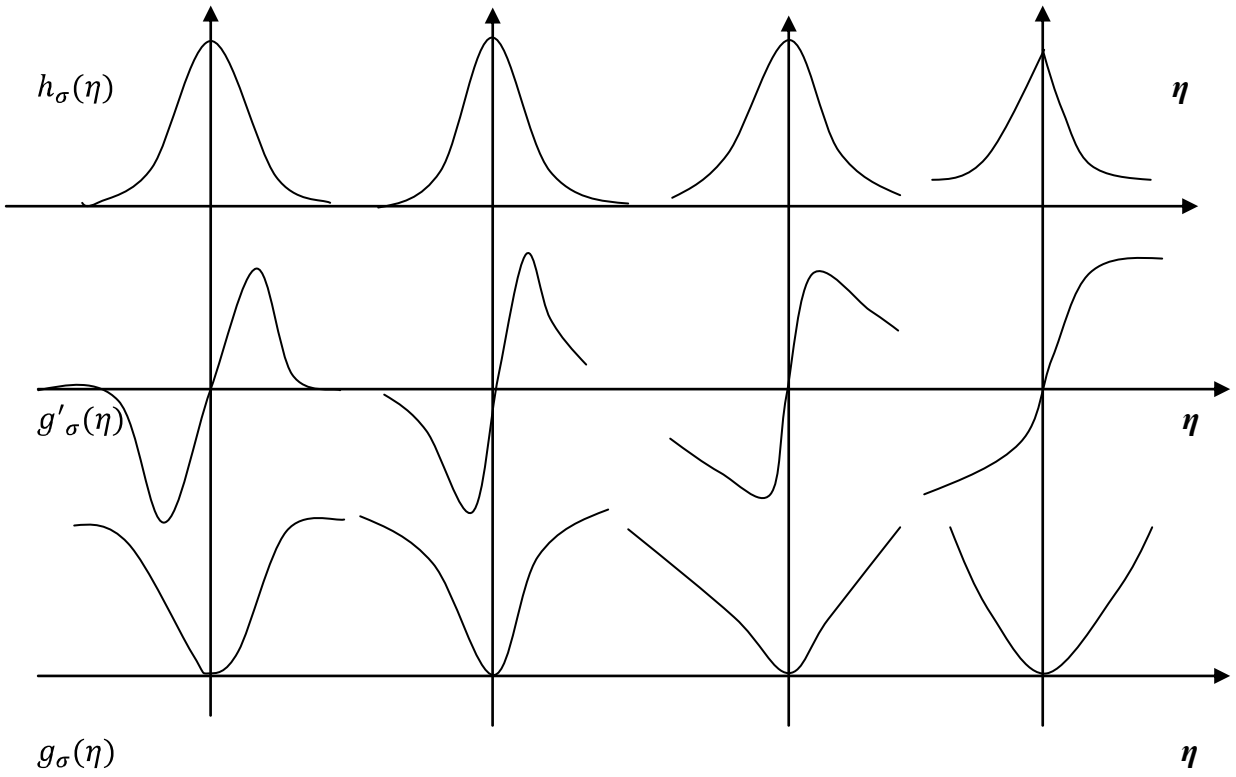

Figure 3.3: Qualitative shape of four DA functions (Li, 1995)

3.4.8 MAXIMUM A POSTERIOR SOLUTION (MAP)

Maximum A Posterior solution can be obtained by minimizing the global posterior energy. The combination of prior energy and conditional energy is the posterior energy solution. According to the Bayesian formula, MAP solution can be obtained as given in Eq 3.39 (Geman and Geman, 1984).

$$P(\mu|d) = \frac{P(d|\mu)P(\mu)}{P(d)} \quad \text{... Eq (3.39)}$$

where,

μ is membership value and,

d is the given dataset.

Minimization of posterior probability can be done as shown by Eq 3.40.

$$\mu = \arg\max\{p(\mu|d)\} \quad \text{... Eq (3.40)}$$

From Eq 3.29, MAP estimate is equivalent to the minimization of global energy function and can be expressed by Eq 3.41.

$$\hat{\mu} = \arg\min\{U(\mu|d) + U(\mu)\} \quad \text{... Eq (3.41)}$$

where,

$\hat{\mu}$ is optimal membership value of a class after minimizing the global energy function,

$U(\mu|d)$ is conditional energy and,

$U(\mu)$ is prior energy function.

The global posterior energy function can be defined by Eq 3.42.

$$U(\mu|d) = U(d|\mu) + U(\mu) \quad \text{... Eq (3.42)}$$

To control the balance between these two energy functions, one additional parameter λ termed as smoothness strength is added. The value of λ varies between 0 and 1. So the function can be re-written as:

$$U(\mu|d) = (1-\lambda)U(d|\mu) + \lambda U(\mu) \quad \text{... Eq (3.43)}$$

Minimization of global posterior energy function is required to obtain the MRF-MAP estimate. Simulated Annealing (SA) algorithm has been used to find out the global minimal energy and it has been proven that SA performs better than the existing method (Tso and Mather, 2009).

In this study, a contextual based FCM, PCM and NC classifiers along with a mixture of entropy has been implemented using Markov Random Field (MRF) models to incorporate contextual information. Smoothness prior and four Discontinuity Adaptive (DA) prior have been used to incorporate contextual information with all entropy and non entropy based contextual classifiers.

3.4.9 SIMULATED ANNEALING AND GIBBS SAMPLING ALGORITHM

In Simulated Annealing, the minimal solution is usually defined as a global one or one of them when there are multiple global minima. Identification of a global minimum is non-trivial, if the energy function contains many local minima. There are two methods to deal with local minimum problem: random search and annealing. In random search, a lower energy configuration is generated with a larger probability. However, annealing is incorporated into a local search method to overcome the problem of local minima. It is of two types, deterministic and stochastic. In MRF, Simulated Annealing as proposed by Geman and Geman (1984) is useful to simulate the behavior of image classification and image segmentation.

Once the posterior energy and associated parameters have been determined, the next step is to determine a solution. Since, Simulated Annealing (SA) was first introduced by Metropolis *et.al*, (1953*)* to simulate particle behavior in a thermal equilibrium, SA is a stochastic relaxation algorithm to determine the global minimum solution. The idea of SA is similar to a process of metallurgy, where the metal is heated up to a certain limit to reconstruct it in a desired shape. Then, as the metal is cools down very slowly, it gets enough time to respond. The SA algorithm is frequently used in MRF based image analysis to obtain the global optimum solutions (Geman and Geman , 1984; Solberg *et.al*, 1996; Li, 2009). In this study, SA has been used to develop an optimum global energy function.

The SA algorithm designed by (Geman and Geman, 1984) is also known as the Gibbs Sampler. It generates a new membership values for each pixel. In order to do so, it depends upon a parameter *T,* called temperature. SA starts with a high value of *T* and then the value of *T* is decreased according to a specific criterion, called the cooling schedule. The process runs till the value of *T* reaches zero. As the name itself suggests, SA emulates the physical annealing process where the solid is first melted by heating it to a very high temperature and then, it is gradually allowed to cool to its desired frozen state which has the minimum energy configuration (Bertsimas and Tsitsiklis, 1993).

In the context of image classification, it implies first perturbing the labels of the pixels randomly which is similar to melting of the metal. Then, the image is passed through the cooling schedule mentioned in Eq 3.44, and by determining the global minima, the final classified image is obtained i.e. the "frozen state". In this study, the cooling schedule as proposed by Dubes and Jain (1988), has been used as mentioned in Eq 3.44.

$$T_{k+1} = \frac{\ln(1+k)}{\ln(2+k)} T_k \qquad \text{... Eq (3.44)}$$

where,

k=number of iterations.

T_k =Temperature of k^{th} iteration.

T_{k+1} =Temperature of $(k+1)^{th}$ iteration

The temperature cooling function mentioned in Eq 3.44 has been used here because it decreases the temperature *T* faster than other existing methods like Maximiser of the Posterior Marginals (MPM) and Iterated Conditional method (ICM) (Tso and Mather, 2009).

3.4.10 FUZZY *C*-MEAN (FCM) WITH CONTEXTUAL INFORMATION

The problem of mixed pixel arises because real world phenomena changes gradually from one class to another as well as due to compatibility of spatial resolution with class size. Therefore, at the boundaries of different classes uncertainty increases and fuzziness or vagueness occurs. To

overcome the problem of multiple classes at boundaries, FCM is one of the popular fuzzy based soft classification techniques which takes care of uncertainty in class definition.

However, standard FCM does not incorporate spatial contextual information of pixels into its classifying algorithm; it only considers the spectral information of pixels. To incorporate spatial contextual information, Markov Random Field (MRF) is being widely used (Geman and Geman, 1984; Li, 2009). MRF theory is able to model context dependent entities such as pixels or correlated features in a convenient and consistent way (Li, 2009). Spatial context implies the presence of correlation of class labels within neighboring pixels (Solberg and Jain, 1996). The actual geographical phenomenon lies in context to others. For example, vegetation pixel has a high probability to have vegetation pixels as its neighbors. So, the chances of isolated vegetation pixels exist rarely. Use of context eliminates the problem of isolated pixels (Tso and Mather, 2009). In this study, MRF has been used to develop the contextual based supervised FCM classifier. To model context, it is important to carefully select MRF models for accurate results. MRF models are also called as MRF priors and regularizes. The various MRF models are standard regularization model, weak string and membrane model, line process model and Discontinuity Adaptive (DA) MRF models.

In this study, standard regularization model Smoothness Prior (SA) and Discontinuity Adaptive (DA) models (edge preserving priors) have been implemented for smoothing effect as well as edge preserving effect in image.

To solve a problem using MAP-MRF, it is important first to formulate the objective function. Here, the objective function of FCM has been formulated for the smoothness prior and for Discontinuity Adaptive priors that are able to incorporate contextual information. The objective function is similar to the objective function of FCM except for the inclusion of neighborhood information.

The objective function in Eq 3.1 calculates the membership values for pixels based on spectral properties, but does not include spatial contextual information. In this study, objective functions have been formulated that incorporate spatial contextual information using either Smoothness prior or Discontinuity Adaptive priors.

Eq 3.45 states the FCM objective function formulated using Smoothness prior. Thus, the objective function in Eq 3.45 will be referred as FCM-S. In this hybrid approach, the contextual information is added in the basic objective function of FCM.

$$\left.\begin{aligned} U(u_{ki}/d) = \; & \underbrace{(1-\lambda)\left[\sum_{i=1}^{c}\sum_{k=1}^{n}(u_{ki})^{m} D(x_k, v_i)\right]}_{} \\ & \underbrace{+\lambda\left[\sum_{i=1}^{c}\sum_{k=1}^{n}\sum_{i' \in n_k}\beta(u_{ki}-u_{ki'})^2\right]}_{}, (m>1) \end{aligned}\right\} \quad \ldots Eq(3.45)$$

where,

$u_{ki} \in [0,1], 1 \le k \le n, 1 \le i \le c$

$U(u_{ki}/d)$ = Posterior energy of image u, in a given image d.

λ= Weight for spectral and contextual information (smoothness strength).

u_{ki} = Membership value of pixel k of class i.

n= Number of pixels.

m= weighing exponent

$D(x_k, v_i) = (x_k - v_i)^T A_i (x_k - v_i)$, Squared distance between pixel vector and mean vector

x_k = vector pixel value,

v_i = mean vector of class i

β= weight for neighbors.

n_k= Neighborhood window around pixel k.

In Eq 3.45, spectral information has been included by using an objective function of FCM and spatial contextual information using smoothness prior.

FCM objective functions incorporating Discontinuity Adaptive priors (DA prior) have been formulated as in Eq 3.35 - 3.38. All the four DA priors (H1, H2, H3 and H4) have been used to formulate the FCM objective function to incorporate spatial contextual information, while avoiding over smoothing at the edges. Let η, be defined as $(u_{ki} - u_{ki'})$ i.e. the difference between target pixels (pixel k) membership value and the membership of its neighboring pixels

membership value in a neighborhood system n_k . The objective function for FCM-DA-MRF model can be expressed as given by Eq 3.46-3.49:

$$U(u_{ki}/d) = \underbrace{(1-\lambda)\left[\sum_{i=1}^{c}\sum_{k=1}^{n}(u_{ki})^{m}D(x_k,v_i)\right]}_{} + \underbrace{\lambda\left[\sum_{i=1}^{c}\sum_{k=1}^{n}\sum_{i'\in n_k}(-\gamma e^{\frac{-\eta^2}{\gamma}})\right]}_{},\ (m>1) \quad \text{...Eq (3.46)}$$

$$U(u_{ki}/d) = \underbrace{(1-\lambda)\left[\sum_{i=1}^{c}\sum_{k=1}^{n}(u_{ki})^{m}D(x_k,v_i)\right]}_{} + \underbrace{\lambda\left[\sum_{i=1}^{c}\sum_{k=1}^{n}\sum_{i'\in n_k}(-\frac{\gamma}{1+\frac{\eta^2}{\gamma}})\right]}_{},\ (m>1) \quad \text{...Eq (3.47)}$$

$$U(u_{ki}/d) = \underbrace{(1-\lambda)\left[\sum_{i=1}^{c}\sum_{k=1}^{n}(u_{ki})^{m}D(x_k,v_i)\right]}_{} + \underbrace{\lambda\left[\sum_{i=1}^{c}\sum_{k=1}^{n}\sum_{i'\in n_k}(\gamma\ln(1+\frac{\eta^2}{\gamma}))\right]}_{},\ (m>1) \quad \text{...Eq (3.48)}$$

$$\left.\begin{aligned} U(u_{ki}/d) = \underbrace{(1-\lambda)\left[\sum_{i=1}^{c}\sum_{k=1}^{n}(u_{ki})^{m}D(x_k,v_i)\right]}_{} \\ \underbrace{+\lambda\left[\sum_{i=1}^{c}\sum_{k=1}^{n}\sum_{i'\in n_k}(\gamma|\eta|-\gamma^2\ln(1+\frac{|\eta|}{\gamma}))\right]}_{},\ (m>1) \end{aligned}\right\} \ldots \text{Eq}\,(3.49)$$

where,

$u_{ki} \in [0,1],\ 1 \le k \le n, 1 \le i \le c$

$U(u_{ki}/d)$ = Posterior energy of image u , in a given image d.

λ= Weight for spectral and contextual information (smoothness strength).

u_{ki} = Membership value of pixel k of class i.

n= Number of pixels.

m= weighing exponent

$D(x_k, v_i)$ = Squared distance between pixel and mean vector.

x_k = vector pixel value,

v_i = mean vector of class i

γ =Adoptive Potential Function or interaction range parameter $\in [0,1]$.

n_k= Neighborhood window around pixel k.

In Eq 3.46-3.49, the second term represents various types of DA models created using Adaptive Interaction Function (AIF) and Adaptive Potential Function (APF). In DA model, addition of γ that is APF as explained in section 3.4.7, with a value varying between 0 and 1. Adaptive Potential Functions (APF) has been used in Eq 3.46 to 3.49 to formulate the objective function of FCM with Discontinuity Adaptive Priors. The objective functions mentioned in Eq 3.46 - 3.49, would be referred as FDM- (H1), FDM-(H2), FDM-(H3) and FDM-(H4) respectively.

The objective functions mentioned in Eq 3.45 - 3.49 involves various parameters**.** It is necessary to estimate these parameters before the objective functions can use for classification

(Li, 2009). The parameters to be optimized are Fuzzifier (m), Initial (T_0) and final temperature(T_f), Lambda(λ), Beta (β),Gamma(γ).

There are no standard methods to estimate these parameters. Several method such as RMSE, total energy etc. have been used in the past to estimate these parameters (Kitaw, 2007; Dutta, 2009). In this study, estimation of parameter has been carried out using the overall accuracy from FERM, SCM and entropy method (Dehghan and Ghassemian, 2006). The entropy method gives an absolute measure of uncertainty and at the same time, checks for preservation of edge by using mean and variance method to estimate the parameters.

3.4.11 POSSIBILISTIC *c*- MEAN (PCM) WITH CONTEXTUAL INFORMATION

The objective function of PCM differs from FCM in terms of representation of neighborhood information. The objective function of PCM (section 3.5), has been minimized with respect to membership function u_{ik} and the mean of the cluster v_{ik} used in computing the square of distance $D(x_k,v_i)$ as given by Eq 3.5. This includes information about the distance of the feature vector (that forms the pixel) from its cluster mean in the feature space. However, it does not incorporate the information on spatial context. The spatial context here includes the influence of the neighboring pixel on the target pixel in the image space.

As discussed in section 3.4.8, the MAP-MRF framework works by maximizing the posterior probability which is related to prior and conditional energy specified by Eq 3.39 -3.43. Eq 3.50 shows the PCM objective function formulated using smoothness prior. From now onwards the objective function in Eq 3.50 will be referred as PCM-S.

$$U(u_{ki}/d) = \left.\begin{aligned} &\underbrace{(1-\lambda)\left[\sum_{i=1}^{c}\sum_{k=1}^{n}(u_{ki})^{m}D(x_k, v_i) + \sum_{i=1}^{c}\eta_i\sum_{k=1}^{n}(1-u_{ki})^{m}\right]}_{} \\ &\underbrace{+\lambda\left[\sum_{i=1}^{c}\sum_{k=1}^{n}\sum_{i'\in n_k}\beta(u_{ki}-u_{ki}')^2\right]}_{}, (m>1) \end{aligned}\right\} \quad \text{...Eq (3.50)}$$

where,

$$\sum_{k=1}^{n} u_{ki} > 0, \quad 1 \le k \le n, 1 \le i \le c$$

$U(u_{ki}/d)$ = Posterior energy of image u in a given image d.

λ= Weight for spectral and contextual information (smoothness strength).

u_{ki} = Membership value of pixel k of class i.

n= Number of pixels.

m= weighing exponent.

$D(x_k, v_i)$ = Squared distance between pixel and mean vector.

x_k = vector pixel value,

v_i = mean vector of class i

β= weight for neighbors (weight given to the neighboring pixels in the window).

n_k= Neighborhood window around pixel k.

η_i = bandwidth or scale parameter

In Eq 3.50, the spectral information has been incorporated by using the objective function of PCM and spatial contextual information has been incorporated using Smoothness prior. PCM objective functions formulated with Discontinuity Adaptive Priors (DA prior) are given by Eq 3.35 - 3.38 as discussed in section 3.4.7, where all the four DA priors (H1, H2, H3 and H4) have been used to formulate the PCM objective function to incorporate spatial contextual information to avoid over smoothing at the edges.

Let η, be defined as $u_{ki} - u_{ki'}$ i.e. the difference between target pixels (pixel *k*) membership value and the membership of its neighboring pixels membership value in a neighborhood system n_k . The objective function for PCM-DA-MRF model is given below:

$$\left.\begin{aligned} U(u_{ki}/d) = & \underbrace{(1-\lambda)\left[\sum_{i=1}^{c}\sum_{k=1}^{n}(u_{ki})^{m}D(x_k, v_i) + \sum_{i=1}^{c}\eta_i\sum_{k=1}^{n}(1-u_{ki})^{m}\right]}_{} \\ & + \underbrace{\lambda\left[\sum_{i=1}^{c}\sum_{k=1}^{n}\sum_{i'\in n_k}(-\gamma e^{\frac{-\eta^2}{\gamma}})\right]}_{}, (m>1) \end{aligned}\right\} \quad ...Eq(3.51)$$

$$\left.\begin{aligned} U(u_{ki}/d) = & \underbrace{\left[\sum_{i=1}^{c}\sum_{k=1}^{n}(u_{ki})^{m}D(x_k, v_i) + \sum_{i=1}^{c}\eta_i\sum_{k=1}^{n}(1-u_{ki})^{m}\right]}_{} \\ & + \underbrace{\lambda\left[\sum_{i=1}^{c}\sum_{k=1}^{n}\sum_{i'\in n_k}(-\frac{\gamma}{1+\frac{\eta^2}{\gamma}})\right]}_{}, (m>1) \end{aligned}\right\} \quad ...Eq(3.52)$$

$$\left.\begin{aligned} U(u_{ki}/d) = & \underbrace{(1-\lambda)\left[\sum_{i=1}^{c}\sum_{k=1}^{n}(u_{ki})^{m}D(x_k, v_i) + \sum_{i=1}^{c}\eta_i\sum_{k=1}^{n}(1-u_{ki})^{m}\right]}_{} \\ & + \underbrace{\lambda\left[\sum_{i=1}^{c}\sum_{k=1}^{n}\sum_{i'\in n_k}(\gamma\ln(1+\frac{\eta^2}{\gamma}))\right]}_{}, (m>1) \end{aligned}\right\} \quad ...Eq(3.53)$$

$$\left.\begin{aligned} U(u_{ki}/d) = & \underbrace{(1-\lambda)\left[\sum_{i=1}^{c}\sum_{k=1}^{n}(u_{ki})^{m}D(x_k, v_i) + \sum_{i=1}^{c}\eta_i\sum_{k=1}^{n}(1-u_{ki})^{m}\right]}_{} \\ & + \underbrace{\lambda\left[\sum_{i=1}^{c}\sum_{k=1}^{n}\sum_{i'\in n_k}(\gamma|\eta| - \gamma^2\ln(1+\frac{|\eta|}{\gamma}))\right]}_{}, (m>1) \end{aligned}\right\} \quad ... Eq(3.54)$$

where,

$$\sum_{k=1}^{n} u_{ki} > 0, \quad 1 \le k \le n, 1 \le i \le c$$

$U(u_{ki}/d)$ = Posterior energy of image u , in a given image d.

λ= Weight for spectral and contextual information (smoothness strength).

u_{ki} = Membership value of pixel k of class i.

n= Number of pixels.

m= weighing exponent

$D(x_k, v_i)$ = Squared distance between pixel and mean vector.

x_k = vector pixel value,

v_i = mean vector of class i

γ =Adaptive Potential Function or interaction range parameter $\in [0,1]$.

n_k= Neighborhood window around pixel k.

In this study, the objective functions mentioned in Eq 3.51 - 3.54 would be referred as PDM- (H1), PDM- (H2), PDM- (H3) and PDM- (H4) respectively.

3.4.12 NOISE CLUSTERING WITH CONTEXTUAL INFORMATION

The idea of using this hybrid approach of soft classification i.e. noise clustering with contextual is a new approach, which helps significantly to eliminate noise pixels while incorporating spatial contextual information and improves the classification accuracy. A conventional NC algorithm does not fully utilize the contextual information in the image. In this study, NC algorithm incorporates spatial information into the membership function for clustering. The spatial function is the summation of membership function in the neighborhood of each pixel under consideration. The advantage of this new method is to yield regions more homogeneous than those of other methods and it reduces spurious information. The basic advantage of this classification approach is that it removes noisy spots. This technique is a powerful method for noisy image segmentation and works for both single and multiple-feature data with spatial information. The spatial context here includes the influence of the neighboring pixel on the target pixel in the image space (Miyamoto *et al.*, 2005).

As discussed in section 3.4.8, the MAP-MRF framework works by maximizing the posterior probability which is related to prior and conditional energy specified in Eqs 3.39 -3.43. Eq 3.55 shows the NC objective function formulated using smoothness prior. From now onwards the objective function in Eq 3.55 will be referred as NC-S.

$$U(u_{ki}/d) = (1-\lambda)\left[\sum_{i=1}^{c}\sum_{k=1}^{n} u_{ki}^{m} D(x_k, v_i) + \sum_{k=1}^{n} u_{k,c+1}^{m}\,\delta\right] + \lambda\left[\sum_{i=1}^{c}\sum_{k=1}^{n}\sum_{i' \in n_k} \beta(u_{ki} - u_{ki}')^2\right], (m>1) \quad \ldots \text{Eq (3.55)}$$

where,

$u_{ki} \in [0,1], 1 \le k \le n,\ 1 \le i \le c+1$

δ = Resolution parameter which is greater than 0.

$U(u_{ki}/d)$ = Posterior energy of image u , in a given image d.

λ= Weight for spectral and contextual information (smoothness strength).

u_{ki} = Membership value of pixel k of class i.

n= Number of pixels.

m= Weighing exponent

$D(x_k, v_i)$ = Squared distance between pixel and mean vector.

x_k = vector pixel value,

v_i = mean vector of class i

β= weight for neighbors (weight given to the neighboring pixels in the window).

n_k= Neighborhood window around pixel k.

η_i = bandwidth or scale parameter

In Eq 3.55, spectral information has been incorporated by using the objective function of NC and spatial contextual information is incorporated using smoothness prior.

NC objective functions formulated using Discontinuity Adaptive Priors (DA prior) all the four DA priors (H1, H2, H3 and H4) have been used to formulate the NC objective function to incorporate spatial contextual information to avoid over smoothing at the edges and reduces

noise. Let η, be defined as $u_{ki} - u_{ki'}$ i.e. the difference between target pixels (pixel k) membership value and the membership of its neighboring pixels membership value in a neighborhood system n_k . The objective function for NC-DA-MRF model is given by Eqs 3.56-3.59.

$$\left.\begin{aligned} U(u_{ki}/d) = (1-\lambda)\left[\sum_{i=1}^{c}\sum_{k=1}^{n} u_{ki}^{m} D(x_k, v_i) + \sum_{k=1}^{n} u_{k,c+1}^{m}\,\delta\right] \\ +\lambda\left[\sum_{i=1}^{c}\sum_{k=1}\sum_{i'\in n_k} (-\gamma e^{\frac{-\eta^2}{\gamma}})\right], (m>1) \end{aligned}\right\} \quad ...Eq\,(3.56)$$

$$\left.\begin{aligned} U(u_{ki}/d) = (1-\lambda)\left[\sum_{i=1}^{c}\sum_{k=1}^{n} u_{ki}^{m} D(x_k, v_i) + \sum_{k=1}^{n} u_{k,c+1}^{m}\,\delta\right] \\ +\lambda\left[\sum_{i=1}^{c}\sum_{k=1}\sum_{i'\in n_k} (-\frac{\gamma}{1+\frac{\eta^2}{\gamma}})\right], (m>1) \end{aligned}\right\} \quad ...Eq\,(3.57)$$

$$\left.\begin{aligned} U(u_{ki}/d) = (1-\lambda)\left[\sum_{i=1}^{c}\sum_{k=1}^{n} \left(u_{ki}\right)^{m} D(x_k, v_i) + \sum_{k=1}^{n} \left(u_{k,c+1}\right)^{m}\delta\right] \\ +\lambda\left[\sum_{i=1}^{c}\sum_{k=1}\sum_{i'\in n_k} (\gamma \ln(1+\frac{\eta^2}{\gamma}))\right], (m>1) \end{aligned}\right\} ...Eq\,(3.58)$$

$$\left.\begin{aligned} U(u_{ki}/d) = (1-\lambda)\left[\sum_{i=1}^{c}\sum_{k=1}^{n} \left(u_{ki}\right)^{m} D(x_k, v_i) + \sum_{k=1}^{n} \left(u_{k,c+1}\right)^{m}\delta\right] \\ +\lambda\left[\sum_{i=1}^{c}\sum_{k=1}\sum_{i'\in n_k} (\gamma|\eta| - \gamma^2 \ln(1+\frac{|\eta|}{\gamma}))\right], (m>1) \end{aligned}\right\} ..Eq\,(3.59)$$

where,

$u_{ki} \in [0,1], 1 \le k \le n,\ 1 \le i \le c+1$

$U(u_{ki}/d)$ = Posterior energy of image u , in a given image d.

δ = Resolution parameter which is greater than 0.

λ= Weight for spectral and contextual information (smoothness strength).

u_{ki} = Membership value of pixel k of class i.

n= Number of pixels.

m= weighing exponent

$D(x_k, v_i)$ = Squared distance between pixel and mean vector.

x_k = vector pixel value,

v_i = mean vector of class i.

γ =Adaptive Potential Function or interaction range parameter $\in [0,1]$.

n_k= Neighborhood window around pixel k.

The objective functions mentioned in Eq 3.56 - 3.59 will be referred as NDM-(H1), NDM-(H2), NDM-(H3) and NDM- (H4) respectively.

3.4.13 NOISE CLUSTERING WITH ENTROPY (NCWE) WITH CONTEXTUAL INFORMATION

This algorithm exploits the spatial contextual information in image data using NCWE as a base classification. The objective function of this method utilizes a new dissimilarity index that takes into account the influence of the neighboring pixels at the centre pixel in a 3×3 window. The algorithm is adaptive to the image content in the sense that any influence from neighboring pixels is suppressed in non homogeneous regions in the image. A cluster merging scheme that merges two clusters based on their closeness and their degree of overlap is presented. Through this merging scheme, an `optimal' number of clusters can be determined automatically as iteration proceeds. Experimental results indicate that the proposed algorithm is more tolerant to noise, efficient in resolving any classification ambiguity and can cope with any cluster shape and size than conventional algorithms.

NCWE objective function using smoothness prior can be formulated as given by Eq 3.60. The objective function mentioned by Eq 3.60 will be referred as NCWE-S.

$$U(u_{ki}/d) = (1-\lambda)\left[\sum_{i=1}^{c}\sum_{k=1}^{n} u_{ki}\ D(x_k, v_i) + \sum_{k=1}^{n} u_{k,c+1}\ \delta + \nu \sum_{i=1}^{c+1}\sum_{k=1}^{n} u_{ki}\log u_{ki}\right] + \lambda\left[\sum_{i=1}^{c}\sum_{k=1}^{n}\sum_{i'\in n_k} \beta(u_{ki}-u_{ki'})^2\right] \quad \text{...Eq (3.60)}$$

where,

$u_{ki} \in [0,1], 1 \le k \le n,\ 1 \le i \le c+1$

δ = Resolution parameter which is greater than 0.

ν = Regularizing parameter has a value greater than 0.

$U(u_{ki}/d)$ = Posterior energy of image u , in a given image d.

λ= Weight for spectral and contextual information (smoothness strength).

u_{ki} = Membership value of pixel k of class i.

n= Number of pixels.

m= Weighing exponent.

$D(x_k, v_i)$ = Squared distance between pixel and mean vector.

x_k = vector pixel value.

v_i = mean vector of class i

β= weight for neighbors (weight given to the neighboring pixels in the window).

n_k= Neighborhood window around pixel k.

η_i = bandwidth or scale parameter.

NCWE objective functions formulated using Discontinuity Adaptive Priors (DA prior) all the four DA priors (H1, H2, H3 and H4) have been used to formulate the NCWE objective function to incorporate spatial contextual information to avoid over smoothing at the edges and reduces noise. The objective function for NCWE-DA-MRF model is given by Eq 3.61-3.64.

$$U(u_{ki}/d) = (1-\lambda)\left[\sum_{i=1}^{c}\sum_{k=1}^{n} u_{ki}\quad D(x_k, v_i) + \sum_{k=1}^{n} u_{k,c+1}\quad \delta + \nu \sum_{i=1}^{c+1}\sum_{k=1}^{n} u_{ki}\log u_{ki}\right] + \lambda\left[\sum_{i=1}^{c}\sum_{k=1}^{n}\sum_{i'\in n_k} (-\gamma e^{\frac{-\eta^2}{\gamma}})\right] \quad \text{...Eq (3.61)}$$

$$U(u_{ki}/d) = (1-\lambda)\left[\sum_{i=1}^{c}\sum_{k=1}^{n} u_{ki}\quad D(x_k, v_i) + \sum_{k=1}^{n} u_{k,c+1}\quad \delta + \nu \sum_{i=1}^{c+1}\sum_{k=1}^{n} u_{ki}\log u_{ki}\right] + \lambda\left[\sum_{i=1}^{c}\sum_{k=1}^{n}\sum_{i'\in n_k} (-\frac{\gamma}{1+\frac{\eta^2}{\gamma}})\right] \quad \text{..Eq (3.62)}$$

$$U(u_{ki}/d) = (1-\lambda)\left[\sum_{i=1}^{c}\sum_{k=1}^{n} (u_{ki})D(x_k, v_i) + \sum_{k=1}^{n} (u_{k,c+1})\delta + \nu \sum_{i=1}^{c+1}\sum_{k=1}^{n} u_{ki}\log u_{ki}\right] + \lambda\left[\sum_{i=1}^{c}\sum_{k=1}^{n}\sum_{i'\in n_k} (\gamma \ln(1+\frac{\eta^2}{\gamma}))\right] \quad \text{...Eq (3.63)}$$

$$U(u_{ki}/d) = (1-\lambda)\left[\sum_{i=1}^{c}\sum_{k=1}^{n} (u_{ki})D(x_k, v_i) + \sum_{k=1}^{n} (u_{k,c+1})\delta + \nu \sum_{i=1}^{c+1}\sum_{k=1}^{n} u_{ki}\log u_{ki}\right] + \lambda\left[\sum_{i=1}^{c}\sum_{k=1}^{n}\sum_{i'\in n_k} (\gamma|\eta| - \gamma^2 \ln(1+\frac{|\eta|}{\gamma}))\right] \quad \text{...Eq (3.64)}$$

where,

$u_{ki} \in [0,1], 1 \le k \le n,\ 1 \le i \le c+1$

δ = Resolution parameter which is greater than 0.

ν = Regularizing parameter has a value greater than 0.

$U(u_{ki}/d)$ = Posterior energy of image u , in a given image d.

λ= Weight for spectral and contextual information (smoothness strength).

u_{ki} = Membership value of pixel k of class i.

n= Number of pixels.

m= Weighing exponent.

$D(x_k, v_i)$ = Squared distance between pixel and mean vector.

x_k = vector pixel value,

v_i = mean vector of class i

γ =Adaptive Potential Function or interaction range parameter $\in [0,1]$.

n_k= Neighborhood window around pixel k.

η_i = bandwidth or scale parameter.

The objective functions mentioned in Eq 3.61 - 3.64 will be referred as NDEM- (H1), NDEM-(H2), NDEM- (H3) and NDEM- (H4) respectively.

3.4.14 FUZZY *C*-MEAN WITH ENTROPY (FCMWE) WITH CONTEXTUAL INFORMATION

Fuzzy c-means algorithm (FCM) is one of the most commonly used clustering methods in image classification. However, the conventional FCM algorithms have some limitation, such as, sensitivity to the noise. However, the same has been rectified by the inclusion of entropy, yet it does not take into consideration contextual information and its convergence to local minimum as it is based on a gradient descent method. In this study, a new approach is being proposed for, spatial fuzzy clustering considers tackle image noise by incorporating spatial contextual information into the membership function. This improves the global performance by taking advantages of global search capability of MRF. Experiments with remote sensing images shows that this FCMWE approach is robust to noise compared to other standard methods such as FCM, PCM and NC.

The incorporation of contextual information using Smoothness prior into the basic representation of FCMWE (Eq 3.23) can be expressed as given by Eq 3.65. The objective function in Eq 3.65 will be referred as FCMWE-S.

$$U(u_{ki}/d) = (1-\lambda)\left[\sum_{i=1}^{c}\sum_{k=1}^{n} u_{ki} D(x_k, v_i) + \nu \sum_{i=1}^{c}\sum_{k=1}^{n} u_{ki}\log u_{ki}\right] + \lambda\left[\sum_{i=1}^{c}\sum_{k=1}^{n}\sum_{i'\in n_k} \beta(u_{ki}-u_{ki'})^2\right],\ (\nu>0) \qquad \ldots \text{Eq}(3.65)$$

where,

$u_{ki} \in [0,1], 1 \le k \le n,\ 1 \le i \le c$

ν = Regularizing parameter having a value greater than 0.

$U(u_{ki}/d)$ = Posterior energy of image u , in a given image d.

λ= Weight for spectral and contextual information i.e. smoothness strength.

u_{ki} = Membership value of pixel k of class i.

n= Number of pixels.

m= Weighing exponent.

$D(x_k, v_i)$ = Squared distance between pixel and mean vector.

x_k = vector pixel value,

v_i = mean vector of class i

β= weight for neighbors (weight given to the neighboring pixels in the window).

n_k= Neighborhood window around pixel k.

η_i = bandwidth or scale parameter.

FCMWE objective functions formulated using Discontinuity Adaptive Priors (DA prior) i.e. all the four DA priors (H1, H2, H3 and H4) have been used to formulate the FCMWE objective function to incorporate spatial contextual information in order to avoid over smoothing at the edges and reduces noise. The objective function for FCMWE-DA-MRF model is given by Eq 3.66-3.69.

$$U(u_{ki}/d) = \left.\begin{aligned}(1-\lambda)\left[\sum_{i=1}^{c}\sum_{k=1}^{n} u_{ki} D(x_k, v_i) + \nu \sum_{i=1}^{c}\sum_{k=1}^{n} u_{ki}\log u_{ki}\right] \\ +\lambda\left[\sum_{i=1}^{c}\sum_{k=1}^{n}\sum_{i'\in n_k} (-\gamma e^{\frac{-\eta^2}{\gamma}})\right], (\nu > 0)\end{aligned}\right\} \text{...Eq (3.66)}$$

$$U(u_{ki}/d) = (1-\lambda)\left[\sum_{i=1}^{c}\sum_{k=1}^{n} u_{ki} D(x_k, v_i) + \nu \sum_{i=1}^{c}\sum_{k=1}^{n} u_{ki}\log u_{ki}\right] + \lambda\left[\sum_{i=1}^{c}\sum_{k=1}^{n}\sum_{i' \in n_k} \left(-\frac{\gamma}{1+\frac{\eta^2}{\gamma}}\right)\right], (\nu > 0) \quad \text{...Eq (3.67)}$$

$$U(u_{ki}/d) = (1-\lambda)\left[\sum_{i=1}^{c}\sum_{k=1}^{n} u_{ki} D(x_k, v_i) + \nu \sum_{i=1}^{c}\sum_{k=1}^{n} u_{ki}\log u_{ki}\right] + \lambda\left[\sum_{i=1}^{c}\sum_{k=1}^{n}\sum_{i' \in n_k} \left(\gamma \ln\left(1+\frac{\eta^2}{\gamma}\right)\right)\right], (\nu > 0) \quad \text{...Eq (3.68)}$$

$$U(u_{ki}/d) = (1-\lambda)\left[\sum_{i=1}^{c}\sum_{k=1}^{n} u_{ki} D(x_k, v_i) + \nu \sum_{i=1}^{c}\sum_{k=1}^{n} u_{ki}\log u_{ki}\right] + \lambda\left[\sum_{i=1}^{c}\sum_{k=1}^{n}\sum_{i' \in n_k} \left(\gamma|\eta| - \gamma^2 \ln\left(1+\frac{|\eta|}{\gamma}\right)\right)\right], (\nu > 0) \quad \text{...Eq (3.69)}$$

where,

$u_{ki} \in [0,1], 1 \le k \le n,\ 1 \le i \le c$

ν = Regularizing parameter has a value greater than 0.

$U(u_{ki}/d)$ = Posterior energy of image u , in a given image d.

λ= Weight for spectral and contextual information (smoothness strength).

u_{ki} = Membership value of pixel k of class i.

n= Number of pixels.

m= Weighing exponent.

$D(x_k, v_i)$ = Squared distance between pixel and mean vector.

x_k = vector pixel value,

v_i = mean vector of class i

γ =Adaptive Potential Function or interaction range parameter $\in [0,1]$.

n_k= Neighborhood window around pixel k.

η_i = bandwidth or scale parameter.

The objective functions mentioned in Eq 3.66 - 3.69 will be referred as FDEM-(H1), FDEM -(H2), FDEM- (H3) and FDEM -(H4) respectively.

3.5 PARAMETERS TO BE ESTIMATED

The objective functions mentioned in Eq 3.1 - 3.69 involves the estimation of the parameters mentioned below**.** It is necessary to estimate the parameters before the objective functions can used for classification (Li, 2009). In this study, the following parameters have been optimized.

(a) Fuzzifier (m)
(b) Resolution parameter (δ)
(c) Regularizing parameter (ν)
(d) Initial (T_0) and final temperature(T_f)
(e) Smoothness strength Lambda (λ)
(f) Weight for Beta (β)
(g) Interaction range parameter Gamma (γ)

There are no standard methods to estimate these parameters. Several method such as RMSE, total energy etc. have been used in the past to estimate these parameters (Dutta, 2009; Chawla, 2010). In this study, estimation of parameter has been carried out using overall accuracy and the entropy method (Dehghan and Ghassemian, 2006). The entropy method gives an absolute measure of uncertainty and at the same time edge preservation is also checked by mean and variance method to estimate the parameters.

Image classification has made tremendous progress in the area of development of advanced classification algorithms using spectral, spatial, and temporal information. However, Hybridized model using contextual information has still not been explored for satellite image classification. The list of classification algorithms along with their associated parameters are listed below:

Table 3.1 Classification methods and associated parameter.

S.No.	Classification Approach	Parameter to be optimized
1	Fuzzy *c*-Mean (FCM)	*m* (fuzzifier)
2	Possibilistic *c*-Mean (PCM)	
3	Noise Clustering (NC)	δ (resolution parameter)
4	NC with entropy	δ (resolution parameter) *v* (regularizing parameter)
5	FCM with entropy	*m* (fuzzifier) *v* (regularizing parameter)
6	FCM with contextual	λ (Smoothness strength) β (weight for neighbors) and γ (interaction range parameter)
7	PCM with contextual	
8	NC with contextual	
9	FCM with entropy with contextual	*v* (regularizing parameter), λ (Smoothness strength) β (weight for neighbors) and γ (interaction range parameter)
10	NC with entropy with contextual	δ (resolution parameter) λ (Smoothness strength) λ (Smoothness strength) β (weight for neighbors) and γ (interaction range parameter)

3.6 ASSESSMENT OF ACCURACY FOR SOFT CLASSIFICATION

The implication of land-cover as an ecological variable has made remote sensing one of the most attractive tools for the production of thematic maps of the earth's surface. However, in order for remote sensing to succeed as a valuable source of land-cover information, reliable accuracy measures are needed (Foody, 2002). In the past few decades, the prevailing concerns on ecological and environmental issues, occurring especially at regional to global scales, have prompted significant advances on the use of remote sensing data for the estimation of land cover information at sub-pixel level (Fisher and Pathirana, 1990; Cross et al., 1991; Roberts et al.,

1993; Gutman and Ignatov, 1998; Carpenter et al., 1999). However, the quality of such classification products, as well as the performance of the classification protocol employed, are difficult to quantify. None of the classification is complete until and unless assessment of accuracy has not been performed (Tortora, 1978, Jensen, 1986; Congalton and Green, 1999).

In hard classification, each pixel is classified to one and only one class. A typical strategy for assessing the accuracy of hard classification is to follow a statistically sound sampling design to select a sample of testing pixels, and to determine whether the class assigned to that pixel matches the actual class represented by pixel on the reference data or not. The sample data is often summarized in an error matrix, which is used to derive various accuracy measures (Congalton, 1991; Congalton and Green, 1999).

In soft classification, where pixels with a mixture of more than one type of land cover, are often dominant in remotely sensed data (Liu and Wu, 2005, Xu et al., 2010). However, the conventional error matrix method falls short in assessing the accuracy of soft classification, because each pixel has partial simultaneous membership in several classes (Pontius and Cheuk, 2006).

Specifically, this study aims to provide answers to the following research questions:

i) How classification performance can be improved using recent developments on fuzzy, entropy and contextual based classifiers?

ii) How can the accuracy of these representations be assessed in a way that is consistent with the standardized confusion matrix of soft classifications?

iii) How can these representations be useful to measure the classification results, and contribute to optimization parameters for various soft classifiers?

The assessment of the conventional (hard) allocation of image pixels to discrete classes has been standardized (to some extent) through the confusion matrix and some derived measures (Congalton, 1991; Stehman and Czaplewski, 1998; Congalton and Green, 1999). However, this method is appropriate only for hard classifications, where it is assumed that each pixel is associated with only one class in both the classified and the reference datasets. In soft classifications, where multiple classes are assigned to a single pixel, a comparable standardized

assessment procedure has not been established yet. Thus, there is an increasing need for sub-pixel assessment of classification products as made evident by recent remote sensing research (Latifovic and Olthof, 2004; Shabanov et al., 2005; Okeke and Karnieli, 2006; Ozdogan and Woodcock, 2006).

For the evaluation of soft classifications in general, various suggestions have been made (Gopal and Woodcock, 1994; Foody, 1995; Binaghi et al., 1999; Congalton and Green, 1999; Townsend, 2000; Lewis and Brown, 2002; Green and Congalton, 2004; Pontius Jr and Cheuk, 2006), amongst which, the Fuzzy Error Matrix (Binaghi et al., 1999) is one of the most commonly used approach, since it is based on fuzzy set theory and represents a generalization of the traditional confusion matrix. In spite of its sound theoretical basis, fuzzy error matrix is not generally adopted as a standard accuracy report for soft classifications. Some of reasons for this have been highlighted as counter-intuitive characteristics (Pontius Jr and Cheuk, 2006). Specifically, for a cross-comparison to be consistent with the traditional confusion matrix, it is desirable that the cross-comparison results in a diagonal matrix when a map is compared to itself, and that its marginal totals match the total of membership grades. More importantly, a cross-comparison should convey readily interpretable information on the confusion among the classes. A composite operator for computing a cross-comparison matrix that exhibits some of the aforementioned desirable characteristics has been proposed as a tool for sub-pixel comparison of maps (Pontius Jr and Cheuk, 2006; Pontius Jr and Connors, 2006). Nevertheless, the applicability of composite operators has not been demonstrated beyond the use of traditional accuracy indices, and neither the use of off-diagonal cells and its interpretation been demonstrated clearly.

To carry out the assessment of an accuracy for soft classified output, a modified error matrix i.e. FERM (Fuzzy Error Matrix) has been proposed by the Binaghi *et al*.(1999) and SCM (Sub-pixel confusion-uncertainty matrix) has been proposed by Silvan and Wang (2008). The Fuzzy Error Matrix is used to derive the accuracy of soft classifier when the outputs are in form of fraction images. FERM is used similar to traditional error matrix but the main difference is that FERM uses fractional images to measure accuracy and the values in FERM are real number (integers in conventional error matrix). The overlap between classified and reference datasets is calculated by using single operators like MIN, LEAST and PROD or composite operators like

MIN-MIN and MIN-LEAST and MIN-PROD (Silván and L. Wang, 2008; Pontius and Cheuk, 2006).

Dehghan and Ghassemian (2006) proposed entropy as a measure to assess the accuracy of the classified output by measuring uncertainty in the results. The entropy gives the absolute measure of uncertainty. This is called absolute since it does not take any reference data to measure the uncertainty. Entropy is an indirect method of assessment of accuracy. Entropy method is used for accuracy measure when there are no references data available for accuracy measurement. Higher entropy implies higher uncertainty and vice-versa in class identification on classified output. The advantage of entropy measure for assessment of accuracy was also proven by Kumar and Dadhwal (2010).

In light of the above study, the objectives of this study, is to assess the classification accuracy using sub-pixel confusion uncertainty matrices, mean and variance method to verify edge preservation for contextual based classification and entropy to identify the uncertainty of class distribution (Wen and Xia, 1999).

3.6.1 GENERATION OF TESTING DATA

Assessment of accuracy is based on the comparison of two datasets: classified image and reference data. Classified image is the product of classified algorithm whereas reference data may be derived from various sources such as existing maps, field survey and any dataset at higher spatial resolution than image to be classified or the combination of these sources. In this study, image to image assessment of accuracy method has been adopted. Thus, to assess the accuracy of soft classification, soft reference data may have to be generated. The simplest way to generate soft reference data is to use fine resolution image of the same area for which coarse resolution image needs to be classified. Each pixel of fine resolution image is allocated to a single class through the assistance of reference data. Therefore, each pixel in this image is assumed to be pure denoting one and only one class. A pixel of coarse resolution image will contain certain number of pure pixels of fine resolution image. After registering the two images and determining the number of pure pixels belonging to each class, class proportions within a

coarse resolution pixel may be assigned. These actual class proportions are named as soft reference data.

3.6.2 METHODS ADOPTED FOR ASSESSMENT OF ACCURACY

Assessment of accuracy of classified output is necessary to obtain the quality of the results. In this work, where an image to image based accuracy assessment technique has been used, the accuracy of classification of a coarser resolution images has been evaluated with the classified output of a finer resolution image. In this section, accuracy assessment techniques for the sub-pixel classified outputs used in this study have been described. The basic approach of assessment of accuracy can be illustrated as shown in Fig. 3.4.

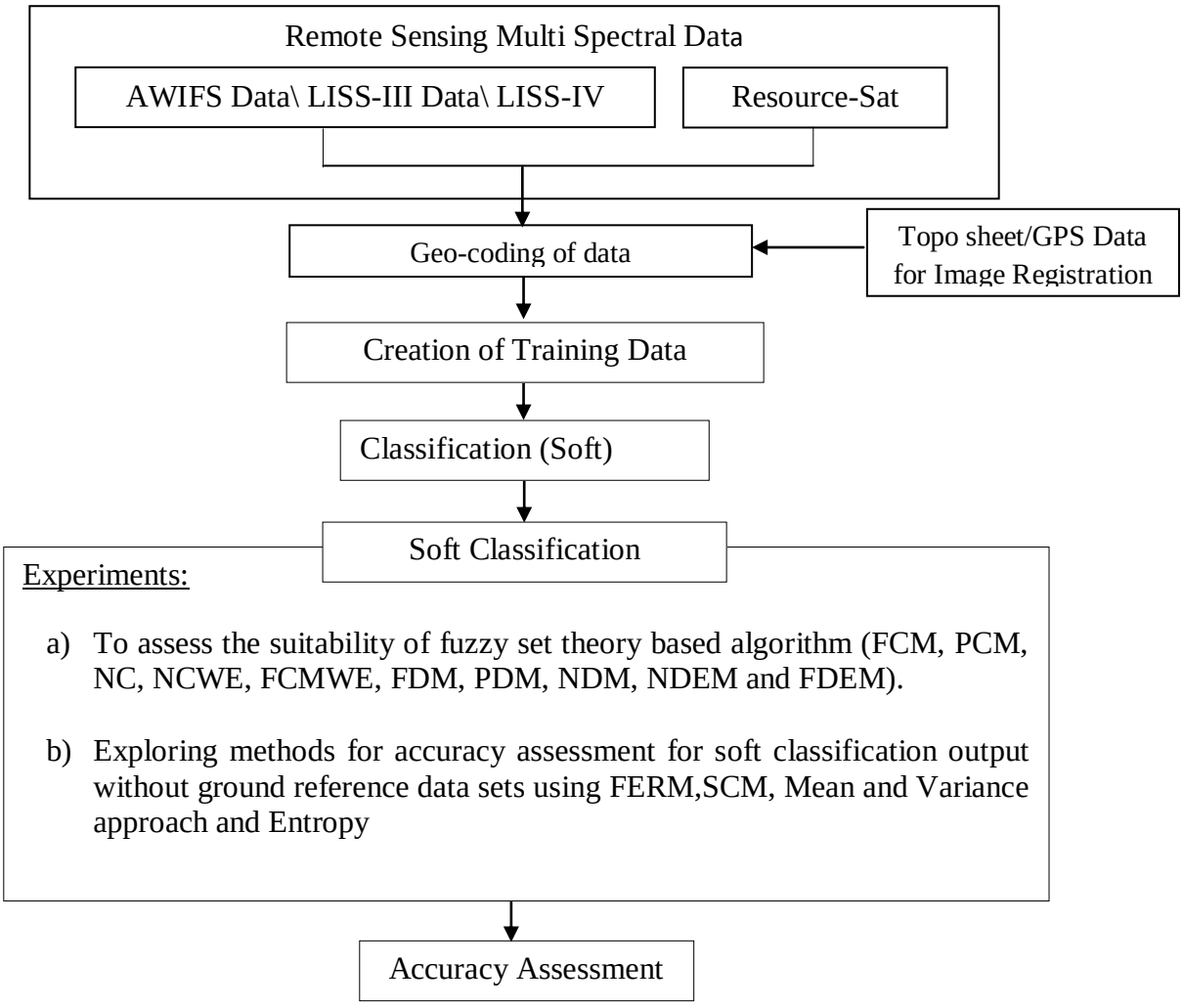

Fig. 3.4 General structure of assessment of accuracy

3.6.2.1 FUZZY ERROR MATRIX

The concept of Fuzzy Error Matrix (FERM) has been put forth to assess the accuracy of soft classification of satellite data (Binaghi et al., 1999). The layout of FERM is similar to the traditional error matrix used for assessing the accuracy of hard classification. For soft classification, where multiple classes are assigned to a single pixel, a comparable standardized procedure is required. In case of soft classification, the elements of fuzzy error matrix can be any non-negative real numbers instead of non-negative integer numbers. The elements of fuzzy error matrix represent class proportions corresponding to reference data (i.e. soft reference data) and classified output (i.e. soft classified image) respectively.

Let R_n and C_m be the sets of reference and classification data assigned to class *n* and *m*, respectively, where the value of *n* and *m* are bounded by one and the number of classes *c*. It may be noted that R_n and C_m are fuzzy sets and $\{R_n\}$ and $\{C_m\}$ are from two fuzzy partitions of the testing sample data set X, where *x* denotes a testing sample in X. The member ship functions of R_n and C_m is given by Eq 3.70.

$$\mu_{R_n} : X \rightarrow [0,1] \text{ and } \mu_{C_n} : X \rightarrow [0,1] \qquad \text{...Eq (3.70)}$$

where [0,1] denotes the interval of real numbers from 0 to 1 inclusive.

Here $\mu_{Rn}(x)$ and $\mu_{Cm}(x)$ is the class membership (or class proportion) of the testing sample *x* in R_n and C_m respectively. Since, in the context of fuzzy classification, these membership functions also represent the proportion of a class in the testing sample, the orthogonality or sum-normalization is often required, which for the fuzzy reference data may be represented as in Eq 3.71

$$\sum_{i=1}^{c} \mu_{R_i}(x) = 1 \qquad \text{...Eq (3.71)}$$

The procedure used to construct the fuzzy error matrix *M* employs fuzzy MIN operator to determine the elements *M(m,n)* in which the degree of membership in the fuzzy intersection $C_m \cap R_n$ is computed as given in Eq 3.72

$$M(\mathrm{m},\mathrm{n}) = \left| C_m \cap R_n \right| = \sum_{x \in X} \min(\mu_{C_\mathrm{m}}, \mu_{R_\mathrm{m}}) \qquad \text{...Eq (3.72)}$$

The layout of a typical FERM is shown in Table 3.2

Table 3.2 Structure of fuzzy error matrix

Soft Classification	Soft Reference data				Total grades
	Class 1	Class 2	…….	Class *c*	
Class 1	$M_{(1,1)}$	$M_{(1,2)}$	……	$M_{(1,c)}$	C_1
Class 2	$M_{(2,1)}$	$M_{(2,2)}$	……	$M_{(2,c)}$	C_2
……	.	.	.	.	.
	.	.	.	.	
Class *c*	$M_{(c,1)}$	$M_{(c,1)}$	……	$M_{(c,1)}$	C_c
Total Grades	R_1	R_2	…….	R_c	
Definition of terms: *M(m,n)* is the member of FERM in the m^{th} class in the soft classified output and nth class of the soft reference data, C_m is the sum of class proportions of class *m* in the classified output and R_n is the sum of class proportions of class *n* from the reference data.					

From FERM, Overall Accuracy (*OA*) may be computed using Eq 3.73.

$$OA = \frac{\sum_{j=1}^{c} M(\mathrm{i},\mathrm{j})}{\sum_{j=1}^{c} R_j} \qquad \text{...Eq (3.73)}$$

Similarly, User and Producer Accuracy of any class *j*, UA_j and PA_j respectively, may be computed, as given in Eq 3.74

$$UA_j = \frac{M_{(\mathrm{j},\mathrm{j})}}{C_j} \quad \text{and} \quad PA_j = \frac{M_{(\mathrm{j},\mathrm{j})}}{R_j} \qquad \text{...Eq (3.74)}$$

The Average user (AA_u) and Average producer (AA_p) accuracy may then be computed from Eq 3.75

$$AA_u = \frac{\sum_{j=1}^{c} UA_j}{c} \quad \text{and} \quad AA_p = \frac{\sum_{j=1}^{c} PA_j}{c} \qquad \text{...Eq (3.75)}$$

Thus, FERM can be used to derive a number of accuracy measures similar to the one obtained from traditional error matrix for hard classification. Therefore, FERM based measures appear more appropriate for the assessment of accuracy of soft classification than using distance measures or correlation coefficients.

3.6.2.2 SUB-PIXEL CONFUSION-UNCERTAINTY MATRIX

The applicability of generating accuracy indices such as Overall Accuracy, User and Producer accuracy, Kappa and conditional Kappa gives different types of accuracy indication coefficients (Binaghi *et al*., 1999; Shabanov et al., 2005; Okeke and Karnieli, 2006). Indeed, derived indices do not account for the off-diagonal cells of the matrix; rather, they are based only on the diagonal cells and the total grades from the reference and assessed datasets (Binaghi *et al*., 1999).

Recently, a composite operator has been proposed for computing a cross comparison matrix that exhibits some of the aforementioned desirable characteristics showed applicability of a composite operator for assessment of a multi-resolution raster maps and compared it with other alternatives, including the traditional hardening pixels, the minimum operator and the product operator (Binaghi et al., 1999; Lewis and Brown, 2001; Pontius and Cheuk, 2006).

This composite operator was also suggested as a viable tool for soft comparison of maps (Pontius and Connors, 2006). Although several desirable properties are found in the composite operator, its utility has only been demonstrated on the use of traditional accuracy indices such as Overall accuracy, User accuracy, Producer accuracy and Kappa coefficient (Kuzera and Pontius, 2004; Pontius and Cheuk, 2006; Pontius and Connors, 2006).

Silván-Cárdenas and Wang (2008), has reviewed the assessment of accuracy for soft classification methods while identifying the major drawbacks and desirable properties based on cross-comparison matrices and provides the theoretical understanding for soft class distribution

uncertainty. Based on Sub-pixel confusion uncertainty matrix (SCM), many assessment indices such as Overall accuracy, User accuracy, Producer accuracy and Kappa coefficient can be calculated to provide a detailed assessment of accuracy for soft classification.

The following symbols are used to describe the sub-pixel confusion-uncertainty matrix:

N number of pixels in the reference and assessed datasets.

K number of classes,

n pixel index, where, $n = 1, ..., N$.

k, l class index, where, $k, l = 1, ..., K$.

s_{nk} grade of membership of pixel n to class k assigned by the assessed dataset,

r_{nl} grade of membership of pixel n to class l assigned by the reference dataset,

s_{+k} total grade of class k from the assessed dataset, $s_{+k} = \sum_n s_{nk}$

r_{+l} total grade of class l from the reference dataset, $r_{+k} = \sum_n r_{nl}$

s'_{nk} overestimation error of class k at pixel n, $s'_{nk} = \max(s_{nk} - r_{nl}, 0)$,

r'_{nl} underestimation error of class l at pixel n, $r'_{nl} = \max(r_{nl} - s_{nk})$,

p_{nkl} agreement-disagreement between membership grades from assessed class k and reference class l at pixel n; it is called agreement when $k = l$ and disagreement (or confusion) when $k \neq l$,

p_{kl} overall agreement-disagreement between assessed class k and reference class l, $p_{kl} = \sum_n p_{nkl}$

p_{k+} marginal row sum of p_{kl} for class k, $p_{k+} = \sum_l p_{kl}$

p_{+l} marginal column sum of p_{kl} for class l, $p_{+l} = \sum_k p_{kl}$

p_{++} total sum of p_{kl}, $p_{++} = \sum_k \sum_l p_{kl}$,

where

$$0 \le r_{nk} \le 1,\ 0 \le s_{nk} \le 1 \text{ and } \sum_k r_{nk} = \sum_k s_{nk} = 1, \quad \forall n \quad \text{...Eq (3.76)}$$

The agreement-disagreement at any pixel n, (P_{nkl}) is computed using a comparison operator in the form $C(s_{nk}, r_{nl})$. The notations p^{C}_{nkl} and P^{C}_{kl} is used to specify the comparison operator, C, employed for overall agreement-disagreement.

In a search of a generalized confusion matrix for soft classification, it is assumed that the matrix should fulfill the following two criterions:

i) *Diagonalization*. The matrix should be diagonal, if and only if, the classified *data matches pe*rfectly with the reference data.

ii) *Marginal sums*. Marginal sums should match with the total grades from the reference and classified data.

The first desirable characteristic is necessary for any assessment matrix to be useful in identifying a perfect matching case, such that it does not constrain the matrix characteristic under slight deviation from perfect match. Therefore, many alternatives can be envisaged that lead to a unique diagonal matrix for a perfect matching case, rather than different matrices when non-perfect match occurs. The second desirable characteristic is (although it may not be necessary) for the matrix to be useful in deriving accuracy indices as given in Eq 3.73, 3.74 and 3.75.

For hard classifications, accuracy indices are customarily written in terms of row and column totals, provided that these marginal sums correspond to class proportions in the classified and reference datasets respectively (i.e. $P_{+l} = r_{+l}, P_{k+} = s_{+k,}$ and $P_{++} = N$). In case of soft classification, marginal sums do not match with the class proportions, are often ignored, and that class proportions are used instead, for the computation of accuracy indices (Binaghi et al., 1999; Shabanov et al., 2005; Okeke and Karnieli, 2006).

First, a meaningful agreement measure does not consider whether the classified pixel membership is above or below the reference pixel membership, i.e., it does not depend on the over or under estimation errors. In contrast, presence and amount of discrepancy are important for defining a disagreement measure. An over estimation of reference pixel membership by a classified pixel membership leads to error of commission and is represented by the off-diagonal cells along the row of the class. Similarly, an under estimation of the reference value by the classified value leads to error of omission. These errors of omission are represented by the off-diagonal cells along the column of the class. Second, agreement and disagreement are, in a way, complimentary to each other, yet are non-negative measures. This is also stated by the constrained marginal sums characteristic. Consequently, when the agreement for a given class achieve its maximum (as in the case of a perfect match), the overall disagreement (i.e. sum of off-diagonal cells) for that class must be minimum (i.e. zero). Conversely, if the overall disagreement is maximum, then agreement is minimum.

It is required that the agreement-disagreement measure to conform to Eq. 3.77, where A and D denote Agreement and Disagreement operators respectively, and s'_{nk} and r'_{nl} denote the over and underestimation errors at pixel n.

$$C(s_{nk}, r_{nl}) = \begin{cases} A(s_{nk}, r_{nl}) & if\ k = l \\ D(s_{nk}, r_{nl}) & if\ k \neq l \end{cases} \quad \text{...Eq(3.77)}$$

$$s'_{nk} = s_{nk} - \min(s_{nk}, r_{nk}) \quad \text{...Eq(3.78)}$$

$$r'_{nl} = s_{nl} - \min(s_{nl}, r_{nl}) \quad \text{...Eq(3.79)}$$

In case of soft classification, pixel-class relationship definition implies that:

i) The pixel-class relationship is defined through the sub-pixel fraction of class coverage, and

ii) The agreement-disagreement is quantified as the proportion of area overlap among the classes at sub-pixel level.

Different operators have been developed under distinct pixel ontologies, listed in Table 3.3.

Table 3.3:Four basic operators

Operator ID	Operator of the form[a] C (s_{nk}, r_{nl})	Traditional interpretation	Soft interpretation
MIN	$\min(s_{nk}, r_{nl})$	Fuzzy set intersection	Maximum overlap
SI	$1 - \frac{\lvert s_{nk} - r_{nl} \rvert}{s_{nk} + r_{nl}}$	Similarity index	Normalized maximum
PROD	$s_{nk} \times r_{nl}$	Joint probability	Expected overlap
LEAST	$\max(s_{nk} + r_{nl} - 1, 0)$	Minimum overlap	Minimum overlap

[a] s_{nk} and r_{nk} denote classified and reference grades of class K at pixel n.

The Minimum operator (MIN) is the classic fuzzy set intersection operator. This operator has been suggested as the natural choice for producing cross-comparison matrices for fuzzy

classifications (Binaghi et al., 1999). In the traditional ontology of fuzzy classifications, the pixel-class relationship describes the admission of the possibility given by a so-called membership function that the pixel is a member of a class. This pixel-class relationship definition is useful for handling the imprecision of meaning of concepts that are characteristic of much of the human reasoning (Gopal and Woodcock, 1994). In the sub-pixel fraction ontology, the MIN operator measures the maximum sub-pixel overlap among the classes. Therefore, if membership values are linearly related to sub-pixel land cover areas (Shabanov et al., 2005), the fuzzy set intersection operator corresponds to the maximum sub-pixel overlap between the classes. However, the MIN matrix can over estimate the actual sub-pixel agreement-disagreement and, consequently, the marginal sums can be greater than the sub-pixel fractions. Also, even in the case of a perfect match, non-null degrees of mismatch are obtained for the off-diagonal cells. These characteristics generally limit the matrix's utility for drawing a conclusion about the confusion among the classes.

A variant of the MIN operator is sometimes used as a Similarity Index (SI) for comparing soft classifications (Townsend, 2000). This variant results after normalizing the MIN operator by the sum of the grade values shown in (Table 3.3). The SI operator is also meaningful for sub-pixel comparison, as it corresponds to a normalized maximum sub-pixel overlap. Nevertheless, it does not satisfy the homogeneity property, as it is invariant under scaling of the grade values. A cross-comparison matrix based on the SI operator does not satisfy the diagonalization and marginal sums characteristics outlined above (Chen et al., 2010).

The Product operator (PROD) arises from a pure probabilistic view of the pixel-class relationship. In the traditional probabilistic ontology, the pixel-class relationship represents the probability that a pixel completely belongs to a class, and the PROD operator gives the joint probability that the reference and classified pixels belong to two given classes, provided that the pixels have been independently classified. In sub-pixel fraction ontology, PROD operator measures the expected class overlap by chance between the reference and assessed sub-pixels partitions. More specifically, consider a randomly drawn point from the space spanned by pixel n. Since all the points within the pixel have the same probability to come out, then the joint probability that the point belongs to class k in the classified map and to class l in the reference map is given by the product ($s_{nk} \times r_{nl}$) provided that the land-cover fractions s_{nk} and r_{nl} have been

generated by an independent processes. A cross-comparison matrix based on the PROD operator has marginal sums that agree with the per-class areas. However, non-null disagreement values can result from the perfect matching case. In fact, it does not satisfy the upper-bound and homogeneity properties. The use of this operator for the assessment of soft classifications has been demonstrated by (Lewis and Brown, 2001), and its counter intuitive characteristics have been illustrated by Pontius and Cheuk (2006).

The LEAST operator was recently introduced in the discussion of sub-pixel comparison of maps (Pontius and Connors, 2006). The expression for LEAST operator is given in Table 3.3. This operator measures the minimum possible sub-pixel overlap between two classes. Even though this operator is meaningful for sub-pixel accuracy assessment, it may be of little use for other contexts, as it has even more counter intuitive characteristics than the PROD operator. Specifically, this operator fails to fulfill all but the commutativity and nullity properties.

None of the basic operators above satisfy the diagonalization characteristic discussed above. Indeed, in order for an operator to exhibit the diagonalization characteristic, it must conform to Eq 3.77. This type of operator is referred to as Composite operator, the only operator from Table 3.3 that satisfies all basic properties i.e. commutativity, positivity, nullity, upper bound and homogeneity for an agreement measure is the MIN operator. The uniqueness of MIN operator as an agreement measure is also mentioned in Eq 3.78 and 3.79, where over and underestimation errors are given in terms of the MIN operator. In this study, only three composite operators that use MIN operator as agreement measure are considered. They are referred to as MIN-PROD, MIN-MIN and MIN-LEAST (Silvan and Wang, 2008). These are defined in Table 3.4.

Table 3.4:List of Composite operators

Operator ID	Agreement[a]	Disagreement[b] (k≠l)	Sub-pixel confusion
MIN-PROD	$\min(s_{nk}, r_{nl})$	$s'_{nk} \times r'_{nl} \Big/ \sum_i r'_{ni}$	Constrained expected
MIN-MIN	$\min(s_{nk}, r_{nl})$	$\min(s'_{nk}, r'_{nl})$	Constrained maximum
MIN-LEAST	$\min(s_{nk}, r_{nl})$	$\min(s'_{nk} + r'_{nl} - \sum_i r'_{ni}, 0)$	Constrained minimum

[a] s_{nk} and r_{nk} denote the assessed and reference grades for class K at pixel n.
[b] s'_{nk} and r'_{nk} denote the over and under estimation errors of class i at pixel n.

The MIN-PROD composite operator was proposed by Pontius and Cheuk (2006). It uses minimum operator for diagonal cells and a normalized product operator for off-diagonal cells, thus combining the fuzzy set view with the probabilistic view as shown in Table 3.4. This operator satisfies the basic properties i.e. commutativity, positivity, nullity, upper bound and homogeneity. In addition, the MIN-PROD matrix satisfies the diagonalization and marginal sum characteristics. The interpretation of composite operator in context of sub-pixel agreement-disagreement is aligned with an assumption of maximum overlap between corresponding categories (diagonal cells), followed by allocation of residual sub-pixel fractions onto other categories (off-diagonal cells). The disagreement measure corresponds to the expected overlap by chance constrained to unmatched sub-pixel fraction. Specifically, disagreement between two membership values, s_{nk} and r_{nl}, corresponds to joint probability that a randomly drawn point within the space spanned by unmatched fraction, $1-\sum_i \min(s_{ni}, r_{ni})$ of pixel *n*, belongs to classes *k* and *l* in the residual class fractions $s_{nk} - min(s_{nk}, r_{nk})$ and $r_{nl} - min(s_{nl}, r_{nl})$ of classified and reference pixels, respectively.

The MIN-MIN composite operator uses minimum operator for both agreement and disagreement. However, it differs from MIN operator such that it assigns agreement in the first step and then, in the second step, it computes the disagreement based on the over and underestimation errors shown in Table 3.4. The MIN-MIN composite operator satisfies all the properties of agreement and disagreement. In addition, it leads to a cross-comparison matrix that satisfies the diagonalization property. However, it does not warrant the marginal sum characteristic. Marginal totals of a MIN-MIN matrix will, generally, overestimate the class proportions from the reference and classified datasets because MIN operator used for computing the off-diagonals cells, accounts for the maximum possible overlapping area among the residual fractions at sub-pixel level (Chen et al., 2010). Thus, the disagreement measure from MIN-MIN operator provides an upper bound for possible sub-pixel overlap constrained to unmatched sub-pixel fraction.

The MIN-LEAST composite operator uses MIN operator for the diagonal cells and a re-normalized LEAST operator for off-diagonal cells. Table 3.4 shows the expressions for agreement and disagreement for this composite operator. While this agreement measure satisfies all the properties i.e. commutativity, positivity, nullity, upper bound and homogeneity, the disagreement measure does not satisfy the required positivity property i.e. Non-null over and under-estimation errors may lead to null disagreement values. The MIN-LEAST operator produces a diagonal matrix for a perfect matching case. However, sub-pixel areas from reference and assessed datasets are generally underestimated by marginal totals. This is because the disagreement measure corresponds to minimum possible sub-pixel overlap constrained to unmatched sub-pixel fraction. Specifically, the re-normalized LEAST operator determines the excess of the sum of two residual class fractions, $s_{nk} - min(s_{nk}, r_{nk})$ and $r_{nl} - min(s_{nl}, r_{nl})$, with respect to the unmatched pixel fraction, $1 - \sum_i \min(s_{ni}, r_{ni})$.

The preceding review of cross-comparison matrices for assessing sub-pixel classifications has shown that:

a) A composite operator is necessary to warrant the diagonalization characteristic, and
b) The MIN operator is the most appropriate candidate for agreement measure.

It is worth noting that the use of a MIN operator for allocating sub-pixel proportions along the diagonal cells accounts only for the agreement at pixel level, i.e., the possible spatial distribution of classes within the pixel is not taken into account, but only the sub-pixel area proportions are matched. In contrast, the sub-pixel disagreement can take into account the possible spatial distribution of classes within the pixel. Nevertheless, there is no unique way to exactly allocate the remaining sub-pixel proportion into the off-diagonal cells. Specifically, the sub-pixel area allocation problem remains underspecified, as there are more unknowns ($K^2 - K$ off-diagonals elements) than equations ($2K$ constraints from column and row totals). One possibility is to use the statistical center of possible confusions, as given by MIN-PROD composite operator. However, sub-pixel distribution uncertainty cannot be accounted in this manner (Silvan and Wang, 2008).

Alternatively to resolve the distribution uncertainty problem associated with mixed pixel, the confusion interval [$P_{kl}^{MIN-LEAST}, P_{kl}^{MIN-MIN}$], formed by MIN-LEAST and MIN-MIN operator, to account soft distribution uncertainty. These intervals express the possible confusions amongst classes. Practically, it is convenient to express each confusion interval in the form of $P_{kl} \pm U_{kl}$, where P_{kl} and U_{kl} are interval center and interval half-width, respectively. These are computed as indicated by Eq 3.80 and 3.81, respectively.

$$P_{kl} = \frac{P_{kl}^{MIN-MIN} + P_{kl}^{MIN-LEAST}}{2} \qquad \text{...Eq (3.80)}$$

$$U_{kl} = \frac{P_{kl}^{MIN-MIN} - P_{kl}^{MIN-LEAST}}{2} \qquad \text{...Eq (3.81)}$$

This notation is preferred, as it provides a center value and allows for explicit documentation of its associated uncertainty. This is necessary for further error propagation analysis. By extension to our definitions, row marginal sum, column marginal sum, and total sum from uncertainty values are defined as mentioned in Eq 3.82

$$U_{k+} = \sum_l U_{kl},\ U_{+l} = \sum_k U_{kl}, U_{++} = \sum_k \sum_l U_{kl}, \qquad \text{Eq (3.82)}.$$

Eq 3.80 defines an operator that satisfies all the basic properties of agreement and disagreement measures. This operator leads to a matrix that exhibits the diagonalization characteristic. However, it does not warrant the marginal sum characteristic. A typical way to circumvent this inconvenience has been the use of area proportions from the reference and classified datasets in place marginal totals (Binaghi et al., 1999). In this way, accuracy indices such as Overall accuracy, User accuracy, Producer accuracy, Expected proportion of agreement, and Kappa coefficient, are readily generalized, where row and column totals are simply replaced by the corresponding area proportions. Unfortunately, the derived accuracy indices cannot reflect the uncertainty of confusion as they do not depend on the off-diagonal cells. Another possibility, which is pursued here, is to consider column and row totals as intervals. These intervals can be used to derive intervals of accuracy indices that reflect the uncertain nature of class soft distribution (Silván-Cárdenas and Wang, 2008). Table 3.5 and 3.6 shows the general structure of

Sub-pixel confusion-uncertainty matrix (SCM) with derive intervals of accuracy indices that reflect the uncertain nature of class soft distribution.

Table 3.5: General structure of the SCM

Class	**Reference**				**Row total**
	Class1	**Class2**	**…**	**Class K**	
Class 1	P_{11}	$P_{12} \pm U_{12}$	…	$P_{1K} \pm U_{1K}$	$P_{1+} \pm U_{1+}$
Class 2	$P_{21} \pm U_{21}$	P_{22}	…	$P_{2K} \pm U_{2K}$	$P_{2+} \pm U_{2+}$
. . .	. . .	. . .	…	…	
Class K	P_{K1}	$P_{K2} \pm U_{K2}$	…	P_{KK}	$P_{K+} \pm U_{K+}$
Column total	$P_{+1} \pm U_{+1}$	$P_{+2} \pm U_{+2}$	…	$P_{+K} \pm U_{+K}$	$P_{++} \pm U_{++}$

Table 3.6: Derived sub-pixel accuracy-uncertainty indices

Sub-pixel Accuracy Index	**Center**	**Uncertainty**
Overall accuracy, AO_s	$\frac{P_{++}\Sigma_k P_{kk}}{P_{++}^2 - U_{++}^2}$	$\frac{U_{++}\Sigma_k P_{kk}}{P_{++}^2 - U_{++}^2}$
k-th User Accuracy, UA_s (k)	$\frac{P_{kk}P_{k+}}{P_{++}^2 - U_{++}^2}$	$\frac{P_{kk}U_{k+}}{P_{++}^2 - U_{++}^2}$
k-th Producer Accuracy, UA_s (k)	$\frac{P_{kk}P_{+k}}{P_{+k}^2 - U_{+k}^2}$	$\frac{P_{kk}U_{+k}}{P_{+k}^2 - U_{+k}^2}$
Kappa Coefficient, K_s	$\frac{(P_0 - P_e)(1-P_e) - (*U_0 + U_e)U_e}{(1-P_e)^2 - U_e^2}$	$\frac{*(1-P_e)U_e + (1-P_e)U_0}{(1-P_e)^2 - U_e^2}$

*=sign of $(1-P_0-U_0)\times(1-P_e-U_e)$

Row and column totals of the SCM are determined as sum of center values (P_{kl}) plus-minus sum of uncertainty values (U_{kl}). The observed proportion of agreement ($P_o \pm U_o$) corresponds to overall accuracy (OA), whereas expected proportion of agreement ($P_e \pm U_e$) is given by Eq 3.83 and 3.84 respectively. The uncertainties from both, observed and expected proportions of agreement are propagated onto Kappa coefficient, which results in an interval of kappa coefficients specified through a center value and its associated uncertainty, as given by Table 3.6

$$P_e = \sum_k \frac{(P_{++}^2 + U_{++}^2)(P_{+k}P_{k+} + U_{+k}U_{k+}) - 2P_{++}U_{++}(U_{+k}P_{k+} + P_{+k}U_{k+})}{(P_{++}^2 - U_{++}^2)^2} \quad \text{...Eq (3.83)}$$

$$U_e = \sum_k \frac{2P_{++}U_{++}(P_{+k}P_{k+} + U_{+k}U_{k+}) - (P_{++}^2 + U_{++}^2)(U_{+k}P_{k+} + P_{+k}U_{k+})}{(P_{++}^2 - U_{++}^2)^2} \quad \text{...Eq (3.84)}$$

On the basis of this study, the following conclusion may be drawn:

i) This study, has shown that problem of sub-pixel area allocation can be resolved using SCM, wherein, membership values correspond to land cover fractions and the agreement and disagreement are defined in terms of the amount of sub-pixel overlap amongst reference and assessed pixels. In this approach, it is necessary to constrain the agreement measure at the pixel level.

ii) MIN-PROD composite operator appears to be meaningful for assessing sub-pixel classifications. However, it is shown that this operator provides one of the (possibly) infinite number of solutions to sub-pixel area allocation problem.

iii) Two new composite operators MIN-LEAST and MIN-MIN has been introduced to provide minimum and maximum possible sub-pixel class overlap constrained to unmatched sub-pixel fraction. The intervals defined by these operators are arranged within a matrix, in the form of a center value plus-minus its uncertainty, termed the Sub-pixel Confusion-uncertainty Matrix (SCM). It was shown that all the confusion intervals are tight i.e., no confusion uncertainty exists. Therefore, uncertainty-free matrices are sufficient to describe a wide variety of land cover characteristics.

3.6.2.3 ENTROPY METHOD

Classification accuracy is generally measured by an error matrix. However, in this study, generation of reference data for LISS-IV image was not possible because of the unavailability of further higher resolution image for the study area as well as it is not possible to generate fraction reference output from ground with large number of samples. In such case, entropy is used as an absolute measure of uncertainty (Dehghan and Ghassemian, 2006). Entropy calculates the

uncertainty from the classified data without using any external data, so it is an indirect method to measure accuracy. The entropy of a classified fraction output can be calculated by Eq 3.85.

For a better classified output, the entropy for a known class will be low and for unknown class, it will be high in a fraction image. For example, if we take fraction image of crop, the entropy value at crop will be low, whereas entropy value other than crop location will be high. Thus, low uncertainty implies more accurate classified output and vice-versa. The mathematical formula for entropy is given in Eq 3.85.

$$Entropy\,(x) = \sum_{i=1}^{C} -\mu(w_i/x)\, log_2(\mu(w_i/x)) \qquad \text{Eq (3.85)}$$

where, c is the total number of classes and $\mu(w_i/x)$ is the estimated membership function of class i for pixel x.

For high uncertainty, the value of entropy in Eq 3.85 is high and inverse. Entropy is defined based on actual output of classifier so it can give the pure uncertainty of classification results (Dehghan and Ghassemian, 2006). In this study, entropy has also been used in the classification process while combining with other measures to optimize the regularization parameters for fuzzy and contextual based classifiers using MRF.

3.6.2.4 MEAN AND VARIANCE METHOD TO VERIFY EDGE PRESERVATION

One of the main aim of this study, is to develop a Smoothening and Discontinuity Adaptive MRF based contextual classifier. Therefore, it is important to verify that any edge within a classified output is correct. An edge represents boundaries between two objects which may be characterized as a step function or slope between two regions (Wen and Xia, 1999).

As per Wen and Xia (1999), if for some specific threshold *c*, $|\mu_1 - \mu_2| \leq c$, then, there is no significant difference between the grey levels on the two sides of the edge, whereas if $|\mu_1 - \mu_2| > c$ then, there is a significant difference between the true averages, where μ_1 and μ_2 are the mean value of the pixels on each sides of the edges. To verify whether or not an edge is significant, an ideal way is to analyze separately the distributions of grey levels of the two regions on either side of the edge, where the difference between the average values within the

two regions indicates the steepness of the edge. To determine the value of *c*, edge point is examined first.

An edge point is retained, if

$$|X_i - Y_i| > c + \sqrt{2}SZ_\alpha \qquad \text{Eq}(3.86)$$

where, Xi and Yi represents the grey level of i^{th} pixel on the two sides of the edge respectively.

S is the standard deviation of the grey levels in the region the point belongs to.

Z_α can be obtained from the standard distribution tables.

In practice the values of α can be assigned as $0.01, 0.05, 0.1, 0.2$ depending upon different requirement. Both low and high thresholds for an edge can be identified by selecting two different α values.

In this study, the developed contextual classifier generates a fraction image for every class. The membership value of a unit in a fraction is high if the pixel exists at a location of a known class and for the unknown class, it is low. In the fraction image, amongst the membership values, variability will be less if the area is homogeneous. Consequently, the mean of the membership value will be high and the variance will be low in case of a homogeneous area for a known class location in a fraction image. This concept has been used here to verify the edge preservation.

The edge preservation method is shown in Fig. 3.5, a homogeneous area of a specific class i.e. crop has been selected which has a high mean value and a low variance. After selecting a homogeneous area, two sets of pixels were selected at either side of the edge. Mean and variance are calculated for these two set of pixels in each iteration of experimentation. The mean difference of these two set of pixels should be high and variance would be low, if the edge is to be preserved (Fig 3.5).

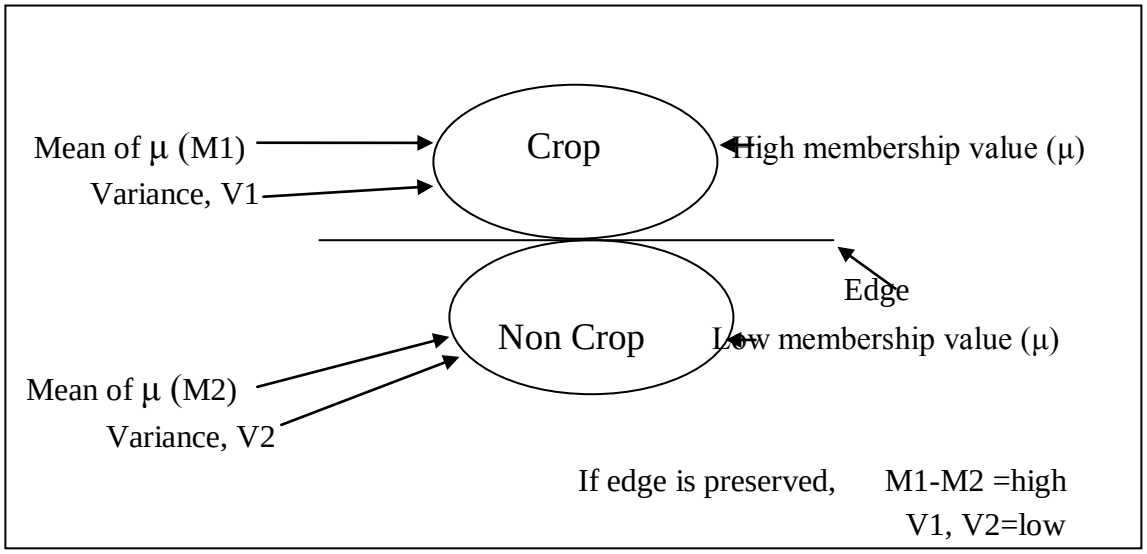

Fig.3.5: Method to verify edge preservation

In this study, soft assessment approach of accuracy has been incorporated using IRS-P6 satellite data, it is possible to acquire spectrally same and spatial different data sets of same area with nearly same acquisition time. Due to the uniqueness of availability of these data sets, soft fraction images generated from coarser resolution data set (e.g. AWIFS, IRS-P6) can be evaluated from fraction images generated from finer resolution data sets (e.g. LISS-III/LISS-IV, IRS-P6) as reference data set acquired at same time.

3.7 SUMMARY

Identification of land cover information accurately from remote sensing is crucial for mapping, assessment, monitoring and management of various resources like agriculture, forestry, geology, water, ocean etc. Since the spatial pattern of land cover information can be smaller than the resolution of sensor, a sub-pixel classification offers a flexible way to infer sub-pixel land cover information. However, accuracy assessment of these representations has been recognized to be far more difficult than traditional crisp classifications. For sub-pixel classifications, where multiple classes are assigned to a single pixel, a comparable standardized assessment procedure FERM, SCM, Entropy and Mean and Variance method for edge preservation has been discussed, to minimize the sub-pixel distribution uncertainty.

The primary objective of this chapter is to provide an understanding of the mathematical formulation of each classifier and accuracy assessment approach used in this study. The implementation of these classification methods along with assessment of accuracy, for soft classification of remote sensing data is highlighted. The knowledge gained in this chapter shall form the basis of developing classification and testing module of the software developed in this research. The next chapter provides the details of the software used, study area and data used.

CHAPTER-4

STUDY AREA AND DATA USED

4.1 INTRODUCTION

The aim of this chapter is to introduce the datasets used in this study to carry out various experiments using soft classification techniques on remote sensing imagery. To study the different aspects of the objectives defined in Chapter 1, *FUZCEN* package has been developed to classify the image. The implementation of soft classification methods through the software has been done using remote sensing data acquired from IRS satellite.

4.2 STUDY AREA

The study area selected for this study is located between the latitude and longitudes ranges of (28°53´57.12´´N to 28°56´31.22´´N) and (79°34´22.92´´E to 79°36´35.27´´E) respectively shown in (Figs. 4.1 and 4.2). Sitarganj Tehsil which is located near Pant Nagar, Uttarakhand state, India. The reason for selecting this area is:-

i) Diversity in terms of land use classes, such as vegetation types, soil and water.

ii) Same date multi-spatial resolution data for this region is available.

Uttarakhand is situated between 28^{o} 43' – 31^{o} 27' N latitudes and 77^{o} 34' – 81^{o} 02' E longitudes. In the vicinity of Kumon, Sitarganj lies in the district of Udham Singh Nagar, and gained a separate status in October 1995. Sitarganj is basically an agricultural and industrial place. The fertile land lends itself to different forms of agriculture giving rise to agriculture related activities and industries making this land a green place which has resulted into prosperity all around. Pantnagar University is a leading institution in the fields of agriculture and technology.

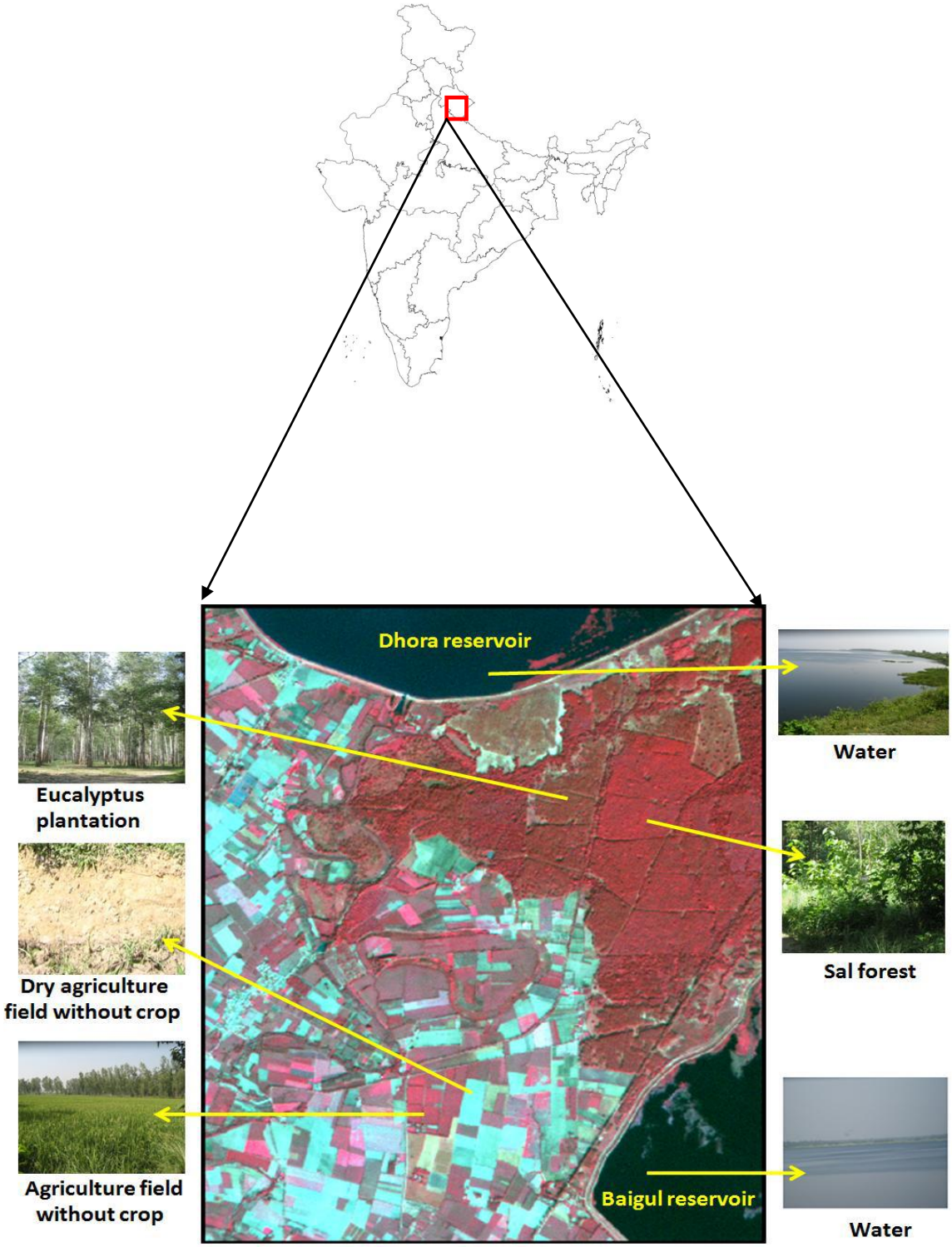

Fig. 4.1: Location map of study area

The population of the Sitarganj primarily depends on agriculture for livelihood about 70% of the population is engaged in agriculture. The climate of the place is quite harsh particularly in winter where the temperature goes occasionally below freezing point. For this study, Sitarganj has been selected as a study area because field work data as well as satellite images of Resourcesat-1 acquired on October 2007 was available.

The study area presents different land cover classes like barren land, sal forest (natural forest), eucalyptus plantation (manmade forest), agricultural land with sugarcane and paddy as major crops. It also has two reservoirs namely, Bhagul and Dhora reservoir (Fig 4.2) along with barren and moist soil areas. Further the study area presents two types of edges or boundaries amongst the land cover classes.

i) The sharp and distinct edges among the agricultures fields and ,

ii) The boundaries which changes gradually from one class to another such as in water class water changes gradually to grass land.

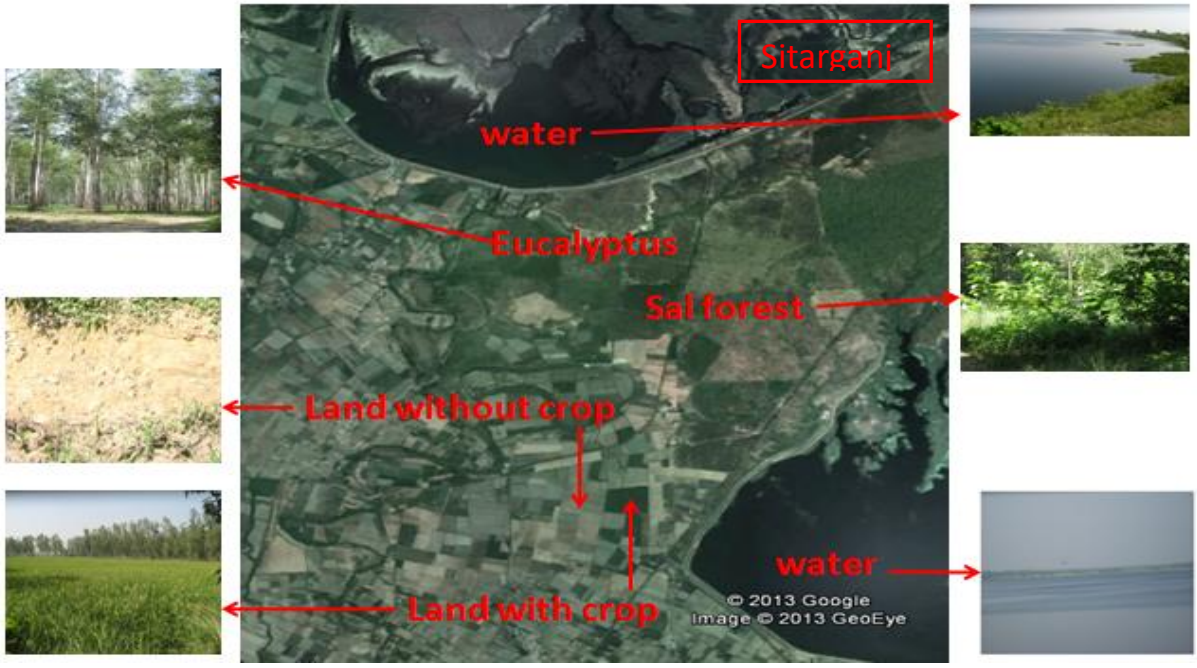

Fig. 4.2: Location of study area (*source*: Google Earth accessed on 11th Jan 2013)

In this study, to assess the accuracy of fraction images, the overall accuracy method suggested by Silván-Cárdenas and Wang (2008) has been used. For this purpose reference fraction images are required of same acquisition time as of classified fraction images.

ResourceSat-1 (IRS-P6), satellite is unique in providing multi-spectral data at different spatial resolution, while preserving the spectral information. In this research work, AWIFS, LISS-III and LISS-IV data sets from ResourceSat-1 (IRS-P6) satellite have been used as classified or reference fraction images generation. The satellite image and field photograph of the study area is shown in Fig. 4.3.

LISS-IV LISS-III AWIFS

Fig. 4.3: Location of study area (Satellite image)

4.2.1 DATA USED

In this study, AWiFS (Advanced Wide Field Sensor), LISS-III (Linear Imaging Self Scanner) and LISS-IV images of same date from the Resourcesat-1 (Indian Remote sensing Satellite-P6) have been used. LISS-III and AWiFS images have been used for classification, whereas the finer resolution of LISS-IV image has been used for the generation of reference data. Table 4.1 describes the basic properties of an image.

The IRS-P6 (Resourcesat-1) satellite was launched by ISRO in October 2003. It is the 10^{th} mission of Indian Remote Sensing (IRS) satellite series. The on-board sensors on this satellite are LISS-IV (Linear Imaging Self Scanner), LISS-III and AWiFS. Table 4.2 describes these sensors characteristics in details.

Table 4.1: Images used for this study

Satellite	**Sensors**	**Image Size**	**Date of Acquisition**	**Path and Row**
Resourcesat-1 (IRS P-6)	LISS-IV	949×745	October 15, 2007	144-40
	LISS-III	238×187		
	AWiFS	80× 63		

Table 4.2: Sensors specification of Resourcesat-1 (source: www.isro.org, on 8th Jan 2013)

Specifications	**Resourcesat-1**		
	LISS-IV	**LISS-III**	**AWiFS**
Spatial resolution (m)	5.8	23.5	56
Swath (KM)	23.9(MX Mode) 70.3(PAN Mode)	141	740
Spectral Bands (microns)	0.52-0.59 0.62-0.68 0.77-0.86	0.52-0.59 0.62-0.68 0.77-0.86 1.55-1.70	0.52-0.59 0.62-0.68 0.77-0.86 1.55-1.70
Quantization (bits)	7	7	10

4.3 INITIAL STATISTICS

In this study, supervised classification approaches have been used, where reference data for training and testing is required. Separate sample data sets have been used for training as well as for testing stage. For collecting the reference data as training data, help from existing topographic map, literature, exiting land use and land cover maps, as well as GPS surveyed data. The statistical information associated with each pixel value for each class in different bands has been shown in Tables 4.3 - 4.11. The size of training data used for supervised sub-pixel classification approach is approximately equal to 10*n* (Jensen, 1996), were *n* is dimension (i.e.

number of bands) of data used. Since, the collection of training data requires lots of effort in terms of time and cost, so in this study, all the classification algorithms have been evaluated using small training data set, in order to assess which classification algorithm gives higher accuracy with small training data sets.

The accuracy assessments of fraction images generated as output have been carried out using Fuzzy Error Matrix (FERM), Sub-pixel Confusion-uncertainty matrix (SCM) and entropy. In FERM and SCM, fuzzy reference data as testing data was required. This testing data have been collected from fine spatial multispectral image, and compared to input image used for classification. A total of 120 testing pixels for each class have been randomly selected, from corresponding outputs and their reference images respectively, such that it fulfills the condition of sample size of 75 to 100 pixels per class as recommended by Congalton (1991) for accuracy assessment purpose. Sample size for training and test were calculated at a confidence level of 99% and a desired precision of ± 5% using equation suggested by (Toratora, 1976, Pathak and Dixit, 2004). Figs. 4.4-4.6 show the histogram of each band for AWiFS, LISS-III and LISS-IV datasets.

Table 4.3: Statistical information of AWiFS data

S. No.	Statistics	Minimum	Maximum	Mean	Median	Mode	Std. dev.
1	Band 1	0	131	94.59	98	92	18.43
2	Band 2	0	133	68.80	70	61	16.79
3	Band 3	0	275	181.44	198.73	201.95	55.32
4	Band 4	0	370	172.77	183.55	0	59.68

Table 4.4: Statistical information of LISS-III data

S. No.	Statistics	Minimum	Maximum	Mean	Median	Mode	Std. dev.
1	Band 1	0	124	80.13	82	76	15.67
2	Band 2	0	89	41.88	42	36	10.36
3	Band 3	0	122	77.56	84	86	23.32
4	Band 4	0	132	57.26	60	57	20.56

Table 4.5: Statistical information of LISS-IV data

S. No.	Statistics	Minimum	Maximum	Mean	Median	Mode	Std. dev.
1	Band 1	0	182	101.12	103	107	18.75
2	Band 2	0	183	81.73	82	74	18.43
3	Band 3	0	136	77.15	83	84	21.37

Table 4.6: Correlation and Co-variance matrix of AWiFS image

AWiFS image	Correlation matrix				Co-variance matrix			
	B1	B2	B3	B4	B1	B2	B3	B4
B1	1				339.69			
B2	0.92	1			286.10	282.19		
B3	0.67	0.59	1		692.50	557.19	3060.44	
B4	0.74	0.83	0.81	1	820.72	841.27	2691.36	3561.65

Table 4.7: Correlation and Co-variance matrix of LISS-III image

LISS-III image	Correlation matrix				Co-variance matrix			
	B1	B2	B3	B4	B1	B2	B3	B4
B1	1				245.83			
B2	0.93	1			151.22	107.48		
B3	0.65	0.54	1		239.84	131.84	544.19	
B4	0.76	0.83	0.77	1	245.20	177.18	371.26	423.05

Table 4.8: Correlation and Co-variance matrix of LISS-IV image

LISS-IV image	Correlation matrix			Co-variance matrix		
	B1	B2	B3	B1	B2	B3
B1	1			351.54		
B2	0.93	1		323.49	339.78	
B3	0.66	0.56	1	268.02	224.18	456.99

Table 4.9: Mean value of pure training data for AWiFS image

S. No.	Class Name	Band 1	Band 2	Band 3	Band 4
1	Agriculture	98	64	243.33	172.33
2	Sal forest	92.05	60.11	240.76	161.11
3	Eucalyptus plantation	92	61.5	198.91	147.83
4	Barren land	125	130	232	345
5	Moist land	105.25	89.5	145.25	221.25
6	Water body	85.41	54.66	59.41	46.41

Table 4.10: Mean value of pure training data for LISS-III image

S. No.	Class Name	Band 1	Band 2	Band 3	Band 4
1	Agriculture	83	39.77	102.45	55.40
2	Sal forest	76.27	36.11	103.83	54.77
3	Eucalyptus plantation	77.78	39.15	84.15	47.31
4	Barren land	113.22	82.27	101.05	125.05
5	Moist land	91.88	54.88	56	71.88
6	Water body	70.76	34	27.03	16

Table 4.11: Mean value of pure training data for LISS-IV image

S. No.	Class Name	Band 1	Band 2	Band 3
1	Agriculture	105.06	81.06	100.16
2	Sal forest	99.64	73.47	98.05
3	Eucalyptus plantation	98.87	77.16	81.61
4	Barren land	136.08	146.02	96.77
5	Moist land	115.10	106.89	60.81
6	Water body	92.8	70.52	35.37

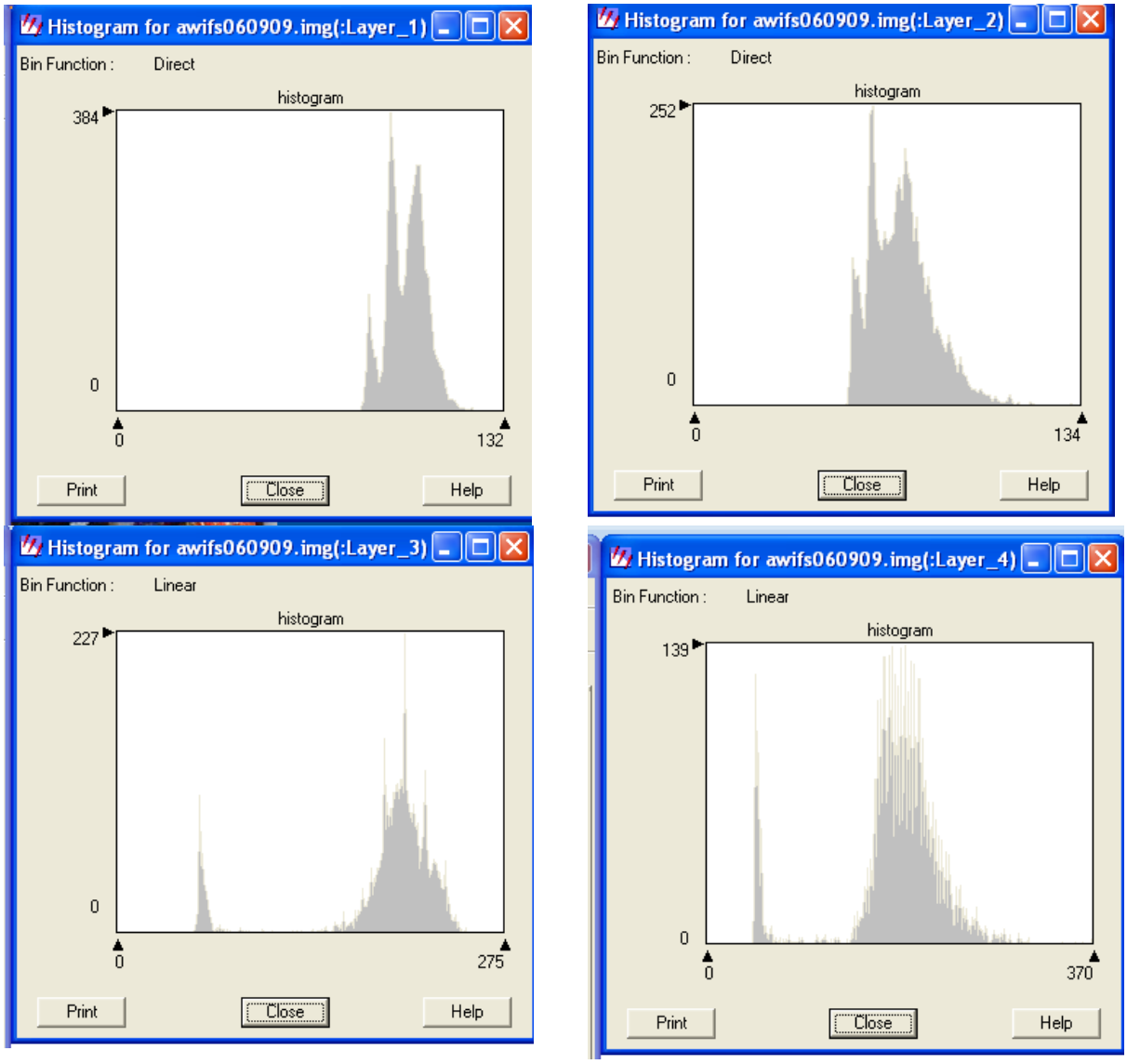

Fig 4.4 Histogram of AWiFS image

Preparation of appropriate reference data is a key for the evaluation of hybrid soft classifiers. Actual class proportions in each pixel of LISS-IV and LISS-III images specified in (Fig. 4.3) has acted as a soft reference data for AWiFS image and LISS-IV image is used an reference image for LISS-III image to identify a particular class in mixed pixels at various stages of supervised classification.

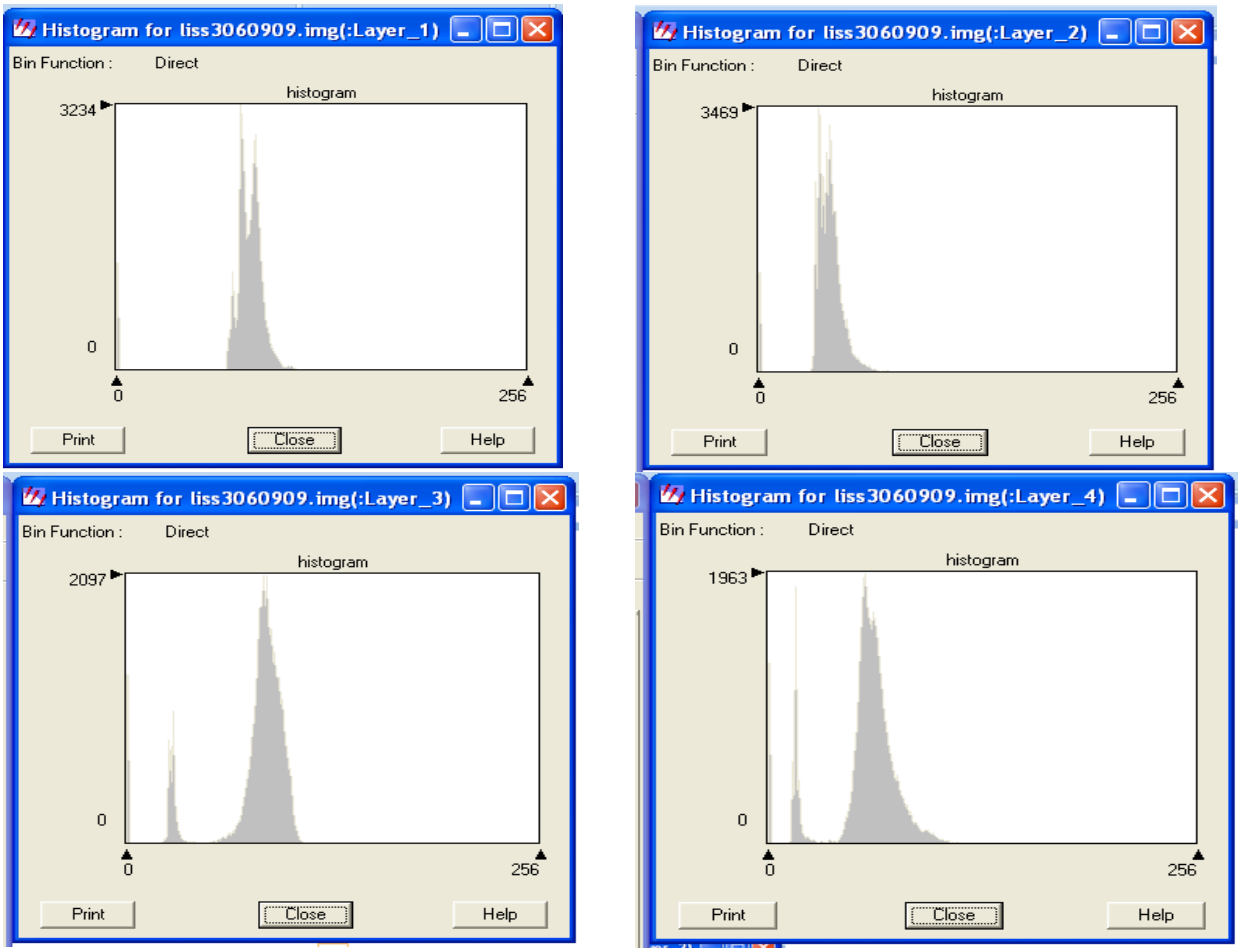

Fig 4.5 Histogram of LISS-III image

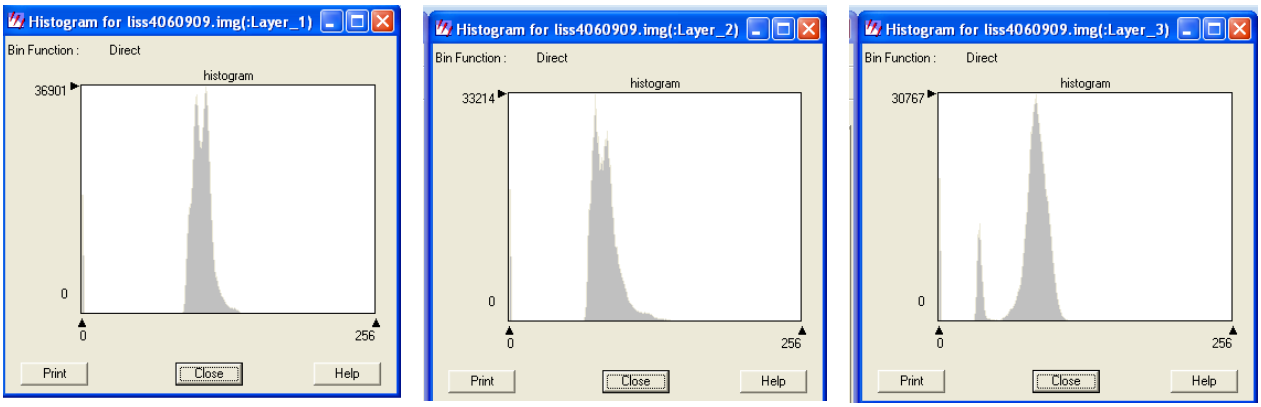

Fig 4.6 Histogram of LISS-IV image

4.4 PREPROCESSING OF DATA

Prior to any application it is important to perform geometric correction for all the images. Coarser resolution images should be co-registered with the fine resolution images. In this study, an image to image accuracy assessment method has been carried out. Also for that reason it is important to co-register the image to compare the coarse spatial resolution images with the fine spatial resolution images.

For geometric correction of the LISS-IV image, the toposheet, numbered $53\frac{P}{9}$ from the Survey of India (SOI) has been used. The LISS-IV image has been geo-registered in UTM projection with WGS84 North spheroid and datum, zone 44. By using nearest neighbor resampling method the LISS-IV image was resampled at a 5m spatial resolution. Resampling is important for an accuracy assessment as finer resolution image has been used as a reference image for classified coarser resolution images. Resampling is required for geometric transformation, and it is like convolving the input image with a uniform weighing function. All the three images (LISS-IV, LISS-III and AWiFS) were resampled at 5m, 20m, and 60m spatial resolution to form a ratio of 1:4:12, respectively. In doing so, correspondence between LISS-III and AWiFS pixels were maintained with particular number of LISS-IV pixels i.e. 16 and 144 pixels respectively. Twenty GCP's were well distributed and 0.33 RMSE value is associated with pixel. Geo-registration of LISS-III image was done with respect to the geometrically corrected LISS-IV image taking similar projection, spheroid and datum as that of LISS-IV image. The LISS-III image was resampled at 20 m spatial resolution.

Geo-registration of AWiFS image was done with respect to the geometrically corrected LISS-III image. The projection, spheroid and datum were same as that of LISS-III and LISS-IV images. The resampling of AWiFS image was done at 60 m spatial resolution.

4.5 GENERATION OF REFERENCE DATASET

In this study, the LISS-III and LISS-IV images have been used as reference data for AWiFS image. The reference dataset has been generated from finer resolution image instead of using field data because of the following listed reasons.

i) It is difficult to locate within pixel classes on the ground exactly.

ii) Reference data generation from field survey is a type of classification and may contain errors (Okeke and Karnieli, 2006).

iii) Correct identification of classes on the ground may be difficult at the sub-pixel level (Okeke and Karnieli, 2006).

iv) As the main issue is land-cover, field data may not provide additional information as compared to high resolution satellite images.

To evaluate the classified dataset, it is also necessary to classify the reference dataset. There are two methods available to generate soft reference data set from finer resolution image. Use sub-pixel classifier to generate soft reference data from fine resolution LISS-IV image and medium resolution LISS-III image. In doing so there may be possibility of error while resampling the dataset.

If the classifier for the reference data set and classified dataset are different, two cases may arise. First, the performance of the classifier used for image classification may be better than reference classifier. Second the performance of classified dataset is better in terms of accuracy than the reference dataset. In this study, the same classifier has been used for both the image classification and reference data generation. This removes the disadvantage of using the different classifiers and error occurred only due to difference in resolution of the images.

4.6 SUMMARY

In this chapter, a description of study area and data used to conduct various experiments has been provided. The investigations shall be based on remote sensing data from IRS P6, AWiFS, LISS-III and LISS-IV sensors. A complete methodology is provided in the next chapter.

CHAPTER 5

METHODOLOGY AND DETAILS OF SOFTWARE PACKAGE DEVELOPED

"Thought and theory must precede all salutary action; yet action is nobler in itself that either thought or theory"- William Wordsworth.

5.1 INTRODUCTION

The aim of this chapter is to provide an overview of methodology for a study planned for soft classifications of remote sensing data along with details of the software package developed for carrying out soft classification with various options. The classification algorithms are based upon Fuzzy Set Theory based algorithms, like Fuzzy *c*-Means (FCM), Possibilistic *c*-Means (PCM) and Noise Clustering (NC). Further, it has the capability to incorporate entropy and contextual information for the hybridization of classifiers. Thus, entropy, contextual and entropy with contextual based hybrid approach has been implemented. The software package developed consists of fuzzy, entropy and contextual based soft classification approaches and has been named as **FUZ**zy soft classification incorporating **C**ontextual, **E**ntropy and **N**oise (FUZCEN).

In some of the commercially available digital image processing software, such as, Environment for Visualizing Images (ENVI), Earth Resource Data Analysis System (ERDAS), Earth Resource Mapping software (ER Mapper) and IDRISI, provide for a few soft classifiers but no corresponding accuracy measures for soft classified output for their evaluation. In general, none of them have incorporated entropy and contextual based hybridization and SCM based approach to assess the accuracy of an classified image. Further, none of the commercial available software packages provide option for entropy and contextual based algorithm using Markov Random Field (MRF) theory for multi-spectral remote sensing data at sub-pixel classification. Thus, it was necessary to develop a package having the sub-pixel classification algorithms used in this study, for different experiments.

5.2 GENERAL METHODOLOGY

The flow chart shown in Fig 5.1 outlines the methodology adopted for carrying the various studies using different types of soft classifiers. The software so developed also follows the same sequence of operations in order to achieve the task. First of all, the initial statistics of input image have been computed and based on this information; the pre-processing of the input image is carried out. In general, atmospheric corrections are provided to eliminate the effects of haze. Since different types of satellite data having varying resolution may be incorporated, hence geo-referencing of these satellites data is must. Thereafter, the training sites are identified and the training data statistics are generated for each class of interest.

Depending on the type of soft classifier to be used, the objective functions are defined. Each objective function has a set of parameters and these have to be optimized before the classification can be carried out. Classification is performed using supervised classification using either Fuzzy, contextual, entropy and noise based classification approaches. The output data is then subjected to assessment of accuracy, in order to identify the efficacy of the algorithms.

The overall methodological flowchart is shown in (Fig. 5.2). Various aspects of this flowchart are now described individually.

5.2.1 GEO-REFERENCING OF SATELLITE IMAGES

Since, a variety of data sets from different remote sensing sensors having varying spatial resolution have been used, thus it was necessary to geo-reference these data sets so that common training as well as testing pixels can be used. Hence, GPS observations pertaining to each sample for each class has been collected using a geodetic single frequency GPS in differential mode. 20 Ground Control Points (GCP) have been used for geo-referencing the data sets and transformation parameters calculated. A root mean square error (RMSE) of 0.33 (in pixel units) has been adopted as the threshold value for geo-referencing. Resampling of the data sets during geo-referencing has been carried out after generation of fraction of images, using Nearest Neigbourhood, in order to avoid the alteration of the pixel values.

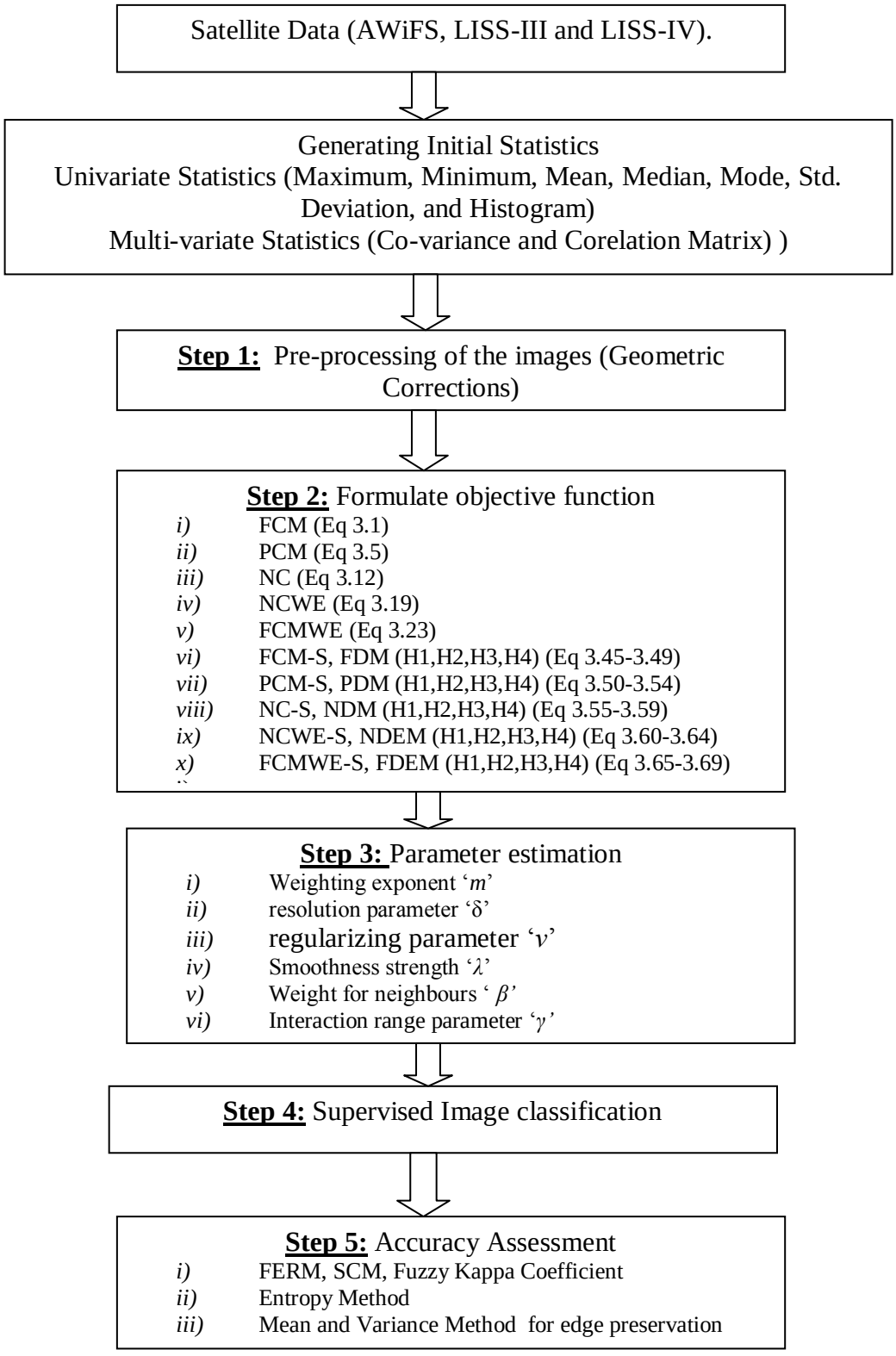

Fig 5.1: Flow chart showing the generalized step of methodology broadly

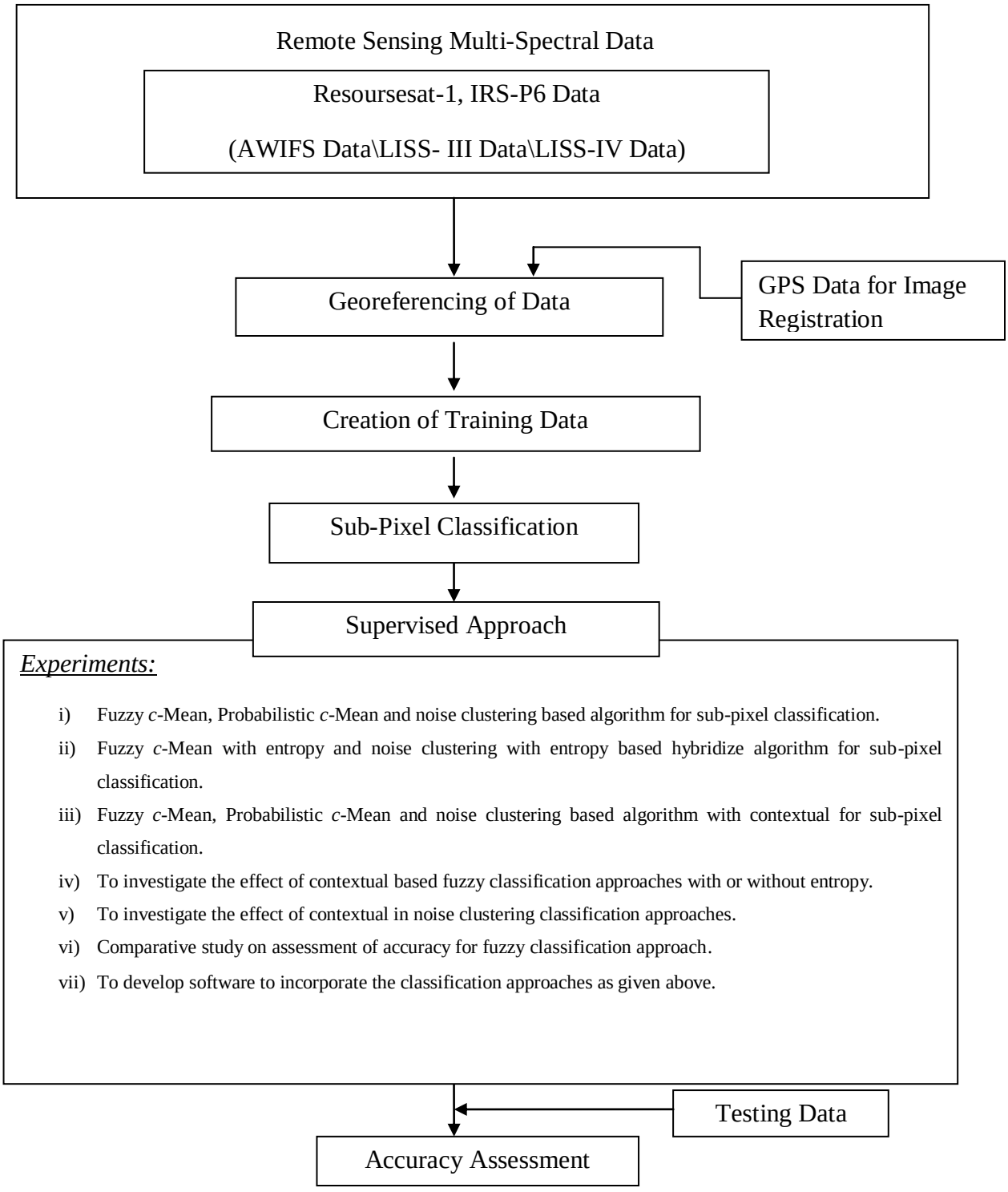

Fig 5.2: General methodology adopted for this study

5.2.2 PREPARATION OF REFERENCE DATA

The sub-pixel classification algorithms evaluated in this study operate in supervised mode. Further, these algorithms have been evaluated using small reference data sets of 10*n* size; where *n* is dimensionality of data sets. First of all, the positional information on ground for each class has been collected using Trimble Juno SB, mobile GIS/GPS. This information has been overlaid on different multi-spectral data sets and pure pixels for training and testing have been collected. Sample size for training and test were computed at a confidence level of 99% and a desired precision of ± 5% as suggested by Toratora (1978).

5.2.3 CLASSIFICATION OF SATELLITE DATA

In this study, supervised classification has been carried out to generate sub-pixel classification output. In all, a total of ten classification algorithms have been tested as mentioned in Fig. 5.2., and the description of tested algorithms are outlined in the following section.

5.2.3.1 EVALUATION OF FUZZY SET THEORY BASED CLASSIFIERS

In this study, fuzzy set theory based sub-pixel classifiers have been tested using multi-spectral remote sensing data. Although, a number of fuzzy set theory based classifiers are available, however in this study, only three classifiers have been taken on to account i.e. Fuzzy *c*-Means (FCM), Possibilistic *c*-Means (PCM) and Noise Clustering (NC) classifiers. FCM, PCM and NC are essentially unsupervised classifiers, however in this study; these classifiers have been implemented in supervised mode. All the algorithms have been evaluated using Euclidian weighting norm for sub-pixel classification and assessment of accuracy has been carried out using Fuzzy Error Matrix (FERM), Sub-pixel confusion uncertainty matrix (SCM), Entropy and Mean and Variance technique. The classification has been carried out using FUZCEN software as described in Section 5.3.

Classification module of FUZCEN software has been used to test the performance these fuzzy set based classifiers, wherein two parameters namely weighting exponent (m) for FCM and PCM classifiers and spatial resolution parameter (δ) for NC classifier have been estimated. The comparative analysis of FCM, PCM and NC classifier has also been performed on the basis of

the classification results and accuracy. The membership values of FCM, PCM and NC can be computed using objective functions defined by Eqs 3.1, 3.5 and 3.12 respectively.

5.2.3.2 EVALUATION OF FUZZY AND ENTROPY BASED CLASSIFIERS

Classification is ordering of information classes in to groups/clusters on the basis of their relationships. Soft or fuzzy methods of classification provide for each pixel a measure of the degree of similarity for every class (Foody, 1996, Maselli *et al*., 1996). The hybridization of entropy with fuzzy nature classifier has been conducted to achieve second and third objective of this study. However, it has been observed that the method proposed by Dunn (1974) and Bezdek (1984) are purely fuzzy in nature, while the entropy based method is more similar to statistical model.

In this study, FCM and NC classifiers has been hybridized with entropy wherein weighting exponent (m) and regularizing parameter (v) has been optimized for FCM with entropy classifier. For NC with entropy classifier, spatial resolution parameter (δ) and regularizing parameter (v) has been optimized. The comparative assessment of FCM with entropy and NC with entropy has also been done. The membership values of NC with entropy and FCM with entropy can be computed using objective functions defined by Eqs 3.19 and 3.23 respectively.

5.2.3.3 EVALUATION OF CONTEXTUAL AND ENTROPY BASED CLASSIFIERS

The coding of Contextual based classifier is based on the mathematical formulation given in Section 3.4.10 for FCM with contextual, Section 3.4.11 for PCM with contextual, Section 3.4.12 for NC with contextual, Section 3.4.13 for NCWE with contextual and Section 3.4.14 for FCMWE with contextual classifiers of Chapter 3. In this approach, the contextual information of an image is used to resolve the problem associated with uncertain boundaries as well as removal of noise in data. Markov Random Field characterizes the spatial contextual information in terms of smoothness prior and Discontinuity Adaptive prior, which helps to improves the classification accuracy and preserves the edges at boundaries and generates smooth output. In this study, the contextual information has been added in FCM, PCM, NC, NCWE and FCMWE classifiers.

One of the objectives of this study is to identify the usefulness of contextual information in fuzzy set theory based and entropy based classifiers. Investigations have been carried out to study the effect of including contextual and entropy in fuzzy and entropy based classifiers on the performance of classifiers.

The mathematical formulation of FCM with contextual based upon smoothness prior model is defined by Eq 3.45 for FCM-S wherein weighting exponent (m), smoothness strength (λ) and weight for neighbours (β) parameters have been optimized. The objective functions incorporating Discontinuity Adaptive (DA) prior model with FCM classifier is defined in Eqs 3.46 to 3.49 for FDM-(H1), FDM-(H2), FDM-(H3) and FDM-(H4) respectively. In DA model, the first objective is the selection of a suitable model amongst H1, H2, H3 and H4 and in the next step, identification of optimized parameters is carried out. In FCM-DA-MRF model, the associated parameters to be optimized are weighting exponent (m), smoothness strength (λ) and interaction range parameter (γ).

The mathematical formulation of PCM with contextual based upon smoothness prior model is defined by Eq 3.50 for PCM-S, wherein weighting exponent (m), smoothness strength (λ) and weight for neighbours (β) parameters have been optimized. The objective functions incorporating Discontinuity Adaptive (DA) prior model with PCM classifier is defined by Eqs3.51 to 3.54 for PDM-(H1), PDM-(H2), PDM-(H3) and PDM-(H4) respectively. In DA model, the first objective is the selection of the suitable model amongst H1, H2, H3 and H4 for PCM with contextual classifier using DA model and in the next step identification of optimized parameters is carried out. In PCM-DA-MRF model, the associated parameters to be optimized are weighting exponent (m), smoothness strength (λ) and interaction range parameter (γ).

The mathematical formulation of NC with contextual based upon smoothness prior model is defined by Eq 3.55 for NC-S, wherein spatial resolution parameter (δ), smoothness strength (λ) and weight for neighbours (β) parameters have been optimized. The objective functions incorporating Discontinuity Adaptive (DA) prior model with NC classifier has been defined in Eq 3.56 to Eq 3.59 for NDM-(H1), NDM-(H2), NDM-(H3) and NDM-(H4) respectively. In DA model, the first objective is the selection of the suitable model amongst H1, H2, H3 and H4 for NC with contextual classifier using DA model and in next step is the identification of suitable

optimized parameters. In NC-DA-MRF model, the associated parameters to be optimized are spatial resolution parameter (δ), smoothness strength (λ) and interaction range parameter (γ).

In this study, hybridization of classification has been done up to third level, wherein at initial stage entropy has been added to the base classifier like NC and in FCM. At lateral stage, the contextual information of an image is also added to investigate the joint effect of entropy and contextual. The mathematical formulation of NC with entropy with contextual based upon smoothness prior model is defined by Eq 3.60 for NCWE-S wherein spatial resolution parameter (δ), regularizing parameter (v) smoothness strength (λ) and weight for neighbours (β) parameters have been optimized. The objective functions incorporating Discontinuity Adaptive (DA) prior model with NCWE classifier has been defined by Eqs 3.61- 3.64 for NDEM-(H1), NDEM-(H2), NDEM-(H3) and NDEM-(H4) respectively. In DA model, the first objective is the selection of the suitable model amongst H1, H2, H3 and H4 for NCWE with contextual classifier using DA model and in next step is the identification of suitable optimized parameters. In NCWE-DA-MRF model, the associated parameters to be optimized are spatial resolution parameter (δ), regularizing parameter (v) smoothness strength (λ) and interaction range parameter (γ).

The mathematical formulation of FCM with entropy with contextual based upon smoothness prior model is defined by Eq 3.65 for FCMWE-S, wherein weighting exponent or Fuzzifier (m), regularizing parameter (v) smoothness strength (λ) and weight for neighbours (β) parameters have been optimized. The objective functions incorporating Discontinuity Adaptive (DA) prior model with FCMWE classifier has been defined by Eqs 3.66 - 3.69 for FDEM-(H1), FDEM-(H2), FDEM-(H3) and FDEM-(H4) respectively. In DA model, the first objective is the selection of the suitable model amongst H1, H2, H3 and H4 for FCMWE with contextual classifier using DA model and in next step is the identification of suitable optimized parameters. In FCMWE-DA-MRF model, the associated parameters to be optimized are Fuzzifier (m), regularizing parameter (v) smoothness strength (λ) and interaction range parameter (γ).

5. 3 COMPARATIVE EVALUATION OF CLASSIFIERS

In this study, three categories of classifiers, namely, fuzzy set based i.e. (FCM, PCM and NC), fuzzy and entropy based i.e. (FCMWE and NCWE) and in third category contextual and entropy

based classifier which includes FCM with contextual, PCM with contextual, NC with contextual, NCWE with contextual and FCM with entropy based classifiers have been analyzed. A comparison between these three approaches of sub-pixel classification has been carried out. The procedure for solving a problem using mathematical framework called formulation of objective function and the comparative assessment of all these mathematical formulation defined in Section 3.2, 3.3 and in Section 3.4, has been described wherein LISS-IV image has been used as a reference image for LISS-III and AWiFS images. The land cover feature which has been taken on to the account is agricultural land, barren land, moist land, sal forest, eucalyptus plantation and water body.

The comparative assessment of classifiers has been done wherein; evaluation of uncertainty has been taken in to account. Uncertainty in the class allocation of a pixel is pronounced in coarse resolution images due to the occurrence of mixed pixels in areas containing mixture of land use land cover classes. So, this uncertainty in the classification can be judged using Shanon's entropy. The comparative model of classifier is depicted in Fig. 5.3. In this flow chart, the classification output of these three category classifiers have been compared with the reference image of high resolution data set.

5. 4 ASSESSMENT OF ACCURACY

Assessment of accuracy is a vital and integral part of digital classification. In fact, no classification is considered to be complete without assessment of accuracy. The purpose of assessment of accuracy is to provide knowledge to the analyst and the user of the classified map regarding the accuracy with which the classes on the ground are identified correctly in the image. In digital image processing, accuracy is a measure of agreement between standard information at a given location to the information at the same location on the classified map. For sub-pixel classification, the assessment of accuracy is carried out using FERM (Section 3.6.2.1), SCM (Section 3.6.2.2). Entropy method has been used as an absolute indicator for uncertainty analysis (Section 3.6.2.3) and Mean and Variance method used to verify edge preservation (Section 3.6.2.4). Initially, classification experimentation has been carried out and thereafter, accuracy measures as specified above have been taken to evaluate and compare the performance of various classification methods.

In hard classification, each pixel is a full member of one specific class. However, in soft classification, each pixel has partial membership pertaining to multiple classes simultaneously. FERM has been widely used technique for image to image assessment of accuracy for soft classification. However, in few cases, it has been observed that the FERM indices are not able to resolve the class overlap problem in remote sensing imagery. Thus, SCM has also been applied to assess the accuracy of all three categories of soft classifiers. As per Pontius and Cheuk (2006), the characteristic of class membership of a pixel can be defined by three types of class membership in soft classification i.e. contemporary, fuzzy and multiple resolutions. For soft classification, the class membership of a pixel equals to the proportion of the area of that class within a pixel, and that the sum of all the class memberships is equal to one. The indices for these soft classification used in this study, has been computed using SCM, as SCM indices are built totally on the area-basis. The general structure of image to image accuracy assessment is shown in Fig. 5.4.

5.5 THE NEED OF FUZCEN

In present arena of digital image processing sofware, various kinds of readymade tools are available to perform digital image analysis. Since last two decades, a large number of image processing software has been developed by various commercial companies offering a suite of modules related to data input, visualization, image enhancement, transformation, classification and assessment of accuracy. Some of the leading image processing software's are ERDAS IMAGINE, IDRISI, ENVI, ER MAPPER and eCognition. Similarly, some individual based soft classification have been developed such as **S**oft **C**lassification **M**ethods and **A**ccuracy Assessment **P**ackage (SCMAP) developed by (Aziz et al., 2004) and **S**ub-pixel **M**ultispectral **I**mage **C**lassifier (SMIC) developed by Kumar and Ghosh (2007), facilitates the image classification based upon statistical learning algorithms and assessment of accuracy using FERM only. However, these tools are not able to fulfil the objectives defined for this study. The need of ***FUZCEN***: ***FUZ****zy Soft Classifier incorporating* ***C****ontextual,* ***E****ntropy and* ***N****oise* has emerged, in order to incorporate the contextual information, entropy and noise in the process of satellite image classification.

Aziz et al. (2004) incorporated the Neural Network based classifier in his study, where in Kumar and Ghosh (2007) has focused primarily on Support Vector Machine (SVM) and statistical based learning algorithms. None of these have provided the hybridized model of classification to incorporate context, entropy, and noise. Further, this tool provides an automated image to image accuracy assessment approach using FERM and SCM.

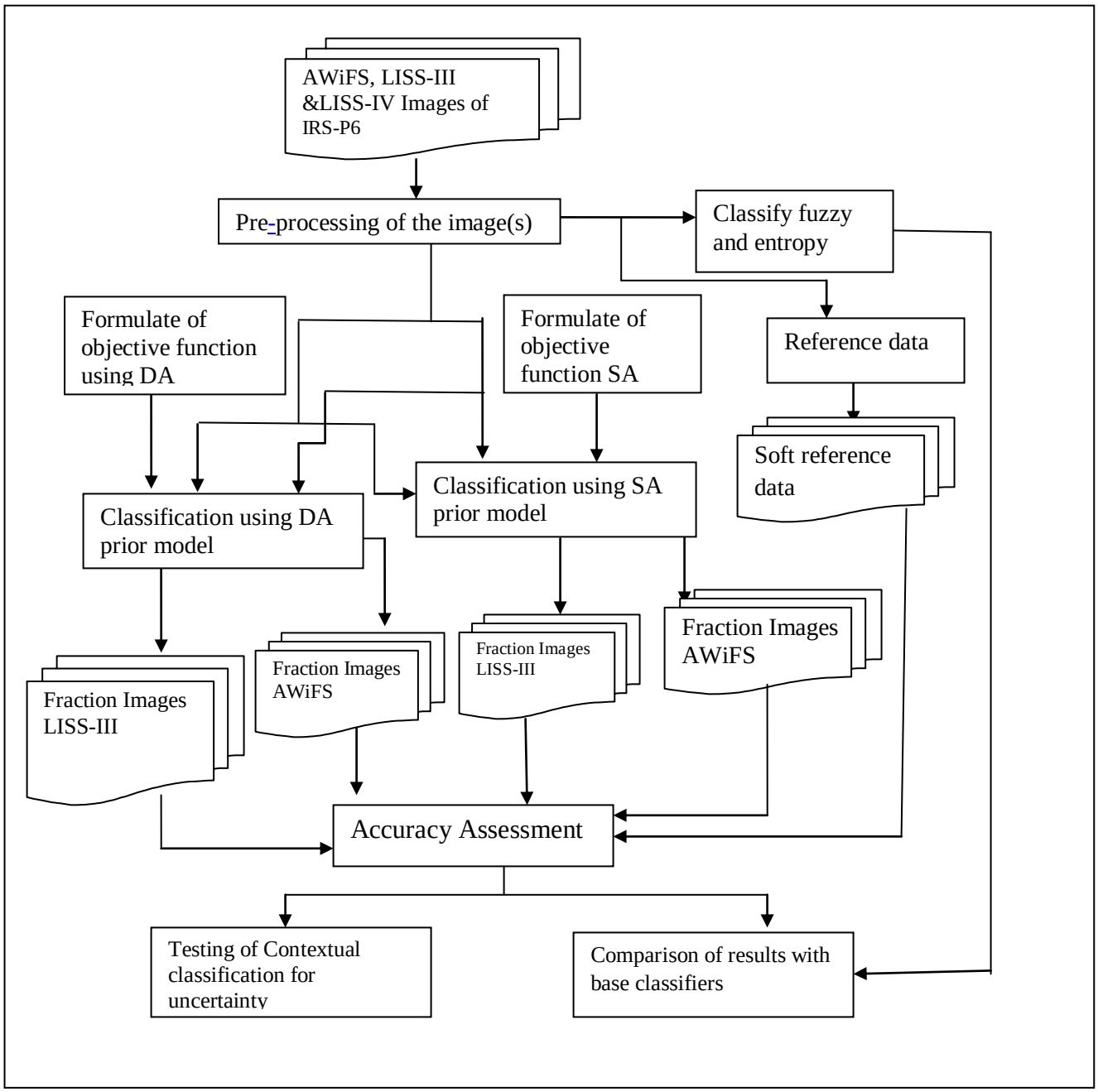

Fig 5.3: Comparative analysis of classifiers

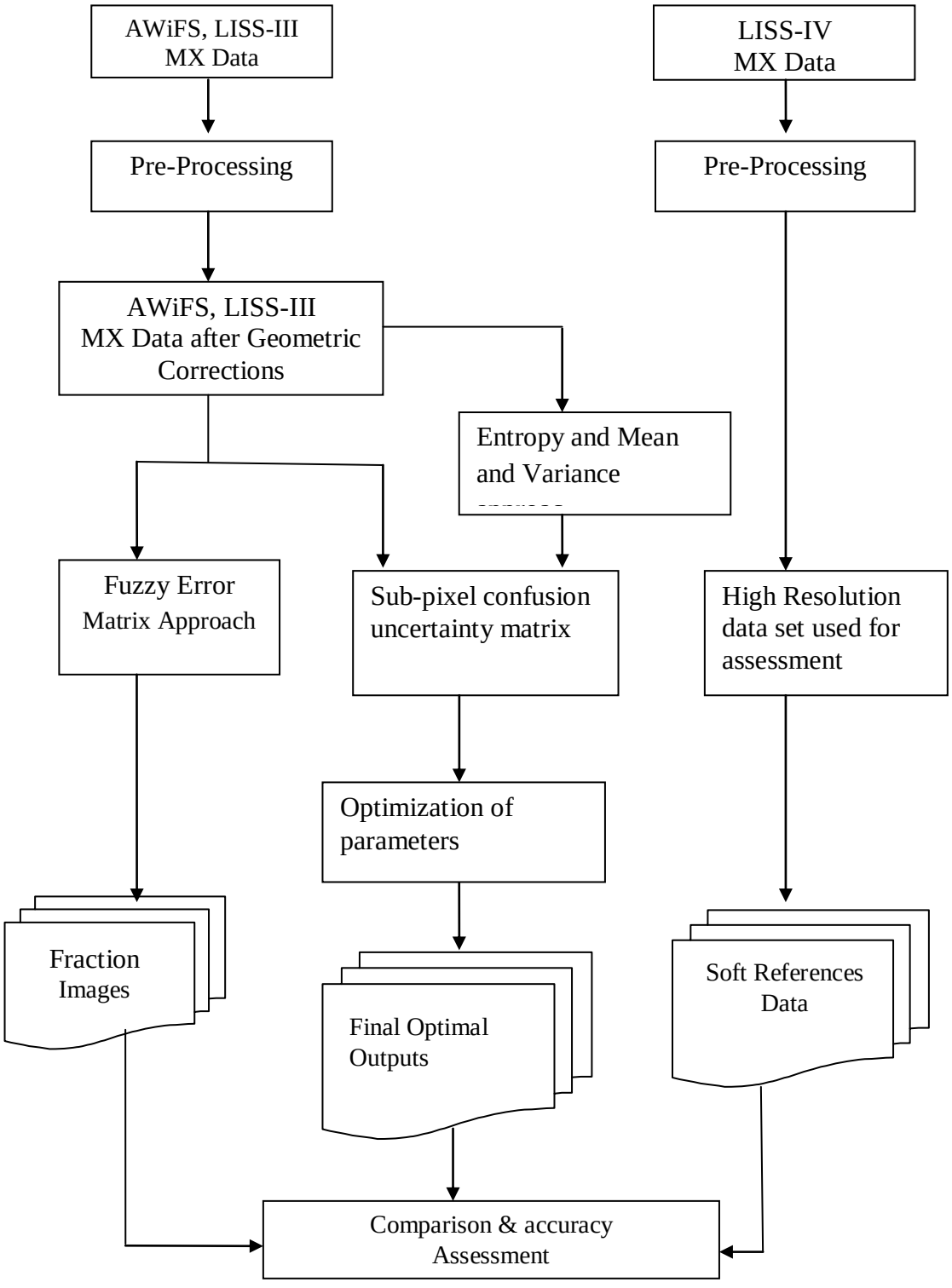

Fig 5.4: Flowchart for image to image assessment of accuracy.

5.6 PROGRAMMING ENVIRONMENT

The coding of *FUZCEN*: *Fuzzy soft classifier incorporating Contextual, Entropy and Noise* package has been done in Java environment. Java can be used to create two types of programs: applications and applets. The output of a Java compiler is not executable code; rather it is a byte-code. Java run-time system is an interpreter for the byte-code. It is simply a highly efficient means of encoding a program for interpretation. It is much easier to allow Java programs to run in a wide variety of environments. Once the run-time package exists for a given system, the byte-code version of any Java program can run on it. Therefore, using byte-code to represent programs is the easiest way to create truly portable programs. Java shares many similarities with C++ as it relates to classes, but there are also several differences. By default, members of a class are accessible by other members of their class, derived classes, and by other members of their package. Therefore, class members are "more public" than they are in C++, however, the private access specifier applies only to the variable or method that it immediately precedes.

All class objects are instantiated in Java using the new operator. Therefore, all class objects are dynamically allocated. When there are no references to an object, then the object is considered inactive. Due to the JAVA environment, FUZCEN package is platform independent. It has also been found that memory management and exceptional conditions are quite difficult in conventional programming environment like C or C++. So, there can be two main reasons for program failure:

i) Memory management issues.
ii) Problem to resolve runtime errors.

Memory management can be a tedious task in traditional programming environments. For example, in C / C++, the programmer must manually allocate and free all dynamic memory. This sometimes leads to problems, because programmers will either forget to free memory that has been previously allocated or, worse, try to free some memory that another part of the code which is still in use. Java virtually eliminates these problems by managing memory allocation and de-allocation. In fact, de-allocation is completely automatic, because Java provides garbage collection for unused objects. Exceptional conditions in traditional environments often arise in

situations such as division by zero or "file not found", and they must be managed with clumsy and hard-to-read constructs. Java helps in this area by providing object oriented exception handling. In a well-written Java program, all run-time errors can be managed by the program itself.

5.7 DIFFERENT MODULES OF THE PACKAGE

The FUZCEN software package has five basic modules mentioned as follows, with main package shown in Fig. 5.5; whereas one plug-in for assessment of accuracy developed by Kumar and Ghosh (2007) , has also been used separately for assessing the accuracy of the various soft classification approaches used in this study.

i) File Module
ii) Display Module
iii) Signature Files Module
iv) Classifiers Module
v) Help Module

5.7.1 DATA INPUT MODULE OR FILE MODULE

This module provides various options related to reading, display and saving of file operations. One of the unique aspects incorporated regarding reading of a file is that any number of bands in a file can be read simultaneously. Thus, high dimensionality data sets can be read and displayed on the screen. This system reads the input multi-spectral image in a generic file (Band Interleaved by Line) BIL format and extracts the rows/columns information from corresponding header file. As different remote sensing satellites have multi-spectral data in different bands as well as different rows/columns, the system dynamically allocates memory to its variables. The GUI of the main window of the package with input data file module is shown in Fig. 5.6. This module has three options, i.e., **OPEN** for opening a file, **SAVE** for saving file information and **EXIT** provides the way to leave the program.

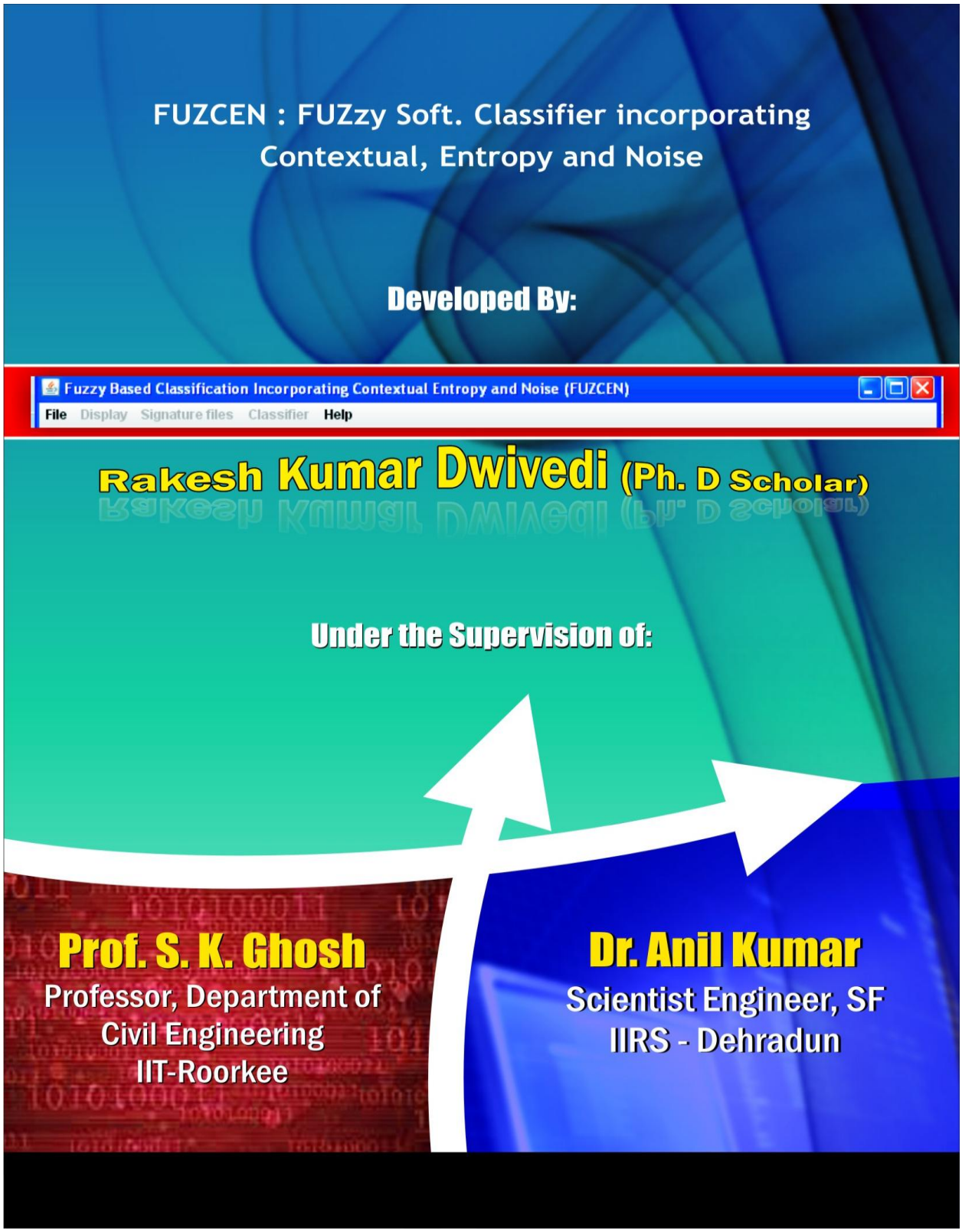

Fig 5.5: The front window of FUZCEN package.

5.7.2 DISPLAY MODULE

This module has three operations, namely, **FCC** for generation of false colour composite, **ENHANCEMENT** for linear enhancement, **ZOOM IN AND ZOOM OUT** for displaying image at different zoom factor. The FCC option allows the user to create a False Colour Composite, while Zoom in and Zoom out allows the user to enlarge or reduce the image view respectively. Both Zoom operations can also be performed with right mouse button, or alternately from the dropdown menu box. The enhancement function allows the user to carry out a simple linear enhancement in order to have a good contrast of the image, while collecting reference data information. As the mouse is moved over the displayed image, the row and column of that pixel is displayed. Fig 5.7 shows the GUI of DISPLAY module.

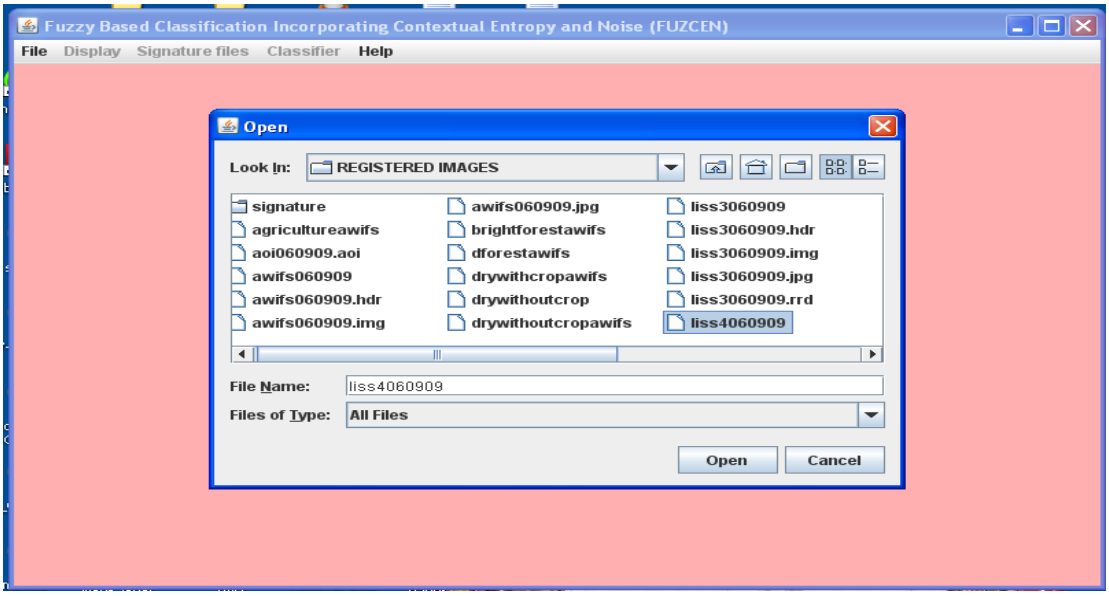

Fig 5.6: The main window of the package with file module.

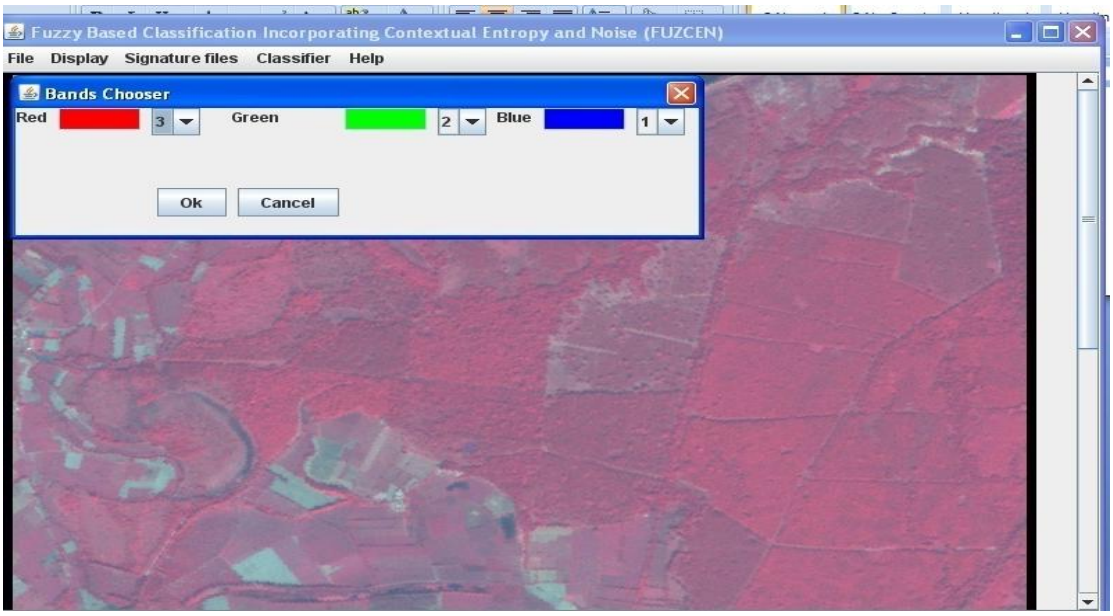

Fig 5.7: GUI of display module.

5.7.3 SIGNATURE FILES MODULE

This module allows the user to create of reference data, both pure and mixed in nature. The reference data can then be used for any of the ten sub-pixel classifiers as provided in FUZCEN package. The signature option, allows the user to collect pure reference pixels so that it can be used as an input by any of the sub-pixel classifiers provided in this package. Fig 5.8 shows the GUI for various options available for collecting pure signature data.

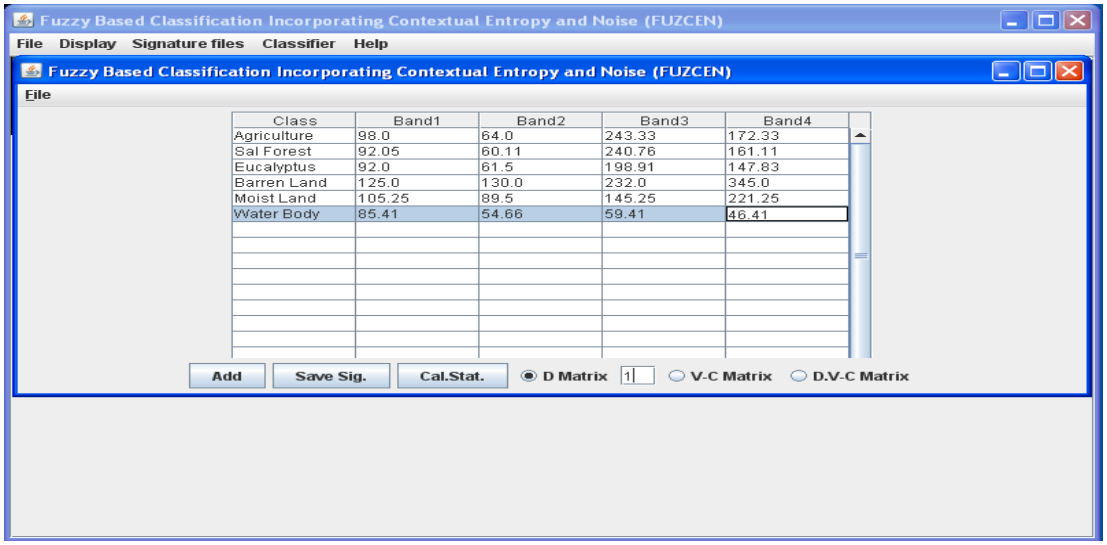

Fig 5.8: Sample training statistics for pure signatures

The **ADD** button allows the user to collect the training data for each class, one by one, by moving the mouse over the desired area or region. In this manner, more areas can be defined for the same class. After all desired training sites for a class has been identified, the same is saved into a file by pressing the **SAVE SIG** button. This process is repeated for the other classes. Now the training data statistics can be computed by pressing the **CAL STAT** button. Fig 5.8 also shows the training statistics of various classes.

Further, amongst a number of *A*-norms available, three norms, namely, Euclidean, Diagonal and Mahalonobis norms, each induced by specific weight matrix have been incorporated in D-Matrix, V-C Matrix and D.V.C Matrix respectively. However, in this study only D-Matrix with value 1 has been used for the classification of satellite imagery.

5.7.4 CLASSIFIER MODULE

This module is the main module of this software package. It provides the options of classifying the input image on the basis of the training data sets described in Section 5.7.3. In this module three fuzzy set based soft classifiers namely FCM, PCM and NC, two entropy based hybrid with fuzzy and five contextual and entropy based soft hybrid classifiers has been incorporated. There is also an option for saving the membership values generated through sub-pixel classifier option using any ten combination of classification algorithms incorporated in the FUZCEN package. Sub-pixel classification option is shown in Fig. 5.9. As mentioned in Fig. 3.1, following classifiers from three different theories have been implemented in this study.

i) Fuzzy set theory based soft classifier
   a) Fuzzy *c*-Means (FCM) classifier.
   b) Possibilistic *c*-Means (PCM) classifier.
   c) Noise Clustering (NC) classifier

ii) Fuzzy Entropy based soft classifier
   a) FCM with entropy classifier.
   b) NC with entropy classifier.

iii) Contextual and Entropy based soft classifiers.
   a) FCM with contextual classifier

b) PCM with contextual classifier

c) NC with contextual classifier

d) FCM with entropy with contextual classifier

e) NC with entropy with contextual classifier

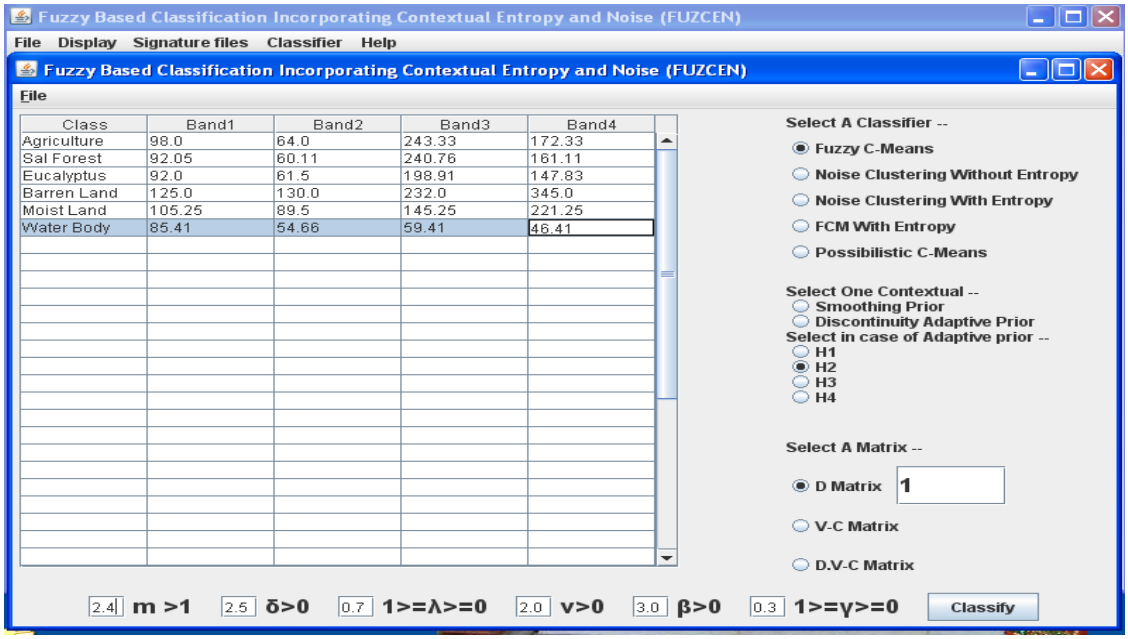

Fig 5.9: The main classification window with different classification algorithm

5.7.4.1 FUZZY SET BASED CLASSIFICATION METHOD

The coding of FCM, PCM and NC classifier is based on the mathematical formulations given in Section 3.2.1, 3.2.2 and Section 3.2.3 of Chapter 3 respectively. For the supervised mode of FCM, only *A*-norm and weighting exponent *m* are required. After getting these parameters, the iterative classification process starts until the least square error is minimized or the number of iteration is over. In supervised mode, the class membership and cluster centers are directly computed from Eq 3.2 and Eq 3.3 for pure training pixels respectively. In this study, FCM algorithms have been incorporated in supervised sub-pixel classification mode and training data has been incorporated as pure pixels using Euclidean weighted norm as shown in Fig. 5.10. The flow diagram of FCM classification algorithm is shown in Fig. 5.11.

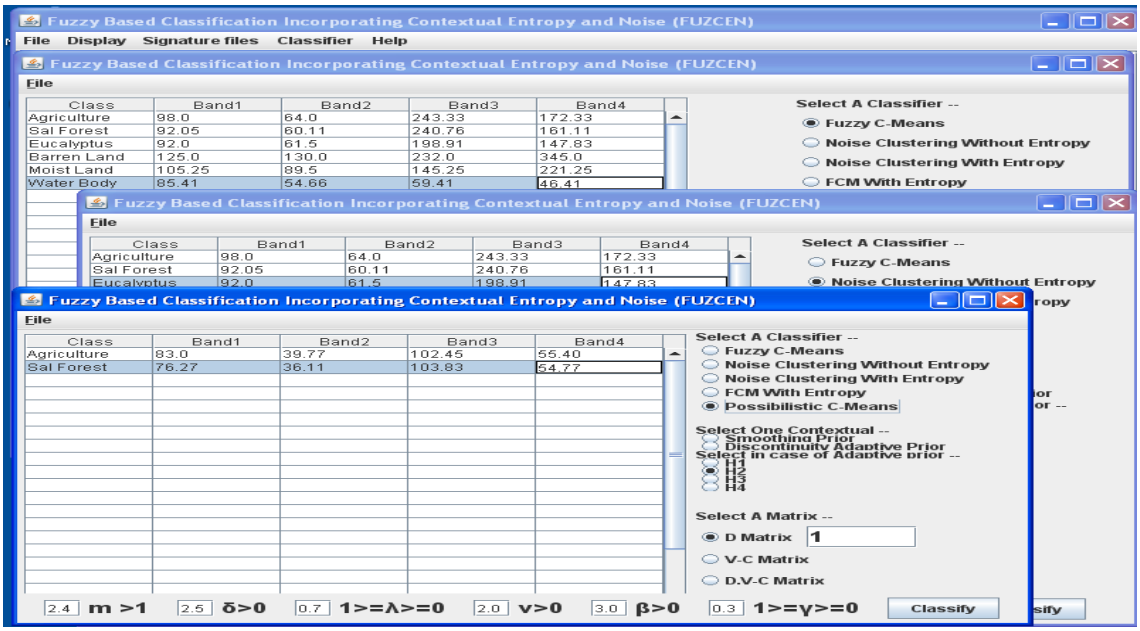

Fig 5.10: FCM, PCM and NC classifier using Euclidean weighted norm

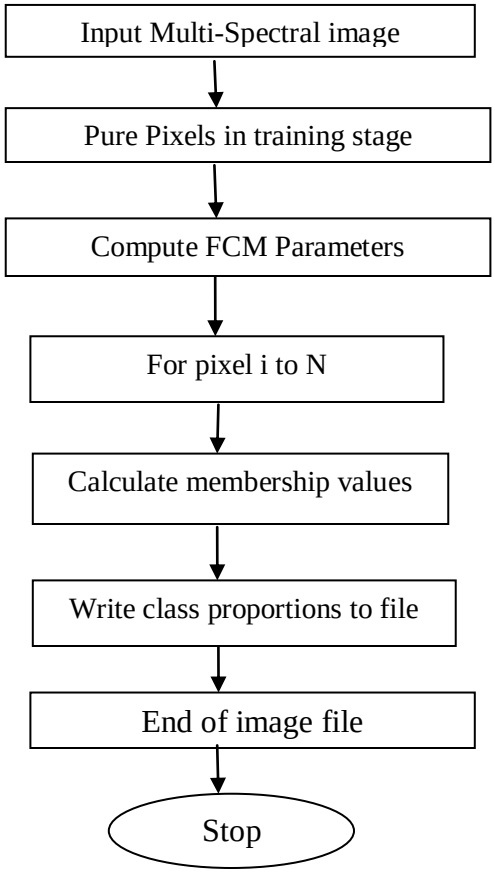

Fig. 5.11: Flow chart of FCM classifier in supervised mode

In PCM, it is also required to compute value of the parameter η_j (Eq 3.9). The value of η_j is computed from the training data in supervised mode. The sequence of operations to classify remote sensing images using PCM is shown in Fig. 5.10 and the flow diagram of PCM classification is shown in Fig. 5.12.

The dialog boxes for running supervised FCM and PCM classifier are shown in Fig 5.10. There are three options for selecting the norm i.e. D Matrix for Euclidean, V-C Matrix for Diagonal and D.V.C Matrix for Mahalonobis norms. Since, these classifiers are iterative in nature, so number of iterations, and weighting exponents and limiting error parameters are provided as an input parameter. To execute algorithm in supervised mode, three basic inputs are required i.e. number of classes, value of weighting exponent (m) and training data along with the input image file type. After receiving all these input parameters, the membership values are computed using Eq 3.1 and Eq 3.5 respectively for FCM and PCM classifiers.

While performing experimentation for FCM and FCM classifier, the value of weighting exponent or Fuzzifier (m) has been iterated between 1.0 to 4.0 with an increment of 0.1. The output has been recorded in form of fraction image for respective classes. On the basis of fraction images, membership values and accuracy indices are computed. The sequence of operation starts with the opening of a satellite image along with its signature data, after which the *A*-norm has to be selected; and the non-negative value of 'm' are assigned in order to carry out FCM and PCM classification in supervised mode.

In a nutshell, the supervised classification approach, where the analyst supervises the pixel categorization process by specifying, to the computer algorithm, numerical descriptors of the various lands cover types present in the scene. Representative samples are used to compile a numerical interpretation key that describes the spectral attributes for each feature type of interest. Each pixel in the data set is then compared numerically to each category in the interpretation key and labelled with the name of category it resembles. The final result is in the form a fraction image which is stored such that each pixel has a class assigned to it.

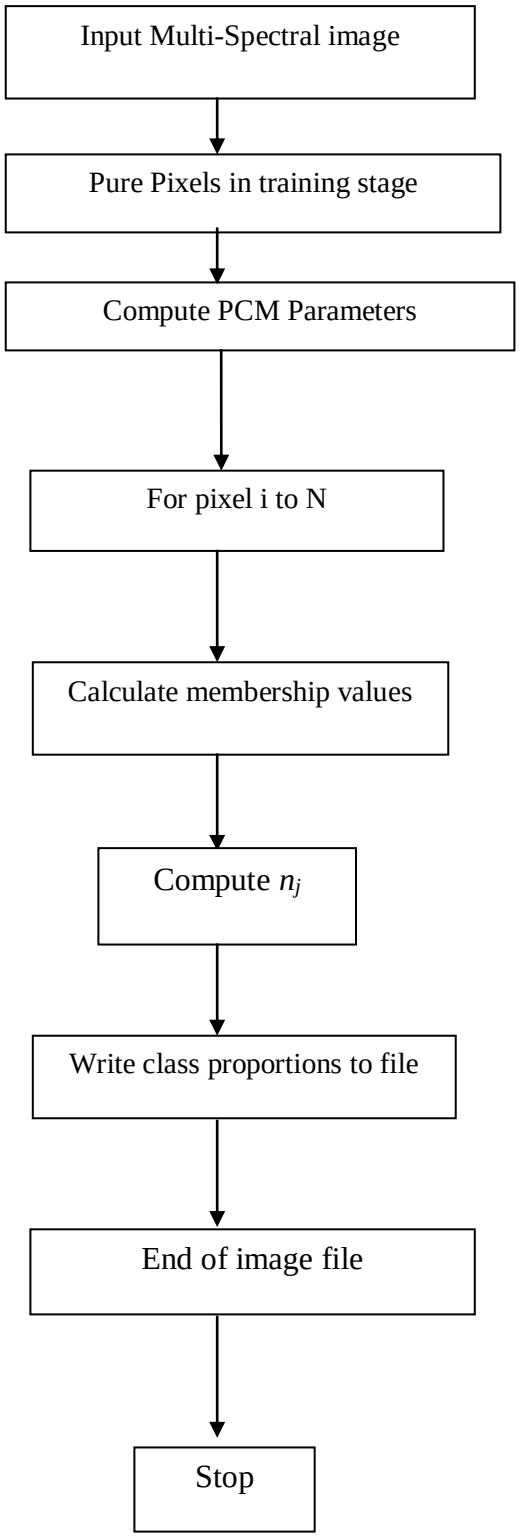

Fig. 5.12: Flow chart of PCM classifier in supervised mode

Fig 5.10 shows the dialog box of executing supervised NC classifier. There are three options for selecting the norm i.e *A*- norm is represented by D Matrix for Euclidean, V-C Matrix for Diagonal and D.V.C Matrix for Mahalonobis norms. Since, this classifier is also iterative in nature, so a number of iterations and fixed optimized value of weighting exponents, limiting error parameters are provided along with the value of spatial resolution parameter (δ) is specified in the input text box. To execute algorithm in supervised mode, three basic inputs are required i.e. number of classes, value of weighting exponent (m), spatial resolution parameter (δ) and training statistics along with the input image file type. After receiving all these input parameters the membership values are computed using Eq 3.12 for NC classifiers.

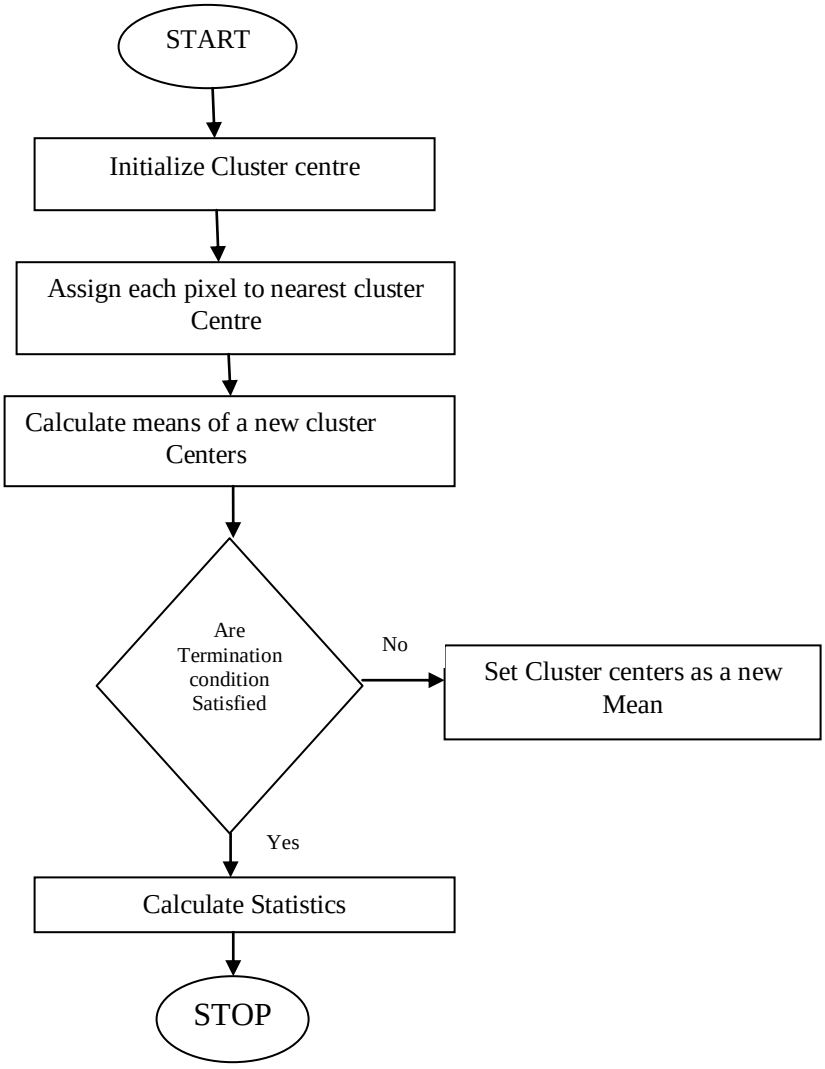

Fig. 5.13: Flow chart of NC classifier in supervised mode

While executing NC classifier, a optimized value of weighting exponent or Fuzzifier (m) is provided as a first input parameter, after which the spatial resolution parameter (δ) is iterated between 1.0 to 10^6 with an increment of 10. The output has been recorded in form of fraction image for respective classes of interest. On the basis of fraction images, membership values and accuracy indices are computed in order to optimize value of spatial resolution parameter (δ). The flow diagram of NC classification is shown in Fig. 5.13.

5.7.4.2 FUZZY AND ENTROPY BASED CLASSIFICATION METHOD

After pre-processing and training dataset collection, the AWiFS and LISS-III images are separately classified FCM with entropy and NC with entropy classifier. Later on the fraction images of both algorithms are validated with respect to soft reference dataset generated from finer resolution dataset. For accuracy assessment, different operators has been used as defined by Silván-Cárdenas and Wang (2008). All the three datasets AWiFS, LISS-III and LISS-IV are geometrically corrected with RMSE <1/3 of a pixel and resampled using nearest neighbour resample method at 60m, 20m and 5m spatial resolution, respectively to maintain the correspondence of a AWiFS pixel with specific number of LISS-III pixels (here 9 LISS III pixels correspond to one AWiFS pixel), while 144 LISS-IV pixels correspond to one AWiFS) with respect to sampling during accuracy assessment. Training data set was collected from the AWiFS imagery with reference to toposheet of the same area. For each of the six classes, 40 pixels were selected as sample according to 10*n* approach (Jensen, 1996) to train the classifiers. For accuracy assessment 100 pixels per class were randomly selected from corresponding classified and reference images, as Congalton (1991) recommended that number of samples for accuracy assessment should be large enough than that of training samples. The flow chart of FCM with entropy and NC with entropy classifiers is shown in Fig. 5.15.

Fig 5.14 shows the dialog box shows for executing supervised NC with entropy and FCM with entropy classifier. Since, this classifier is also iterative in nature, so numbers of iterations, and an optimized value of resolution parameter (δ), limiting error parameters are provided along with the varying value of regularizing parameter *(ν)* as specified in an input text box. To execute algorithm in supervised mode three basic inputs are required i.e. number of classes, value of resolution parameter *(δ)*, spatial regularizing parameter *(ν)* and training statistics along with the

input image file type. After receiving all these input parameters, the membership values are computed using Eq 3.19 and 3.23 for NC with entropy and FCM with entropy classifiers respectively.

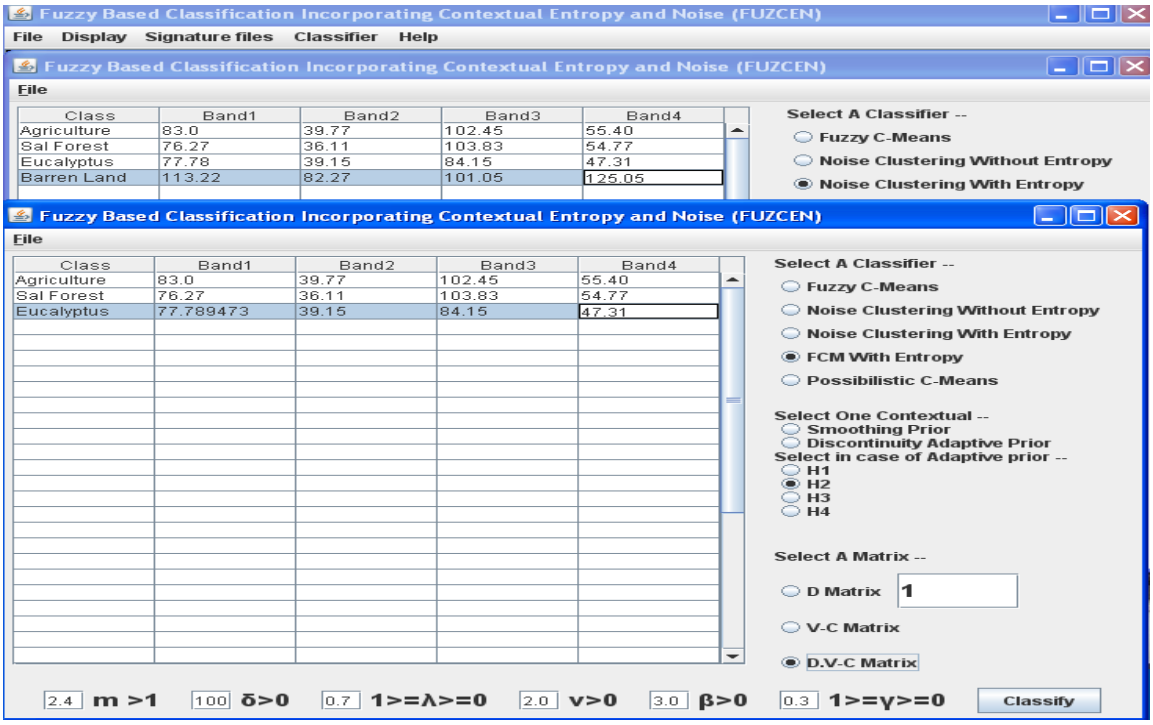

Fig 5.14: General working of FCM and NC with entropy classifier in FUZCEN package

While carrying out classification using FCM with entropy and NC with entropy classifier the optimized value of weighting exponent or Fuzzifier (m) is provided thereafter the regularizing parameter (ν) is iterated between 1.0 to 10^9 with an increment of 10. The output has been recorded in form of fraction image for respective classes of interest. On the basis of fraction images generated, membership values and accuracy indices are computed in order to decide the optimized value of regularizing parameter (ν) for FCM with entropy classifier. In case of NC with entropy the optimized value of resolution parameter *(δ)* has been provided as a first input.

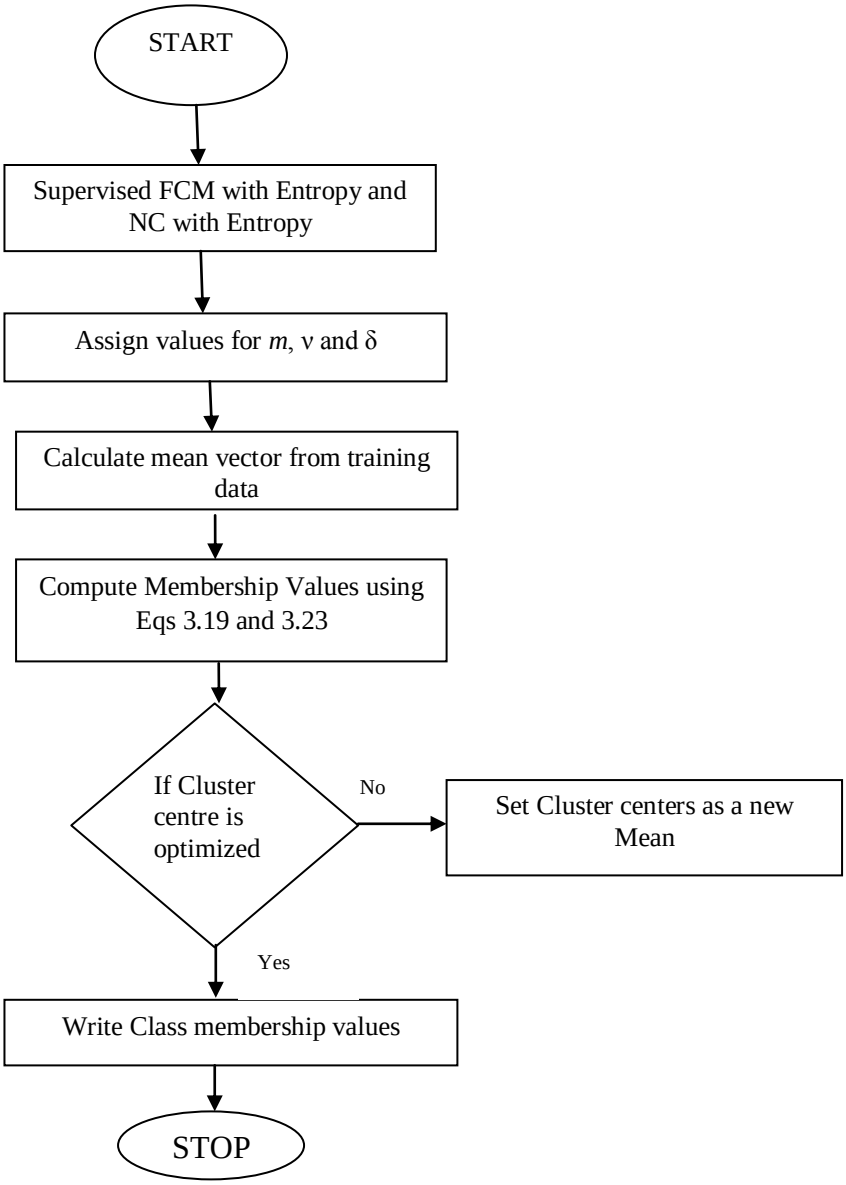

Fig 5.15: Flow chart of FCM and NC with entropy classifier

5.7.4.3 ENTROPY AND CONTEXTUAL BASED HYBRID CLASSIFICATION METHOD

To enhance the classification performance, contextual information is added in FCM, PCM, NC, NCWE and FCMWE classifier. In contextual and entropy based hybrid classification approach the optimized values of weighting exponent *(m)*, spatial resolution parameter *(δ)* and regularizing parameter *(ν)* are provided as input parameters; after which experiments are conducted to further optimize initial (T_o) and final temperature (T_f), smoothness parameter *(λ)*, weight for neighbours

(β) and interaction range parameter *(γ)* for FCM with contextual, PCM with contextual, NC with contextual, NC with entropy with contextual and FCM with entropy with contextual classifier. The classification approach using FUZCEN software package is shown in (Fig. 5.16).

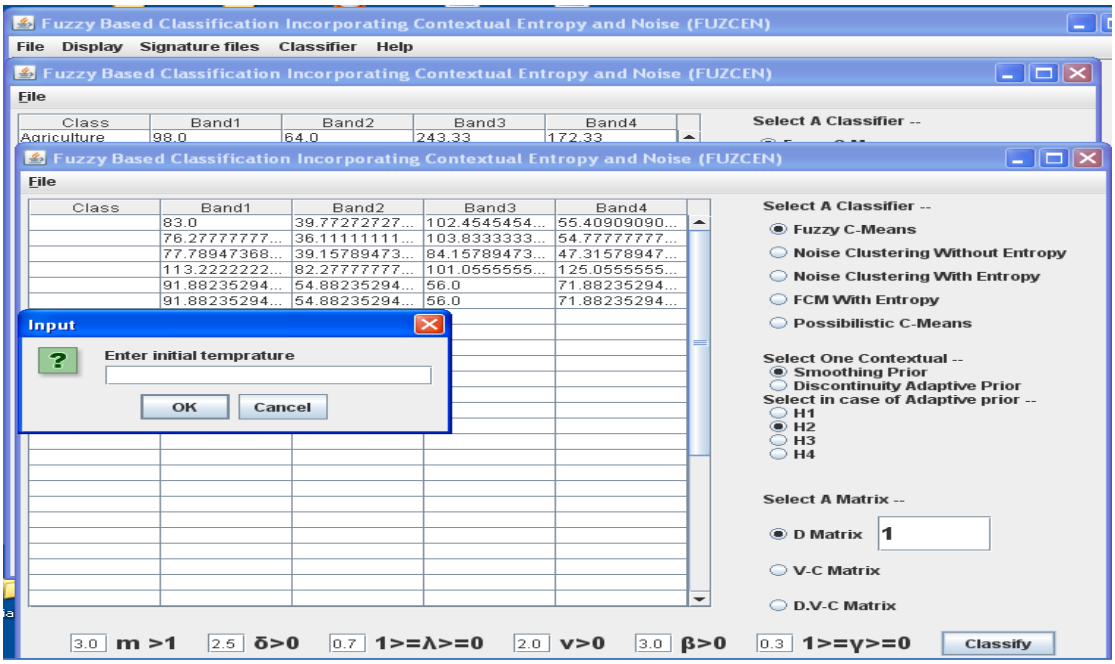

Fig. 5.16: General working model of contextual classifier in FUZCEN package

To execute contextual based algorithms in supervised mode, three basic inputs are required i.e. the optimized values of weighting exponent *(m)*, spatial resolution parameter *(δ)* and regularizing parameter *(ν)* are being used as an input parameter for FCM/PCM with contextual, NC with contextual and FCMWE/NCWE with contextual classifier respectively. In case of Smoothness prior, first optimize initial (T_o) and final temperature (T_f), smoothness parameter *(λ)*, weight for neighbours *(β)* to classify the input image. However, in case of DA prior, first optimize initial (T_o) and final temperature (T_f), smoothness parameter *(λ)*, and interaction range parameter *(γ)* to classify the image using FCM with contextual, PCM with contextual, NC with contextual, NC with entropy with contextual and FCM with entropy with contextual classifier. The flowchart of contextual approach is shown in Fig. 5.18.

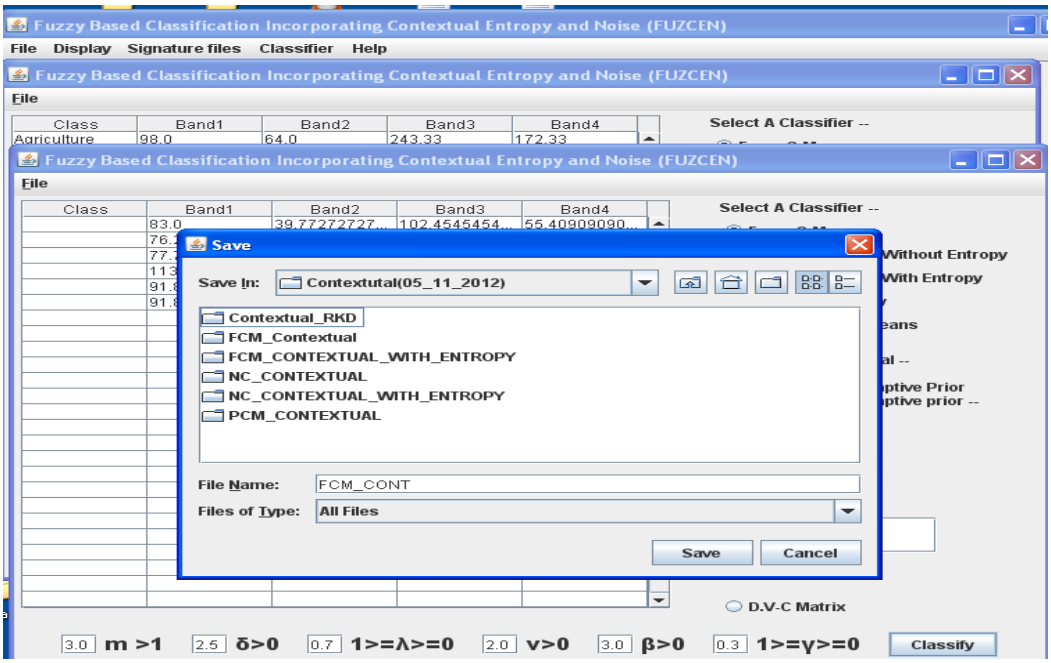

Fig 5.17: Dialog box with contextual classifier of output generation.

To perform execution of various hybrid models with contextual, which in-turn is divided into two stream, first one is called Smoothness prior, wherein our objective is to optimize the initial and final temperature parameters (T_0 and T_f) along with smoothness parameter *(λ)*, weight for neighbours (*β*). Further, the experimentation has been performed for the following values of (*λ*) i.e. $0.1 \leq \lambda \leq 1.0$, with interval of 0.1 and weight for neighbours (*β*) has been tested between 0.5 up to 6.0, i.e. $0.5 \leq \beta \leq 6.0$. The another stream of contextual is called discontinuity prior model wherein four DA priors (H1,H2,H3,H4) have been tested and smoothness parameter *(λ)* along with interaction range parameter *(γ)* have been optimized. The range of *(γ)* is lying between 0 and 1, wherein classification experiment has been performed for the following range i.e. $0.1 \leq \gamma \leq 1.0$, to identify the optimized value of interaction range parameter *(γ)*.

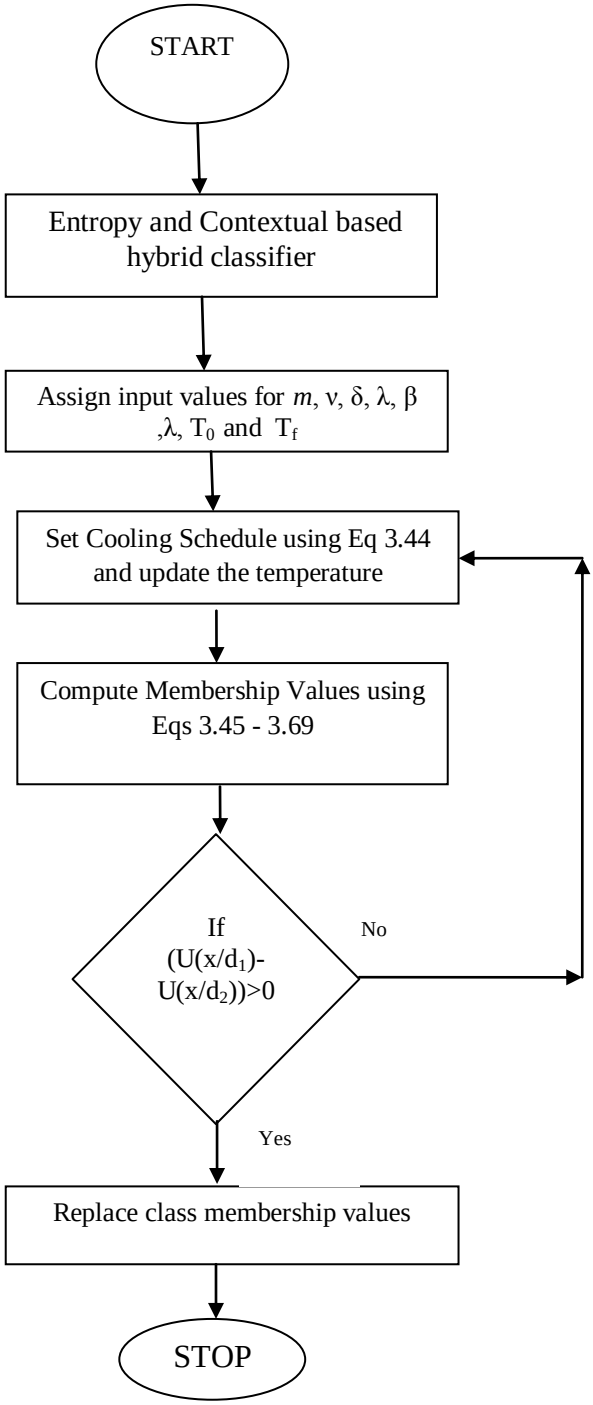

Fig 5.18: Flow chart of contextual and entropy based hybrid classifiers

5.8 SUMMARY

In this chapter, the overall methodologies of the work along with the execution model of various classification approaches are incorporated in this study have been provided. All hybrid approaches of soft classification has been executed using FUZCEN software package and results are obtained in form of class wise fraction images along with the text files which specifies all the accuracy indices of FERM and SCM. A complete data analysis and results of all the approaches incorporated in this study is provided in next chapter.

CHAPTER 6

DATA ANALYSIS AND RESULTS

"Building Insight. Breaking Boundaries"-Elseiver

6.1 INTRODUCTION

In this chapter, a detailed discussion on the results obtained from various studies as outlined in Chapter 3 and Chapter 5 are given. The analytical investigations have been carried out on multi-spectral remote sensing datasets as described in Chapter 4. All the analysis have been carried out using *FUZCEN: Fuzzy Soft Classification incorporating Contextual, Entropy and Noise* package as described in Chapter 5. To understand and demonstrate the efficiency and the capability of the Fuzzy based, Entropy based and Contextual based classification methods developed in this study, it is pertinent to perform the accuracy assessment and review the results. Therefore, as stated in Section 3.6of Chapter 3, various methods have been employed for the same. All the results obtained from different classifiers have been discussed as outlined below. Section 6.2, 6.3and 6.4 describes the results obtained from Fuzzy set based classifiers i.e. FCM, PCM and NC respectively, while Section 6.5 and 6.6 describes the results of Fuzzy and Entropy based classifiers i.e. FCM with entropy, and NC with entropy. Section 6.7, 6.8, 6.9, 6.10 and 6.11 describes contextual and entropy based classifiers i.e. FCM with contextual, PCM with contextual, NC with contextual, FCM with entropy with contextual and NC with entropy with contextual classification algorithms respectively.

In this study, assessment of accuracy has been carried for all the classification results based upon fuzzy set theory, entropy theory and contextual. Since, there is no commercially available tool to assess the accuracy of the sub-pixel classified output. Thus a JAVA based in house tool *FUZCEN* has been used for classification and assessment of accuracy purpose. It works on the basis of random sampling approach. As per the Congalton's rule (1991), 75 to 100 pixels per class have been considered while generating testing data. The fuzzy based accuracy measures used in this study namely FERM and SCM also follows the mean aggregation method

to bring the reference dataset at the same scale of classified datasets (Binaghi et al., 1999, Silvan and Wang, 2008). Once the reference dataset has been brought at the scale of classified images, different accuracy measurement techniques such as FERM and SCM have been used. In order to measure the uncertainty in the image classification, entropy method has been utilized.

In a nutshell, the following fuzzy based accuracy measures namely FERM, SCM, MIN-MIN, MIN-PROD, and MIN-LEAST operator has been used to assess the accuracy of fraction images derived from different hybrid classification approaches.

6.2 RESULTS OF FUZZY *C*-MEAN (FCM) CLASSIFIER

In this study, FCM is the first classifier which has been taken for consideration. It has been observed that the performance of the FCM classifier depends upon the value of the weighting exponent or Fuzzifier (*m*). To obtain the best result from this classifier, the optimization of *m* is important, since the value of *m* is directly related to class membership. For a good classification, the membership value of a particular class should be high while its corresponding entropy value be minimum. In order to determine the optimum value of weighting exponent *m* the following measures have been adopted:

i) Class membership based upon mathematical formulation of FCM.

ii) Producer's accuracy has been computed to determine the class based optimized value for classification.

iii) Image to image assessment of accuracy for soft classification using FERM, SCM, MIN-MIN, MIN-LEAST and Entropy techniques.

6.2.1 CLASS MEMBERSHIP OF FCM CLASSIFIER

Fig. 6.1 (a), (b) & (c) shows the variation of weighting exponent *m* with class membership for different classes such as agriculture, sal forest, eucalyptus plantation, barren land, moist land and water body of IRS-P6 for AWIFS, LISS-III and LISS-IV dataset

respectively. For all the three datasets, class membership has been generated for the different values of *m* ranging from 1.1 to 4.0 at an interval of 0.1. The class membership values of a pixel denote the class proportions, which in turn may represent the soft classified output for a pixel. It has been observed from the Fig. 6.1 (a), (b) &(c) that for *m* =1.8 to 3.2, the class membership lies between 0.80 to 0.99. According to Pal and Bezdek (1995) and Chen and Lee (2001), the value of *m* should be in between 1.3 to 2.5.

The class membership 'μ' increases till *m*=2.5, and thereafter the membership value starts to decrease or almost becomes constant {Fig. 6.1(a), (b), (c)}. Thus, as per class membership, the optimum value of *m* for FCM lies within the range of 1.8 to 3.2 for AWiFS, LISS-III and LISS-IV datasets. However, in this study, the optimization of a parameter for the classification would be analyzed and verified via entropy method and the classification performance is assessed using sub-pixel accuracy indices such as FERM, SCM, MIN-MIN, MIN-LEAST and Fuzzy Kappa coefficient.

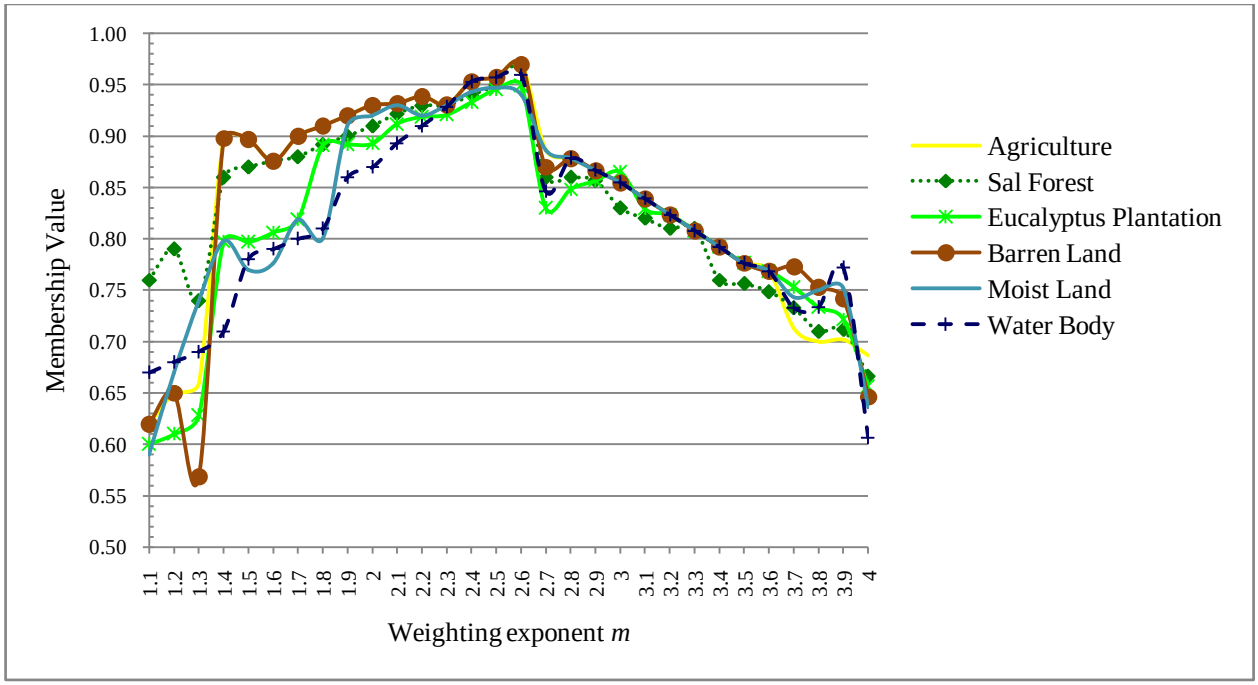

Fig. 6.1(a) Class membership for FCM classifier using AWiFS dataset

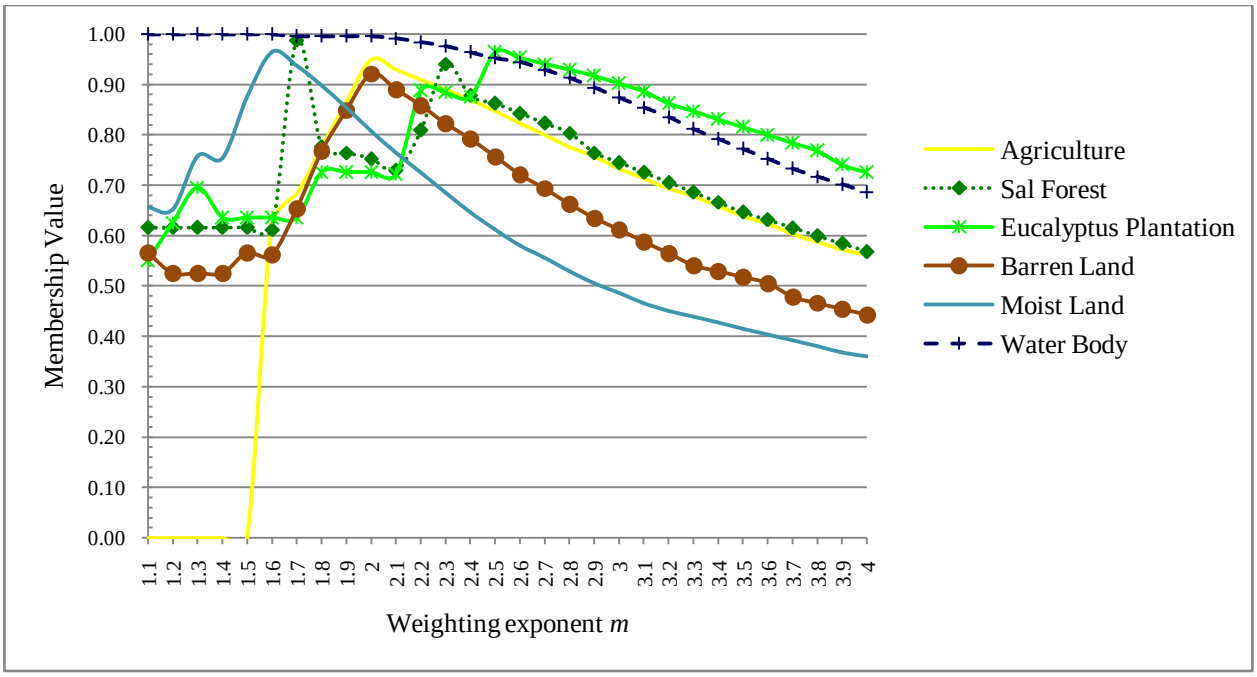

Fig. 6.1(b) Class membership for FCM classifier using LISS-III dataset

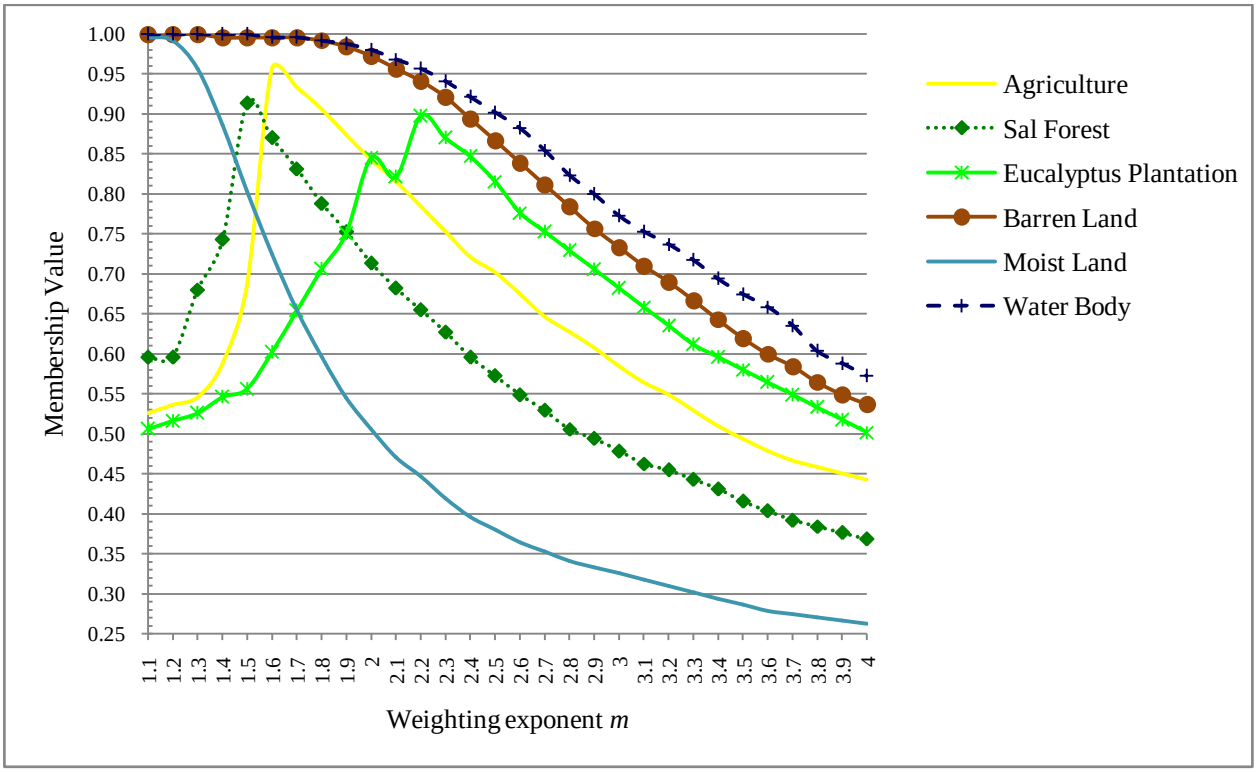

Fig. 6.1(c) Class membership for FCM classifier using LISS-IV datasets

6.2.2 ENTROPY OF FCM CLASSIFIER

Generally, the accuracy of classified images are measured by accuracy indices. However, in this study, generation of reference data for LISS-IV image was not possible due to unavailability of higher resolution image for the study area. In such cases, entropy can be used as an absolute measure of an uncertainty (Dehghan and Ghassemian, 2006). The entropy of a classified fraction images can be computed by using Eq 3.85. For a better classified output, the entropy should be low or reaches up-to the level of saturation or starts to decrease at the optimized point. As shown in Fig. 6.2 (a), (b) and (c), the computed entropy of FCM classifier for homogenous and heterogeneous land cover classes lies between the range of [0,3]. This indicates that the information of uncertainty is not exceeding more than 3%. Measuring the spatial statistics of a satellite image using entropy, for six land cover classes can be obtained by using Eq 3.85 i. e. $6*(-1/6*\log_2 1/6)=2.585$ (Stein et al., 2002).

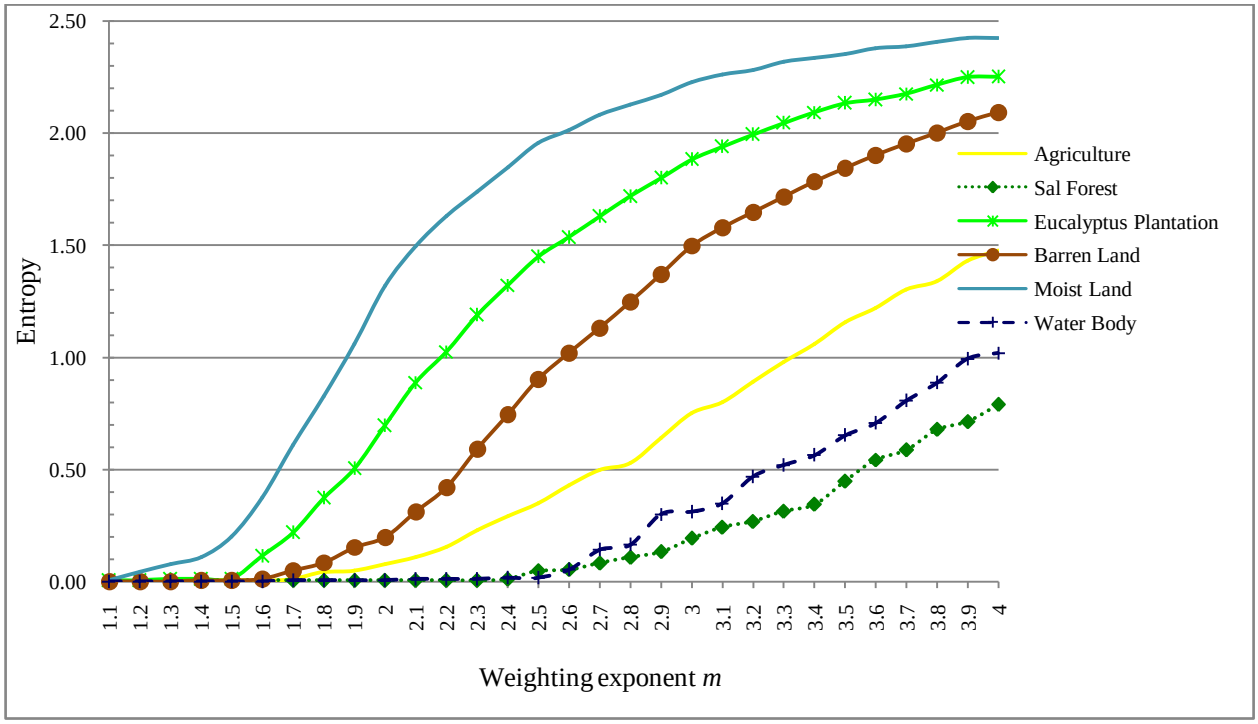

Fig. 6.2 (a): Entropy for FCM classifier using AWiFS dataset

This states that if the computed entropy values of classified image are lying within this range; then this indicates a better classification results with minimum uncertainty. It has been observed from Fig. 6.3 (a), (b) and (c) that for *m*=1.8 to 2.9 either the entropy value is low or it reaches up-to the level of saturation. This indicates that within this specified range of *m* the uncertainty is in its lower range. However, for initial *m* values for *m*=1.1 to 1.6 the entropy value is close to zero which implies that classified results are crisp, thereafter it starts to soften.

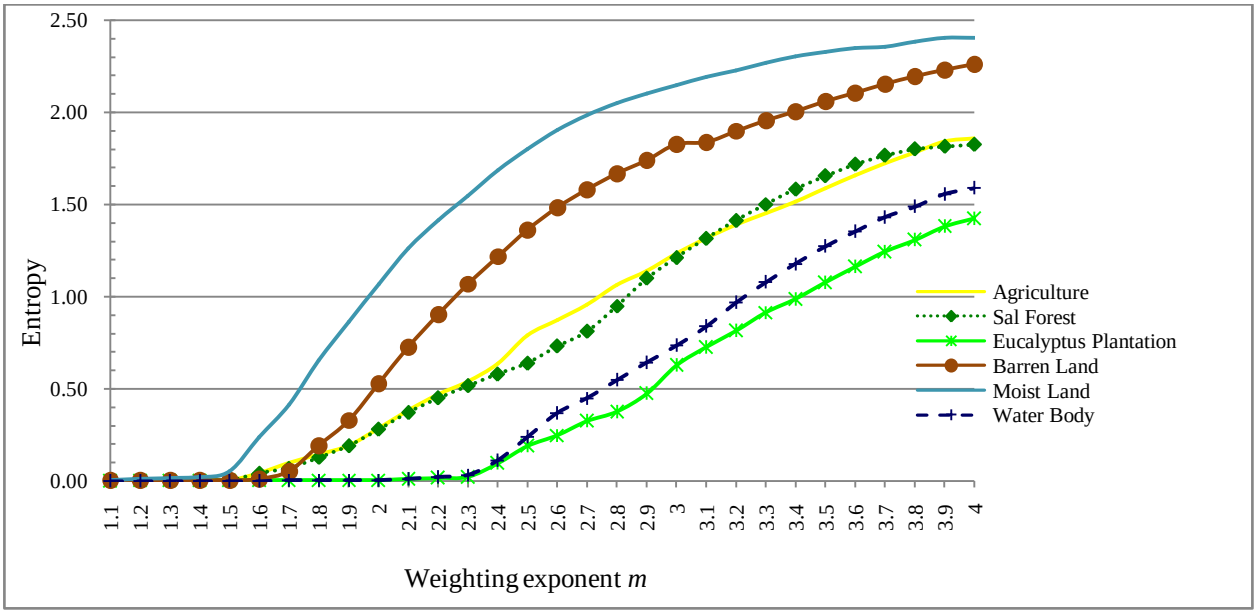

Fig. 6.2 (b): Entropy for FCM classifier using LISS-III dataset

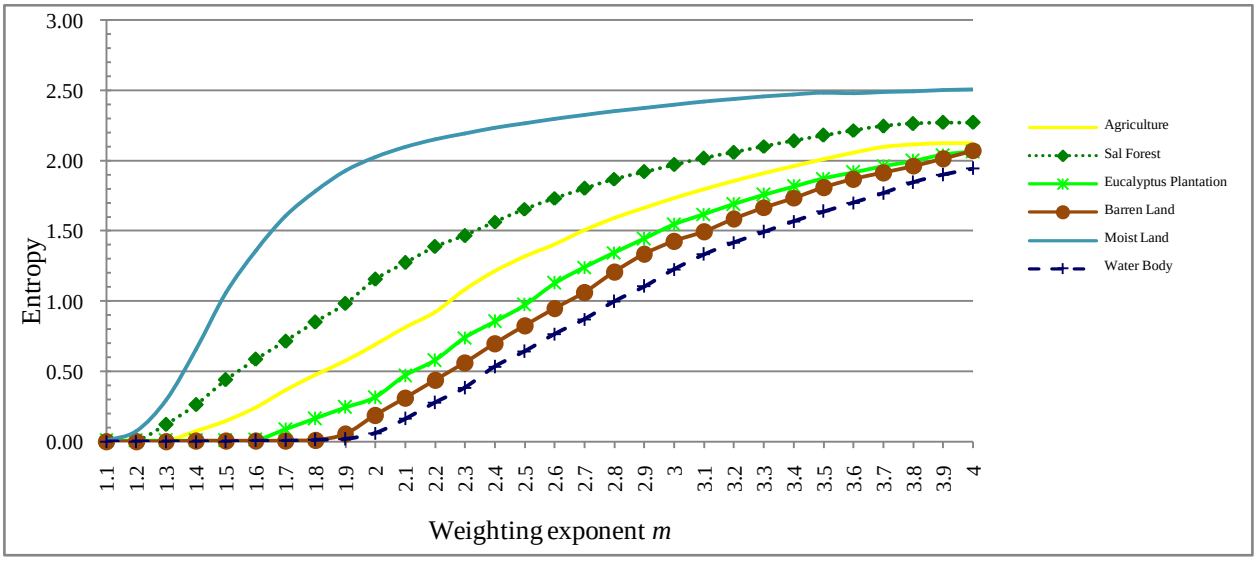

Fig. 6.2 (c): Entropy for FCM classifier using LISS-IV dataset

6.2.3 PRODUCER'S ACCURACY OF FCM CLASSIFIER

To determine the accuracy of individual classes Producer's Accuracy (PA) has been computed for FCM classifier {Fig. 6.3 (a) and (b)}. In this case, AWiFS image have been used for classification, while LISS-III and LISS-IV images are used as a reference image to determine the Producer Accuracy. It is observed that for *m*=2.4 to 2.6, FCM classifier produces highest accuracy for all six land cover classes present in the image.

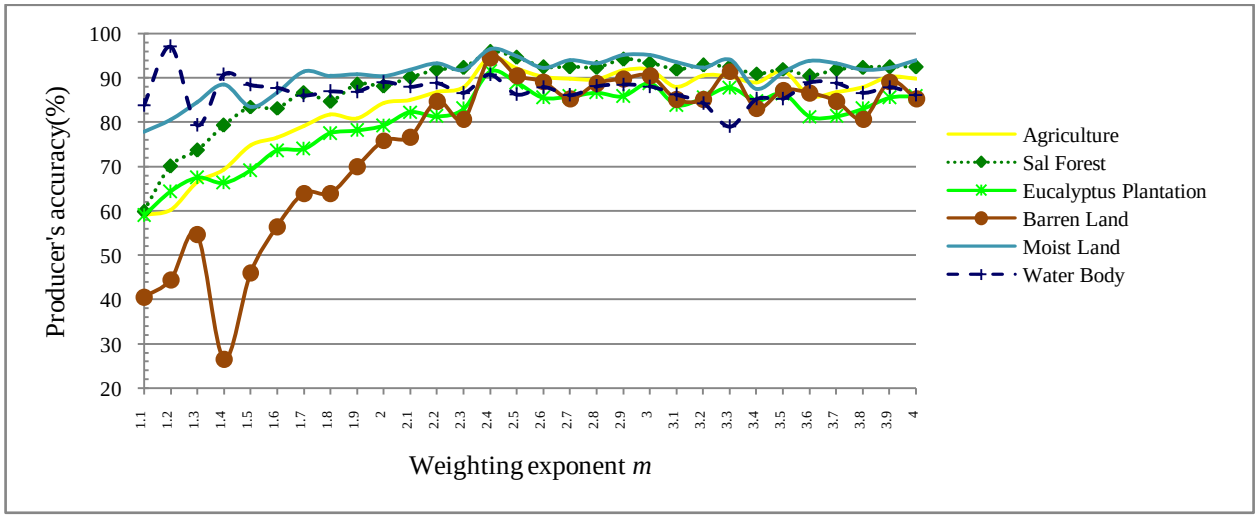

Fig. 6.3(a): Producer's accuracy of FCM classifier for AWiFS dataset using LISS-III as reference dataset.

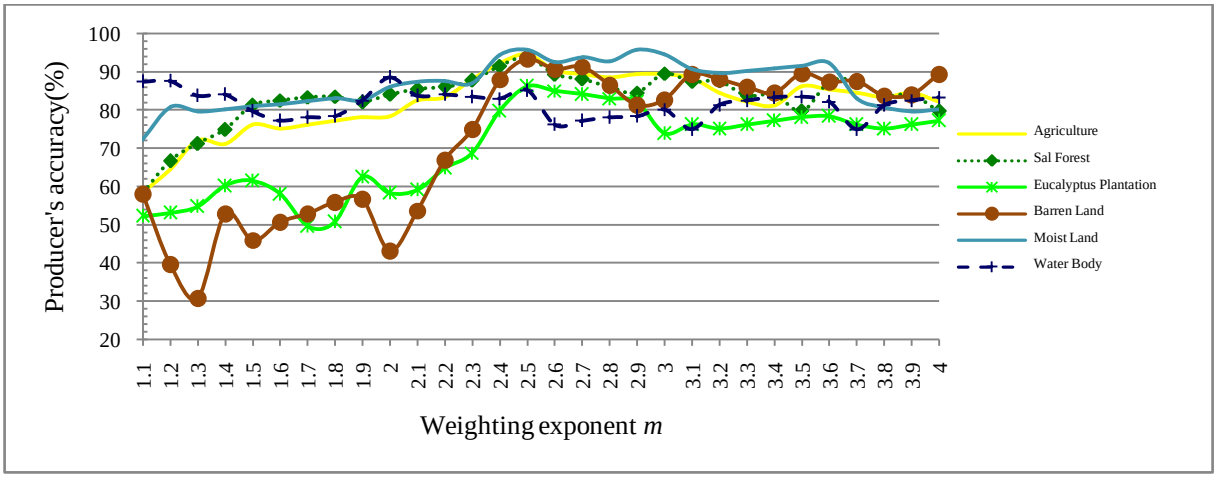

Fig. 6.3(b): Producer's accuracy of FCM classifier for AWiFS dataset using LISS-IV as reference dataset.

6.2.4 CLASS WISE PARAMETER OPTIMIZATION OF FCM CLASSIFIER

On the basis of highest class membership, lower entropy and highest producers accuracy produced by classified imagery, class wise optimized values of weighting exponent *m* have been shown in Table 6.1. It is observed that irrespective of datasets, the optimized value of *m* for agriculture, sal forest, eucalyptus plantation, barren land, moist land and water body is 2.0, 2.1, 2.3, 2.2, 1.9 and 1.8 respectively.

Table 6.1: Class wise parameter optimization of weighting exponent (*m*) for FCM on the basis of class membership/Entropy and Producer's accuracy.

Class	Class membership			Entropy			Producer's accuracy		Optimized Mean Value
	AWiFS	LISS-III	LISS-IV	AWiFS	LISS-III	LISS-IV	AWiFS-LISS-III	AWiFS-LISS-IV	
Agriculture	2.6	2.0	1.6	1.6	1.6	1.6	2.4	2.5	2.0
Sal Forest	2.6	1.7	1.5	2.4	1.6	2.0	2.4	2.5	2.1
Eucalyptus plantation	2.6	2.5	2.2	2.3	2.0	1.8	2.4	2.5	2.3
Barren land	2.6	2.0	2.3	1.5	1.5	2.1	2.4	2.5	2.2
Moist land	2.5	1.6	1.1	1.2	1.3	2.1	2.4	2.5	1.9
Water body	2.5	1.6	1.4	2.0	2.1	2.0	1.2	2.0	1.8

6.2.5 GENERALIZED PARAMETER OPTIMIZATION OF FCM CLASSIFIER

To resolve the sub-pixel area allocation problem, Sub-pixel Confusion Uncertainty Matrix (SCM) has been introduced. The FCM classification algorithm has been used in supervised mode along with the Euclidian weighted norm to classify the remote sensing imagery. Results of the

Overall Accuracy of FCM classifier using LISS-III as reference data is shown in Fig. 6.4 (a). It is found that for *m*=2.6, all the accuracy measures yield a minimum of 85% accuracy. Further, MIN-LEAST operator achieves the threshold criterion of 85% for *m*=1.8.

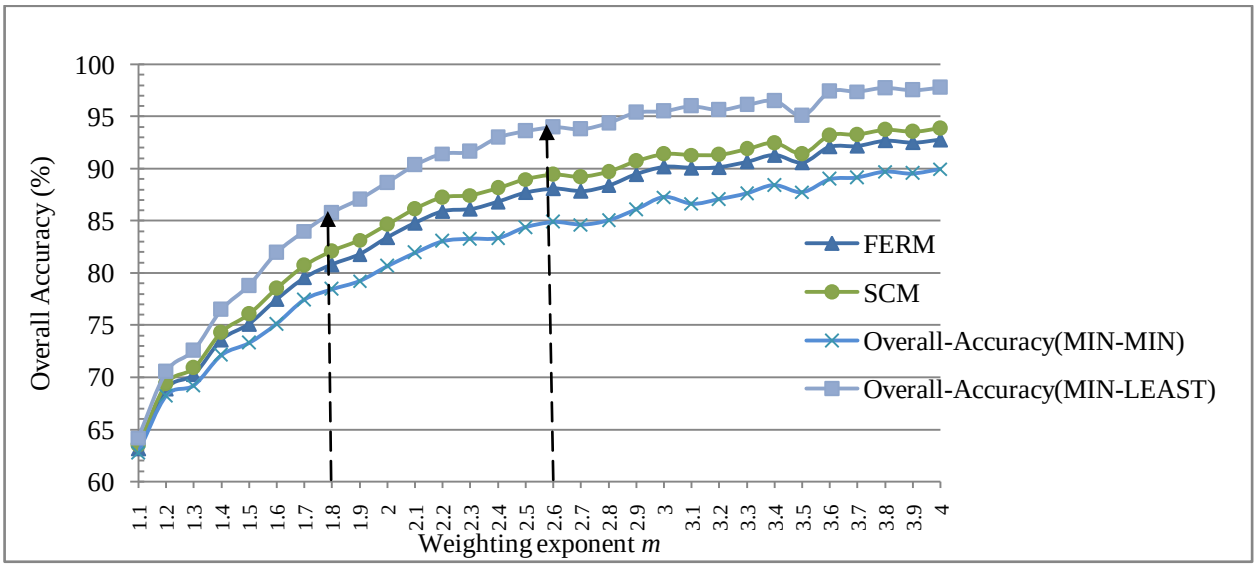

Fig. 6.4(a): Overall accuracy of FCM classifier for AWiFS dataset using LISS-III as reference dataset.

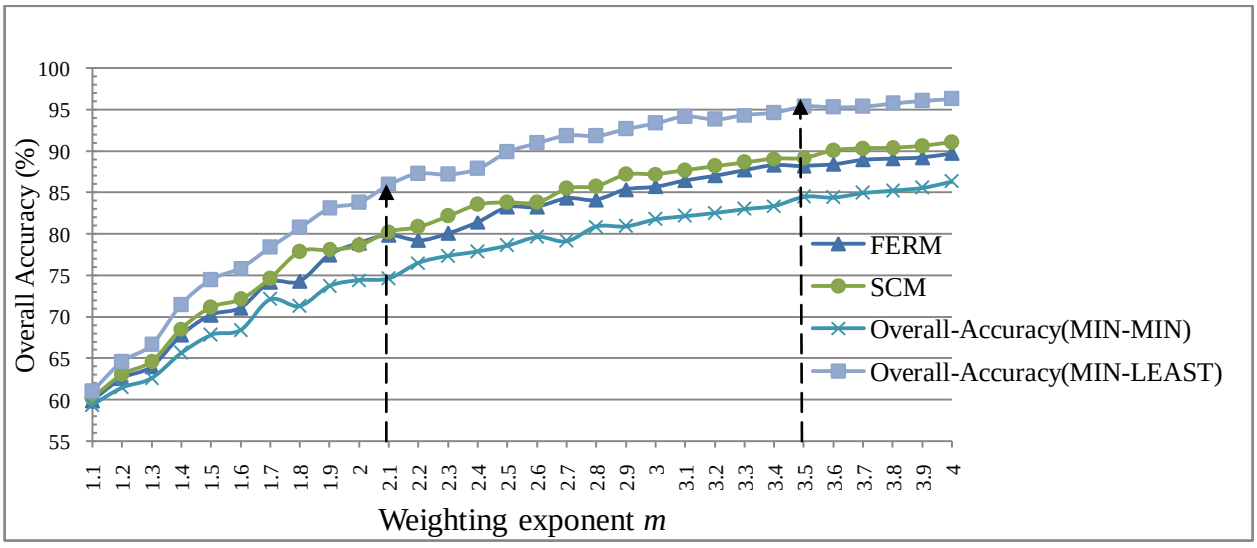

Fig. 6.4(b): Overall accuracy of FCM classifier for AWiFS data using LISS-IV as reference dataset.

The Overall Accuracy of AWiFS using LISS-IV as reference data is shown in Fig. 6.4 (b). It is observed that for *m*=3.5, all the accuracy measures yield a minimum of 85% accuracy. However, MIN-LEAST operator achieves the threshold criterion of 85% for *m*=2.1.

From Fig. 6.4 (a) and (b), the range of weighting exponent (*m*) varies from 1.8 to 3.5 corresponding to threshold criterion of 85%. Therefore, in order to determine a single optimized value for all class and independent of dataset, Chen et al. (2010), have proposed Fuzzy Kappa coefficient. The advantage of using this measure of accuracy is that overall accuracy and Fuzzy Kappa coefficient are less affected by distribution of error among classes. The Fuzzy Kappa coefficient values have been computed for SCM, MIN-MIN and MIN-LEAST operator.

The Fuzzy Kappa coefficient value of AWiFS image using LISS-III as reference data is shown in Fig. 6.5 (a). It is observed that for *m*=3.4, Fuzzy Kappa coefficient of SCM, MIN-MIN and MIN-LEAST operator yield a desired value 0.85. However, MIN-LEAST operator achieves the threshold criterion of 0.85 for *m*=2.0. Further, it is observed from Fig. 6.5 (b) that for *m*=3.4, Fuzzy Kappa coefficient for all SCM, MIN-MIN and MIN-LEAST operators yield a desired value 0.85 while MIN-LEAST operator achieves this for *m* = 2.5.

On the basis of Overall Accuracy and Fuzzy Kappa values, it is observed that it is difficult to state a single value for the optimized parameter (*m*). Thus, to resolve this situation, it may be advisable to compare uncertainty values of AWiFS using LISS-III and LISS-IV datasets.

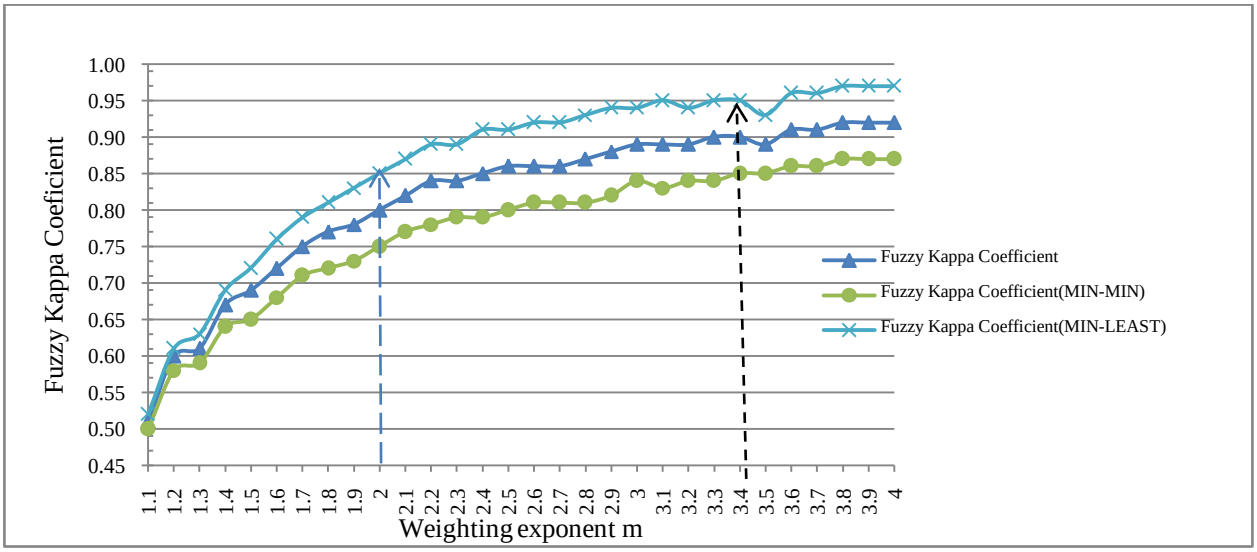

Fig. 6.5(a): Fuzzy Kappa of FCM classifier using AWiFS dataset and LISS-III as reference dataset

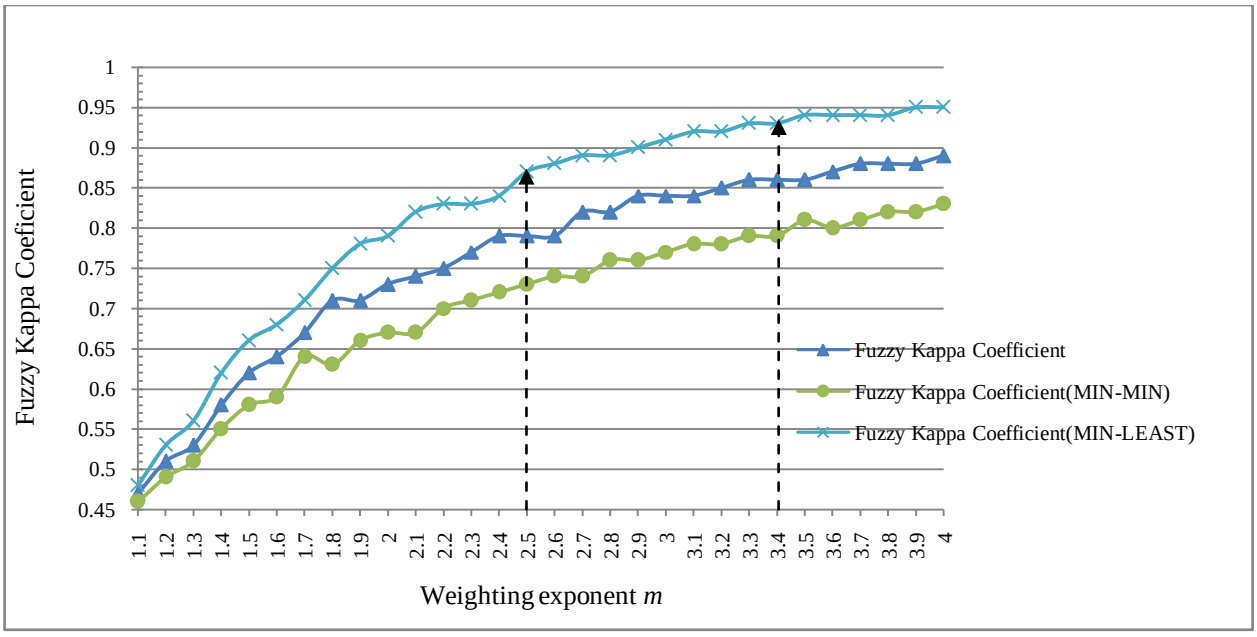

Fig. 6.5(b): Fuzzy Kappa of FCM classifier using AWiFS dataset and LISS-IV as reference dataset

From Fig. 6.6, it is found that classification uncertainty does not exceed beyond 6%, for all values of *m* ranging from 1.1 to 4.0. However, this is minimum for *m*=2.4. This indicates that the uncertainty measures of SCM, MIN-MIN and MIN-LEAST are able to distinguish between sub-pixel classifications having distinct error distributions, even though the overall accuracy is same.

The uncertainty associated with Overall accuracy signifies that the uncertainty proportion lies in the classified imagery. The uncertainty values also indicate the consistency amongst classified output. This can be seen in Fig. 6.6, where the value of weighting exponent *m* reaches to 2.1, the SCM uncertainty starts to decrease and that for optimized value of *m* =2.4, it reaches to its minimum level. This correlates the degree of mathematical correspondence between overall accuracy and Fuzzy Kappa coefficient (Chen, 2010).

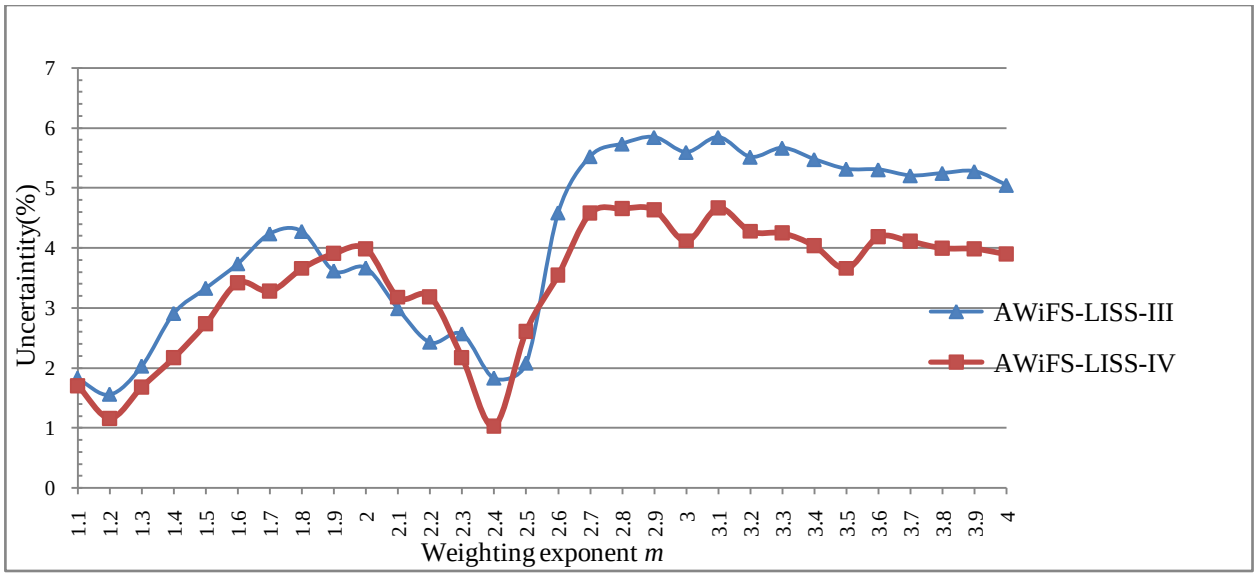

Fig. 6.6: SCM uncertainty of FCM classifier

Table 6.2 shows all the accuracy measures for the optimized value of weighting exponent *m*=2.4, where AWiFS image has been used as the classified image and LISS-IV image has been used as reference image. The Fuzzy Overall Accuracy, FERM, SCM, MIN-PROD, MIN-MIN, and MIN-LEAST of all classes are 81.45%, 83.54%, 82.41%, 77.87% and 87.87% respectively. It is observed that when LISS-III and LISS-IV data is used as reference data to classify AWiFS data, the trends of Overall Accuracy is more or less similar {Fig. 6.4(a) and (b)}. This indicates that an appropriate classification has been performed. It further strengthens the fact that FERM and SCM are suitable measures of assessment of accuracy of soft classification using soft reference data. Thus, the optimum value of *m* may be fixed as 2.4 for classification using FCM classifier. Further, when LISS-IV image is used as a reference image, the overall accuracy using MIN-LEAST increases by 0.44%, while uncertainty almost reduces by 1%. Thus, the classification trend shown by all the measures are of similar nature when LISS-III data is used as reference. It is also observed that amongst all measures of accuracy MIN-LEAST operator is found to be more suitable to assess the accuracy of FCM classifier.

Table 6.2: Accuracy values for optimized value of *m*=2.4 for FCM classifier of AWiFS data with LISS-IV as reference data

Land-Use Classes	**Accuracy assessment methods**				
	FERM	**SCM**	**MIN-PROD**	**MIN-MIN**	**MIN-LEAST**
Fuzzy User's accuracy (%)					
Agriculture	79.87	81.82±5.10	80.17	75.84	83.85
Sal forest	86.71	87.61 ±6.0	87.30	83.35	91.65
Eucalyptus plantation	90.16	93.03±1.92	92.51	89.56	91.86
Barren Land	68.56	70.90±17.35	70.49	57.94	92.20
Moist Land	61.19	63.21±7.72	60.74	51.90	72.46
Water Body	93.56	94.60±1.03	94.74	94.93	96.77
Fuzzy Producer's accuracy (%)					
Agriculture	87.52	88.90±4.90	89.14	83.44	93.11
Sal forest	87.45	89.42±3.0	89.51	84.07	92.06
Eucalyptus plantation	77.28	73.25±6.11	71.39	67.95	79.01
Barren Land	82.03	84.97±10.41	82.14	77.01	92.10
Moist Land	92.64	93.14±4.31	93.01	91.75	94.20
Water Body	77.26	83.26±9.60	78.21	74.95	87.61
Fuzzy Overall Accuracy (%)	81.45	83.54±5.83	82.41	77.87	87.87
Fuzzy Kappa	-	0.79±0.07	0.78	0.72	0.84

Fig. 6.7 shows the classified fraction images of AWiFS datasets for the optimized value of m = 2.4, generated by FCM classifier. The derived fraction images matches closely with the reference data for all classes. These images also show that the classes like agriculture, sal forest, barren land and water bodies have been correctly identified using FCM approach. The visual interpretation of classified fraction images have further strengthen the belief that soft classification technique is able to resolve the problem of mixed pixel.

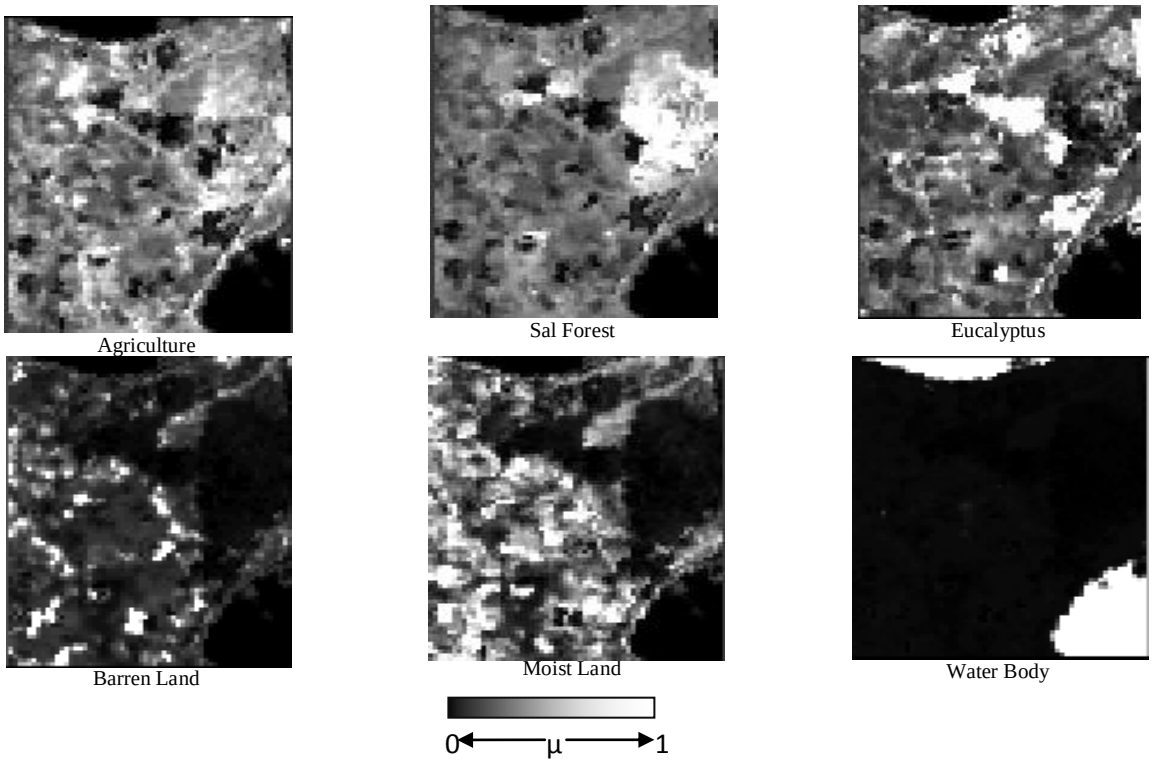

Fig. 6.7: FCM classification output of AWiFS image

6.3 RESULTS OF POSSIBILISTIC *C*-MEAN (PCM) CLASSIFIER

The main motivation behind the use of PCM relates to the relaxation of the probabilistic constraint of FCM (Eq 3.4). Therefore, one additional term called the regularizing term is added to form the objective function of PCM (Eq 3.5). The degree of fuzziness in the FCM and PCM classifier is controlled by a parameter *m* known as the weighting exponent. In past one decade, many attempts have been made to fix the value of *m* for these classifiers. Shalan et al. (2003) have suggested a value of 2.0 for *m* to produce the most accurate fuzzy classification. On the other hand, Ibrahim et al. (2005) suggested, that *m* has a fixed value of 2.3 and 2.2 for FCM and PCM respectively. However, all these analyses do not cater to all the dimensions of parameter optimization, where the analysis is based upon hard classification and accuracy using FERM only. In this study, the assessment of accuracy has been done using FERM, SCM along with entropy.

6.3.1 CLASS MEMBERSHIP OF PCM CLASSIFIER

Fig. 6.8 (a), (b) and (c) shows the variation of the weighting exponent *m* with class membership of different classes using AWIFS, LISS-III and LISS-IV datasets respectively. For all the three datasets, class membership has been generated for the different values of weighting exponent *m* ranging from 1.1 to 4.0 at an interval of 0.1. The class membership values of a pixel denote the class proportions, which in turn may represent the soft classified output for a pixel. It has been observed from Fig. 6.8 (a), (b) and (c), that for *m* =1.5 to 2.6, the class membership values lies between 0.85 to 0.99 for homogenous classes like agriculture, sal forest, and eucalyptus plantation, whereas, for heterogeneous classes barren land, moist land and water body, the class membership lies between 0.75 to 0.99. However, it has been observed that for both categories of classes produced highest class membership for *m* =2.2 to 2.4 with almost stable entropy values ranging between 1.0 to 2.0 {Fig. 6.9 (a), (b) and (c)}.

PCM classifier takes care of both i.e., class membership or relative typicalities and possibilities or absolute typicalities, for correct interpretation of a classified fraction image. Unlike FCM classifier, membership generated by PCM would be interpreted as "*degree of belongingness*" instead of "*degree of sharing*". To optimize the value of *m*, a number of iterations have been conducted by varying *m* from 1.1 to 4.0. The class membership μ is higher till *m*=2.4, and thereafter membership starts to decrease or becomes almost constant {Fig. 6.8(a) (b) and (c)}. Thus, as per the analysis of class membership, the optimum value of *m* for PCM has been identified between 2.2 to 2.4. However, the optimization of a parameter for the classification would be further analyzed and verified via entropy method and the classification performance assessed using Sub-pixel accuracy indices such as Producer's Accuracy, FERM, SCM, MIN-MIN, MIN-LEAST and Fuzzy Kappa coefficient.

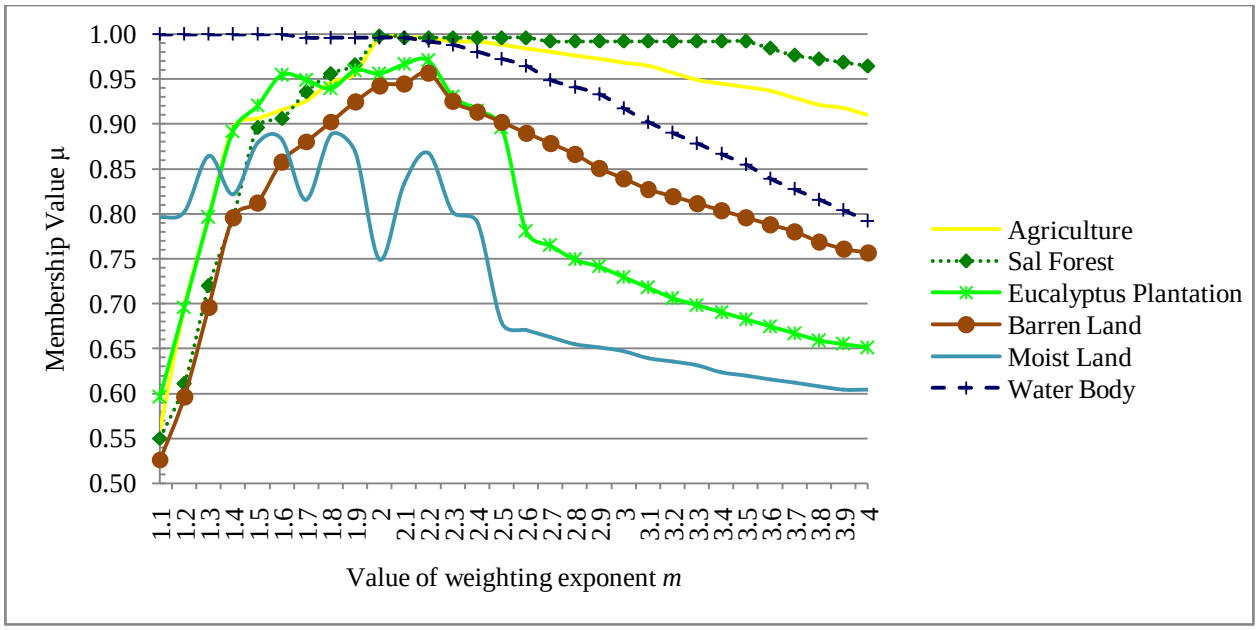

Fig. 6.8(a): Class membership for PCM classifier using AWiFS dataset.

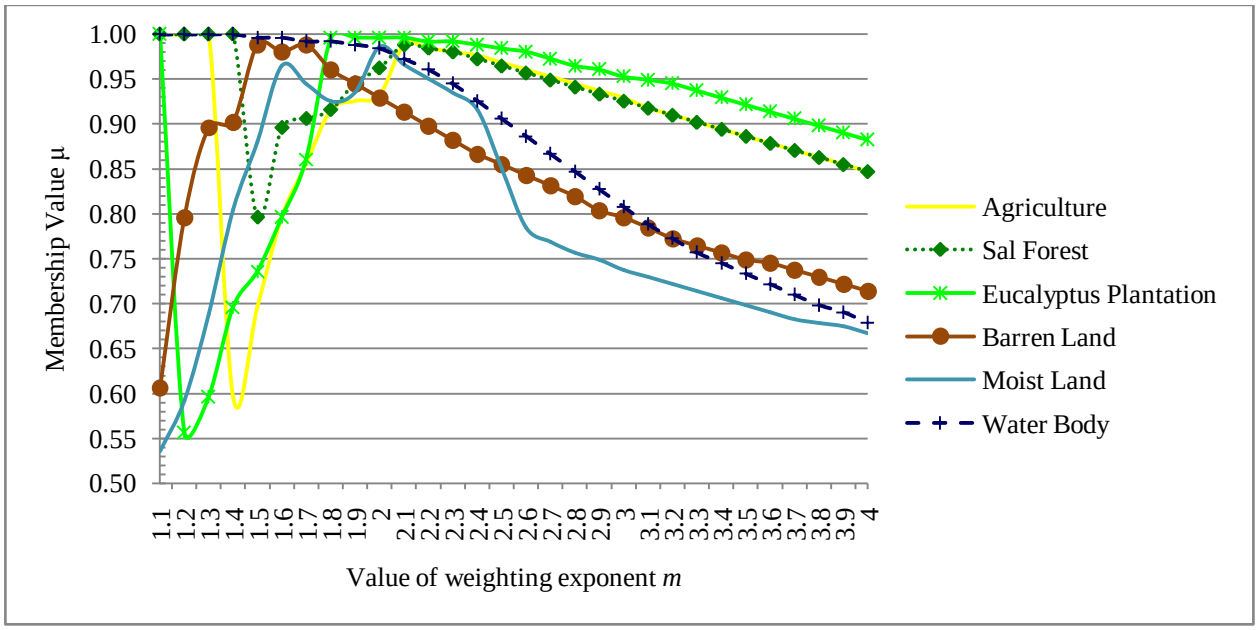

Fig. 6.8(b): Class membership for PCM classifier using LISS-III dataset.

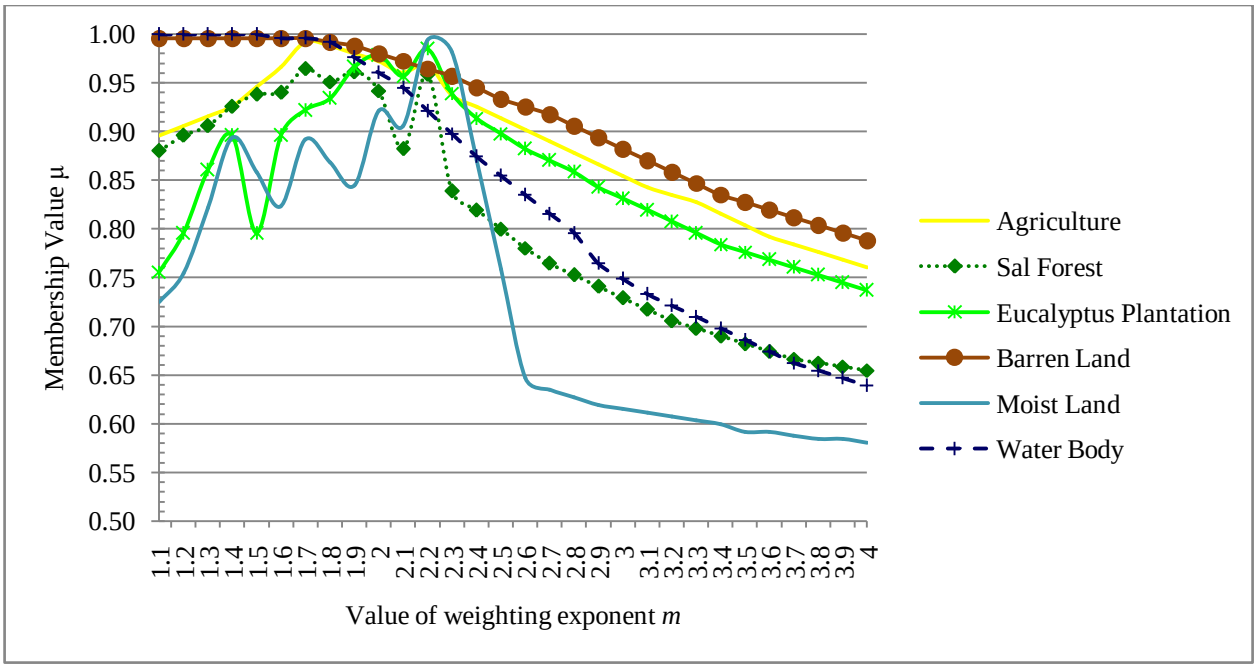

Fig. 6.8(c): Class membership for PCM classifier using LISS-IV dataset.

6.3.2 ENTROPY OF PCM CLASSIFIER

Fig. 6.9 (a), (b) and (c) shows the entropy of PCM classifier for agriculture, sal forest, eucalyptus plantation, barren land, moist land and water body. The entropy values for these land cover classes lie between a close interval range of [0, 3]. This indicates that if the computed entropy values of classified images are lying within this range; then the classification results have been obtained with minimum uncertainty. Further, it has been observed that for *m*=2.2 to 2.4 either the entropy value is low or it reaches up-to the level of saturation. Low entropy or saturated entropy it indicates better performance of the classifier.

From Fig.6.9 (a), (b) and (c) for m=2.2 to 2.4, the membership of all classes are high and the entropy criterion is not at the lowest level. This phenomenon occurs because the other class membership is also high for same pixel position. This indicates that classifier has correctly labeled the pixel to a class; simultaneously it also indicates the presence of another class.

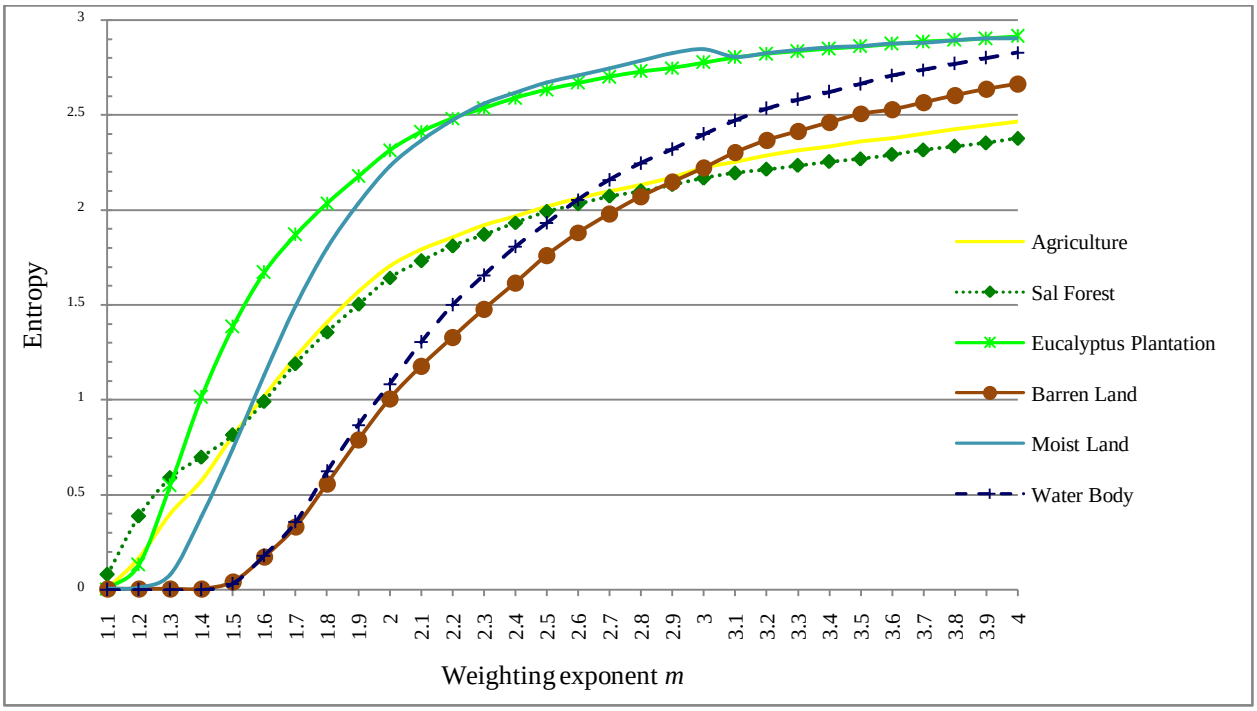

Fig. 6.9(a): Entropy for PCM classifier using AWiFS dataset

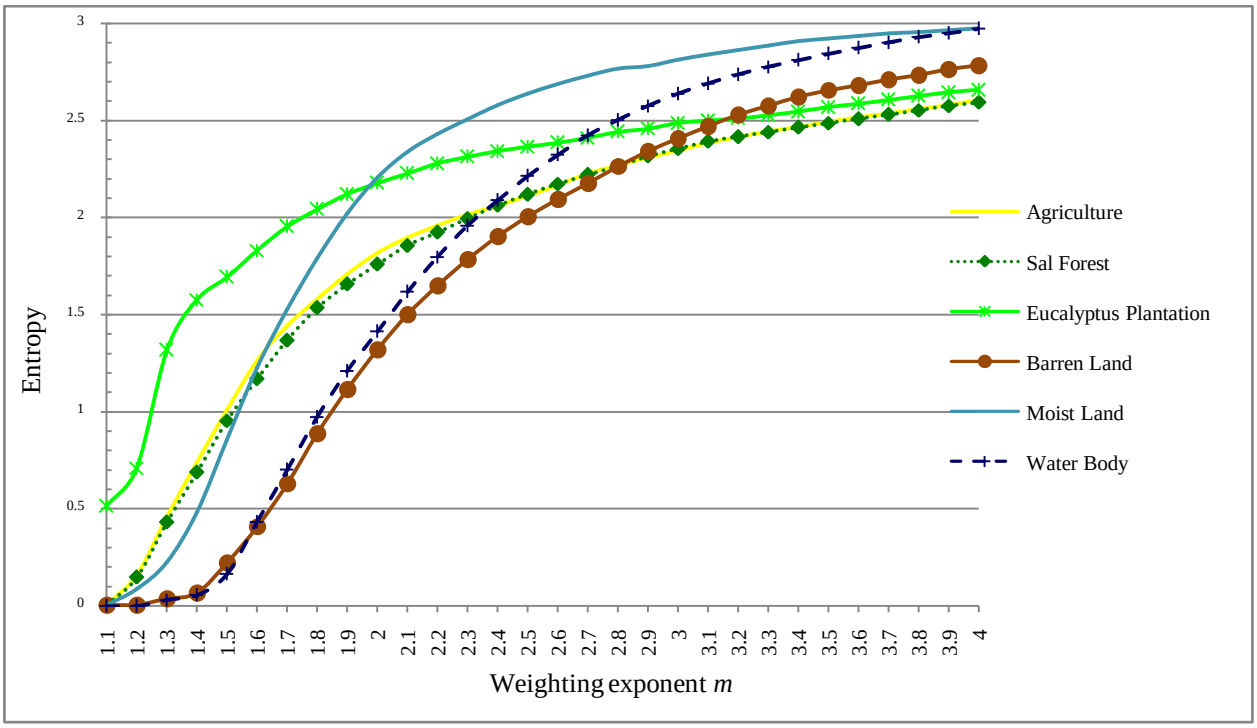

Fig. 6.9(b): Entropy for PCM classifier using LISS-III dataset

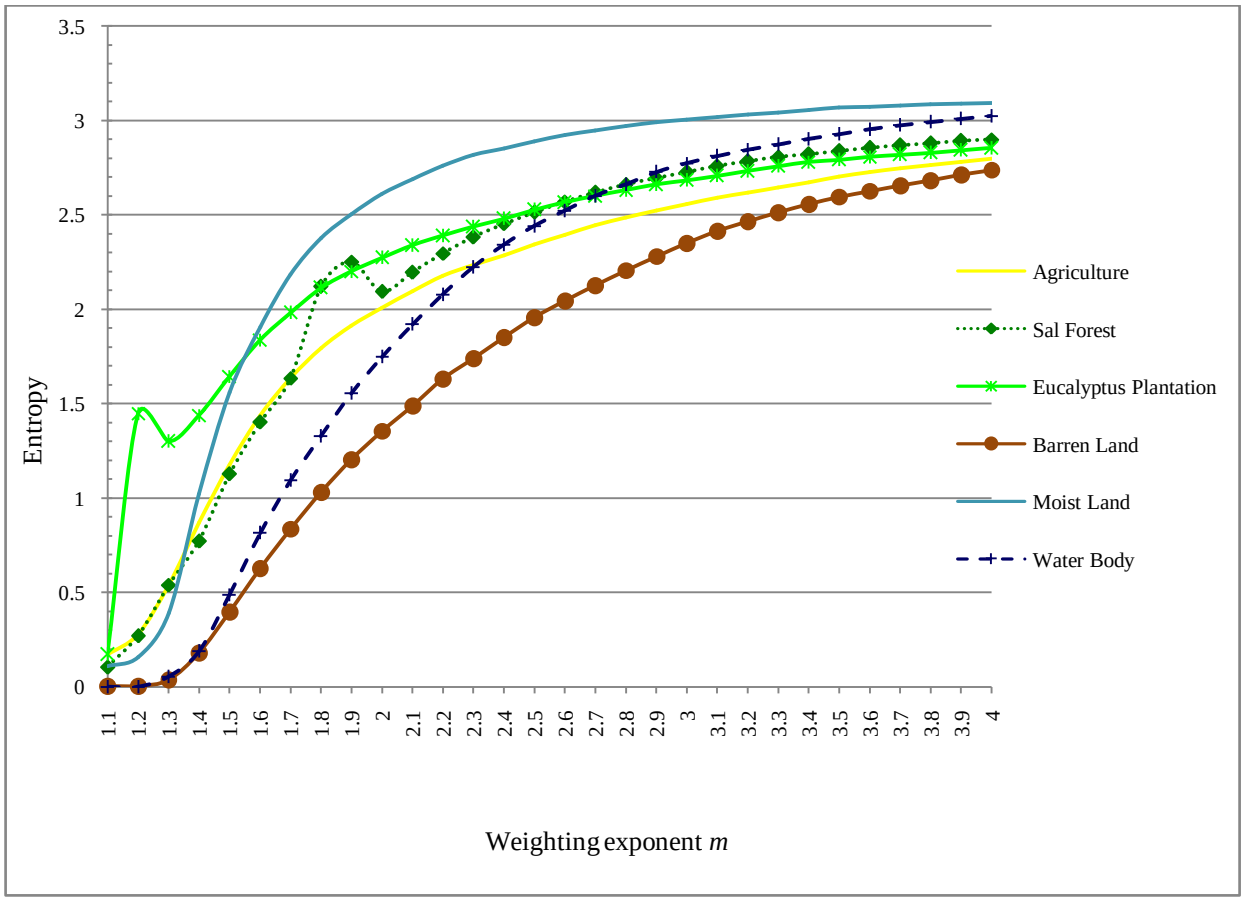

Fig. 6.9(c): Entropy for PCM classifier using LISS-IV dataset

6.3.3 PRODUCER'S ACCURACY OF PCM CLASSIFIER

To assess the accuracy of individual classes, Producer's Accuracy has been computed for PCM classifier {Fig. 6.10 (a) and (b)}. To determine Producer's Accuracy, AWiFS image has been used for classification while LISS-III and LISS-IV images are used as reference image. It has been observed that while classifying AWiFS with LISS-III reference dataset, the optimized value of m=2.2 is obtained, while the optimized value of m, is 2.4 when LISS-IV dataset are being used as a reference. For these values of m, a threshold criterion of 85% accuracy for MIN-PROD operator is also achieved.

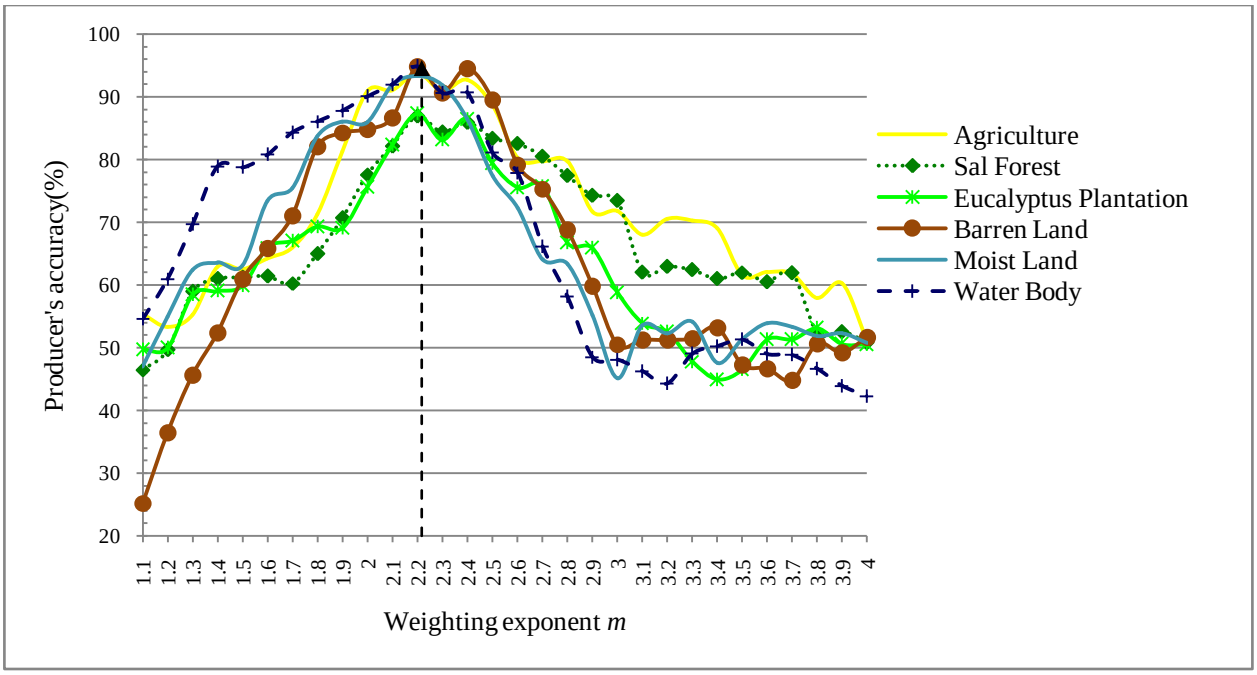

Fig. 6.10(a): Producer's accuracy of PCM classifier for AWiFS dataset using LISS-III as reference dataset.

Fig. 6.10(b): Producer's accuracy of PCM classifier for AWiFS dataset using LISS-IV as reference dataset.

6.3.4 CLASSWISE PARAMETER OPTIMIZATION OF PCM CLASSIFIER

On the basis of class membership, entropy and Producer's Accuracy of the classified imagery, class wise optimized values of weighting exponent (*m*) has been shown in Table 6.3. This value of *m* has been stated for each class where class membership and Producer's Accuracy is high and entropy is up to the level of saturation. It has been observed that irrespective of dataset *m*=2.1 have been found to be more suitable to classify agriculture. For barren land, moist land and water body *m*=2.2 yield good classification while for sal forest, and eucalyptus plantation *m*=2.3 gives the best result.

Table 6.3: Class wise parameter optimization of weighting exponent (*m*) for PCM classifier

Class	Class membership			Entropy			Producer's accuracy		Optimized Mean Value
	AWiFS	LISS-III	LISS-IV	AWiFS	LISS-III	LISS-IV	AWiFS-LISS-III	AWiFS-LISS-IV	
Agriculture	2.2	2.0	1.7	2.2	2.1	2.2	2.2	2.4	2.1
Sal Forest	2.2	2.0	2.2	2.3	2.5	2.6	2.2	2.4	2.3
Eucalyptus plantation	2.2	2.2	2.3	2.4	2.4	2.4	2.2	2.4	2.3
Barren land	2.2	2.1	2.0	2.6	2.1	2.6	2.2	2.4	2.2
Moist land	2.2	1.9	1.3	2.5	2.6	2.7	2.2	2.4	2.2
Water body	1.9	1.7	1.7	2.4	2.7	2.7	2.2	2.4	2.2

6.3.5 GENERALIZED PARAMETER OPTIMIZATION OF PCM CLASSIFIER

One of the major concerns is to verify the correctness and certainty of the information in a classified imagery. The PCM classification algorithm has been used in supervised mode along with the Euclidian weighted norm to classify the remote sensing imagery. Results of PCM classifier is shown in Fig. 6.11 (a) and (b). In comparison with FCM, PCM relaxes the unity norm of class membership which helps to mitigate the effect of uncertainty.

Fig. 6.11 (a) and (b) shows that for values of weighting exponent *m* ranging from 1.1 to 4.0, the Overall accuracy, FERM, and MIN-MIN are varying between 60% to 92% in both cases, where AWiFS dataset is used for classification and LISS-III/LISS-IV dataset is used as a reference image. However, SCM and MIN-LEAST operator indicates lower accuracy. The SCM accuracy is ranging between 30% to 55% for all classes, where the accuracy of MIN-LEAST is ranging between 5% to 15%. The overall accuracy as computed by FERM and MIN-MIN operator is consistent with PCM, wherein SCM and MIN-LEAST results of PCM classifier do not show similar pattern like in FCM. The MIN-LEAST is a new operator; introduced by Silavn (2008), measures the minimum possible sub-pixel overlap between two classes. So, the basic reason of its lower accuracy is that, it is not able to minimize the class overlap problems of homogenous and heterogeneous groups. It produces a higher accuracy in case of perfect matching case only. However, sub-pixel area from the reference and classified datasets are generally underestimated by marginal totals.

In the process of identifying the optimized value of weighting exponent *m*, all these accuracy measures has been analyzed for all six classes selected for this study and it is found that, for $m = 2.2$ to 2.8 produces highest accuracy for all classes whenever, AWiFS image has been used for classification and LISS-III/LISS-IV image is used as a reference image.

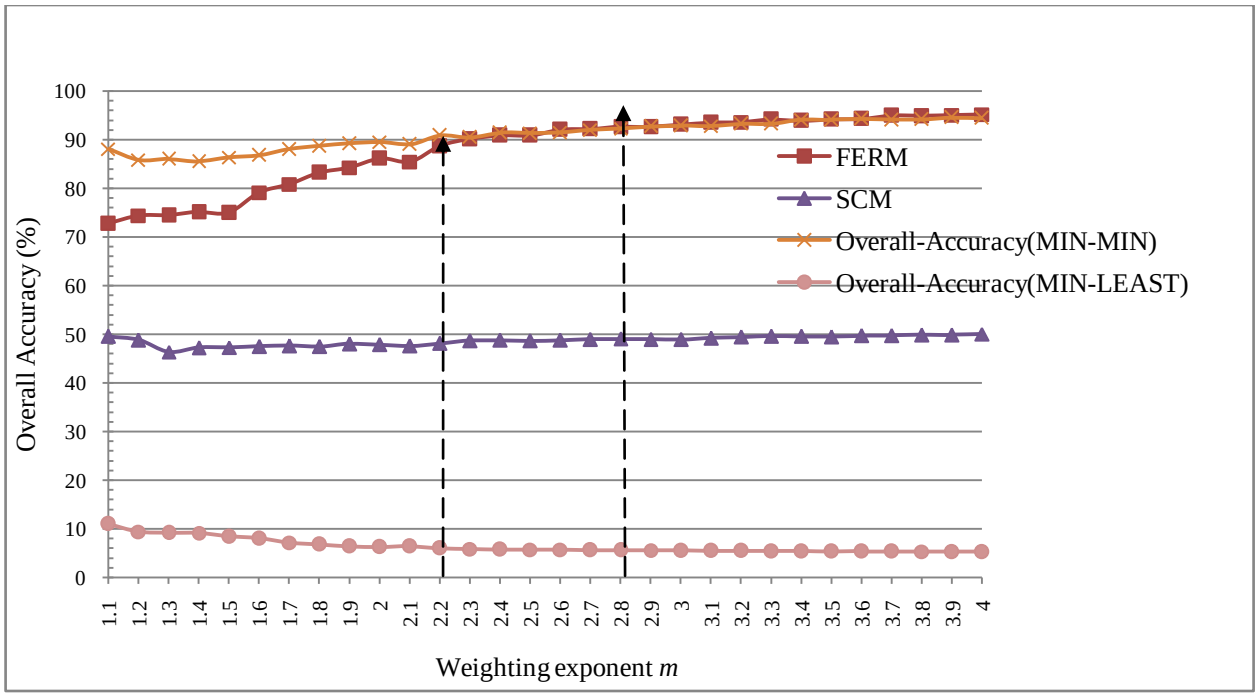

Fig. 6.11(a): Overall accuracy of PCM classifier for AWiFS dataset using LISS-III as reference dataset

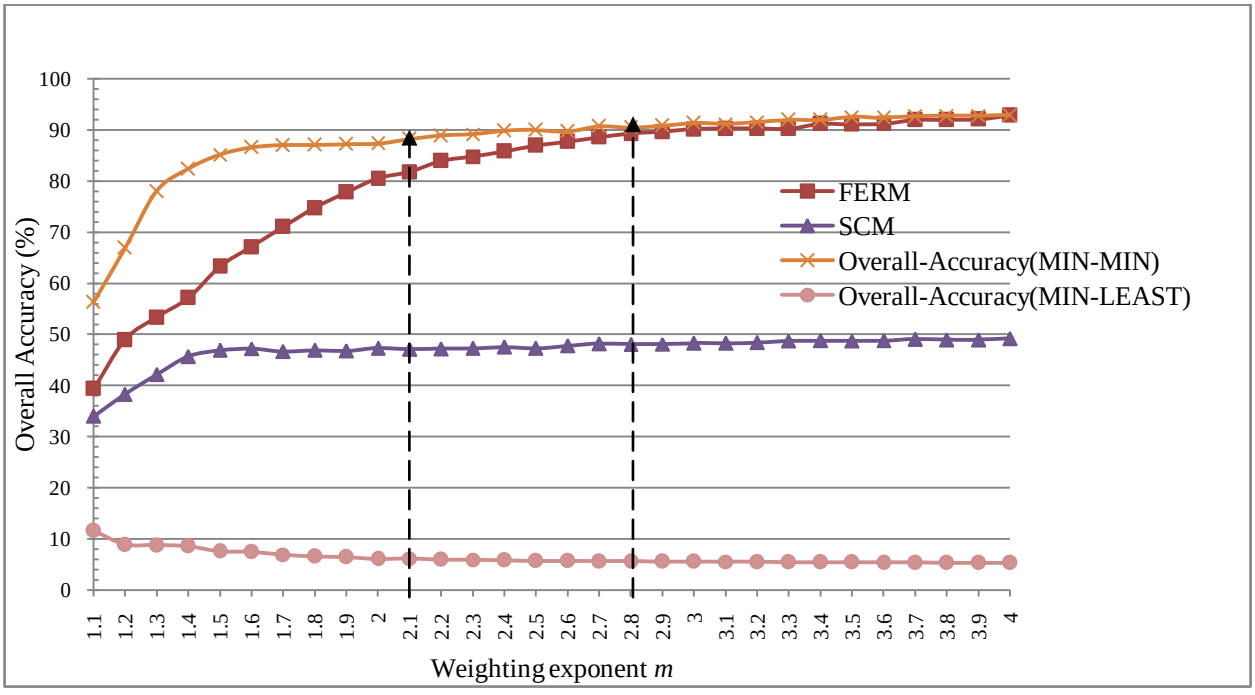

Fig. 6.11(b): Overall accuracy of PCM classifier for AWiFS dataset using LISS-IV as reference dataset

The Overall Accuracy (FERM and MIN-MIN) and class membership of PCM classifier increases till the value of *m* up to 2.8 and thereafter either it decreases or become stable as shown in Fig. 6.8 (a), (b) and (c). At this point entropy values are also becomes stable for certain classes, as shown in Fig.6.9 (a), (b) and (c). Therefore, in order to determine a single optimized value for all classes and independent of dataset Fuzzy Kappa coefficient have been used for PCM classifier.

Fig. 6.12 (a) and (b) shows that the value of Fuzzy Kappa coefficient is greater than 0.80 for SCM approach and is of increasing nature. This signifies that the classification performed using PCM classifier is consistent with respect to classified image and reference image. However, for MIN-LEAST, it is on the lower side as shown in Fig. {6.12 (a) and (b)}. The Overall Accuracy and Fuzzy Kappa coefficient shows similar trends, which indicates appropriateness in classification. However, the Fuzzy Kappa values for MIN-LEAST operator do not produce very high values, due to intermixing of class at boundary points. It has also been observed that MIN-LEAST operator is not suitable to assess the accuracy of PCM.

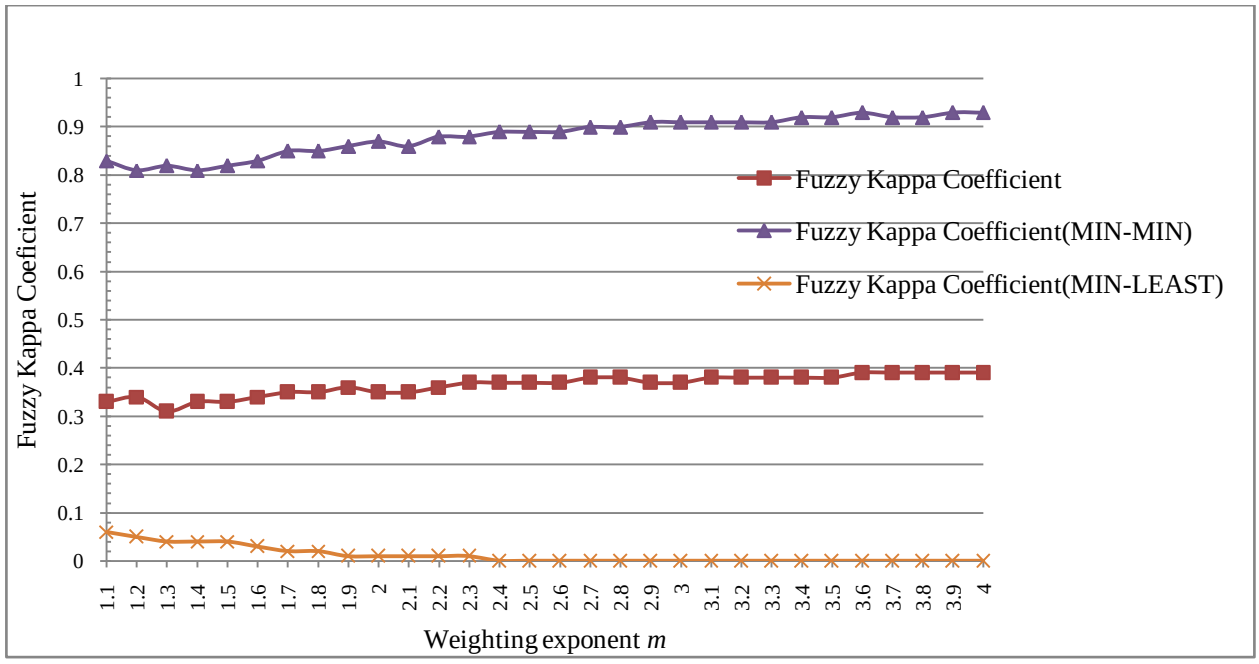

Fig. 6.12(a): Fuzzy Kappa of PCM classifier using AWiFS dataset and LISS-III as reference

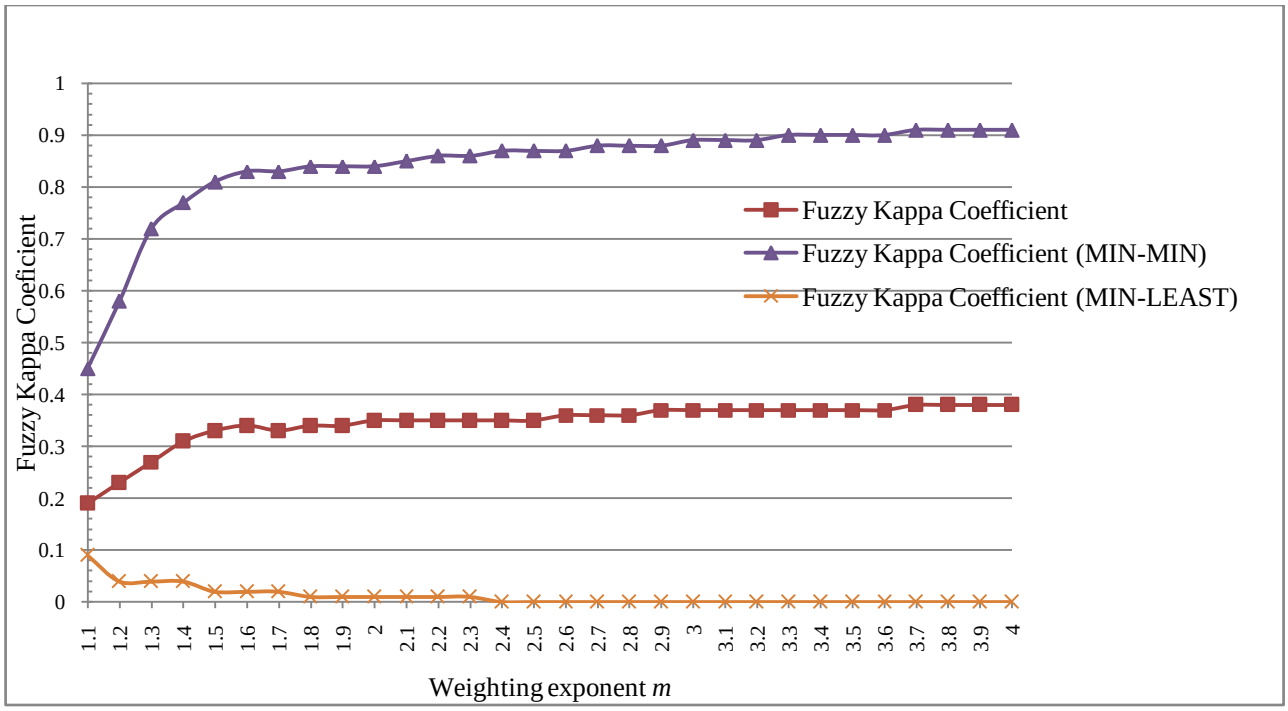

Fig. 6.12(b): Fuzzy Kappa of PCM classifier using AWiFS dataset and LISS-IV as reference

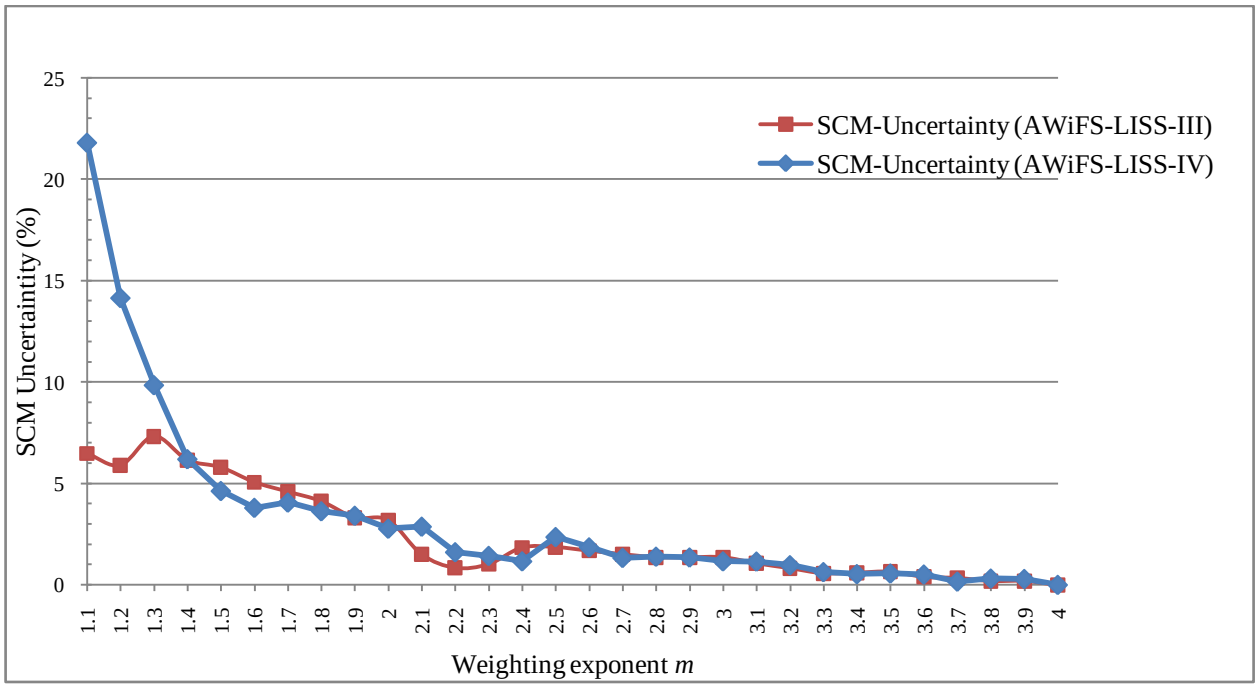

Fig. 6.13: SCM uncertainty of PCM classifier

From Fig. 6.13, it is observed that classification uncertainty is not exceeding beyond 22% for all the values of *m* ranging from 1.1 to 4.0. However, this produces minimum uncertainty value for *m* =2.2. From Fig. 6.8 (a), (b) and (c) and Fig. 6.13, it is observed that lower uncertainty of an index indicates that the center value is useful for classification. In a nutshell, the accuracy-uncertainty index has the capability to identify the distribution of error, even in the case when the entire operator has same overall accuracy. In this study, the uncertainty acceptability criterion of 5% has been followed and for optimized values of *m*, it is around less than 1% for both category of classification.

Table 6.4 shows all the accuracy measures for the optimized value of weighting exponent *m*=2.2, where AWiFS image has been used as a classified image and LISS-III image has been used a reference image. This output reflects that the user's accuracy for agriculture, sal forest, eucalyptus plantation, moist land, and water body is higher and reaches up to the level of 95%. This indicates that the error of omission and error of commission is less. The Fuzzy overall accuracy, FERM, SCM, MIN-PROD, MIN-MIN, and MIN-LEAST of all classes are 88.71%, 48.80%, 93.98%, 90.87% and 6.05% respectively. From Table 6.5, it is observed that composite MIN-LEAST operator is not found suitable to assess the accuracy of PCM classifier, because it does not follow the unity constraint like FCM. As per the obtained results, the FERM, and MIN-MIN accuracy measures fulfills the accuracy acceptability criterion of 85% for optimized value of *m*. However, other measures like SCM and MIN-LEAST are not found suitable to assess the classification accuracy based upon PCM classifier.

Fig. 6.14 shows the fraction images of AWiFS dataset for optimized weighting exponent (*m*). After examining the fraction images generated by PCM classifier, it is found that water body has been identified clearly. On the other hand, sal forest and eucalyptus plantation have a significant amount of merging at the boundary of each other. In case of agriculture land, merging with sal forest and eucalyptus plantation is observed. This indicates that, in this image has a high extent of inter-grade phenomena existing.

For the initial values of weighting exponent *m*, its class membership is not very high (0.55), but with the increase in value of *m* i.e. at 1.6 the class membership starts to increase.

Further, for *m*= 2.2, all the accuracy measures yield highest values with low uncertainty {see Fig. 6.8(a), (b) and (c) and Fig. 6.11(a), (b) and (c)}. This result has also been verified using Entropy and Producer's Accuracy as shown in Fig. 6.9 (a), (b) and (c) and 6.10 (a) and (b).

Table 6.4: accuracy values for optimized value of *m*=2.2 for PCM classification of AWiFS data with LISS-III as a reference data.

Land-Use Classes	**Accuracy assessment methods**				
	FERM	**SCM**	**MIN-PROD**	**MIN-MIN**	**MIN-LEAST**
Fuzzy user's accuracy (%)					
Agriculture	94.59	50.70±1.12	97.17	93.07	8.08
Sal forest	94.09	50.24±2.32	97.06	92.39	7.55
Eucalyptus plantation	91.13	49.56±2.81	97.30	91.52	6.96
Barren Land	93.69	44.81±1.51	95.95	82.56	4.39
Moist Land	95.40	49.69±3.65	94.93	90.51	6.65
Water Body	98.29	46.21±1.78	92.21	94.24	2.39
Fuzzy producer's accuracy (%)					
Agriculture	89.67	50.73±2.72	90.40	93.51	8.03
Sal forest	89.30	50.38±2.12	91.65	93.32	7.54
Eucalyptus plantation	86.65	49.34±2.71	92.54	90.91	6.94
Barren Land	94.50	49.90±1.37	92.30	91.54	4.51
Moist Land	87.81	48.09±3.65	94.06	87.86	6.55
Water Body	82.49	40.53±1.77	91.61	83.06	2.39
Fuzzy overall accuracy (%)	88.71	48.80±3.47	93.98	90.87	6.05
Fuzzy Kappa	-	0.37±0.07	0.87	0.88	0.12

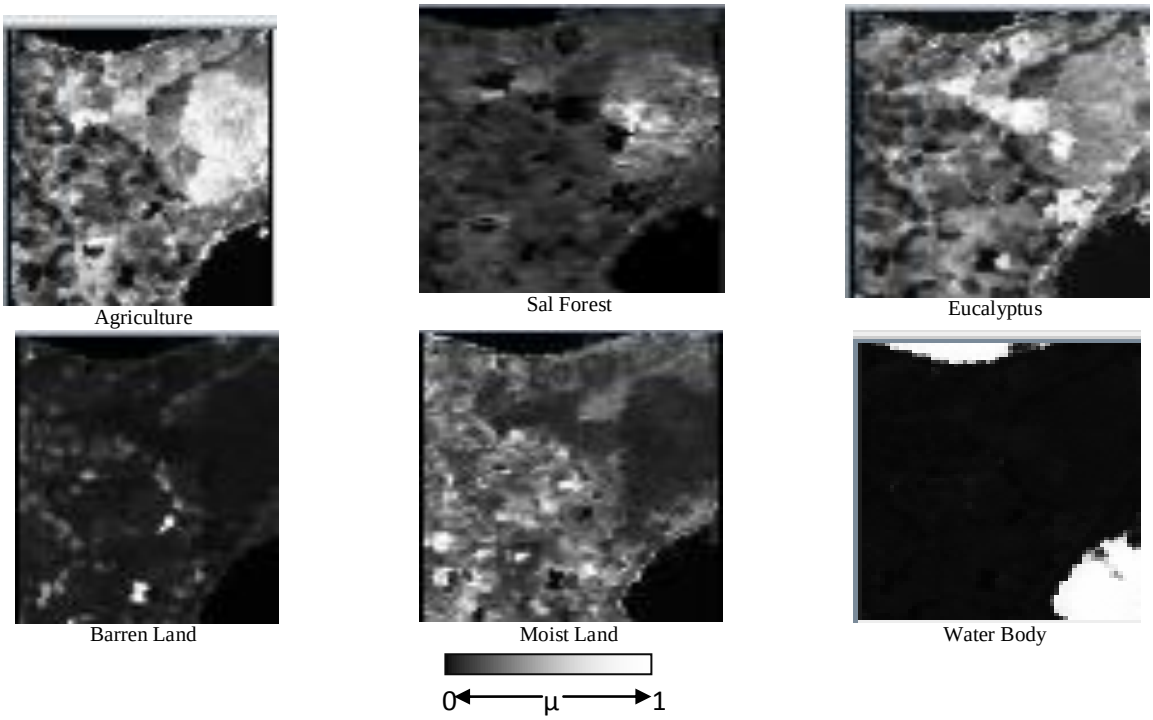

Fig. 6.14: PCM classification output of AWiFS image

In a nutshell, it is observed that *m*=2.2, can be used as a generalized optimized value for the classification irrespective of dataset. However, for a particular class *m*=2.1 may be use to classify agriculture. For barren land, moist land and water body *m*=2.2 yield good classification while for sal forest, and eucalyptus plantation *m*=2.3 gives the best result.

6.4 RESULTS OF NOISE CLUSTERING (NC) CLASSIFIER

The basic aim of NC classifier is to assess the suitability of noise clustering based algorithm for sub-pixel classification. Depending upon the type of satellite data used, there is a problem of mixed pixel, where more than one information class is present within a pixel. In order to resolve such situations, NC classifier has been used to overcome the problem of noisy data points. The classifier has been formulated in such a manner so that it can extract a multiple land cover class at a time, at sub-pixel level. The performance of NC classifier is dependent upon the optimized value of weighting exponent (*m*) and varying value of resolution parameter (δ). The optimized value of weighting exponent *m* is class dependent, while resolution parameter δ is dependent upon the class characteristic, yet both are interdependent to perform the classification using NC

classifier. Here, a fixed value of m=2.4 has been used while varying the values of δ. Resolution parameter δ is a fixed parameter ($0 \leq \delta < \infty$) which controls the distance between the feature vectors from the central point of the line of cluster.

6.4.1 CLASS MEMBERSHIP OF NC CLASSIFIER

Fig. 6.15 (a), (b) and (c) shows the variation of the resolution parameter δ with class membership of different classes such as agriculture, sal forest, eucalyptus plantation, barren land, moist land and water body for AWIFS, LISS-III and LISS-IV dataset respectively. For all three datasets, class membership has been generated for the different values of δ ranging from 1.0 to 10^9at an interval of $\log_{10}10$. The class membership value of a pixel denotes the class proportions, which in turn represents the soft classified output for a pixel. From the Fig. 6.15 (a), (b) and (c), it is observed that for $\delta = 10^5$, the class membership (μ) lies between 0.78 to 0.98 for all classes.

The class membership μ increases till $\delta=10^5$, and thereafter the membership value starts to decrease or almost becomes constant {Fig. 6.15(a), (b) and (c)}. Thus, as per class membership, the optimum value of δ for NC classification has been fixed as10^5. However, the optimization of a resolution parameter δ would be analyzed and verified using entropy method and the classifier performance is tested by using Sub-pixel accuracy indices such as FERM, SCM, MIN-MIN, MIN-LEAST and Fuzzy Kappa coefficient along with their associated uncertainty.

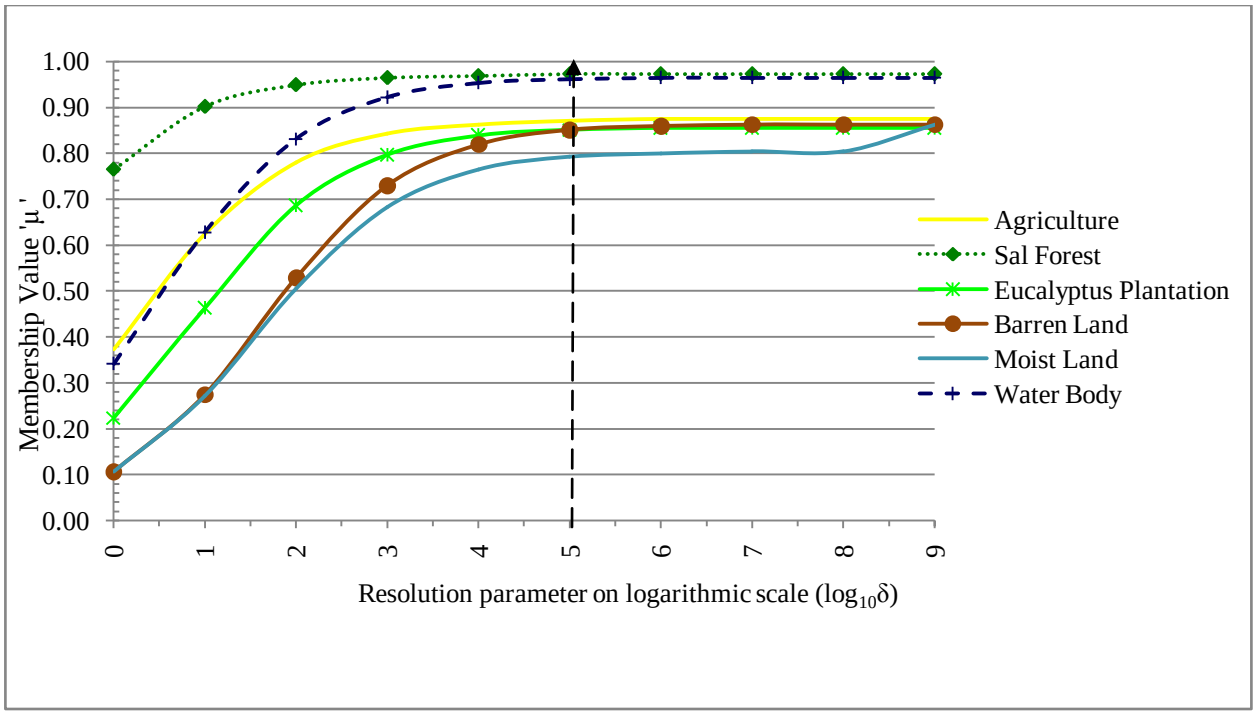

Fig. 6.15(a): Class membership for NC classifier using AWiFS datasets.

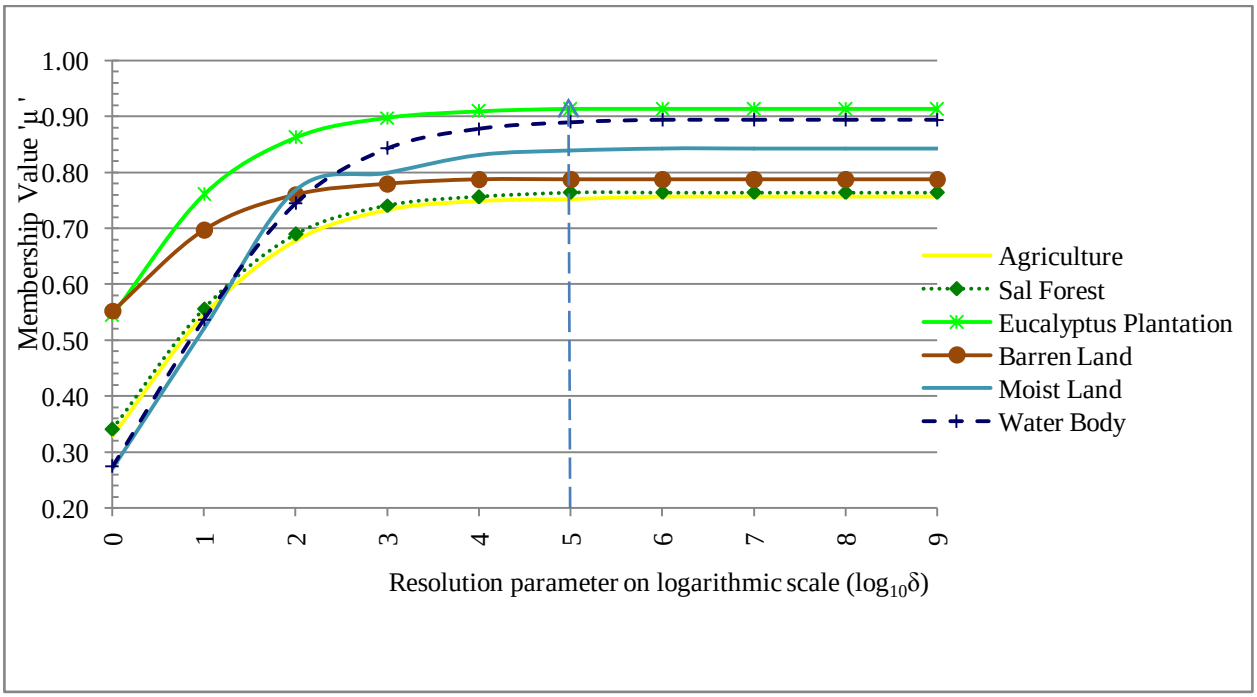

Fig. 6.15(b): Class membership for NC classifier using LISS-III datasets.

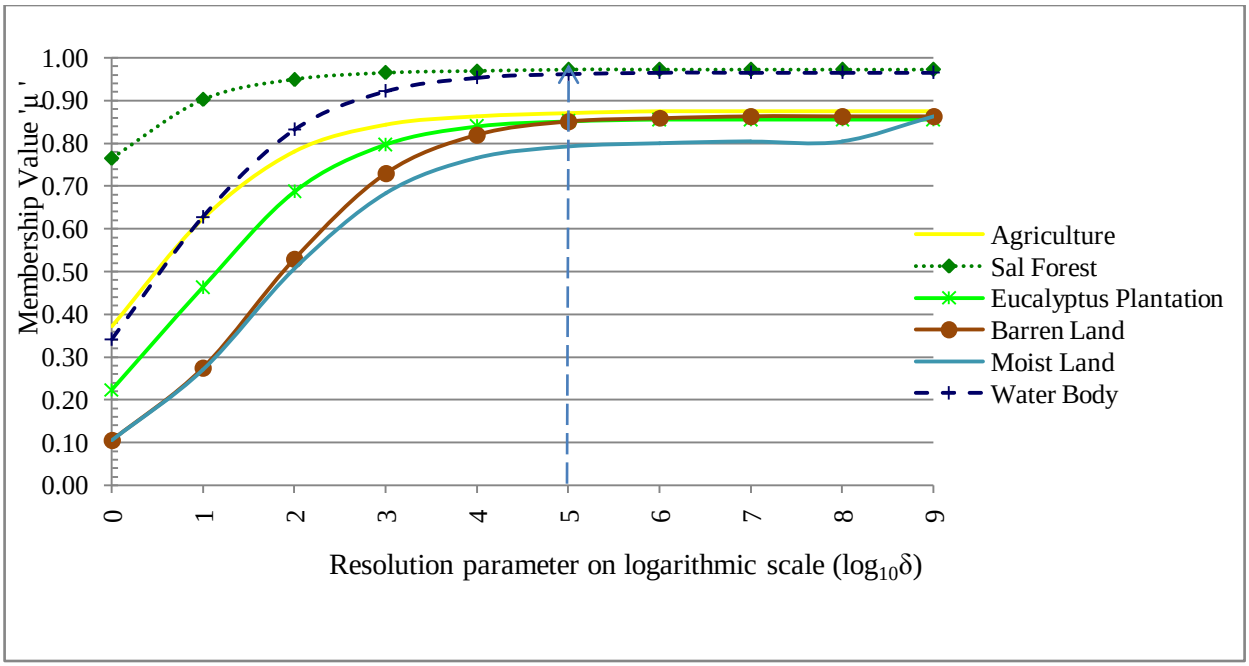

Fig. 6.15(c): Class membership for NC classifier using LISS-IV datasets.

6.4.2 ENTROPY OF NC CLASSIFIER

The assessment of uncertainty in classified results is important and necessary to evaluate the classifier performance. For a better classified output, the entropy should be low or it reaches up-to the level of saturation or starts to decrease after at certain points (Dehghan and Ghassemian, 2006). As shown in Fig. 6.16 (a), (b) and (c), the computed entropy for AWiFS, LISS-III and LISS-IV fraction images of NC classifier for all six land cover classes lies between the specified range of [0,3]. Measuring the spectral uncertainty of a classified satellite image using an entropy, of six land cover classes can be computed using Eq 3.85 i. e. $6*(-1/6*\log_2 1/6)=2.585$ (Stein et al., 2002). This states that if the computed entropy value of classified fraction image is lying within this range then this indicates a better classification results with minimum uncertainty.

Further, it has been observed from Fig. 6.16 (a), (b) and (c) that at $\delta=10^5$, the entropy values for all classes are low. For this optimized value of δ, the class membership is high i.e. up to 94% and the computed entropy is between 0.6 to 1.0. This trend indicates that the uncertainty in classified results is low. Entropy has been used as assessment parameter of accuracy for various land cover classes i.e. agriculture, sal forest, eucalyptus plantation, barren land, moist land and water body. In a nutshell, it can be stated that this study on spatial variation has

identified that total uncertainty has not exceeded the referential value (2.585) for six classes. This mathematical model of entropy computation is used as an absolute indicator of measuring uncertainty without using any ground reference data.

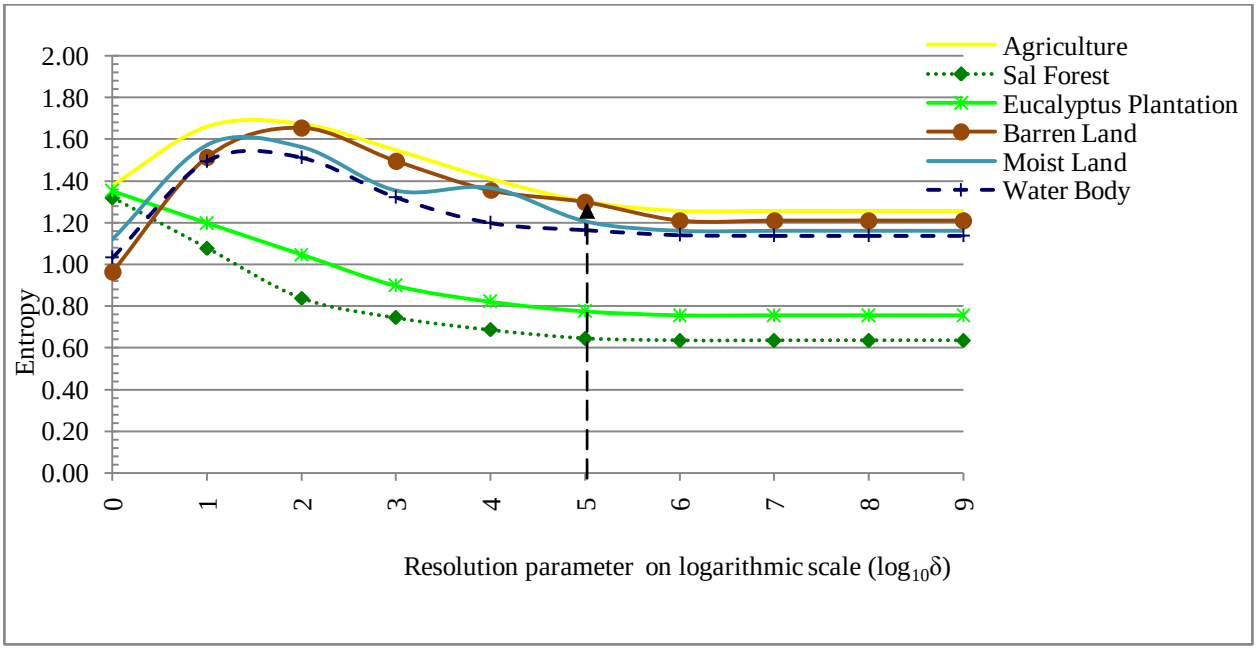

Fig. 6.16(a): Entropy for NC classifier using AWiFS dataset

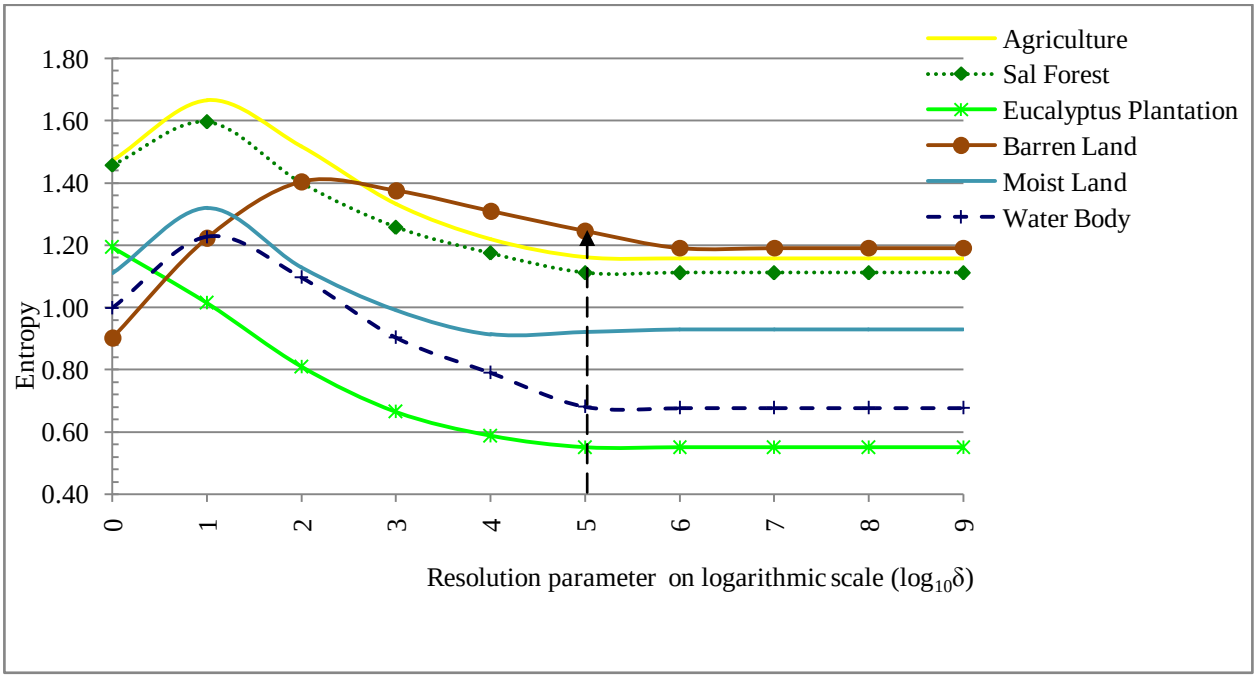

Fig. 6.16(b): Entropy for NC classifier using LISS-III dataset

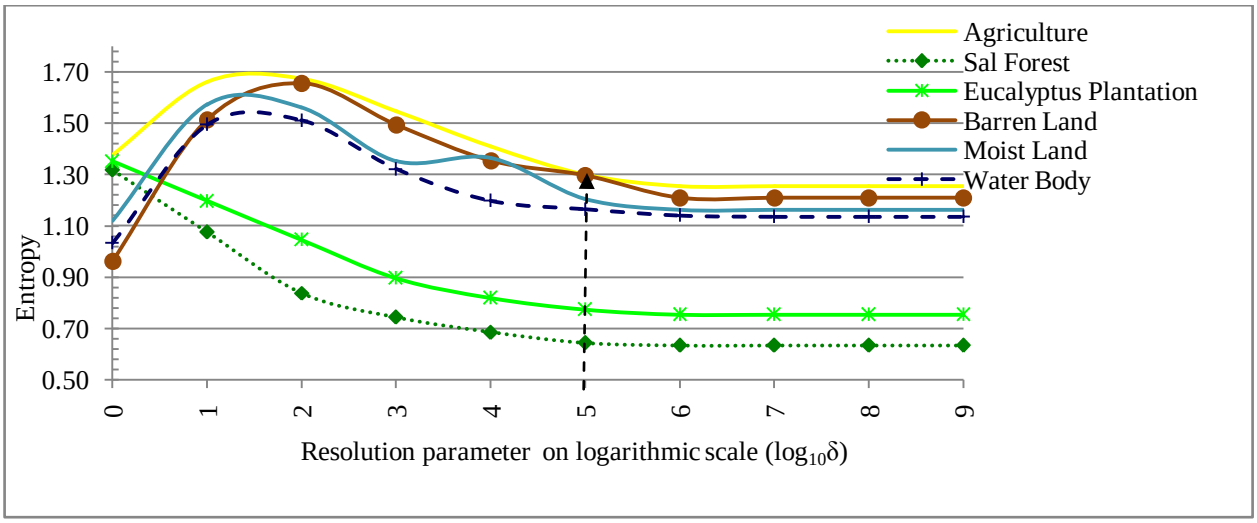

Fig. 6.16(c): Entropy for NC classifier using LISS-IV dataset

6.4.3 PRODUCER'S ACCURACY OF NC CLASSIFIER

To determine the accuracy of individual classes, Producer's Accuracy (PA) has been computed for NC classifier {Fig. 6.17 (a) and (b)}. AWiFS image has been used for classification while LISS-III and LISS-IV images are used as a reference image to determine the Producer Accuracy. It is observed that while for $\delta=10^5$, NC classifier produces highest accuracy for all six land cover classes present in the image.

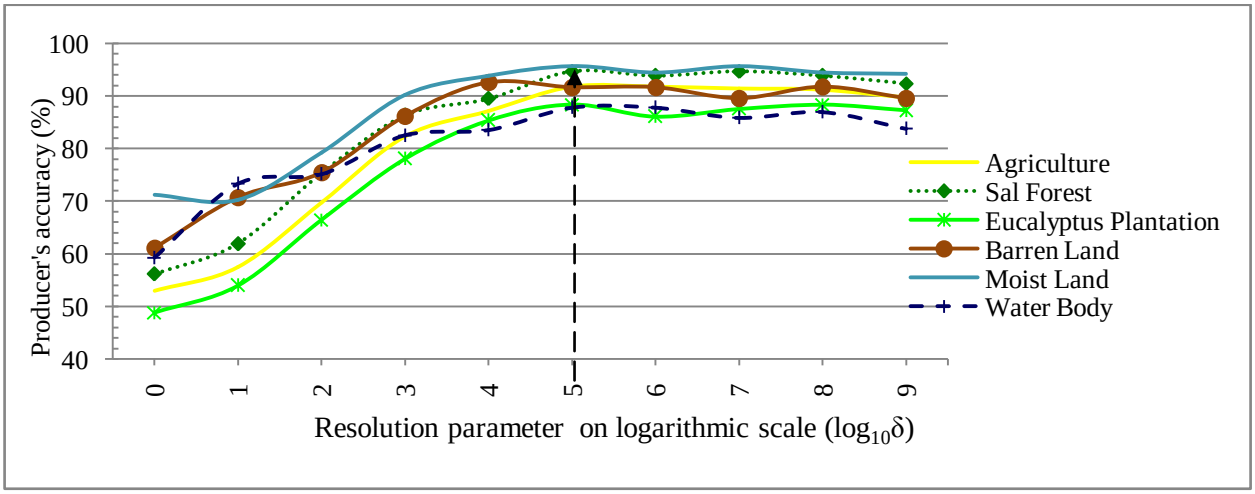

Fig. 6.17(a): Producer's accuracy of NC classifier for AWiFS dataset using LISS-III as reference dataset.

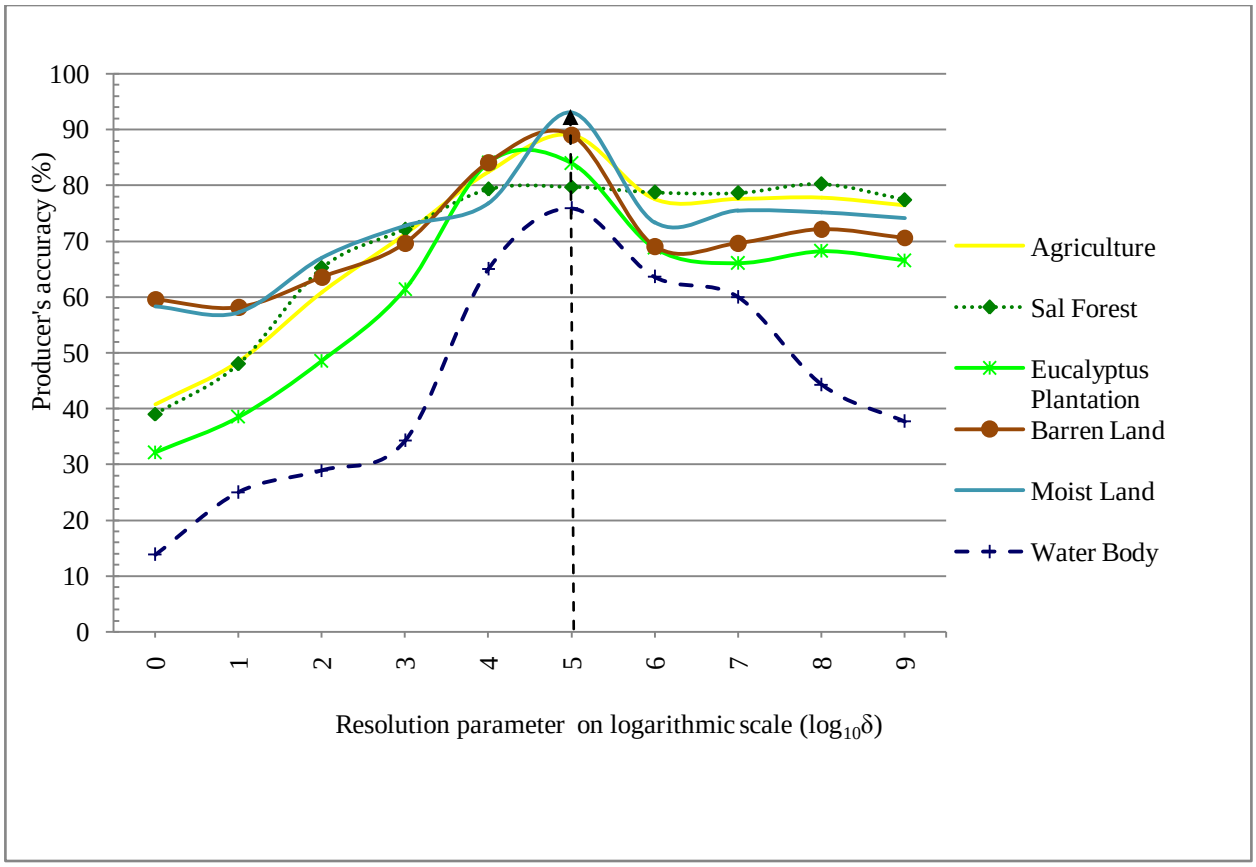

Fig. 6.17(b): Producer's accuracy of NC classifier for AWiFS dataset using LISS-IV as reference dataset.

6.4.4 CLASS WISE PARAMETER OPTIMIZATION OF NC CLASSIFIER

On the basis of highest class membership, lower entropy and highest producers accuracy produced by classified imagery, the class wise optimized values of resolution parameter (δ) have been shown in Table 6.5. It is observed that irrespective of datasets, the optimized value of (δ)for agriculture, sal forest, eucalyptus plantation, barren land, moist land and water body is 3.2×10^5, 0.8×10^5, 3.1×10^5,4.1×10^5,27.8×10^5, and 3.1×10^5 respectively.

Table 6.5: Class wise parameter optimization of (δ) for NC classifier

Class	Class membership			Entropy			Producer's accuracy		Optimized Mean Value
	AWiFS	LISS-III	LISS-IV	AWiFS	LISS-III	LISS-IV	AWiFS-LISS-III	AWiFS-LISS-IV	
Agriculture	10^6	10^5	10^6	10^5	10^4	10^5	10^5	10^5	3.2×10^5
Sal Forest	10^5	10^5	10^5	10^4	10^5	10^5	10^5	10^5	0.8×10^5
Eucalyptus plantation	10^6	10^5	10^6	10^3	10^5	10^5	10^5	10^5	3.1×10^5
Barren land	10^5	10^5	10^6	10^4	10^6	10^6	10^4	10^5	4.1×10^5
Moist land	10^7	10^6	10^7	10^5	10^4	10^6	10^5	10^5	27.8×10^5
Water body	10^5	10^5	10^5	10^3	10^5	10^6	10^5	10^5	3.1×10^5

6.4.5 GENERALIZED PARAMETER OPTIMIZATION OF NC CLASSIFIER

In this study, a comparative assessment of fuzzy based classifiers has been carried out to identify the agriculture, sal forest, eucalyptus plantation, barren land, moist land and water body. For a good classification, training data should be available for all representative classes present in the imagery.

The NC classifier has been used in supervised mode along with the Euclidean weighted norm to classify the remote sensing imagery. A result of NC classifier is shown in Fig. 6.18 (a) and (b), wherein AWiFS image has been classified using LISS-III and LISS-IV images as a reference.

The overall accuracy shown in Fig. 6.18(a) and (b) has been computed for varying values of resolution parameter δ which is ranging from 1 to 10^9along with constant value of weighting exponent *m*=2.4 (optimized), taken from FCM classifier. The overall accuracy, FERM, SCM, MIN-MIN and MIN-LEAST are varying between 55% to 95% in both cases, where AWiFS is used as a classified image and LISS-III or LISS-IV dataset is used as a reference image. In the process of identifying the optimized value of resolution parameter δ, all these accuracy measures has been analyzed for all six classes incorporated for this study. It is found that for $\delta = 10^5$, all accuracy measures are higher and achieving the threshold criterion of accuracy measures of 85% with lesser uncertainty values.

The value of resolution parameter δ lies between one to infinity. However, in this study, the value of δ has been tested from 1to 10^9. The output of NC soft classification is represented in form of the fraction image corresponding to the land cover classes incorporated for this study. The output values of known pixels have been plotted against the varying values of δ for all the accuracy measures in Fig. 6.18 (a) and (b).

It is observed that the membership values of all six classes are increasing when δ varies from 1 to10^5 and thereafter it increases slowly and then attains a constant value at a fixed point, where the membership value is close to 0.954 {Fig. 6.15 (a), (b) and (c)}. Any further increment in resolution parameter δ, increases the membership values of non-interest classes which increases the noise in the outputs. Thus, the value of resolution parameter δ which corresponds to the fixed point yields the best results for AWiFS, LISS-III and LISS-IV datasets.

To further strengthening our belief for the optimization of resolution parameter (δ), Fuzzy Kappa coefficient has been chosen as a better alternative to measure the accuracy of any classifier when the sample size is limited (Chen et al., 2010). This accuracy index is less affected by distribution of error among classes. Fuzzy Kappa signifies the amount of certainty proportion lying in the classified imagery. The values of Fuzzy Kappa coefficient is of increasing nature, which indicates that the classification done using NC classifier is consistent with respect to classified image and reference image. The overall accuracy and Fuzzy Kappa coefficient shows the same trend, and this indicates the consistent classification has been performed.

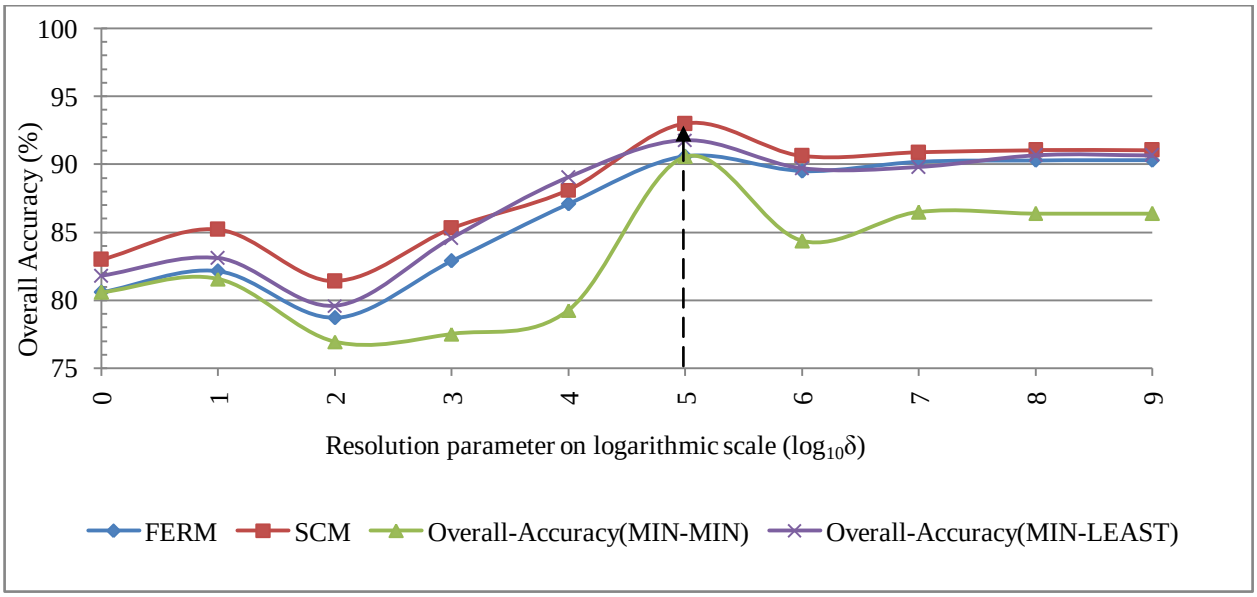

Fig. 6.18(a): Overall accuracy of NC classifier for AWiFS dataset using LISS-III as reference dataset

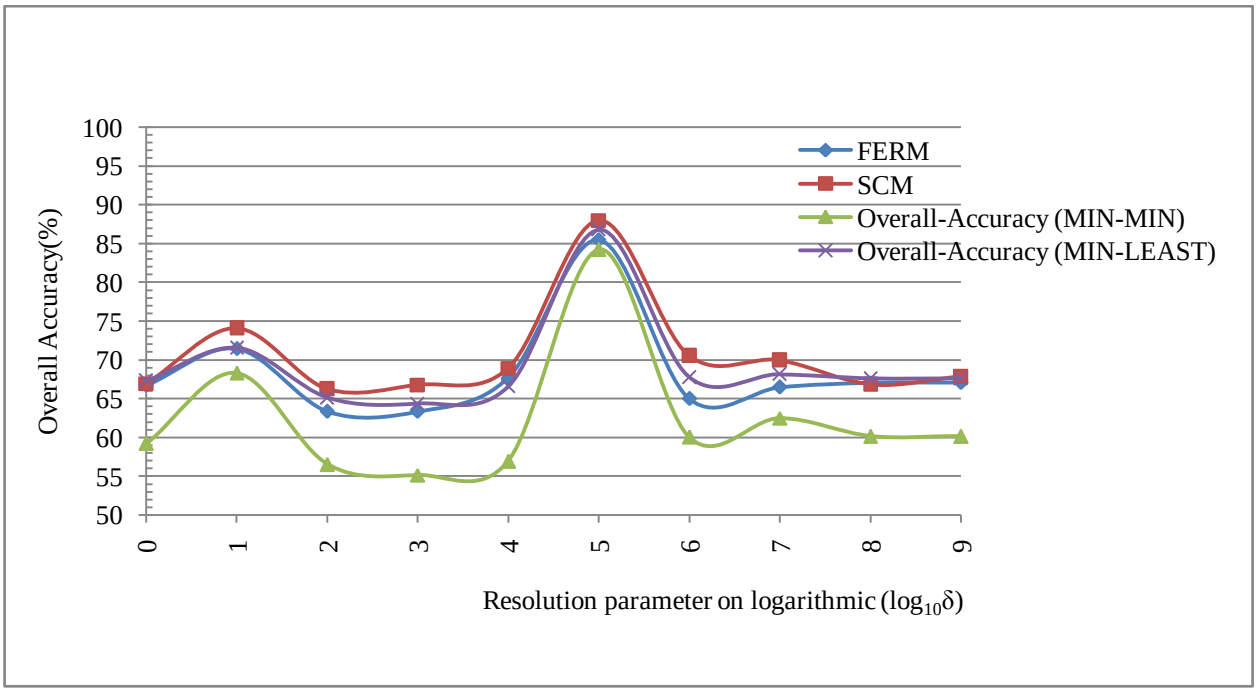

Fig. 6.18(b): Overall accuracy of NC classifier for AWiFS dataset using LISS-IV as reference dataset

The Fuzzy Kappa coefficient value of AWiFS image using LISS-III as reference data is shown in Fig. 6.19 (a). It is observed that for $\delta=10^5$, Fuzzy Kappa coefficient of SCM, MIN-MIN and MIN-LEAST operator yield a desired value 0.85. However, MIN-MIN operator has achieves the threshold criterion of 0.85 for $\delta=10^5$. Further, it is observed from Fig. 6.19 (b) that for $\delta=10^5$, Fuzzy Kappa coefficient for all SCM, MIN-MIN and MIN-LEAST operators yield a desired value 0.85 while MIN-LEAST operator achieves this for $\delta=10^4$.

On the basis of Overall Accuracy and Fuzzy Kappa values, it is observed that the optimized value of resolution parameter (δ) is 10^5. However, to further verify this fact; it may be advisable to compare uncertainty values of AWiFS using LISS-III and LISS-IV datasets.

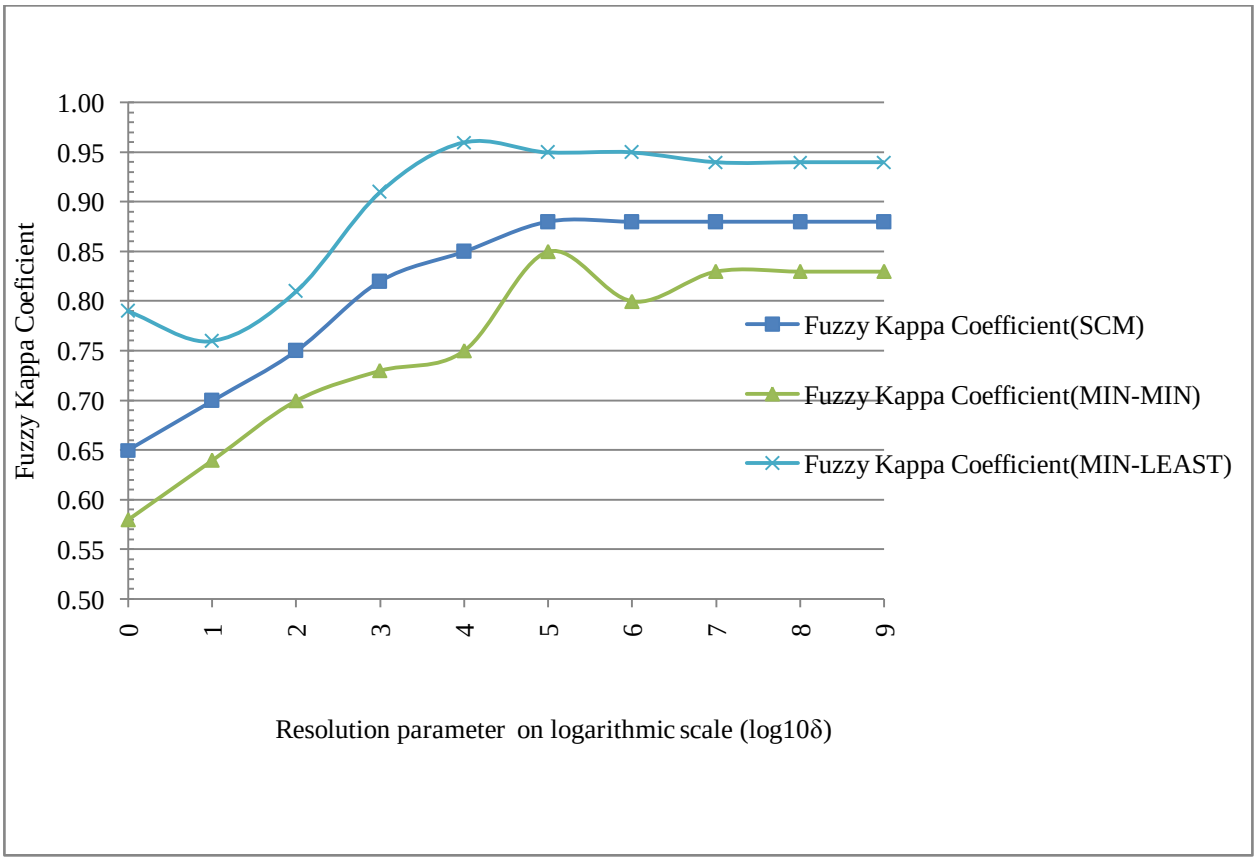

Fig. 6.19(a): Fuzzy Kappa of NC classifier using AWiFS dataset and LISS-III as reference dataset

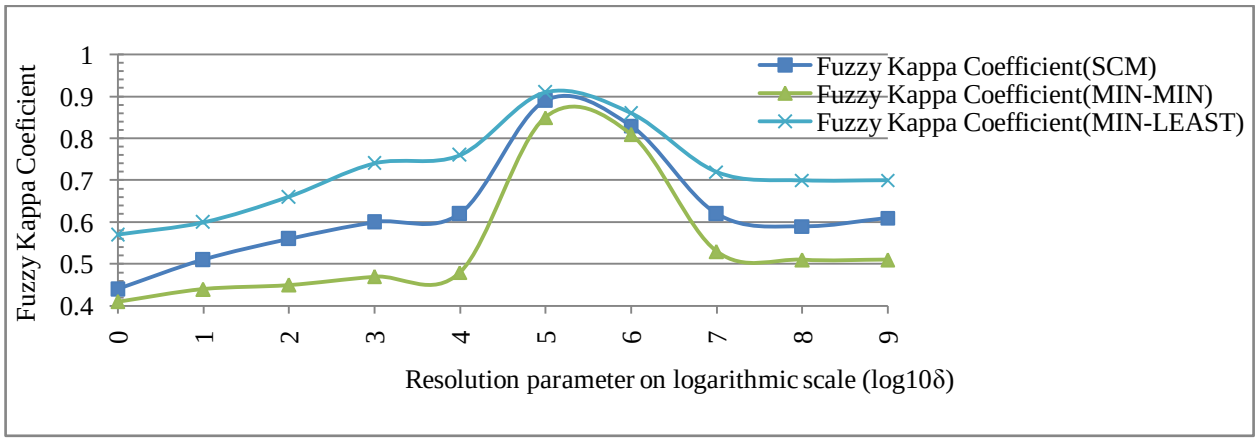

Fig. 6.19 (b): Fuzzy Kappa of NC classifier using AWiFS dataset and LISS-IV as reference dataset

Fig. 6.20 shows that classification uncertainty does not exceed by more than 14% for all values of δ ranging from 1 to 10^9. However, minimum uncertainty value is obtained for $\delta = 10^5$. It has been observed that lower uncertainty of an index indicates that the center value is useful for classification. In a nutshell, the accuracy-uncertainty index from SCM has the capability to identify the distribution of error, even though all operators have same overall accuracy. From {Figs. 6.15 (a), (b) and (c), 6.16 (a), (b) and (c), and 6.18 (a) and (b)}, it can be observed that for the optimized value of resolution parameter $\delta = 10^{5,}$ uncertainty has been reduced due to noisy pixels has been minimized using NC classification approach.

Table 6.6 shows all the accuracy indices for the optimized value of resolution parameter $\delta=10^5$, where AWiFS image has been used as a classified image and LISS-III image has been used a reference image. This output reflects that the User's and Producer's Accuracy for agriculture, sal forest, eucalyptus plantation, moist land, and water body is higher than the threshold value of 85% for MIN-LEAST, MIN-PROD and SCM. Further, it also indicates that the error of omission and error of commission is less in classified imagery (Chen and Zhu, 2010). The Fuzzy overall accuracy, FERM, SCM, MIN-PROD, MIN-MIN, and MIN-LEAST of all classes are 88.84%, 89.56±6.60%, 90.32%, 82.95% and 96.09% respectively. These accuracy measures provide detailed information about the uncertainty which is associated with any particular class. The SCM approach of assessment of accuracy also determines the interclass confusion ratio with the help of MIN-PROD, MIN-MIN, and MIN-LEAST operator.

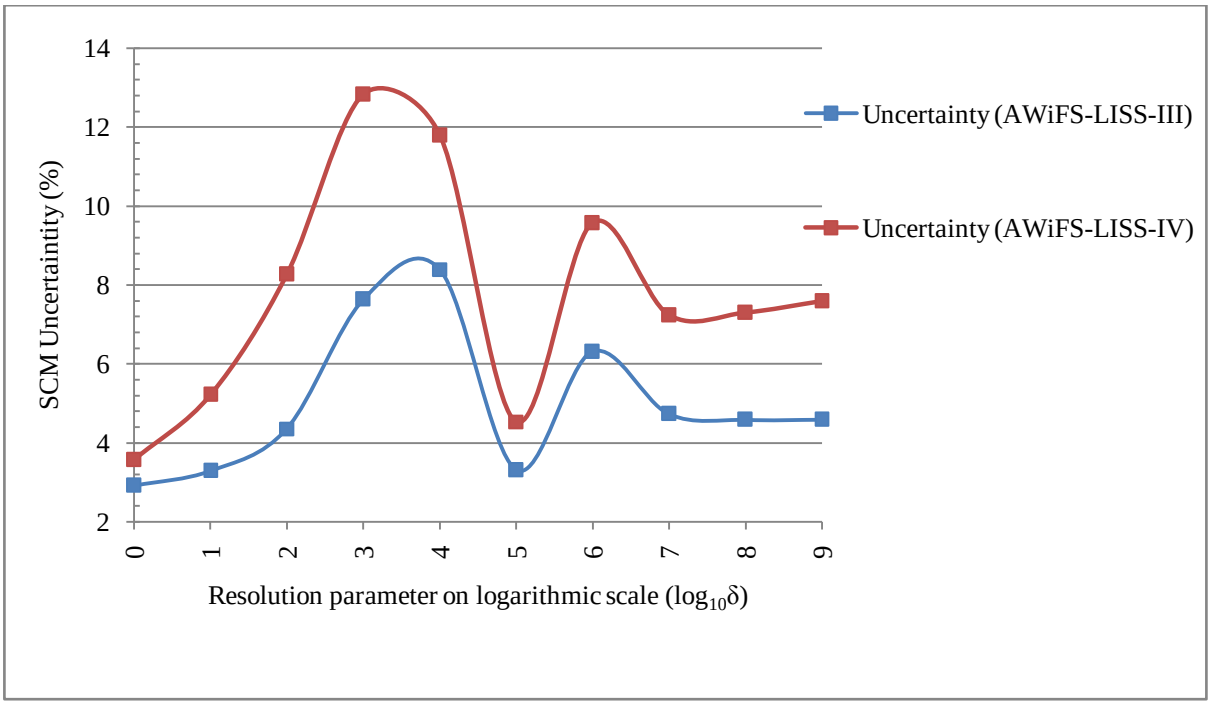

Fig. 6.20: SCM uncertainty of NC classifier

In comparison with PCM classification output Table 6.4, the observed accuracy indices from Table 6.6, are found to be more reliable and accurate. In this study, it has also been observed that MIN-LEAST operator is found more suitable to assess the classification accuracy of NC classifier. In general, to make full use of the multiple features of different sensors data, selecting a suitable variable for inputting into a classification procedure is important. For setting the optimized value of δ, a number of experiments have been performed by varying δ from 1 to 10^9. The accuracy of NC classifier increases with an increase in value of δ until $\delta=10^5$ and thereafter, the class membership is either decreases or become stable as shown in {Fig. 6.15(a), (b) and (c)}. At this point, the corresponding entropy values are also low for all six classes, {Fig.6.16(a), (b) and (c)}. Thus, the optimum value of δ for NC classification has been fixed as 10^5 for NC classifier.

Table 6.6: Accuracy values optimized value of $\delta=10^5$ for NC classifier of AWiFS data with LISS-IV as reference data.

Land-Use Classes	**Accuracy assessment methods**				
	FERM	**SCM**	**MIN-PROD**	**MIN-MIN**	**MIN-LEAST**
Fuzzy user's accuracy (%)					
Agriculture	93.04	93.27±3.01	94.90	91.50	97.02
Sal forest	91.03	91.61±4.30	92.72	88.07	96.12
Eucalyptus plantation	92.20	92.80±3.05	93.37	89.63	96.02
Barren Land	85.42	85.57±11.72	87.09	70.17	97.53
Moist Land	80.77	84.48±9.92	81.94	72.18	92.81
Water Body	95.64	96.37±2.54	96.11	95.01	98.01
Fuzzy producer's accuracy (%)					
Agriculture	90.09	89.73±6.99	91.26	83.02	96.03
Sal forest	91.84	92.40±5.35	93.60	87.02	97.29
Eucalyptus plantation	84.91	87.25±7.10	85.63	79.13	93.87
Barren Land	86.27	89.59±8.37	91.19	79.70	98.76
Moist Land	93.57	94.19±4.66	94.09	89.78	98.33
Water Body	84.98	83.81±8.29	87.24	78.06	94.56
Fuzzy overall accuracy (%)	88.84	89.56±6.60	90.32	82.95	96.09
Fuzzy Kappa	-	0.87±0.08	0.88	0.79	0.95

Fig. 6.21 shows the classified fraction images of AWiFS datasets for the optimized value of $\delta = 10^5$, generated by NC classifier. The derived fraction images matches accurately with the reference data for all classes. These images also show that classes like agriculture, sal forest, barren land and water bodies have been correctly identified using NC approach. The visual interpretations of classified fraction images have further strengthen the belief that NC classifier is able to resolve the problem of mixed pixel.

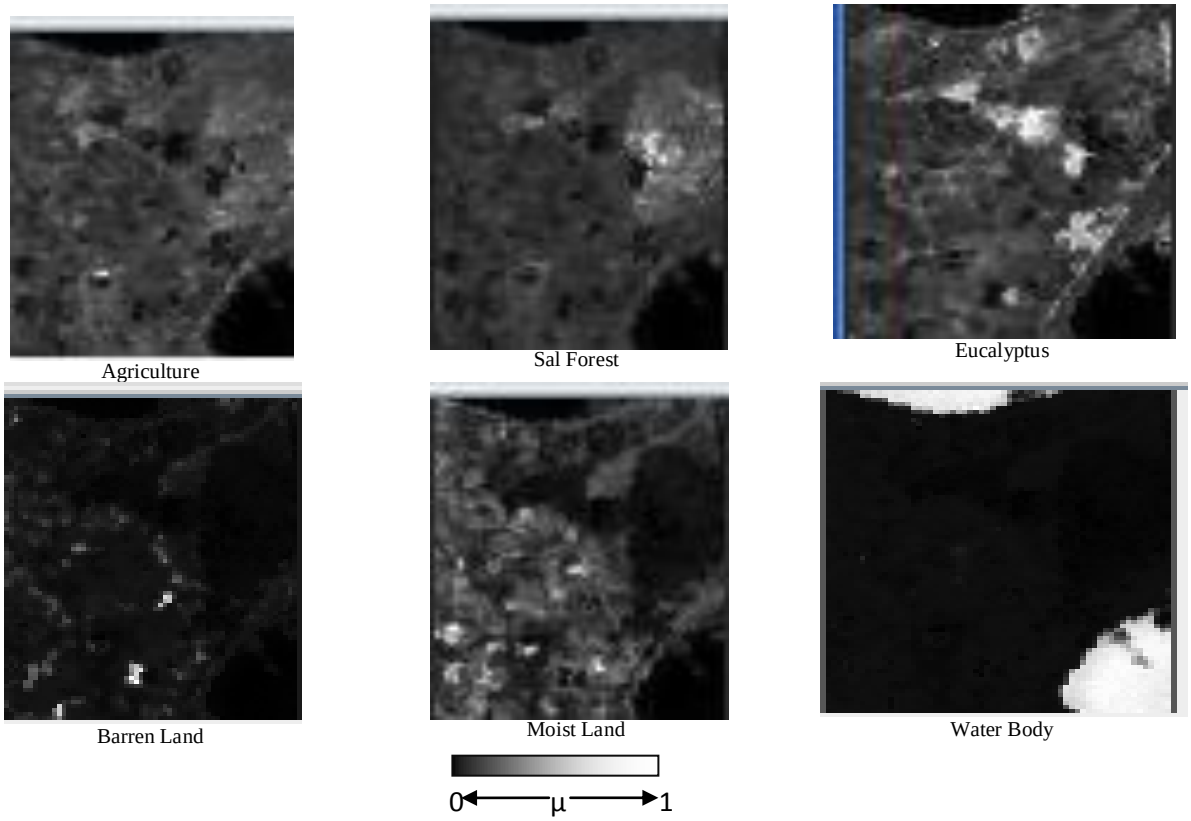

Fig. 6.21: NC classification output of AWiFS image

6.5 RESULTS OF NOISE CLUSTERING WITH ENTROPY (NCWE) CLASSIFIER

To analyze the effect of hybridized model of Fuzzy and entropy based supervised classifier which includes NC with Entropy (NCWE) and FCM with Entropy (FCMWE), classification. The resampling of AWiFS, LISS-III and LISS-IV image has been done at 60m, 20m, and 5m resolution. The resampling is important for assessment of accuracy as each finer resolution image is used as a reference data set for classified image of a coarser data set. The resampling of these datasets has been done in such a way such that the pixel size in all three images formed a ratio of 1:4:12, for LISS-IV, LISS-III and AWiFS datasets.

The basic objective of this study is to hybridize two fuzzy based methods FCM and NC with entropy to identify the join effect of two purely fuzzy models and entropy models which is similar to statistical model. The NCWE classifier has been used in this study, to extract the multiple land cover class at a time, at sub-pixel level. The performance of this classifier is dependent on the constant value of resolution parameter δ and regularizing parameter ν (Eq. 3.19). To obtain accurate information from the classifier, the optimization of regularizing parameter ν is required.

The optimized constant value of resolution parameter δ and varying value of regularizing parameter ν is class dependent but both are mutually dependent to perform the classification using NCWE approach. To perform NCWE classification, a fixed value of $\delta=10^5$has been used for all varying values of ν (from 0 to 10^9).

6.5.1 CLASS MEMBERSHIP OF NCWE CLASSIFIER

Fig. 6.22 (a), (b) and (c) shows the variation of the of the regularizing parameter (ν) with class membership of different classes such as agriculture, sal forest, eucalyptus plantation, barren land, moist land and water body of IRS-P6 for AWIFS, LISS-III and LISS-IV dataset respectively. For all three datasets, class membership has been generated for the different values of ν ranging from 0 to 10^9. The class membership values of a pixel denote the class proportions, which indicate the soft classified output for a pixel. It has been observed from the Fig. 6.22 (a), (b) and (c) that for the initial values of regularizing parameter ν hard classification has been performed by the classifier due to the effect of entropy. However, after certain iteration when ν reaches up to 1, it starts to soften and for $\nu =10^2$, class membership lies between 0.85 to 0.99 for all classes. Regularizing parameter ν is the fixed parameter, $0\leq \nu < \infty$ which regularizes the fuzzified solution to crisp solution.

The class membership μ increases till $\nu=10^2$, and thereafter it starts to decrease or becomes almost constant {Fig. 6.22(a), (b) and (c)}. Thus, as per the analysis of class membership, the optimum value of ν for NCWE classification has been fixed as 10^2, when

AWiFS image has been used as classified image and LISS-III and LISS-IV images has been used as a reference image. In this study, the optimization of a regularizing parameter ν for the classification would also be analyzed and verified via entropy method. The classification performance are also being assessed by using Sub-pixel accuracy indices such as FERM, SCM, MIN-MIN, MIN-LEAST and Fuzzy Kappa coefficient along with their associated uncertainty. For identifying the class-wise optimized value Producer's Accuracy have been computed for all six classes.

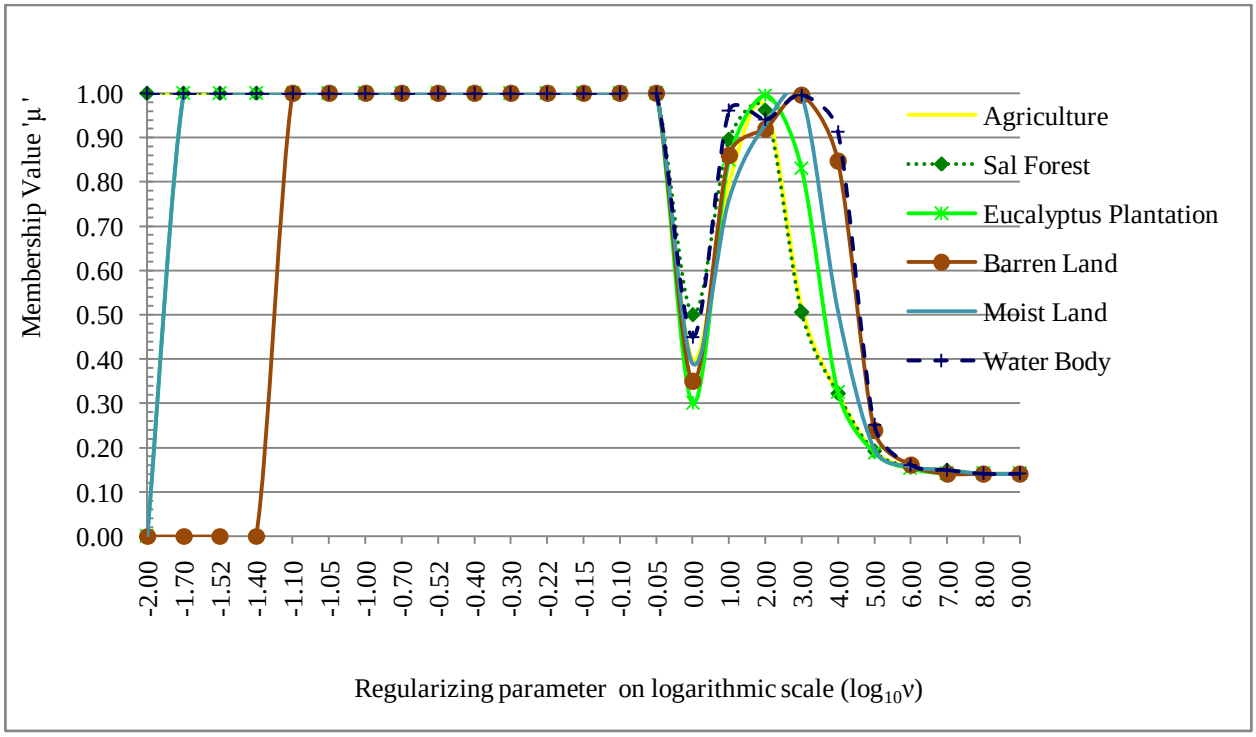

Fig. 6.22(a): Class membership for NCWE classifier using AWiFS dataset.

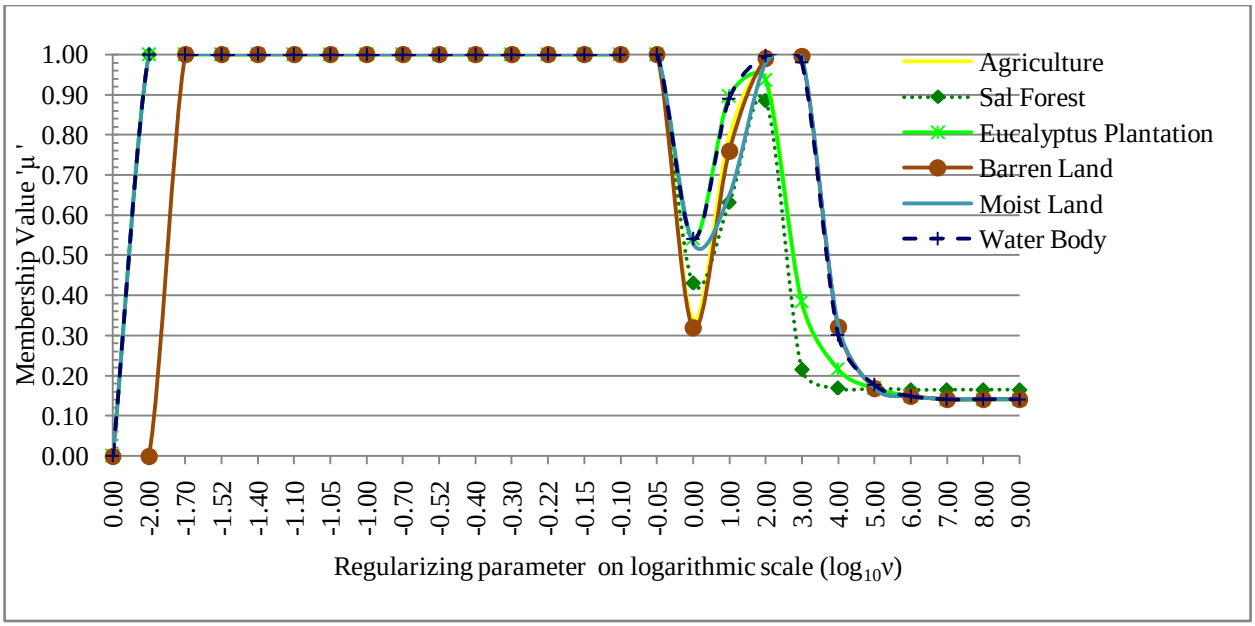

Fig. 6.22(b): Class membership for NCWE classifier using LISS-III dataset.

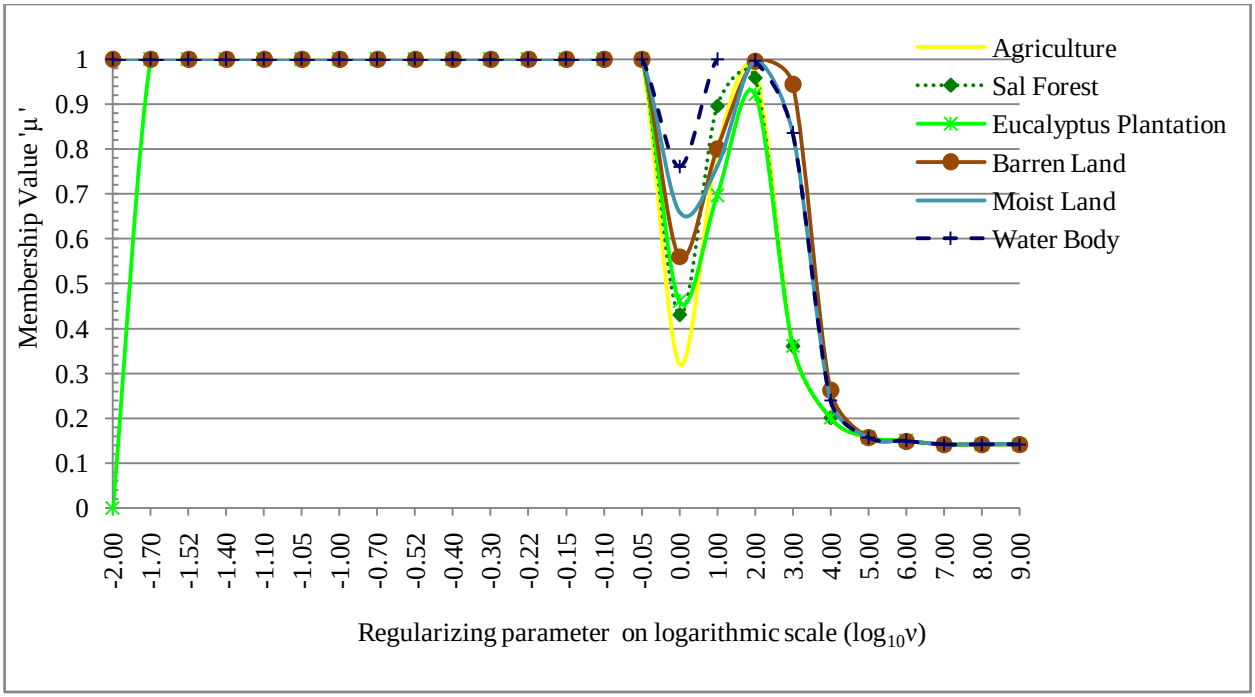

Fig. 6.22(c): Class membership for NCWE classifier using LISS-IV dataset.

6.5.2 ENTROPY OF NCWE CLASSIFIER

Fig. 6.23 (a), (b) and (c) shows that the computed entropy for AWiFS, LISS-III and LISS-IV fraction images of NCWE classifier for agriculture, sal forest, eucalyptus plantation, barren land and water body land cover classes lies between the specified range of [0,3]. This indicates that the information uncertainty is not exceeding more than 3% (Stein et al., 2002). It has been observed from Fig. 6.23 (a), (b) and (c) that for $\nu=10^2$, the entropy values for all classes are at lowest level. For this optimized value of ν, the membership value is high i.e. up to 0.995 and the computed entropy is low (0.005). This trend reflects that the uncertainty in classified result is low. In a nutshell, this study on spatial variation has identified that the mixture of entropy in NCWE classifier initially hardens the output, but when ν reaches towards 1, its starts to soften. However, for $\nu= 10^2$, it produces optimum membership with minimum entropy.

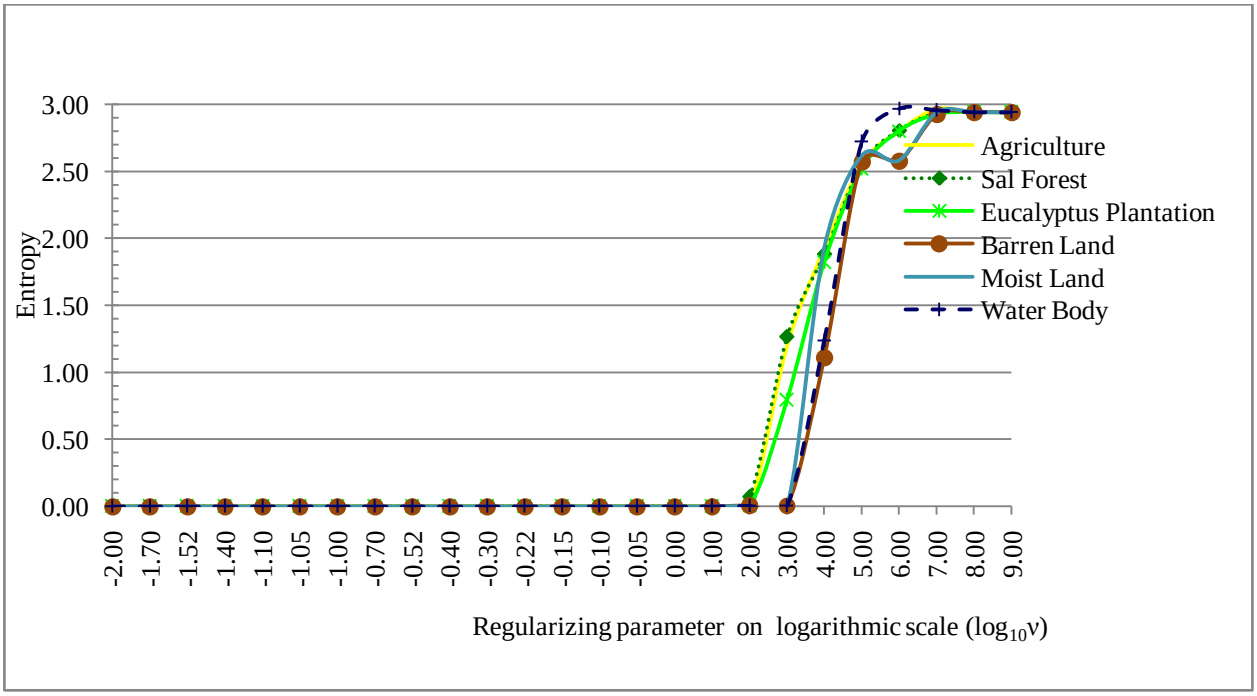

Fig. 6.23(a): Entropy for NCWE classifier using AWiFS dataset

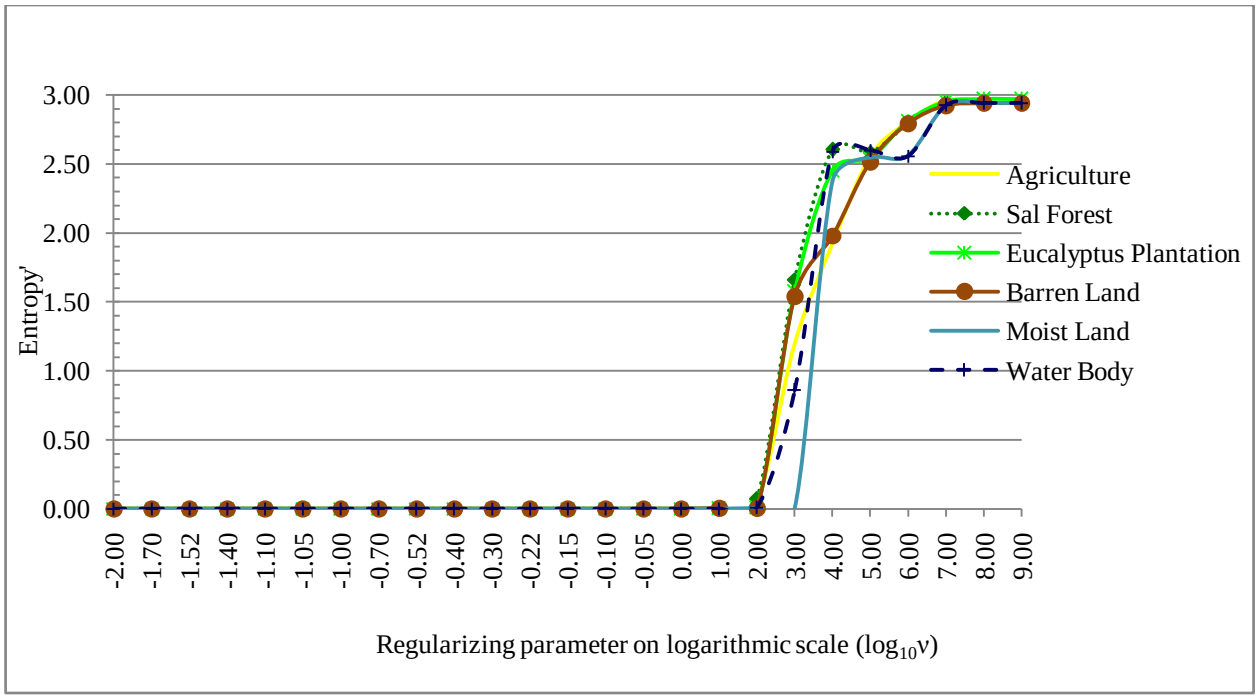

Fig. 6.23(b): Entropy for NCWE classifier using LISS-III dataset

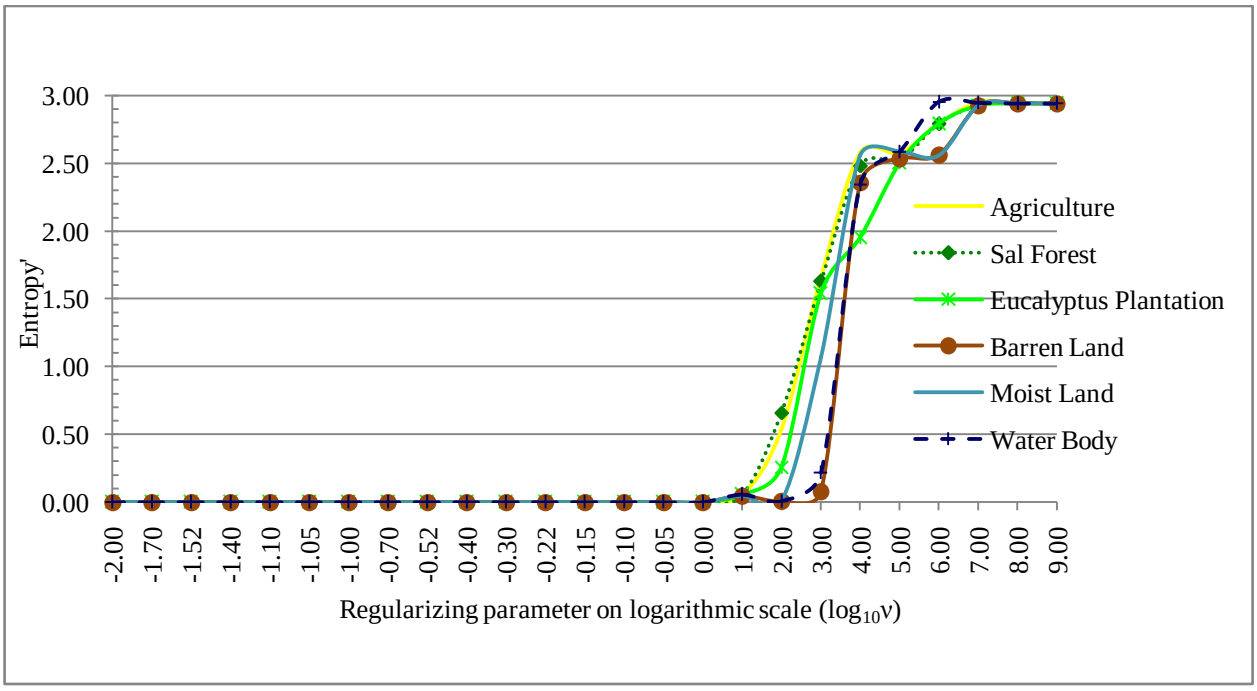

Fig. 6.23(c): Entropy for NCWE classifier using LISS-IV dataset

6.5.3 PRODUCER'S ACCURACY OF NCWE CLASSIFIER

To ascertain the accuracy of individual classes, Producer's Accuracy (PA) has been computed for NCWE classifier {Fig. 6.24 (a) and (b)}. AWiFS image has been used for classification while LISS-III and LISS-IV images are used as a reference image to determine the Producer Accuracy. It is observed that for $\nu=10^2$, NCWE classifier produces highest accuracy for all six land cover classes present in the image.

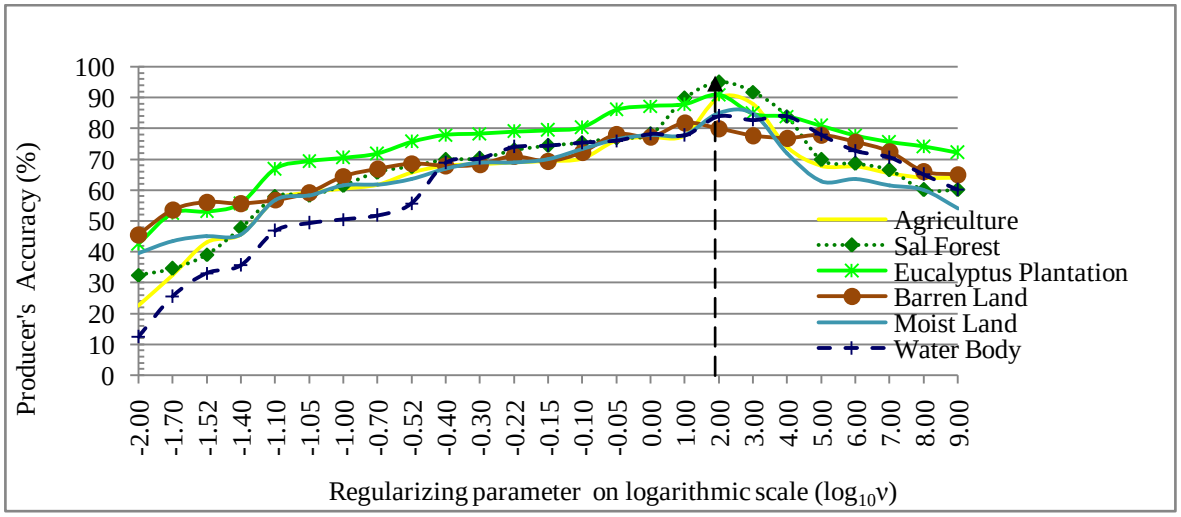

Fig. 6.24(a): Producer's accuracy of NCWE classifier for AWiFS dataset using LISS-III as reference dataset.

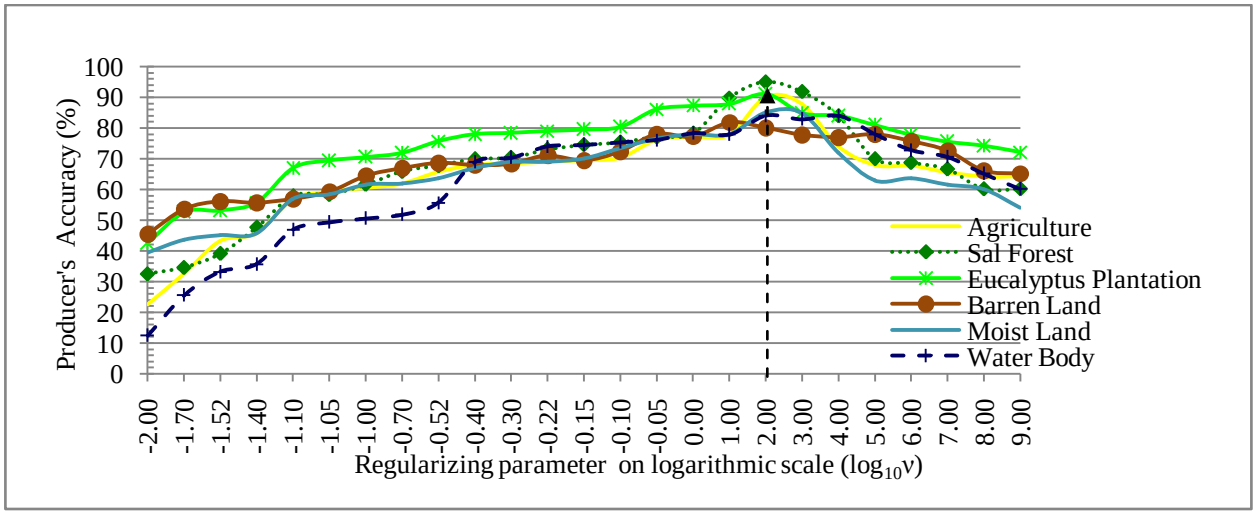

Fig. 6.24(b): Producer's accuracy of NCWE classifier for AWiFS dataset using LISS-IV as reference dataset.

6.5.4 CLASS WISE PARAMETER OPTIMIZATION OF NCWE CLASSIFIER

On the basis of highest class membership, lower entropy and highest Producers Accuracy produced by classified imagery, the class wise optimized values of regularizing parameter (ν) have been shown in Table 6.7. It is observed that irrespective of datasets, the optimized value of (ν)for agriculture and barren land is 2.12×10^2. While, for sal forest, eucalyptus plantation, moist land and water body it is 10^2.

Table 6.7: Class wise parameter optimization of (ν) for NCWE classifier

Class	Class membership			Entropy			Producer's accuracy		Optimized Mean Value
	AWiFS	LISS-III	LISS-IV	AWiFS	LISS-III	LISS-IV	AWiFS-LISS-III	AWiFS-LISS-IV	
Agriculture	10^3	10^2	10^2	10^2	10^2	10^2	10^2	10^2	2.12×10^2
Sal Forest	10^2	10^2	10^2	10^2	10^2	10^2	10^2	10^2	10^2
Eucalyptus plantation	10^2	10^2	10^2	10^2	10^2	10^2	10^2	10^2	10^2
Barren land	10^3	10^2	10^2	10^2	10^2	10^2	10^2	10^2	2.12×10^2
Moist land	10^2	10^2	10^2	10^2	10^2	10^2	10^2	10^2	10^2
Water body	10^2	10^2	10^2	10^2	10^2	10^2	10^2	10^2	10^2

6.5.5 GENERALIZED PARAMETER OPTIMIZATION OF NCWE CLASSIFIER

In this study, a noise and entropy based hybridized classifiers has been used to identify the agriculture, sal forest, eucalyptus plantation, barren land, moist land and water body. For a good classification, training data should be available for all representative classes present in the

imagery. The NCWE classifier is capable of performing soft classification when the user has supplied the information for specified land cover classes.

The performance of NCWE classifier can be assessed by various accuracy indices like FERM, SCM, MIN-MIN, and MIN-LEAST is shown in Fig. 6.25 (a) and (b). To obtain the result mentioned in Fig. 6.25 (a) and (b), the optimized value of resolution parameter $\delta=10^5$ has been taken as a constant and the regularizing parameter ν is ranging from 0 to 10^9, while Overall accuracy, FERM, SCM, MIN-MIN and MIN-LEAST are varying between 25% to 95% in both cases, when AWiFS datasets are used as a classified image and LISS-III or LISS-IV dataset has been used as a reference image. In the process of identifying the optimized value of regularizing parameter (ν), FERM, SCM and other accuracy indices have been analyzed for all six classes. It is found that for $\nu = 10^2$, all the accuracy indices have high value i.e. up to (95%) and less uncertainty value (0.005).

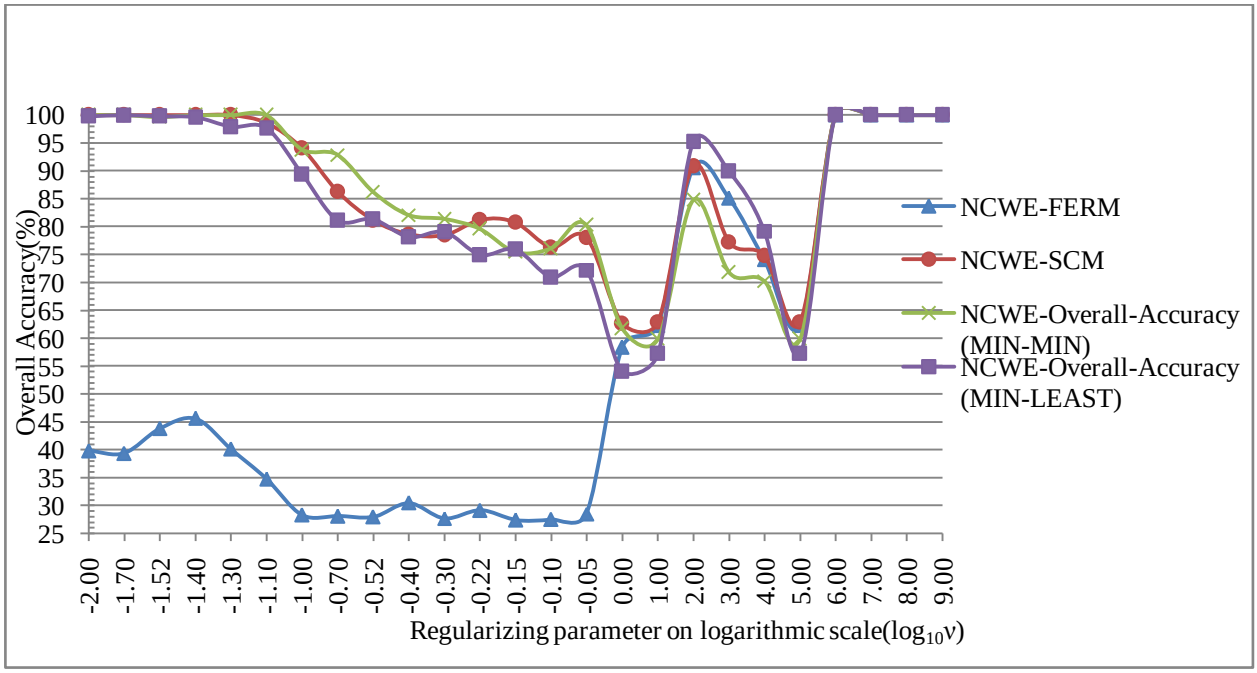

Fig. 6.25(a): Overall accuracy of NCWE classifier for AWiFS dataset using LISS-III as reference dataset

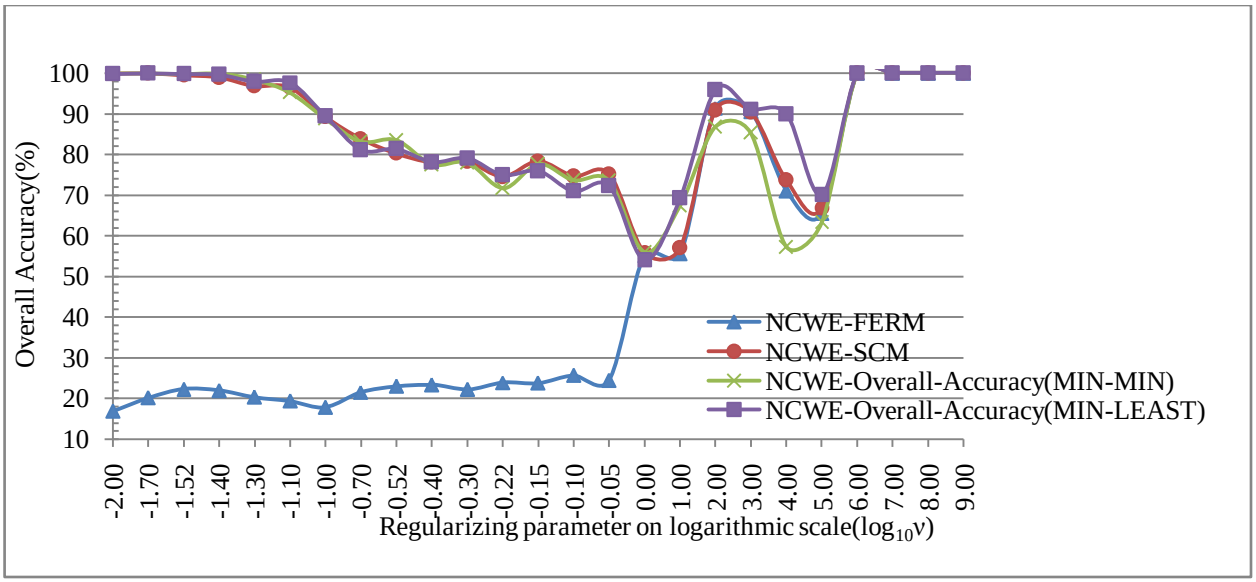

Fig. 6.25(b): Overall accuracy of NCWE classifier for AWiFS dataset using LISS-IV as reference dataset

The computed Fuzzy Kappa coefficient for NCWE classifier is shown in Fig. 6.26 (a) and (b) which shows that the value of Fuzzy Kappa coefficient lies between 0.38 to 1.0 for SCM, MIN-MIN and MIN-LEAST accuracy indices. The value of Fuzzy Kappa coefficient signifies that for initial values of ν, it is almost one. This indicates that the inclusion of statistical approach via entropy in fuzzy based classification approach (NC) perform hard classification for initial values of ν till it reaches to 0.5, and thereafter it starts to soften. This trend indicates that the classification done using NCWE classifier is appropriate and consistent with respect to accuracy measures.

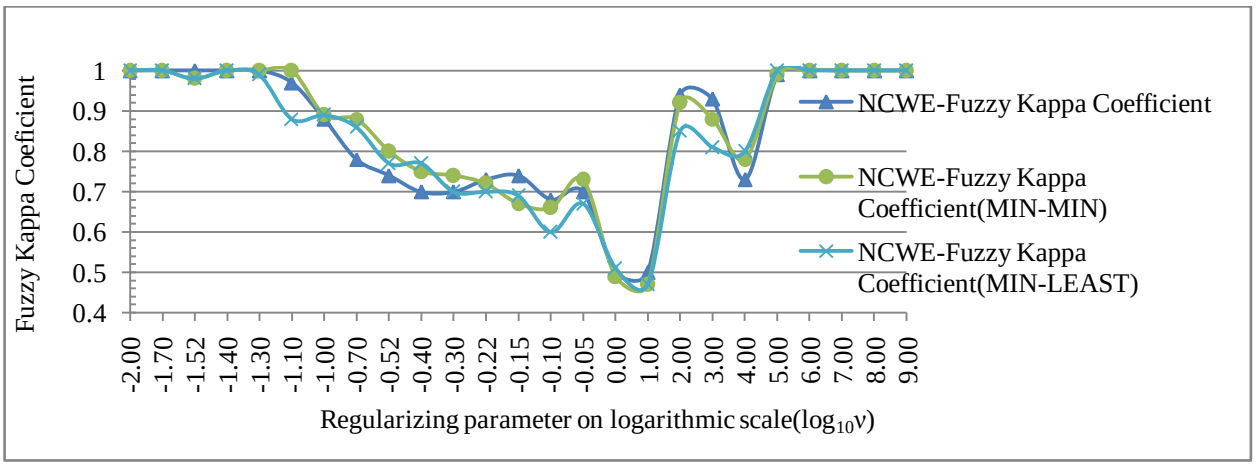

Fig. 6.26(a): Fuzzy Kappa of NCWE classifier using AWiFS dataset and LISS-III as reference dataset

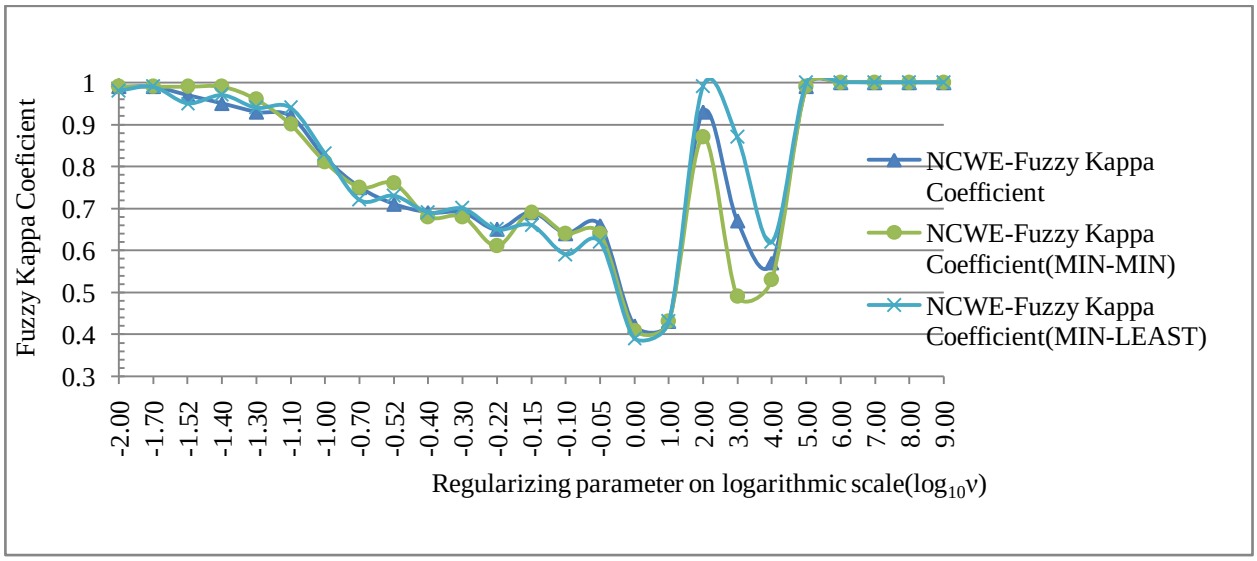

Fig. 6.26(b): Fuzzy Kappa of NCWE classifier using AWiFS dataset and LISS-III as reference dataset

Fig. 6.27 shows the classification uncertainty is not more than 8% for all values of ν ranging from 0 to 10^9. However, this accuracy index produces minimum value for the optimized values of ν $=10^2$.The uncertainty index of SCM has the capability to identify the error distributions among classes and it is shown in Fig. 6.27 that for $\nu=10^2$ the distribution of error in classification is minimum in both cases where AWiFS dataset has been assessed using LISS-III and LISS-IV dataset.

The estimation of an uncertainty of classification results is important and necessary to evaluate the performance of a classifier. In this study, the evaluation of performance of NCWE classifier has been addressed. For estimating the uncertainty in a classified imagery, various soft accuracy indices such as fuzzy overall accuracy, fuzzy kappa coefficient with varying spatial resolution of classification and reference sub-pixel outputs have been considered. The uncertainty criteria have been estimated from SCM based on actual and desired outputs of classifier. Therefore, these criteria are dependent on the error of the results and sensitive to error variations. This fact has also been verified using entropy-based criterion on actual outputs of classifier and hence it is sensitive to uncertain variations.

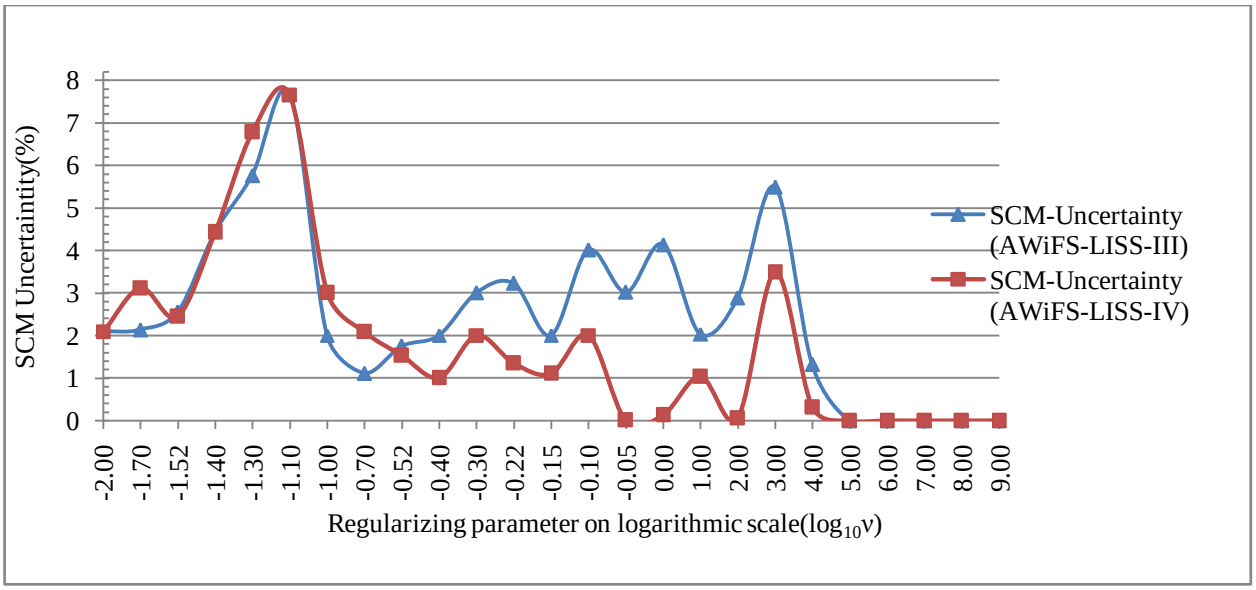

Fig. 6.27: SCM uncertainty of NCWE classifier

Table 6.8 shows all the accuracy indices for the optimized value of regularizing parameter $\nu=10^2$, where AWiFS image has been used as a classified image and LISS-IV image has been used a reference image. The Fuzzy overall accuracy, FERM, SCM, MIN-PROD, MIN-MIN, and MIN-LEAST of all classes are 90.20%, 90.80±4.89%, 90.48%, 85.40% and 95.24% respectively. Thus, the optimum value of ν for NCWE classification has been fixed as 10^2toclassify coarser resolution imagery.

Fig. 6.27 shows the fraction images of AWiFS datasets for NCWE classification. After examining the fraction images generated by NCWE classifier, it has been observed that intergrades phenomena within pixel have been resolved in AWiFS. The inclusion of entropy and regularizes the classifier to remove pixel uncertainty. However, one of the major drawbacks of this classifier is, it tends towards hard classification for the initial values of regularizing parameter ν. After a certain value of ν when it reaches to 0.5, the classification starts to soften and after the analysis of each fraction images generated by NCWE classifier, it can be concluded that for $\nu=10^2$, the class membership and overall accuracy is higher.

Table 6.8: Accuracy assessment report of NCWE classification for AWiFS image of Resourcesat-1 with LISS-IV as a reference image for optimized value of $\nu=10^2$

Land-Use Classes	**Accuracy assessment methods**				
	FERM	**SCM**	**MIN-PROD**	**MIN-MIN**	**MIN-LEAST**
Fuzzy user's accuracy (%)					
Agriculture	89.96	91.19±6.44	90.75	83.68	97.94
Sal forest	94.66	94.71±4.53	94.43	88.58	99.21
Eucalyptus plantation	94.18	94.66±3.69	94.34	90.92	97.85
Barren Land	65.00	73.47±4.53	79.25	69.06	81.06
Moist Land	80.99	82.79±6.98	80.88	76.85	87.43
Water Body	85.72	87.71±1.46	87.45	85.39	89.03
Fuzzy producer's accuracy (%)					
Agriculture	97.48	97.42±1.48	97.33	96.38	98.59
Sal forest	94.43	94.85±3.36	94.77	91.99	97.69
Eucalyptus plantation	90.98	91.72±3.49	91.66	88.96	94.66
Barren Land	53.16	69.50±13.41	60.35	50.15	81.69
Moist Land	86.99	87.60±5.99	88.76	80.90	93.28
Water Body	75.61	77.77±11.97	72.65	61.21	90.17
Fuzzy overall accuracy (%)	90.20	90.80±4.89	90.48	85.40	95.24
Fuzzy Kappa	-	0.88±0.06	0.87	0.81	0.94

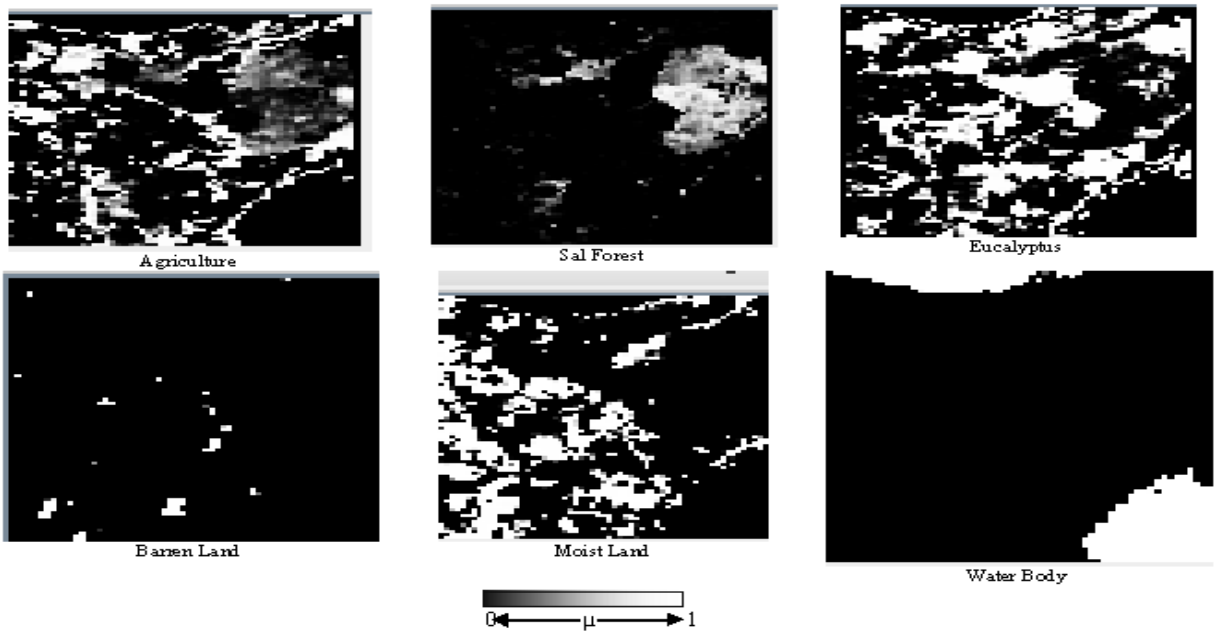

Fig. 6.28: NCWE classification output of AWiFS image

6.6 RESULTS OF FUZZY *C*-MEAN WITH ENTROPY (FCMWE) CLASSIFIER

In this study, Fuzzy *C*-means (FCM) has been used as a base soft classifier and entropy has been added to investigate the effect of this hybridized model known as FCMWE. The basic objective of this study is to identify the optimized value of regularizing parameter ν for FCMWE classifier which generates classified output with minimum uncertainty. The performance of this classifier is dependent on the constant value of weighting exponent *m*=1 and regularizing parameter ν. To obtain accurate information from this classifier, the optimization of regularizing parameter ν is required. To perform the FCMWE classification, fixed value of *m*=1 has been used for all varying values of ν (from 0 to 10^9).

6.6.1 CLASS MEMBERSHIP OF FCMWE CLASSIFIER

Fig. 6.29 (a), (b) and (c) shows the variation of the of the regularizing parameter ν with class membership of different classes such as agriculture, sal forest, eucalyptus plantation, barren land, moist land and water body for AWIFS, LISS-III and LISS-IV dataset respectively. For all three datasets, class membership has been generated for the different values of ν ranging from 0 to 10^9. It has been observed from Fig. 6.29 (a), (b) and (c) that for initial values of ν, this classifier performs hard classification and the effect of entropy is higher. However, when ν reaches to 1, the classifier starts to soften. For ν =$10^2$and 10^3, the class membership is higher and lies between 0.85 to 0.99 for all the six classes. Regularizing parameter ν is the fixed parameter, $0 \leq \nu < \infty$ which regularizes the fuzzified solution to crisp solution.

The class membership μ increases till ν=10, 10^2 and 10^3, and thereafter it starts to decrease or becomes almost constant {Fig. 6.29 (a), (b) and (c)}. Thus, as per the analysis of class membership, the optimum value of ν for FCMWE classifier has been fixed as 10^2. However, this optimization would be further verified by entropy and other accuracy measure such as FERM, SCM and Fuzzy Kappa coefficient.

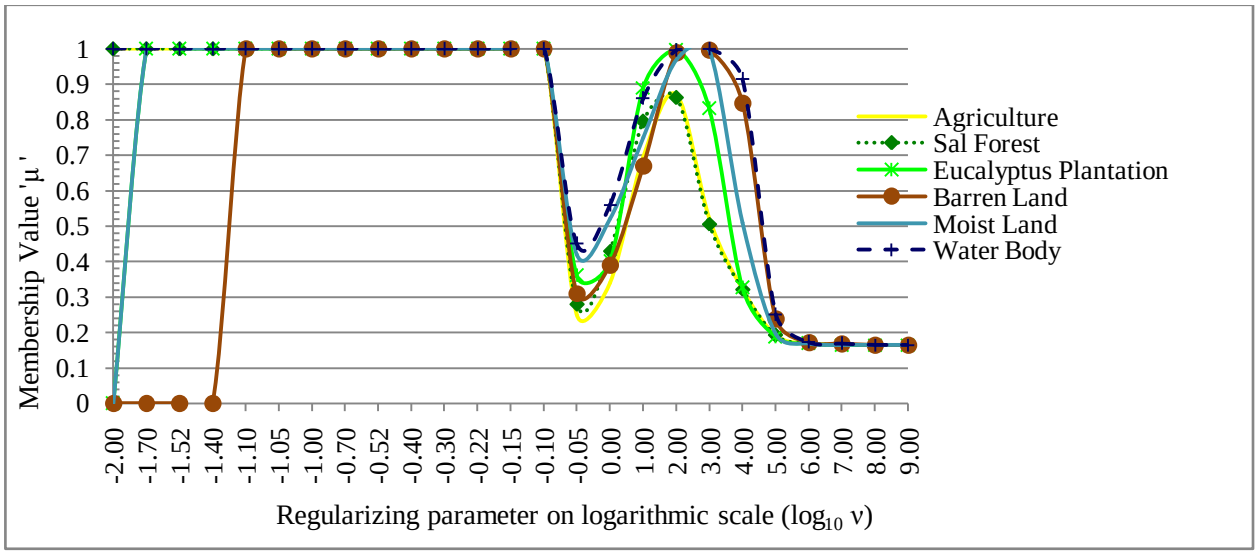

Fig. 6.29 (a): Class membership for FCMWE classifier using AWiFS datasets.

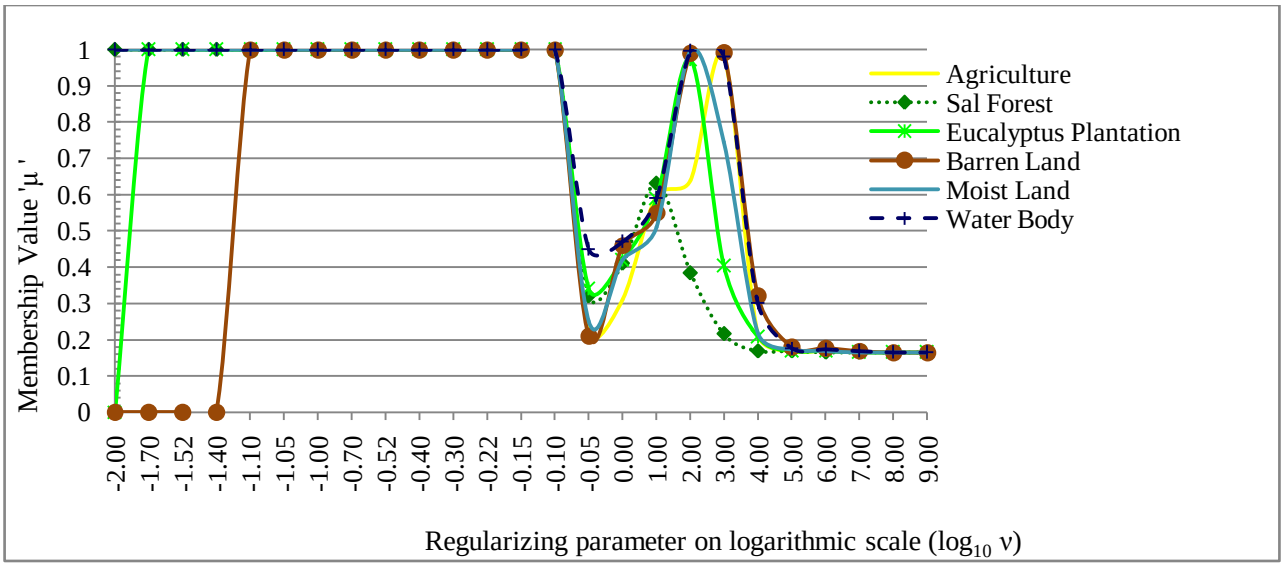

Fig. 6.29 (b): Class membership for FCMWE classifier using AWiFS datasets.

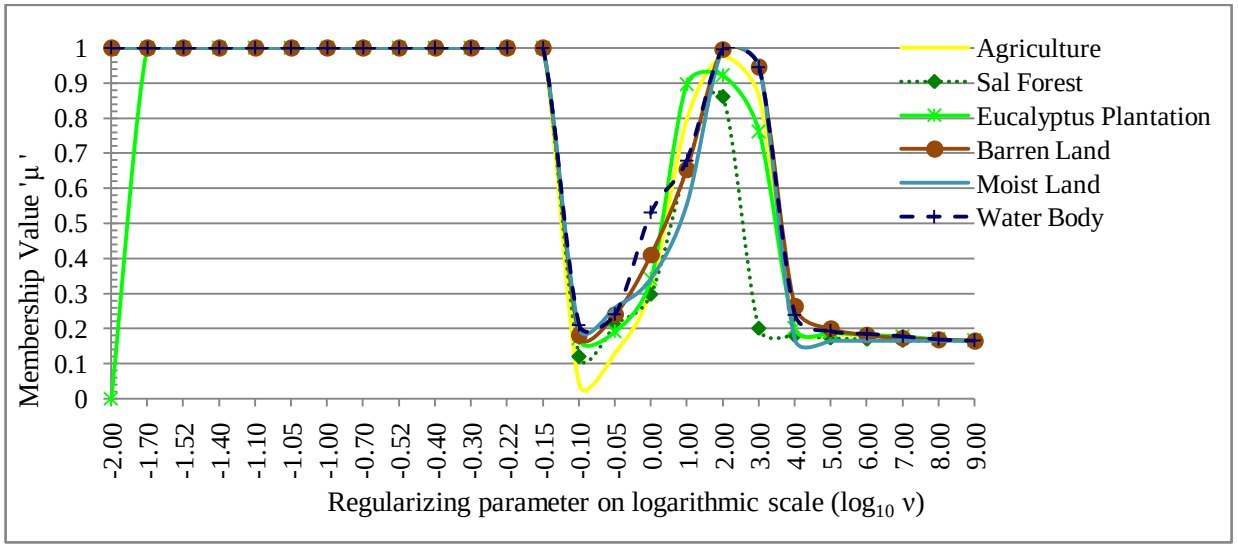

Fig. 6.29 (c): Class membership for FCMWE classifier using AWiFS datasets.

6.6.2 ENTROPYOF FCMWE CLASSIFIER

The entropy of FCMWE classifier of classified fraction images can be computed by using Eq 3.85. Fig. 6.30 (a), (b) and (c) shows the computed entropy for AWiFS, LISS-III and LISS-IV fraction images of FCMWE classifier. It has been observed from Fig. 6.30 (a), (b) and (c) that for $\nu=10^2$ and 10^3 the entropy values for all classes are low. For this optimized value of ν, the membership is high i.e. up to 0.995 and the computed entropy is low (0.005). This trend reflects

that the uncertainty in results is low. In a nutshell, it can be concluded that whenever entropy has been used as an indirect accuracy measure and this shows the classification consistency with respect to a particular class.

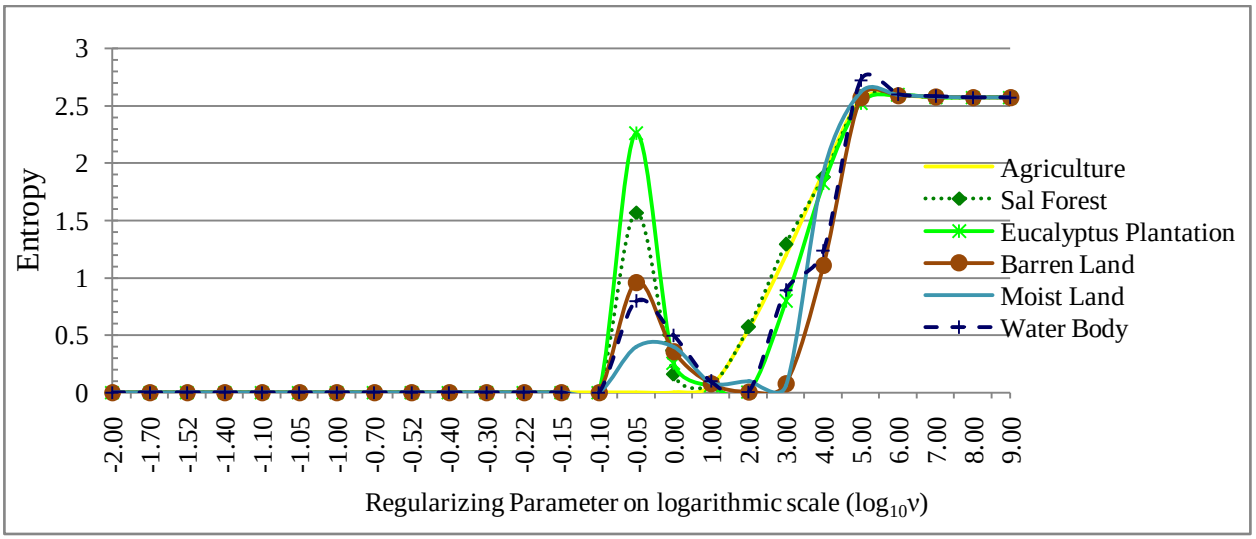

Fig. 6.30(a): Entropy for FCMWE classifier using AWiFS dataset

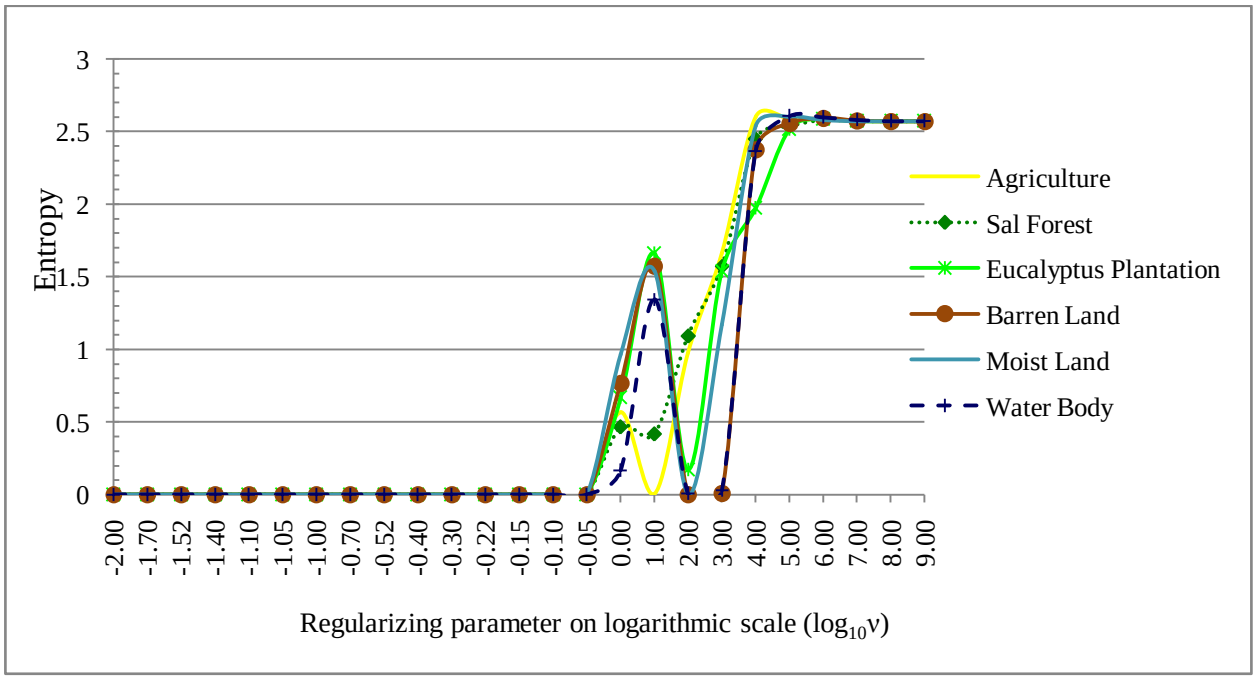

Fig. 6.30(b): Entropy for FCMWE classifier using LISS-III dataset

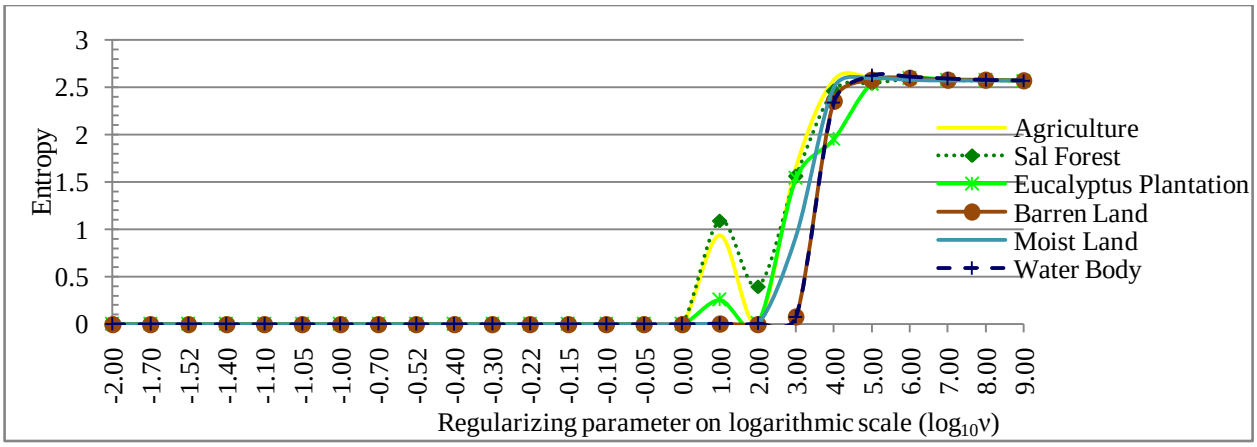

Fig. 6.30(c): Entropy for FCMWE classifier using LISS-IV dataset

6.6.3 PRODUCER'S ACCURACY OF FCMWE CLASSIFIER

To find out the accuracy of an individual class, Producer's Accuracy has been computed for FCMWE classifier {Fig. 6.31 (a) and (b)}. To compute Producer's Accuracy, AWiFS image has been used for classification, while LISS-III and LISS-IV images have been used as reference image. It has been observed that while classifying AWiFS with LISS-III and LISS-IV dataset, the optimized value of regularizing parameter $\nu=10^3$ for agriculture, sal forest and eucalyptus plantation. However, for barren land, moist land and water body $\nu=10^2$ produce highest accuracy values.

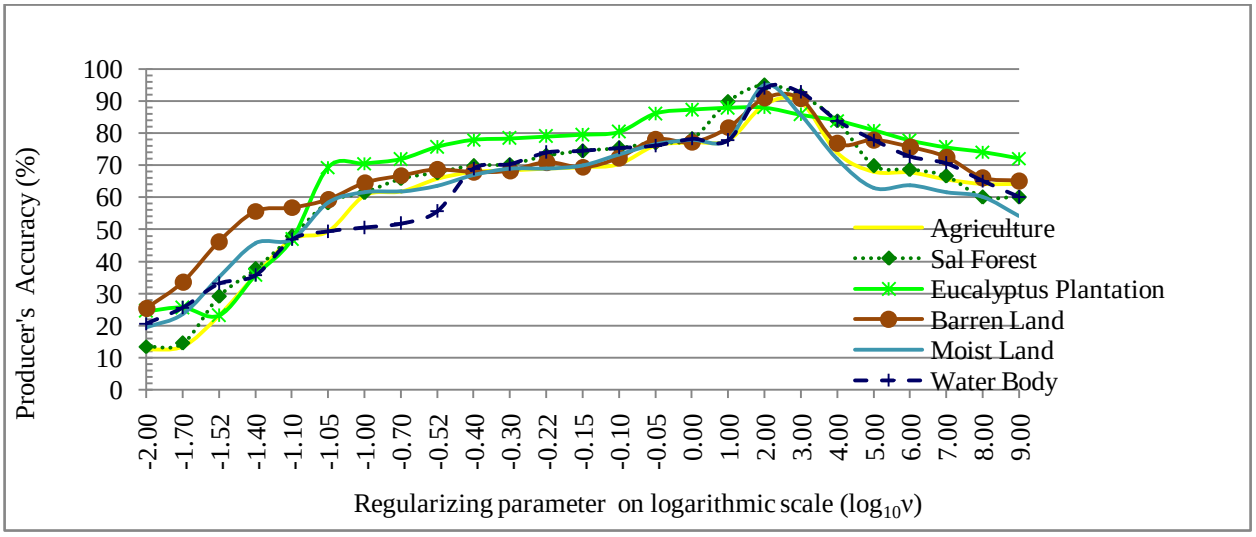

Fig. 6.31(a): Producer's accuracy of FCMWE classifier for AWiFS dataset using LISS-III as reference dataset.

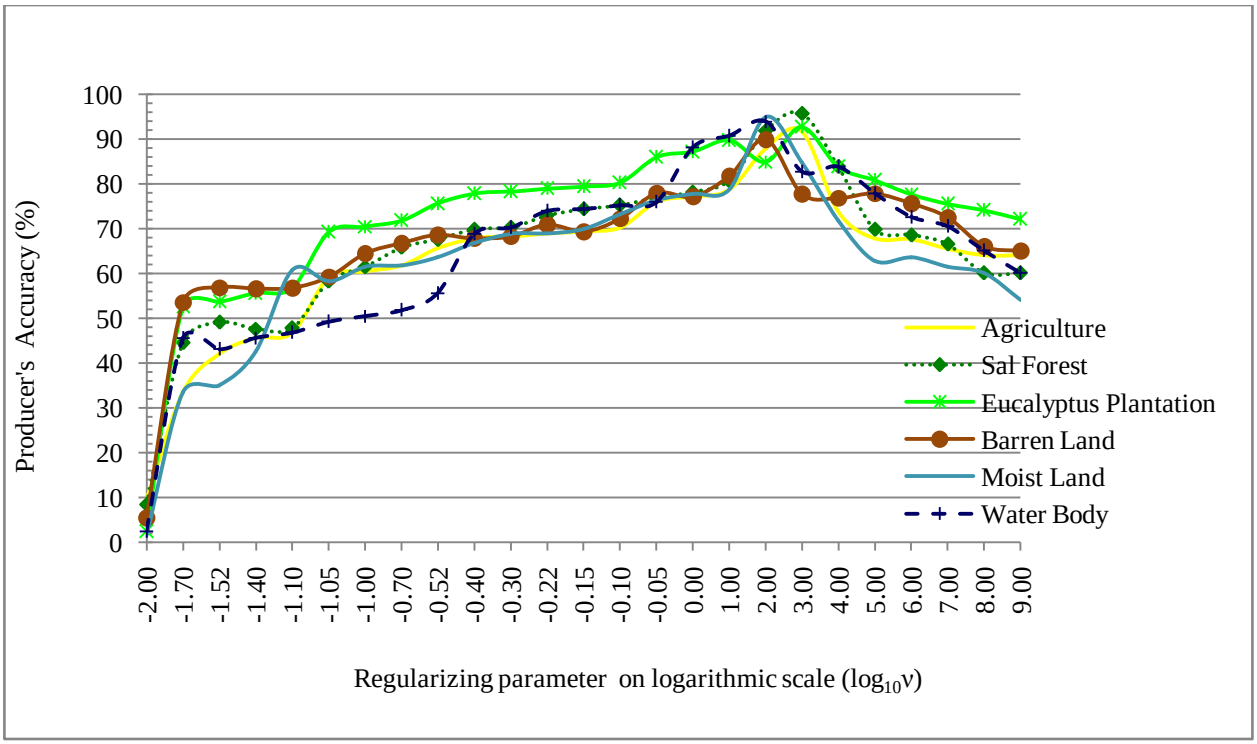

Fig. 6.31(b): Producer's accuracy of FCMWE classifier for AWiFS dataset using LISS-IV as reference dataset.

6.6.4 CLASS WISE PARAMETER OPTIMIZATION OF FCMWE CLASSIFIER

On the basis of class membership, entropy and producer's accuracy produced by classified imagery. The class wise optimized values of regularizing parameter ν have been shown in Table 6.9. This value of ν has been recorded for each class where class membership and Producer's accuracy is high and entropy is low. It has been recognized from the obtained results that irrespective of datasets $\nu = 6.6 \times 10^2$ found more suitable to classify agriculture and eucalyptus plantation. However, for barren land, moist land and water body, $\nu = 10^2$ is found to be more suitable for the classification using FCMWE classification approach. For sal forest $\nu = 7.7 \times 10^2$ is found to be more appropriate for classification. To perform classification a constant value of weighting exponent m =1 has been used.

Table 6.9: Class wise parameter optimization of (ν) for FCMWE classifier

Class	Class membership			Entropy			Producer's accuracy		Optimized Mean Value
	AWiFS	LISS-III	LISS-IV	AWiFS	LISS-III	LISS-IV	AWiFS-LISS-III	AWiFS-LISS-IV	
Agriculture	10^3	10^3	10^3	10^2	10^2	10^2	10^3	10^3	6.6×10^2
Sal Forest	10^3	10^3	10^3	10^3	10^2	10^2	10^3	10^3	7.7×10^2
Eucalyptus plantation	10^3	10^3	10^3	10^2	10^2	10^2	10^3	10^3	6.6×10^2
Barren land	10^2	10^2	10^2	10^2	10^2	10^2	10^2	10^2	10^2
Moist land	10^2	10^2	10^2	10^2	10^2	10^2	10^2	10^2	10^2
Water body	10^2	10^2	10^2	10^2	10^2	10^2	10^2	10^2	10^2

6.6.5 GENERALIZED PARAMETER OPTIMIZATION OF FCMWE CLASSIFIER

The FCMWE classification algorithm has been used in supervised mode along with the Euclidian weighted norm to classify the remote sensing imagery. A result of FCMWE classifier in form of various accuracy indices like FERM, SCM, MIN-MIN, and MIN-LEAST is shown in Fig. 6.32 (a), (b) and (c).

To obtain the result mentioned in Fig. 6.32(a), (b) and (c), a constant value of weighting exponent m=1 has been taken for regularizing parameter ν ranges from 0 to 10^9. The Overall accuracy, FERM, SCM, MIN-MIN and MIN-LEAST are varying between 10% to 99% in both cases, where, AWiFS dataset is used for classification and LISS-III or LISS-IV dataset is used as a reference image. In the process of identifying the optimized value of regularizing parameter (ν), all these accuracy indices has been analyzed for all six classes incorporated in this study and it is found that for $\nu = 10^2$, all the accuracy indices are higher i.e. up to (92%) except FERM, and has lesser uncertainty value (0.005).

The FERM based measures are not suitable for initial ν values to assess the accuracy of FCMWE hybrid soft classifier. This phenomenon occurs because when class proportions are hardened to their corresponding class allocation with the inclusion of entropy, FERM accuracy drops marginally. This is due to the fact that hardening has resulted in over estimation of some classes and under estimation of others. Another important observation is that after ν $=10^5$, the classifier totally starts to behave like hard statistical classifier where the effect of entropy is dominant and fuzzied effect reduces. It is observed that the role of regularizing parameter is vital for both classifiers. However, for FCMWE, after a certain point ($\nu=10^5$), it over estimates the class proportions.

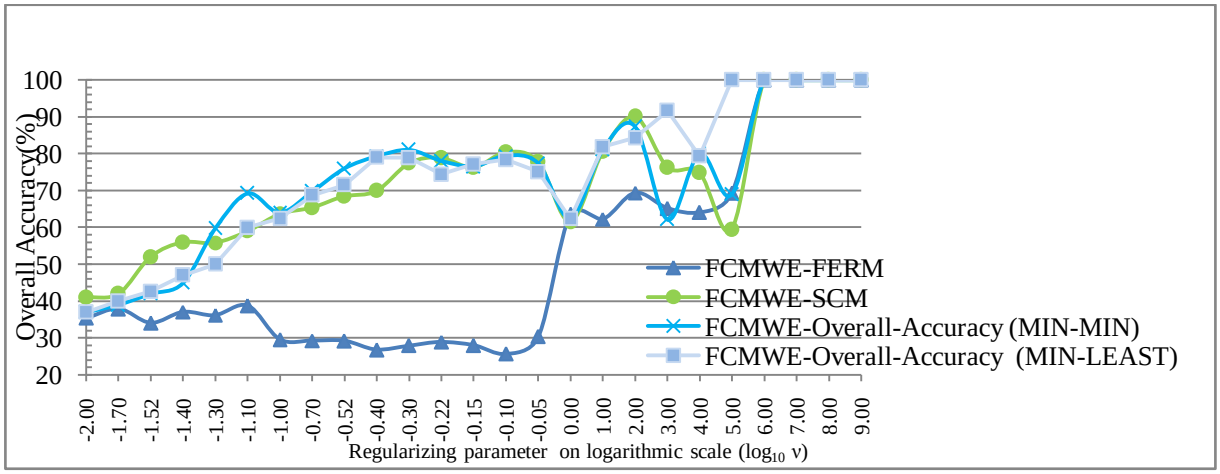

Fig. 6.32(a): Overall accuracy of FCMWE classifier of AWiFS dataset using LISS-III as reference dataset

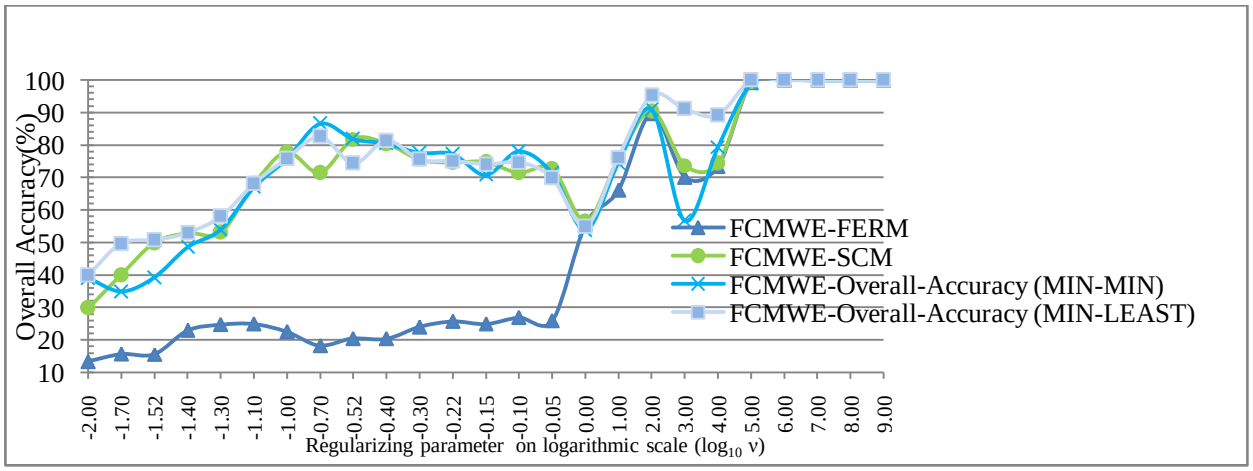

Fig. 6.32(b): Overall accuracy of FCMWE classifier of AWiFS dataset using LISS-IV as reference dataset

Fig. 6.33 (a) and (b) shows that the values of Fuzzy Kappa coefficient is greater than 0.40 and is of increasing nature, which indicates that the classification using FCMWE classifier is consistent with respect to classified image and reference image. Further, it is observed that for almost all cases using the optimized value of $\nu = 10^2$, the value of Fuzzy Kappa is higher for all classes. The Fuzzy Kappa values have been computed for SCM, MIN-MIN and MIN-LEAST operator. The consistency in Overall accuracy and Fuzzy Kappa is found that after $\nu = 10^5$, the effect of regularizing parameter becomes dominant.

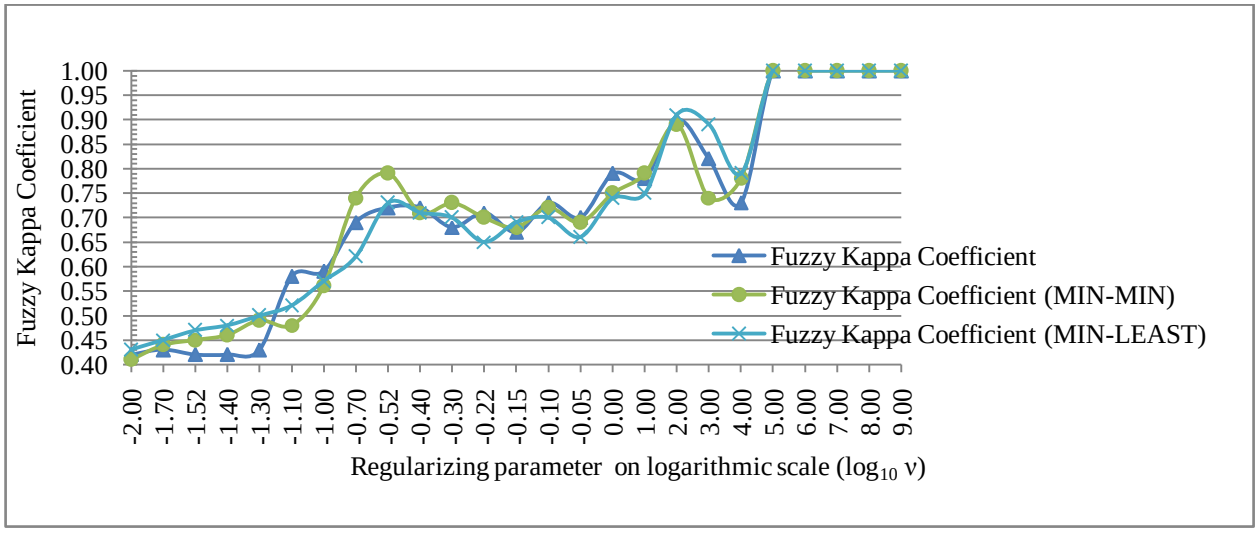

Fig. 6.33(a): Fuzzy Kappa of FCMWE classifier using AWiFS dataset and LISS-III as reference dataset

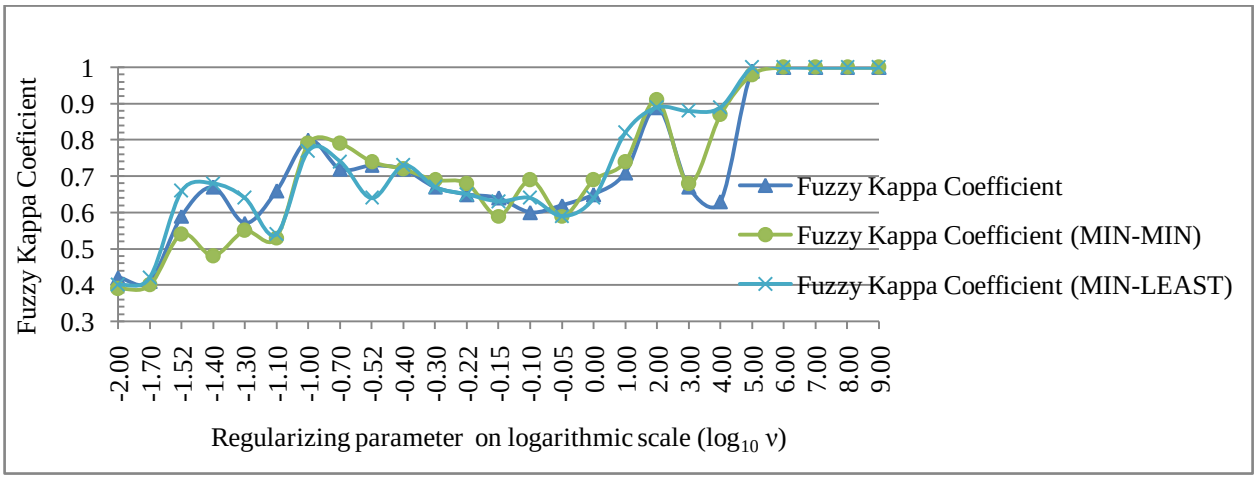

Fig. 6.33(b): Fuzzy Kappa of FCMWE classifier using AWiFS dataset and LISS-IV as reference dataset

Fig. 6.34 shows the classification uncertainty which is not more than 9% for all values of ν ranging from 0 to 10^9. However, this accuracy index produces minimum uncertainty value for the optimized values of ν =10^2. It is observed that when FCMWE classifier starts to soften, some unidentified land cover classes produce high membership. This indicates that low uncertainty has not been achieved for all values of ν. In a nutshell, the accuracy-uncertainty index from SCM has the capability to identify the error distributions among classes. This shows that a noisy point has a substantial impact on the FCMWE classification but virtually no effect on the robustness of the classifiers performance. The consistency between SCM uncertainty and Fuzzy Kappa coefficient depicts similar trend which signifies the smoothness in classified result.

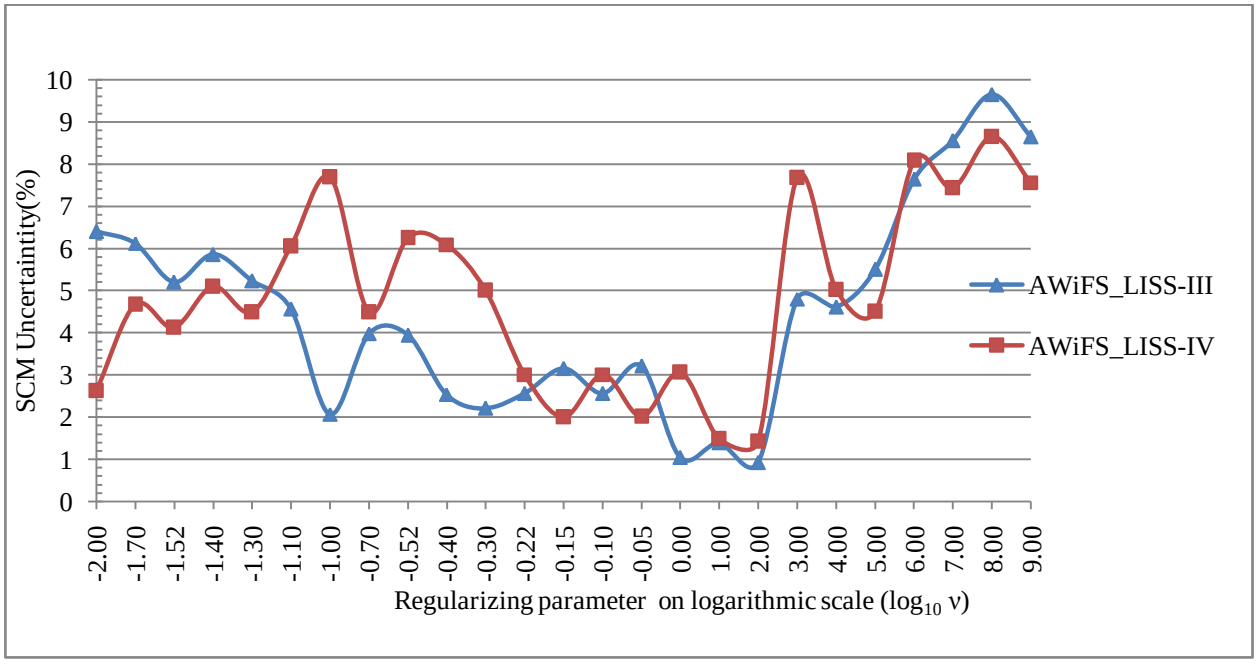

Fig. 6.34: SCM uncertainty of FCMWE classifier

Table 6.10 shows all the accuracy indices for the optimized value of regularizing parameter ν=10^2, where AWiFS image has been used as a classified image and LISS-IV image has been used a reference image. The Fuzzy overall accuracy, FERM, SCM, MIN-PROD, MIN-MIN, and MIN-LEAST of all classes are 89.73%, 90.46±5.18%, 90.92%, 84.96% and 95.26% respectively. Thus, the optimum value of ν for FCMWE classification has been fixed as 10^2toclassify coarser resolution imagery.

Table 6.10: Accuracy values for optimized value of $\nu = 10^2$ for FCMWE classifier of AWiFS data with LISS-IV as reference data.

Land-Use Classes	**Accuracy assessment methods**				
	FERM	**SCM**	**MIN-PROD**	**MIN-MIN**	**MIN-LEAST**
Fuzzy user's accuracy (%)					
Agriculture	90.11	90.91±6.63	91.52	83.68	97.54
Sal forest	94.51	94.41±4.71	94.84	88.19	98.78
Eucalyptus plantation	94.23	94.20±3.88	94.36	90.84	97.89
Barren Land	70.80	70.32±8.12	80.20	62.12	77.36
Moist Land	79.93	81.25±7.46	81.41	75.85	89.55
Water Body	82.75	86.29±1.22	88.02	85.98	88.19
Fuzzy producer's accuracy (%)					
Agriculture	97.15	97.60±1.42	97.40	96.17	98.82
Sal forest	94.38	94.58±3.33	94.47	91.96	97.97
Eucalyptus plantation	91.01	91.91±3.51	92.45	86.71	94.81
Barren Land	58.46	57.58±17.59	53.09	48.72	75.33
Moist Land	87.14	87.61±7.20	88.58	79.64	93.83
Water Body	70.13	73.60±12.57	78.40	66.87	89.00
Fuzzy overall accuracy (%)	89.73	90.46±5.18	90.92	84.96	95.26
Fuzzy Kappa	-	0.87±0.06	0.88	0.81	0.94

In this study, the performance evaluation of FCMWE classifier has been addressed. In first part of the classification procedure of FCMWE, it has been tried to add entropy-based regularizing function with FCM and optimize the regularizing parameter (ν) in (Eq 3.23) with respect to fuzzy overall accuracy and fuzzy kappa coefficient. From these outputs, it has been observed that as regularizing parameter increases, fuzzy overall accuracy as well as fuzzy kappa coefficient also increases. However, it has also observed that uncertainty in fuzzy overall accuracy as well as in fuzzy kappa coefficient also increases. However, uncertainty starts decreasing when ν reaches to 1 and it produces minimum value for $\nu = 10^2$. So, it is important to decide what should be the appropriate regularizing parameter value to be used in entropy-based

fuzzy classifier. For this value of regularizing parameter (ν), entropy remains minimum and fuzzy overall accuracy as well as fuzzy kappa coefficient is higher. So, from the above mentioned discussion, it becomes easy to interpret that the optimum value of regularizing parameter for AWIFS LISS-III and LISS-IV can be set as 10^2 for FCMWE classifier.

Fig. 6.35 shows the fraction images of AWiFS datasets for FCMWE classification. After examining the fraction images generated by FCMWE classifier, it has been observed that an intergrades phenomenon within pixel is more dominant in AWiFS imagery. It is shown in fraction images that regularizing parameter ν regularizes the output to remove inter-grade phenomena by using FCMWE classifier which removes uncertainty among classes. In FCMWE classifier the effect of regularizing parameter (ν) is dominant because of unity value of weighting exponent. This trend can be seen from fraction images {Fig. 6.35} where actual class produces high membership and all remaining classes are reflecting very low membership i.e. almost zero.

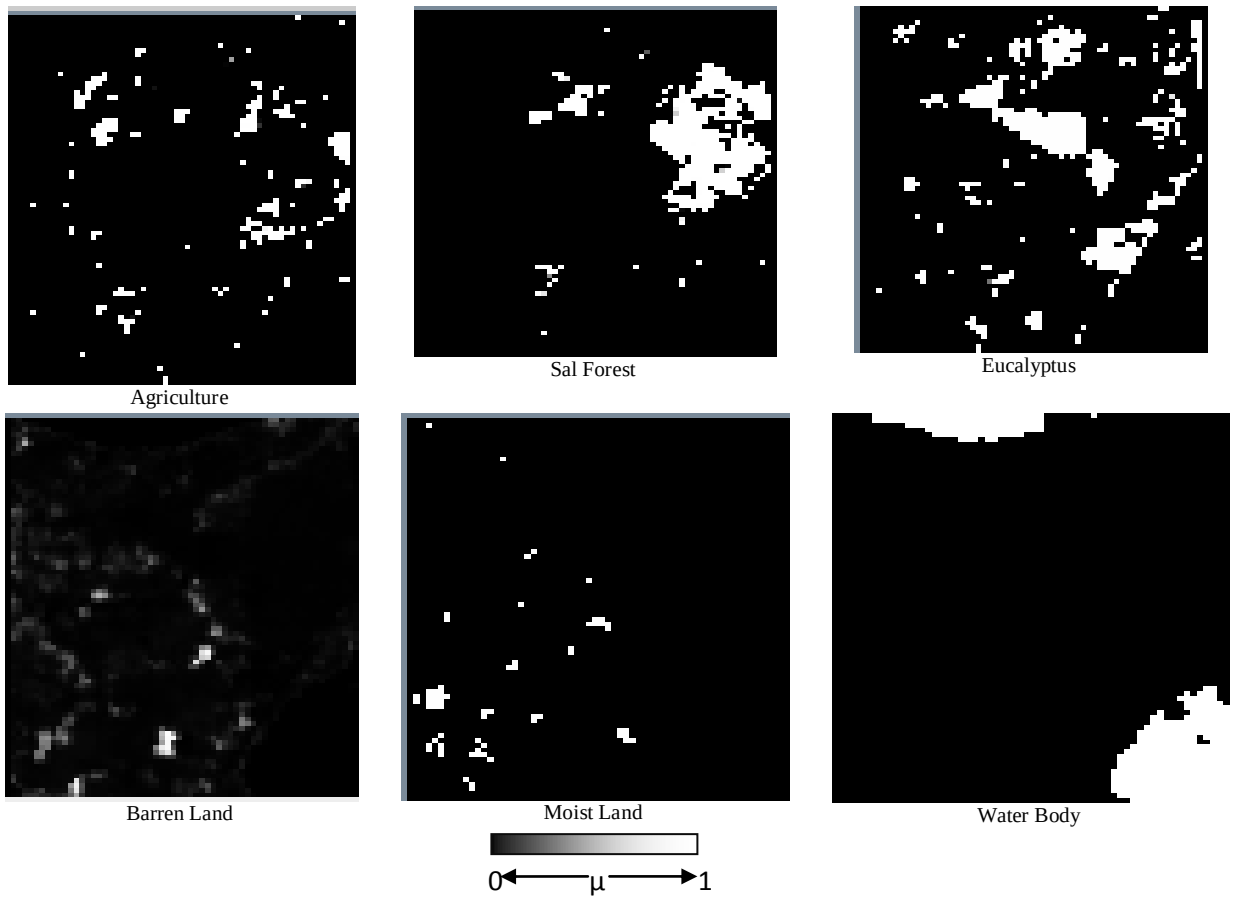

Fig. 6.35: FCMWE classification output of AWiFS image

6.7 RESULTS OF CONTEXTUAL FUZZY AND ENTROPY BASED CLASSIFIER

This study, elaborates the parameter optimization related with contextual based hybrid classification approaches specified in Section 3.4.10, 3.4.11, 3.4.12, 3.4.13 and 3.4.14. The associated parameters are described in Table 3.1. The parameters required to be estimated in Sections 6.7 -6.11 is as follows:

i) Weighting exponent or Fuzzifier, *m* is the membership weighing exponent, $1 \leq m < \infty$, controls the degree of fuzziness in classification. In this study, the optimized value of weighting exponent (*m*) is taken as 2.4 from FCM classifier.

ii) Resolution parameter, δ is the fixed parameter, $0 \leq \delta < \infty$ which controls the distance between the feature vectors from the central point of line cluster. In this study, the optimized value of δ is taken as10^5.

iii) Regularizing parameter ν is the fixed parameter, $0 \leq \nu < \infty$ which regularizes the fuzzified solution to crisp solution. In this study, the optimized value of ν is taken as10^2.

iv) Initial temperature(T_0): According to Geman and Geman (1984) initial temperatureT_0 should be 3 or 4 for the most image analysis application. Thus, in this study, to find out the optimize value of T_0, entropy value of the classified output has been calculated. During the optimization process, other parameters were kept fixed and it is found that the value of $T_0 > 4$ does not provide any improvement. Hence, for this study $T_0 = 3$ has been selected for all experiments.

v) Smoothness strength (λ) is a smoothness parameter that controls the balance between spectral and spatial information. This parameter is required in both models i.e. SA and DA, of all contextual based hybrid classifiers. To optimize this parameter, the class membership, various accuracy indices, and entropy has been computed and edge preservation has been verified parallely. It is important to verify edge preservation in this study in order to solve the problem related with inter class boundary.

vi) Weight for neighbor (β) is the weight given to the neighboring pixel in a window in SA model (Section 3.4.10-3.4.14). It is similar to optimization of λ, the entropy and edge preservation has to be checked in order to determine the optimized value for β.

vii) Interaction range parameter (γ) is required in DA models. It determines the rate at which AIF reaches zero and controls the interaction between two pixels (Li, 1995). Estimation of γ has been done by calculating entropy values as well as by verifying edge preservation.

All the experimentation of contextual based classifiers has been carried out by using *FUZCEN* software. The results of these hybrid soft classifiers have now been analyzed and discussed in the following sections.

6.7.1 RESULTS OF FCM WITH CONTEXTUAL CLASSIFIER

To perform supervised classification for FCM with contextual of AWiFS, LISS-III and LISS-IV datasets, a total 50 training pixels have been selected for each land cover class. This soft classification approach uses only the Euclidean norm, since from literature it is found that Euclidean weighted norm performs better in comparison to Mahalanobis and Diagonal norm considered (Kumar and Ghosh, 2007). The hybrid classification approach of FCM with contextual has been perform in two categories i.e. FCM with Smoothness prior (FCM-S) and four categories of FCM with Discontinuity Adaptive prior (FDM-H1, FDM-H2, FDM-H3, FDM-H4). The following sections describe the findings of the FCM with contextual classifiers in both the categories.

6.7.1.1 RESULTS OF FCM WITH SMOOTHNESS PRIOR

To incorporate the spatial contextual information along with spectral information, the hybridized model has been devised to resolve the problem of mixed pixel. The contextual information has been added in FCM classifier to generate smoothness effect. Two basic variables associated are smoothness parameter (λ) and weight for neighbours (β). The performance of this classifier is

dependent on the constant value of weighting exponent *m* and smoothness parameter λ along with weight for neighbours parameter β (Eq. 3.45). The optimized constant value of weighting exponent *m* and varying value of smoothness parameter λ along with weight for neighbours parameter β has been tested. For FCM-S classification, both the parameters are mutually dependent upon each other for incorporating spatial contextual information. To perform the FCM-S classification, a fixed value of *m*=2.4 has been taken for all varying values of λ from 0.1 to 1.0 with the interval 0.1 and β is varied from 0.5 to 5.0 at an interval of 0.5.

Fig. 6.36 (a), (b) and (c) shows the variation of the of the varying value of smoothness parameter (λ) and weight for neighbours parameter (β)with class membership of different classes such as agriculture, sal forest, eucalyptus plantation, barren land, moist land and water body for AWIFS, LISS-III and LISS-IV dataset respectively. For all three datasets, class membership has been generated for the different values of λ and β. The class membership values of a pixel denote the class proportions, which in turn may represent the soft classified output for a pixel.

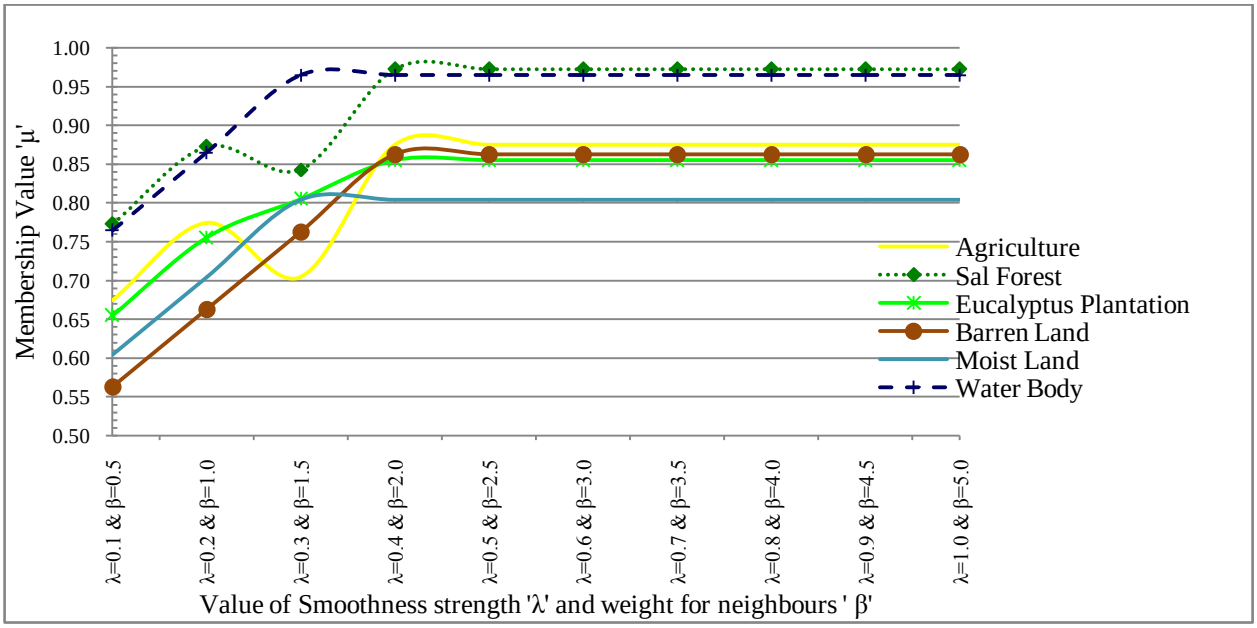

Fig. 6.36 (a): Class membership for FCM-S classifier using AWiFS dataset.

It has been observed from the Fig. 6.36 (a), (b) and (c), the optimized value of λ=0.7 and β =3.5 produces highest membership. The class membership lies between 0.75 to 0.95 for all six classes. On the basis of highest class membership produced by classified imagery, the class wise

optimized values of λ and β have been identified. For agriculture, barren land, and water body λ=0.7 and β=3.5, found suitable for the classification using FCM-S classifier. However, for sal forest, λ=0.7 and β=5.0, eucalyptus plantation λ=0.6 and β=3.0 and moist land λ=0.5 and β=2.5 is found to be more appropriate for classification.

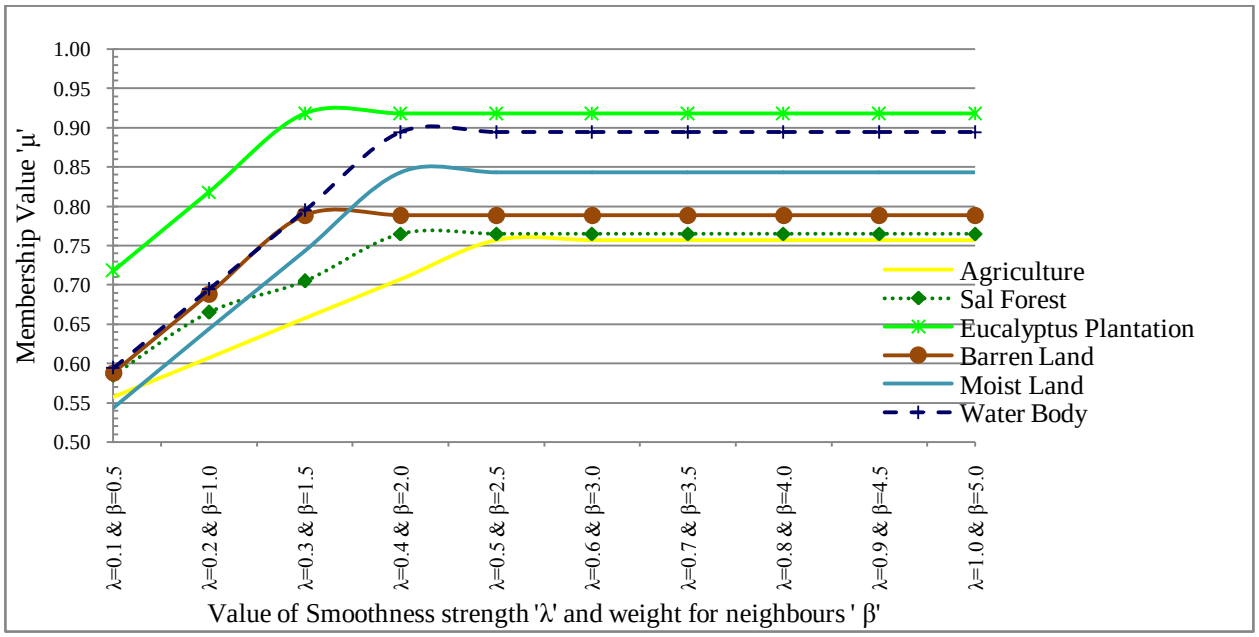

Fig. 6.36 (b): Class membership for FCM-S classifier using LISS-III dataset.

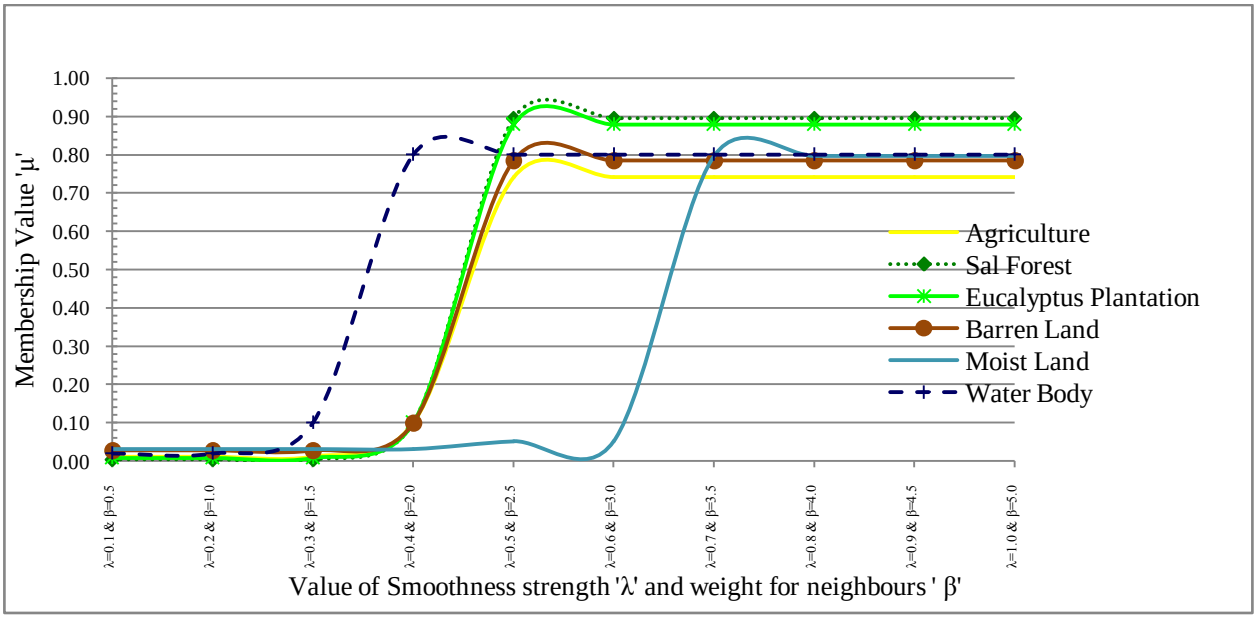

Fig. 6.36 (c): Class membership for FCM-S classifier using LISS-IV dataset.

Fig. 6.37 (a), (b) and (c) shows the computed entropy for AWiFS, LISS-III and LISS-IV fraction images of FCM-S classifier. The range of entropy visualizes the uncertainty in classification. Fig. 6.37 (a), (b) and (c) shows that for λ=0.7 and β= 3.5 entropy values are minimum for agriculture, sal forest, eucalyptus plantation, barren land, moist land and water body. This trend shows that uncertainty in classified results is low. This mathematical model of entropy computation is used as an absolute indicator of measuring uncertainty without using any ground reference data. This output of entropy is computed on classified output to visualize the pure uncertainty and it is found that for optimized values it is low for all three images.

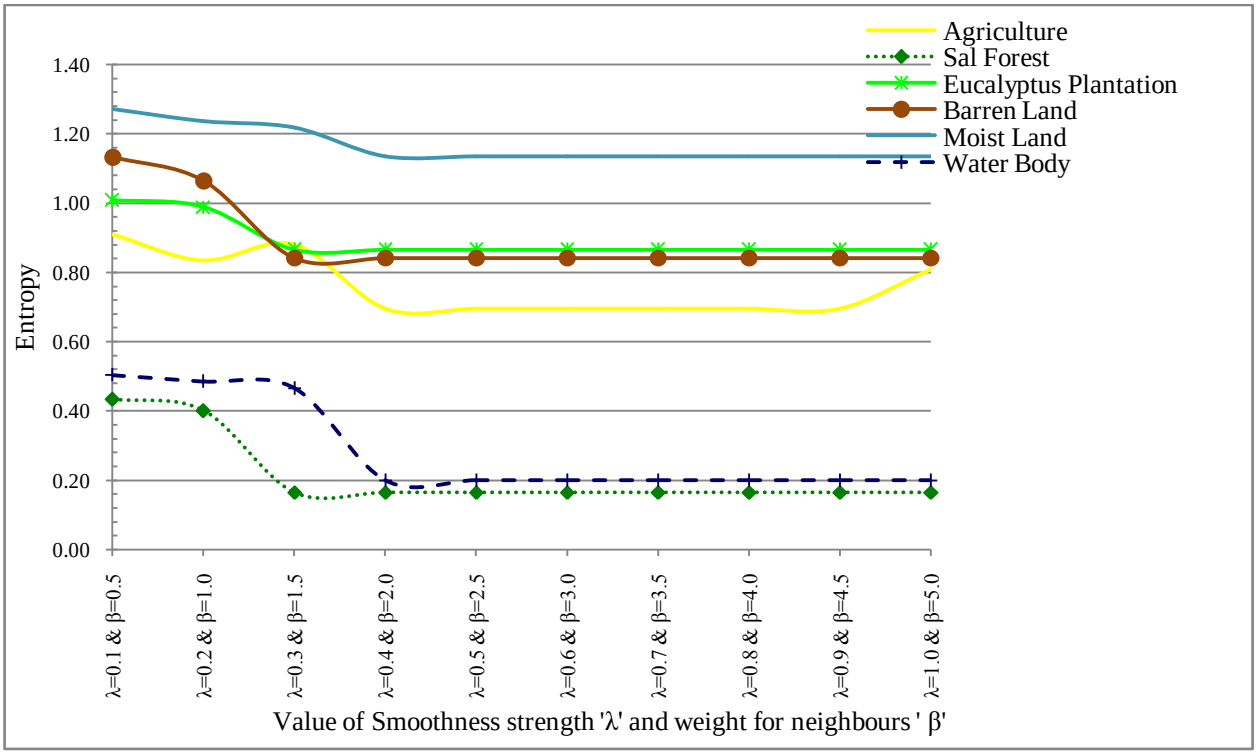

Fig. 6.37 (a): Entropy for FCM-S classifier using AWiFS dataset

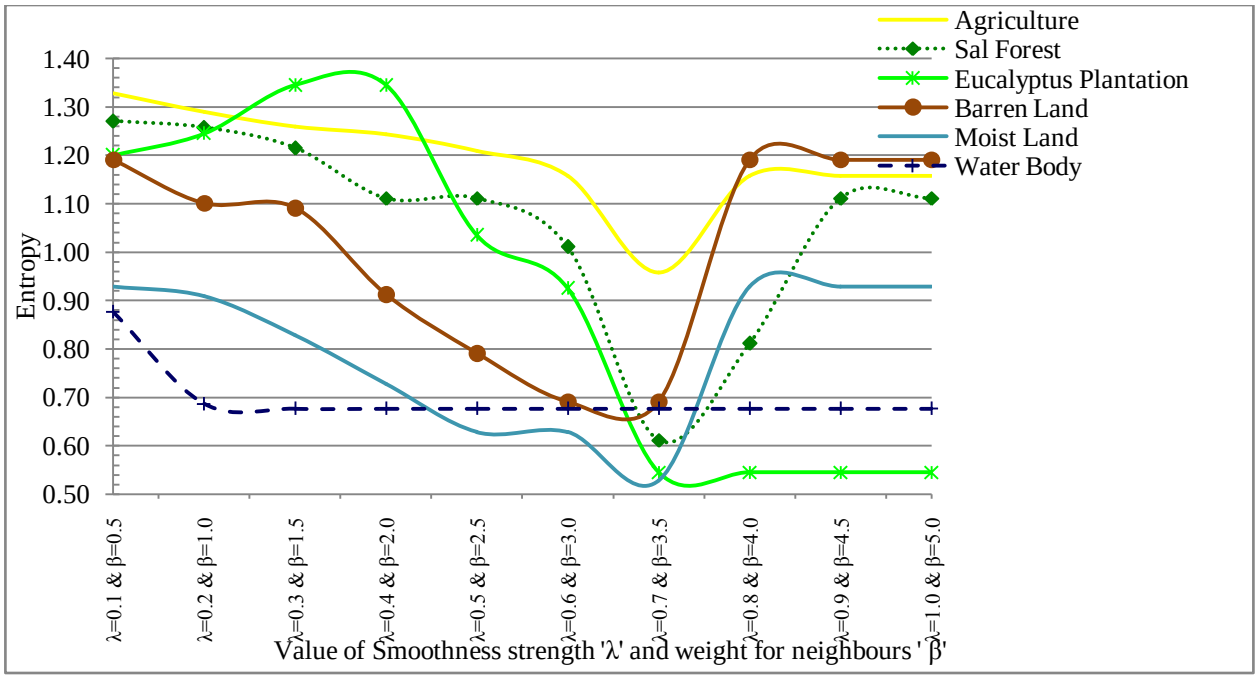

Fig. 6.37 (b): Entropy for FCM-S classifier using AWiFS dataset

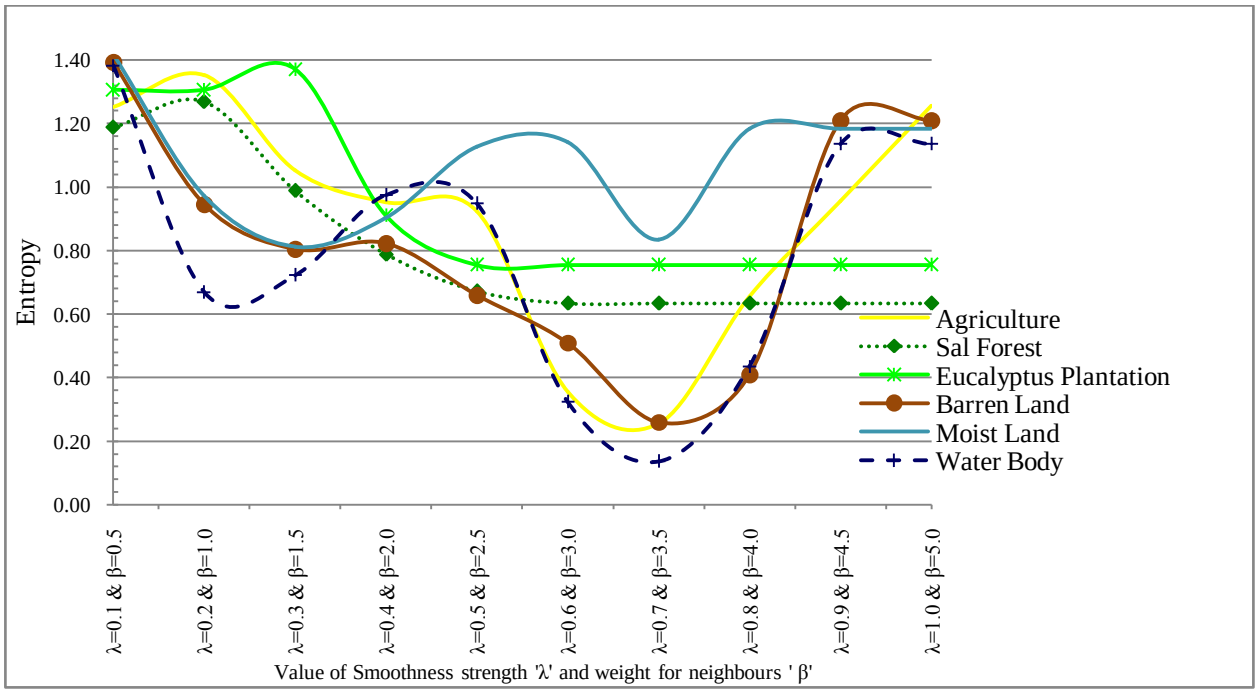

Fig. 6.37 (c): Entropy for FCM-S classifier using AWiFS dataset

In generally, the error occurs close to the boundary edges, thus preserving the edge, may increase the classification accuracy (Melgani and Serpico, 2003). On the basis of class membership {Fig. 6.36(a), (b) and (c)} and entropy {Fig. 6.37(a), (b) and (c)}, the optimized

value of λ and β can be fixed as λ=0.7 and β=3.5. However, the edge preservation has also been verified.

In this study, the membership value of a unit in a fraction image indicates belongingness of class proportions. If the pixel exists at a location of a known class, then it is high or else for an unknown class it is low. In the classified imagery, the variability among membership values is less for homogenous area. Subsequently, the mean of the membership value will be high and the variance will be low (Wen and Xia, 1999). Tables 6.11 and 6.12 shows difference in mean and variance for AWiFS (classified)-LISS-III (referenced) and AWiFS (classified) - LISS – IV (referenced) datasets for different λ and β values. It has been observed that for the optimized values of λ =0.7 and β=3.5, the difference of mean is high (**208.666**) and variance is low (**66.166, 3.366**). The verification of edge preservation is very important to measure the effect contextual based hybridized approach and is calculated at the either sides of the edge. In Tables 6.11 and 6.12, the calculated mean and variance of the grey level is presented for all six lands cover classes i.e. Agriculture, Sal forest, Eucalyptus plantation, Barren land, and Moist land and Water body. Thus, it can be concluded that for value of λ=0.7 and β=3.5, the edge between classes have been preserved.

Table 6.11: Verification of edge preservation for FCM-S classification of AWiFS image for optimized value of 'λ'=0.7 and 'β'=3.5

Values of (λ and β)	**Difference in mean**	**Variance**
0.2,1.0	1.33	0.166, 0.566
0.3,1.5	176.66	7822.167, 6.966
0.4,2.0	209.666	66.166, 7.666
0.5,2.5	208.5	66.166, 3.866
0.6,3.0	208.5	66.166, 3.866
0.7,3.5	**208.666**	**66.166, 3.366**
0.8,4.0	208.666	66.166, 3.366
0.9,4.5	208.5	66.166, 3.866

Table 6.12: Verification of edge preservation for FCM-S classification of LISS-III image for optimized value of 'λ'=0.7 and 'β'=3.5

Values of (λ and β)	Difference in mean	Variance
0.2,1.0	-0.2	0.3,0.2
0.3,1.5	241.4	27.5, 3.8
0.4,2.0	243.8	27.5, 2.2
0.5,2.5	243.8	27.5, 2.2
0.6,3.0	243.8	27.5, 2.2
0.7,3.5	**245.4**	**27.5, 1.2**
0.8,4.0	243.8	27.5, 2.2
0.9,4.5	-0.2	0.3,0.2

To perform FCM-S classification, the optimized value of weighting exponent *m*=2.4 has been taken as a constant. The smoothness parameter 'λ' and weight for neighbours 'β' have been computed by varying between 0.1 to 1.0 and 0.5 to 5.0 respectively. The Overall accuracy, FERM, SCM, MIN-MIN and MIN-LEAST are varying between 65% to 98% in both cases, where AWiFS dataset is used as a classified image and LISS-III or LISS-IV dataset is used as a reference. In the process of identifying the optimized value of smoothness parameter λ and weight for neighbours β, all accuracy indices (FERM, SCM, MIN-MIN and MIN-LEAST) has been analyzed for all six classes selected for this study. It is found that for λ=0.7 and β=3.5, class membership is higher and having lesser uncertainty {Fig. 6.37(a), (b) and (c)}.

Table 6.13 shows the accuracy indices for optimized value of smoothness parameter λ and weight for neighbours β of AWiFS (classified) and LISS-IV (referenced) combinations. The value of smoothness parameter λ is greater than zero and it is tested from 0.1 to 1. Another parameter weight for neighbours β is also greater than zero. However, in this study, the value of β is varying from 0.5 to 6.0. The output membership values and entropy of known pixels have been plotted against the varying values of λ and β for AWiFS, LISS-III and LISS-IV datasets as shown in {Figs. 6.36 (a), (b) and (c) and Figs. 6.37 (a), (b) and (c)} respectively.

It is observed that the membership values of all six classes increases when λ and βare increasing till 0.3 and 1.5 respectively. Thereafter, it increases slowly and then attains a constant value at a fixed point, where the membership value is close to 0.934.Any further increment in λ and β increases the membership values of noninterest classes which increases the noise in the outputs. Thus, thevalue of λ and β, which corresponds to the fixed point, yields the best results for AWiFS, LISS-III and LISS-IV datasets. All the accuracy indices for optimized values of smoothness parameter λ and weight for neighbours β are presented in Tables 6.13.

Table 6.13: Accuracy values for optimized value of λ=0.7 and β=3.5 for FCM-S classifier of AWiFS data using LISS-IV as reference data.

Land-Use Classes	**Accuracy assessment methods**				
	FERM	**SCM**	**MIN-PROD**	**MIN-MIN**	**MIN-LEAST**
Fuzzy user's accuracy (%)					
Agriculture	96.29	98.57±1.28	98.79	97.28	99.85
Sal forest	50.40	80.98±14.01	80.93	66.96	95.00
Eucalyptus plantation	65.92	87.62±6.82	87.82	80.79	94.44
Barren Land	62.73	90.91±6.46	91.54	84.44	97.38
Moist Land	41.98	82.03±15.01	81.80	67.01	97.05
Water Body	96.29	98.57±1.28	98.79	97.28	99.85
Fuzzy producer's accuracy (%)					
Agriculture	86.54	88.61±6.75	89.53	81.85	95.37
Sal forest	89.63	90.36±6.56	91.07	83.79	96.93
Eucalyptus plantation	89.84	90.76±8.52	91.72	82.24	99.29
Barren Land	79.38	81.76±13.97	80.90	67.79	95.73
Moist Land	86.54	88.61±6.75	89.53	81.85	95.37
Water Body	94.37	95.71±1.80	95.85	93.91	97.51
Fuzzy overall accuracy (%)	87.02	88.43±8.47	88.97	79.99	96.87
Fuzzy Kappa		0.85±0.10	0.86	0.74	0.96

Fig. 6.38 shows the fraction images of AWiFS datasets for FCM-S classification. After examining the fraction images generated by FCM-S classifier, it is observed that the value of λ and β changes across the spatial resolution of image. It has also been observed that for optimized values of λ and β, coarser resolution dataset has low variability in the image and vice-versa. In this study, for AWiFS imagery (60m), LISS-III (20m) and LISS-IV (5m) spatial resolution, the optimized λ and β values are 0.7 and 3.5. It is also found in Figs. 6.38, that incorporation of contextual information in FCM the classifier is spectrally and spatially consistent {Fig 6.36(a), (b) and (c)} and uncertainty has been minimized. The FCM classifier considers only the spectral properties for classification, but after hybridizing this with contextual information, it also considers the spatial properties of the image which increases the overall classification accuracy of an image.

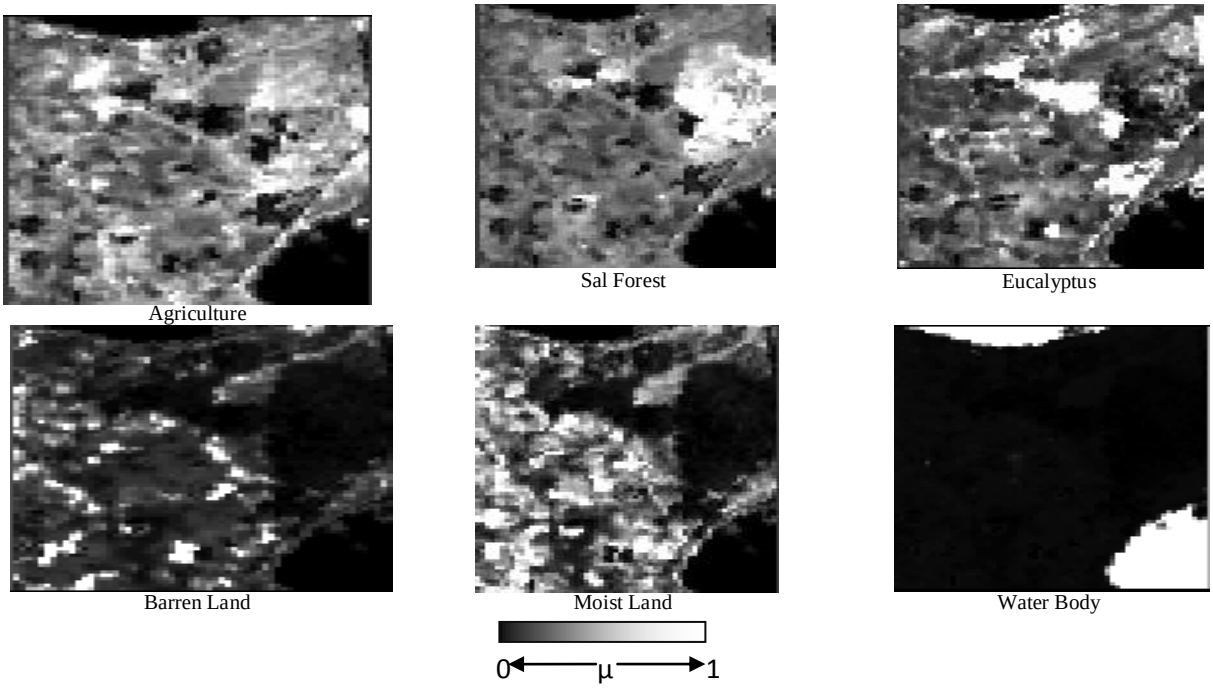

Fig. 6.38: FCM-S classification output of AWiFS image

6.7.1.2 RESULTS OF FCM WITH DISCONTINUITY ADAPTIVE PRIOR

To incorporate the spatial contextual information with FCM, smoothness prior and four DA-MRF described in Section 3.4.7.2 has been widely used in Electrical Engineering (Li, 2009). So, to incorporate the spatial contextual information along with spectral information, the hybridized model of DA approach has been devised to resolve the problem of mixed pixel. The objective function of FCM with Discontinuity Adaptive prior is defined in (Eq 3.46-3.49) and known as FDM-(H1), FDM-(H2), FDM-(H3), and FDM-(H4). The smoothness parameter (λ) controls the balance between spectral and spatial information. Another parameter which is added with the objective function of FCM with Discontinuity Adaptive prior classifier is the Adoptive Potential Function (AIF) or Interaction Range Parameter (γ). This determines the rate of decay at that point where AIF reaches to zero and also controls the interaction between two pixels (Moser and Serpico, 2010). The basic objective of this study is to optimize the parameters λ and γ to get better classification. Another aspect of this study, is to identify the optimize DA-model, yields the best image classification.

The performance of this classifier is dependent on the constant value of weighting exponent (*m*) and smoothness parameter (λ) along with Interaction Range Parameter (γ).The optimized value of weighting exponent *m* and varying value of smoothness parameter λ along with interaction range parameter γ has been tested. These parameters are mutually dependent on each other in FDM-(H1), FDM-(H2), FDM-(H3), and FDM-(H4) classification approaches. To carry out the classification, a fixed value of *m*=2.4 has been used while varying the values of λ and γ between 0.1 to 1.0 at an interval of 0.1. For an appropriate classification, the membership value of a particular class shall be very high and that its corresponding entropy value should be minimum.

Fig. 6.39 (a), (b), (c),(d) shows the variation of the varying value of λ and γ with class membership of different classes such as agriculture, sal forest, eucalyptus plantation, barren land, moist land and water body for AWIFS dataset of FDM-(H1), FDM-(H2), FDM-(H3), FDM-(H4) classifier. For all three datasets, class memberships have been generated for the different values of λ and γ. The class membership values of a pixel denote the class proportions,

which represents the soft classified output for a pixel. It has been observed that the optimized value of λ and γ is 0.8. The optimized value of λ and γ is finalized on the basis of membership values, which is higher for all classes and lying between **0.80** to **0.996** for FDM-(H1), FDM-(H2), FDM-(H3), FDM-(H4) classifier.

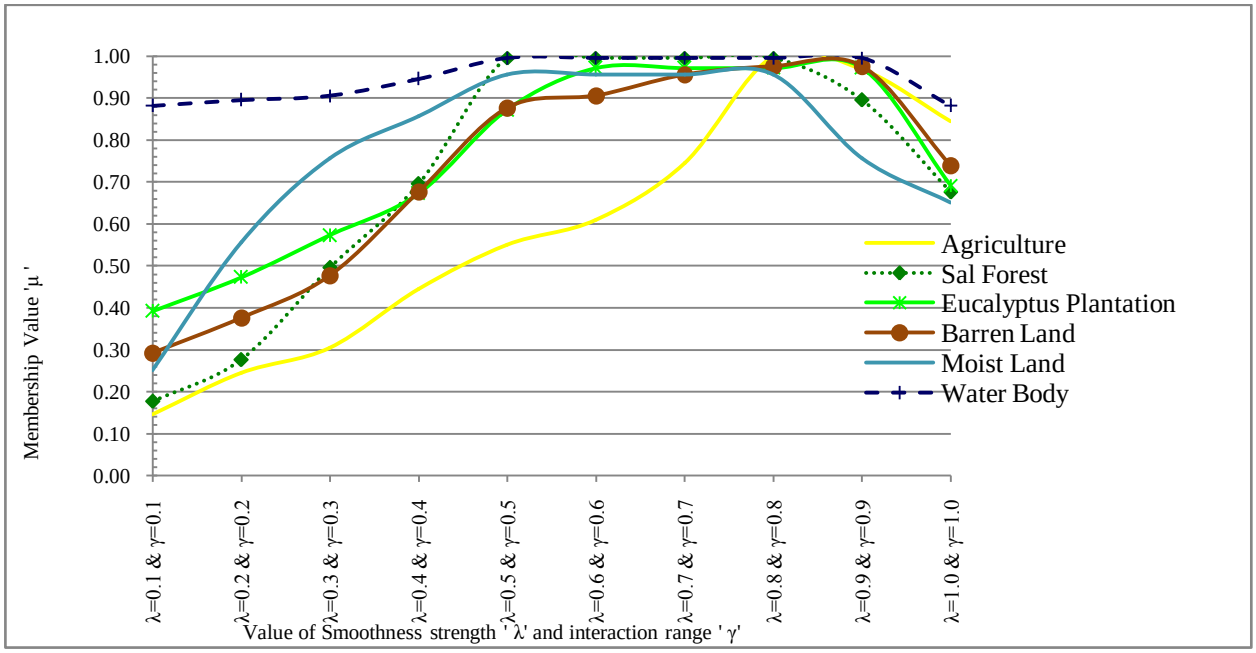

Fig. 6.39 (a): Class membership for FDM-(H1) using AWiFS dataset.

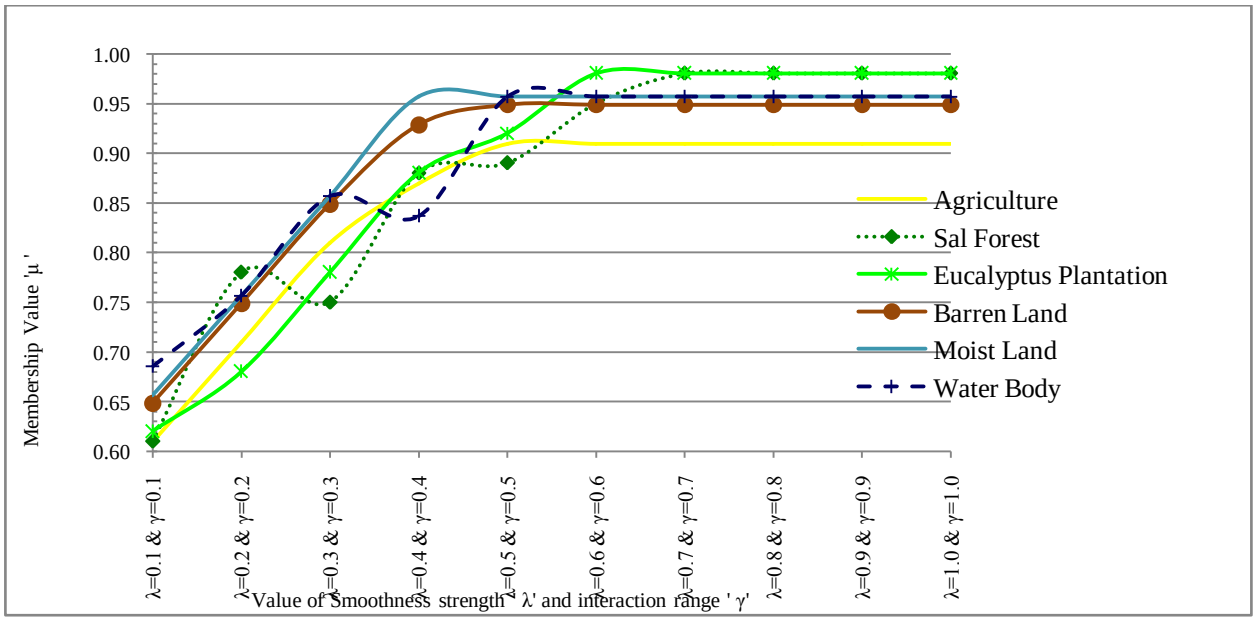

Fig. 6.39 (b): Class membership for FDM-(H2) using AWiFS dataset.

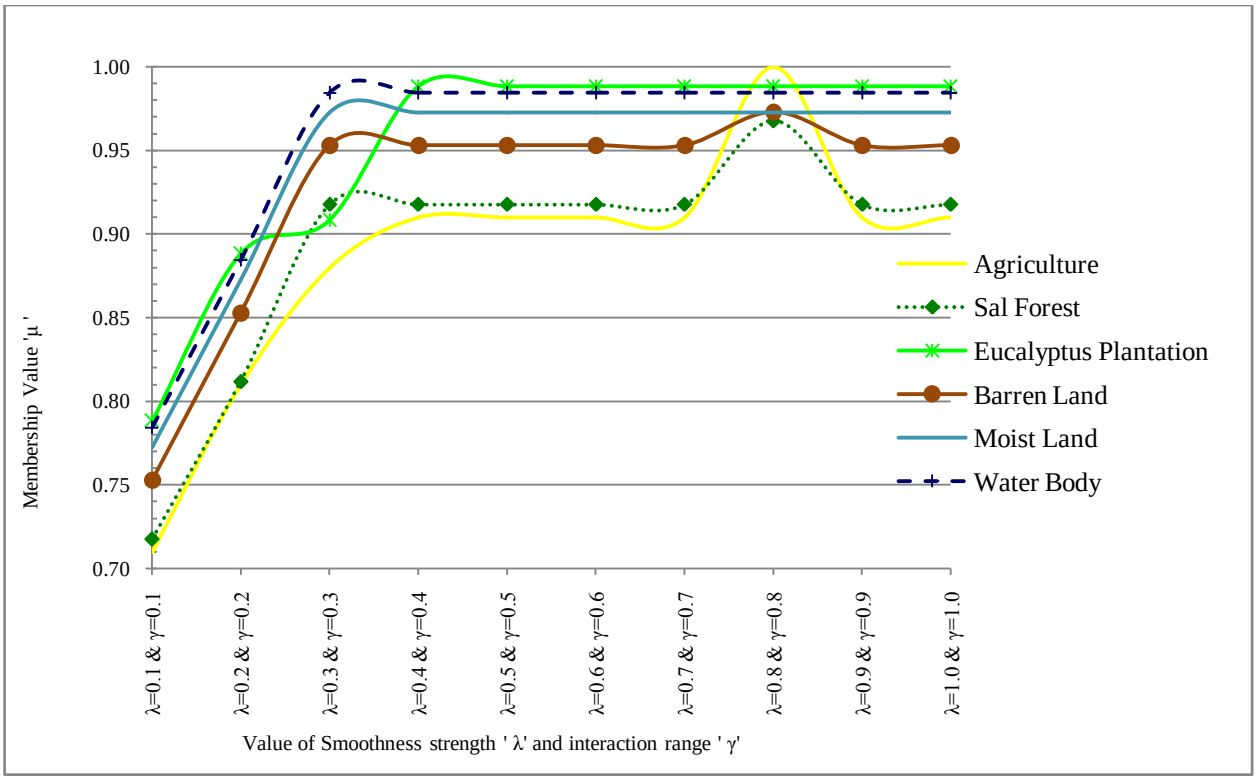

Fig. 6.39 (c): Class membership for FDM-(H3)using AWiFS dataset.

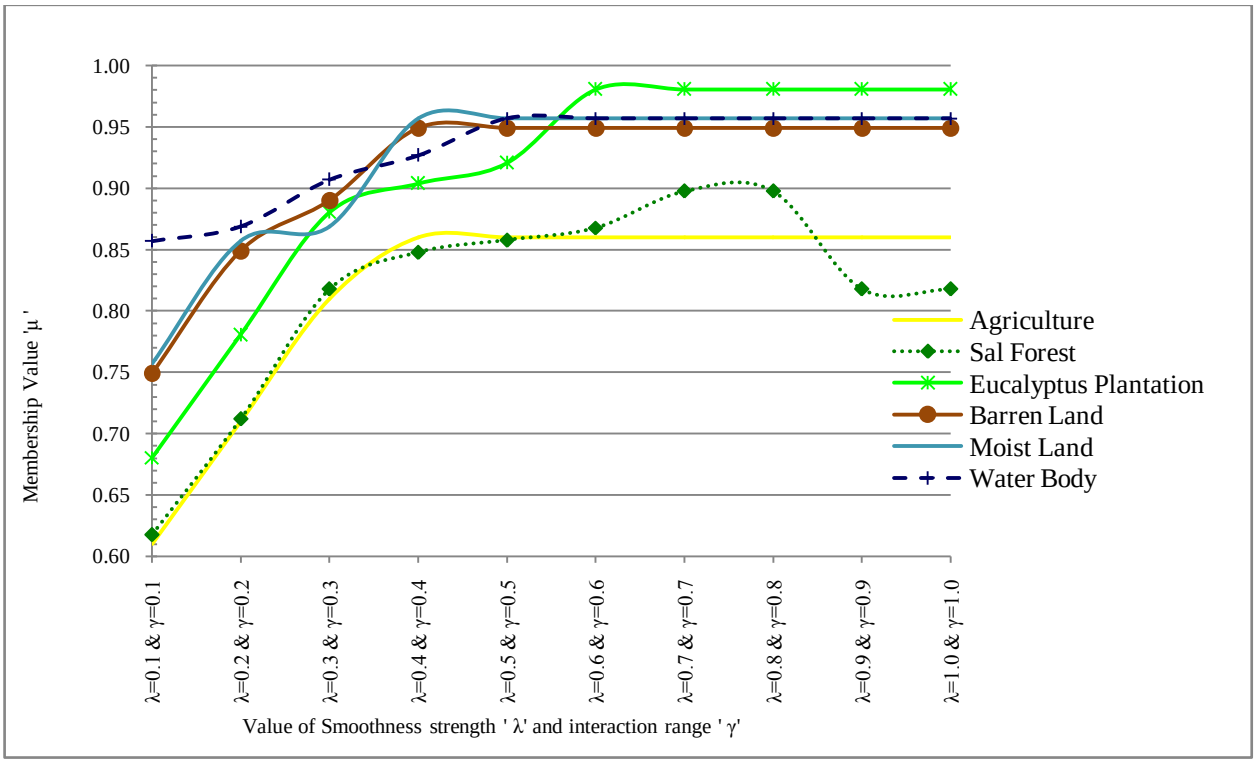

Fig. 6.39 (d): Class membership for FDM-(H4) using AWiFS dataset.

Table 6.14 shows FERM, SCM and MIN-LEAST accuracy measures for the optimized value of λ =0.8 and γ=0.8. The accuracy values are presented for all four DA prior models. From Table 6.5, it has been observed that FDM-(H3) model produces the highest accuracy. The assessment of accuracy shows that FDM-(H3) model produces higher values for FERM, SCM and MIN-LEAST operator. The MIN-LEAST approach of assessment of accuracy determines the interclass confusion ratio and a high value indicates minimal interclass confusion (Chen, 2010). The entropy value has been computed for optimized λ and γ for all four DA models and it is found to be 0.07, 0.08, 0.03, and 0.85 for FDM-(H1, H2, H3, and H4) models respectively. This reflects that FDM-(H3) has lowest entropy (**0.3**) when compared to other models. The basic advantage of hybridization DA model with FCM classifier is that classes are well classified and edges were not over smoothed (Fig. 6.40).

Table 6.14: Comparative assessment of accuracy values for FDM (H1, H2, H3, and H4) classifier of AWiFS data using LISS-III and LISS-IV as reference data

Images → / Indices ↓	AWiFS-LISS-III				AWiFS-LISS-IV			
FDM-Classifier	H-1	H-2	H-3	H-4	H-1	H-2	H-3	H-4
FERM(%)	83.86	83.76	**87.85**	85.29	84.13	85.01	**88.00**	79.23
SCM(%)	84.98	89.24	**90.12**	89.12	80.37	84.24	**86.12**	81.12
MIN-LEAST(%)	87.97	93.63	**98.14**	98.14	88.65	93.05	**95.34**	91.14

The classification performance of FDM-(H3) has been compared with FCM and FCM-S and it has been observed that it reduces the problem of over smoothing of FCM-S and reduces the uncertainty up to 4% to 6% for agriculture, sal forest, eucalyptus plantation and 7% to 9% for barren land, moist land and water body classes {Tables 6.2 and 6.13}.

For checking and verifying the edge preservation for classified output at its optimized point, mean and variance method has been used. The edges have been checked, on per- pixel basis for all the classified output of AWiFS image (See Table 6.15). As per the output in form of class membership {Fig. 6.39 (a), (b), (c) and (d)} and Table 6.5, it has been observed that the FDM-(H3) is effective for inspection of preservation of edges. It has been observed that, for the optimized value of λ=0.8 and γ=0.8, the edges have been preserved more correctly with high mean difference and low variance than smoothness prior (Table 6.12). It may be concluded that, while using contextual based classifier, the verification of edge preservation is important to avoid the problem of over smoothing on the classified imagery.

Table 6.15: Verification of edge preservation for FDM-(H3) classification of AWiFS image for optimized value of 'λ'=0.8 and 'γ'=0.8

Values of (λ and γ)	Difference in mean	Variance
0.1,0.1	242.3	23.5, 3.7
0.2,0.2	232.3	43.5, 2.01
0.3,0.3	247.2	37.5, 0.2
0.4,0.4	247.2	37.5, 0.2
0.5,0.5	247.2	37.5, 0.2
0.6,0.6	247.2	37.5, 0.2
0.7,0.7	247.2	37.5, 0.2
0.8,0.8	**247.2**	**37.5, 0.2**
0.9,0.9	247.2	37.5, 0.2

Fig. 6.40 shows the classified fraction image for optimized values of λ and γ of AWiFS dataset for FDM-(H3) classification. This model performs better than other models as smoothing strength (λ) increases monotonically as scale parameter 'η'>0 increases within the neighbourhood window. As shown in Fig. 6.40, FDM-(H3) model controls over smoothing for homogenous category of classes, by applying zero smoothing principle when 'η' is almost zero. This aspect of zero smoothing and over smoothing has also been verified by Li (2009), where smoothness prior model allows boundless smoothening when $\eta \rightarrow \infty$.

On the basis of highest class membership, the class wise optimized value of λ and γ has been identified. For agriculture, and barren land, λ=0.7 and γ=0.7 has been found suitable for the classification using FDM-(H3) classifier. However, for sal forest and moist land, λ=0.8 and γ=0.8, eucalyptus plantation (λ=0.6 and γ =0.6) and water body (λ=0.5 and γ =0.5) is found to be appropriate for classification irrespective of datasets.

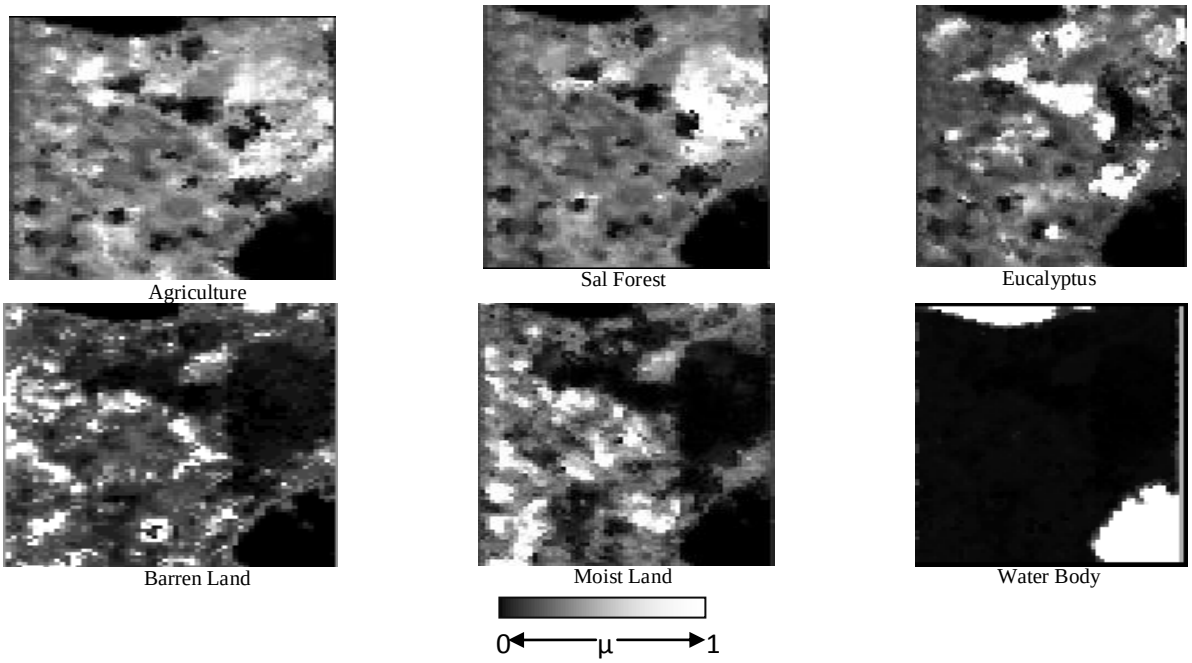

Fig. 6.40: FDM-(H3) classification output of AWiFS image

Fig. 6.40 shows the classified fraction images of AWiFS dataset for the optimized value of λ and γ. To incorporate the spatial contextual information with FCM, smoothness prior and four DA-MRF models have been tested. From Table 6.14, it has been observed that DA models increases Overall accuracy (SCM) up to 10% when compared to FCM-S and FCM. In FDM classifier, the interactions amongst the pixels are constant everywhere in the classified imagery and avoid the problem of over smoothing at edges. Thus, adding the contextual information using DA-MRF models reduces the problem of over smoothing at edges while preserving it at boundary points (Fig. 6.40) and produces more consistent classified fraction imagery.

6.8 RESULTS OF PCM WITH CONTEXTUAL CLASSIFIER

To perform supervised classification for PCM with contextual information of AWiFS, LISS-III and LISS-IV datasets, a total of 50 training pixels have been selected for each land cover class. The hybrid classification approach of PCM with contextual has been carried out in two categories i.e. PCM with Smoothness prior (PCM-S) and four categories of PCM with Discontinuity Adaptive prior (PDM-H1, PDM-H2, PDM-H3, PDM-H4). The following sections, describes the results of the PCM with contextual classifiers in both the categories.

6.8.1 RESULTS OF PCM WITH SMOOTHNESS PRIOR (PCM-S)

To incorporate the spatial contextual information along with spectral information, the hybridized model has been devised to resolve the problem of mixed pixel. The contextual information has been added in PCM classifier to generate smoothness effect and it is defined as PCM-S (Eq 3.50). Two basic variables are associated with the defined objective function are smoothness parameter (λ) and weight for neighbours (β). The smoothness parameter controls the balance between spectral and spatial information, while β analyzes the weight to be given to a neighbouring pixel in a window. The basic objective of this study is to optimize these parameters to get better classification.

The performance of this classifier is dependent on the constant value of weighting exponent *m* and smoothness parameter λ along with weight for neighbours parameter β(Eq. 3.50). The optimized constant value of weighting exponent *m* and varying value of smoothness parameter λ along with weight for neighbours parameter β has been tested. To perform the PCM-S classification, a fixed value of m=2.4 has been used for all varying values of λ and β.

Fig. 6.41 shows the variation of smoothness parameter (λ) and weight for neighbours parameter (β) with class membership for different classes such as agriculture, sal forest, eucalyptus plantation, barren land, moist land and water body for AWIFS, datasets. It has been observed from Fig. 6.41, that for λ=0.6 and β =3.0, all classes produces highest membership. For

λ=0.6 and β=3.0, the class membership lies between 0.85 to 0.99 for all six classes selected for this study. It has been further verified via entropy and observed that the value of optimized parameter is not deviating (Fig. 6.42).

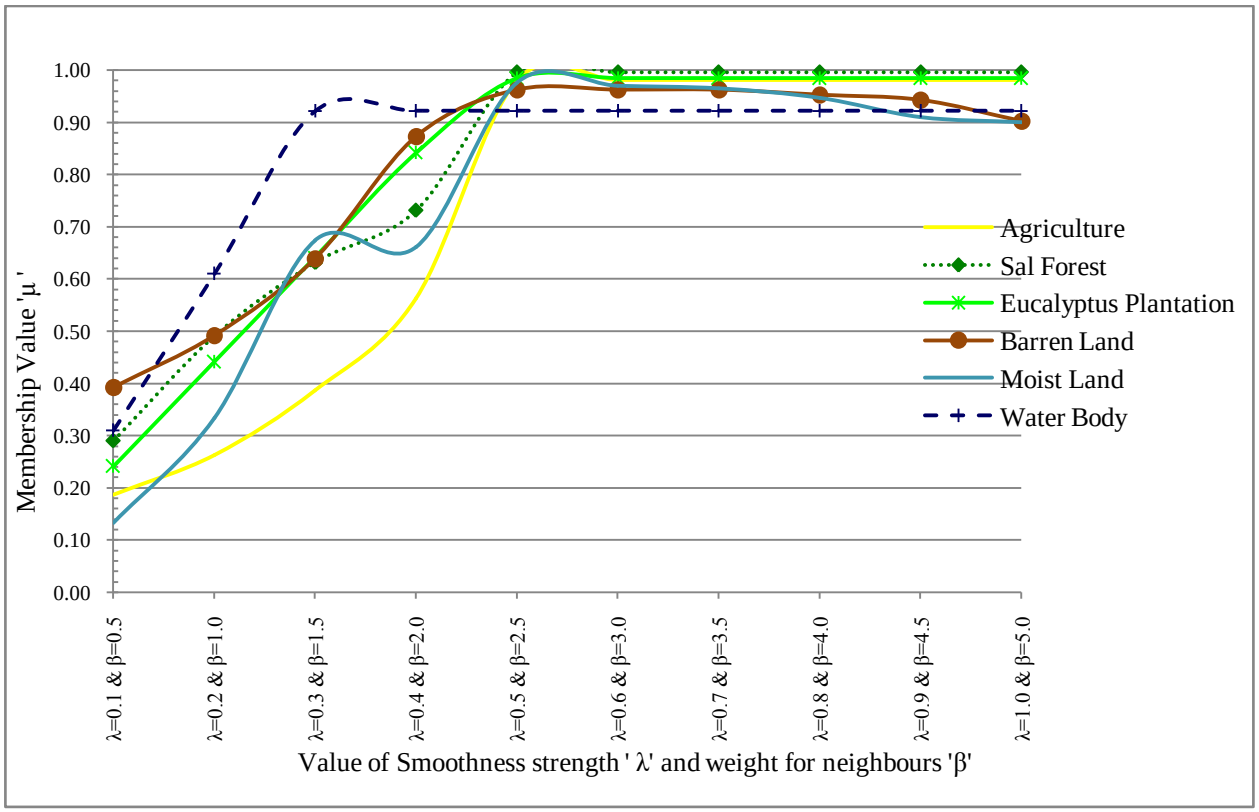

Fig. 6.41: Class membership for PCM-S classifier using AWiFS datasets

The prime objective of image classification using PCM-S classifier is to establish a relationship between spectral and spatial information with adequate land cover type. The correctness of the classification results are evaluated using class membership and accuracy indices criterion. However, this criterion is not sufficient to measure the quality of certainty of the classification results. For the visualization and evaluation of uncertainty in the classified imagery, the entropy criterion is proposed. This can be express by a single number to show the distribution and extent of uncertainty in the classified results.

Fig. 6.42 shows the computed entropy for AWiFS fraction images of PCM-S classifier for agriculture, sal forest, eucalyptus plantation, barren land, moist land, and water body land

cover classes. The entropy values are lying between the specified range of [0.8, 2.5]. If the entropy value of classified fraction imagery is less; this indicates better classification with minimum uncertainty. It has been observed from Fig. 6.42, that at λ= 0.6 and β=3.0 for AWiFS dataset, the entropy values for all classes are lowest. For these optimized values of λ and β, the membership is high i.e. up to 98% and the computed entropy is lying between 0.8 to 1.9. This trend indicates that the uncertainty in classified results is low at optimized point for smoothness parameter λ= 0.6 and weight for neighbours parameter β=3.0. This mathematical model of entropy computation is used as an absolute indicator of measuring uncertainty without using any ground reference data.

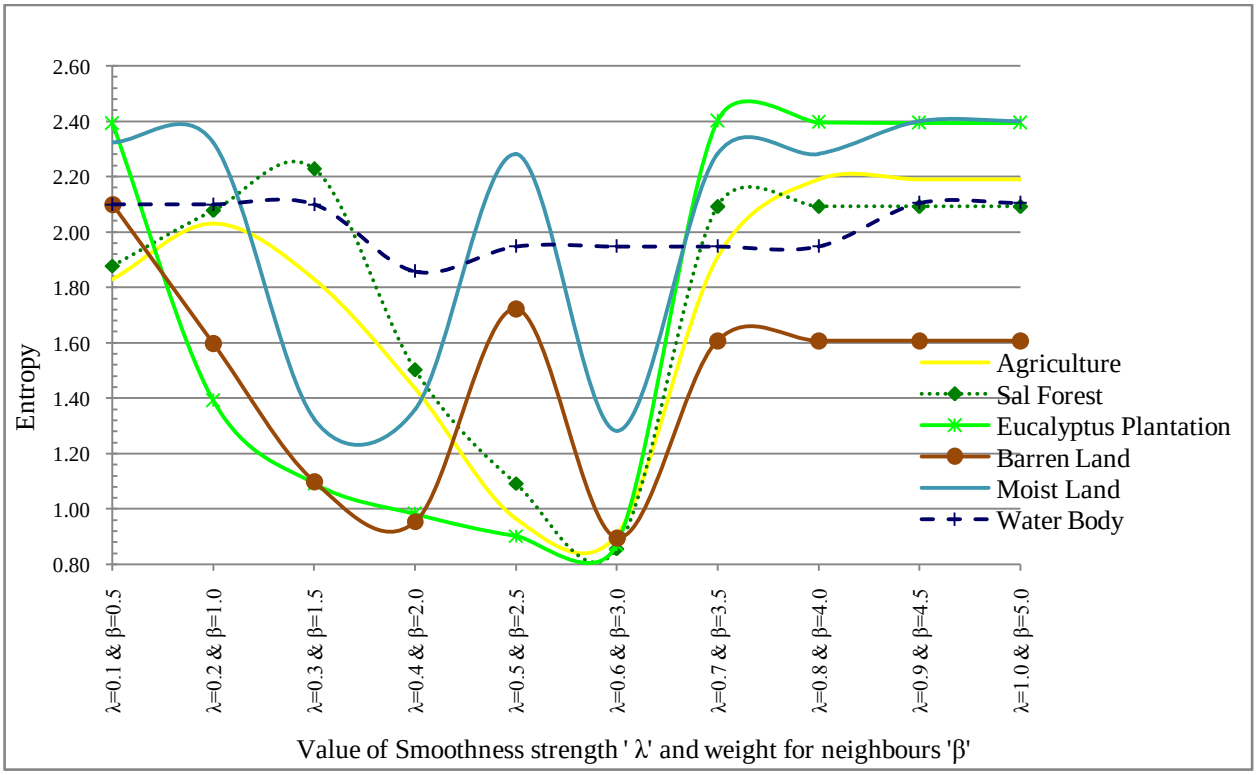

Fig. 6.42: Entropy for PCM-S classifier using AWiFS dataset.

To verify the preservation of edges, a homogenous area of a class has been selected such that it should have high mean and low variance. After the identification of homogenous class, two set of pixels have been selected, where each set lie on either side of the edge. Table 6.16 shows that the difference of the mean between two pixels is high and variance within each pixel set is low. This phenomenon describes the low variability within the classified fraction imagery.

The error usually occurs around the edges and by preserving the edges it increases the classification accuracy (Tso and Oslen, 2005).

Table 6.16: Verification of edge preservation for PCM-S classifier of AWiFS image for optimized value of λ=0.6 and β=3.0.

Class	Difference in mean	Variance
Agriculture	98.63	117.29, 292.41
Sal forest	107.23	83.33, 228.01
Eucalyptus plantation	110.91	272.25,56.25
Barren Land	105.18	256.32,75.34
Moist Land	157	114.5,0.5
Water Body	171.80	1604.66,388.54

To perform PCM-S classification, the optimized value of weighting exponent *m*=2.4 has been taken and λ and β are varying between 0.1 to 1.0 and 0.5 to 6.0 respectively. Table 6.17 shows that Overall accuracy, FERM, SCM, MIN-MIN and MIN-LEAST are varying between 66% to 96% when, AWiFS dataset is used for classification image and LISS-III or LISS-IV dataset is used as a reference. In the process of identifying the optimized value of λ and β, all accuracy indices (FERM, SCM, MIN-MIN and MIN-LEAST) has been analyzed for all six classes selected for the study and it is found that for λ=0.6 and β=3.0, all the accuracy measures are higher and have lesser uncertainty (Fig. 6.42).

Tables 6.17 shows the accuracy indices for optimized value of smoothness parameter (λ) and weight for neighbours (β) of AWiFS (classified)-LISS-IV (referenced) combination. One important aspect as observed from Tables 6.4 and 6.17 is that PCM-S classification performs better than ordinary PCM classification, with 25% improvement in SCM accuracy.

Table 6.17: Accuracy values for optimized value of λ=0.6 and β=3.0 for PCM-S classifier of AWiFS data using LISS-IV as reference data.

Land-Use Classes	**Accuracy assessment methods**				
	FERM	**SCM**	**MIN-PROD**	**MIN-MIN**	**MIN-LEAST**
Fuzzy user's accuracy (%)					
Agriculture	92.33	88.18±1.07	87.34	86.76	86.34
Sal forest	91.61	82.65±2.06	82.87	71.39	85.92
Eucalyptus plantation	88.66	68.59±3.38	79.82	67.20	89.97
Barren Land	97.08	80.2±5.06	67.64	65.13	85.27
Moist Land	94.47	85.07±3.98	95.41	81.21	88.93
Water Body	96.52	85.33±2.64	91.25	72.66	88.56
Fuzzy producer's accuracy (%)					
Agriculture	89.22	87.01±3.51	89.69	85.48	88.58
Sal forest	91.69	91.08±6.47	91.76	81.60	87.55
Eucalyptus plantation	86.30	85.26±1.42	87.96	71.85	78.66
Barren Land	85.77	92.41±7.17	93.23	84.03	79.58
Moist Land	87.23	78.51±14.25	75.56	65.36	92.77
Water Body	66.10	93.61±4.24	92.88	89.36	97.85
Fuzzy overall accuracy (%)	86.20	84.40±4.60	86.28	76.83	87.49
Fuzzy Kappa	-	0.83±0.12	0.83	0.70	0.95

Fig. 6.43 shows the fraction images of AWiFS datasets for PCM-S classification. After examining the fraction images generated by PCM-S classifier, it is found that the value of λ and β changes across the spatial resolution of image. The inclusion of contextual information in PCM resolves the inter-grade homogeneity problem, while PCM is unable to distinguish between homogenous classes. It is also found that by incorporating contextual information in PCM, the output is spectrally and spatially consistent and that overlapping of classes has been resolved effectively (Fig. 6.43).

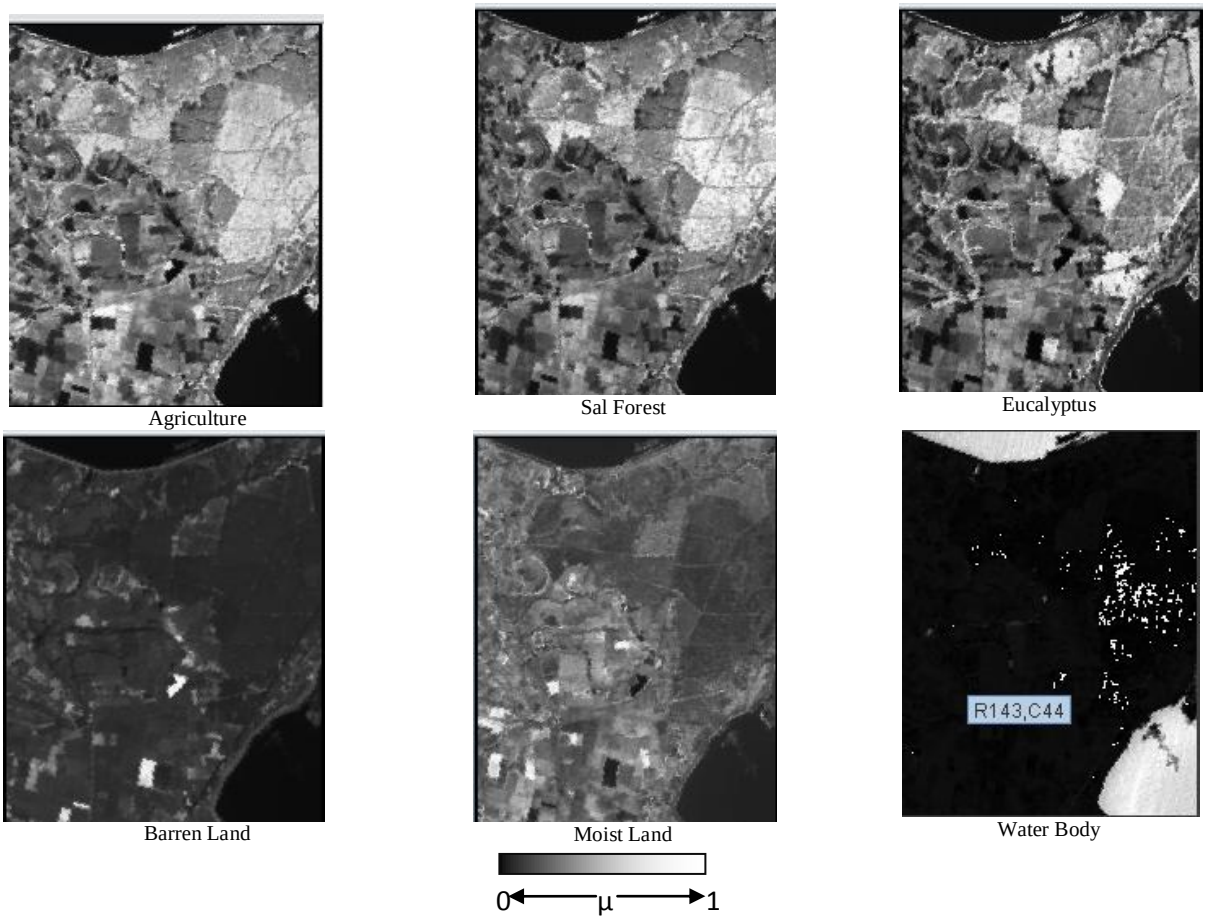

Fig. 6.43: PCM-S classification output of AWiFS image

6.8.2 RESULTS OF PCM WITH DISCONTINUITY ADAPTIVE PRIOR

The basic objective of this study is to develop PCM based hybridized sub-pixel classifier for classifying moderate and coarser spatial resolution multi-spectral data set using PCM-MRF model. In ordinary PCM based classifier, no spatial context of an image was incorporated, so to incorporate the spatial contextual information with PCM, smoothness prior and four DA-MRF described in Section 3.4.11 has been developed. The PCM with contextual classifier incorporates spatial context using DA model and performs sub-pixel classification in supervised mode. Another aspect of this method is to verify the preservation of edge at boundary points.

The objective function of PCM with Discontinuity Adaptive Prior is defined by (Eq 3.51-3.54) and has been designated as PDM-(H1), PDM-(H2),PDM-(H3),PDM-(H4) classifier. As

mentioned in Section 3.4.11, the smoothness parameter (λ) controls the balance between spectral and spatial information. Another parameter which is added with the objective function of PCM with Discontinuity Adaptive (DA) prior classifier is the Adaptive Potential Function (AIF) or Interaction Range Parameter (γ). This determines the rate of decay at that point where AIF reaches to zero and also controls the interaction between two pixels (Moser and Serpico, 2010). The basic objective of this study is to optimize these parameters λ and γ to get better classification. Another aspect of this study, is to identify the optimize DA-model, which yield best classification and also preserves the edges.

The performance of this classifier is dependent on the constant value of weighting exponent (*m*) and smoothness parameter (λ) along with interaction range parameter (γ) (Eq. 3.51-3.54). The optimized constant value of weighting exponent (*m*) and varying value of (λ) and (γ) has been tested. Both parameters are mutually dependent to perform the classification using PDM-(H1), PDM-(H2), PDM-(H3), and PDM-(H4) classifiers. To perform the classification, fixed value of *m*=2.4 has been used while varying the values of λ and γ between 0.1 to 1.0 at an interval of 0.1.

Fig. 6.44 (a), (b), (c) and (d) shows the variation of the class membership for varying value of λ and γ for different classes such as agriculture, sal forest, eucalyptus plantation, barren land, moist land and water body of AWIFS dataset of PDM-(H1), PDM-(H2), PDM-(H3), and PDM-(H4) classifier. For all three datasets, class membership has been generated for the different values of λ and γ. It has been observed from the Fig. 6.44 (a), (b), (c) and (d), that the optimized value of λ and γ is 0.5. The optimized value of λ and γ is finalized on the basis of membership values, for all classes and lying between **0.80** to **0.996** for PDM-(H1), PDM-(H2), PDM-(H3), and PDM-(H4) classifier.

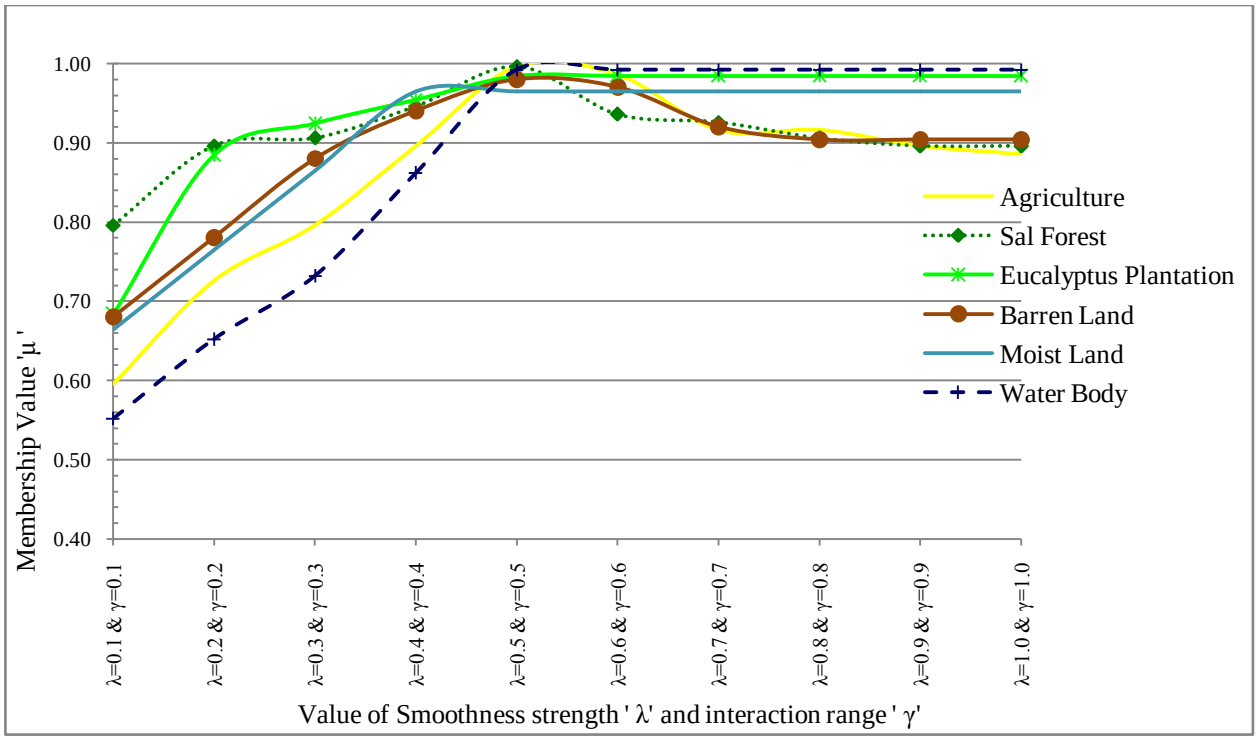

Fig. 6.44(a): Class membership for PDM-(H1) classifier using AWiFS dataset.

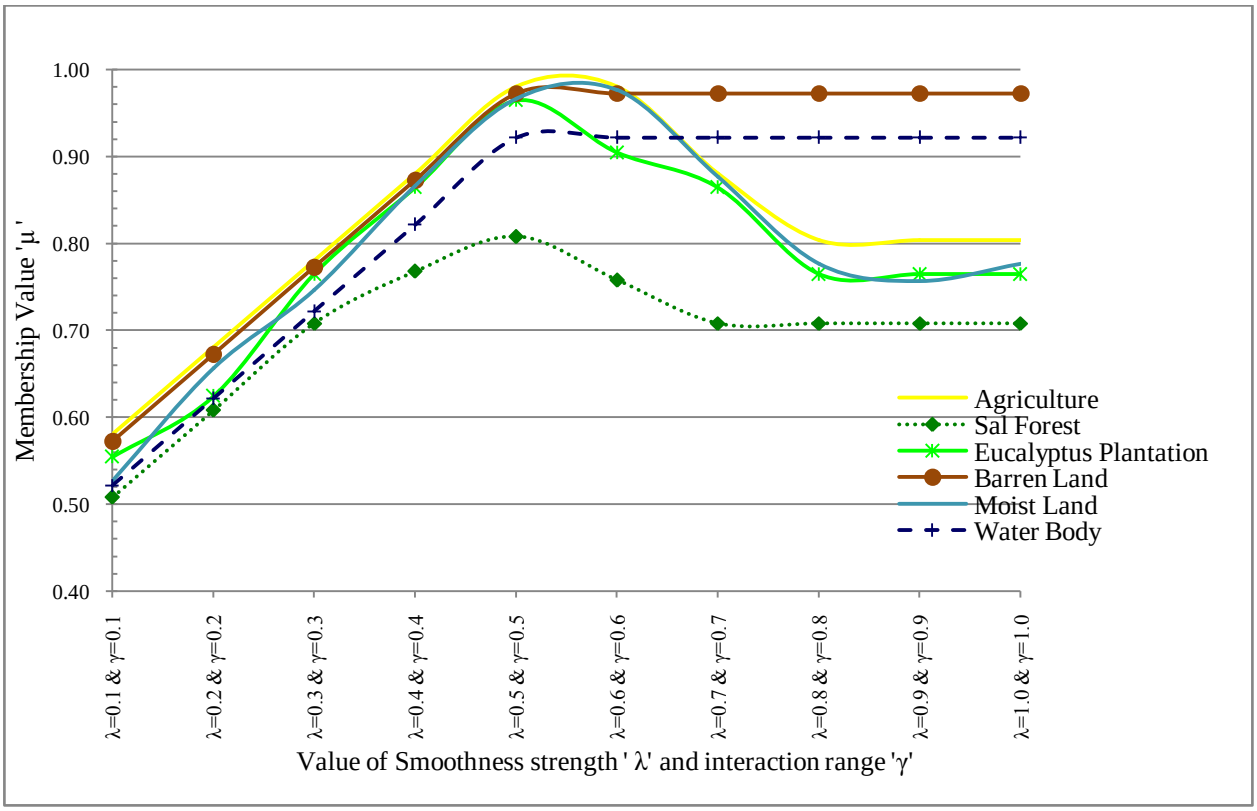

Fig. 6.44(b): Class membership for PDM-(H2) classifier using AWiFS dataset.

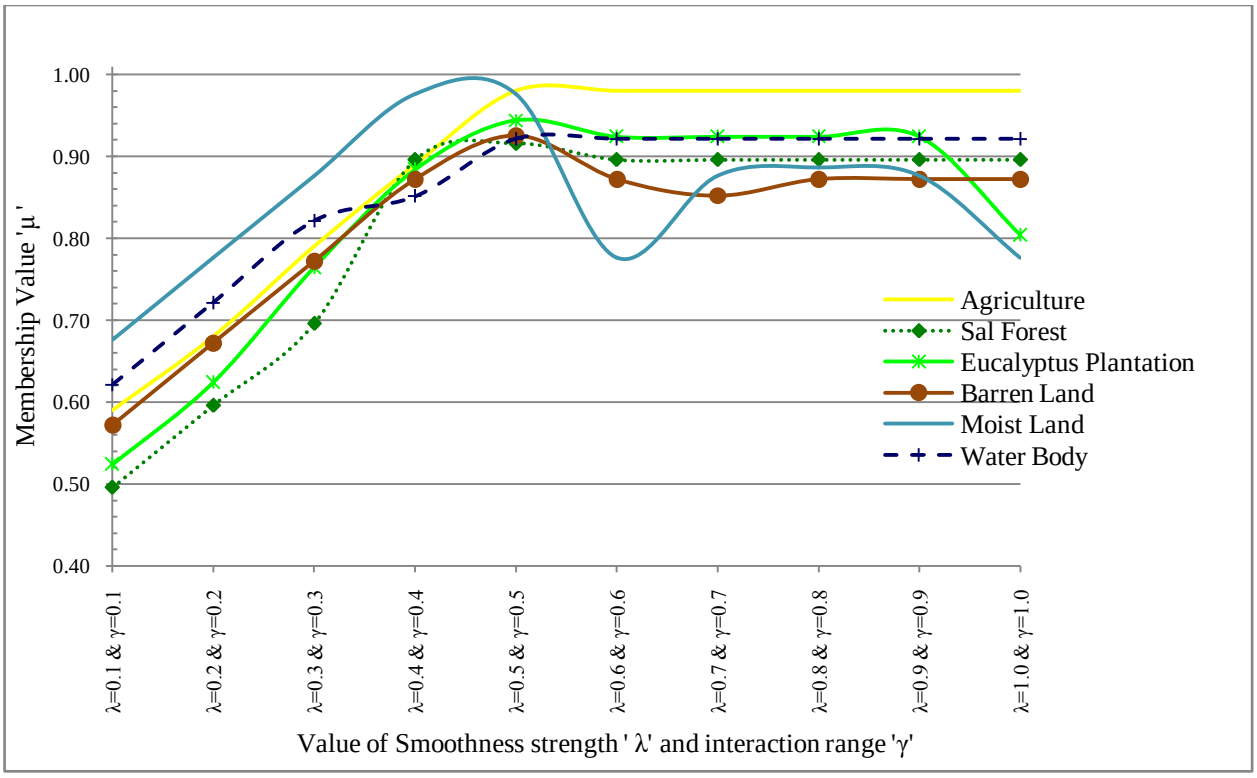

Fig. 6.44(c): Class membership for PDM-(H3) classifier using AWiFS dataset.

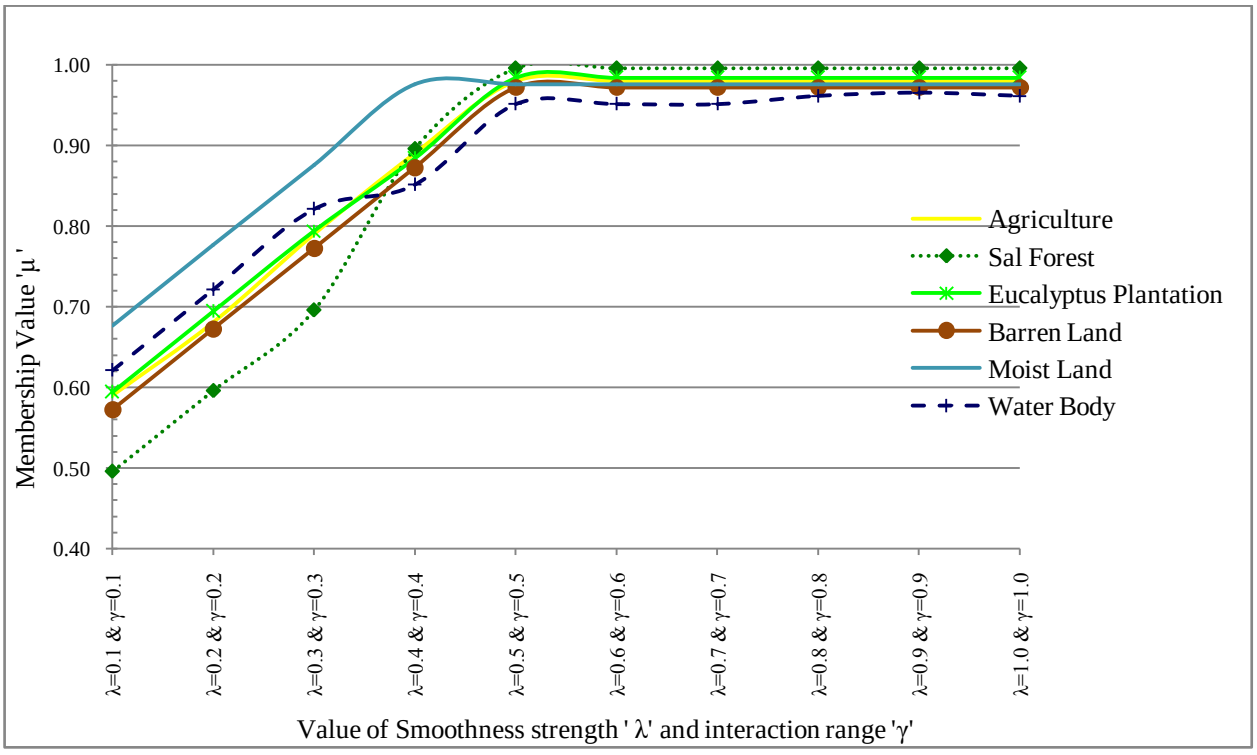

Fig. 6.44(d): Class membership for PDM-(H4) classifier using AWiFS dataset.

Table 6.18 shows the accuracy values for the optimized value of λ =0.5 and γ=0.5, where AWiFS image has been used as a classified image and LISS-III or LISS-IV image has been used a reference image. The accuracy values are presented for all four DA models. From Table 6.18, it has been observed that PDM-(H4) model produces higher accuracy in all cases. All approaches of assessment accuracy shows that PDM-(H4) model produces higher values for FERM, SCM and MIN-LEAST operator. The MIN-LEAST approaches for assessment of accuracy also determines the interclass confusion ratio. The lower values of MIN-LEAST operator states higher interclass confusion (Chen, 2010). The entropy values have also been computed for optimized λ and γ for all four DA models and it is found to be 2.31, 2.85, 2.23, and 1.85 for PDM-(H1, H2, H3, and H4) models respectively. This also indicates that PDM-(H4) has lower entropy (**1.85**) when compared to other models. The basic advantage of hybridization DA model with PCM classifier is that classes are well classified and edges were not over smoothened (Fig. 6.45).

The classification performance of PDM-(H4) has been compared with PCM and PCM-S and it has been found that it reduces the problem of over smoothing of PCM-S and reduces the uncertainty up to 1.5% to 3% for agriculture, sal forest, eucalyptus plantation and 0.5% to 6% for barren land, moist land and water body classes (Tables 6.5, 6.18 and 6.19). Further, it has been observed that FERM and SCM are more robust to assess the accuracy of PCM with contextual classifier. However, it is found that MIN-LEAST is not suitable to assess the accuracy of PCM based hybrid sub-pixel classifier, as it does not follow the hyper-line constraint. PCM-S classification approach follows constant interaction among the pixels within the image space, which sometimes leads to over smoothening and thus it is not able to preserve the edges as efficiently as DA models.

Table 6.18: Comparative accuracy values for optimized value of λ=0.5 and γ=0.5 for PDM (H1, H2, H3 and H4) classifier of AWiFS data using LISS-III and LISS-IV as reference data.

Images → / Indices ↓	AWiFS-LISS-III				AWiFS-LISS-IV			
PDM-Classifier	H-1	H-2	H-3	H-4	H-1	H-2	H-3	H-4
FERM(%)	89.24	89.34	88.95	**89.46**	61.25	92.35	90.17	**90.90**
SCM(%)	82.38	79.04	80.12	**84.43**	80.37	81.23	76.14	**84.50**
MIN-LEAST (%)	57.76	63.61	58.14	**68.32**	58.61	63.05	65.34	**71.21**

To verify the preservation of edges, a homogenous area of a class has been selected by verifying that it should have high mean and low variance. After the identification of homogenous class, two set of pixels have selected lying on the either side of the edge. Table 6.19 shows that the difference of the mean between two pixels is high and that variance within each pixel set is low. This phenomenon describes the low variability within the dataset. It may be conclude that, while using contextual based classifier avoids the problem of over smoothing on the classified imagery.

Table 6.19: Verification of edge preservation for PDM-(H4) classification of AWiFS image for optimized value of 'λ'=0.5 and 'γ'=0.5

Class	Difference in mean	Variance
Eucalyptus plantation	171.84	142.25, 179.56
Barren Land	139.7	256.32,75.34
Water Body	152.05	129.96, 214.92

Fig. 6.45 shows the classified fraction image for optimized values of λ and γ of AWiFS dataset using PDM-(H4) classifier. This classifier performs best in comparison to other DA models. It is observed that first three DA-MRF models with PCM (Eq 3.51-3.53) behave

similarly to PCM-S. However, in case of PDM-(H4) model, the bandwidth or scale parameter does not follow this criterion (η^2«1) (Li, 1990). As observed from Fig. 6.45, PDM-(H4) model controls over smoothing for all category of classes effectively. On the basis of highest class membership, the class wise optimized value of λ and γ has also been identified and it is found to same as that of generalized optimized value i.e. λ= 0.5 and γ=0.5 for all classes.

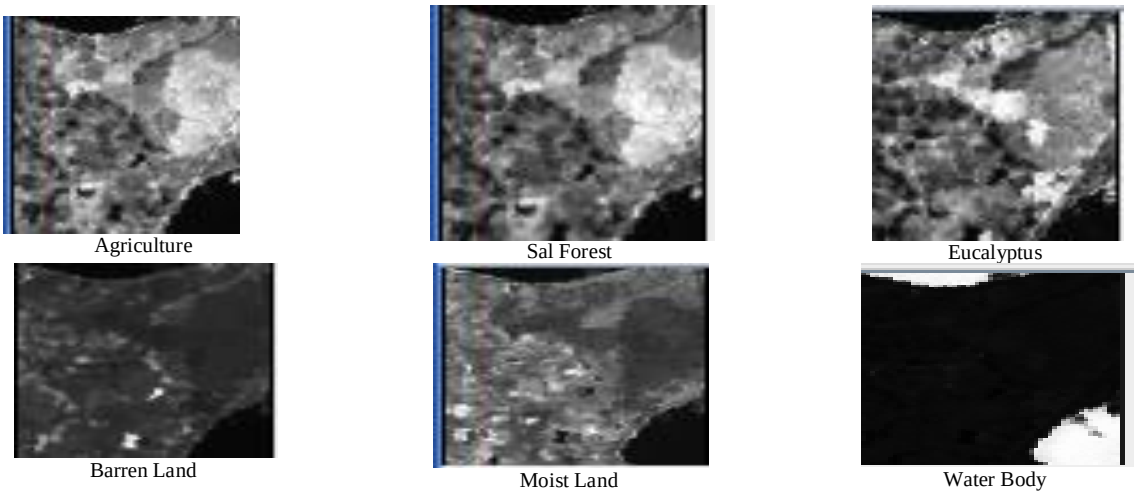

Fig. 6.45: PDM-(H4) classification output of AWiFS image

Fig. 6.45 shows the classified fraction images of AWiFS dataset for the optimized value of λ and γ. To incorporate the spatial contextual information with PCM, smoothness prior and four DA-MRF models have been tested. From Tables 6.18, it has been observed that DA models increases overall accuracy up to 8% when compared to PCM-S (Table 6.17). In PCM and PCM-S classifier, the interactions among the pixels are constant everywhere in the classified imagery. This leads to over smoothing at edges in PCM-S classifier. However, in PDM classification approach, the smoothing strength λ is proportional to η. Thus, adding the contextual information using DA-MRF models reduces the problem of over smoothing at edges, while preserving it at boundary points (Figs. 6.45) and produces more accurate results. Although, it is a fact that hybridization of contextual with PCM incorporate some level of uncertainty because, the computed entropy values for optimized λ =0.5 and γ =0.5 for all four DA models are not at minimal level and is found to 2.31, 2.85, 2.23, and 1.85 for PDM-(H1, H2, H3, and H4) models

respectively. Thus, inclusion of contextual information in PCM classifier has not efficiently utilized the spatial information of an image.

6.9 RESULTS OF NC WITH CONTEXTUAL CLASSIFIER

The idea of using this hybrid approach of soft classification i.e. Noise Clustering (NC) with contextual is a new approach which helps significantly to eliminate noise pixels while incorporating spatial contextual information. The hybrid classification approach of NC with contextual information has been performed in two categories i.e. NC with Smoothness prior (NC-S) and four categories of NC with Discontinuity Adaptive (DA) prior i.e. (NDM-H1,NDM-H2,NDM-H3, NDM-H4). The following sections, describes the results of the NC with contextual classifiers.

6.9.1 RESULTS OF NC WITH SMOOTHNESS PRIOR

The contextual information has been added in NC classifier to generate smoothness effect and it has been designated as NC-S. The inclusion of Standard Regularizes in NC assumes a constant interaction among the pixels in image space. Two basic variables are associated with the defined objective function are smoothness parameter (λ) and weight for neighbours (β). The function of these parameters has been indicated in Section 6.7. The basic objective of this study is to optimize these parameters to acquire better classified fraction imagery.

The performance of this classifier is dependent on the constant value of resolution parameter δ and smoothness parameter λ along with weight for neighbours parameter β. The optimized constant value of δ and varying value of λ along with β has been tested. Both parameters are mutually dependent to perform the classification using NC-S approach. To perform the NC-S classification, the fixed optimized value of $\delta=10^5$ has been used for all varying values of λ from 0.1 to 1.0 at an interval of 0.1 and β is varied from 0.5 to 5.0 at an interval of 0.5.

Fig. 6.46 shows the variation of varying value of smoothness parameter (λ) and weight for neighbours parameter (β) with class membership of different classes such as agriculture, sal forest, eucalyptus plantation, barren land, moist land and water body of AWIFS, dataset. For AWiFS dataset, class membership has been generated for the different values of λ and β. The class membership values of a pixel denote the class proportions, which in turn may represent the soft classified output for a pixel. It has been observed from the Fig. 6.46 that for λ=0.7 and β =3.5, class membership lies between 0.90 to 0.99 for all six classes selected for this study.

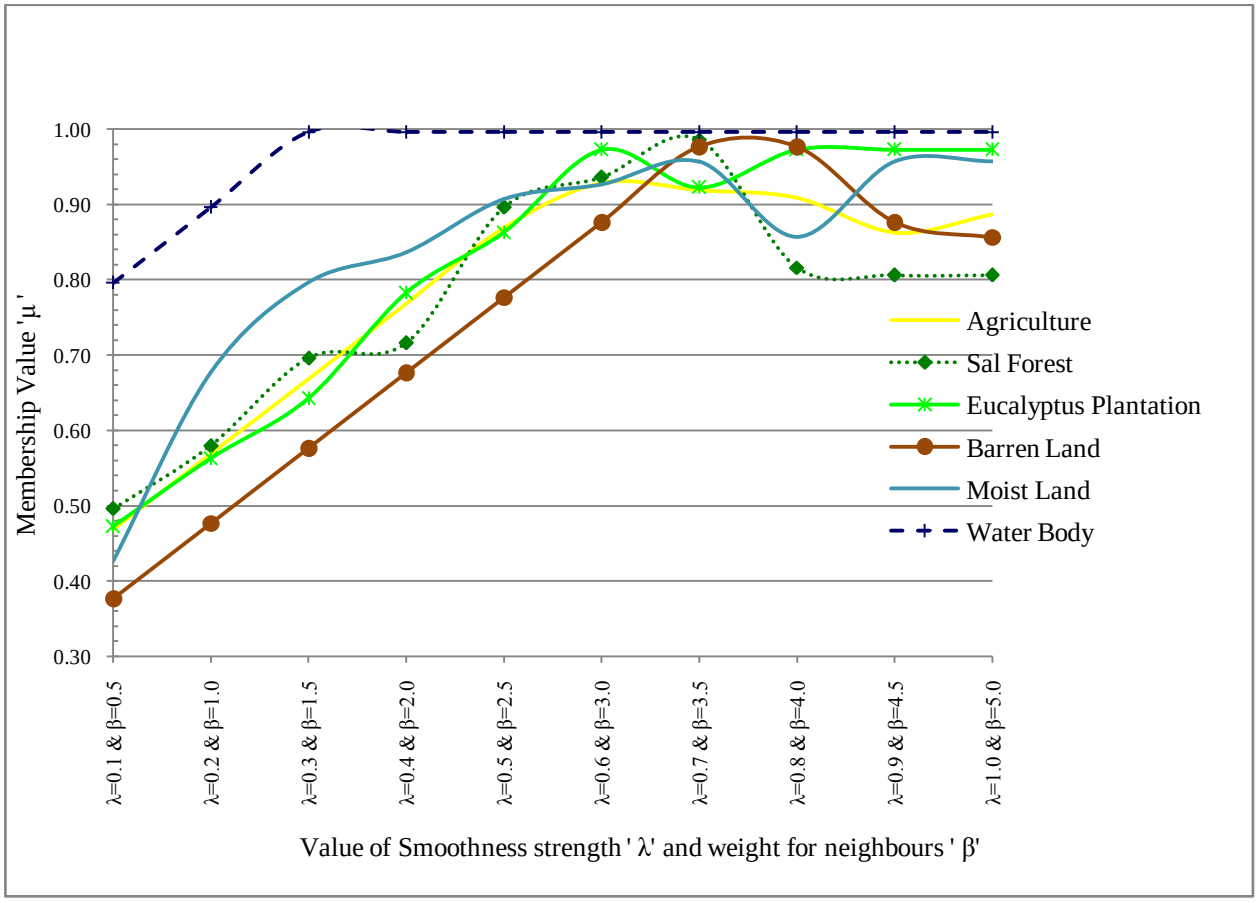

Fig. 6.46: Class membership for NC-S classifier using AWiFS dataset.

Fig. 6.47 shows the computed entropy for AWiFS fraction images of NC-S classifier for agriculture, sal forest, eucalyptus plantation, barren land, moist land, and water body land cover classes. The entropy values are lying between the specified range of [0.005, 0.65]. If the entropy values of classified fraction imagery are less; this indicates better classification results with

minimum uncertainty. It has been observed from Fig. 6.47 that at λ= 0.7 and β=3.5 for AWiFS dataset, the entropy values for all classes are at the lowest level. For these optimized values of λ and β, the membership is high i.e. up to 99% and the computed entropy is lying between 0.005 to 0.65. This trend indicates that the uncertainty in classified results is lowest at optimized point for smoothness parameter λ= 0.7 and weight for neighbours parameter β=3.5. This mathematical model of entropy computation is used as an absolute indicator of measuring uncertainty without using any ground reference data.

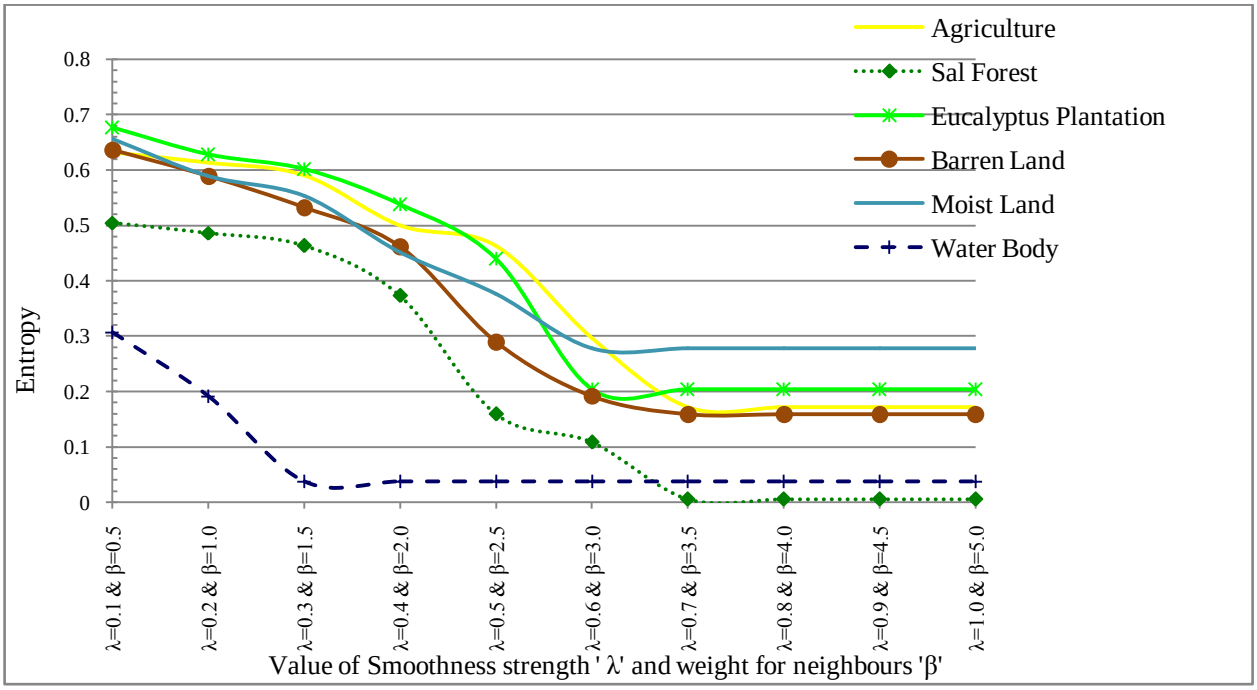

Fig. 6.47: Entropy for NC-S classifier using AWiFS dataset.

To perform NC-S classification, the optimized value of resolution parameter $\delta=10^5$, has been taken and λ and β are varying between 0.1 to 1.0 and 0.5 to 6.0 respectively. Table 6.20 shows that the Overall accuracy, FERM, SCM, MIN-MIN and MIN-LEAST are varying between 83% to 95% where, AWiFS dataset has been used for classification image and LISS-III or LISS-IV dataset is used as a reference image. In the process of identifying the optimized value of λ and β, all accuracy indices (FERM, SCM, MIN-MIN and MIN-LEAST) has been analyzed for all six classes selected for the study and it is found that for λ=0.7 and β=3.5, all the accuracy measures are highest and having lowest uncertainty{Fig. 6.47}.

Tables 6.20 shows the accuracy indices for optimized value of smoothness parameter (λ) and weight for neighbours (β) of AWiFS (classified)-LISS-IV (referenced) combination. One important aspect that can be seen from Tables 6.6 and 6.20 is that NC-S classifier performs slightly better than ordinary NC classifier, where entropy values are on the lower side (**0.005**) when compare to NC classifier (Fig. 6.16(a), (b) and (c)).

Table 6.20: Accuracy values for optimized value of λ=0.7 and β=3.5 for NC-S classifier of AWiFS data using LISS-IV as reference data.

Land-Use Classes	**Accuracy assessment methods**				
	FERM	**SCM**	**MIN-PROD**	**MIN-MIN**	**MIN-LEAST**
Fuzzy user's accuracy (%)					
Agriculture	69.03	83.20±8.53	82.26	74.67	91.73
Sal forest	78.95	89.33±8.19	88.83	81.14	97.52
Eucalyptus plantation	86.73	94.98±3.05	94.80	91.93	98.03
Barren Land	73.46	83.96±12.73	81.89	71.22	96.70
Moist Land	67.88	78.52±8.92	77.28	69.60	87.45
Water Body	95.88	98.50±1.31	98.14	97.19	99.81
Fuzzy producer's accuracy (%)					
Agriculture	95.03	95.53±2.63	95.38	92.89	98.17
Sal forest	92.69	93.31±3.34	93.06	89.96	96.66
Eucalyptus plantation	80.93	83.36±8.07	81.72	75.28	91.43
Barren Land	91.33	81.78±14.45	81.01	67.33	96.23
Moist Land	91.81	92.38±5.27	91.98	87.10	97.66
Water Body	66.10	91.52±7.16	92.41	84.36	98.68
Fuzzy overall accuracy (%)	88.19	89.33±6.24	88.82	83.09	95.57
Fuzzy Kappa	-	0.86±0.07	0.85	0.78	0.94

Table 6.21 presents the values of mean and variance which has been computed to verify the edge preservation. To verify the preservation of edges of AWiFS image to land cover classes i.e. barren land and water body has been selected and mean and variance has been computed at

the two sides of the edge. The mean difference is high and variance is low in NC-S classifier. Table 6.21 shows that the difference of the mean between two pixels is high and variance within each pixel set is low. This phenomenon describes the low variability within the image set.

Table 6.21: Verification of edge preservation for NC-S classifier of AWiFS image for optimized value of λ=0.7 and β=3.5

Class	Difference in mean	Variance
Barren Land	216.5	4.5,2.0
Water Body	231.5	8,4.5

Fig 6.48 shows the results in form of fraction image generated using NC-S classifier. It is observed that results have not improved by including spatial context with NC using standard regularizer. As discussed in Section 3.4.12, standard regularizer tends to over smoothing and hence, in spite of adding contextual information in NC classifier using smoothening prior, the results do not improved when compared to NC and NCWE (Tables 6.6 and 6.8). The fraction images generated by NC-S classifier are spectrally and specially consistent and uncertainty is lesser than NC and NCWE classifier (Figs. 6. 16(a), 6.23(a) and 6.47). However, it does not show any improvement in terms of accuracy measures such as FERM and SCM.

6.9.2 RESULTS OF NC WITH DISCONTINUITY ADAPTIVE PRIOR

To incorporate the spatial contextual information with NC, smoothness prior and four DA-MRF described in Section 3.4.12 has been hybridized to resolve the problem of mixed pixel. The objective function of NC with Discontinuity Adaptive prior is defined in (Eq 3.56-3.59) and designated as NDM-(H1), NDM-(H2), NDM-(H3), NDM-(H4).The smoothness parameter (λ) controls the balance between spectral and spatial information. Another parameter which is added with the objective function of FCM with Discontinuity Adaptive prior classifier is the Adaptive Potential Function (AIF) or Interaction Range Parameter (γ). This determines the rate of decay at that point where AIF reaches to zero and also controls the interaction between two pixels (Moser and Serpico, 2010). The basic objective of this study is to optimize these parameters λ and γ to

get better classification. Another aspect of this study, is to identify the optimize DA-model, which suites for the satellite image classification.

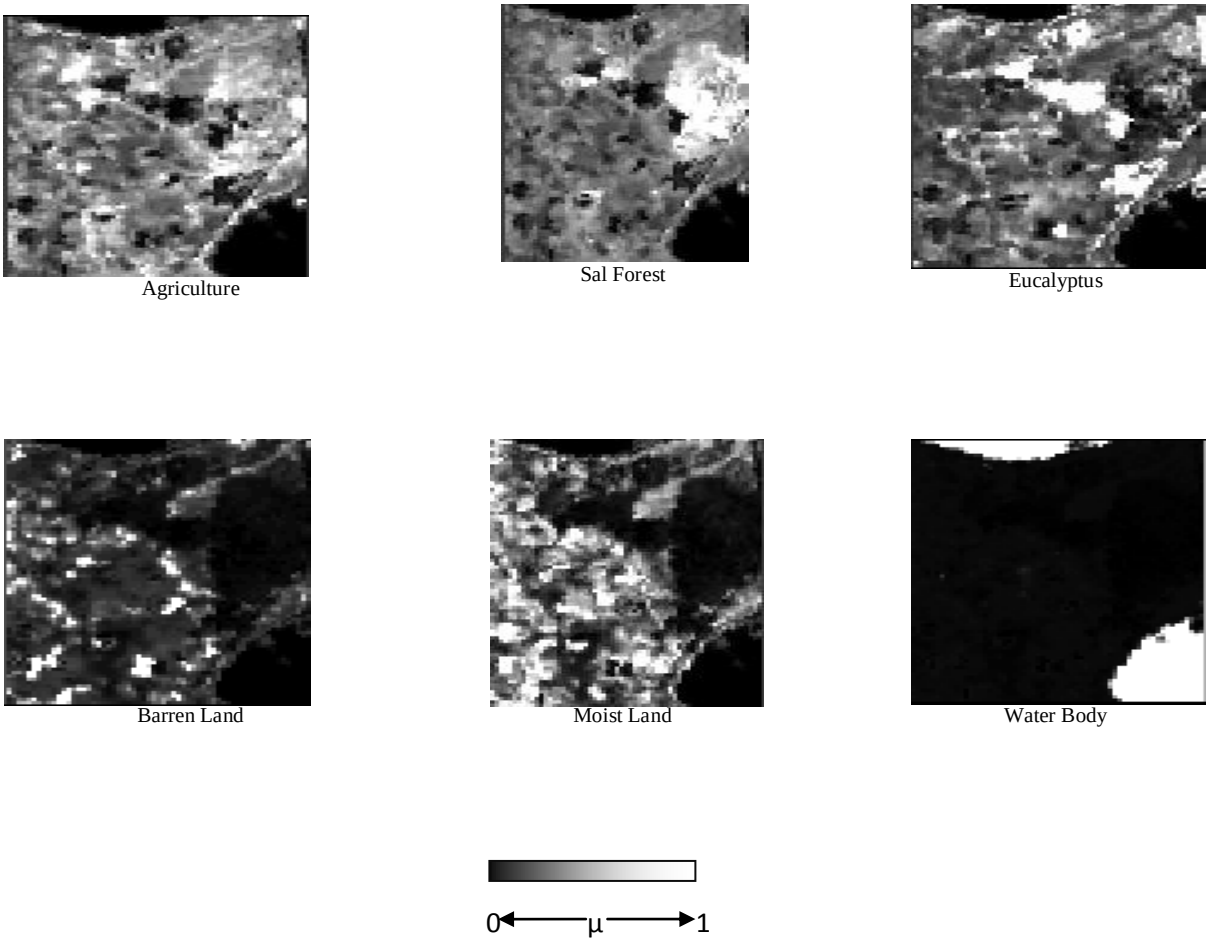

Fig. 6.48: NC-S classification output of AWiFS image

The performance of this classifier is dependent on the constant value of resolution parameter (δ) and smoothness parameter (λ) along with Interaction Range Parameter (γ). The optimized value of δ and varying value of λ and γ has been tested. These parameters are mutually dependent on each other in NDM-(H1), NDM-(H2), NDM-(H3), and NDM-(H4) classification approaches. To carry out the classification, a fixed value of $\delta=10^5$, has been used while varying the values of λ and γ between 0.1 to 1.0 at an interval of 0.1. For an appropriate classification, the membership value of a particular class should be very high and that its corresponding entropy value should be minimum.

Fig. 6.49 (a), (b), (c),(d) shows the variation of the of the varying value of λ and γ with class membership of different classes such as agriculture, sal forest, eucalyptus plantation, barren land, moist land and water body for AWIFS dataset of NDM-(H1), NDM-(H2), NDM-(H3), NDM-(H4) classifier. For all three datasets, class membership has been generated for different values of λ and γ. It has been observed that the optimized value of λ and γ is 0.4. The optimized value of λ and γ is finalized on the basis of membership values, which is highest for all classes and is lying between **0.92** to **0.99** for NDM-(H1), NDM-(H2), NDM-(H3), NDM-(H4) classifier.

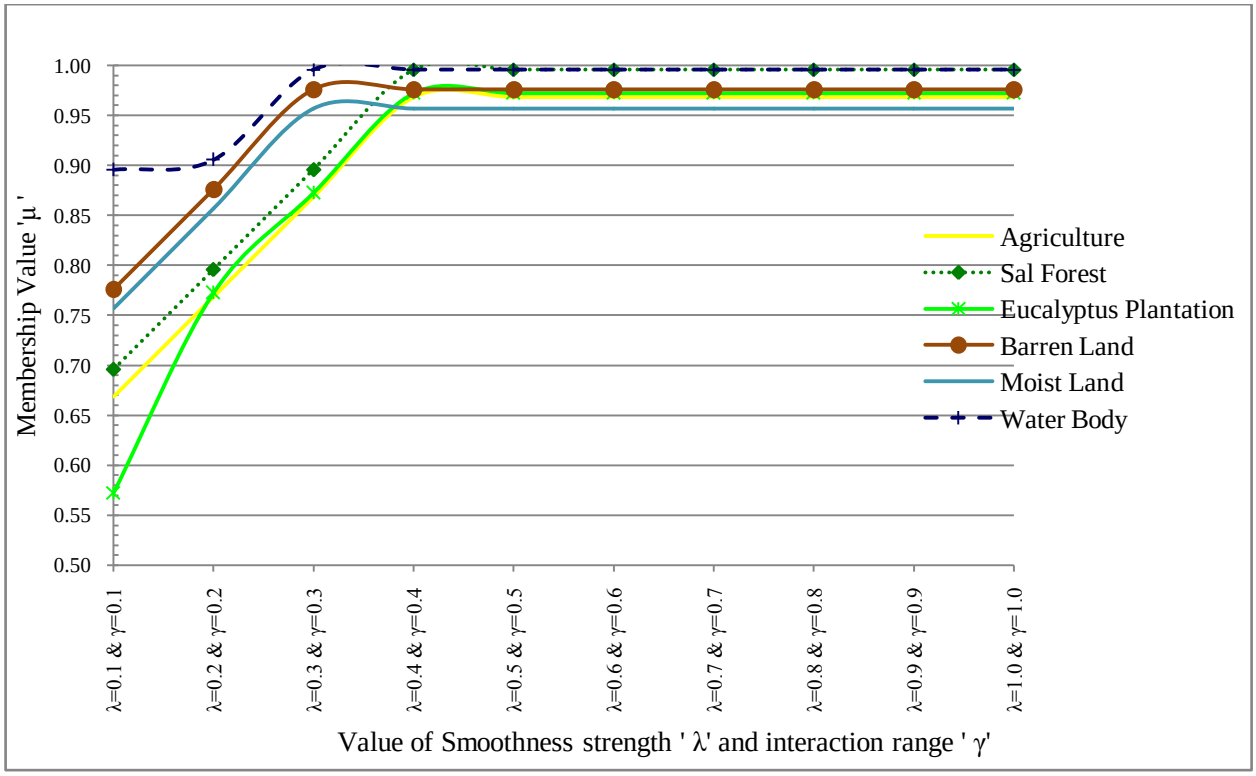

Fig. 6.49 (a): Class membership for NDM-(H1) classifier using AWiFS dataset.

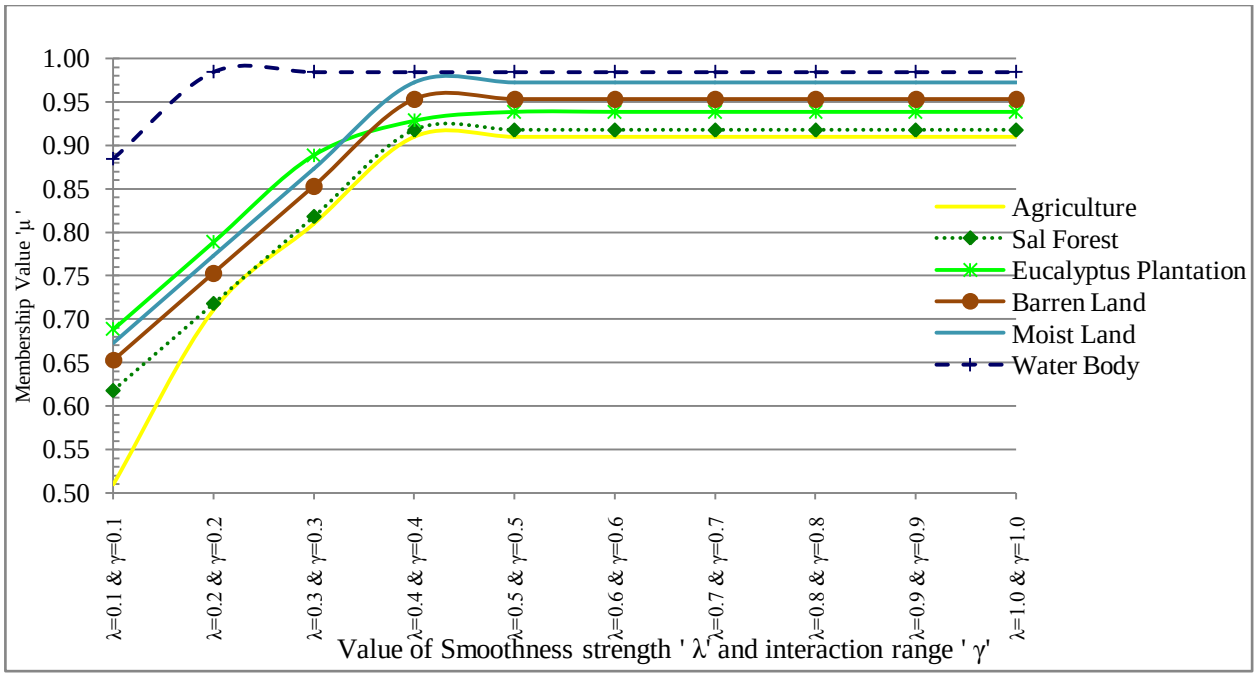

Fig. 6.49 (b): Class membership for NDM-(H2) classifier using AWiFS dataset.

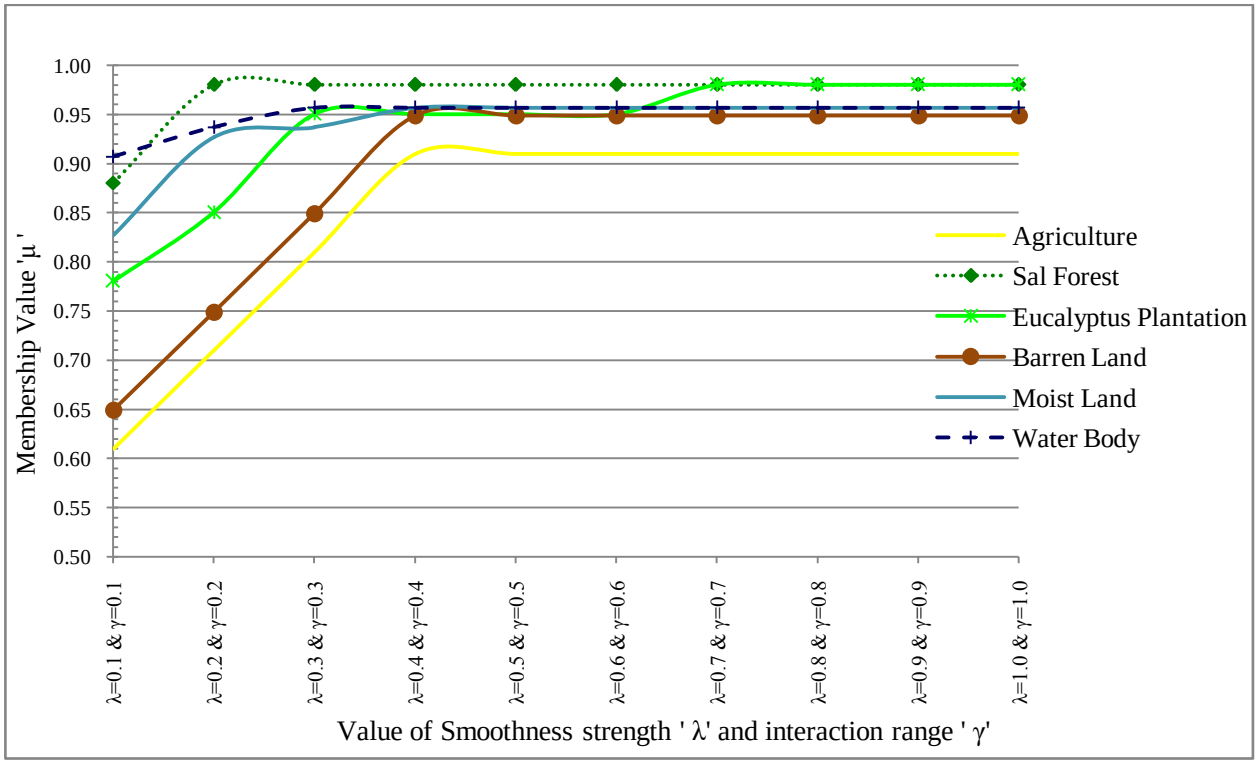

Fig. 6.49 (c): Class membership for NDM-(H3) classifier using AWiFS dataset.

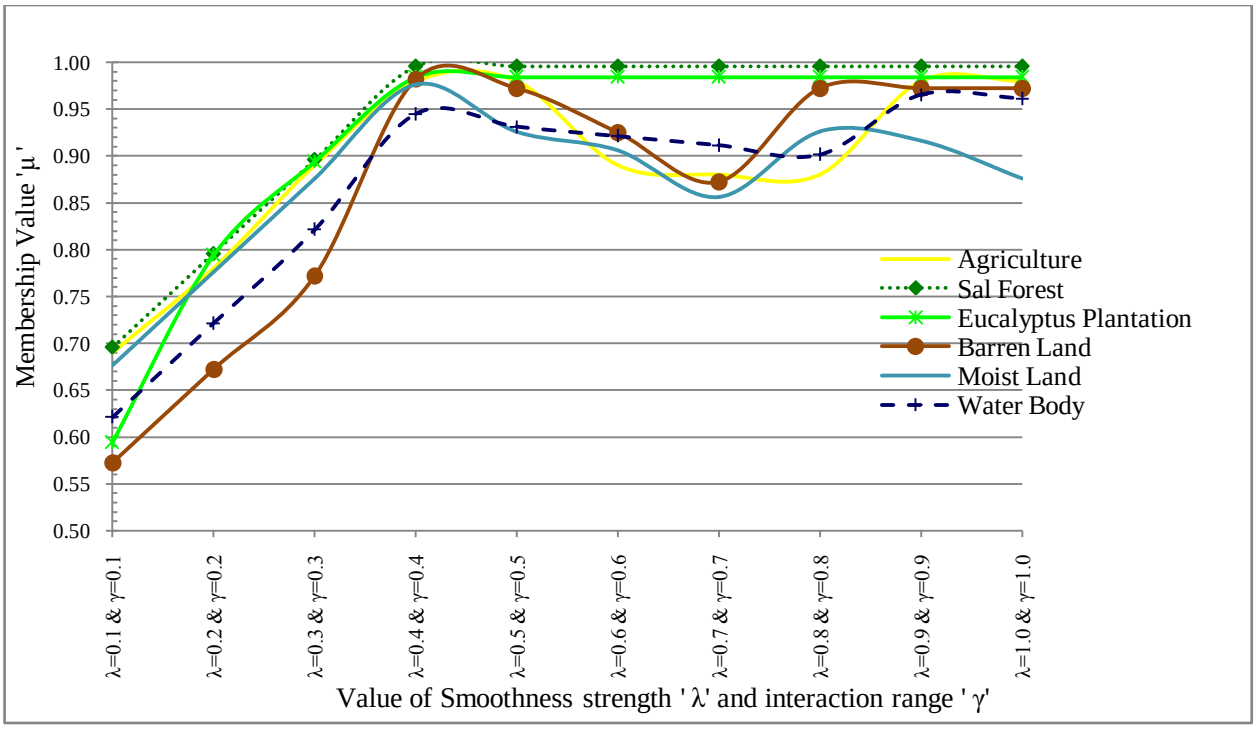

Fig. 6.49 (d): Class membership for NDM-(H4) classifier using AWiFS dataset.

To perform NDM classification with all four DA-MRF models, the optimized value of resolution parameter $\delta=10^5$ has been taken and λ and γ are varying between 0.1 to 1.0 at an interval of 0.1. Table 6.22 shows all the accuracy values for the optimized value of λ =0.4 and γ=0.4, where AWiFS image has been used as a classified image and LISS-III or LISS-IV image has been used reference image. Table 6.22 shows the accuracy values for all four DA models. It has been observed that NDM-(H4) model produces highest accuracy for all cases. All approaches of assessment accuracy shows that NDM-(H4) model produces higher values for FERM, SCM and MIN-LEAST operator. The entropy values have also been computed for optimized λ and γ for all four DA models and it is found to be 1.08, 0.52, 1.23, and 0.005 for NDM-(H1, H2, H3, and H4) models respectively. This also reflects that NDM-(H4) has lower entropy (**0.005**) when compared to other models. The basic advantage of hybridization DA model with NC classifier is that classes are well classified and edges were not over smoothed (Fig. 6.50).

The classification performance of NDM-(H4) has been compared with NC, NCWE and NC-S. It has been observed that it reduces the problem of over smoothing of NC-S and increases the SCM accuracy approximately by 8% (Tables 6.6, 6.8, 6.20 and 6.22). Further, it has also

been observed that FERM, SCM and MIN-LEAST are more robust to assess the accuracy of PCM with contextual classifier. NC-S (standard regularizes) classification approach follows constant interaction among the pixels in image space, which sometimes lead to over smoothening and not able to preserves the edges efficiently as DA models do. Tables 6.22 shows the accuracy indices for optimized value of Smoothness parameter (λ) and Interaction Range Parameter (γ) of AWiFS (classified)-LISS-III/LISS-IV (referenced) combination. One important aspect that can be seen from Tables 6.6, 6.20 and 6.22 is NDM-(H4) classifier performs best in comparison to ordinary NC, NCWE and NC-S classifier. All the accuracy measures are highest and entropy values are lower (**0.005**) when compare to NC, NCWE and NC-S classifier (Figs. 6.16(a), (b) and (c), 6.46).

Table 6.22: Comparative accuracy values for optimized value of λ=0.4 and γ=0.4 NDM (H1, H2, H3, H4) classifier of AWiFS data using LISS-III and LISS-IV as reference data.

Images → / Indices ↓	AWiFS-LISS-III				AWiFS-LISS-IV			
NDM-Classifier	H-1	H-2	H-3	H-4	H-1	H-2	H-3	H-4
FERM(%)	85.87	85.88	85.51	**85.56**	41.88	94.25	89.27	**99.83**
SCM(%)	87.29	87.30	86.88	**87.95**	58.92	93.65	89.18	**99.79**
MIN-LEAST(%)	82.89	86.86	91.26	**91.29**	72.10	99.48	98.26	**98.05**

To verify the edge preservation for AWiFS image two land cover classes i.e. barren land and water body have been selected and mean and variance were computed on both sides of the edges as shown in Table 6.23. The difference of the mean value is high and variance is low in NDM-(H4) classifier in comparison to NC-S (Table 6.21), it implies that NDM-(H4) preserves the edges.

Table 6.23: Verification of edge preservation for NDM-(H4) classification of AWiFS image for optimized value of λ=0.4 and γ=0.4

Class	Difference in mean	Variance
Barren Land	298.5	3.3,2
Water Body	264.5	8,4.5

The smoothness parameter (λ) and Interaction Range Parameter (γ) has been optimized and Fig. 6.50 shows the classified fraction images of AWiFS dataset. To incorporate the spatial contextual information with NC, smoothness prior and four DA-MRF models have been tested. From Tables 6.22, it has been observed that DA models increases Overall accuracy by 9% when compared to NC-S. In NC and NC-S classifier (Eq 3.12 and Eq 3.55), the interactions among the pixels are constant everywhere in the classified imagery. This leads to over smoothing at edges in NC-S classifier. However, in NDM classification approach, the smoothing strength λ is proportional to η (Eq 3.56-3.59). Thus, adding the contextual information using DA-MRF models reduces the problem of over smoothing at edges while preserving it at boundary points (Figs. 6.50) and thus produces better results. It has been observed that hybridization of contextual with NC classifier, minimizes uncertainty since, the computed entropy values for optimized λ =0.4 and γ =0.4 for all four DA models are at minimal level NDM-(H4) models. Thus, it can be concluded that incorporation of contextual information with NC classifier produces spectrally and spatially consistent and robust results.

6.10 RESULTS OF FCMWE WITH CONTEXTUAL CLASSIFIER

The idea of using Fuzzy *c*-Mean with Entropy, a hybrid approach of soft classification i.e. FCMWE with contextual information is a new approach which helps significantly to reduce uncertainty among pixels while incorporating spatial contextual information. The hybrid classification approach of FCMWE with contextual information has been performed in two categories i.e. FCMWE with Smoothness prior (FCMWE-S) and four categories of FCMWE with Discontinuity Adaptive (DA) prior i.e. (FDEM-H1, FDEM -H2, FDEM -H3, FDEM -H4). The following sections, describes the results of the FCMWE with contextual classifiers. It is

believed that inclusion of entropy and contextual information in FCM classifier gives better impact to classify various land cover classes.

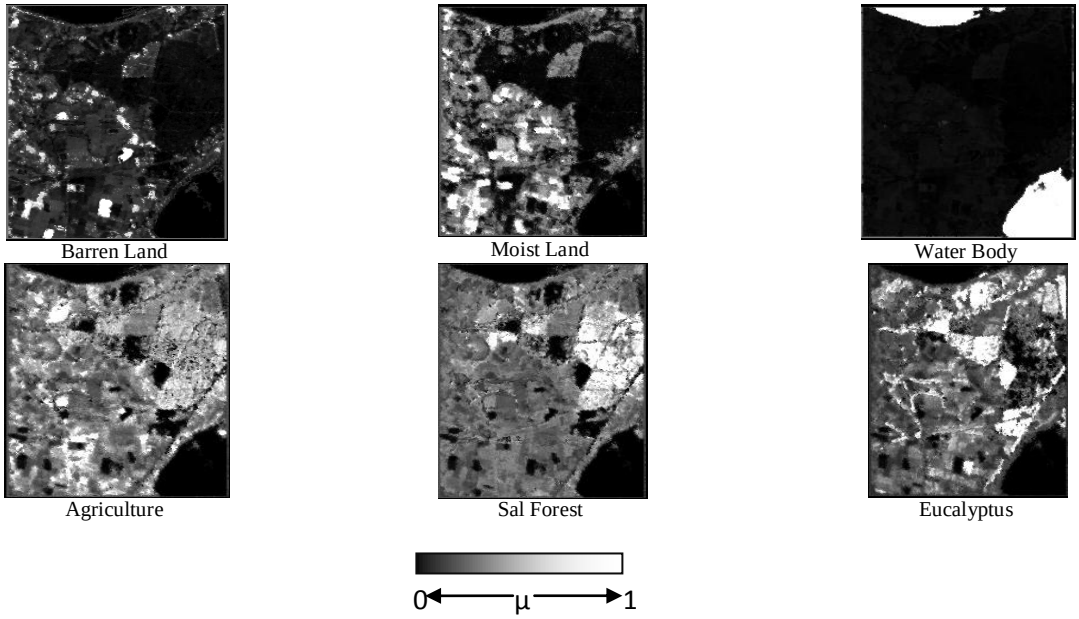

Fig. 6.50: NDM-(H4) classification output of AWiFS image

6.10.1 RESULTS OF FCMWE WITH SMOOTHNESS PRIOR

To incorporate spatial contextual information, spectral information along with entropy as a regularizer, a hybridized model has been devised to resolve the problem of mixed pixel. The contextual information has been added in FCMWE classifier to generate smoothness effect and it is defined as FCMWE-S (Eq 3.65). Two basic variables are associated with the defined objective function are smoothness parameter (λ) and weight for neighbours (β). The smoothness parameter controls the balance between spectral and spatial information, while β analyzes the weight to be given to a neighboring pixel in a window. The basic objective of this study is to optimize these parameters to get better classification output with minimum uncertainty.

The performance of this classifier is dependent on the constant value of Regularizing parameter (ν) and smoothness parameter (λ) along with weight for neighbor's parameter β(Eq. 3.65). The optimized constant value of Regularizing parameter (ν) and varying value of

smoothness parameter (λ) along with weight for neighbors parameter β has been tested. To perform FCMWE-S classification, a fixed value of ν =10^2 has been used by varying the values of λ ranges between 0.1 to 1.0 at an interval of 0.1, while β has been varied from 0.5 to 5.0 at an interval of 0.5.

Fig. 6.51 shows the variation of smoothness parameter (λ) and weight for neighbour's parameter (β) with class membership for different classes such as agriculture, sal forest, eucalyptus plantation, barren land, moist land and water body for AWIFS datasets. The class membership values of a pixel denote the class proportion, and indicate the soft classified output for a pixel. It has been observed from Fig. 6.51, that for λ=0.4 and β =2.0, agriculture, barren land, moist land and water body produces highest membership. However, for λ=0.5 and β =2.5, λ=0.6 and β =3.0, sal forest and eucalyptus plantation produces highest membership respectively. For the above values of λ and β values, the class membership lies between 0.95 to 0.99 for all six classes selected for this study. It has been further verified via entropy and observed that the value of optimized parameter is not deviating (Fig. 6.52).

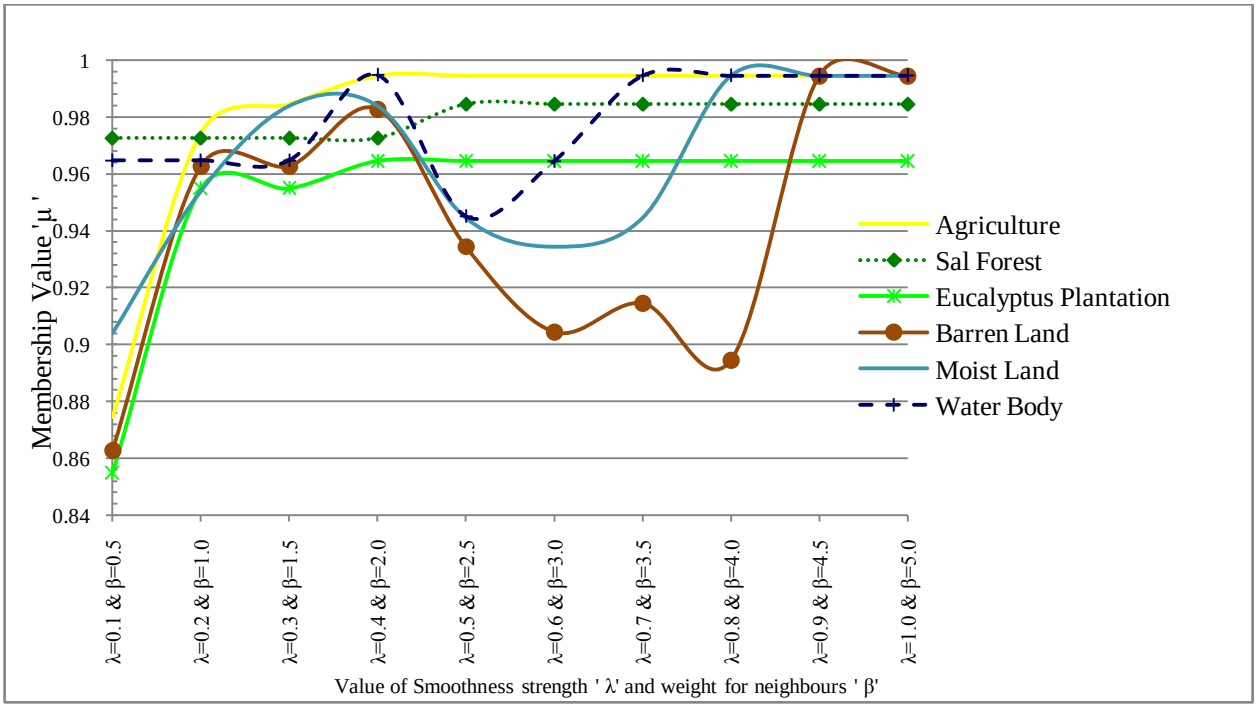

Fig. 6.51: Class membership for FCMWE-S classifier using AWiFS datasets

The prime objective of image classification using FCMWE-S classifier is to establish a relationship between the spectral and spatial information with adequate land cover type. The correctness of the classification results are evaluated using class membership and accuracy indices criterion. However, this criterion is not sufficient to measure the quality of certainty of the classification results. For the visualization and evaluation of uncertainty in the classified imagery, the entropy criterion is proposed. This can be express by a single number to show the distribution and extent of uncertainty in the classified results.

Fig. 6.52 shows the computed entropy for AWiFS fraction images of FCMWE-S classifier for agriculture, sal forest, eucalyptus plantation, barren land, moist land, and water body land cover classes. The entropy values are lying between the specified range of [0.005, 0.35]. If the entropy value of classified fraction imagery is less; this indicates better classification with minimum uncertainty. It has been observed from Fig. 6.52, that at λ= 0.4 and β=2.0 for AWiFS dataset, the entropy values for agriculture, barren land, moist land and water body classes are lowest. However, for sal forest and eucalyptus plantation the optimized value of λ=0.5 and β=2.5, λ=0.6 and β=3.0 respectively. For these optimized values of λ and β, the membership is high i.e. up to 99% and the computed entropy is 0.005. This trend indicates that the uncertainty in classified results is lowest at optimized point for smoothness parameter (λ) and weight for neighbor parameter (β). This mathematical model of entropy computation is used as an absolute indicator of measuring uncertainty without using any ground reference data.

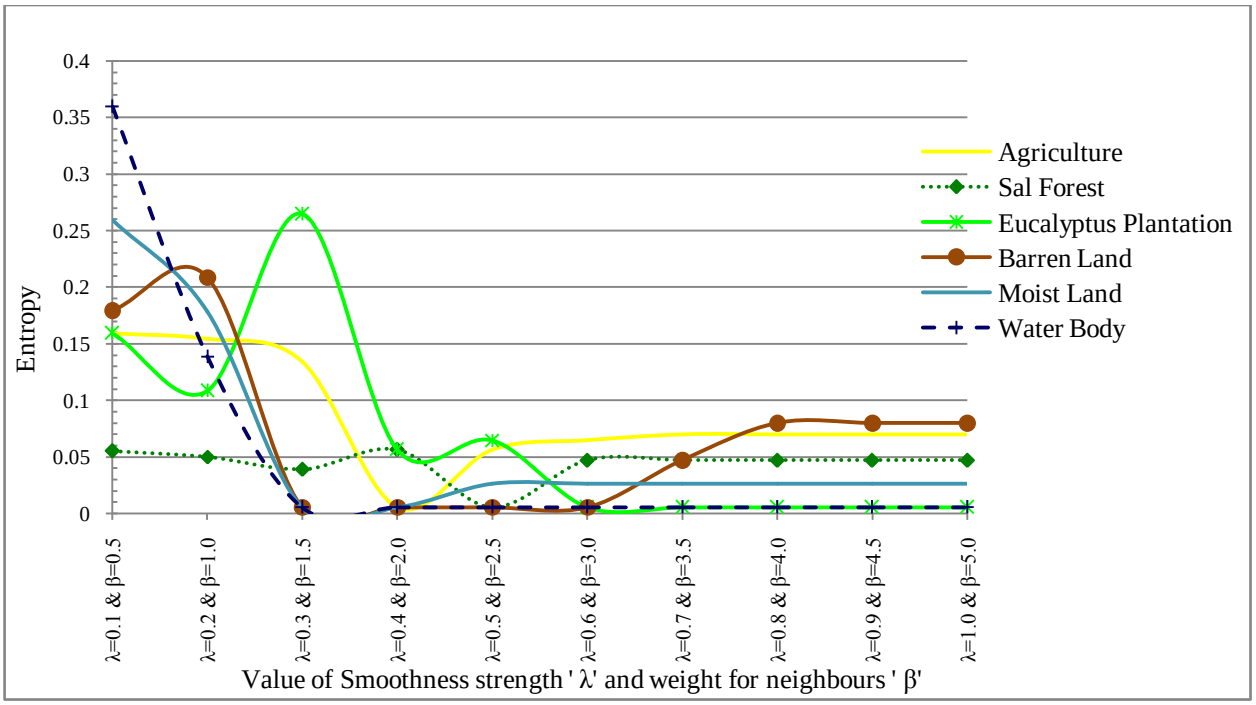

Fig. 6.52: Entropy for FCMWE-S classifier using AWiFS dataset.

To verify the preservation of edges, a homogenous area of a class has been selected such that it should have high mean and low variance. After the identification of homogenous class, two set of pixels have been selected, where each set lie on either side of the edge. Table 6.24 shows that the difference of mean between two pixels is high and variance within each pixel set is low. This phenomenon describes the low variability within the classified fraction imagery. The error usually occurs around the edges and by preserving the edges it increases the classification accuracy (Tso and Oslen, 2005). However, inclusion of entropy and contextual information with FCM reduces the uncertainty in classification but it is not able to remove the problem of class overlapping.

Table 6.24: Verification of edge preservation for FCMWE-S classifier of AWiFS image for optimized value of λ=0.4 and β=2.0.

Class	Difference in mean	Variance
Barren Land	242	8, 0.5
Water Body	224.5	264.5, 2

To perform FCMWE-S classification, the optimized value of Regularizing parameter ν $=10^2$has been taken and λ and β are varying between 0.1 to 1.0 and 0.5 to 6.0 respectively. Table 6.26 shows that Overall accuracy, FERM, SCM, MIN-MIN and MIN-LEAST are varying between 86% to 98% when, AWiFS dataset is used for classification image and LISS-III or LISS-IV dataset is used as a reference. In the process of identifying the optimized value of λ and β, all accuracy indices (FERM, SCM, MIN-MIN and MIN-LEAST) has been analyzed for all six classes selected for the study and it is found that for λ=0.4 and β=2.0, all the accuracy measures are higher and have lesser uncertainty (Fig. 6.52).

Table 6.25: Accuracy values for optimized value of λ=0.4 and β=2.0 for FCMWE-S classifier of AWiFS data using LISS-IV as reference data.

Land-Use Classes	**Accuracy assessment methods**				
	FERM	**SCM**	**MIN-PROD**	**MIN-MIN**	**MIN-LEAST**
Fuzzy user's accuracy (%)					
Agriculture	61.68	84.27±3.16	84.36	71.10	97.44
Sal forest	56.34	85.55±3.39	85.21	72.16	98.94
Eucalyptus plantation	67.60	92.04±2.30	92.30	85.73	98.35
Barren Land	77.25	91.09±3.05	91.03	86.03	96.15
Water Body	95.26	97.61±2.02	98.02	95.58	99.64
Fuzzy producer's accuracy (%)					
Agriculture	78.96	88.09±4.40	87.65	78.68	97.49
Sal forest	91.89	94.33±2.87	94.62	91.46	97.21
Eucalyptus plantation	79.15	85.98±1.20	85.39	74.77	97.19
Barren Land	86.31	90.81±8.66	91.48	82.14	99.48
Water Body	91.81	94.10±4.97	95.36	89.13	99.07
Fuzzy overall accuracy (%)	85.29	90.31±3.81	90.65	82.50	98.12
Fuzzy Kappa		0.87	0.88	0.78	0.97

Tables 6.25 shows the accuracy indices for optimized value of smoothness parameter (λ) and weight for neighbors (β) of AWiFS (classified) with LISS-IV as (referenced) combination.

One important aspect as observed from Tables 6.2, 6.10, 6.13 and 6.25 is that FCMWE-S classification performs better than ordinary FCM, FCMWE and FCM-S classification, with 2% improvement in SCM accuracy and uncertainty confusion ratio decreased by 5%.

Fig. 6.53 shows the fraction images of AWiFS datasets for FCMWE-S classification. After examining the fraction images generated by FCMWE-S classifier, it is found that the value of λ and β changes across the spatial resolution of image. The inclusion of contextual information in FCMWE resolves the inter-grade homogeneity problem, while FCM, FCMWE and FCM-S are unable to distinguish between homogenous classes. It is also found that by incorporating contextual information and entropy together in FCMWE classifier, the output is spectrally and spatially consistent but due to entropy factor class overlapping of classes has not been resolved effectively (Fig. 6.53).

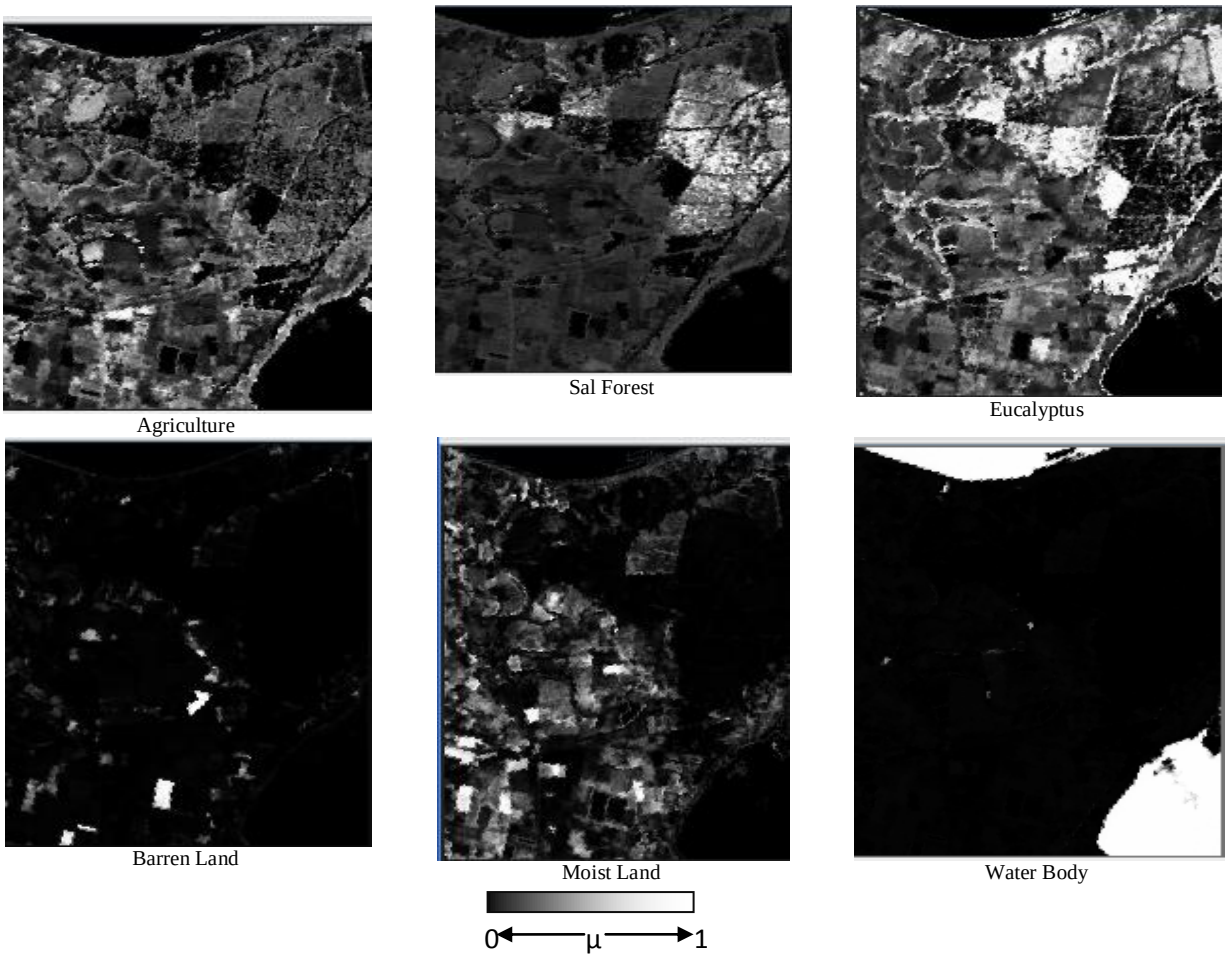

Fig. 6.53: FCMWE-S classification output of AWiFS image

6.10.2 RESULTS OF FCMWE WITH DISCONTINUITY ADAPTIVE PRIOR

The basic objective of this study is to develop FCMWE based hybridized sub-pixel classifier for classifying moderate and coarser spatial resolution multi-spectral data set using FCMWE-MRF model. In ordinary FCMWE based classifier, no spatial context of an image was incorporated, so to incorporate the spatial contextual information with FCMWE, smoothness prior and four DA-MRF, as described in Section 3.4.14, has been developed. The FCMWE with contextual classifier incorporates spatial context using DA model and performs sub-pixel classification in supervised mode. Another aspect of this method is to verify the preservation of edge at boundary points and investigate the joint effect of entropy and contextual in FCM classifier.

The objective function of FCMWE with Discontinuity Adaptive Prior is defined by Eqs 3.66-3.69 and has been designated as FDEM-(H1), FDEM - (H2), FDEM - (H3), FDEM - (H4) classifier. As mentioned in Section 3.4.14, the smoothness parameter (λ) controls the balance between spectral and spatial information. Another parameter which is added with the objective function of FCMWE with Discontinuity Adaptive (DA) prior classifier is the Adaptive Potential Function (AIF) or Interaction Range Parameter (γ). This determines the rate of decay at that point where AIF reaches to zero and also controls the interaction between two pixels (Moser and Serpico, 2010). The basic objective of this study is to optimize these parameters λ and γ to get better classification. Another aspect of this study, is to identify the optimize DA-model, which yield best classification and also preserves the edges.

The performance of this classifier is dependent on the constant value of Regularizing parameter (ν) and smoothness parameter (λ) along with interaction range parameter (γ) (Eq. 3.66-3.69). The optimized constant value of Regularizing parameter (ν) and varying value of (λ) and (γ) has been tested. Both parameters are mutually dependent to perform classification using FDEM-(H1), FDEM-(H2), FDEM-(H3), and FDEM-(H4) classifiers. To perform the classification, fixed value of $\nu=10^2$has been used while varying the values of λ and γ between 0.1 to 1.0 at an interval of 0.1.

Fig. 6.54 (a), (b), (c) and (d) shows the variation of the class membership for varying value of λ and γ for different classes such as agriculture, sal forest, eucalyptus plantation, barren land, moist land and water body of AWIFS dataset of FDEM -(H1), FDEM -(H2), FDEM -(H3), and FDEM -(H4) classifier. For all three datasets, class membership has been generated for the different values of λ and γ. It has been observed from the Fig. 6.54 (a), (b), (c) and (d), that the optimized value of λ and γ is 0.7. The optimized value of λ and γ is finalized on the basis of membership values, for all classes and lying between **0.90** to **0.996** for FDEM-(H1), FDEM-(H2), FDEM -(H3), FDEM -(H4) classifier. The membership trends indicates that for λ=0.7 and γ=0.7 all classes produces highest membership values and thereafter either it starts to decrease or it reaches up to the level of saturation.

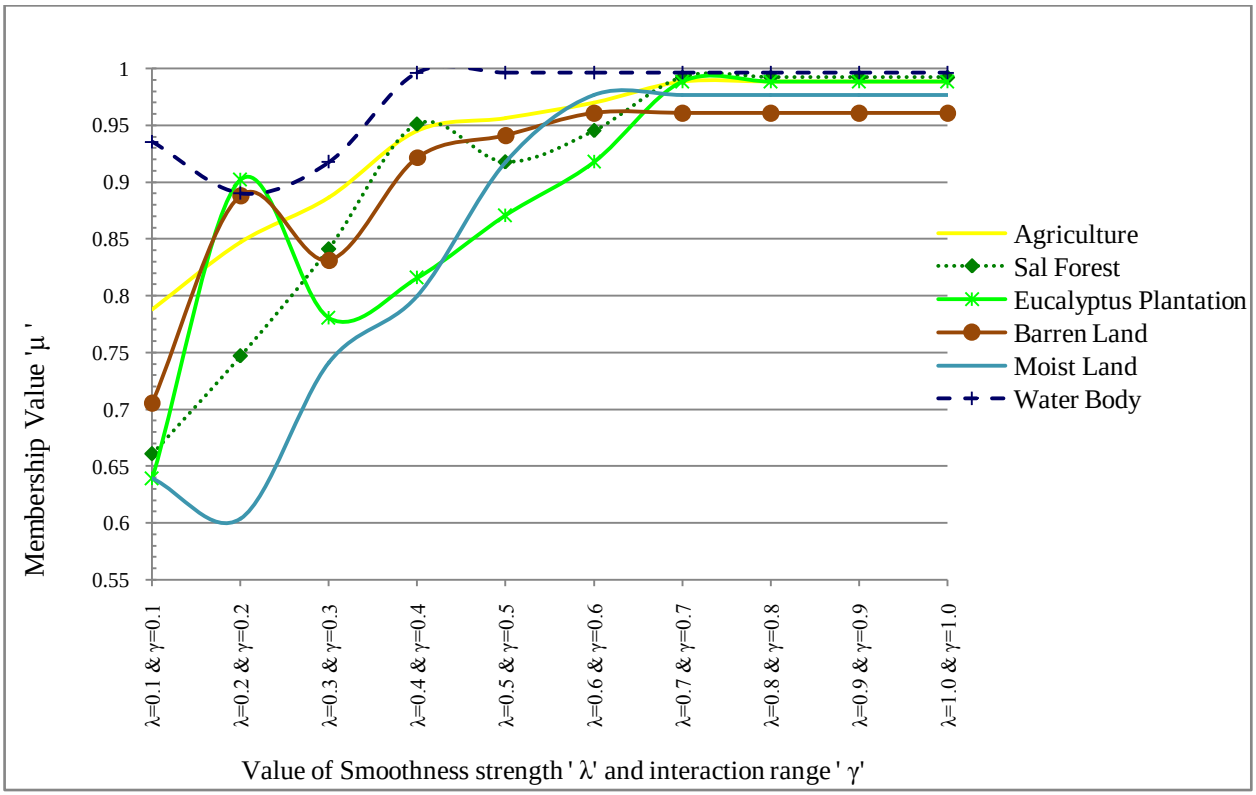

Fig. 6.54(a): Class membership for FDEM-(H1) classifier using AWiFS dataset.

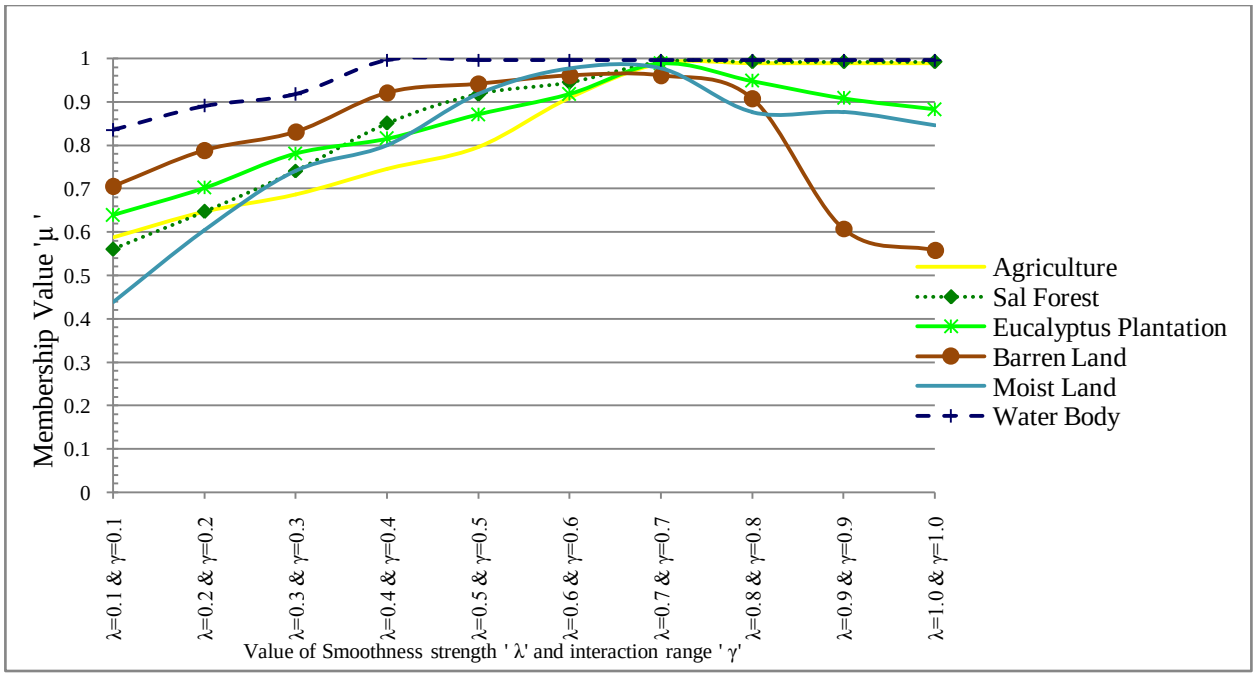

Fig. 6.54(b): Class membership for FDEM-(H2) classifier using AWiFS dataset.

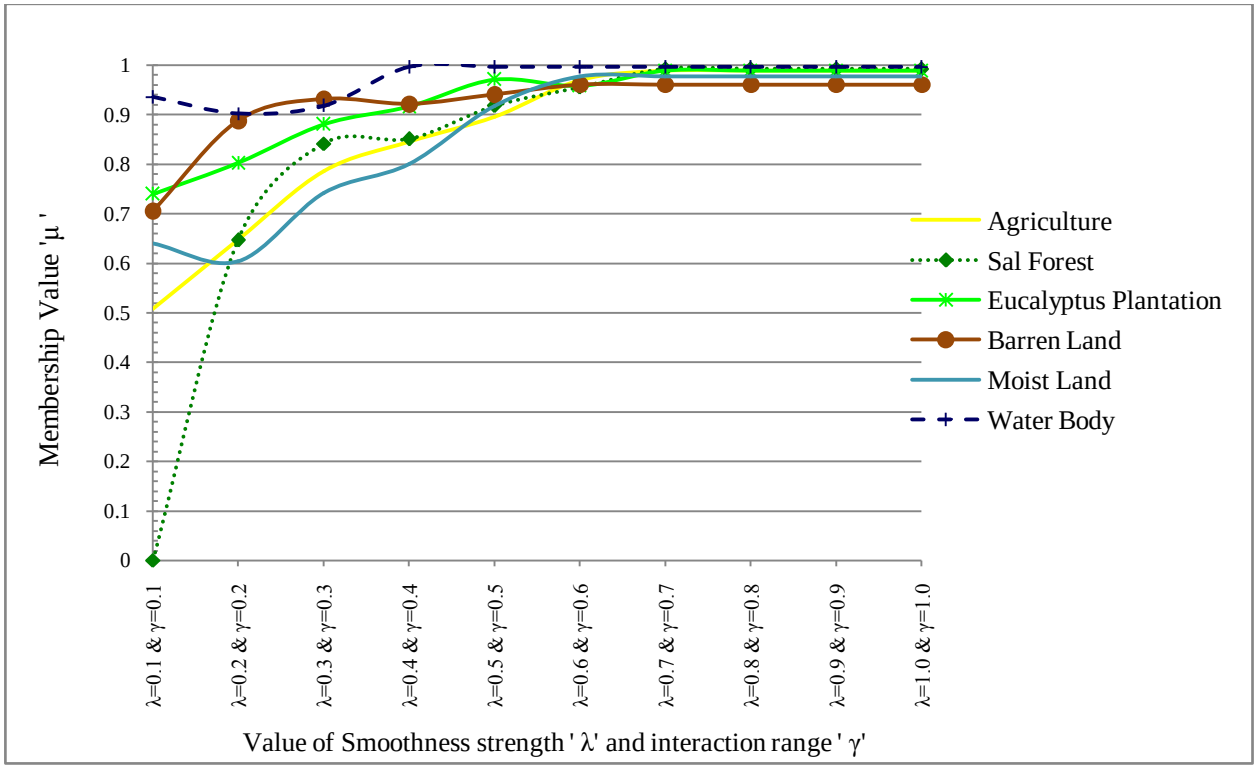

Fig. 6.54(c): Class membership for FDEM-(H3) classifier using AWiFS dataset.

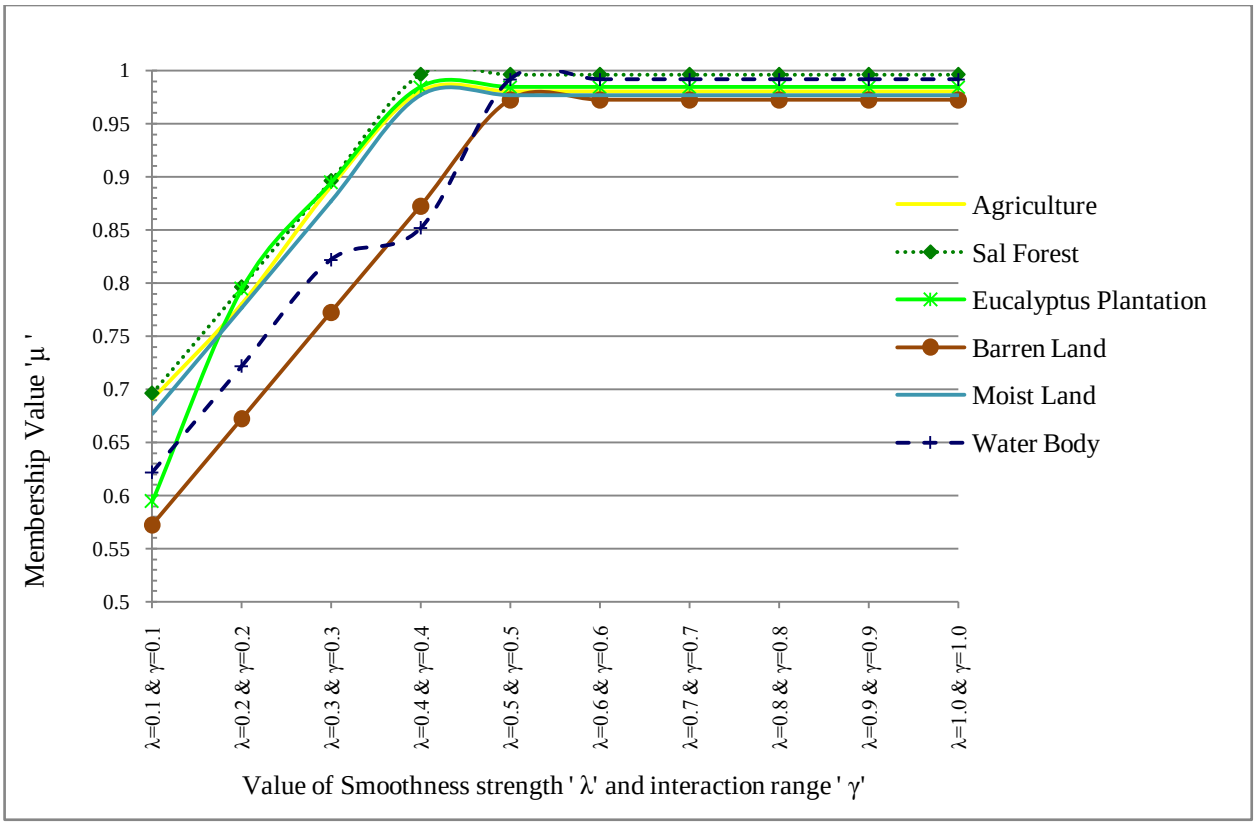

Fig. 6.54(d): Class membership for FDEM-(H4) classifier using AWiFS dataset.

Table 6.26 shows the accuracy values for the optimized value of λ =0.7 and γ=0.7, where AWiFS image has been used as a classified image and LISS-III or LISS-IV image has been used a reference image. The accuracy values are presented for all four DA models. From Table 6.26, it has been observed that FDEM-(H1) model produces higher accuracy in all cases. All approaches of assessment accuracy shows that FDEM-(H1) model produces higher values for FERM, SCM and MIN-LEAST operator. The entropy values have also been computed for optimized λ and γ for all four DA models and it is found to be 0.45, 0.85, 0.94, and 2.34 for FDEM-(H1, H2, H3, and H4) models respectively. This also indicates that FDEM-(H1) has lower entropy (**0.45**) when compared to other models. The basic advantage of hybridization DA model with FCMWE classifier is that classes are well classified and edges were not over smoothened (Fig. 6.55).

The classification performance of FDEM-(H1) has been compared with FCM, FCMWE FCM-S, FDM-(H3) and FCMWE-S and it has been found that the inclusion of contextual

information and entropy together does not improving the performance of classification (Tables 6.2, 6.10, 6.13, 6.14, 6.25). Although FDEM-(H1) is able to classify all six land cover classes precisely using λ =0.7and γ=0.7. However, in view of classification performance FDM-(H3) model performs better than FDEM-(H1) model. This indicates that inclusion of entropy along with contextual information is not able to remove uncertainty completely; instead it increases the problem of class overlapping. From Table 6.26, all accuracy measures are not higher when compared with other hybrid classifiers using FCM, thus edge preservation has not been checked for FDEM-(H1) classifier.

Fig. 6.55 shows the classified fraction image for optimized values of λ and γ of AWiFS dataset using FDEM-(H1) classifier. This classifier performs best in comparison to other DA models. It is observed that last three DA-MRF models with FCMWE (Eq 3.67-3.69) behave similarly to FCM-S and FCMWE-S. However, in case of FDEM-(H1) model, the bandwidth or scale parameter does not follow this criterion (η^2«1) (Li, 1990). As observed from Fig. 6.55, FDEM-(H1) model controls the over smoothing for all categories of classes effectively however, due to entropy factor, it hardens the output and is not able to resolve inter-grade class phenomena precisely. On the basis of highest class membership, the class wise optimized value of λ and γ has also been identified and it is found to same as that of generalized optimized value i.e. λ= 0.7 and γ=0.7 for all classes.

Table 6.26: Comparative accuracy values for optimized value of λ=0.7 and γ=0.7 for FDEM (H1, H2, H3, H4) classifier of AWiFS data using LISS-III and LISS-IV as reference data.

Images → / Indices ↓	AWiFS-LISS-III				AWiFS-LISS-IV			
FDEM-Classifier	H-1	H-2	H-3	H-4	H-1	H-2	H-3	H-4
FERM(%)	**87.85**	85.88	85.51	85.56	**91.88**	84.26	82.27	79.84
SCM(%)	**82.29**	81.30	81.00	77.95	**85.92**	83.65	79.18	79.79
MIN-LEAST(%)	**82.89**	76.86	81.26	83.29	**82.10**	79.48	78.26	78.05

Fig. 6.55 shows the classified fraction images of AWiFS dataset for the optimized value of λ and γ. To incorporate spatial contextual information with FCMWE, smoothness prior and four DA-MRF models have been tested. From Tables 6.26, it has been observed that DA models are not able to increase overall accuracy when compared to FCMWE-S. In FCM, FCMWE, FCM-S, FDM-(H3) and FCMWE-S classifier (Eqs 3.1, 3.23, 3.45, 3.48 and Eq 3.65), the interactions among pixels are constant everywhere in the classified imagery. This leads to over smoothing at edges when classification using these classifier is carried out. However, in FDEM-(H1) classifier, the smoothing strength λ is proportional to η (Eq 3.66-3.69). Thus, adding contextual information using DA-MRF models reduces the problem of over smoothing at edges but is not able to preserve the edges at boundary points (Figs. 6.55) and also does not produce more accurate results. Although, it is a fact that hybridization of contextual with FDEM reduces some level of uncertainty because, the computed entropy values for optimized λ =0.7 and γ =0.7 for all four DA models are at minimal level and is found to 0.45, 0.85, 0.94, and 2.34 for FDEM-(H1, H2, H3, and H4) models respectively. Thus, inclusion of contextual information in FCMWE classifier is not able to utilize efficiently the spatial information of an image.

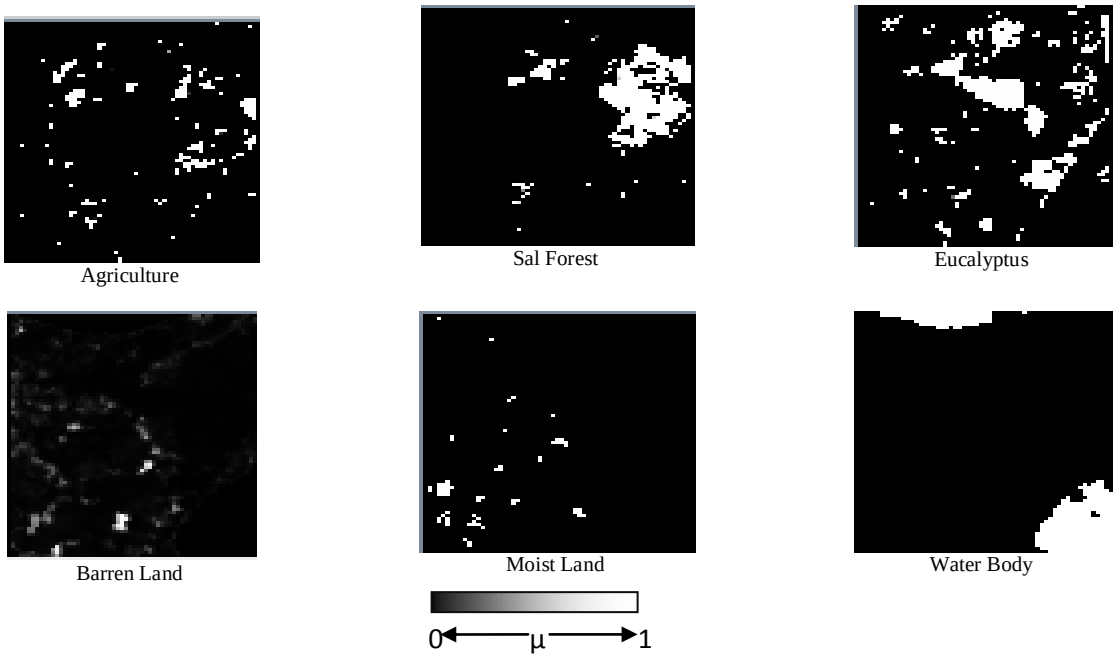

Fig. 6.55: FDEM-(H1) classification output of AWiFS image

6.11 RESULTS OF NCWE WITH CONTEXTUAL CLASSIFIER

The idea of using Noise Clustering with Entropy (NCWE), a hybrid approach of soft classification i.e. NCWE with contextual information is a new approach which helps significantly to reduce noise pixels while incorporating spatial contextual information. The hybrid classification approach of NCWE with contextual information has been performed in two categories i.e. NCWE with Smoothness prior (NCWE-S) and four categories of NCWE with Discontinuity Adaptive (DA) prior i.e. (NDEM-H1, NDEM -H2, NDEM -H3, NDEM -H4). The following sections, describes the results of the NCWE with contextual classifiers. It is believed that inclusion of entropy and contextual information in NC classifier is ably separate the noise pixels and reduces the uncertainty while classifying various land cover classes.

6.11.1 RESULTS OF NCWE WITH SMOOTHNESS PRIOR

To incorporate spatial contextual information, spectral information along with entropy as a regularizer, a hybridized model has been devised to resolve the problem of mixed pixel. The contextual information has been added in NCWE classifier to generate smoothness effect and it is defined as NCWE-S (Eq 3.60). Two basic variables are associated with the defined objective function are smoothness parameter (λ) and weight for neighbours (β). The smoothness parameter controls the balance between spectral and spatial information, while β analyzes the weight to be given to a neighbouring pixel in a window. The basic objective of this study is to optimize these parameters to get better classification output with minimum uncertainty.

The performance of this classifier is dependent on the constant value of Regularizing parameter (ν) and smoothness parameter (λ) along with weight for neighbours parameter β(Eq. 3.60). The optimized constant value of Regularizing parameter (ν) and varying value of smoothness parameter (λ) along with weight for neighbours parameter (β) has been tested. To perform the NCWE-S classification, a fixed value of $\nu = 10^2$ has been used for all varying values of λ ranges from 0.1 to 1.0 at an interval of 0.1, while β ranges from 0.5 to 5.0 at an interval of 0.5.

Fig. 6.56 shows the variation of smoothness parameter (λ) and weight for neighbours parameter (β) with class membership for different classes such as agriculture, sal forest, eucalyptus plantation, barren land, moist land and water body for AWIFS, datasets. The class membership values of a pixel denote the class proportion, which in turn indicates the soft classified output for a pixel. It has been observed from Fig. 6.56, that for λ=0.6 and β =3.0, all six classes such as agriculture, sal forest, eucalyptus plantation, barren land, moist land and water body produce the highest membership. For the above mentioned values of λ and β, the class membership lies between 0.95 to 0.99 for all six classes selected for this study. It has been further verified via entropy and observed that the value of optimized parameter does not deviate (Fig. 6.56).

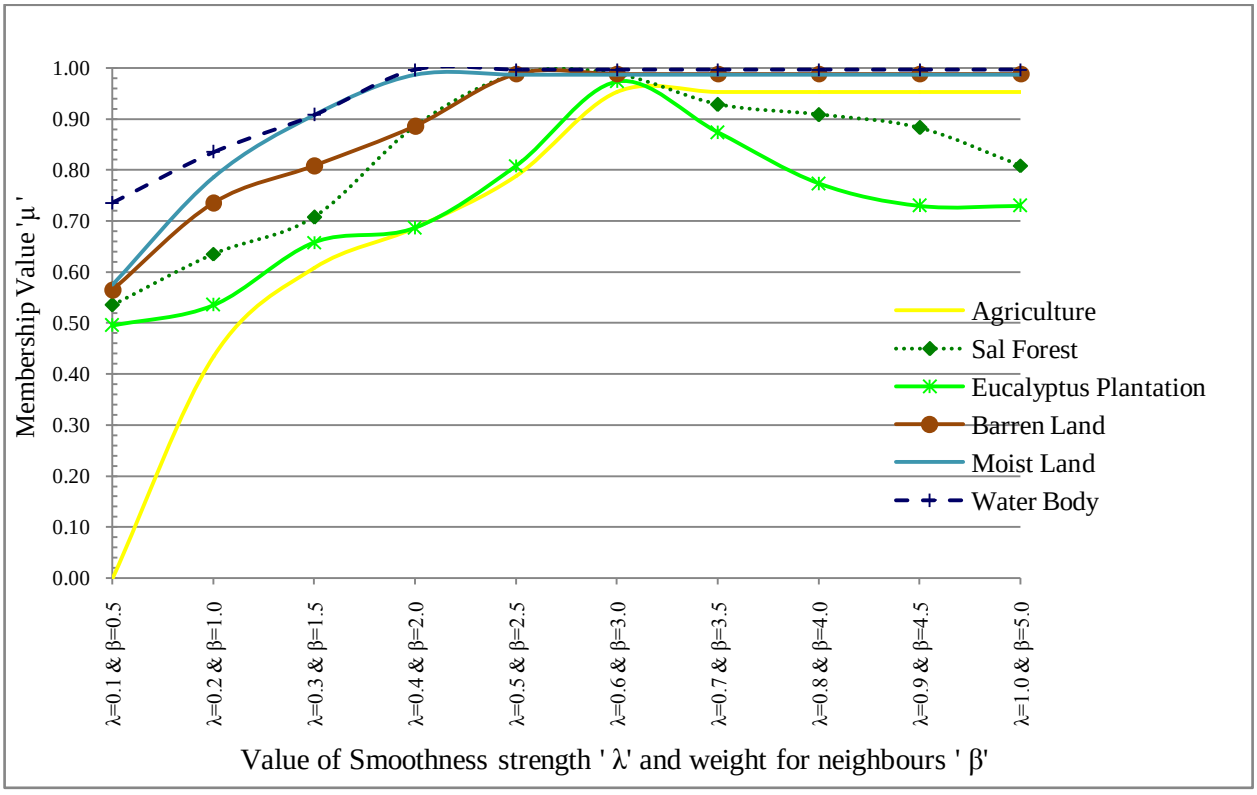

Fig. 6.56: Class membership for NCWE-S classifier using AWiFS dataset.

Fig. 6.57 shows the computed entropy for AWiFS fraction images of NCWE-S classifier for agriculture, sal forest, eucalyptus plantation, barren land, moist land, and water body land

cover classes. The entropy values are lying between the specified range of [0.005, 2.45]. If the entropy value of classified fraction imagery is less; it indicates better classification with minimum uncertainty. It has been observed from Fig. 6.57, that at λ= 0.6 and β=3.0 for AWiFS dataset, the entropy values for all six classes are lowest. For these optimized values of λ and β the membership is high i.e. up to 99% and the computed entropy is less than 0.05. This trend indicates that the uncertainty in classified results is lowest at optimized point for smoothness parameter (λ) and weight for neighbours parameter (β). This mathematical model of entropy computation is used as an absolute indicator of measuring uncertainty without using any ground reference data.

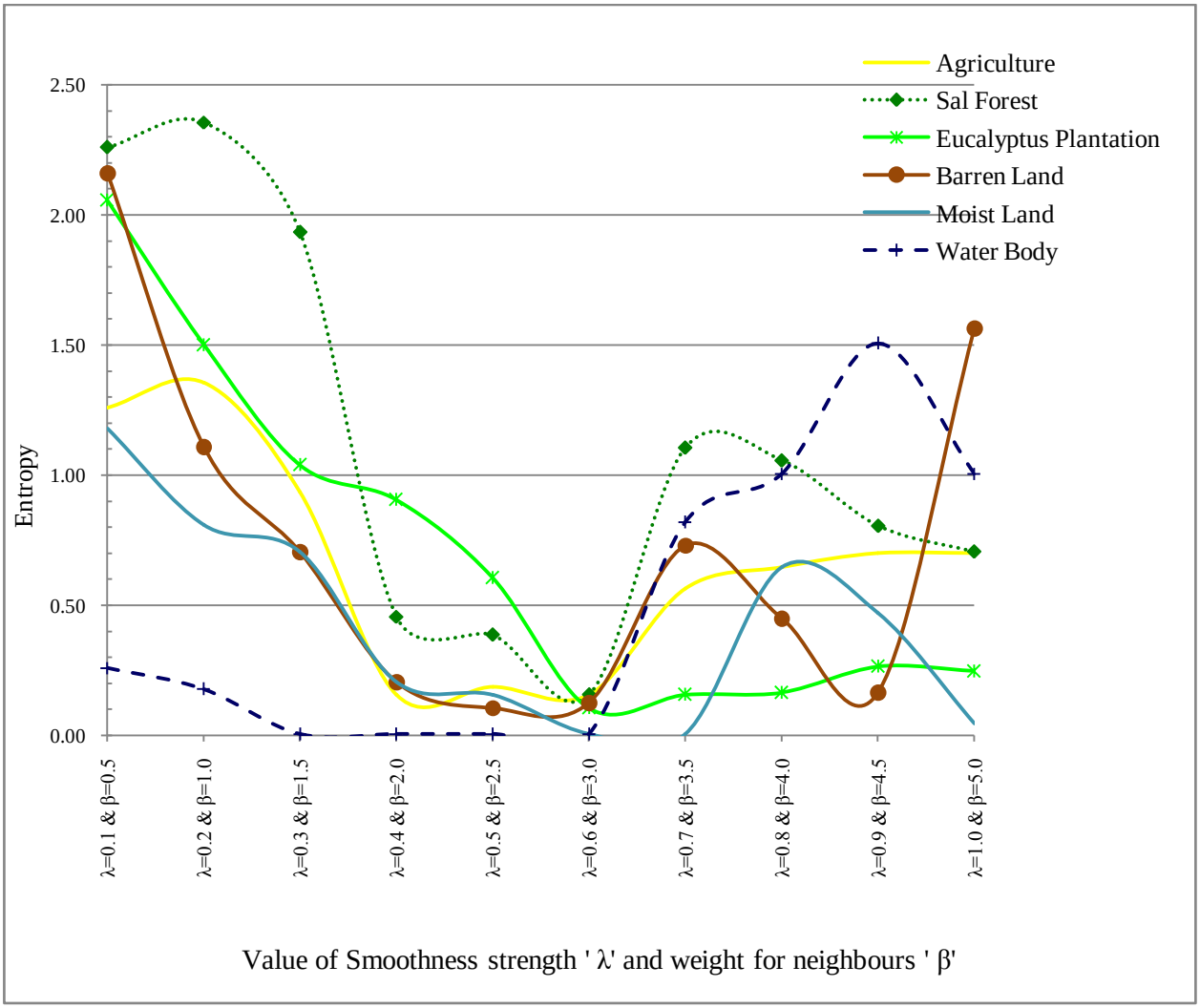

Fig. 6.57: Entropy for NCWE-S classifier using AWiFS dataset.

To verify the preservation of edges, a homogenous area of a class has been selected such that it should have high mean and low variance. After the identification of homogenous class, two set of pixels have been selected, where each set lie on either side of the edge. Table 6.27 shows that the difference of the mean between two pixels is high and variance within each pixel set is low. This phenomenon describes the low variability within the classified fraction imagery. The error usually occurs around the edges and by preserving the edges it increases the classification accuracy (Tso and Oslen, 2005). However, the inclusion of entropy and contextual information with NC reduces the uncertainty in classification and ably removes the noise pixel from classified imagery. Further, this also removes the class overlapping problem as previously it exists with FCMWE-S in Section 6.10.1.

Table 6.27: Verification of edge preservation for NCWE-S classifier of AWiFS image for optimized value of λ=0.6 and β=3.0.

Class	Difference in mean	Variance
Barren Land	229.5	4.5, 2.0
Water Body	239.5	8 ,4.5

To perform NCWE-S classification, the optimized value of Regularizing parameter $\nu = 10^2$has been taken and λ and β are varying between 0.1 to 1.0 and 0.5 to 6.0 respectively. Table 6.28 shows that Overall accuracy, FERM, SCM, MIN-MIN and MIN-LEAST are varying between 83% to 95% when, AWiFS dataset is used for classification image and LISS-III or LISS-IV dataset is used as a reference. In the process of identifying the optimized value of λ and β, all accuracy indices (FERM, SCM, MIN-MIN and MIN-LEAST) has been analyzed for all six classes selected for the study and it is found that for λ=0.6 and β=3.0, all the accuracy measures are higher and have least uncertainty (Fig. 6.57).

Tables 6.28 shows the accuracy indices for optimized value of smoothness parameter (λ) and weight for neighbours (β) of AWiFS (classified)-LISS-IV (referenced) combination. One important aspect as observed from Tables 6.6, 6.8, 6.20 and 6.28 is that NCWE-S classification does not performs better than ordinary NC, NCWE and NC-S classification. However, uncertainty confusion ratio decreased marginally by 0.39% when compared to NC-S classifier.

Table 6.28: Accuracy values for optimized value of λ=0.6 and β=3.0 for NCWE-S classifier of AWiFS data using LISS-IV as reference data.

Land-Use Classes	**Accuracy assessment methods**				
	FERM	**SCM**	**MIN-PROD**	**MIN-MIN**	**MIN-LEAST**
Fuzzy user's accuracy (%)					
Agriculture	73.01	82.91±9.01	82.14	73.90	91.92
Sal forest	81.96	88.88±8.23	88.36	80.65	97.12
Eucalyptus plantation	89.86	94.34±2.84	94.31	91.49	97.19
Barren Land	77.60	85.85±12.92	84.77	72.92	98.77
Moist Land	73.05	82.06±10.32	80.58	71.73	92.38
Water Body	94.09	96.61±1.81	96.68	94.80	98.42
Fuzzy producer's accuracy (%)					
Agriculture	90.13	93.65±3.53	93.92	90.12	97.18
Sal forest	86.74	90.28±4.33	90.21	85.95	94.62
Eucalyptus plantation	75.54	83.72±9.54	81.33	74.17	93.26
Barren Land	73.18	81.79±11.55	82.29	70.23	93.34
Moist Land	88.96	92.82±6.07	93.52	86.75	98.90
Water Body	91.34	93.81±5.44	95.77	88.36	99.26
Fuzzy overall accuracy (%)	83.90	89.13±6.63	88.77	82.50	95.77
Fuzzy Kappa		0.86±0.08	0.85	0.77	0.94

Fig. 6.58 shows the fraction images of AWiFS datasets for NCWE-S classification. After examining the fraction images generated by NCWE-S classifier, it is found that the value of λ and β changes across the spatial resolution of image. The inclusion of contextual information in NCWE resolves the inter-grade homogeneity problem and removes the noise from classified imagery, while NC, NCWE and NC-S are unable to distinguish between homogenous classes precisely. It is also found that by incorporating contextual information and entropy together in NCWE classifier, the output is spectrally and spatially consistent but due to entropy factor class overlapping of classes has not been resolved effectively (Fig. 6.58).

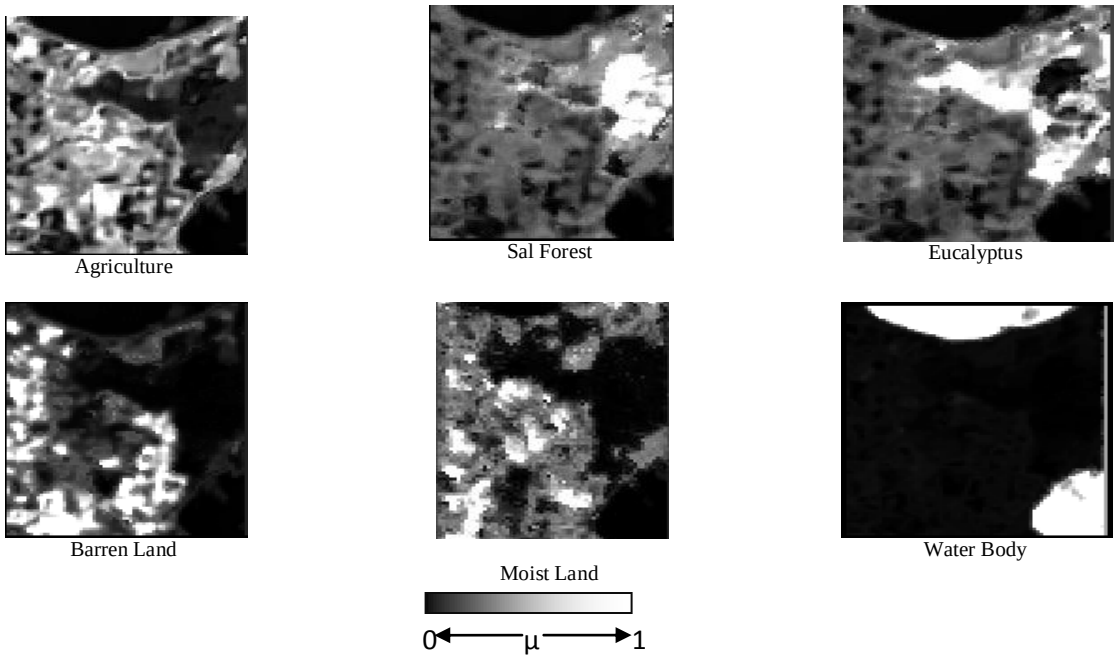

Fig. 6.58: NCWE-S classification output of AWiFS image

6.11.2 RESULTS OF NCWE WITH DISCONTINUITY ADAPTIVE PRIOR

The basic objective of this study is to develop NCWE based hybridized sub-pixel classifier for classifying moderate and coarser spatial resolution multi-spectral data set using NCWE-MRF model. In ordinary NCWE based classifier, no spatial context of an image was incorporated, thus to incorporate the spatial contextual information with NCWE, smoothness prior and four DA-MRF described in Section 3.4.13 has been developed. The NCWE with contextual classifier incorporates spatial context using DA model and performs sub-pixel classification in supervised mode. Another aspect of this method is to verify the preservation of edge at boundary points and investigate the joint effect of entropy and contextual in NC classifier.

The objective function of NCWE with Discontinuity Adaptive Prior is defined by Eqs 3.61-3.64 and has been designated as NDEM-(H1), NDEM - (H2), NDEM - (H3), NDEM - (H4) classifier. As mentioned in Section 3.4.13, the smoothness parameter (λ) controls the balance between spectral and spatial information. Another parameter which is added with the objective function of NCWE with Discontinuity Adaptive (DA) prior classifier is the Adaptive Potential

Function (AIF) or Interaction Range Parameter (γ). This determines the rate of decay at that point where AIF reaches to zero and also controls the interaction between two pixels (Moser and Serpico, 2010). The basic objective of this study is to optimize these parameters λ and γ to get better classification. Another aspect of this study, is to identify the optimize DA-model, which yield best classification and also preserves the edges.

The performance of this classifier is dependent on the constant value of Regularizing parameter (ν) and smoothness parameter (λ) along with interaction range parameter (γ) (Eq. 3.61-3.64). The optimized constant value of Regularizing parameter (ν) and varying value of (λ) and (γ) has been tested. Both parameters are mutually dependent to perform the classification using NDEM-(H1), NDEM-(H2), NDEM-(H3), and NDEM-(H4) classifiers. To perform the classification, fixed value of $\nu=10^2$has been used while varying the values of λ and γ between 0.1 to 1.0 at an interval of 0.1.

Fig. 6.59 (a), (b), (c) and (d) shows the variation of the class membership for varying value of λ and γ for different classes such as agriculture, sal forest, eucalyptus plantation, barren land, moist land and water body of AWIFS dataset of NDEM -(H1), NDEM -(H2), NDEM -(H3), and NDEM -(H4) classifier. For all three datasets, class membership has been generated for different values of λ and γ. It has been observed from Fig. 6.59 (a), (b), (c) and (d), that the optimized value of λ and γ is 0.5. The optimized value of λ and γ is finalized on the basis of membership values, for all classes and lying between **0.92** to **0.996** for NDEM-(H1), NDEM-(H2), NDEM - (H3), NDEM - (H4) classifier. The membership trends indicates that for λ=0.5 and γ=0.5 all classes produces highest membership values and thereafter either it starts to decrease or it reaches up to the level of saturation. The basic difference between NC with entropy with contextual and FCM with entropy with contextual is that NC with entropy with contextual classifier starts producing very high membership for early values of λ and γ (Fig. 6.59).

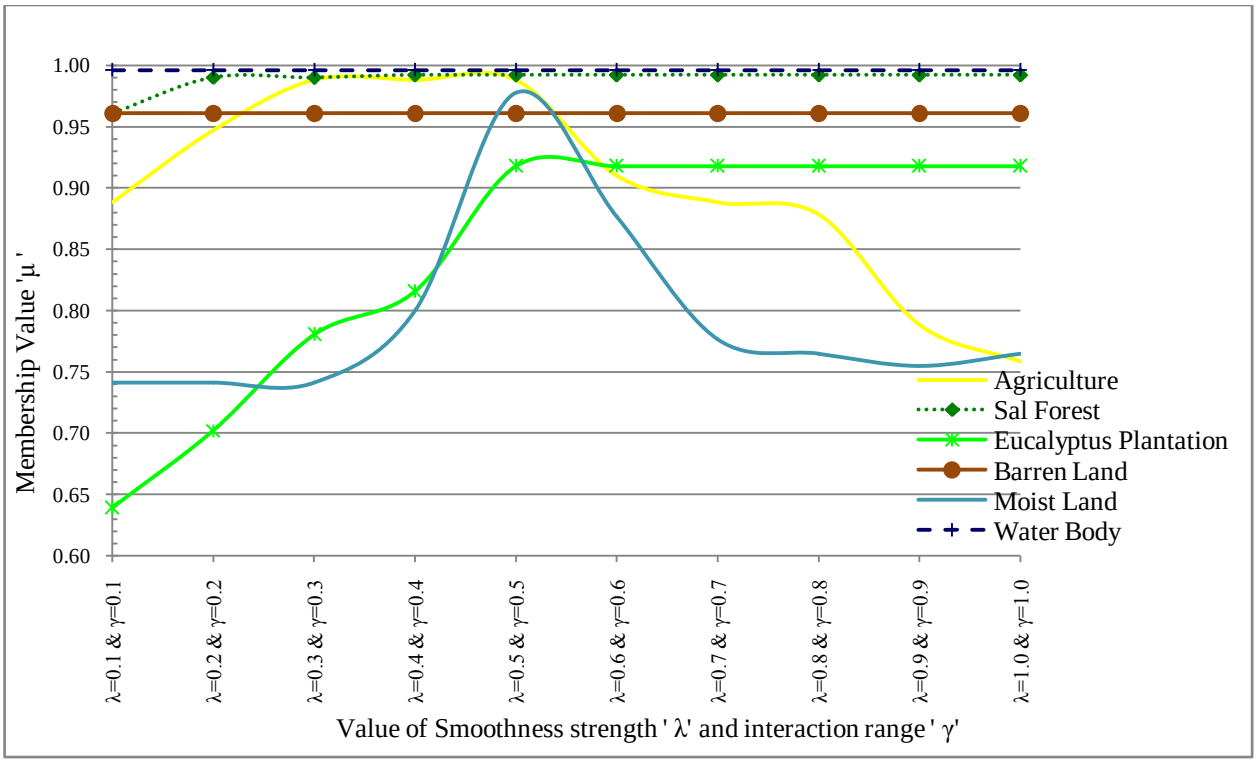

Fig. 6.59(a): Class membership for NDEM-(H1) classifier using AWiFS dataset.

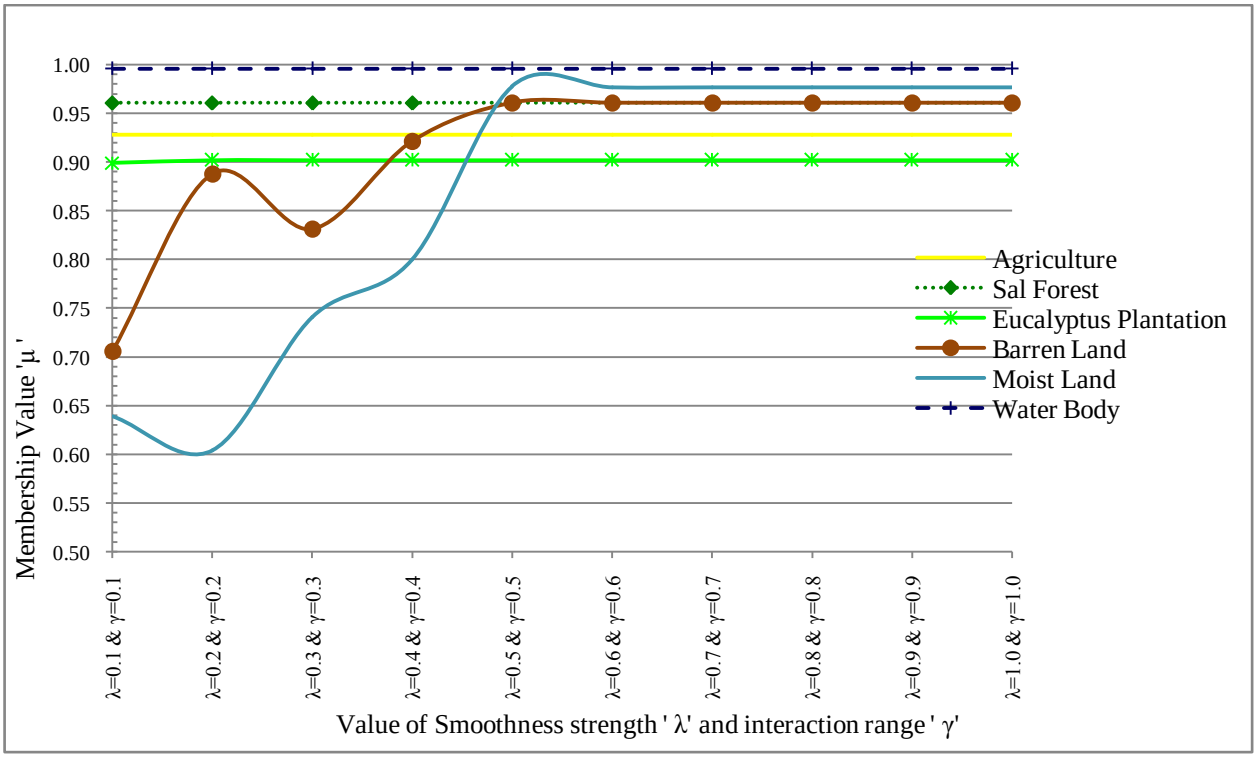

Fig. 6.59(b): Class membership for NDEM-(H2) classifier using AWiFS dataset.

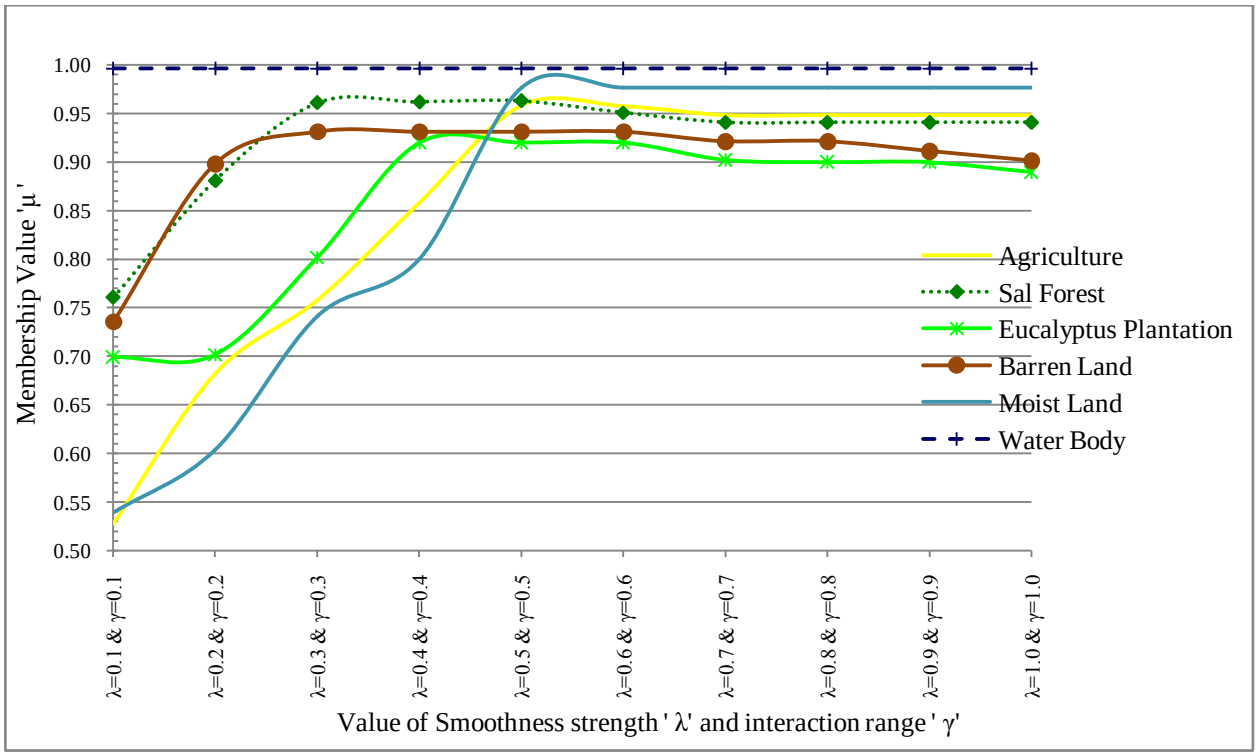

Fig. 6.59(c): Class membership for NDEM-(H3) classifier using AWiFS dataset.

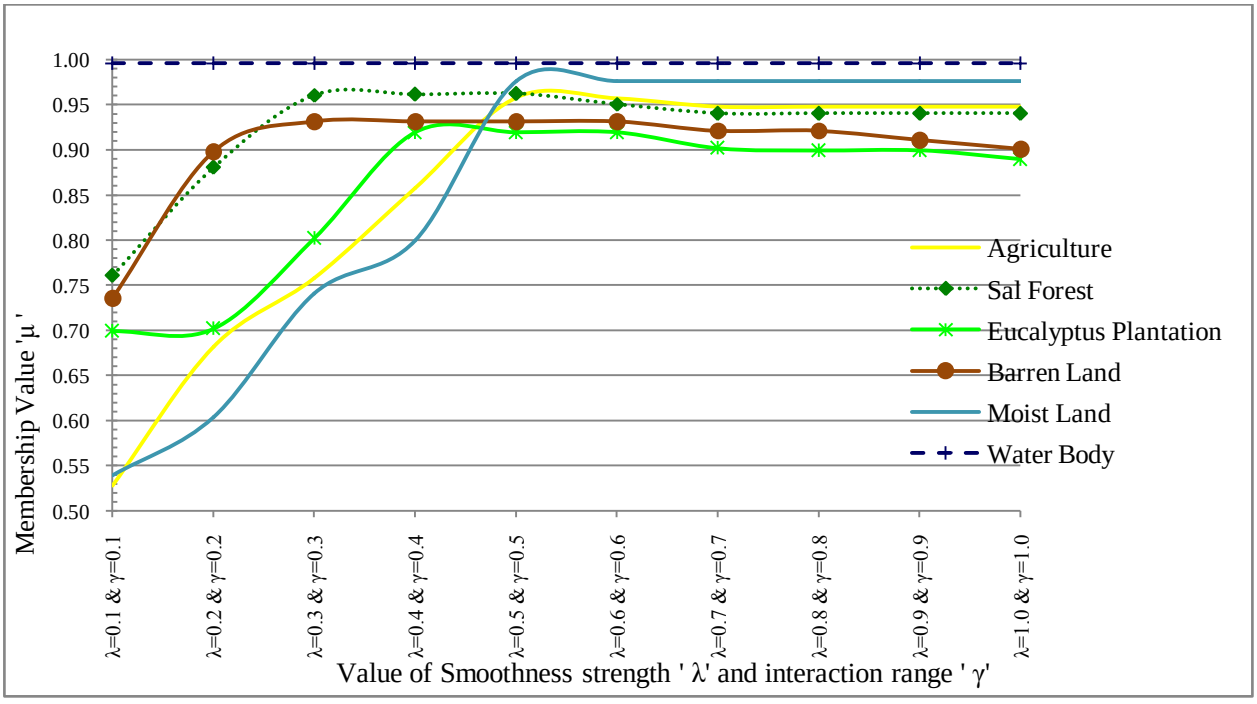

Fig. 6.59(d): Class membership for NDEM-(H4) classifier using AWiFS dataset.

Table 6.29 shows the accuracy values for the optimized value of λ =0.5 and γ=0.5, where AWiFS image has been used as a classified image and LISS-III or LISS-IV image has been used a reference image. The accuracy values are presented for all four DA models. From Table 6.29, it has been observed that NDEM-(H2) model produces higher accuracy in all cases. All approaches of assessment accuracy shows that NDEM-(H2) model produces higher values for FERM, SCM and MIN-LEAST operator. The entropy values have also been computed for optimized λ and γ for all four DA models and it is found to be 0.32, 0.01, 0.43, and 0.74 for NDEM-(H1, H2, H3, and H4) models respectively. This also indicates that NDEM-(H2) has lower entropy (**0.01**) when compared to other models. The basic advantage of hybridization DA model with NCWE classifier is that classes are well classified and edges were not over smoothened (Fig. 6.60).

The classification performance of NDEM-(H2) has been compared with NC, NCWE NC-S, NDM-(H4) and NCWE-S and it has been found that it inclusion of contextual information and entropy together is not improving the classification performance (Tables 6.6, 6.8, 6.20, 6.22, and 6.29). Although NDEM-(H2) is able to classify all six land cover classes precisely using λ =0.5 and γ=0.5. However, in view of classification performance NDM-(H4) model performs better than NDEM-(H2) model. This indicates that inclusion of entropy along with contextual information is not able to remove uncertainty completely; instead it increases the problem of class overlapping. From Table 6.29, it is observed that all the accuracy measures are not higher when compared with other hybrid classifiers using NC.

Table 6.29: Comparative accuracy values for optimized value of λ=0.5 and γ=0.5 for NDEM (H1, H2, H3, H4) classifier of AWiFS data using LISS-III and LISS-IV as a reference data.

Images → / Indices ↓	AWiFS-LISS-III				AWiFS-LISS-IV			
NDEM-Classifier	H-1	H-2	H-3	H-4	H-1	H-2	H-3	H-4
FERM(%)	82.94	**86.74**	85.51	86.40	76.79	**86.69**	88.63	89.74
SCM(%)	88.62	**90.45**	89.40	83.95	81.32	**81.85**	89.43	79.46
MIN-LEAST(%)	91.69	**93.30**	93.26	93.26	91.10	**92.38**	88.36	88.15

To verify the preservation of edges, a homogenous area of a class has been selected such that it should have high mean and low variance. After the identification of homogenous class, two set of pixels have been selected, where each set lie on either side of the edge. Table 6.30 shows that the difference of the mean between two pixels is high and variance within each pixel set is low. This phenomenon describes the low variability within the classified fraction imagery. The error usually occurs around the edges and by preserving the edges it increases the classification accuracy (Tso and Oslen, 2005). However, the inclusion of entropy and contextual information with NC reduces the uncertainty in classification and ably removes the noise pixel from classified imagery. Further, this also removes the class overlapping problem as previously it exists with NCWE-S in Section 6.11.1. From Table 6.27 and Table 6.30 it has been observed that NDEM-(H2) classifier has high mean difference when compared with NCWE-S classifier. This indicates that NDEM-(H2) preserves the edges at boundary points and removes the problem of over smoothening.

Table 6.30: Verification of edge preservation for NDEM-(H2) classifier of AWiFS image for optimized value of λ=0.5 and γ=0.5.

Class	Difference in mean	Variance
Barren Land	247.5	8.0,4.5
Water Body	239	0.7,0.5

Fig. 6.60 shows the classified fraction image for optimized values of λ and γ of AWiFS dataset using NDEM-(H2) classifier. This classifier performs best in comparison to other DA models. It is observed that other DA-MRF models with NCWE behave similar to NC-S and NCWE-S. However, in case of NDEM-(H2) model, the bandwidth or scale parameter does not follow this criterion (η^2«1) (Li, 1990). As observed from Fig. 6.60, NDEM-(H2) model controls over smoothing for all categories of classes effectively but due to entropy factor it hardens the output and not able to resolve inter-grade class phenomena precisely. On the basis of highest class membership, the class wise optimized value of λ and γ has also been identified and it is found to same as that of generalized optimized value i.e. λ= 0.5 and γ=0.5 for all classes. However, for few classes like barren land, moist land and water body it produces highest membership for the initial values of λ and γ.

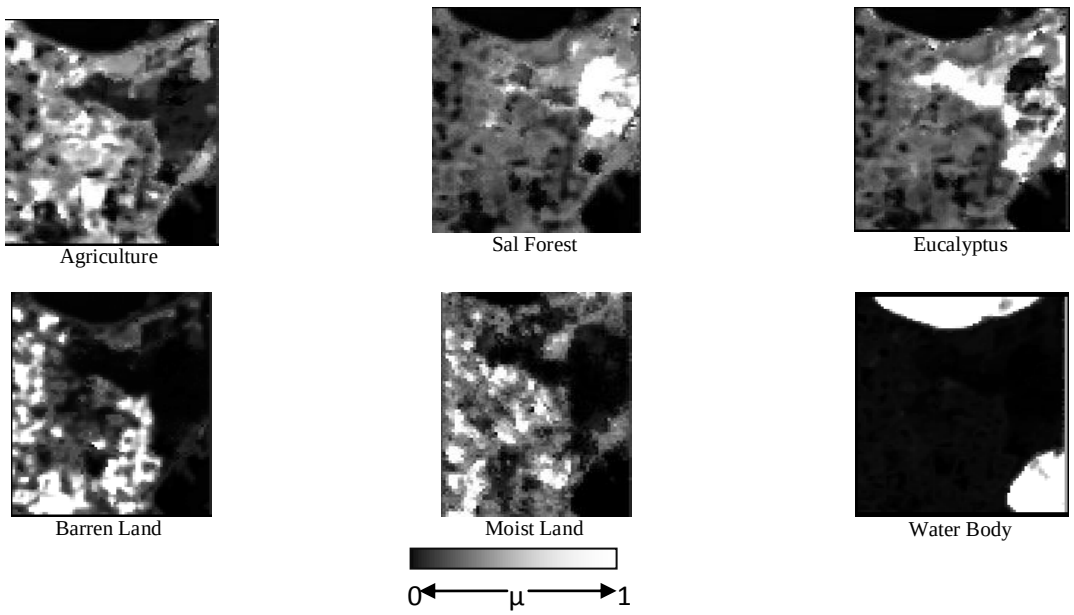

Fig. 6.60: NDEM-(H2) classification output of AWiFS image

Fig. 6.60 shows the classified fraction images of AWiFS dataset for the optimized value of λ and γ. To incorporate the spatial contextual information with NCWE, smoothness prior and four DA-MRF models have been tested. From Tables 6.30, it has been observed that DA models are not able to increase overall accuracy when compared to NDM-(H4) classifier, the interactions among the pixels are constant everywhere in the classified imagery. Thus, adding the contextual

information using DA-MRF models along with entropy reduces the problem of over smoothing at edges but not able to preserve the edges at boundary points (Figs. 6.60). Although, it is a fact that hybridization of contextual with NCWE reduces some level of uncertainty because, the computed entropy values for optimized λ =0.5 and γ =0.5 for all four DA models are at minimal level and is found to be 0.32, 0.01, 0.43, and 0.74 for NDEM-(H1, H2, H3, and H4) models respectively. Thus, inclusion of contextual information in NCWE classifier is not efficiently utilizes the spatial information of an image.

6.12 COMPARATIVE ANALYSIS OF CLASSIFIERS

Assessment of accuracy plays a vital role in the implementation of soft classification. The comparative assessment of a classifier has been presented using Sub-pixel Confusion uncertainty Matrix (SCM). The SCM approach is chosen because it is based on the sub-pixel class distribution uncertainty. The third aspect of this study is to evaluate the performance of classifiers on the basis of computed accuracy measures. Fig. 6.61 shows the comparative assessment of classifier based upon Overall accuracy. On the basis of Fig. 6.61, NDM (H4) classifiers produce highest accuracy (99.79%) with minimum entropy (0.005). This classifier also preserves the edges at boundaries produces homogenous representation of a classified image shown in Fig. 6.50. This shows that the combination of noise clustering classifier with contextual classifier using DA model produces lesser uncertainty as compare to other classifiers. The achieved results have been discussed in Section 6.1 to 6.11.

In this study, three categories of classifiers have been tested. The first category base classifier FCM, PCM and NC have been tested and found that NC performs best with 89.56 % Overall accuracy. In second category classifier where entropy has been added in FCM and NC classifier and new classifier has been created i.e. FCMWE and FCMWE and found that classification performance is almost similar. However, NCWE shows slightly better accuracy i.e. (0.34%) when compared with FCMWE. In third category of classifier where contextual information and entropy has been added in base classifier and twenty five combinations have been tested. Amongst all these combinations NDM-(H4) model found to be more robust and consistent for the classification of medium and coarser resolution dataset. This trend also indicates that

inclusion of spatial contextual information without entropy regularizer controls the problem of over smoothing and preserves the edges at boundary points.

The computation of uncertainty is independent of the reference dataset and it is an absolute measure of uncertainty of the classified imagery. Thus, NDM-(H4) model is less affected by uncertainty because of less entropy value and hence it can be used to generate spectrally and spatially consistent thematic maps which preserve the edges.

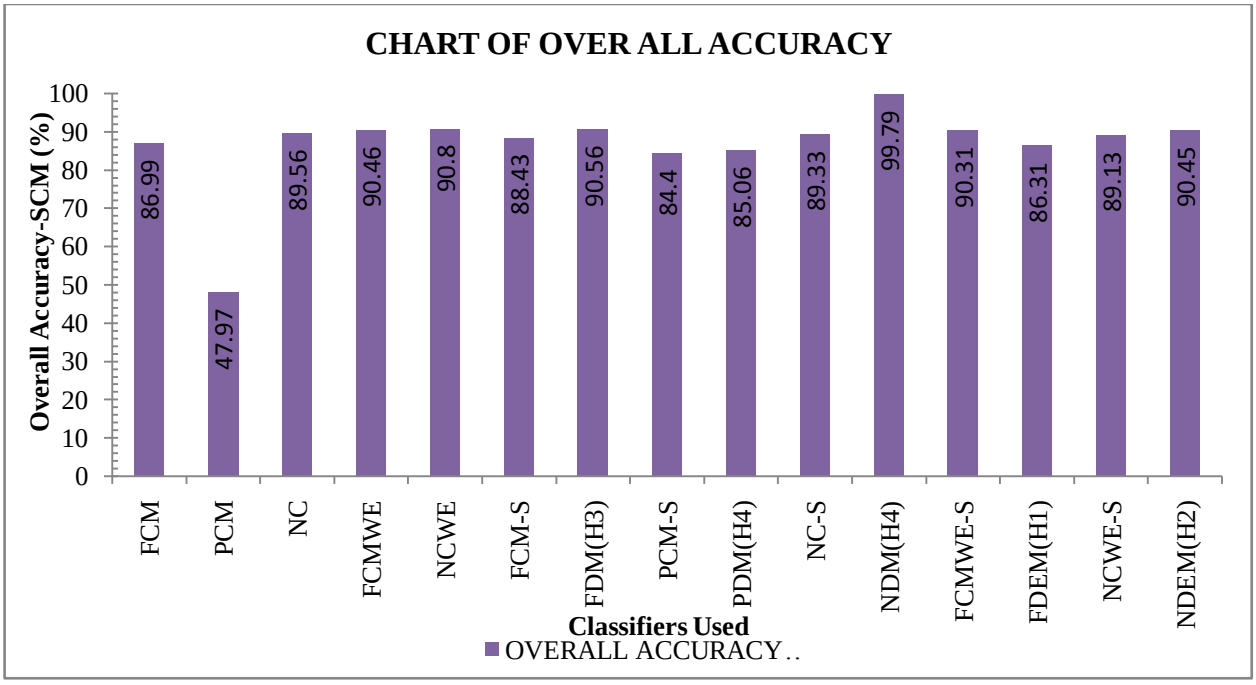

Fig. 6.61: Comparative Analysis of Classifiers

6.13 SUMMARY

In this chapter, the results of the classifications produces from various soft classifiers have been provided, analyzed and discussed. A number of experiments are being conducted using Resourcesat-1 data. Full use of *FUZCEN* software was made in executing these experiments. These results can be summarized in the following.

i) Through the use of entropy, the uncertainty or class mixture in the classified imagery was quantified.

ii) Overall accuracy (FERM, SCM, MIN-MIN and MIN-LEAST) and Fuzzy Kappa coefficient shows similar trend for the assessment of accuracy of soft classification. There was no significant difference between the values of these measures for classification produced from AWiFS data while using LISS-III and LISS-IV as a reference data.

iii) Accuracy measures based upon FERM, SCM, MIN-MIN, and MIN-LEAST can be used for the assessment of image to image accuracy of soft classification. However, entropy could be used as an absolute indicator without using any reference data.

iv) After several experimental trials, class based and generalized optimized parameters have been drawn for FCM, PCM,NC, NCWE,FCMWE, FCM-S, FDM-(H3), PCM-S, PDM-(H4), NC-S, NDM-(H4), FCMWE-S, FDEM-(H1), NCWE-S and NDEM-(H2) classifiers using Euclidean norm.

v) All the classifiers have been tested using supervised classification approach using AWiFS as a classified dataset and LISS-III or LISS-IV as a reference dataset.

vi) Supervised NDM-(H4) classifier was found to be more appropriate which utilizes the contextual information in effective manner and produces robust and consistent classified fraction imagery.

vii) It has also been observed that non-contextual based classifiers were found to be inferior to contextual and entropy based classifiers for classification of remote sensing data.

viii) The optimized values of 'm', 'δ', 'ν','λ', 'β' and 'γ' for different classifiers have been obtained. These optimum values of constants ('m', 'δ', 'ν','λ', 'β' and 'γ') for fuzzy-set based, entropy based and contextual based classifiers shall now be used to generate appropriate outputs of the classifiers. Identified classes have shown low entropy (0.005), which means that uncertainty in the results, is low.

ix) Amongst the three fuzzy set based supervised classifiers (FCM, PCM and NC), NC gives the highest accuracy in identification of various land cover classes.

x) Amongst the two fuzzy and entropy based supervised classifiers (FCMWE, and NCWE), NCWE performs slightly better in identification of various land cover classes.

xi) Amongst twenty five hybrid combinations of fuzzy, entropy and contextual based classifiers, NDM-(H4) gives highest accuracy (99.79%) with lowest entropy (0.005) for $\delta=10^5$, $\lambda=0.4$ and $\gamma=0.4$, to classify various land cover classes with minimum uncertainty.

xii) In a nutshell it has been observed that contextual based hybridized approach of classification performs best when compared to entropy based and fuzzy –set based classifiers. Further, this indicates that while classifying the satellite imagery, spectral as well as spatial information content is required to enhance the class of interest.

CHAPTER 7

SUMMARY, CONCLUSIONS AND FURTHER RESEARCH

7.1 INTRODUCTION

The conventional hard and soft classification methods may produce erroneous classification of images containing mixed pixels thereby resulting in erroneous area estimation of land use land cover classes. The fuzzy, entropy and contextual based hybrid soft classification methods may be preferred to retrieve appropriate classified imagery. Moreover, the utilization of hybrid soft classification approaches has enormous potential in Indian conditions where by land cover classes are of mixed nature. The major findings of this study were targeted to advance the work on classification of images contaminated with mixed pixels, which is critical to the current needs of the society. This study also provides the basis for modeling contextual information in image classification and presented a comprehensive study on the use of hybridized soft classifications for solving the mixed pixel problem..

7.2 CONCLUSIONS

From the analysis of the studies carried out in Chapter 6, following general conclusions can be drawn:

(i) To resolve the sub-pixel area allocation problem, class membership, Sub-pixel Confusion Uncertainty Matrix (SCM), FERM, MIN-MIN, MIN-LESAT and ENTROPY methods has been introduced to assess the accuracy of fuzzy, entropy and contextual based hybrid soft classifiers. All the classification algorithms of this study have been tested in supervised mode using Euclidian weighted norm to classify the remote sensing imagery.

(ii) In this study, entropy has been used to measure the accuracy in terms of uncertainty without using any kind of ground reference data. Entropy is an absolute indicator of an uncertainty.

(iii) Class wise setting of optimum values of parameters for fuzzy set based, entropy based and contextual based classifiers are crucial for their successful implementation. The class

wise optimized values for all classifiers are shown in Table 7.1. The following parameters have been optimized i.e. weighting exponent (*m*), resolution parameter (δ), regularizing parameter (ν), smoothness parameter (λ), weight for neighbours (β) and interaction range parameter (γ).

Table 7.1: Class wise parameter optimization

Classifier	Parameters	Agriculture	Sal forest	Eucalyptus plantation	Barren land	Moist land	Water body
FCM	*m*	2.0	2.1	2.3	2.2	1.9	1.8
PCM	*m*	2.1	2.3	2.3	2.2	2.2	2.2
NC	*m* and δ	2.4 and 3.2×10^5	2.4 and 0.8×10^5	2.4 and 3.1×10^5	2.4 and 4.1×10^5	2.4 and 27.8×10^5	2.4 and 3.1×10^5
NCWE	δ and *v*	10^5 and 2.12×10^2	10^5 and 10^2	10^5 and 10^2	10^5 and 2.1×10^2	10^5 and 10^2	10^5 and 10^2
FCMWE	*m* and *v*	1 and 6.6×10^2	1 and 7.7×10^2	1 and 6.6×10^2	1 and 10^2	1 and 10^2	1 and 10^2
FCM-S	λ and β	0.7 and 3.5	0.7 and 3.5	0.7 and 3.5	0.7 and 3.5	0.7 and 3.5	0.7 and 3.5
PCM-S	λ and β	0.6 and 3.0	0.6 and 3.0	0.6 and 3.0	0.6 and 3.0	0.6 and 3.0	0.6 and 3.0
NC-S	λ and β	0.7 and 3.5	0.7 and 3.5	0.7 and 3.5	0.7 and 3.5	0.7 and 3.5	0.7 and 3.5
FCMWE-S	λ and β	0.4 and 2.0	0.5 and 2.5	0.6 and 3.0	0.4 and 2.0	0.4 and 2.0	0.4 and 2.0
NCWE-S	λ and β	0.6 and 3.0	0.6 and 3.0	0.6 and 3.0	0.6 and 3.0	0.6 and 3.0	0.6 and 3.0
FDM(H3)	λ and γ	0.7 and 0.7	0.8 and 0.8	0.6 and 0.6	0.7 and 0.7	0.8 and 0.8	0.5 and 0.5
PDM(H4)	λ and γ	0.5 and 0.5	0.5 and 0.5	0.5 and 0.5	0.5 and 0.5	0.5 and 0.5	0.5 and 0.5
NDM(H4)	λ and γ	0.4 and 0.4	0.4 and 0.4	0.4 and 0.4	0.3 and 0.3	0.4 and 0.4	0.4 and 0.4
FDEM(H1)	λ and γ	0.7 and 0.7	0.7 and 0.7	0.7 and 0.7	0.7 and 0.7	0.7 and 0.7	0.7 and 0.7
NDEM(H2)	λ and γ	0.5 and 0.5	0.5 and 0.5	0.5 and 0.5	0.5 and 0.5	0.5 and 0.5	0.5 and 0.5

(iv) Another aspect of this study is to identify the generalized optimized value for any land cover class which is found suitable to classify any satellite imagery using fuzzy set based, entropy based and contextual based classifier. Table 7.2 shows the generalized optimized values for all dataset combinations wherein AWiFS classified dataset has been assessed using LISS-III and LISS-IV classified dataset as a reference. The basic objective is to propose a dataset independent optimized value of all the classifiers incorporated in this study.

Table 7.2: Classifier's generalized optimized values

Classifier	Associated parameters	Optimized Value
FCM	m	2.4
PCM	m	2.2
NC	m and δ	2.4 and 10^5
NCWE	δ and v	10^5 and 10^2
FCMWE	m and v	1 and 10^2
FCM-S	m, λ and β	2.4, 0.7 and 3.5
PCM-S	m, λ and β	2.4, 0.6 and 3.0
NC-S	δ, λ and β	10^5, 0.7 and 3.5
FCMWE-S	ν, λ and β	10^2,0.4 and 2.0
NCWE-S	ν, λ and β	10^2,0.6 and 3.0
FDM(H3)	m, λ and γ	2.4, 0.8 and 0.8
PDM(H4)	m, λ and γ	2.4, 0.5 and 0.5
NDM(H4)	δ, λ and γ	10^5, 0.4 and 0.4
FDEM(H1)	ν, λ and γ	10^2,0.7 and 0.7
NDEM(H2)	ν, λ and γ	10^2,0.5 and 0.5

(v) On the basis of Table 7.1 and 7.2, appropriate optimized parameter have been identified and Table 7.3 shows the accuracy values for optimized parameters of fuzzy set based, entropy based and contextual based classifiers.

(vi) The parameters weighting exponent (m) for FCM and PCM, resolution parameter (δ) for NC and regularizing parameter (ν) for FCMWE and NCWE has been optimized, with respect to different land cover classes of AWiFS, LISS-III and LISS-IV dataset of the study.

(vii) For smoothness adaptive prior model, the smoothness strength (λ) and weight for neighbours (β) has been optimized. However, in DA model smoothness strength (λ) and interaction range parameter (γ) has been optimized for all contextual based classifiers.

Table 7.3: Accuracy values for generalized optimized parameter of a classifier for AWiFS data using LISS-IV as reference data

Classifiers	Optimized parameters	Accuracy measures				AWiFS Entropy
		FERM (%)	SCM (%)	MIN-LEAST (%)	Fuzzy Kappa coefficient of SCM	
FCM	m=2.4	81.45	83.54	87.87	0.79	2.0
PCM	m=2.2	88.71	48.80	6.05	0.37	2.3
NC	m=2.4 and $\delta=10^5$	88.84	89.56	96.09	0.87	0.92
NCWE	$\delta=10^5$ and $\nu=10^2$	90.20	90.80	95.24	0.88	0.005
FCMWE	m=1 and $\nu=10^2$	89.73	90.46	95.25	0.87	0.005
FCM-S	m=2.4, λ=0.7 and β=3.5	87.02	88.43	96.87	0.85	1.35
PCM-S	m=2.4, λ=0.6 and β=3.0	86.20	84.40	87.49	0.83	1.9
NC-S	$\delta=10^5$, λ=0.7 and β=3.5	88.19	89.33	95.57	0.86	0.7
FCMWE-S	$\nu=10^2$, λ=0.4 and β=2.0	85.29	90.31	98.12	0.87	0.35
NCWE-S	$\nu=10^2$,λ=0.6 and β=3.0	83.90	89.13	95.77	0.86	0.53
FDM(H3)	m=2.4, ,λ=0.8 and γ=0.8	87.85	90.12	98.14	0.89	0.3
PDM(H4)	m=2.4, λ=0.5 and γ=0.5	90.46	84.50	71.21	0.83	1.85
NDM(H4)	$\delta=10^5$, λ=0.4 and γ=0.4	99.83	99.79	98.05	0.93	0.005
FDEM(H1)	$\nu=10^2$,λ=0.7 and γ=0.7	91.88	85.92	82.10	0.81	0.45
NDEM(H2)	$\nu=10^2$,λ=0.5 and γ=0.5	86.69	81.85	92.38	0.81	0.01

(viii) The joint effect of two purely fuzzy models (FCM and NC) and entropy models which is similar to statistical model have been investigated. The Noise Clustering with Entropy (NCWE) and FCM with entropy classifiers are able to extract the multiple land cover class at a time, at sub-pixel level. The performance of both classifiers is dependent on the constant value of resolution parameter (δ), weighting exponent (m) and regularizing parameter (ν).

(ix) It has been observed that MIN-LEAST operator is not able to assess the accuracy of PCM classifier. This phenomenon occurs because it is not able to measure the minimum sub-pixel overlap between two classes.

(x) To incorporate the spatial contextual information along with spectral information, the hybridized model has been devised to resolve the problem of mixed pixel. The contextual information has been added in FCM, PCM, NC, NCWE and FCMWE classifier to generate smoothness effect, preserving the edges at boundary points and reducing the classification uncertainty.

(xi) The hybrid classification approach with contextual information has been performed in two categories i.e. Smoothness prior and four categories of Discontinuity Adaptive prior. The basic advantage of hybridization DA model with FCM, PCM, NC, NCWE and FCMWE classifier that it undertakes classification with less uncertainty and prevents overshooting of edges.

(xii) The classification performance of FDM-(H3) has been compared with FCM and FCM-S. It has been observed that it reduces the problem of over smoothing of FCM-S and reduces uncertainty by 4% to 6% for agriculture, sal forest, eucalyptus plantation and 7% to 9% for barren land, moist land and water body classes.

(xiii) It has been observed that PDM-(H4) model produces higher accuracy in all cases. The classification performance of PDM-(H4) has been compared with PCM and PCM-S and it has been found that it reduces the problem of over smoothing of PCM-S and reduces the uncertainty by 1.5% to 3% for agriculture, sal forest, eucalyptus plantation and 0.5% to 6% for barren land, moist land and water body classes.

(xiv) It has been observed that NDM-(H4) model produces highest accuracy for all cases. The basic advantage of hybridization DA model with NC classifier is that all classes are well classified and edges are not over smoothed.

(xv) The classification performance of NDM-(H4) has been compared with NC, NCWE and NC-S. It has been observed that it reduces the problem of over smoothing of NC-S and increases the SCM accuracy approximately by 8%. NC-S (standard regularizes) classification approach follows constant interaction among the pixels in image space, which sometimes lead to over smoothening and thus it is not able to preserves the edges efficiently as DA models do.

(xvi) The idea of using Fuzzy *c*-Mean with Entropy and Noise Clustering with Entropy besed hybrid approach of soft classification i.e. FCMWE and NCWE with contextual information is a new approach which helps significantly to reduce uncertainty among pixels while incorporating spatial contextual information and entropy together.

(xvii) It has been observed that inclusion of entropy as a regularizer along with contextual information reduces the uncertainty in terms of entropy. However, it does not make much impact on accuracy values.

(xviii) On the basis of SCM accuracy, the comparative performance analysis has been done for all the classifiers, and it is found that NDM (H4) classifier produces highest accuracy (99.79%) with minimum entropy (0.005). It also preserves edges and produces homogenous representation of a classified image. This reflects that the combination of noise clustering classifier with contextual information using DA model produces lesser uncertainty when compared to other classifiers. Thus, NDM-(H4) model is less affected by uncertainty because of less entropy value and hence it can be used to generate spectrally and spatially consistent thematic maps which preserve the edges. At this point the fifth objective of the study which was related to the performance comparison amongst classifier has been achieved.

(xix) By optimizing parameters for fuzzy set based algorithms for different land cover classes, the first and second objective of the study has been achieved. After hybridizing the FCM, PCM and NC classifier with contextual second and fourth objective of the study has been achieved. Further, hybridizing the FCM and NC classifier with entropy and contextual third and fourth objective of the study has been achieved.

(xx) It has been observed that hybrid approach of soft classification based upon contextual is effective for the land cover identification.

(xxi) It has been observed that Noise Clustering with contextual classifier produces higher accuracy amongst all classifiers. This indicates that stochastic modeling with fuzzy based modeling is suitable for soft classification.

(xxii) The edge perseverations have been verified using mean and variance approach suggested by Wen and Xia (1999).

7.3 MAJOR CONTRIBUTION

The outcome of this study has resulted in to the following major contributions,

(i) Development of an indigenous, user-friendly, interactive and comprehensive software tool (*FUZCEN*) exclusively designed for hybrid soft classification and its assessment of accuracy, is a novelty since there appears to be no such software currently available for image classification.

(ii) The advantage of entropy and contextual based classifier in dealing with noise and uncertainty in the dataset has been validated, which is novel in the sense that no such study has been reported earlier in the remote sensing literature.

(iii) The use of FERM, SCM, MIN-MIN, MIN-LEAST and entropy based accuracy measures for the assessment of accuracy of hybrid soft classifications have been advocated.

(iv) The inclusion of entropy in FCM and NC classifier significantly removes the classification uncertainty.

(v) The use of spatial information has been attempted through contextual classifier, which is unique. Further research may required in understanding the characteristics of these classifiers so that it is acceptable at the operational level.

7.4 FURTHER RESEARCH

This study has focused its attention on the use of satellite data in identifying various land cover classes with adequate boundaries using fuzzy-set based, entropy based and contextual based classifiers. However, there are some areas which require further investigations. Based on this work further research scope can be identified as follows:

(i) All the classifiers based upon entropy and contextual needs to be further examined using unsupervised approach.

(ii) For energy minimization instead of Simulated Annealing other method like Maximizing of the Posterior Marginal's (MPM) may be adopted.

(iii) DA-MRF models may also be tested for other classification techniques such as Decision tree classifier, Support Vector Machine (SVM) and Linear Mixture Modeling (LMM) etc.

(iv) To assess the classification uncertainty other than entropy criterion like Mean Relative Error (MRE) and Root Mean Square Error (RMSE) approach may be used.

(v) While adding the regularizing parameter (ν) sometimes barren land and moist land has not been discriminated properly in NCWE classifier, so it is further recommended to test this algorithm using unsupervised approach.

(vi) In contextual based classifier λ, β and γ needs to be optimized separately using unsupervised approach.

(vii) There is no doubt that hybrid approach of sub-pixel classifications can result in accurate and meaningful land use land cover classification. Contextual based classifiers have exploited the spatial distribution of classes within a pixel. However, MRF model may be attempted to account for this spatial information in super-resolution land cover mapping.

(viii) This research has clearly advocated the use of FERM, SCM, MIN-LEAST, MIN-MIN and entropy based measures for assessment of accuracy of remote sensing classifications. Generally, FERM and SCM is created using sample of testing data, the statistical confidence limits of the measures need to be devised before these can be accepted as accuracy standards.

(ix) The contextual based hybrid soft classifier needs to be tested for large, complex and heterogeneous regions, so that edge perseveration can be checked accurately.

(x) The use of soft reference data for the assessment of accuracy is still an active area of research in Geomatics Engineering and needs more exploration.

REFERENCES

1. Abe, S. and Thawonmas, R., 1997. Fuzzy classifier with ellipsoidal regions, *IEEE Transactions on Fuzzy Systems*, **5**, 358-367.
2. Abler, R. F., 1993, Everything in its Place: GPS, GIS and Geography in 1990s, *Professional Geographer*, **45 (2)**: 131-139.
3. Adams, J.B., Smith, M.O. and Johnson, P.E., 1985. Spectral mixture modeling: a new analysis of rock and soil types at the Viking Lander 1 site, *Journal of Geophysical Research*, **91**, 8098-8112.
4. Adams, J.B., Sabol, D.E., Kapos, V., Filho, R.A., Roberts, D.A., Smith, M.O., Gillespie, A.R., 1995, Classification of multispectral images based on fractions of endmembers: application to land cover change in the Brazilian Amazon. *Remote Sensing of Environment*, **52**, 137–154.
5. Ahmad, H., Yeats, R.S. and Lisa, M., 2008. Geological setting of the 8 October 2005 Kashmirearthquake, *Journal of Seismology*, **13**, 315-325.
6. Aniekwu, A.N. and Orie, O.U., 2005. The determination of severity indices of variables that cause collapse of engineering facilities in Nigeria: A case study of Benin City, *The Journal of Engineering Science and Applications*, **4**, 63-70.
7. Aplin, P., Atkinson, P.M. and Curran, P.J., 1999a, Per-field classification of land use using the forthcoming very fine spatial resolution satellite sensors: problems and potential solutions. In P.M. Atkinson and N.J. Tate (Eds), *Advances in Remote Sensing and GIS Analysis*, 219–239 (New York: John Wiley and Sons).
8. Aplin P. and Atkinson, P. M., 2001, Sub-pixel land cover mapping for per-field classification, *International Journal of Remote Sensing*, **22(14)**, 2853–2858.
9. Archer, D.R. and Fowler, H.J., 2008. Using meteorological data to forecast seasonal runoff on the River Jhelum, Pakistan, *Journal of Hydrology*, **361**, 10-23.
10. Ardizzone, F., Cardinali,M., Galli,M., Guzzetti, F. and Reichenbach, P., 2007. Identification and mapping of recent rainfall-induced landslides using elevation data collected by airborne Lidar, *Natural Hazards and Earth System Sciences*, **7**, 637-650.
11. Arora M. K. and Foody G. M., 1997, Log-linear modeling for the evaluation of the variable

affecting the accuracy of probabilistic, fuzzy and neural network classifications. *International Journal of Remote Sensing* **18(4)**: 785-798.

12. Arora, M. K., 2002, Land cover classification from remote sensing data, *GIS development*, **6**, 24-25, 30-31.
13. Arrowsmith, C. A. and Williamson, I. P., 1990. Land Information Systems in Local Government and the Role of the Private Sector. *The Australian Surveyor*, **35(1)**, 29-39.
14. Arulndandan, K., Yogachandran, C., Meegoda, N.J., Ying, L. and Zhauji, S., 1986.Comparison of the SPT, CPT, SV and electrical methods of evaluating earthquake induced liquefaction susceptibility in Ying Kou City during the Haicheng earthquake. *Proc. Use of In Situ Tests in Geotech. Engg.*, **6**, ASCE, New York, N. Y., 389-415.
15. Asner, G.P. and Heidebrecht, K.B., 2002. Spectral unmixing of vegetation, soil and dry carbon cover in arid regions: comparing multispectral and hyperspectral observations. *International Journal of Remote Sensing*, **23**, 3939–3958.
16. Atkinson, P.M. and Aplin, P., 2004. Spatial variation in land cover and choice of spatial resolution for remote sensing, *International Journal of Remote Sensing*, **25**, 3687-3702.
17. Atkinson, P.M., Cutler, M.E.J. and Lewis, H., 1997. Mapping subpixel proportional land cover with AVHRR imagery, *International Journal of Remote Sensing*, **18**, 917-935.
18. Atkinson, P.M. and Tatnall, A.R., 1997. Introduction: neural networks in remote sensing, *International Journal of Remote Sensing*, **18**, 699-709.
19. Aziz, M. A. 2004. Evaluation of soft classifiers for remote sensing data, unpublished Ph.D thesis, Indian Institute of Technology Roorkee, Roorkee, India.
20. Babovic, V. and Keijzer, M., 2000, Genetic programming as a model induction engine. *Journal of Hydroinformatics*. **2 (1)**, 35-60.
21. Balafar, M. A., Ramli, A. R. ,Saripan, M. I. and Mashohor, S. 2010. Review of brain MRI image segmentation methods. *Artificial Intelligence Review* March 2010, **33(3)**, 261-274
22. Balz, T. and Liao, M., 2010. Building-damage detection using post-seismic high-resolution SAR satellite data, International *Journal of Remote Sensing*, **31**, 3369-3391.
23. Bandyopadhyay, S., Maulik, U. and Mukhopadhyay, A., 2007. Multiobjective Genetic Clustering for Pixel Classification in Remote Sensing Imagery, *IEEE Transactions on Geoscience and Remote Sensing*, **45(5)**, 1506-1511, 2007.

24. Bannari, A., Morin, D., Bonn, F. and Huete, A.R., 1995. A review of vegetation indices, *Remote Sensing Reviews*, **13**, 95-120.

25. Baraldi, A. and Parmiggiani, F., 1995, An investigation of the textural characteristics associated with gray level cooccurrence matrix statistical parameters. *IEEE Transactions on Geoscience and Remote Sensing*, **33**, 293–304.

26. Barandela, R. and Juarez, M., 2002, Supervised classification of remotely sensed data with ongoing learning capability. *International Journal of Remote Sensing*, **23**, 4965–4970.

27. Barlow, J., Martin, Y. and Franklin, S.E., 2003. Detecting translational landslide scars using segmentation of Landsat ETM+ and DEM data in the northern Cascade Mountains, British Columbia, *Canadian Journal of Remote Sensing*, **29**, 510-517.

28. Barni, M., Cappellini, V., and Mecocci, A., 1996. A possibilistic approach to clustering, *IEEE Trans. Fuzzy Syst.*, **4(3)**, 393 -396,

29. Barnsley, M. and Barr, S., 1996. Inferring urban land use from satellite sensor images using kernel-based analysis and classification. *Photogrammetric Engineering and Remote Sensing*, **62**, 949-958.

30. Bastin, L., 1997. Comparison of fuzzy *c*-mean classification, linear mixture modelling and MLC probabilities as tools for unmixing coarse pixels, *International Journal of Remote Sensing*, **18**, 3629-3648.

31. Baugh, W.M. and Groeneveld, D.P., 2006. Broadband vegetation index performance evaluated for a low-cover environment, *International Journal of Remote Sensing*, **27**, 4715-4730.

32. Benediktsson, J.A., Swain, P.H. and Ersoy, O.K., 1990. Neural network approaches versus statistical methods in classification of multisource remote sensing data, *IEEE Transactions on Geoscience and Remote Sensing*, **28**, 540-552.

33. Benz, U.C., Hofmann, P., Willhauck, G., Lingenfelder, I. and Heynen, M., 2004, Multi-resolution, object-oriented fuzzy analysis of remote sensing data for GIS ready information. *ISPRS Journal of Photogrammetry & Remote Sensing*, **58**, 239–258.

34. Bertsimas, D. and Tsitsiklis, J., 1993. Simulated Annealing, Statistical Science, **8(1)**, 10-15.

35. Besag, J., 1974. Spatial interaction and the statistical analysis of lattice systems, *Journal of the Royal Statistical Society. Series B (Methodological)*, 192–236.

36. Bezdek, J.C., 1981. *Pattern Recognition with Fuzzy Objective Function Algorithm*. Plenum, New York, USA, ISBN: 978-1-4757-0452-5.

37. Bezdek, J.C., Ehrlich, R. and Full, W., 1984. FCM: The fuzzy *c*-means clustering algorithm, *Computers and Geosciences*, **10**, 191-203.

38. Bezdek, J.C., Hathaway, R.J., Sabin, M.J., and Tucker, W.T., 1987. Convergence theory for fuzzy c-means: counterexamples and repairs. *IEEE Trans. on Syst., Man, Cybern*, SMC-**17(5)**, 873-877.

39. Biehl, L. and Landgrebe, D., 2002, MultiSpec—a tool for multispectral-hyperspectral image data analysis. *Computers and Geosciences*, **28**, 1153–1159.

40. Bilham, R. and Hough, S.E., 2006. Future earthquakes on the Indian Continent: Inevitable hazard, preventable risk, *South Asia Journal*, **12**, 1-9.

41. Binaghi, J.E., Madella, P., Montesano, M.G. and Rampini, A., 1997. Fuzzy contextual classification of multisource remote sensing images, *IEEE Transactions on Geoscience and Remote Sensing*, **35**, 326-340.

42. Binaghi, E., Brivio, P.A., Chessi, P. and Rampini, A., 1999. A fuzzy set based accuracy assessment of soft classification,*Pattern Recognition Letters*, **20**, 935-948.

43. Binaghi,E., Pedoia, V., Guidali,A. and Guglielmin, M.,2013. Snow cover thickness estimation using radial basis function networks. *The Cryosphere*, An Interactive Open Access Journal of the European Geosciences Union, 7, 841-854, doi:10.5194/tc-7-841-2013, 2013.

44. Birth, G.S. and Mc-Vey, G., 1968. Measuring the color of growing turf with a reflectance spectroradiometer, *Agronomy Journal*, **60**, 640-643.

45. Biswas, S.K., 1987. Regional tectonic framework, structure and evolution of the western marginal basins of India, *Tectonophysics*, **135**, 307-327.

46. Blaschke,T., 2004. Objec tbased image analysis for remote sensing. , **65**, 2-16.

47. Bloch, I., 1996, Information combination operators for data fusion: a comparative review with classification. *IEEE Transactions on Systems, Man, and Cybernetics*, **26**, 52–67.

48. Boardman, J.W., 1989. Inversion of imaging spectrometry data using singular value decomposition, *Proc. IGARSS'89, 12th Canadian Symposium on Remote Sensing*, **4**, 2069-2072.

49. Bock, M., Xofis, P., Mitchley, J., Rossner, G., and Wissen, M., 2005. Object-oriented methods for habitat mapping at multiple scales – case studies from Northern Germany and Wye Downs, UK. *Journal for Nature Conservation*, 13: 75-89.

50. Brier, G.W. and Allen, R.A., 1951.*Verification of Weather Forecasts*, Compendium of Meteorology,American Meteorological Society **(**T.Malone, ed.), 841-848.

51. Boser, H., Guyon I. M. and Vapnik, V. N., 1992, A training algorithm for optimal margin classifiers. *Proceedings of 5th Annual ACM Workshop on computational Learning Theory*, Pittsburgh, PA, 144-152.

52. Brodley, C. E., and Utgoff, P. E., 1995, Multivariate decision trees. *Machine Learning*, **19**, 45–77.

53. Brown, M., Gunn, S.R. and Lewis, H.G., 1999. Support vector machines for optimal classification and spectral unmixing, *Ecological Modelling*, **120**, 167-179.

54. Bruzzone, L. , Conese, C., Maselli, F. and Roli, F., 1997, Multi source classification of complex rural areas by statistical and neural-network approaches. *Photogrammetric Engineering and Remote Sensing*, **63**, 523–533.

55. Carpenter, G. A., Gopal, S., Martens, S., and Woodcock, C. E., 1999. A neural network method for mixture estimation for vegetation mapping. *Remote Sensing of Environment*, **70**, 138–152.

56. Chandra, A. M. & Ghosh, S. K. 2006. Remote Sensing and Geographical Information System, ISBN 81-7319-685-0.

57. Chang, C., 2002, Target Signature-Constrained Mixed Pixel Classification for Hyper-spectral Imagery, *IEEE Transactions on Geoscience And Remote Sensing*, Vol. 40, No. 5.

58. Chang, R.T. and Liu, J.K., 2004. Landslide features interpreted by neural network method using high-resolution satellite image and digital topographic data, *Proc.of ISPRS04*, Istambul, Turkey.

59. Chawla, S., 2010. Possibilistic c - means - spatial contextual information based sub - pixel classification approach for multi - spectral data, University of Twente Faculty of Geo-Information and Earth Observation (ITC), Enschede.

60. Chen, C. F. and Lee,J. M., 2001. The validity measurement of fuzzy c-means classifier for remotely sensed images, in *Paper presented at the 22nd Asian Conference on Remote Sensing*, **5**, 9.

61. Chen, D., Stow, D.A. and Gong, P., 2004. Examining the effect of spatial resolution and texture window size on classification accuracy: An urban environment case, *International Journal of Remote Sensing*, **25**, 2177-2192.

62. Chen, J., Zhu, X., Imura, H. and Chen, X., 2010. Consistency of accuracy assessment indices for soft classification: Simulation analysis. *ISPRS Journal of Photogrammetry and Remote Sensing*, **65**, 156-164.

63. Chen, K.S., Tzeng, Y.C., Chen, C.F. and Kao, W.L., 1995, Land-cover classification of multispectral imagery using a dynamic learning neural network. *Photogrammetric Engineering and Remote Sensing*, **61**, 403–408.

64. Chen, X., Vogelmann, J.E., Rollins, M., Ohlen, D., Key, C.H., Yang, L., Huang, C. and Shi, H., 2011. Detecting post-fire burn severity and vegetation recovery using multitemporal remote sensing spectral indices and field-collected composite burn index data in a ponderosa pine forest, *International Journal of Remote Sensing*, **32**, 7905-7927.

65. Chotiwattana, W.,2009. Noise Clustering Algorithm based on Kernel Method. *IEEE International Advance Computing Conference (IACC-2009)*, Patiala, India, 6-7 March.

66. Cihlar, J., 2000, Land cover mapping of large areas from satellites: status and research priorities. *International Journal of Remote Sensing*, **21**, 1093–1114.

67. Clausius, R., 1865. Über die Wärmeleitung gasförmiger Körper", Annalen der Physik 125: 353–400.

68. Cihlar, J., Xiao, Q., Chen, J., Beaubien, J., Fung, K. and Latifovic, R., 1998, Classification by progressive generalization: a new automated methodology for remote sensing multispectral data. *International Journal of Remote Sensing*, **19**, 2685–2704.

69. Congalton, R. G., 1988, Using Spatial Autocorrelation Analysis to Explore the Errors in Maps Generated from Remotely Sensed Data, *Photogrammetric Engineering and Remote Sensing*, **54 (5)**, 587-592.

70. Congalton, R. G., 1991, A review of assessing the accuracy of classifications of remotely sensed data. *Remote Sensing of Environment*, **37**, 35-47.

71. Congalton, R. G., and Green, K., 1999. Assessing the accuracy of remotely sensed data: Principles and practices. Boca Raton, FL: Lewis.

72. Cortes, C. and Vapnik, V., 1995, Support vector networks, *Machine Learning*, **20**, 273– 297.

73. Cortijo, F.J. and De La Blanca, N.P., 1998, Improving classical contextual classification. *International Journal of Remote Sensing*, **19**, 1591–1613.

74. Côté S. and Tatnall A. R. L., 1997, The Hopfield neural network as a tool for feature tracking and recognition from satellite sensor images. *International Journal of Remote Sensing*, **18(4)**, 871–885.

75. Cross, A. M., Settle, J. J., Drake, N. A., and Paivinen, R. T. M., 1991. Sub-pixel measures of tropical forest cover using AVHRR data. *International Journal of Remote Sensing*, **12**, 1119–1129.

76. Dadhwal, V. K., Sehgal, V. K., Singh, R. P. and Rajak.,D. R., 2002. Wheat yield modeling using satellite remote sensing with wheather data : Recent Indian Experience, Crop Inventory and Modelling division, ARG, RESA Space Application centre (ISRO), MAUSAM, **54**, 252-262

77. Dav´e, R.N., 1990: An adaptive fuzzy c-elliptotype clustering algorithm. Proc. of the North American Fuzzy Information Processing Society: Quarter Century of Fuzziness 1, 9–12

78. Dave, R.N., 1991. Characterization and detection of noise in clustering. *Pattern Recognition Letters*, **12**, 657-664.

79. Dav´e, R.N., Krishnapuram, K., 1997: Robust clustering methods: A unified view. *IEEE Trans. on Fuzzy Systems*, **5**, 270–293

80. Daniel K. W., Tripathi, N. K., Honda K., 2003, Artificial neural network analysis of laboratory and in situ spectra for the estimation of macronutrients in soils of Lop Buri, Thailand. Aust. J. Soil Res. **41**, 47-59.

81. Dean, A.M. and Smith, G.M., 2003, An evaluation of per-parcel land cover mapping using maximum likelihood class probabilities. *International Journal of Remote Sensing*, **24**, 2905–2920.

82. Debayle, J. and Pinoli,J. C., 2006. General adaptive neighborhood image processing, *Journal of Mathematical Imaging and Vision*, vol. **25**, no. 2, 245–266.

83. Debella-Gilo, M. and Kaab, A., 2011. Sub-pixel precision image matching for measuring surface displacements on mass movements using normalized cross-correlation, *Remote Sensing of Environment*, **115**, 130-142.

84. Defries, R.S., Hansen, M., Townshend, J.R.G. and Sohlberg, R., 1998, Global land cover classification at 8 km spatial resolution: the use of training data derived from Landsat imagery in decision tree classifiers. *International Journal of Remote Sensing*, **19**, 3141–3168.

85. De-Luca, A. and Termini, S., 1972.A definition of a nonprobabilistic entropy in the setting of fuzzy sets theory, *Information and Control*, **20**, 301-312.

86. Deering, D.W.,Rouse, J.W., Haas, R.H. and Schall, J.A., 1975. Measuring forage production of grazing units from Landsat MSS data, *Proc. of Tenth International Symposium on Remote Sensing of Environment*, Ann Arbor, ERIM, **2**, 1169-1178.

87. Defries, R. S., Hansen, M., Townshend, J. R. G., and Sohlberg, R., 1998, Global land cover classifications at 8km spatial resolution: the use of training data derived from Landsat imagery in decision tree classifiers. *International Journal of Remote Sensing*, **19**, 3141–3168.

88. Defries, R.S. and Chan, J.C., 2000, Multiple criteria for evaluating machine learning algorithms for land cover classification from satellite data. *Remote Sensing of Environment*, **74**, 503–515.

89. Dehghan, H. andGhassemian, H., 2006. Measurement of uncertainty by the entropy: application to the classification of MSS data, *International journal of remote sensing*, vol. **27**, no. 18, 4005–4014.

90. Derin, H., and Elliott, H., 1987. Modeling and segmentation of noisy and textured images using Gibbs random fields. *IEEE Trans. on Pattern Anal. Machine Intell., PAMI* **-9(1)**: 39–55.

91. Devasthale, A., Mohan Krishna B., and Rao E. P., 2004.The Evaluation of JPEG-2000 Compression Standard for Remote Sensing Applications.Asian *Journal of Geoinformatics*, vol. **4**, no. 4, 69-80.

92. Dibike, Y. B., Velickov, S., Solomatine, D. and Abbott, M. B., 2001, Model Induction with Support Vector Machines: Introduction and Applications. *ASCE Journal of Computing in Civil Engineering*, vol. **15**, No. 3, 208-216.

93. Dikshit, O. and Behl, V., 2009. Segmentation-Assisted Classification for IKONOS Imagery, *Journal of Indian Society of Remote Sensing*. **37**, 551–564.

94. Dulyakarn, P. and Rangsanseri, Y., 2001. Fuzzy c-means clustering using spatial information with application to remote sensing, in *Paper presented at the 22nd Asian Conference on Remote Sensing*, vol. **5**, 5-9, Singapore., November,2001

95. Dunn, J.C., 1974. Well Separated Clusters and Optimal Fuzzy Partitions, *Journal of Cybernetics*, **4**, 95-104.

96. Dutta,A., 2009. Fuzzy c-means classification of multispectral data incorporation spatial contextual information, ITC, Enschede.

97. Eastman, J.R. and Laney, R.M., 2002. Bayesian soft classification for sub-pixel analysis: critical evaluation, *Photogrammetric Engineering and Remote Sensing*, **68**, 1149-1154.

98. Ebanks, B.R., 1983. On measures of fuzziness and their representations, *Journal of Mathematical Analysis and Applications*, **94**, 24-37.

99. Emrahoglu, N., Yegingil, I., Pestemalci, V., Senkal, O. and Kandirmaz, H.M., 2003, Comparison of a new algorithm with the supervised classifications. *International Journal of Remote Sensing*, **24**, 649–655.

100. Erbek, F.S., Ozkan, C. and Taberner, M., 2004, Comparison of maximum likelihood classification method with supervised artificial neural network algorithms for land use activities. *International Journal of Remote Sensing*, **25**, 1733–1748.

101. Espindola G., Câmara G., Reis I., Bins L. and Monteiro A. M.V., 2006, Parameter Selection for Region-Growing Image Segmentation Algorithms using Spatial Autocorrelation. *International Journal of Remote Sensing*, Vol. **27** (14/20): 3035-3040.

102. Fassnacht, K.S., Cohen, W.B. and Spies, T.A., 2006. Key issues in making and using satellite-based maps in ecology: A primer, *Forest Ecology and Management*, **222**, 167-181.

103. Ferna´ Ndez-Prieto, D., 2002, An iterative approach to partially supervised classification problems. *International Journal of Remote Sensing*, **23**, 3887–3892.

104. Fisher, P. F. and Pathirana, S., 1990. The Evaluation of Fuzzy Membership of Land Cover Classes in the Suburban Zone. *Remote Sensing of Environment*, **34**, 121-132.

105. Fisher, P., 1997. The pixel: a snare and a delusion, *International Journal of Remote Sensing*, vol **18**, no.3, 679-685.

106. Flygare, A-M., 1997, A comparison of contextual classification methods using Landsat TM. *International Journal of Remote Sensing*, **18**, 3835–3842.

107. Foody, G.M., Campbell, N.A., Trodd, N.M. and Wood, T.F., 1992. Derivation and application of probabilistic measures of class membership from maximum likelihood classification, *Photogrammetric Engineering and Remote Sensing*, **58**, 1335-1341.

108. Foody, G.M. and Cox, D.P., 1994. Sub-pixel land cover composition estimation using a linear mixture model and fuzzy membership functions, *International Journal of Remote Sensing*, **15**, 619-631.

109. Foody, G.M., 1996. Approaches for the production and evaluation of fuzzy land cover classifications from remotely-sensed data, *International Journal of Remote Sensing*, vol. **17**, no. 7, 1317–1340.

110. Foody, G. M., 2000.Estimation of sub-pixel land cover composition in the presence of untrained classes," *Computers & Geosciences*, vol. **26**, no. 4, 469–478.

111. Foody, G.M., and Zhang, J., 2001. Fully-fuzzy supervised classification of sub-urban land cover from remotely sensed imagery: statistical and artificial neural network approaches. *International Journal of Remote Sensing*, **22(4)**, 615–628.

112. Foody, G. M., 2002. Status of land cover classification accuracy assessment, *Remote Sensing of Environment*, **80**, 185– 201.

113. Foody, G. M. and Mathur A., 2004, A Relative Evaluation of Multiclass Image Classification by Support Vector Machines, *IEEE Transactions on Geoscience and Remote Sensing*, Vol.**42**, No. 6.

114. Foody, G. M. and Mathur, A., 2006, Toward intelligent training of supervised image classifications: directing training data acquisition for SVM classification. *Remote Sensing of Environment*, **93** , 107 – 117

115. Franklin, S.E., Peddle, D.R., Dechka, J.A. and Stenhouse, G.B., 2002, Evidential reasoning with Landsat TM, DEM and GIS data for land cover classification In support of grizzly bear habitat mapping. *International Journal of Remote Sensing*, **23**, 4633–4652.

116. Friedl, M. A., and Brodley, C. E., 1997, Decision tree classification of land cover from remotely sensed data. *Remote Sensing of Environment*, **61**, 399–409.

117. Friedman J. H., 1994, Flexible metric nearest neighbor classification. Technical report, Department of Statistics and Stanford University.

118. Fung, T. and Siu, W., 2000. Environmental quality and its changes, an analysis using NDVI, *International Journal of Remote Sensing*, **21**, 1011-1024.

119. Gallego, F.J., 2004, Remote sensing and land cover area estimation. *International Journal of Remote Sensing*, **25**, 3019–3047.

120. Geman, S. and Geman D., 1984. Stochastic Relaxation, Gibbs Distributions, and the Bayesian Restoration of Images, *IEEE Transactions on Pattern Analysis and Machine Intelligence*, vol. **PAMI-6**, no. 6, 721 –741.

121. Gao, B.C., 1996. NDWI-a normalized difference water index for remote sensing of vegetation liquid water from space, *Remote Sensing of Environment*, **58**, 257-266.

122. Garcia-Haro, F.J., Gilabert, M.A. and Melia, J., 1996. Linear spectral mixture modelling to estimate vegetation amount from optical spectral data, *International Journal of Remote Sensing*, **17**, 3373-3400.

123. Gattinoni, P., 2009. Parametrical landslide modeling for the hydrogeological susceptibility assessment: from the Crativalley to the Cavallerizzo landslide (Southern Italy), *Natural Hazards*, **50**, 161-178.

124. Geneletti, D. and Gorte, B.G.H., 2003, A method for object-oriented land cover classification combining Landsat TM data and aerial photographs. *International Journal of Remote Sensing*, **24**, 1273–1286.

125. Ghosh, S. K., 2013, Digital Image Processing. Narosa Publishing House, New Delhi.

126. Gillespie, A.R., 1992. Spectral mixture analysis of multi-spectral thermal infrared images, *Remote Sensing of Environment*, **42**, 137-145.

127. Gitas, I.Z., Mitri, G.H. and Ventura, G., 2004, Object-based image classification for burned area mapping of Creus Cape Spain, using NOAA-AVHRR imagery. *Remote Sensing of Environment*, **92**, 409–413.

128. Goel, N.S. and Qin, W., 1994. Influences of canopy architecture on relationships between various vegetation indices and LAI and FPAR: a computer simulation, *Remote Sensing Reviews*, **10**, 309-347.

129. Gong, P. and Howarth, P.J., 1992, Frequency-based contextual classification and gray-level vector reduction for land-use identification. *Photogrammetric Engineering and Remote Sensing*, **58**, 423–437.

130. Gong, P., Marceau, D.J. and Howarth, P.J., 1992, A comparison of spatial feature extraction algorithms for land-use classification with SPOT HRV data. *Remote Sensing of Environment*, **40**, 137–151.

131. GopalNaik M., Rao E. P. and Eldho T. I., (2009). Finite element method and GIS based distributed model for soil erosion and sediment yield in a watershed, *Journal of Water Resources Management*, Vol. **23**, 553-579.

132. Gopal, S. and Woodcock, C., 1994, Theory and methods for accuracy assessment of thematic maps using fuzzy sets, *Photogrammetric Engineering and Remote Sensing*, **60**, 181-188.

133. Grégoire, M., and Lennon, M., 2003, Support Vector Machines for Hyper-spectral Image Classification with Spectral-based kernels, *Proceeding of IGARSS*.

134. Grimson, W. E. L., 1981.*From images to surfaces: A computational study of the human early visual system*, vol. **4**.

135. Guerschman, J.P., Paruelo, J.M., Bella, C.D., Giallorenzi, M.C. and Pacin, F., 2003. Land cover classification in the Argentine Pampas using multi-temporal Landsat TM data, *International Journal of Remote Sensing*, **24**, 3381-3402.

136. Guo, Q., Kellya, M. and Graham, C. H., 2005, Support vector machines for predicting distribution of Sudden Oak Death in California, *Ecological Modelling*, **182**, 75–90.

137. Gutman, G. and Ignatov, A., 1998. The derivation of the green vegetation fraction from NOAA/AVHRR data for use in numerical weather prediction models. *International Journal of Remote Sensing*, **60(2)**, 181–188.

138. Hall, F.G., Townshend, J.R. and Engman, E.T., 1995. Status of remote sensing algorithms for estimation of land surface state parameters, *Remote Sensing of Environment*, **51**, 138-156.

139. Hansen, M., Dubayah, R., and DeFries, R., 1996, Classification trees: an alternative to traditional land cover classifiers. *International Journal of Remote Sensing*, **17**, 1075–1081.

140. Hansen, M., DeFries, R. S., Townshend, J. R. G., and Sohlberg, R., 2000, Global land cover classification at 1 km spatial resolution using a classification tree approach. *International Journal of Remote Sensing*, **21**, 1331–1364.

141. Hardisky, M.A., Klemas, V. and Smart, R.M., 1983. The influences of soil salinity, growth form, and leaf moisture on the spectral reflectance of spartinaalterniflora canopies, *Photogrammetric Engineering and Remote Sensing*, **4**9, 77-83.

142. Harris R., 1980, Spectral and spatial image processing for remote sensing, *International Journal of Remote Sensing,* **1**, 361-375.

143. Harris R., 1981, An experiment in probabilistic relaxation for terrain cover classification of Kuwait from Landsat imagery, Fifteenth International *Symposium on Remote Sensing of Environment,* Ann Arbor, Michigan, USA, 1245-1252.

144. Harris, R., 1981a. Frameworks for the analysis of Landsat digital data, *Environment and Planning, **A*-13**, 1553-1562.

145. Harris R., 1983, A comparative study of the effects of data reduction on terrain cover mapping from Landsat, *International Journal of Remote Sensing*, **4**, 723-728.

146. Harris, R., 1985. Contextual classification post processing of Landsat data using a probabilistic relaxation model, *International Journal of Remote Sensing*, **6**, 847-866.

147. Harris R., 2005, Data policy challenges for remote sensing, *Remote Sensing Arabia*, Riyadh, Saudi Arabia, conference proceedings of, *International Society of Photogrammetry and Remote Sensing*.

148. Hastie T. J. and Tibshirani R. J., 1996, Discriminant adaptive nearest neighbor classification. *IEEE Transactions on Pattern Analysis and Machine Intelligence,* **18(6),** 607-615.

149. Hathaway, R.J., Bezdek, J.C. and Pedrycz, W., 1996. A parametric model for fusing heterogeneous fuzzy data, *IEEE Transactions on Fuzzy Systems*, **4**, 1277-1282.

150. Hebsur, A. V.,Muniappan N. and Rao,E.P., 2012, application of gpr in urban utility detection ranging and characterization, *14th International Conference on Ground Penetrating Radar(GPR)* June 4-8, Shanghai, China ISBN: 978-1-4673-2663-6.

151. Hebsur, A. V.,Muniappan N. Rao,E.P. and G., Venkatachalam, 2010, A Methodology for Detecting Buried Solids in Second-use Sites Using GPR, *Indian Geotechnical Conference – 2010, GEOtrendz December 16–18,*

152. Heremans,S., Bossyns, B., Eerens,H., Orshoven, J., 2012. Efficient collection of training data for sub-pixel land cover classification using neural networks. *International Journal of Applied Earth Observation and Geoinformation*. Volume **13**, Issue **4**, 657-667.

153. Hermes, L., Frieau D., Puzicha, J. and Buhmann J. M., 1999, Support Vector Machines for Land Usage Classification in Landsat TM Imagery, *Proceeding of IGARSS 1999*, vol. **1**, 348-350.

154. Herold, M., LIU, X. and Clarke, K.C., 2003, Spatial metrics and image texture for mapping urban land use. *Photogrammetric Engineering and Remote Sensing*, **69**, 991–1001.

155. Hore, P., Hall, P. and Goldgof, D. B., 2007 "Creating Streaming Iterative Soft Clustering Algorithms," *NAFIPS 07* , San Diego, pages 484-488,

156. Horn, B. K. P. and Schunck, B. G., 1981. Determining optical flow, *Artificial intelligence*, vol. **17**, no. **1**, 185–203.

157. Hou, Z., Qian, W., Huang, S., Hu, Q., and Nowinski, W.L., 2007. Regularized fuzzy *c*-means method for brain tissue clustering, *Pattern Recognition Letters*, vol **28**, no. **13**, 1788-1794.

158. Huang, C., Davis, L., S. and Townshend, J., R., G., 2002, An assessment of support vector machines for land cover classification, *International Journal of Remote Sensing*, vol. **23**, no. **4**, 725–749.

159. Hung, M. and Ridd, M.K., 2002, A subpixel classifier for urban land-cover mapping based on a maximum-likelihood approach and expert system rules. *Photogrammetric Engineering and Remote Sensing*, **68**, 1173–1180.

160. Hubert-Moy, L., Cotonnec, A., Le Du, L., Chardin, A. and Perez, P., 2001, A comparison of parametric classification procedures of remotely sensed data applied on different landscape units. *Remote Sensing of Environment*, **75**, 174–187.

161. Huete, A.R., 1988. A soil-adjusted vegetation index (SAVI), *Remote Sensing of Environment*, **25**, 3295-309.

162. Hughes G. F., 1968, On the mean accuracy of statistical pattern recognizers. *IEEE Transactions on Information Theory*, vol. **IT-14(1)**, 55–63.

163. Huguenin, R.L., Karaska, M.A., Blaricom, D.V. and Jensen, J.R., 1997, Subpixel classification of Bald Cypress and Tupelo Gum trees in Thematic Mapper imagery. *Photogrammetric Engineering and Remote Sensing*, **63**, 717–725.

164. Ibrahim, M. A., Arora, M. K., and Ghosh, S. K., 2005. Estimating and accommodating uncertainty through the soft classification of remote sensing data, *International Journal of Remote Sensing*, vol. **26**, no. **14**, 2995–3007.

165. Ishibuchi, H., Nozaki, K., Yamamoto, N. and Tanaka, H., 1995. Selecting fuzzy If-Then rules for classification problems using genetic algorithms, *IEEE Transactions on Fuzzy Systems*, **3**, 260-270.

166. Jackson, Q. andLandgrebe,D. A., 2002. Adaptive Bayesian contextual classification based on Markov random fields, *IEEE Transactions on Geoscience and Remote Sensing*, vol. **40**, no. **11**, 2454 – 2463.

167. Jacobsen, K., 2013**.** Characteristics of very high resolution optical satellites for topographic mapping. ISPRS WG IV/2 Workshop Interexpo GEO-Siberia- 2013, Novosibirsk, proceedings, 58-78.

168. Jain, A. K. and Dubes, R. C., 1988, Algorithms for Clustering Data. Prentice Hall, USA.

169. Jensen, J. R., 1996, *Introductory Digital Image Processing: A Remote Sensing Perspective* (2nd ed.) Prentice Hall PTR, USA, ISBN: 978-0131453616.

170. Jensen, J.R., 2000. *Remote sensing of the environment: An earth resource perspective*, (3rd ed.) Prentice-Hall, Inc., New Jersey,ISBN: 978-0131889507.

171. Jensen, J.R., 2005. *Introductory digital image processing: A remote sensing perspective*, (3rd ed.). Upper Saddle River: Prentice-Hall,ISBN: 978-0131453616,526.

172. Jeyakanthan V. S. and Sanjeevi, S.,2006, Capacity Estimation of Vaigai Reservoir Using Remote Sensing Data-A Soft Classification Approach, *International Conference on Environmental Geosciences-2006,* 15-16 February, Chennai.

173. Ji, M., 2003. Using fuzzy sets to improve cluster labeling in unsupervised classification, *International Journal of Remote Sensing*, **24**, 657-671.

174. Jordan, C.F., 1969. Derivation of leaf area index from quality of light on the forest floor, *Ecology*, **50**, 663-666.

175. Ju, J., Gopal, S. and Kolaczyk, E.D., 2005. On the choice of spatial and categorical scale in remote sensing land cover classification, *Remote Sensing of Environment*, **96**, 62-77.

176. Ju, J., Kolaczyk, E.D. and Gopal, S., 2003. Gaussian mixture discriminant analysis and sub pixel land cover characterization in remote sensing, *Remote Sensing of Environment*, **84**, 550-560.

177. Kamp, U., Growley, B.J., Khattak, G.A. and Owen, L.A., 2008. GIS-based landslide susceptibility mapping for the 2005 Kashmir earthquake region, *Geomorphology*, **101**, 631-642.

178. Kang, D.J.and Roh, K.S., 2001. A discontinuity adaptive Markov model for color image smoothing, *Image and Vision Computing*, vol. **19**, no. **6**, 369–379.

179. Kannan,S. R., Devi, R., Ramathilagam, S., and Takezawa, K., 2013. Effective FCM noise clustering algorithms in medical images, *Computers in Biology and Medicine*, vol. **43**, no. **2**, 73–83.

180. Kartikeyan, B., Sarkar, A. and Majumder, K.L., 1998. A segmentation approach to classification of remote sensing imagery. *International Journal of Remote Sensing*, **19**, 1695 - 1709.

181. Kasetkasem, T.,Arora,M. K. and Varshney,P. K., 2005. Super-resolution land cover mapping using a Markov random field based approach, *Remote Sensing of Environment*, vol. **96**, no. **3–4**, 302–314.

182. Kavzoglu, T. and Mather, P.M., 2004. The use of backpropagating artificial neural networks in land cover classification. *International Journal of Remote Sensing*, **24**, 4907–4938.

183. Keerthi, S. S., 2002. Efficient Tuning of SVM Hyperparameters Using Radius/Margin Bound and Iterative Algorithms, *IEEE Transactions on Neural Networks*, Vol. **13**, No. **5**.

184. Keramitsoglou, I., Sarimveis, H., Kiranoudis, C.T., Kontoes, C., Sifakis, N., and Fitoka, E., 2006. The performance of pixel window algorithms in the classification of habitats using VHSR imagery. *ISPRS Journal of Photogrammetry & Remote Sensing*, **60**: 225–238.

185. Kerle, N. and Oppenheimer, C., 2002. Satellite remote sensing as a tool in Lahar disaster management,*Disasters*, **26**, 140-160.

186. Keshava, N. and Mustard, J.F., 2002. Spectral unmixing, *IEEE Signal Processing*, **19**, 44-57.

187. Keuchel, J., Naumann, S., Heiler, M., and Siegmund, A., 2003. Automatic land cover analysis for Tenerife by supervised classification using remotely sensed data, *Remote Sensing of Environment* , **86**, 530–541.

188. Kirkpatrick, S., Gelett, C. D., and Vecchi, M.P., 1983. Optimization by simulated annealing, *Statistical Science*, vol **220**, 621-630.

189. Kivinen, J. and Warmuth, M., 1999: Boosting as Entropy Projection. In: *Proc. 12th Ann. Conf. Computational Learning Theory*, 134–144.

190. Kitaw, H. G., 2007. Image pan-sharpening with Markov random field and simulated annealing.

191. Klir, G.J., 1990. A principle of uncertainty and information variance, *International Journal of General System*, **17**, 249-275.

192. Klir, G.J., and Yuan, B., 1995. Fuzzy Sets and Fuzzy Logic Theory and Applications. Prentic Hall, USA.

193. Kontoes, C.C. and Rokos, D., 1993. The integration of spatial context information in an experimental knowledge based system and the supervised relaxation algorithm: two successful approaches to improving SPOT-XS classification. *International Journal of Remote Sensing*, **17**, 3093–3106.

194. Kontoes, C.C. and Rokos, D., 1996, The integration of spatial context information in an experimental knowledge based system and the supervised relaxation algorithm: two successful approaches to improving SPOT-XS classification. *International Journal of Remote Sensing*, **17**, 3093–3106.

195. Koggalage R., and Halgamuge, S., 2004. Reducing the Number of Training Samples for Fast Support Vector Machine Classification, *Neural Information Processing – Letters and Reviews* Vol. **2**, No. **3**.

196. Kolaczyk, E. D., 2003. On the Use of Prior and Posterior Information in the SubpixelProportion Problem, *IEEE Transactions on Geoscience And Remote Sensing*, Vol. **41**, No. **11**.

197. Koza, J. R., 1992. *Genetic Programing: on the programming of computers by natural selection*, MIT, Cambridge, MA.

198. Krishnapuram, R. and Keller, J.M., 1993. A possiblistic approach to clustering. *IEEE Transactions on Fuzzy Systems*, **1**, 98-108.

199. Krishnapuram, R. and Keller, J.M., 1996. The possibilistic c-means algorithm: Insights and recommendations, *IEEE Transactions on Fuzzy Systems*, **4**, no. **3**, 385-393.

200. Kuzera, K. and Pontius Jr, R., 2004. Categorical coefficients for assessing soft-classified maps at multiple resolutions. In Conference proceedings of the joint meeting of The Fifteenth *Annual Conference of The International Environmetrics Society and The Sixth Annual Symposium on Spatial Accuracy Assessment in Natural Resources and Environmental Sciences*. Portland ME, volume **28**.

201. Kulkarni, A.D. and Lulla, K., 1999. Fuzzy neural network models for supervised classification: multispectral image analysis. *Geocarto International*, **14**, 42–50.

202. Kumar, A., Ghosh, S. K., and Dadhwal, V. K., 2006. Sub-Pixel Land Cover Mapping: SMIC System. *ISPRS International Symposium on "Geospatial Databases for Sustainable Development*" Goa, India, September 27- 30.

203. Kumar, A., Ghosh, S.K. and Dadhwal, V.K., 2007. Full fuzzy land cover mapping using remote sensing data based on fuzzy c-means and density estimation. *Can. J. Remote sensing*, **33(2)**: 81-87.

204. Kumar, A. Ghosh, S. K & Dadhwal, V. K., 2007a. Subpixel classifiers: fuzzy theoryversus *statistical learning algorithm.SPIE*, vol **27**, no. **1-2**, 153-176.

205. Kumar, A. Ghosh. S. K.&Dadhwal, V. K., 2007b. A comparison of the performance of fuzzy algorithm versus statistical algorithm based sub-pixel classifier for remote sensing data, *ISPRS Commission VII Mid-term Symposium, Remote Sensing : From Pixels to Processes*Enscheded, Netherlands, 8-11 May 2006.

206. Kumar, A. and Dadhwal, V. K., 2010. Entropy-based fuzzy classification parameter optimization using uncertainty variation across spatial resolution, *Journal of the Indian Society of Remote Sensing*, vol. **38**, no. **2**, 179–192.

207. Landgrebe, D.A., 2003, *Signal Theory Methods in Multispectral Remote Sensing* (Hoboken, NJ: John Wiley and Sons).

208. Lakshmi, S. V. and Sanjeevi, S., 2003. Spatial Resolution and Classification Accuracy – Implications for sub-pixel Classification. *Proceedings of the International Conference on Geomatics* 2003: Retrospect and Prospect. New Delhi 2003. Remote Sensing Technology Trends and Geomatics Applications.

209. Latifovic, R., & Olthof, I., 2004. Accuracy assessment using sub-pixel fractional error matrices of global land cover products derived from satellite data. *Remote Sensing of Environment* ,90 , 153 − 165.

210. Lawrence, R., Bunn, A., Powell, S. and Zmabon, M., 2004. Classification of remotely sensed imagery using stochastic gradient boosting as a refinement of classification tree analysis. *Remote Sensing of Environment*, **90**, 331–336.

211. Lee, T.W., Lewicki, M.S. and Sejnowski, T.J., 2000. ICA mixture models for unsupervised classification of non-gaussian classes and automatic context switching in blind signal

separation. *IEEE Transactions on Pattern Analysis and Machine Intelligence*, **22**, 1078–1089.

212. Lee, S. and Lathrop, R. G., 2005. Sub-pixel estimation of urban land cover components with linear mixture model analysis and Landsat Thematic Mapper imagery, Volume **26**, Number 22 / 20 November, 4885 – 4905.

213. Lewis, H. G., & Brown, M., 2002. A generalized confusion matrix for assessing area estimates from remotely sensed data.*International Journal of Remote Sensing*, **22**, 3223−3235.

214. Li, J., 2013. " Texture Classification of Landsat TM Imagery using Bayes Point Machine". Published in: *Proceeding ACMSE '13 Proceedings of the 51st ACM Southeast Conference* Article No. 16.ISBN: 978-1-4503-1901-0. ACM New York, NY, USA.

215. Li, R.P. and Mukaidono, M., 1999. Gaussian clustering method based on maximum-fuzzy entropy interpretation. *Fuzzy Sets and Systems* **102**, 253–258

216. Li, S. Z., 1990. Reconstruction without discontinuities, in *Computer Vision, Proceedings, Third International Conference on Computer Vision,* 709-712.

217. Li, S. Z., 1995. On discontinuity-adaptive smoothness priors in computer vision, *IEEE Transactions on Pattern Analysis and Machine Intelligence*, vol. **17**, no. **6**, 576 –586.

218. Li, S. Z.,1995a. Discontinuous mrf prior and robust statistics: a comparative study, *Image and Vision Computing*, vol. **13**, no. **3**, 227–233.

219. Li, S. Z., 2009.*Markov random fields modeling in image analysis: e-book*, Third edition. London: Springer.

220. Lillesand, T.M. and Kiefer, R.W., 1999. *Remote Sensing and Image Interpretation* (4th ed.). John Wiley & Sons, Inc, ISBN: 978-0470052457.

221. Lillesand, T.M., Kiefer, R.W. and Chipman, J.W., 2008. *Remote sensing and image interpretation*. New York: John Wiley and Sons.

222. Lippman, R. P., 1987, An introduction to computing with neural nets. *IEEE ASSP Magazine*, **4**, 2–22.

223. Little, R.J., Rubin, D.B., 2002.Statistical Analysis with Missing Data, 2nd edn. John Wiley and Sons, New York.

224. Liu, W. and Wu, E. Y., 2005. Comparison of nonlinear mixture models: Sub-pixel classification. *Remote Sensing of Environment*, **94**, 145–154.

225. Lobell, D.B., Asner, G.P., Law, B.E. and Treuhaft, R.N., 2002. View angle effects on canopy reflectance and spectral mixture analysis of coniferous forests using AVIRIS. *International Journal of Remote Sensing*, **23**, 2247–2262.

226. Lobo, A., Chic, O. and Casterad, A., 1996, Classification of Mediterranean crops with multisensor data: per-pixel versus per-object statistics and image segmentation. *International Journal of Remote Sensing*, **17**, 2385–2400.

227. Lu, D., Mausel, P., Batistella, M. and Moran, E., 2004. Comparison of land cove classification methods in the Brazilian Amazon basin, *Photogrammetric Engineering and Remote Sensing*, **70**, 723-732.

228. Lu, D. and Weng, Q., 2007. A survey of image classification methods and techniques for improving classification performance. *International Journal of Remote Sensing*, **28 (5)**, 823–870.

229. Lucas, N. S., Sanjeevi, S., and Barnsley, M. J., 2002, Sub-pixel habitat mapping of a coastal dune ecosystem, *Applied Geography*, **22**, 253-270.

230. Lyon, J.G.,Yuan, D., Lunetta, R.S. and Elvidge, C.D., 1997. A change detection experiment using vegetation indices, *Photogrammetric Engineering and Remote Sensing*, **64**, 143-150.

231. MacAlister, C., and Mahaxay, M., 2008. Mapping wetlands in the Lower Mekong Basin for wetland resource and conservation management using Landsat ETM images and field survey data. *Journal of Environmental Management*, xxx (2008), 1–8.

232. MacKay, H., Finlayson, C.M., Ferna´ ndez-Prieto, D., Davidson, N., Pritchard, D., Rebelo, L.M., 2009. The role of Earth Observation (EO) technologies in supporting implementation of the Ramsar Convention on Wetlands. *Journal of Environmental Management*, xxx (2009), 1–9.

233. Macleod, R.D., and Congalton, R.G., 1998. A quantitative comparison of change-detection algorithms for monitoring eelgrass from remotely sensed data. *Photogrammetric Engineering and Remote Sensing*, **64**, 207–216.

234. Magnussen, S., Boudewyn, P., and Wulder, M., 2004. Contextual classification of Landsat TM images to forest inventory cover types, *International Journal of Remote Sensing*, vol. **25**, no. **12**, 2421–2440.

235. Manfred, O. and Winther, O. 2000, Gaussian Processes for Classification: Mean Field Algorithm, Neural Computation, vol. **12**, No. **11**, 2655-2684.

236. Mannan, B. and Ray, A.K., 2003, Crisp and fuzzy competitive learning networks for supervised classification of multispectral IRS scenes. *International Journal of Remote Sensing*, **24**, 3491–3502.

237. Mantero, P., Moser, G. and Serpico, S. B., 2005, Partially Supervised Classification of Remote Sensing Images Through SVM-Based Probability Density Estimation. *IEEE Transactions on Geoscience and Remote Sensing*, Vol. **43**, No. **3**.

238. Markham, B.L. and Barker, I.J., 1986. Landsat MSS and TM post-calibration dynamic ranges, exoatmospheric reflectances and at-satellite temperatures. *EOSAT Landsat Technical Notes*, **1**, 3-8.

239. Maselli, F., Rodolf, A. and Conese, C., 1996. Fuzzy classification of spatially degraded Thematic Mapper data for the estimation of sub-pixel components, *International Journal of Remote Sensing*, **17**, 537-551.

240. Massone, A.M., Masulli, F. and Petrosini, A., 2000. Fuzzy clustering algorithms and Landsat images for detection of waste areas: A comparison. In Advances in Fuzzy Systems and Intelligent Technologies,*Proc. WILF '99, Italian Workshop on Fuzzy Logic*, Shaker Publishing, Maastricht, The Netherlands, 165-175.

241. Mather, P. M., 1999, *Computer processing of remotely –sensed images: an introduction* 2nd edition. John Wiley and Sons.Chichester, NY.

242. Mattera, D. and Haykin, S., 1999, Support vector machines for dynamic reconstruction of a chaotic system. In Scholkopf et al, editors, Advances in Kernel Methods – Support Vector Learning, Cambridge, MA, MIT Press, 211-242.

243. Maulik, U. and Bandyopadhyay, S., 2003, "Performance Evaluation of Some Clustering Algorithms and Validity Indices", *IEEE Transactions on Pattern Analysis and Machine Intelligence*, vol. **24**, no. **12**, 1650-1654,

244. Maulik, U. and Sarkar,A., 2013 "Efficient Parallel Algorithm for Pixel Classification in Remote Sensing Imagery", *Geoinformatica* (accepted)

245. Mausel, P.W., Kramber, W.J. and Lee, J.K., 1990, Optimum band selection for supervised classification of multispectral data. *Photogrammetric Engineering and Remote Sensing*,**56**, 55–60.

246. Melgani, F. and Serpico, S. B., 2003. A Markov random field approach to spatio-temporal contextual image classification, *Geoscience and Remote Sensing, IEEE Transactions on*, vol. **41**, no. **11**, 2478–2487.

247. Mercier, G. and Marc, L. 2003, Support Vector Machines for Hyper-spectral Image Classification with Spectral-based kernels, *Proceeding of IGARSS 2003*.

248. Mertens, K. C., Verbeke, L. P. C., Ducheyne, E. I. and De Wulf, R. R., 2003, Using genetic algorithms in sub-pixel mapping, *International Journal of Remote Sensing*, 10 November, Vol. **24**, No. **21**, 4241–4247.

249. Metropolis, N.,Rosenbluth, A. W.,Rosenbluth, M. N., Teller, A. H. and Teller, E., 1953. Equation of state calculations by fast computing machines, *The journal of chemical physics*, vol. **21**, 1087.

250. Metternicht, G.I. and Zinck, J.A., 1998. Evaluating the information contents of JERS-1 SAR and LANDSAT TM data for discrimination of soil erosion features, *Photogrammetric Engineering and Remote Sensing*, **53**, 143-153.

251. Meyer, M. and L. Werth, 1990, Satellite Data: Management Panacea or Potential Problem? *Journal of Forestry*, **88 (9)**, 10-13.

252. Mitra, P., Shankar, B.U. and Pal, S.K., 2004, Segmentation of multispectral remote sensing images using active support vector machines. *Pattern Recognition Letters*, **25**, 1067–1074.

253. Miyamoto, S., Ichihashi, H. and Honda, K., 2008. *Algorithms for Fuzzy Clustering: Methods in c-Means Clustering with Applications*, Springer, ISBN: 978-3-540-78737-2, 46-66.

254. Miyamoto, S., Yasukochi, T., Inokuchi, R., 2005. A Family of Fuzzy and Defuzzified c Means Algorithms. In: *Proc. of the International Conference on Computational Intelligence for Modelling, Control and Automation*, Vienna, Austria, 170–176.

255. Miyamoto, S., Mukaidono, M., 1997. Fuzzy c-means as a regularization and maximum entropy approach. In: Proc. of the *7th International Fuzzy Systems Association World Congress (IFSA 1997)*, Prague, Czech, June 25-30, 1997, vol. **II**, 86–92.

256. Mohan B.K., Devasthale A.D. and Rao E. P., 2002. Generation Of Optimial Quantization Table For A Rate Constrained Version Of JPEG Using *Genetic Algorithm. International Symposium ISPRS 2002,* Hyderabad, 3-6 Dec. 2002.

257. Mohan B.K.,Satish U., and Rao E. P.,2003. Segmentation of high resolution imagery. *International Conference MAP ASIA 2003* at Kuala Lumpur, Malaysia.

258. Mohan B.K.,RaviBabu A., Bimal G., and Rao E. P., 2004. Region segmentation and classification of high resolution imagery. *Proc. Asian Conference on Remote Sensing*, Chiang Mai, Thailand, November 2004.

259. Moody, A., 1998, Using Landsat spatial relationships to improve estimates of land-cover area from coarse resolution remote sensing. *Remote Sensing of Environment*, **64**, 202–220.

260. Moreira, F., Almeida-Filho R. and Câmara G., 2003, Evaluation of The Performance of Fuzzy Logic Applied In Spatial Analysis For Mineral Prospecting. *Revista Brasileira de Geociências*, v.**33**, 183 – 190.

261. Moser, G. andSerpico, S. B., 2010. Contextual remote-sensing image classification by support vector machines and Markov random fields, *Geoscience and Remote Sensing Symposium (IGARSS), IEEE International*, **25**, 3728–3731.

262. Mukherjee, S. Osuna, E. and Girosi, F., 1997, Nonlinear prediction of chaotic time series using support vector machine. In *proceedings of the IEEE Workshop on Neural Networks for Signal Processing*, 7, Amerlia Island, FL, 511-519.

263. Muller, K.R., Smola, A. Ratsch, G., Scholkopf, B., Kohlmorgen, J. and Vapnik, V., 1997, Predicting time series with support vector machines. In proceedings, *International Conference on Artificial Neural Networks, Springer Lecture Notes in Computer Science*, 999.

264. Murai, H. and Omatu S., 1997, Remote sensing image analysis using a neural network and knowledge-based processing. *International Journal of Remote Sensing*, Vol. **18**, no**. 4**, 811–828.

265. Murtagh, B. A. and Saunders, M. A., 1987, *MINOS 5.1 user's guide. (SOL 83-20R)*, Standford University.

266. Myint, S.W., 2001, A robust texture analysis and classification approach for urban land-use and land-cover feature discrimination. *Geocarto International*, 16, 27–38.

267. Myint, S. W., 2006, Urban vegetation mapping using sub-pixel analysis and expert system rules: A critical approach, Volume **26**, Number 22 / 20 November, 4885 – 4905.

268. Neville, R.A., Levesque, J., Staene, K., Nadeau, C., Hauff, P. and Borstad, G.A., 2003,Spectral unmixing of hyperspectral imagery for mineral exploration: comparison of results from SFSI and AVIRIS. *Canadian Journal of Remote Sensing*, **29**, 99–110.

269. Nguyen, H.H. and Cohen, P., 1993. Gibbs random fields, fuzzy clustering, and the unsupervised segmentation of textured images. Graphical Models and Image Processing, **55(1):**1 - 19.

270. Okeke, F.,and Karnieli, A., 2006 Methods for fuzzy classification and accuracy assessment of historical aerial photographs for vegetation change analyses. Part I: Algorithm development, *International journal of remote sensing*, vol. **27**, no. **1**, 153–176.

271. Oki, K., Uenishi, T.M., Omasa, K. and Tamura, M., 2004. Accuracy of land cover area estimation from coarse spatial resolution images using an unmixing method, *International Journal of Remote Sensing*, **25**, 1673-1683.

272. Okin, G.S., Roberts, D.A., Murray, B. and Okin, W.J., 2001, Practical limits on hyperspectral vegetation discrimination in arid and semiarid environments. Remote Sensing of Environment, **77**, 212–225.

273. Olgun, E., 2000. Izmit (Turkey) earthquake, August 17, 1999 and the Application of Change Detection Techniques for Damage Assessment Using Spot4 Satellite Images (Individual Final Assignment). Enschede: *International Institute of Aerospace Survey and Earth Observation.*

274. Olthof, I., King, D.J. and Lautenschlager, R.A., 2004, Mapping deciduous forest ice storm damage using Landsat and environmental data. *Remote Sensing ofEnvironment*, **89**, 484–496.

275. Oommen, T. and Baise, L.G., 2008. A new approach to liquefaction potential mapping using satellite remote sensing and support vector machine algorithm, *IEEE Geoscience and Remote Sensing Symposium*, 7-11 July 2008,Bostan, Massachusetts, U.S.A.,**III**, 51-54.

276. Opper, M. and Winther O., 2000, Gaussian Processes for Classification: Mean Field Algorithms, *Neural Computation*, vol. **12**, No.**11**, 2655-2684.

277. Osoba, O., Mitaim, S., & Kosko, B., 2013. Noise benefits in the expecta-tion–maximization algorithm: NEM theorems and models. In *The 2013 inter- national joint conference on neural networks(IJCNN)* (3178–3183)

278. Osuna, E., Freund, R. and Girosi, F., 1997, An improved training algorithm for support vector machines. In Proceedings of the *IEEE Workshop on Neural Networks for Signal Processing* VII, New York, 276-285.

279. Ozdarici, A. and Turker, M., 2006. Field-based classification of agricultural crops using multi-scale images. *1st international conference on geographic object-based image analysis*, 4-5 July 2006. Salzburg, Austria.

280. Ozdogan, M., & Woodcock, C. E., 2006. Resolution dependent errors in remote sensing of cultivated areas. *Remote Sensing of Environment*, **103**,203−217

281. Pal M., and Mather, P. M., 2001a, Decision Tree classifiers and land use classification. In Proceedings of the *27th Annual Conference of the Remote Sensing Society*, 12-14 September, London, UK.

282. Pal M. and Mather, P. M., 2001b, Decision Tree Based Classification of Remotely Sensed Data.In Proceedings of the *22nd Asian Conference of Remote Sensing*,5-9 November, Singapore.

283. Pal M. and Mather, P. M., 2002, A Comparison of Decision Tree and Backpropagation Neural Network Classifiers for Land Use Classification. *IEEE Geoscience and Remote Sensing Symposium 2002*, Toronto, Canada. 24-28 June 2002. Published.

284. Pal M. and Mather, P. M., 2003a, Decision tree and support vector classifiers for land cover classification: a case study using InSAR data. *Symposium on Microwave Remote Sensing, IIT Bombay*, Mumbai, 21-24 January 2003.

285. Pal, M. and Mather, P., M., 2003b, Support Vector classifiers for Land Cover Classification, *Proceeding of Map India 2003 Conference*, New Delhi, India.

286. Pal, M. and Mather, P. M., 2003c, An Assessment of the Effectiveness of Decision Tree Methods for Land cover Classification. *Remote Sensing of Environment*. **86**, 554-565.

287. Pal, M., and Mather, P. M., 2004, Assessment of the effectiveness of support vector machines for hyperspectral data. *Future Generation Computer Systems*, **20(7)**, 1215-1225.

288. Pal, M., 2005, Multiclass Approaches for Support Vector Machine Based Land Cover Classification. Proc.Map India, *8th annual international conference and exhibition in the field of GIS, GPS, Arial Photography, and Remote Sensing*, New Delhi.

289. Pal M. and Mather P. M., 2005, Support Vector Machines for Classification in Remote Sensing. *International Journal of Remote Sensing*, **26(5)**, 1007-1011.

290. Pal, M. 2006a, M5 Model Tree for Land Cover Classification. *International Journal of Remote Sensing*, **27(4)**, 825-831.

291. Pal, M., 2006b, Class decomposition Approaches for land cover classification, *International Symposium of Geoinformation*, 19-21 September, Universititechnologi MARA, Shah Alam, Selangor, Malaysia.

292. Pal, M., 2006c, Error Corrected Output Coding Based Class Decomposition approach for Remote Sensing Classification.*International Journal of Remote Sensing*, Vol. **27**, No. **14**, 2863–2876.

293. Pal, M., 2006d, Support Vector Machines Based Feature Selection for land cover classification: a case study with DIAS Hyperspectral Data. *International Journal of Remote Sensing*, Vol. **27**, No. **14**, 2877–2894.

294. Pal, M. and Mather, P. M., 2006, Some issues in the classification of DAIS hyper-spectral data, *International Journal of Remote Sensing*, Vol. **27**, No. **14**, 20 July, 2895–2916.

295. Pal, N.R. and Bezdek, J.C., 1995. On cluster validity for the Fuzzy c-Means model,*IEEE Transaction on Fuzzy System*, **3**, 370-379.

296. Palanisamy S.,Yu-Hwan A. and Sanjeevi, S., 2006,A comparison of the classification of wetland characteristics by linear spectral mixture modelling and traditional hard classifiers on multispectral remotely sensed imagery in southern India, *Ecological Modelling*, **194**, 379–394.

297. Palubinskas, G., Lucas, R.M., Foody, G.M. and Curran, P., 1995. An evaluation of fuzzy and texture based classification approaches for mapping regenerating tropical forest classes from Landsat TM data, *International Journal of Remote Sensing*, **16**, 747-759.

298. Paola, J.D. and Schowengerdt, R.D., 1995. Review article: A review and analysis of backpropagation neural networks for classification of remotely sensed multispectral imagery, *International Journal of Remote Sensing*, **16**, 3033-3058.

299. Paulsson, B., 1992. *Urban Applications of Satellite Remote Sensing and GIS Analysis*, (Urban Management Program, No 9), Washington D.C., ISBN: 978-0821322666.

300. Pateriya, B., Siva Subramanian, K.S., Kar, D., Ranjan, R. and Razdan, N., 2007. Reliable remote sensing – test case – a comparison with supply chain-mandis/millers. Map World Forum 2007: MWF PN 36.

301. Pathak, V. and Dikshit, O., 2004. Segment based classification of Indian urban environment. In: *3rd International Symposium on New Technologies for Urban Safety of Mega Cities in Asia*, 18-19, Agra, India.

302. Peddle, D.R. and Ferguson, D.T., 2002, Optimization of multisource data analysis: an example using evidential reasoning for GIS data classification. *Computers & Geosciences*, **28**, 45–52.

303. Penaloza, M.A. andwelch, R.M., 1996, Feature selection for classification of polar regions using a fuzzy expert system. *Remote Sensing of Environment*, **58**, 81–100.

304. Perez, P 1998. Markov Random Fields and Images, *CWI Quarterly*, vol 11, no. 4, pp 413-437.

305. Pham, D., 2001. Spatial Models for Fuzzy Clustering, *Computer Vision and Image Understanding*, vol. **84**, no. **2**, 285–297.

306. Pinoli, J.C., and Debayle, J., 2009. General Adaptive Neighborhood Mathematical Morphology,in *2009 16th IEEE International Conference on Image Processing (ICIP)*, 2009, 2249 –2252.

307. Pizurica, A 2002. Image Denoising using Wavelets and Spatial Context Modelling, PhD Thesis, Ghentt University.

308. Platt, R.V. and Goetz, A.F.H., 2004. A comparison of AVIRIS and Landsat for land use classification at the urban fringe. *Photogrammetric Engineering and Remote Sensing*, **70**, 813–819.

309. Pontius Jr, R. G. and Cheuk, M. L., 2006. A generalized cross tabulation matrix to compare soft classified maps at multiple resolutions, *International Journal of Geographical Information Science*, vol. **20**, no. **1**, 1–30.

310. Pontius Jr, R. G. and Connors, J., 2006. Expanding the conceptual, mathematical and practical methods for map comparison. In Spatial Accuracy Meeting, Lisbon, Portugal. Available from www. clarku. edu/rpontius.

311. Powell, R.L., Matzke, N., De Souza JR, C., Clark, M., Numata, I., Hess, L.L. and Roberts, D.A., 2004, Sources of error in accuracy assessment of thematic land-cover maps in the Brazilian Amazon. *Remote Sensing of Environment*, **90**, 221–234.

312. Price, J.C., 2003, Comparing MODIS and ETM+ data for regional and global land classification. *Remote Sensing of Environment*, **86**, 491–499.

313. Rashed, T., Weeks, J.R., Gadalla, M.S. and Hill, A.G., 2001, Revealing the anatomy of cities through spectral mixture analysis of multispectral satellite imagery: a case study of the Greater Cairo region, Egypt. *Geocarto International*, **16**, 5–15.

314. Refaat M M. and Farag A. A, 2003, A New Unsupervised Approach for the Classification of Multispectral Data, Proc. *6th International Conference on Information Fusion*, Queensland, Australia, 951-958, Jul. 8-11.

315. Refaat, M. M. and Farag, A. A., 2004, Mean Field Theory for density Estimation Using Support Vector Machines, Computer Vision and Image Processing Laboratory, University of Louisville, Louisville, KY, 40292.

316. Rehm, F., Klawonn, F., Kruse, R., 2007. A novel approach to noise clustering for outlier detection. *Soft Computing* 11 (2007): 489–494.

317. Reulke,R. and Lippock,A., 2008. Markov Random Field based texture segmentation for road extraction, The *International Archives of Photogrammetry, Remote Sensing and Spatial information Sciences*, vol **XXXVII**, part **B3b**, Beijing.

318. Richards, J. A. and Jia, X., 2005, Remote sensing digital image analysis: an introduction, 3rd edition. Springer Verlag, berlin, Heidelberg, New York.

319. Ricotta, C., 2004. Evaluating the classification accuracy of fuzzy thematic maps with a simple parameteric measure, *International Journal of Remote Sensing*, vol **25**, no. **11**, 2169-2176.

320. Ricotta, C. and Avena, G. C. 2006. Evaluating the degree of fuzziness of thematic maps with a generalized entropy function: a methodological outlook, *International Journal of Remote Sensing*, vol **23**, no. **20**, pp 4519-4523.

321. Roberts, D. A., Smith, M. O., and Adams, J. B., 1993. Green vegetation, non-photosynthetic vegetation and soils in AVIRIS data. *Remote Sensing of Environment*, **44**, 255–269.

322. Roberts, D.A., Gardner, M., Church, R., Ustin, S., Scheer, G. and Green, R.O., 1998b, Mapping chaparral in the Santa Monica mountains using multiple end member spectral mixture models. *Remote Sensing of Environment*, **65**, 267–279.

323. Royle, J.A., Koneff, M.D., and Reynolds, R.E., 2002. Spatial modeling of wetland condition in the U.S. Prairie pothole region. Biometrics, **58 (2)**: 270-279.

324. Safavian, S. R., and Landgrebe, D., 1991, A survey of decision tree classifier methodology. *IEEE Transactions on Systems, Man, and Cybernetics*, **21**, 660–674.

325. Saha,I.,Maulik, U., Bandyopadhyay, S. and Plewczynsk,D. "Unsupervised and Supervised learning approaches together for Microarray Analysis", *Fundamenta Informatica*, vol. **106**, no. **1**, 45-73, 2010.

326. Salzenstein, F., and Collet, C., 2006. Fuzzy markov random fields versus chains for multispectral image segmentation. *IEEE Trans. on Pattern Anal. Machine Intell*., **PAMI-28(11)**, 1753–1767.

327. San Miguel-Ayanz, J. and Biging, G.S., 1997, Comparison of single-stage and multi-stage classification approaches for cover type mapping with TM and SPOT data. *Remote Sensing of Environment*, **59**, 92–104.

328. Sanchez-Hernandez, C., Boyed, D.S. and Foody, G.M. "One-Class Classification for Mapping a Specific Land-Cover Class: SVDD Classification of Fenland*." IEEE Transactions on Geoscience and Remote Sensing*, 45(2007), 1061-1073.

329. Sanjeevi, S. and Barnsley, M., 1998, Linear Spectral Unmixing of *CASI* data for habitat mapping and management in a coastal dune system. *Proceedings of the International Symposium on Geoscience and Remote sensing (IGARSS 98)* Seattle, USA.

330. Sanjeevi, S., and Barnsley, M. J., 2000, Spectral unmixing of Compact Airborne Spectrographic Imager (CASI) data for quantifying sub-pixel proportions of parameters in a coastal dune system, Photonirvachak , *Journal of the Indian Soc. of Remote Sensing*, **28 (2-3)**, 187-204.

331. Sanjeevi, S. and Lucas, N., 2000, Sub-pixel Habitat Mapping in Coastal Dune Ecosystems Using Linear Mixture Model and Fuzzy Membership Functions. Proceedings of the *28th International Symposium on Remote Sensing of Environment*. Cape Town. South Africa.

332. Schmidt, K.S., Skidmore, A.K., Kloosterman, E.H., Van Oosten, H., Kumar, L. and Janssen, J.A.M., 2004, Mapping coastal vegetation using an expert system and hyper spectral imagery. *Photogrammetric Engineering and Remote Sensing*, **70**, 703–715.

333. Schowengerdt, R.A., 1996, On the estimation of spatial-spectral mixing with classifier likelihood functions. *Pattern Recognition Letters*, **17**, 1379–1387.

334. Seetha, M., Muralikrishna, I.V. and Deekshatulu, B.L., 2007. Comparison of Advanced Techniques of Image Classification, *Proc. of Map World Forum*, Hyderabad, India, 22-25 January.

335. Sellers, P.J., Meeson, B.W., Hall, F.G.,Asrar, G., Murphy, R.E.,Schiffer, R.A.,Bretherton, F.P., Dickinson, R.E., Ellingson, R.G., Field, C.B., Huemmrich, K.F., Justice, C.O., Melack, J.M., Roulet, N.T., Schimel, D.S. and Try, P.D., 1995. Remote sensing of the land surface for studies of global change: models-algorithms-experiments, *Remote Sensing of Enviro.*, **51**, 3-26.

336. Sengar, S. S., Kumar,A., Ghosh, S.K. & Wason, H. R.,2013. Liquefaction Identification Using IRS-1D Temporal Indices Data. *Journal of the Indian Soc. of Remote Sensing* (June 2013) **41(2)** ,355–363 DOI 10.1007/s12524-012-0239-y

337. Shaban, M.A. and Dikshit, O., 2001. Improvement of classification in urban areas by the use of textural features: The case study of Lucknow city, Uttar Pradesh, *International Journal of Remote Sensing*, **22**, 565-593.

338. Shabanov, N. V., Lo, K., Gopal, S., and Myneni, R. B., 2005. Subpixel burn detection in Moderate Resolution Imaging Spectro-radiometer 500-m data with ARTMAP neural networks. *Journal of Geophysical Research,* **110**, 1−17.

339. Shah, C.A., Arora, M.K. and Varshney, P.K., 2004, unsupervised classification of hyperspectral data: an ICA mixture model based approach. *International Journal of Remote Sensing*, **25**, 481–487.

340. Shalan, M.A., Arora, M.K. and Ghosh, S.K., 2003. An evaluation of fuzzy classifications from IRS 1C LISS III imagery: a case study, *International Journal of Remote Sensing*, **24**, 3179-3186.

341. Shannon, C. E., 1948. A Mathematical Theory of Communication. *Bell System Technical Journal* **27 (3)**, 379–423.

342. Shannon, C. E., 1951. Prediction and Entropy of Printed English. *Bell System Technical Journal* **30 (1)**, 50–64.

343. Sharma, K.M.S. and Sarkar, A., 1998. A modified contextual classification technique for remote sensing data. *Photogrammetric Engineering and Remote Sensing*, **64**, 273–280.

344. Shi, W. Z., Ehlers, M. and Temphli, K., 1999, Analytical modeling of positional and thematic uncertainty in integration of remote sensing and geographical information systems, *Transactions in GIS*, **3**, 119-136.

345. Sidle, R.C. and Ochiai, H., 2006. Landslides: processes, prediction, and landuse. American Geophysical Union, Washington, D.C., *Water Resources Monograph*, **18**, 312.

346. Silván-Cárdenas, J. L., and Wang,L., 2008. Sub-pixel confusion–uncertainty matrix for assessing soft classifications, *Remote Sensing of Environment*, vol. **112**, no. **3**, 1081–1095.

347. Silva M., Câmara G., Souza R., Valeriano D. and Escada I., 2005, Mining Patterns of Change in Remote Sensing Image Databases. Fifth *IEEE International Conference on Data Mining*. Houston, TX, USA, November.

348. Simone, G., Farina, A., Morabito, F.C., Serpico, S.B. and Bruzzone, L., 2002, Image fusion techniques for remote sensing applications. *Information Fusion*, **3**,3–15.

349. Singhroy, V. and Mattar, K., 2000. SAR image techniques for mapping areas of landslides *Proc. of International Society for Photogrammetry and Remote Sensing Conference*, Amsterdam, 1395-1402.

350. Sluiter, R., 2005. *Mediterranean land cover change*. Doctoral dissertation. Utrecht: Universiteit Utrecht, Department of Physical Geography.

351. Sohn, Y., Moran, E. and Gurri, F., 1999, Deforestation in north-central Yucatan (1985–1995): mapping secondary succession of forest and agricultural land use in Sotuta using the cosine of the angle concept. *Photogrammetric Engineering and Remote Sensing*, **65**, 947–958.

352. Sohn, Y. and Rebello, N.S., 2002, Supervised and unsupervised spectral angle classifiers. *Photogrammetric Engineering and Remote Sensing*, **68**, 1271–1281.

353. Solaiman, B., Pierce, L.E. and Ulaby, F.T., 1999, Multisensor data fusion using fuzzy concepts: application to land-cover classification using ERS-1/JERS-1 SAR composites. *IEEE Transactions on Geoscience and Remote Sensing*, **37**, 1316–1326.

354. Solberg, A. H. S., Taxt,T., and Jain, A. K. 1996. "A Markov random field model for classification of multisource satellite imagery," *IEEE Transactions on Geoscience and Remote Sensing*, vol. **34**, no. **1**, 100 –113.

355. Smits, P. C. and Dellepiane,S., 1996. Information fusion in a Markov random field-based image segmentation approach using adaptive neighbourhoods, in *Pattern Recognition, Proceedings of the 13th International Conference on*, 1996, vol. **2**, 570–575.

356. Smits, P. C. andDellepiane,S., 1997. Discontinuity adaptive MRF model for remote sensing image analysis, in *Geoscience and Remote Sensing, IGARSS97. Remote Sensing - A Scientific Vision for Sustainable Development, IEEE International*, vol. **2**, 907 –909.

357. Smits, P. C. and Dellepiane,S., 1997a. Discontinuity Adaptive MRF Model for the Analysis of Synthetic Aperture Radar Images, *IEEE Transactions of Geoscience and Remote Sensing*, vol **35**, no. **4**, 837-840.

358. Solomatine, D. P. and Torres, L. A., 1996, Neural network approximation of a hydrodynamic model in optimizing reservoir operation - *Proc. 2nd Intern. Conference on Hydroinformatics*, Zurich, September 9-13, 201-206.

359. Stehman, S. V. and Czaplewski, R. L., 1998. Design and analysis for thematic map accuracy assessment: Fundamental principles. *Remote Sensing of Environment*, **64**, 331–344.

360. Stein, A**.**, 2002. Pattern recognition. In: *Encyclopedia of environmentrics* Vol. 4. / ed. by A.H. El-Shaarawi and W. Piegorsch. - Chichester: Wiley & Sons, ISBN: 0-471-89997-6. 1534-1542.

361. Stein, A**.,** 2005, Image - mining for solving spatial and spatio - temporal uncertainty. In: *Proceedings of the International Symposium on Spatial Data Quality* '2005, August 25-26, 2005, Beijing / ed. by Lun Wu, Wenzhong Shi, Yu Fang and Qingxi Tong. Hong Kong: The Hong Kong Polytechnic University, 2005. 27-39.

362. Stein, A**.,** 2006, Developments in image mining for vague objects: abstract. In: *Abstracts of the workshop on modern aspects of remote sensing and geospatial data processing*, NRSA - ITC, Hyderabad, India, 24-25 November 2006 / ed by. K.M.M. Rao, A. Stein, P.S. Roy and A.S. Manjunath. Hyderabad: National Remote Sensing Agency (NRSA), 2006.

363. Stuckens, J., Coppin, P.R. and Bauer, M.E., 2000, Integrating contextual information with per-pixel classification for improved land cover classification. *Remote Sensing of Environment*, **71**, 282–296.

364. Swain, P.H. and Davis, S.M., 1978. *Remote sensing: the quantitative approach*, McGraw-Hill, New York, USA, ISBN: 978-0070625761, 136-187.

365. Szeliski, R., Zabih, R., Scharstein, D., Veksler, O., Kolmogorov, V., Agarwala, A., Tappen, M.,andRother, C., 2008. A comparative study of energy minimization methods for markov random fields with smoothness-based priors. *IEEE Trans. on Pattern Anal. Machine Intell.*, ***PAMI*- 30(6)**, 1068–1080.

366. Tan,C.P., Koay,J.Y.,Lim, K.S.,Ewe, H.T., and Chuah, H.T., 2007.classification of multi-temporal sar images for rice crops using combinedentropy decomposition and support vector machine technique, *Progress In Electromagnetics Research*, **PIER71**,19–39.

367. Tayyebi, A., M.R. Delavar, S. Saeedi, J. Amini and H. Alinia, 2008. monitoring land use change by multi-temporal landsat remote sensing imagery, *International Archives of the Photogrammetry, Remote Sensing and Spatial Information Sciences*. Vol. **XXXVII**. Part **B7**. Beijing.

368. Thai, B. and Healey, G., 2002, Invariant Subpixel Material Detection in Hyper-spectral Imagery, *IEEE Transactions on Geoscience And Remote Sensing*, Vol. **40**, No. **3**.

369. Thomas, N., Hendrix, C. and Congalton, R.G., 2003, A comparison of urban mapping methods using high-resolution digital imagery. *Photogrammetric Engineering and Remote Sensing*, **69**, 963–972.

370. Tihonov, A.N., Arsenin, V.Y., 1977. Solutions of Ill-Posed Problems. Wiley, New York.

371. Thornton, M. W. Atkinson, P. M. and Holland, D. A., 2006, Sub-pixel mapping of rural land cover objects from fine spatial resolution satellite sensor imagery using super resolution pixel swapping, Volume 27, Number 3 / 10 February, 473 – 491.

372. Tolpekin, V. A. and Stein, A. 2009. Quantification of the effects of the land-coverclass seperability on the accuracy of Markov-Random-Field-Based superresolution mapping, *IEEE Transactions on Geoscience and Remote Sensing*, vol **23**,no. **20**, 4519-4523.

373. Tortora, R., 1978. A note on sample size estimation for multinomial populations. *The American Statistician*, **32 (3)**, 100-102.

374. Townshend, J.R.G., 1992. Land cover, *International Journal of Remote Sensing*, **13**, 1319-1328.

375. Townsend, P. A., 2000. A quantitative fuzzy approach to assess mapped vegetation classifications for ecological applications. *Remote Sensing of Environment*, **72**, 253–267.

376. Townsend, P.A., and Walsh, S.J., 2001. Remote sensing of forested wetlands: application of multi-temporal and multispectral satellite imagery to determine plant community composition and structure in southeastern USA. *Plant Ecology*, **157** , 129–149.

377. Trinder, J., Maulik U., and Bandyopadhyay,S.,2012. "Semi-automated Feature Extraction Using Simulated Annealing", *International Archives on Photogrammetry and Remote Sensing (ISPRS)*, vol. **33 (3/2)**, 905-909,

378. Tso B., and Olsen, R. C., 2005. A contextual classification scheme based on MRF model with improved parameter estimation and multiscale fuzzy line process, *Remote Sensing of Environment*, vol. **97**, no. **1**, 127–136.

379. Tso, B. and Mather, P.M., 2001, *Classification Methods for Remotely Sensed Data* ,New York: Taylor and Francis Inc.

380. Tso, B. and Mather, P.M., 2009. *Classification Methods for Remotely Sensed Data*, CRC Press, Boca Raton,ISBN: 978-0415259095, 56-69.

381. Tsoukalas, L. H. and Uhrig, R. E., 1997, *Fuzzy and Neural Approaches in Engineering*. John Wiley and Sons, N.Y., 587.

382. Tuia, D. and Camps-Valls, G., 2011. Urban Image Classification With Semisupervised Multiscale Cluster Kernels. *IEEE journal of selected topics in applied earth observations and remote sensing*, vol. **4**, no. **1**. 1401-1404.

383. Tucker, C.J., 1979. Red and photographic infrared linear combinations for monitoring vegetation, *Remote Sensing of Environment*, **8**, 127-150.

384. Tuladhar, A.M., 2004. *Parcel-based Geo-Information System: Concept and Guidelines*. ITC Dissertation 115, ISBN: 90-6164-224-8.

385. Upadhyay, P., Ghosh, S.K., and Kumar, A., 2013. Moist deciduous forest identification using temporal MODIS data — A comparative study using fuzzy based classifiers, *Ecological Informatics*, **18**, 117–130.

386. Valls, G. C., Chova, L. G. and Maravilla, J. C., 2004, Robust Support Vector Method for Hyper-spectral Data Classification and Knowledge Discovery, *IEEE Transactions on Geoscience And Remote Sensing*, vol. **42**, no. **7**.

387. Van Der Sande, C.J., De Jong, S.M. and De Roo, A.P.J., 2003, A segmentation and classification approach of IKONOS-2 imagery for land cover mapping to assist flood risk and flood damage assessment. International *Journal of Applied Earth Observation and Geoinformation*, **4**, 217–229.

388. Van de Vlag, D. E. and Stein, A., 2005, Uncertainty propagation in beach classification using fuzzy decision trees. In: *Proceedings of the International Symposium on Spatial Data Quality* '2005, August 25-26, 2005, Beijing / ed. by Lun Wu, Wenzhong Shi, Yu Fang and Qingxi Tong. The Hong Kong Polytechnic University, Hong Kong, 2005. 257-269.

389. Vanderbei R. J., 1997, User's manual – version 3.10. (SOR-97-08), Statistics and Operations Research, Princeton University, Princeton, NJ.

390. Vapnik, V., and Chervonenkis, 1974, *Theory of Pattern Recognition* [in Russian], Nauka, Moscow.

391. Vapnik, V., 1995, *The Nature of Statistical Learning Theory*, Springer Verlag, New York.

392. Vapnik, V., 1998, *Statistical Learning Theory*, John Wiley and Sons, New York.

393. Vapnik V. N., 1999, An overview of statistical learning theory. *IEEE Transactions of Neural Networks*, **10** , 988-999.

394. Vapnik V. N., 2000, *The Nature of Statistical Learning Theory*. Springer, 2nd Edition.

395. Van-Westen, C., 2000. Remote Sensing and Geographic Information Systems for Natural Disaster Management. *International Archives of Photogrammetry and Remote Sensing*. Vol. **XXXIII**, Part **B7**. Amsterdam 2000, 1609-1617.

396. Venkatachalam, P., 1981. Utilization of remote sensing in resources identification and landuse in India - An integrated approach. Proceedings of *15th International Symposium on Remote Sensing of Environment*, Ann Arbor, Michigan, USA, May 1981.

397. Verhoeye J.and Robert D. W. 2000."Sub-pixel Mapping of Sahelian Wetlands using Multi-temporal SPOT Vegetation Images. Laboratory of Forest Managementand Spatial Information Techniques," Faculty of Agricultural and Applied Biological Sciences, University of Gent.

398. Vijaya, M., Kumar, A., Roy, P.S. and Kale, K., 2012. "Evaluation of fuzzy-based classifiers for cotton crop identification". *Geocarto International,*Vol. **28**, Issue **3**, 243-257

399. Volpi, M., Tuia, D. and M. Kanevski, 2011. "Transfer component analysis for domain adaptation in image classification," , 12

400. Walter, V., 2004, Object-based classification of remote sensing data for change detection. *ISPRS Journal of Photogrammetry & Remote Sensing*, **58**, 225–238.

401. Wan, S., Lei, T.C. and Chou, T.Y., 2010. A novel data mining technique of analysis and classification for landslide problems, *Natural Hazards*, **52**, 211-230.

402. Wang, F., 1990. Fuzzy supervised classification of remote sensing images, *IEEE Transactions on Geoscience and Remote Sensing*, **28**, 194-201.

403. Wang, F., 1990a, Improving Remote Sensing Image Analysis Through Fuzzy Information Representation. *Photogrammetric Engineering & Remote Sensing*, **56(8)**, 1163-1169.

404. Wang, J., Price, K.P. and Rich, P.M., 2001. Spatial patterns of NDVI in response to precipitation and temperature in the Central Great Plains, *International Journal of Remote Sensing*, **22**, 3827-3844.

405. Wang, L., Sousa, W.P. and Gong, P., 2004. Integration of object-based and pixel-based classification for mapping mangroves with IKONOS imagery, *International Journal of Remote Sensing*, **25**, 5655-5668.

406. Wang, Q., Zhang,Q., and Zhou,W., 2012. Study on Remote Sensing Image Segmentation Based on ACA–FCM, *PhysicsProcedia*, vol. **33**, no. **0**, 1286–1291.

407. Watkins, C. J., C. H. and Dayan, P., 1992, *Q-learning. Machine learning*, 8, 279-292.

408. Wei, W. and Jerry, M.M., 1999. A fuzzy logic method for modulation classification in non-ideal environment, *IEEE Transactions on Fuzzy Systems*, **7**, 333-344.

409. Wen, W. and Xia, A., 1999. Verifying edges for visual inspection purposes, *Pattern recognition letters*, vol. **20**, no. **3**, 315–328.

410. Woodcock, C.E. and Gopal, S., 2000, Fuzzy set theory and thematic maps: accuracy assessment and area estimation. *International Journal of Geographic Information Science*, **14**, 153–172.

411. Wu, Xiao-Hong and Zhou, Jian-Jiang, 2006. Alternative Noise Clustering Algorithm. *IEEE-ICSP 2006 Proceedings*, 0-7803-9737-1/06.

412. Xu, B., Gong, P., Seto, E. and Spear, R., 2003, Comparison of gray-level reduction and different texture spectrum encoding methods for land-use classification using a panchromatic IKONOS image. *Photogrammetric Engineering and Remote Sensing*, **69**, 529–536.

413. Xu, M., Cao, C., Zhang, H., Guo, J., Nakane, K., He, Q., Guo, J., Chang, C., Bao, Y., Gao,M. and Li, X., 2010. Change detection of an earthquake-induced barrier lake based on remote sensing image classification, *International Journal of Remote Sensing*, **31**, 3521-3534.

414. Xuan, S.U.,Wang, X., Wang, Z. and Xiao, Y., 2010. Annew fuzzy clustering algorithm based on entropy weighting, *Journal of Computational Information Systems*, **6**, 3319-3326.

415. Yang,M&Wu,K., 2006. Unsupervised Possibilistic Clustering, *Pattern Recognition*, vol **39**, 5-21.

416. Yannis, S. A., and Stefanos, D. K. 1999."Fuzzy Image Classification Using Multi-resolution Neural with Applications to Remote Sensing." Electrical Engineering Department, National Technical University of Athens, Zographou 15773, Greece.

417. Yeow, L.S., 2010. *Spatial kernel-based generalized c-mean clustering for medical image segmentation*, Ph.D. thesis, School of computer sciences, UniversitySains Malaysia.

418. Zadeh, L. A., 1965 "*Fuzzy sets," Information and control*, vol. **8**, 338–353.

419. Zhang, J. and Foody, G.M., 2001. A fuzzy classification of sub-urban land cover from remotely sensed imagery, *International Journal of Remote Sensing*, **19**, 2721-2738.

420. Zhang, J. and Foody, G.M., 2001a. Fully-fuzzy supervised classification of sub-urban land cover from remotely sensed imagery: Statistical and artificial neural network approaches," *International Journal of Remote Sensing*, vol. **22**, no. **4**, 615–628.

421. Zhang, Z., Gong, H., Zhao, W. and Zhang, Y., 2005. Application of remote sensing to study of landslides, *Proc. of IEEE IGARSS International 2005*, 1546-1549.

422. Zhang, L. and Huang, X., 2007. Classification of high-spatial resolution imagery based on distance-weighted Markov random field. *International Journal of Remote Sensing* Vol. **30**, No. **8**, 1977–1987.

423. Zhang,G., and Jia,X., 2011. Spectral-Spatial Based Super Pixel Remote Sensing Image Classification. *4th IEEE International Congress on Image and Signal Processing*.978-1-4244-9306-7/11.

424. Zhou, Y., 2007, Utilizing geometric attributes of spatial information to improve digital image classification. *Remote Sensing Reviews*, **16**, 233–253.

425. Zhu, A.X., 1997. Measuring of uncertainty in class assignment for natural resource maps under fuzzy logic, *Photogrammetric Engineering and Remote Sensing*, **63**, 1195-1202.

426. Zhu, G. and Blumberg, D.G., 2002, Classification using ASTER data and SVM algorithms: the case study of Beer Sheva, Israel. *Remote Sensing of Environment*, **80**, 233–240.

APPENDIX

LIST OF PUBLICATIONS

Refereed Journals

i) Dwivedi, R.K., Ghosh, S. K. and Kumar, A., 2012. Study of Fuzzy based Classifier Parameter across Spatial Resolution. *International Journal of Computer Applications, (0975–8887).Volume,50–No.11,17-24.* http://www.ijcaonline.org/archives/volume50/number11/7814-1074

ii) Dwivedi, R.K., Ghosh, S. K. and Kumar, A., 2012. Study of Fuzzy Based Classifier Parameter Using Fuzzy Matrix. *International Journal of Soft Computing and Engineering (IJSCE) ISSN: 2231-2307, Volume-2, Issue-3, 358-365.* http://www.ijsce.org/attachments/File/v2i3/C0818062312.pdf

iii) Dwivedi, R.K., Ghosh, S. K. and Kumar, A., 2012. Investigation of Image Classification Techniques For Performance Enhancement. *Viewpoint "An International Journal of Management and Technology" ISSN-2229-3825. Volume 3, number 2, 3-10.* http://www.tmu.ac.in/pdf/viewpointjultodec2012/final_inner_05.pdf

iv) Dwivedi, R.K., Ghosh, S. K. and Kumar, A., 2013. Proposed Model To Measure The Effect of Discontinuity Adaptive MRF Models In Fuzzy Based Classifier On Satellite Images. *MATRIX Academic International Online Journal Of Engineering And Technology, Volume 1 Issue 1, 19-29.* *http://maioj.org/data/documents/005April2013.pdf*

v) Dwivedi, R.K., Ghosh, S. K. and Kumar, A., 2013. Parameter Optimization for Noise Clustering with Contextual Classifier on satellite Images. *International Journal of Trends in Computer Science (IJTICS), Volume 2, Issue 11. 191-202.* *http://www.academicjournalonline.co.in/pdf/new_ijtics/Parameter%20Optimization%20for%20Noise%20Clustering%20with%20Contextual%20Classifier%20on%20satellite%20Images%20By%20Rakesh%20Dwivedi.pdf*

Conferences

i) Dwivedi, R.K., Ghosh, S. K. and Kumar, A., 2011. Optimisation of Fuzzy based Soft classifiers for Remote Sensing Data AWIFS with LISS-IV DATASET. *Indian Society of Remote Sensing*, Bhopal, India. November 9-10, 2011.

ii) Dwivedi, R.K**.,** Ghosh, S. K. and Kumar, A., 2011. Optimisation of Fuzzy based Soft Classifiers for Remote Sensing Data USING LISS-III and LISS-IV DATASET. *International Conference on Information and Communication Technology*, Dehradun, India. November, 2011.

iii) Dwivedi, R.K., Ghosh, S. K. and Kumar, A., 2012. Optimization of Fuzzy Based Soft Classifiers For Remote Sensing Data Comparative Analysis Using Entropy. *International Archives of the Photogrammetry, Remote Sensing and Spatial Information Sciences*, Volume XXXIX-B3, pp 385-390 2012. XXII ISPRS Congress, 25 August – 01 September 2012, Melbourne, Australia. http://www.int-arch-photogramm-remote-sens-spatial-inf-sci.net/XXXIX-B3/385/2012/isprsarchives-XXXIX-B3-385-2012.pdf

iv) Dwivedi, R.K., Ghosh, S. K. and Kumar, A., 2012. Investigation of parameter optimization of noise clustering algorithm using entropy. *National Symposium on Space Technology for Food & Environmental Security*, New Delhi, India, December 5-7, 2012.

v) Dwivedi, R.K., Ghosh, S. K. and Kumar, A., 2012. Estimation of Uncertainty using entropy on noise based soft classifiers. *2nd International Conference on Soft Computing (SocPros-2012)*, Jaipur, India, December 28 – 30, 2012.

vi) Dwivedi, R.K., Ghosh, S. K. and Kumar, A., 2012. Investigation of Image classification Techniques For Performance. *International Conference on System modeling and Advancement in research trends (SMART-1)*, Moradabad, India, October 20-21, 2012. (*Awarded Best paper*).

vii) Dwivedi, R.K., Ghosh, S. K. and Kumar, A., 2013. Visualization of Uncertainty using entropy on Noise clustering with entropy classifier. *3rd IEEE International Advance Computing Conference (IACC-2013)*. ISBN:-978-1-4673-4528-6. Ghaziabad (UP)-201009, India, February, 22-23, 2013. http://ieeexplore.ieee.org/stamp/stamp.jsp?tp=&arnumber=6514415.

viii) Dwivedi, R.K., Ghosh, S. K. and Kumar, A., 2013. Analyze The Effect of Contextual

Based Fuzzy MRF Models In Satellite Images. *The 19th International Conference on Parallel and Distributed Processing Techniques and Applications (PDPTA-2013. WORLDCOMP-13*), Las Vegas, Nevada, USA, July 22-25, 2013. *worldcomp-proceedings.com/proc/p2013/PDP7043.pdf*

ix) Dwivedi, R.K., Ghosh, S. K. and Kumar, A., 2013. Effect of smoothening and Discontinuity Adaptive MRF Models in Noise Based Classifier on Satellite Images. *Latin American Remote Sensing Week (LARS, 2013), Regional ISPRS conference*, Chile, 23-25 October, 2013.

x) Dwivedi, R.K., Ghosh, S. K. and Kumar, A., 2013. Parameter Optimization for Noise Clustering with Contextual Classifier on satellite Images. International Conference on System modeling and Advancement in research trends(SMART-2), Moradabad, India, November 15,16, 2013.

xi) Dwivedi, R.K., Ghosh, S. K. and Kumar, A., Analyzing the Effect of Contextual Information in Noise Based Classifier On Satellite Images. *The 20th International Conference on Parallel and Distributed Processing Techniques and Applications (PDPTA-2014. WORLDCOMP-14*, Las Vegas, Nevada, USA, July 22-25, 2014 (*Accepted*).